NI-CATALYZED FIXATION OF HETEROCUMULENES INTO ORGANIC MATTER AND C-H FUNCTIONALIZATION REACTIONS

Xueqiang Wang

2015

Ni-catalyzed Fixation of Heterocumulenes into

Organic Matter and C-H Functionalization Reactions

DOTORAL THESIS

DOTORAL THESIS

Institute of Chemical Research of Catalonia

ICIQ
Institut Català d'Investigació Química

UNIVERSITAT ROVIRA I VIRGILI

2015

DOCTORAL THESIS

Ni-catalyzed Fixation of Heterocumulenes into Organic Matter and C-H Functionalization Reactions

Xueqiang Wang

Supervised by Prof. Ruben Martin

Tarragona, Spain

2015

Institute of Chemical Research of Catalonia (ICIQ)

ICIQ
Institut Català d'Investigació Química

UNIVERSITAT ROVIRA I VIRGILI

Avinguda Països Catalans, 16
43007, Tarragona, Spain
Tel: +34 977 920 200
Fax: +34 977 920 222

Department de Quimica Fisia Inorganica
C/Marcelli Domingo s/n
Edifici N4, Campus Sescelades
43007, Tarragona, Spain
Tel: +34 977 558 137 9696
Fax: +34 977 559 563

Prof. **Ruben Martin**, Group Leader of Research Group and ICREA Research Professor at the Institute of Chemical Research of Catalonia (ICIQ).

CERTIFIES, that the present Doctoral Thesis entitled: "**Ni-catalyzed Fixation of Heterocumulenes into Organic Matter and C-H Functionalization Reactions**" presented by Xueqiang Wang to receive the degree of Doctor, has been carried out under his supervision at the Institute of Chemical Research of Catalonia (ICIQ).

Tarragona, October 6, 2015.

PhD Thesis Supervisor:

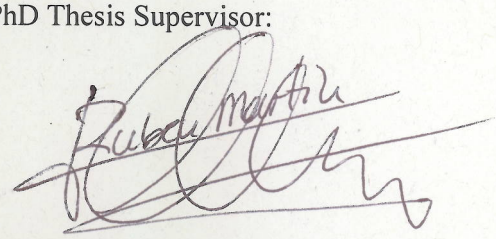

Prof. Ruben Martin

Acknowledgements

First of all, I would like to sincerely express my gratitude to Prof. Ruben Martin for offering me a great opportunity to pursue my PhD within his group. Working with him considerably expanded my chemistry knowledge, taught me the importance of quality and excellent day-to-day work. Thank you very much for teaching me so many things, for the guidance and support you gave me during my time in this amazing group.

During my last three years at ICIQ I got to know a lot of people. I have to say that it is very hard to do a PhD without my family, but I am blessed that I had so many good friends around who were more than willing to help me out. A simple thank you is far from enough to express my gratitude but even so: thank you very much. Thanks for all your kind help to make my life much easier here.

I remember when I arrived at ICIQ, I almost could not speak English. The guys from lab 2.10 were patient to talk to me, to explain me lots of things. I really had a great time in such a international lab, Caye, Pep and David from Spain, Rene from Germany, Indranil and Sandeep from India, Xu Tian from China, Lucasz from Poland, Rodeligo from Brazil. Thanks, guys.

Being a member of the Martin group provided me the privilege of sharing my time with extraordinary people that are not just colleagues but precious friends: Dr. Arkaitz Correa, Dr. Yu Liu, Dr. Thierry León, Dr. Rubén Manzano, Dr. Josep Cornellà, Dr. Areli Flores, Dr. Asraa Ziadi, Dr. Antoni Moragas, Dr. Francisco Julià, Dr. Masaki Nakajima, Dr. Morgane Gaydou, Dr. Manuel van Gemmeren, Dr. Xiang-Wei Liu, Dr. Daniel Gallego, Álvaro Gutiérrez, Miriam Sau, Eloisa Serrano, Cayetana Zárate, Marino Rolando Börjesson, Yangyang Shen, Javier Echavarren, Andreu Tortajada. Thank you all for the wonderful moments you allowed me to spend with you. I will miss you very much.

My special thanks to my project mates: Dr. Yu Liu, Dr. Masaki Nakajima, Marino Rolando Börjesson. Thanks for your incredible work to help me finishing all the projects, for the high quality of your results presented in my thesis, for all the laughs and funny time that we had. Apart from their important help from a scientific point of view, I am grateful to them for always being such supportive, patient and cheerful

friends. I also would like to thank my friends Cayetana Zárate and Marino Rolando Börjesson with particular affection for helping me to find a department and being ‘professional’ translators to help me out. My special appreciation is also for our group administrative support: Ingrid Mateu. Thanks a lot for all of the help and support and all of the fun times we had.

I would like specially to thank the management department and research support departments. Thanks for your unbelievable help during my PhD at ICIQ. Undoubtedly, I would not have been able to finish my PhD studies without all your support.

I also would like to say thank you to my flat mate: Peilin Han. I am grateful to him for always being such encouraging, patient and cheerful friend.

Thanks to Dr. Morgane Gaydou, Dr. Antoni Moragas, Dr. Masaki Nakajima, Dr. Manuel van Gemmeren, Dr. Daniel Gallego, Eloisa Serrano, and Rosie Somerville for helping me correct my thesis

My deepest gratitude goes to my family. A billion thanks to my wife, Sijie Huang who encourage me to pursue my PhD abroad and took care of our son during all these years. My deepest thankfulness to my parents, my parents-in-law, my sister and my brother-in law will not ever be enough for their altruistic support.

值此博士论文完成之际，我要由衷的感谢我辛劳的父母，感谢他们在这三十几年里对我养育之恩！我也要真挚的感谢我的妻子和岳父母，正是由于你们对我生活上的关心和照顾、学业上的支持，才使我能安心学习和研究，感谢你们对小宝贝子西无微不至的照顾！我也衷心的感谢我的妹妹和妹夫对我学业上的支持，在家里对父母悉心的照顾，今天可以完成学业有你们很大的一份功劳！感谢各位亲朋好友对我的关爱！你们的默默支持和无私奉献是我学业的支柱，谨以我的博士论文，献给一直以来关爱、呵护我的家人们。

Tarragona, August 4, 2015.

Abbreviations

CO_2	Carbon dioxide
Conv.	Conversion
eq.	Equivalents
Vb	Valence bond
DCM	Dichloromethane
THF	Tetrahydrofuran
PhMe	Toluene
MeCN	Acetonitrile
DMF	Dimethylformamide
DMA	Dimethylacetamide
t-BuOH	*tert*-butanol
NMP	*N*-Methyl-2-pyrrolidone
DMSO	Dimethyl sulfoxide
ArI	Aryl iodide
AcOH	Acetic acid
AcO_2H	Peracetic acid
PIDA	(Diacetoxyiodo)benzene
PIFA	[Bis(trifluoroacetoxy)iodo]benzene
rt	Room temperature
TMS	Trimethylsilyl
δ	Chemical shift
J	Coupling constant
$CDCl_3$	Deuterated chloroform
s	Singlet
d	Doublet
t	Triplet
m	Multiplet
NMR	Nuclear Magnetic Resonance
ppm	Parts per million
Me	Methyl
OPiv	Pivalate

The rest of abbreviations and acronyms: "Guideline for authors" *J. Org. Chem.* **2008**, *73*, 23A-24A.

List of Publications

The results of this PhD thesis have delivered the following publications:

1) Ni-catalyzed Regioselective Hydroamidation of Alkynes with Isocyanates
   Wang, X.; Nakajima, M.; Martin, R. Manuscript in preparation.

2) Ni-catalyzed Regioselective Hydrocarboxylation of Alkynes with CO_2 by Using Simple Alcohols as Proton Sources
   Wang, X.; Nakajima, M.; Martin, R. *J. Am. Chem. Soc.* **2015**, *137*, 8924.
   Most read JACS articles in July 2015

3) Ni-catalyzed Divergent Cyclization/Carboxylation of Unactivated Primary and Secondary Alkyl Halides with CO_2
   Wang, X.; Liu, Y.; Martin, R. *J. Am. Chem. Soc.* **2015**, *137*, 6476.
   Among the most read JACS articles in May 2015

4) Mild ArI-catalyzed C(sp^2)-H or C(sp^3)-H Functionalization/C-O Formation: An Intriguing Catalyst-Controlled Selectivity Switch
   Wang, X.; Gallardo, D. J.; Martin, R, *Angew. Chem. Int. Ed.* **2014,** *53*, 11084.
   Highlighted in *Synfacts* **2014**, *10*(12), 1255.

Content

Chapter 1: General Introduction

1.1 Introduction to CO_2

During the last decades, the increasing level of atmospheric carbon dioxide (CO_2) has oftentimes been associated with global warming, and has created serious environmental concerns about the continuous use of carbon-based fuels. Currently, the CO_2 concentration in the atmosphere exceeds 402.8 ppm in 2015.[1] Analyses of ocean sediments for seawater pH and calcium, ice core data, magnesium and carbonate mineralogy, have led to a conclusion that the atmospheric concentration has not reached such a level over the last 400,000 years.[2,3] Over the last decades, global industrial development has produced anthropogenic sources of CO_2, leading to an increase of the concentration of CO_2, and the level attained is well above to the one from natural fluctuations.

As exhibited in Figure 1.1, the combustion of fossil fuels represents more than half of the worldwide greenhouse gas release.[4] Global CO_2 production has increased by nearly 80% over the period of 1970-2004 (from 21 to 38 Gt/year). Unfortunately, these emission levels are expected to rise further over the next few decades due to the increase in energy requests related to a growing global population. As a consequence, average global temperatures are estimated to increase between 1.8 and 6.4 °C by the end of this century based on the potential scenarios presented in the recent IPCC climate report in 2007.[5]

---

[1] Earth System Research Laboratory: http://www.esrl.noaa.gov/gmd/ccgg/trends/

[2] Fischer, H.; Wahlen, M.; Smith, J.; Mastroianni, D.; Deck, B. *Science* **1999**, *283*, 1712.

[3] Demicco, R. V.; Lowenstein, T. K.; Hardie, L. A. *Geology* **2003**, *31*, 793.

[4] Pachauri, R. K.; Reisinger, A. I*PCC Fourth Assessment Report, Intergovernmental Panel on Climate Change*, **2007**.

[5] Sumida, K; Rogow, D. L.; Mason, J. A.; McDonald, T. M.; Bloch, E. D. Herm, Z. R.; Bae, T.; Long, J. R. *Chem. Rev.* **2012**, *112*, 724.

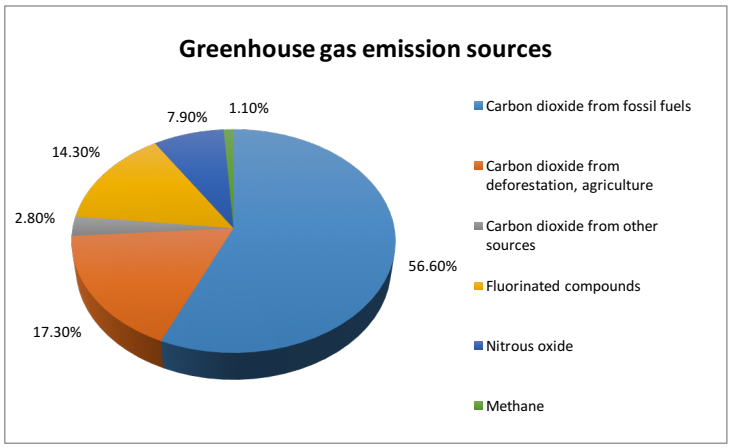

Figure 1.1. Global greenhouse gas emission sources in 2004.

Despite all the advances realized to reduce CO_2 emissions, the increasing demand for energy is constant and there is no doubt that CO_2 emissions will rise even further. That being set, chemists have been challenged to design CO_2 fixation techniques since CO_2 is probably the most abundant C1 source. Although, the utilization of CO_2 as a chemical feedstock will not reduce its atmospheric concentration significantly, this may pave the way to precious products from a nontoxic, renewable, and low-cost resource. Such sustainable methodologies would reduce waste and make a better use of energy and carbon.

1.2 General Coordination Modes and Activation Routes

According to the valence bond (*VB*) theory, CO_2 is a linear molecule with a total of sixteen bonding electrons in its valence shell (Figure 1.2). Carbon is the central atom of the molecule and the *z*-axis goes through the center of carbon and the two oxygen atoms. The C-O σ-bond is formed by the interaction between the hybrid *sp* orbital of carbon and the *Pz* orbital of oxygen. Meanwhile a *P* orbital from the carbon and one from the oxygen make up the π bonds.

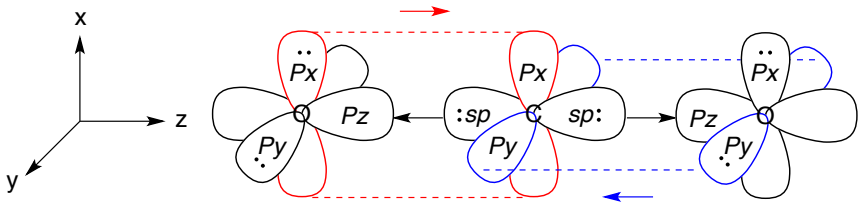

Figure 1.2. Simple *VB* model of CO_2.

The most important coordination modes of CO_2 to transition metals is depicted in

Figure 1.3, σ bonding of the metal to the carbon atom (**A**); the σ bonding of the carbon atom to the metal with the metal coordinated to the oxygen atom (**B**); the π coordination of one carbonyl bond to the metal center (**C**) and σ-O coordinated CO_2 (**D**). Although catalytic modes significantly lower the barrier of thermodynamically and kinetically inert CO_2, the transformation of the coordinated CO_2 still becomes rather problematic, particularly in a catalytic fashion.

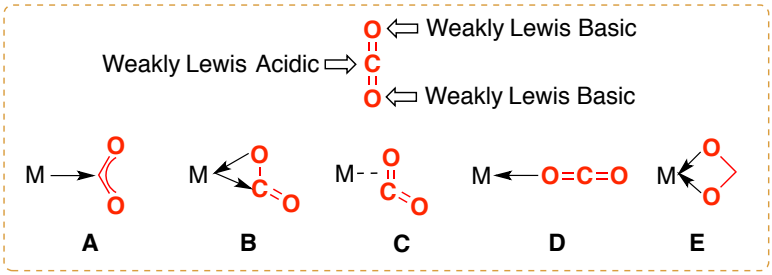

Figure 1.3. Possible coordination modes of CO_2 to a transition metal complex.

Surprisingly, the recently published protocols are still associated with the initial studies from the 1970's-1980's, reported by Inoue, Musco, Hoberg, Walther, Behr and their coworkers, which were well reviewed in several reviews.[6] Essentially, two general routes can be found (Scheme 1.1): (a) Cycloaddition reaction of π-components (b) Insertion of CO_2 into reactive R-metal bonds. The basicity and capability for binding CO_2 through back bonding makes late-transition metals (Fe^0, Rh^I, Ni^0, Pd^0, Pd^{II}) particularly useful for activating and further functinalizing CO_2.[7]

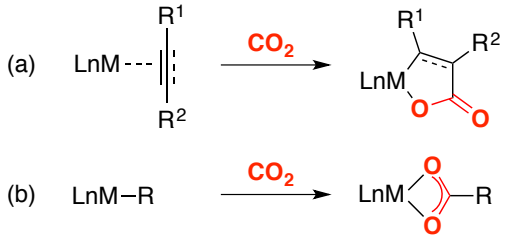

Scheme 1.1. General CO_2 activation routes.

[6] (a) Palmer, D. A.; Eldik, R. V. *Chem. Rev.* **1983**, *83*, 651. (b) Behr, A. *Angew. Chem. Int. Ed.* **1988**, *27,* 661. (c) Gibson, D. H. *Chem. Rev.* **1996**, *96*, 2063. (d) Leitner, W. *Coord. Chem. Rev.* **1996**, *153*, 257. (e) Gibson, D. H. *Coord. Chem. Rev.* **1999**, *185 – 186*, 335. (f) Lin, X.; Moss, J. R. *Coord. Chem. Rev.* **1999**, *181*, 27.

[7] (a) Cokoja, M.; Bruckmeier, C.; Rieger, B.; Herrmann, W. A.; Kühn F. E. *Angew. Chem. Int. Ed.* **2011**, *50*, 8510. (b) Huang, K.; Sun, C.; Shi, Z. *Chem. Soc. Rev.* **2011**, *40*, 2435. (c) Riduan, S. N.; Zhang, Y. *Dalton Trans.* **2010**, *39*, 3347. (d) Louie, J. *Curr. Org. Chem.* **2005**, *9*, 605. (e) Yu, D.; Teong, S. P.; Zhang Y. *Coord. Chem. Rev.* **2015**, *293 - 294,* 279. (f) Tsuji, Y.; Fujihara, T. *Chem. Commun.,* **2012**, *48*, 9956. (g) Martin, R.; Kleij, A. W. *ChemSusChem* **2011**, *4*, 1259.

1.3 Stoichiometric Coupling of CO_2

1.3.1 Coupling of CO_2 with Nucleophilic Organometallic Reagents

Scheme 1.2. CO_2 coupling with organolithium or Grignard reagents.

Due to its thermodynamic stability and kinetic inertness, it is not surprising that highly reactive Grignard reagents or organolithium derivatives have been effectively sued for fixating CO_2, resulting in the synthesis of carboxylic acids. It is worth noting that these protocols proceed easily even without transition metal catalysts. Unfortunately, the high reactivity of Grignard reagents or organolithiums makes the chemoselectivity profile particularly problematic, thus motivating the use of less-base and less-reactive organometallic entities.[8]

In 2002, Olah's group realized the direct carboxylation of benzene and derivatives via the intermediacy of organoaluminum reagents. Although generally good results were obtained, this technique required high pressure of CO_2, certainly a drawback that needs to b overcome (Scheme 1.3).[9]

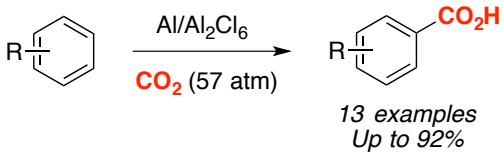

Scheme 1.3. CO_2 coupling with organoaluminum reagents.

In 2005, the Ebert group described the carboxylation of organocopper reagents generated *in situ* from the corresponding aryl iodides.[10] The corresponding copper benzoates were found to react with alkyl halides to form aryl esters (Scheme 1.4). Unlike the utilization of Grignard reagents or organolithiums This methodology

[8] (a) Correa, A.; Martin, R. *Angew. Chem. Int. Ed.* **2009**, *48,* 6201. (b) Goossen, L. J.; Rodriguez, N.; Goossen, K. *Angew. Chem. Int. Ed.* **2008**, *47*, 3100. (c) Bew, S. P.; Katritzky, A. R.; Taylor R. J. K. (Eds.), *Comprehensive Organic Functional Groups Transformation II*, Elsevier, Oxford, **2005**, p. 19.

[9] Olah, G. A.; Torok, B.; Joschek, J. P.; Pierre, I. P.; Esteves, M.; Rasul, G.; Prakash, G. K. S. *J. Am. Chem. Soc.* **2002**, *124*, 11379.

[10] Ebert, G. W.; Juda, W. L.; Kosakowski, R. H.; Ma, B.; Dong, L.; Cummings, K. E.; Phelps, M. V. B.; Mostafa, A. E.; Luo, J. *J. Org. Chem.* **2005***, 70,* 4314.

afforded the possibility of using sensitive functional groups.

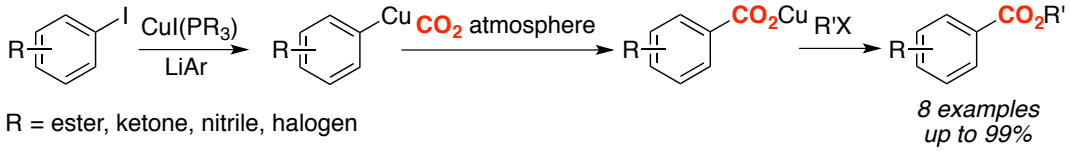

Scheme 1.4. CO_2 coupling with organocopper reagents.

A carboxylation of organozinc reagents in the presence of LiCl with atmospheric pressure CO_2 (1 atm) was described by Kondo and coworkers.[11] The reaction conditions were mild, allowing for the coupling of a wide variety of arylzinc iodides that containing electron-donating or electron-withdrawing substituents in good to excellent yields. However, the authors did not explain the role of LiCl. (Scheme 1.5).

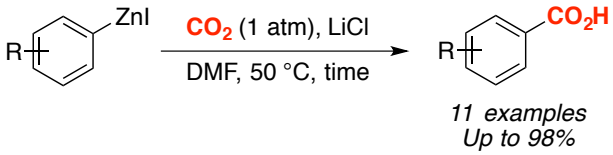

Scheme 1.5. CO_2 coupling with organozinc reagents.

1.3.2 Coupling of CO_2 with Unsaturated Bonds

In the 1980's, the research groups of Hoberg and Walther pioneered the oxidative coupling of CO_2 with Ni(0) complexes and alkenes to form stable nickelalactones.[12] Typically, these reactions required bulky σ donor ligands (PCy_3, etc.) or bidentate ligands (dcpe, bipy, etc) to form a highly reactive NiL_2 species *in situ*, thus promoting the cyclization of alkenes and CO_2. A final acid hydrolysis of the metallacycle yields the desired acid. As for the regioselectivity profile, Hoberg *et al*. observed that a selectivity switch depending on the alkene motif. While styrenes resulted in **I** with the Ni-center located adjacent to the aromatic ring, the use of aliphatic olefins in **II** where the Ni-center is located at the less hindered site (Scheme 1.6).[13]

[11] Kobayashi, K.; Kondo, Y. *Org. Lett.* **2009**, *11*, 2035.

[12] (a) Hoberg, H.; Schaefer, S. *J. Organomet. Chem.* **1982**, *236*, C28. (b) Hoberg, H.; Schaefer, S. *J. Organomet. Chem.* **1983**, *251*, C51. (c) Walther, D.; Dinjus, E.; Sieler, J.; Andersen, L.; Lindqvist, O.; *J. Organomet. Chem.* **1984**, *276*, 99.

[13] Hoberg, H.; Schaefer, S.; Burkhart, G.; Krüger, C.; Romao, M. J. *J. Organomet. Chem.* **1984**, *266*, 203.

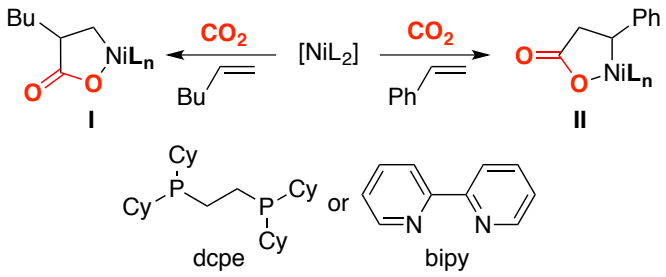

Scheme 1.6. Regioselective oxidative coupling.

In 2001, Mori's group the Ni-mediated carboxylation of 1,3-diene with CO_2 in the presence of DBU as ligand. Interestingly, while these reactions resulted in double decarboxylation when stoichiometric amounts of Me_2Zn were used, the use of ArZn reagents ended up in arylative carboxylation reaction. The carboxylic acids could be further converted into the corresponding ester with Me_2Zn reagents or CH_2N_2 in a highly stereoselective manner (Scheme 1.7).[14]

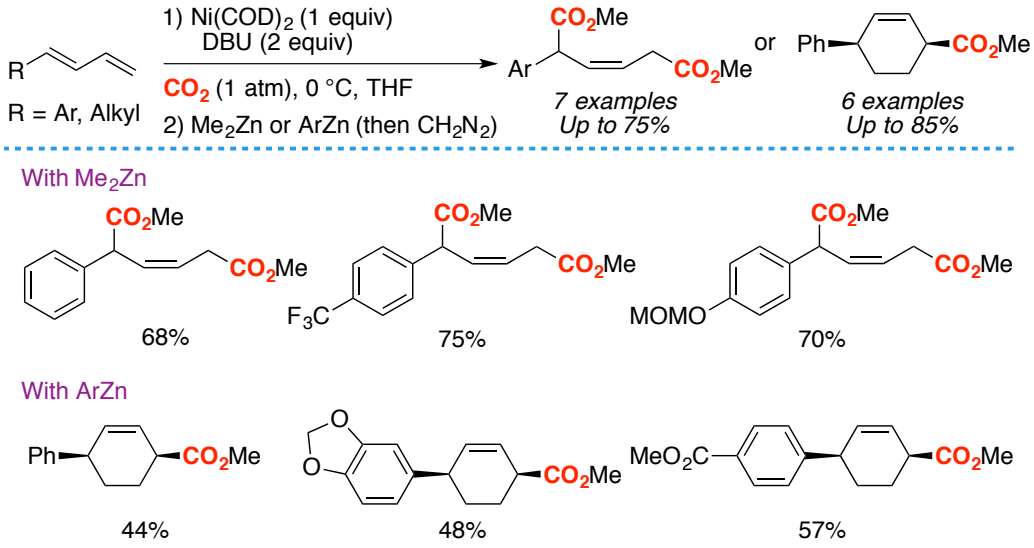

Scheme 1.7. Dicarboxylation or arylative carboxylation.

Allenes have also been employed in Ni-mediated carboxylation processes. In 2004, Mori and coworkers developed an interesting Ni-mediated hydrocarboxylation reaction with silane-containing allenes and hydride source to synthesis the corresponding silane esters in satisfactory yields (45-78%).[15] The authors proposed a mechanism involving the formation of nickelalactone, which subsequent reacts with hydride source to break

[14] Takimoto, M.; Mori, M. *J. Am. Chem. Soc.* **2001,** *123,* 2895.
[15] Takimoto, M.; Kawamura, M.; Mori, M. *Synthesis* **2004**, 791.

the C-Ni(II) (Scheme 1.8).

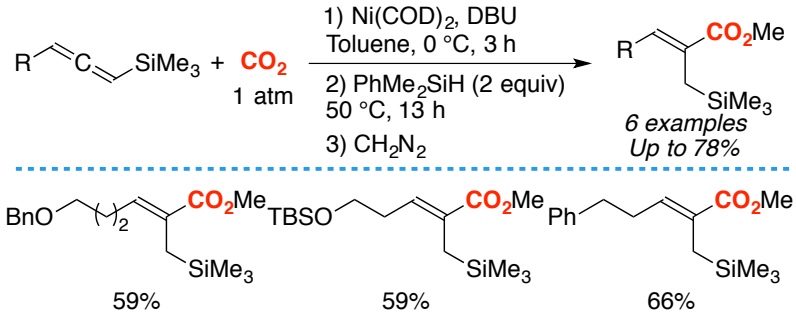

Scheme 1.8. Oxidative coupling of CO_2 with allenes.

Following up their interest on CO_2 fixation reactions, the Hoberg and Walter's groups reported the preparation of acrylic acids via the formation of nickelalactones.[16] Later on, Walther's group studied this transformation. The unsaturated nickelalactones were easily accessible by nickel-catalyzed oxidative coupling of CO_2 employing internal alkynes and different ligands at the Ni(0) center (Scheme 1.9).

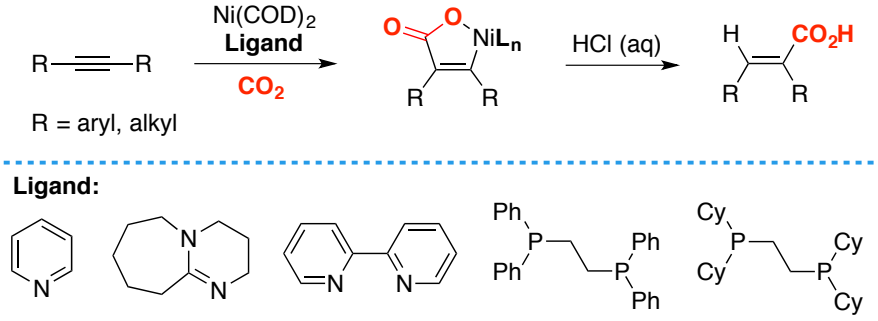

Scheme 1.9. General oxidative coupling of CO_2 with internal alkynes.

In 1999, the Yamamoto group developed a nickel-mediated carboxylation of terminal alkynes. The reaction was carried out under very mild conditions, and operated in a highly regio- and chemoselectivity. The reaction was found to be rather general, including the use of diynes, thus ending up in carboxylic acids embedded in an enyne backbone. The author believed that the high selectivity observed in this reaction could be rationalized by the stability and the reactivity of the nickelalactone intermediate

[16] (a) Hoberg, H.; Schaefer, D.; Burkhart, G.; Krüger, C.; Romão, M. J. *J. Organomet. Chem.* **1984**, *266*, 203. (b) Walther, D.; Schönberg, H.; Dinjus, E.; Sieler, J. *J. Organomet. Chem.* **1987**, *334*, 377. (c) Langer, J.; Walther, D.; Görls, H. *J. Organomet. Chem.* **2006**, *691*, 4874. (c) Langer, J.; Görls, H.; Walther, D. *Polyhedron* **2012**, *32*, 60.

(Scheme 1.10).[17]

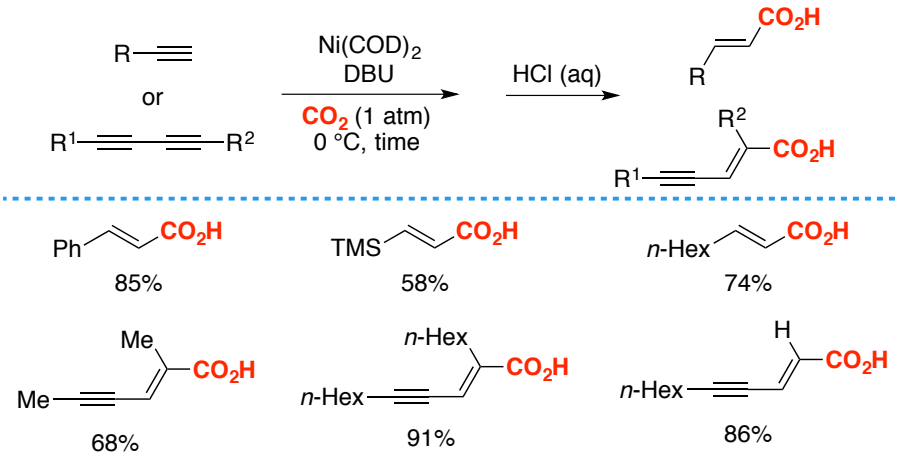

Scheme 1.10. Oxidative coupling of CO_2 with alkynes.

Inspired by the work of Yamamoto, the Iwasawa group developed a new family of bidentate nitrogen ligand that promoted the hydrocarboxylation of terminal alkynes in good yields. Interestingly, the absence of substituents in the chain resulted in selectivity switch, forming preferentially the 1,1-substituted product, although in low yield (Scheme 1.11).[18]

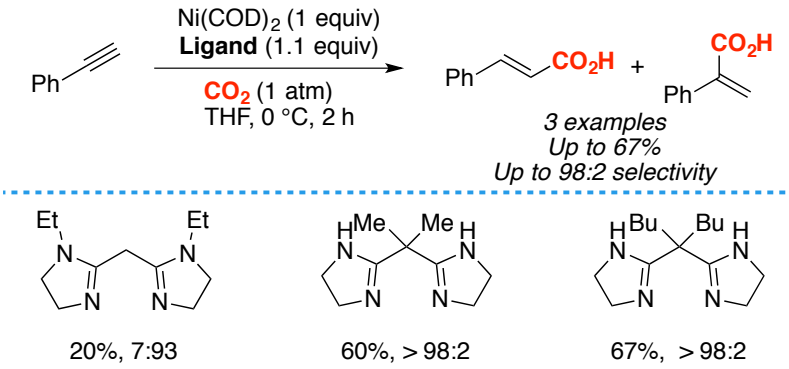

Scheme 1.11. Oxidative coupling of CO_2 with terminal alkynes.

1.4 Transition Metal-catalyzed Carboxylation Reactions

1.4.1 Pd- and Ni-catalyzed Carboxylation of Organotin and Organozinc Reagents

Inspired by the observation that CO_2 can be readily inserted into C-metal bonds, several groups have described the development of transition metal-catalyzed CO_2 fixation process. In 1997, Nicholas and coworkers developed Pd- or Pt-catalyzed

[17] Saito, S.; Nakagawa, S.; Koizumi, T.; Hirayama, K.; Yamamoto, Y. *J. Org. Chem.* **1999**, *64*, 3975.
[18] Aoki, M.; Kaneko, M.; Izumi, S.; Ukai, K.; Iwasawa, N. *Chem. Commum.* **2004**, 2568.

carboxylation reactions of allyltin reagents in the presence of phosphine ligands at under high pressure of CO_2 (33 atm), the products were obtained in good selectivity.[19] Ten year later, the Wendt group improved the selectivity by using pincer-type palladium complexes. The proposed mechanism was based on transmetallation of the allyltin reagent, followed by CO_2 insertion to generate the final products (Scheme 1.12).[20] In 2011, the Hazari group described a more efficient carboxylation of allylstannanes and –boranes using Pd(I)-bridging allyl dimers containing N-heterocyclic carbene, with yields up to 91% with 5 mol% of catalyst loading.[21]

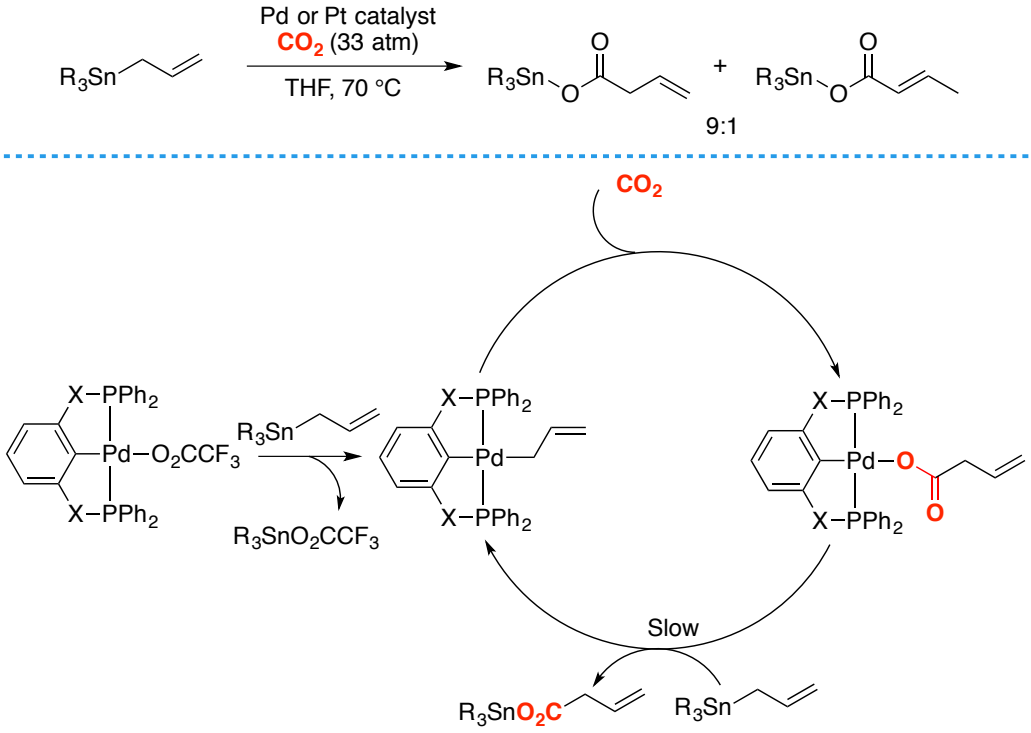

Scheme 1.12. Wendt's pincer-type Pd ligand complex for carboxylation of allyl stannanes.

Although the utilization of stannane derivatives promoted a significant step-forward in transition metal-catalyzed carboxylation methodolodies, the toxicity of Organotin reagents constituted a serious concern to be overcome. In 2008, the Oshima group published the carboxylation of aryl- and alkylzinc reagents with CO_2 in the presence of $Ni(acac)_2$ and PCy_3 as the supporting ligand. They managed to isolate the carboxylated

[19] Shi, M.; Nicholas, K. M. *J. Am. Chem. Soc.* **1997**, *119*, 5057.
[20] Johansson, R.; Wendt, O. F. *Dalton Trans.* **2007**, 488.
[21] (a) Hruszkewycz, D. P.; Wu, J.; Hazari, N.; Incarvito, C. D. *J. Am. Chem. Soc.* **2011**, *133*, 3280. (b) Wu, J.; Hazari, N. *Chem. Commum.* **2011**, *47*, 1069.

products in moderate yields as shown in Scheme 1.13.[22]

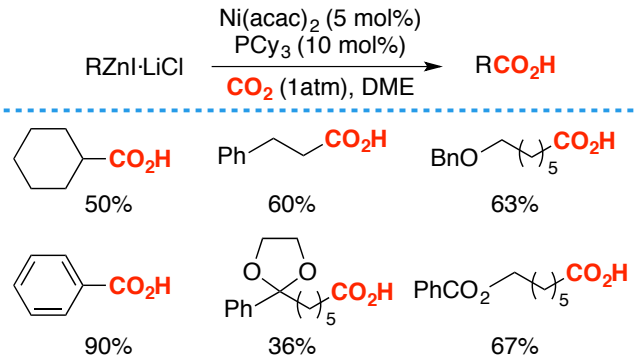

Scheme 1.13. Ni-catalyzed carboxylation of organozinc reagents.

Similarly, the Dong group reported the carboxylation of aryl- and alkylzinc reagents with an *in situ* generated Aresta complex $[(Cy_3P)_2M(\eta^2\text{-}CO_2)]$ (M = Pd, Ni). Interestingly, the authors discovered that $Pd(OAc)_2$ can be used for similar process as a convenient catalyst precursor for CO_2 activation. Unlike Oshima's work, Dong found that LiCl was not required as an additive for the reaction to occur (Scheme 1.14).[23]

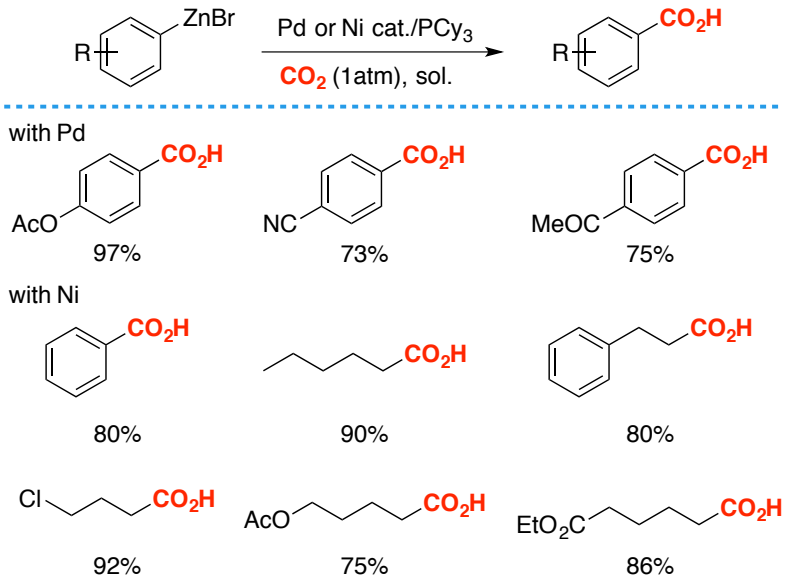

Scheme 1.14. Pd- and Ni-catalyzed carboxylation of organozinc reagents.

The proposed mechanism for this reaction consists of an initial coordination of CO_2 to intermediate **III**, producing η^2-coordinated complex **IV**, which subsequently undergoes a transmetallation with the organozinc reagent leading to Ni(II) species **V**.

[22] Ochiai, H.; Jang, M.; Hirano, K.; Yorimitsu, H.; Oshima, K. *Org. Lett.* **2008**, *10*, 2681.
[23] Yeung, C. S.; Dong, V. M. *J. Am. Chem. Soc.* **2008**, *130*, 7826.

Finally, rapid reductive elimination releases RCO_2ZnX and recover back complex **III** to complete the catalytic cycle. Mostly likely, the electron-donating properties of PCy_3 increases the electron density of the oxygen of intermediate **IV**, facilitating the following transmetallation event. Its bulkiness accelerates the corresponding the reductive elimination while suppressing β-hydride elimination (Scheme 1.15).

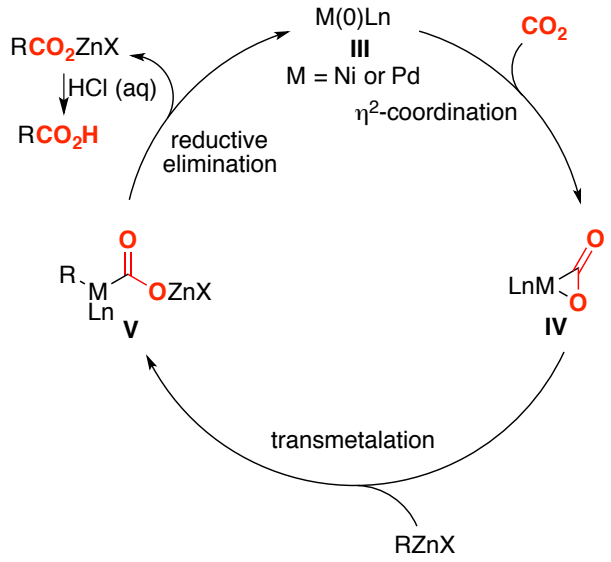

Scheme 1.15. General mechanism for Pd- and Ni-catalyzed carboxylation of organozinc reagents.

1.4.2 Rh- and Cu-catalyzed Carboxylation of Organoborane Reagents

Owing to their air- and moisture-stability, organoboranes have widely been employed in the cross-coupling process, becoming ideal reagents for both pharmaceutical and industrial laboratories. In 2006, the Iwasawa group developed the carboxylation of bronic esters with CO_2 at atmospheric pressure of CO_2 (Scheme 1.16).[24]

[24] Ukai, K.; Aoki, M.; Takaya, J.; Iwasawa, N. *J. Am. Chem. Soc.* **2006**, *128*, 8706.

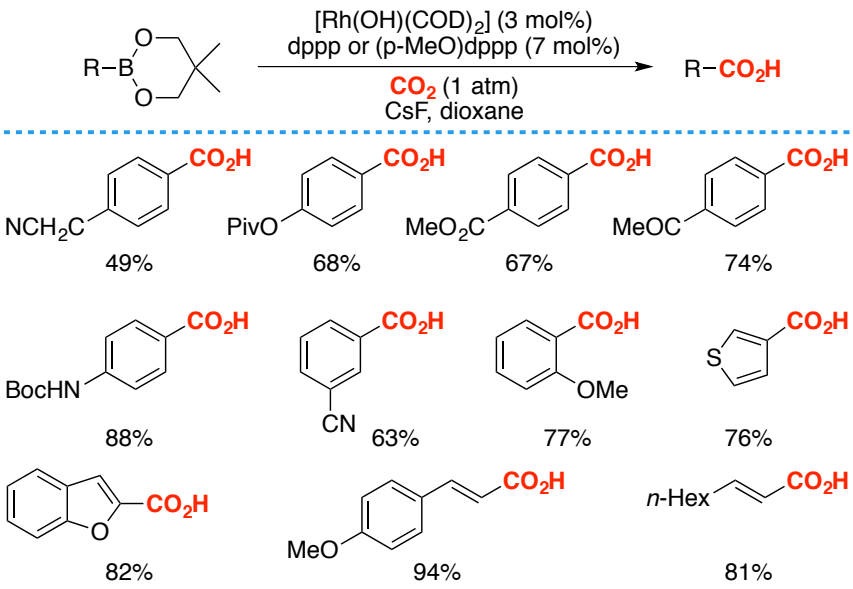

Scheme 1.16. Rh-catalyzed carboxylation of boronic esters.

The proposed mechanism starts with a transmetallation of **VI** with boronic ester to afford intermediate **VII**, followed by CO_2 insertion to generate the Rh-carboxylate **VIII**. A final transmetallation with $ArB(OR)_2$ results in **VII** while delivering a boranecarboxylate that upon acidic workup generates the desired carboxylic acids. (Scheme 1.17).

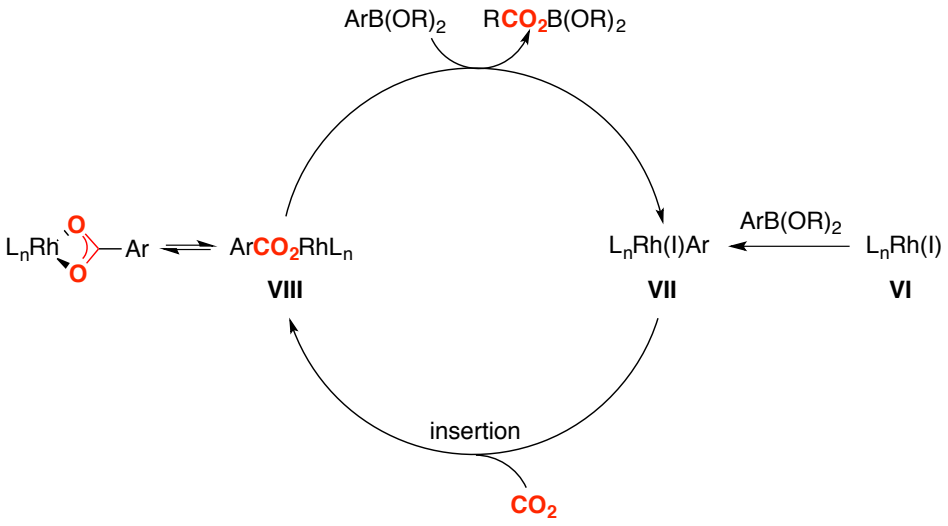

Scheme 1.17. Proposed mechanism for Rh-catalyzed carboxylation of boronic esters.

Taking into consideration the price of Rh species, Iwasawa and co-workers reported a follow-up using Cu-catalyst supported by bisoxazoline ligand. This protocol displayed better functional group tolerance than the Rh and the desired products were

obtained in 60-99% yields. The proposed mechanism is similar to that described for rhodium catalyst.[25]

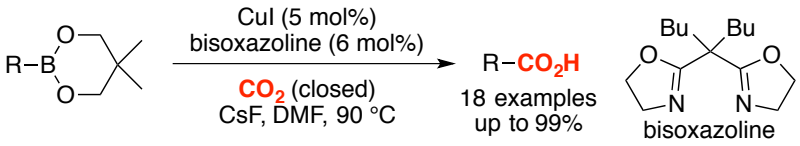

Scheme 1.18. Cu-catalyzed carboxylation of boronic esters.

Independently, Hou and co-workers published the Cu-catalyzed carboxylation of boronic esters in the presence of a N-heterocycle carbene as ligand to afford carboxylic acids in 73-99% yields.[26] Importantly, stoichiometric reactions supported the mechanism of this reaction. Specifically, the reaction of [(IPr)CuCl] with one equivalent of *t*-BuOK in THF at room temperature resulted in [(IPr)Cu(O*t*-Bu)] in 92% isolated yield. Subsequently, the authors managed to isolate arylcopper complex **X** in 91% isolated yield. Treatment of the arylcopper complex **X** and the carboxylate species **XI** in high yield. Exposure of carboxylate Cu-complex **XI** to one equivalent of *t*-BuOK in THF regenerated complex **VIIII** [(IPr)Cu(O*t*-Bu)], with quantitative release of potassium 4-methoxybenzoate as a white precipitate. Remarkably, the complex **VIIII**, aryl **X** and **XI** all exhibited high catalytic activity for the carboxylation of 4-MeOC$_6$H$_4$-boronic ester with CO_2, affording acids in essentially quantitative yields.

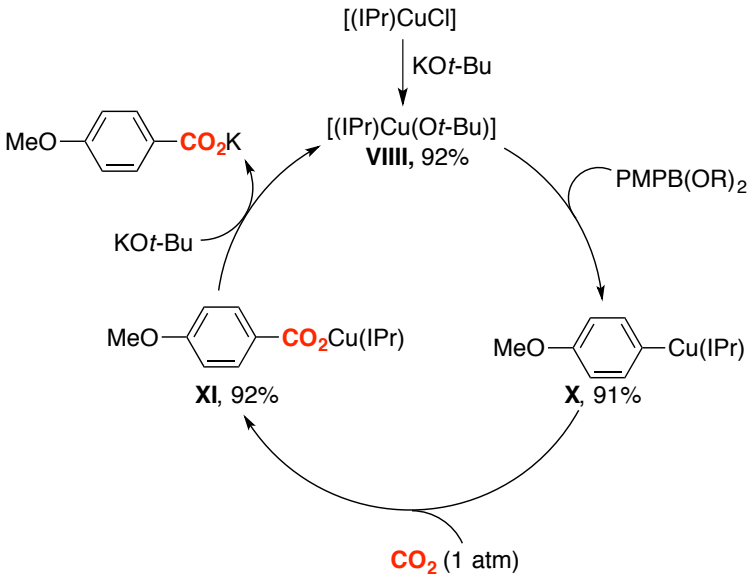

Scheme 1.19. Stoichiometric studies on Cu-complexes.

[25] Takaya, J.; Tadami, S.; Ukai, K.; Iwasawa, N. *Org. Lett.* **2008**, *10*, 2697.
[26] Ohishi, T.; Nishiura, M.; Hou, Z. *Angew. Chem. Int. Ed.* **2008**, *47*, 5792.

In 2011, the Hou group extended this transformation to alkylboronic esters generated *in situ* by hydroboration of olefins with 9-BBN dimer (Scheme 1.20, path a).[27] The authors demonstrated that the combination of [(IPr)CuCl] with MeOLi could serve as an excellent catalyst system for the carboxylation of alkylboranes with CO_2. The isolation of the copper adduct complex and its CO_2 insertion product provided important information for the mechanism. Similarly, Sawamura's group described the carboxylation of alkylboron compounds (alkyl-9-BBN) in the presence of CuOAc and 1,10-phenanthroline with a stoichiometric amount of KO*t*-Bu as boranephile (Scheme 1.20, path b).[28]

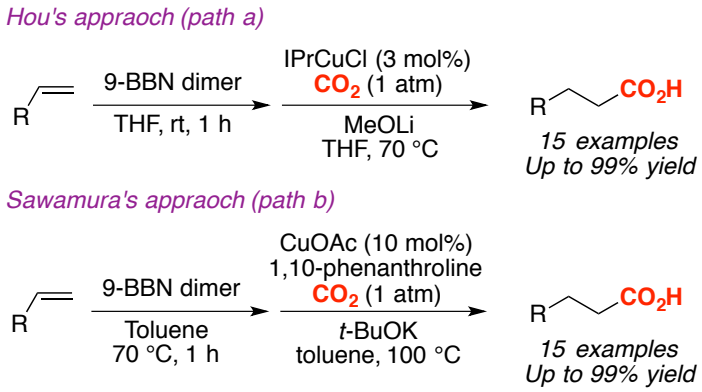

Scheme 1.20. Copper-catalyzed carboxylation of alkylboranes.

Inspired by the recent developments using organoboranes, Duong's group developed the carboxylation reaction of allylboronic esters in the presence of IPrCuCl as catalyst. The reaction is distinguished by high regioselectivity, delivering branched-unsaturated carboxylic acids in most cases. A wide range of functionalized carboxylic acids were prepared following this methodology, including the products containing all-carbon quaternary centers (Scheme 1.24).[29]

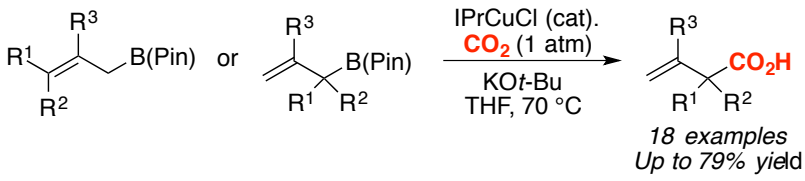

Scheme 1.21. Cu-catalyzed carboxylation of allylboronic esters.

[27] Ohishi, T.; Zhang, L.; Nishiura, M.; Hou, Z. *Angew. Chem. Int. Ed.* **2011**, *50*, 8114.
[28] Ohmiya, H.; Tanabe, M.; Sawamura, M. *Org. Lett.* **2011**, *13*, 1086.
[29] Duong, H. A.; Huleatt, P. B.; Tan, Q. W.; Shuying, E. L. *Org. Lett.* **2013**, *15*, 4034.

1.4.3 Pd-, Ni- and Cu-catalyzed Carboxylation of C-X Bonds

While the carboxylation of well-defined organometallic reagents represents an advance in CO_2 fixation process, these species are typically prepared from the corresponding organic halides. Therefore, the development of a direct carboxylation of organic halides with CO_2 constitute an advantage from a both conceptual and practical standpoint.

Inspired by the initial work of Osanede using stoichiometric amounts of metal compounds, our group established the first catalytic carboxylation of $C(sp^2)$-Br bonds with 5 mol% of $Pd(OAc)_2$ as precatalyst, *t*-Bu-XPhos as ligand and in the presence of Et_2Zn as reducing reagent.[30] The corresponding acids were obtained in 40-82% isolated yields after hydrolytic workup (Scheme 1.25). Although a detailed mechanistic picture requires further studies, a catalytic cycle consisting of implies a challenging CO_2 insertion into the Pd-aryl bond of an initially formed **XIII** to form **XIIII** was proposed. Subsequently, transmetallation with Et_2Zn might deliver the zinc carboxylate, with concomitant release of **XV**, which ultimately would lead to the regeneration of the catalytic LnPd(0) species. While one might argue that Et_2Zn could trigger the formation of ArZnEt or Ar_2Zn derivatives, control experiments in the absence of CO_2 and D_2O quchch revealed that no ArD was formed in the reaction mixture, thus ruling out the intermediate of ArZnBr species

[30] Correa, A.; Martin, R. *J. Am. Chem. Soc.* **2009**, *131*, 15974.

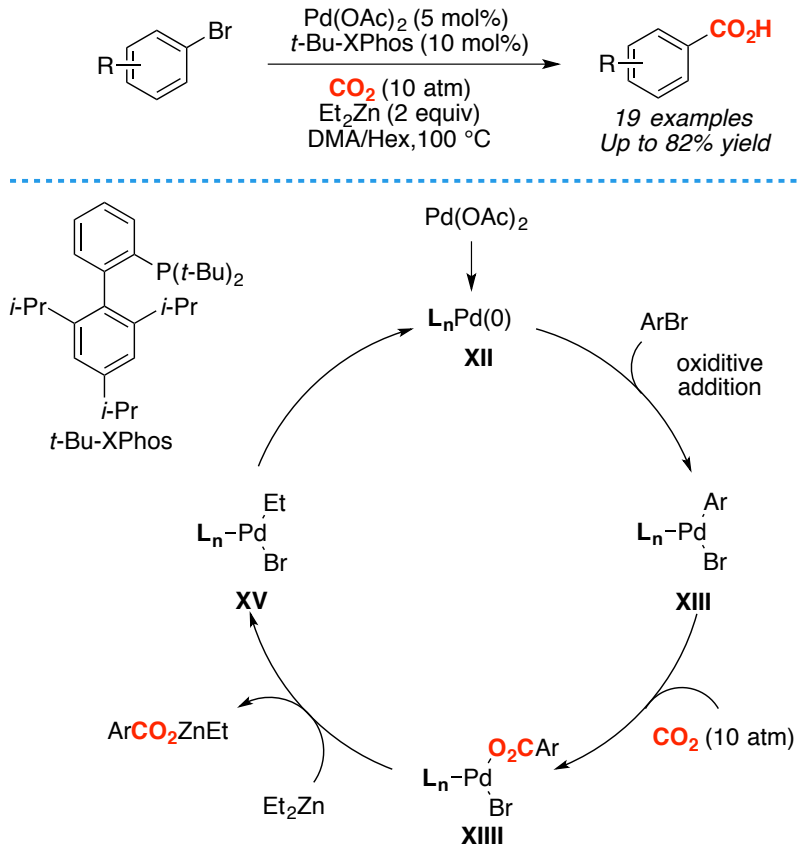

Scheme 1.22. Pd-catalyzed carboxylation of aryl bromides and the proposed mechanism.

In 2012, Tsuji and colleagues published the Ni-catalyzed carboxylation of aryl and vinyl chlorides with CO_2. The reactions were performed under an atmospheric pressure of CO_2 at room temperature in the presence of Mn powder as reductant. A wide array of aryl chlorides and vinyl chlorides could be transformed to the corresponding benzoic acids or acrylic acids in good to excellent yields. The authors also carried out mechanistic studies, revealing that a Mn/Et_4NI system could act as an efficient reducing agent, and that a Ni(I) species might be involved in the catalytic cycle (Scheme 1.23, path a).[31] Shortly after, our group described an novel, direct, and efficient Ni-catalyzed carboxylation of primary, secondary, and tertiary benzyl halides with CO_2, yielding benzolic acids in high yields. This protocol constitutes a user-friendly and operationally simple coupling reaction for the preparation of phenylacetic acids in high yields under mild reaction conditions (Scheme 1.23, path b).[32]

[31] Fujihara, T.; Nogi, K.; Xu, T.; Terao, J.; Tsuji, Y. *J. Am. Chem. Soc.* **2012**, *134*, 9106.
[32] León, T.; Correa, A.; Martin, R. *J. Am. Chem. Soc.* **2013**, *135*, 1221.

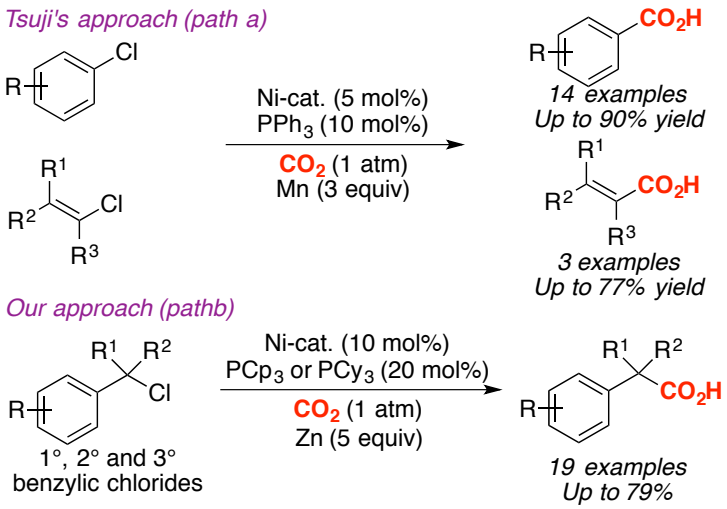

Scheme 1.23. Ni-catalyzed carboxylation of aryl, vinyl, benzyl chlorides.

The mechanism of these reaction is believed to proceed via initial formation of Ni(0), followed by oxidative addition of the organic chloride to generate Ni(II) intermediate **XVII**. In line with the ability of Mn to promote single-electron-transfer process in electrochemical reactions, Ni(II) intermediate **XVII** might be reduced to Ni(I) intermediate **XVIII**, which might be nucleophilic enough to react with CO_2 to form carboxylateonickel complex **XVIIII**. Finally, reduction of **XVIIII** by Mn regenerate Ni(0) catalyst with formation of Ni(0) species A (Scheme 1.24).

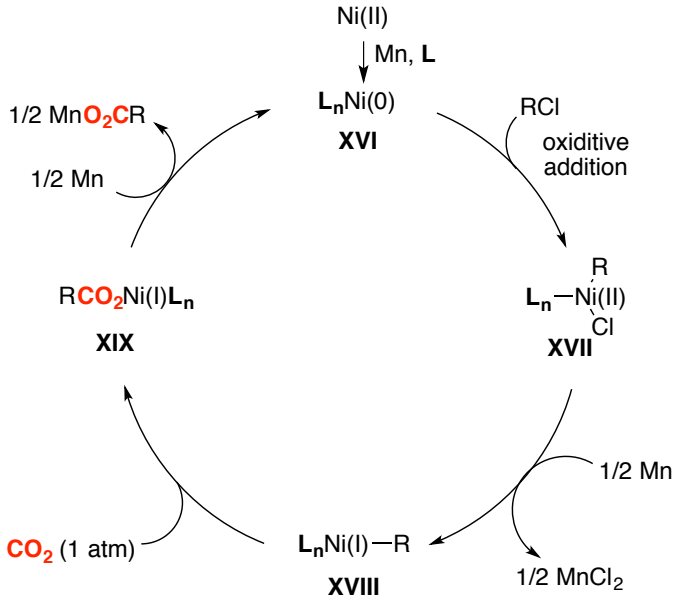

Scheme 1.24. Proposed mechanism.

In addition to Pd- and Ni-catalyzed carboxylation of organic halides with CO_2. Daugulis describe that benzoic acids are within reach via Cu-catalyzed carboxylation

of aryl iodides with TMEDA or DMEDA as ligand and Et_2Zn as the reducing agent in DMSO or DMA. As compared to Ni- and Pd-catalysts, the CuI catalyst is less active since only aryl iodides can be employed as coupling partners. As for the mechanism, the authors proposed an otherwise similar rationale to the one suggested for in Scheme 1.4 (Scheme 1.25).[33]

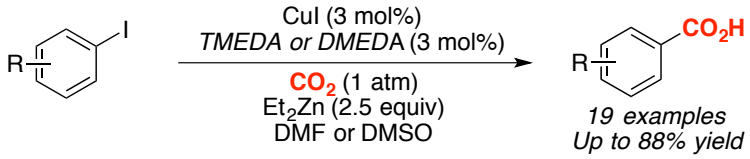

Scheme 1.25. Cu-catalyzed carboxylation of aryl iodides.

In 2014, the Ma group developed a highly regioselective indium-mediated carboxylation of simple allylic halides with CO_2. The reaction is user-friendly and operationally simple as no transition metal catalyst is needed and an inert atmosphere is not imperative. The protocol endures a wide number of synthetically interesting functional groups with a reasonably high branched-regioselectivity (Scheme 1.26).[34]

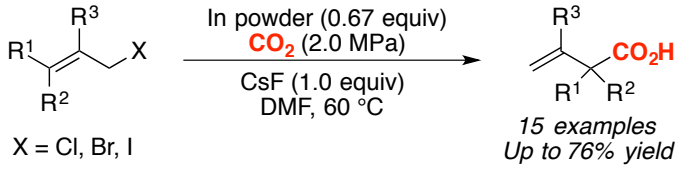

Scheme 1.26. In-mediated carboxylation of allyl halide.

Ideally, the reductive carboxylation field should not be limited to substrates that readily undergo oxidative addition, such as aryl or benzyl halides. These substrates are quite challenging for transition metal-catalyzed cross coupling reactions due to poor reactivity, a tendency of *in situ* formed alkylmetal species to undergo homodimerization, and a possible hydrogen abstraction or *β*-hydride elimination pathway. In 2014, our group reported a mild Ni-catalyzed carboxylation of unactivated primary alkyl bromides and sulfonates with CO_2 (Scheme 1.27). The protocol represents a convenient way to access carboxylic acids from simple starting materials and it operates with high chemoselectivity profile in line with previous carboxylation processes. Mechanistic study showed that the reaction might go through a SET-type pathway via Ni(I)

[33] Tran-Vu, H.; Daugulis, O. *ACS Catal.* **2013**, *3*, 2417.
[34] Miao, B.; Ma, S. *Chem. Commum.* **2014**, *50*, 3285.

intermediate.[35]

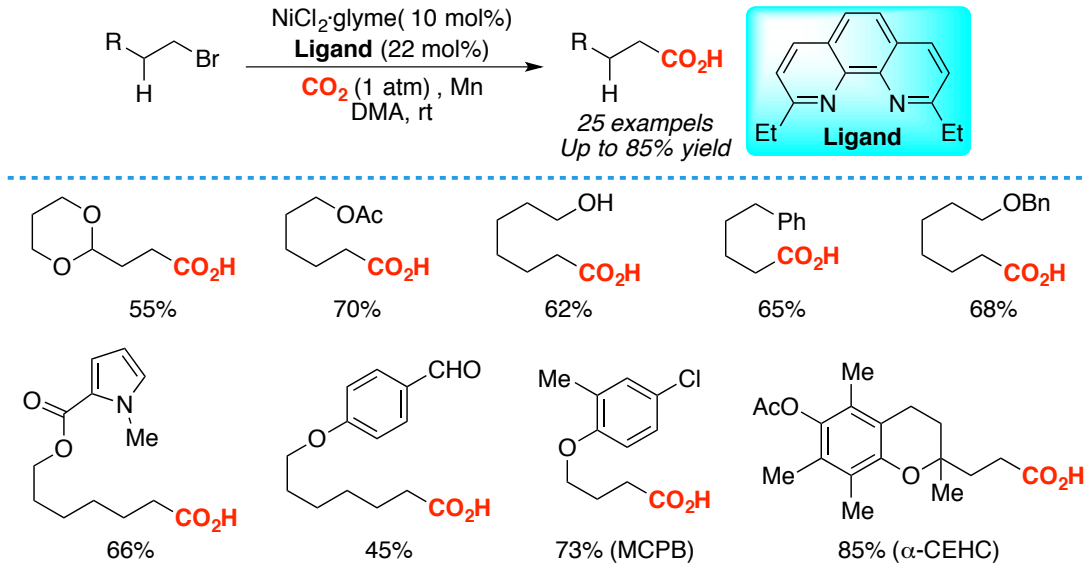

Scheme 1.27. Ni-catalyzed carboxylation of unactivated alkyl bromides.

1.4.4 Ni-catalyzed Carboxylation of C-O Bonds

Phenol derivatives are versatile and low-cost alternatives to aryl halides in the cross-coupling area due to their general low-cost, ready availability, high thermal stability and lack of toxicity. Unlike activated aryl triflates, mesylates, aryl sulfonates or tosylates, catalytic cross-coupling reaction with simple aryl esters via C−O bond-cleavage is less explored. This is probably due to the factor that esters are less willing to act as leaving groups when compared to sulfonate derivatives as well as easy to cleavage the O-CO bond using transition metal catalysts.[36]

In 2014, our group described the first example of Ni-catalyzed direct carboxylation of aryl or benzylic esters with CO_2 via C−O bond cleavage. The transformation occurred with a wide substrate scope, including challenging substrate combinations. While aromatic motif could be coupled with no problem, the use of benzylic motifs required directing groups on the side chain. The reaction was believed to undergo via

[35] Liu, Y.; Cornella, J.; Martin, R. *J. Am. Chem. Soc.* **2014**, *136*, 11212.

[36] For recent reviews: (a) Mesganaw, T.; Garg, N. K. *Org. Process Res. Dev.* **2013**, *17*, 29. (b) Correa, A.; Cornella, J.; Martin, R. *Angew. Chem. Int. Ed.* **2013,** *52*, 1878. (d) Rosen, B. M.; Quasdorf, K. W.; Wilson, D. A.; Zhang, N.; Resmerita, A. M.; Garg, N. K.; Percec, V. *Chem. Rev.* **2011**, *111*, 1346. (e) Li, B. J.; Yu, D. G.; Sun, C. L.; Shi, Z. J. *Chem.-Eur. J.* **2011**, *17*, 1728. (f) Yu, D. G.; Li, B. J.; Shi, Z. J. *Acc. Chem. Res.* **2010**, *43*, 1486.

Ni(I) intermediate (Scheme 1.28).[37]

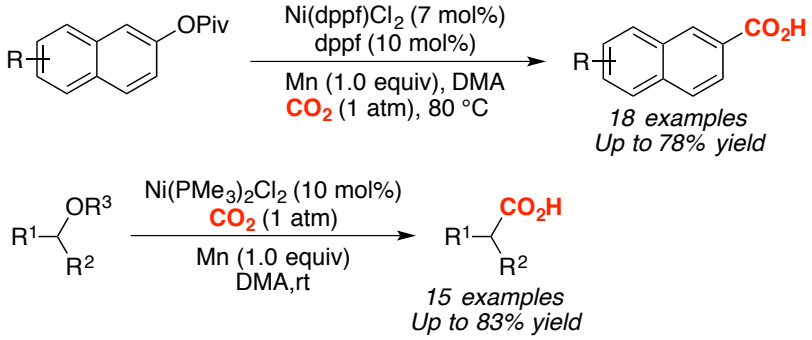

Scheme 1.28. Ni-catalyzed carboxylation of esters.

This same year, our group established another interesting carboxylation of C-O bonds. The authors described a novel, mild, and user-friendly Ni-catalyzed regiodivergent carboxylation of allyl acetates with CO_2. This protocol showed that the choice of ligand is crucial for controlling the regioselectivity profile. The mechanistic studies disclosed that the regiodivergent carboxylation events underwent different mechanistic pathways. While the use of neocuproine led to a SEP-type pathway, the quarterpyridine might act similarly to pincer-type ligands in related carboxylation reactions through a η^1-allyl intermediates,[38] and the additional pyridine motif might be behaving as a hemilabile ligand (Scheme 1.29).[39]

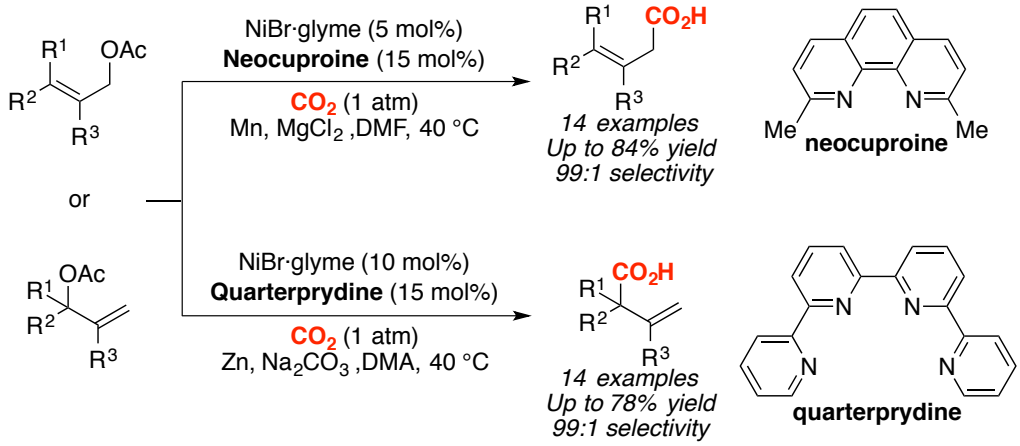

Scheme 1.29. Ligand-controlled regiodivergent carboxylation of allyl esters.

[37] Correa, A.; León, T.; Martin, R. *J. Am. Chem. Soc.* **2014**, *136*, 1062.
[38] (a) Suh, H.W.; Guard, L. M.; Hazari, N. *Chem. Sci.* **2014**, *5*, 3859. (b) Takaya, J.; Iwasawa, N. *J. Am. Chem. Soc*. **2008**, *130*, 15254.
[39] Moragas, T.; Cornella, J.; Martin, R. *J. Am. Chem. Soc.* **2014**, *136*, 17702.

1.4.5 Transition Metal-catalyzed Carboxylation of Alkenes

In 1979, the Inoue group reported the synthesis of five-membered lactones by Pd-catalyzed carboxylation of methylenecyclopropanes with CO_2 at high pressure (40 bar).[40] The authors managed to control the selectivity by employing different ligands. While the utilization of PPh_3 resulted in A, bidentate dppe ligand led to lactone **B** (Scheme 1.30).

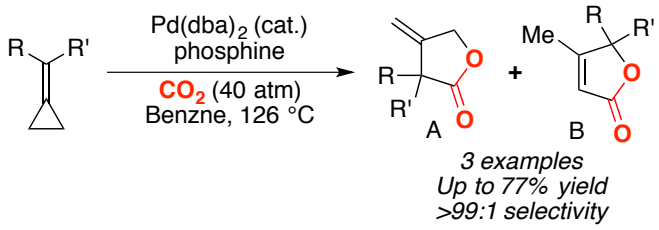

Scheme 1.30. Pd-catalyzed carboxylation of methylenecyclopropanes.

Surprisingly, the catalytic carboxylation of simple alkenes was not described until 2008, when Rovis and coworkers reported the formation of phenylacetic acids from styrene derivatives. The reactions were performed under mild conditions using $Ni(acac)_2$ as pre-catalyst (10 mol%), Et_2Zn (2.5 equiv) as reducing reagent and $CsCO_3$ (20 mol%) as an additive. The resulting branched acids were obtained in 56-92% yields. This protocol is suitable for a variety of styrene analogues possessing electron deficient and neutral substituents. The authors proposed a mechanism involving a nickel-hydride active catalyst (Scheme 1.31).[41]

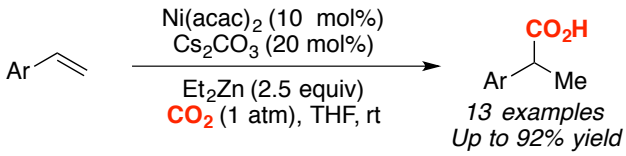

Scheme 1.31. Ni-catalyzed carboxylation of styrenes.

Few years later, the Thomas group described the first iron-catalyzed hydrocarboxylation of sytrenes with Grignard reagents. An efficient and bench-stable combination of $FeCl_2$ precatalyst (1 mol %) and bis(imino)pyridine (1 mol%) produced the branched phenylacetic acids in excellent yields and regioselectivity. A number of

[40] Inoue, Y.; Hibi, T.; Satake, M.; Hashimoto, H. *J. Chem. Soc. Chem. Commun.* **1979**, 982.
[41] Williams, C. M.; Johnson, J. B.; Rovis, T. *J. Am. Chem. Soc.* **2008**, *130*, 14936.

styrene analogues that were differentiated both sterically and electronically were converted to the targeted acids. The catalyst was found to be equally active with a much lower loading of 0.1 mol%. However, due to the presence of RMgX reagents, a lack of functional group tolerance was found. Preliminary mechanistic study shows that the catalytic cycle proceeds through via transmetallation, β-hydride elimination, olefin insertion and CO_2 fixation with newly formed Grignard reagent (Scheme 1.31).[42]

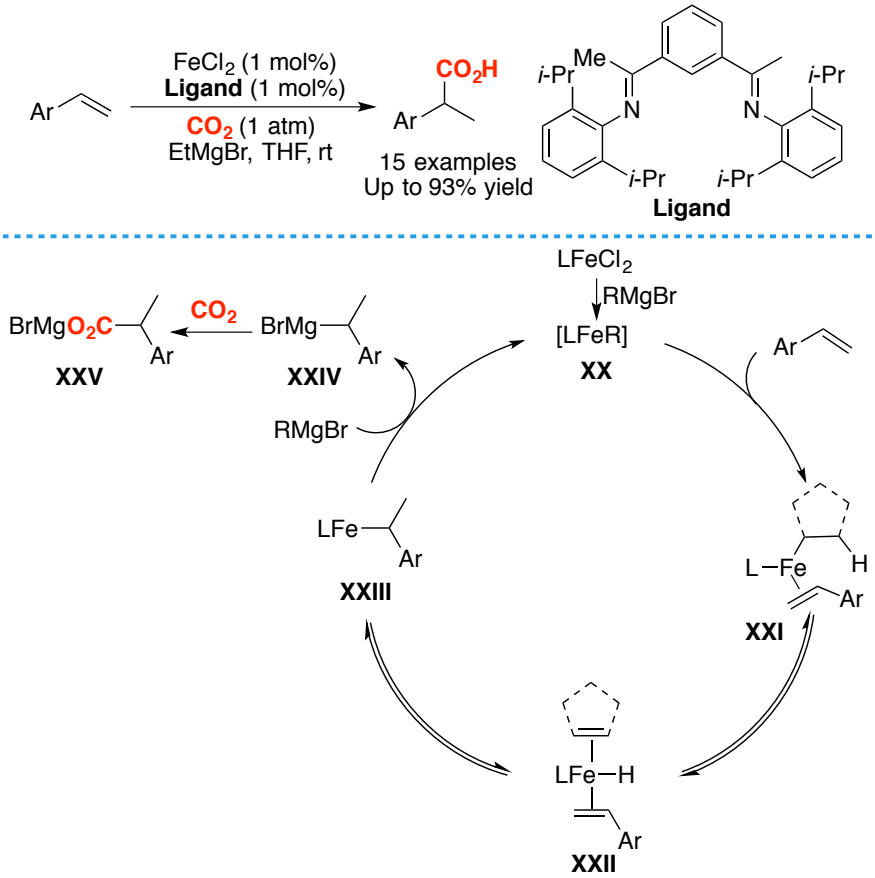

Scheme 1.32. Fe-catalyzed carboxylation of styrenes and the proposed mechanism.

Recently, Leitner and coworkers developed a Rh system for the hydrocarboxylation of non-activated olefins with CO_2 and H_2.[43] Although several disadvantages can be noted in this protocol (high pressure of CO_2 and H_2, elevated temperatures and poor selectivity profile). Simple internal and terminal olefins could be converted to the corresponding products in moderate to excellent yields. Remarkably, primary and secondary alcohols can be used as substrates for this transformation to provide similar

[42] Greenhalgh, M. D.; Thomas, S. P. *J. Am. Chem. Soc.* **2012**, *134*, 11900.
[43] Ostapowicz, T. G.; Schmitz, M.; Krystof, M.; Klankermayer, J.; Leitner, W. *Angew. Chem. Int. Ed.* **2013**, *52*, 12119.

outcomes as compared to substituted alkene analogues. However, low selectivity was observed (Scheme 1.33).

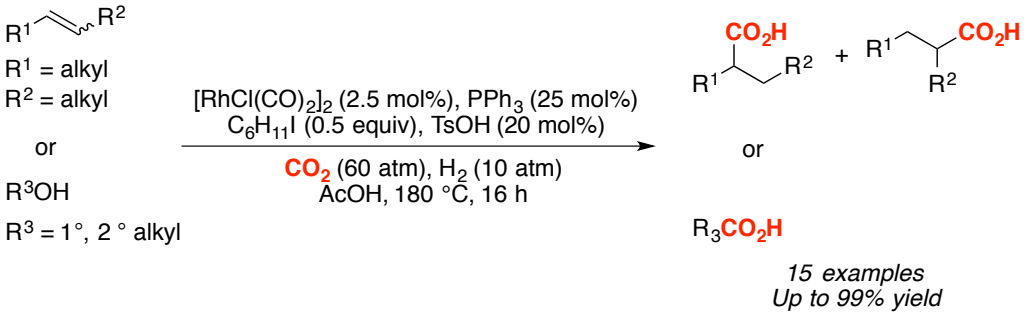

Scheme 1.33. Rh-catalyzed carboxylation of styrenes with CO_2 and H_2.

The synthesis of acrylic acid from readily available and inexpensive ethylene and CO_2 is particularly attractive from an industrial viewpoint, since acrylic acid is widely used for polyacrylate synthesis. Since, more than $3x10^6$ tons of acrylic acid are produced every year through the industrial SOHIO process, involving the oxidation of acrolein over heterogeneous molybdenum/ vanadium oxide catalysts at 300 °C.[44] Thus, establishing a low-cost route to produce acrylic acid under mild conditions is highly desirable.

Recently, nickel-mediated carboxylation of ethylene with CO_2 has been studied in detail.[45] The first example was published by Rieger and colleagues, showing that *β*-H elimination could be achieved by breaking the Ni-O bond in the presence MeI.[46a] In 2010, Limbach and colleagues reported the first Ni-catalyzed carboxylation of ethylene to form sodium acrylates.[46c] The reaction is believed to operate through binding of ethylene to Ni(0) species **XXIV**, followed by cycloaddition with CO_2 to form nickelalactone **XXV**. Subsequently, the presence of NaO*t*-Bu greatly accelerates *β*-H elimination en route to **XXVI**, which undergoes ligand exchange with ethylene to

[44] Herrmann, W. A. in *Applied Homogeneous Catalysis with Organometallic Compounds*, Vol. *3* (Eds.: B. Cornils, W. A. Herrmann), 2nded., Wiley-VCH Weinheim, **2002**, pp.1297.

[45] (a) Bruckmeier, C.; Lehenmeier, M. W.; Reichardt, R.; Vagin, S.; Rieger, B. *Organometallics* **2010**, *29*, 2199. (b) Plessow, P. N.; Schäfer, A.; Limbach, M.; Hofmann, P. *Organometallics* **2014**, *33*, 3657. (c) Jin, D.; Williard, P. G.; Hazari, N.; Bernskoetter, W. H. *Chem. Eur. J.* **2014**, *20*, 3205. (d) Plessow, P. N.; Weigel, L.; Lindner, R.; Schäfer, A.; Rominger, F.; Limbach, M.; Hofmann, P. *Organometallics* **2013**, *32*, 3327. (e) Jin, D.; Schmeier, T. J.; Williard, P. G.; Hazari, N.; Bernskoetter, W. H. *Organometallics* **2013**, *32*, 2152.

[46] Lejkowski, M. L.; Lindner, R.; Kageyama, T.; Bódizs, G. É.; Plessow, P. N.; Müller, I. B.; Schäfer, A.; Rominger, F.; Hofmann, P.; Futter, C.; Schunk, S. A.; Limbach, M. *Chem. Eur. J.* **2012**, *18*, 14017.

regenerate catalyst **XXIV** (Scheme 1.34).

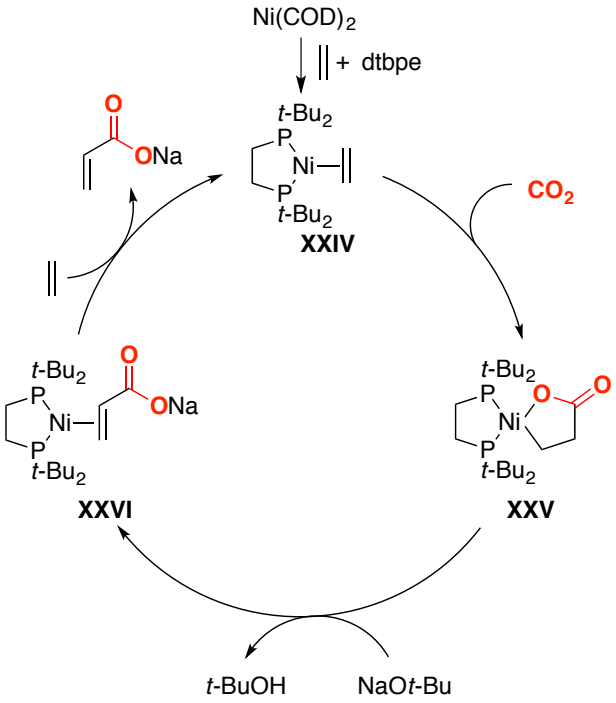

Scheme 1.34. Proposed mechanism.

Promoted by the work of Inoue and Musco with Pd-catalysts. In 2002, Mori and co-workers successfully developed a nickel-catalyzed cycloisomerization/carboxylation of 1,3-dienes, generating allic acids in good to excellent yields. The protocol was highly regio- and stereoselective, and it was believed to proceeded through CO_2 insertion into bisallyl nickel complex **XXVIII** to generate carboxylate nickel species **XXIX**. Subsequent treatment with a R_2Zn reagent delivers Ni-complex **XXX**. The following reductive elimination results in the final product and regenerates active catalyst **XXVII** (Scheme 1.35).[47]

[47] Takimoto, M.; Mori, M. *J. Am. Chem. Soc.* **2002**, *124*, 10008.

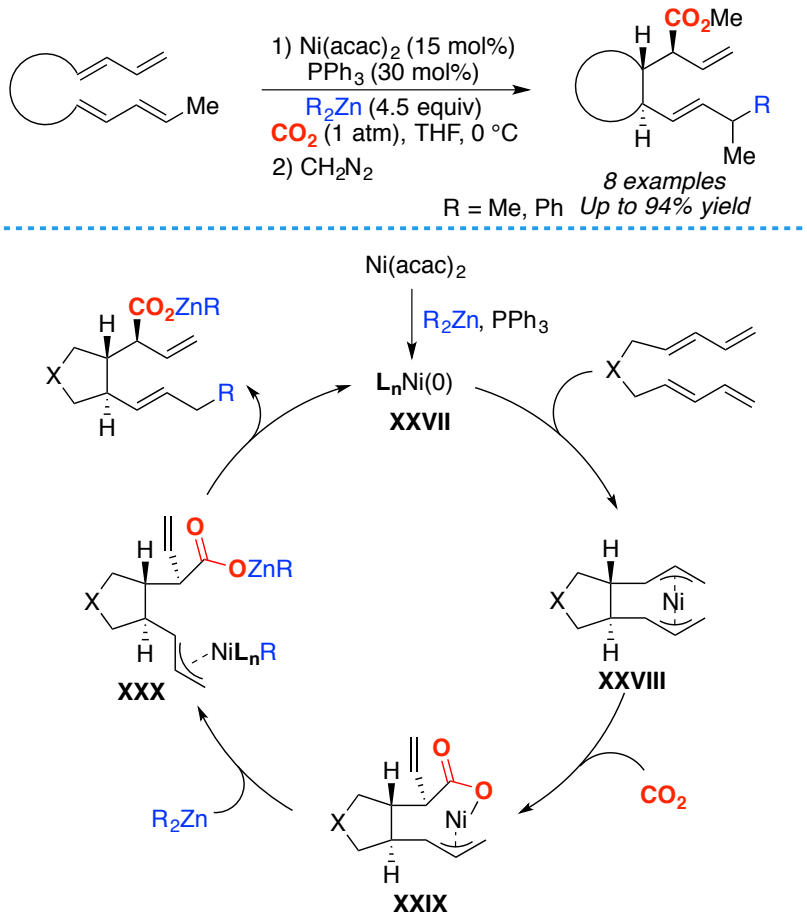

Scheme 1.35. Ni-catalyzed carboxylation of 1,3-diene and the proposed mechanism.

Soon after, Mori's group successfully established the nickel-catalyzed asymmetric CO_2 incorporation of various 1,3-dienes.[48] The transformation operated with high enantioselectivities in the presence of a catalytic amount of $Ni(acac)_2$, (*S*)-MeO-MOP and an organozinc reagent (Me_2Zn or Ph_2Zn). (Scheme 1.36).

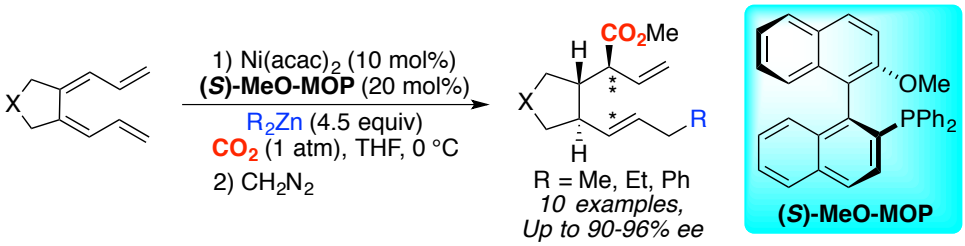

Scheme 1.36. Ni-catalyzed asymmetric carboxylation of 1,3-dienes.

The carboxylation of simple 1,3-dienes was also extended to palladium catalysts using pincer-type complexes (Scheme 1.37). In 2011, Iwasawa and coworkers

[48] Takimoto, M.; Nakamura, Y.; Kimura, K.; Mori, M. *J. Am. Chem. Soc.* **2004**, *126*, 5956.

developed an efficient Pd-PSiP complex capable of promoting the catalytic hydrocarboxylation with high efficiency and exclusive branched selectivity..[49]

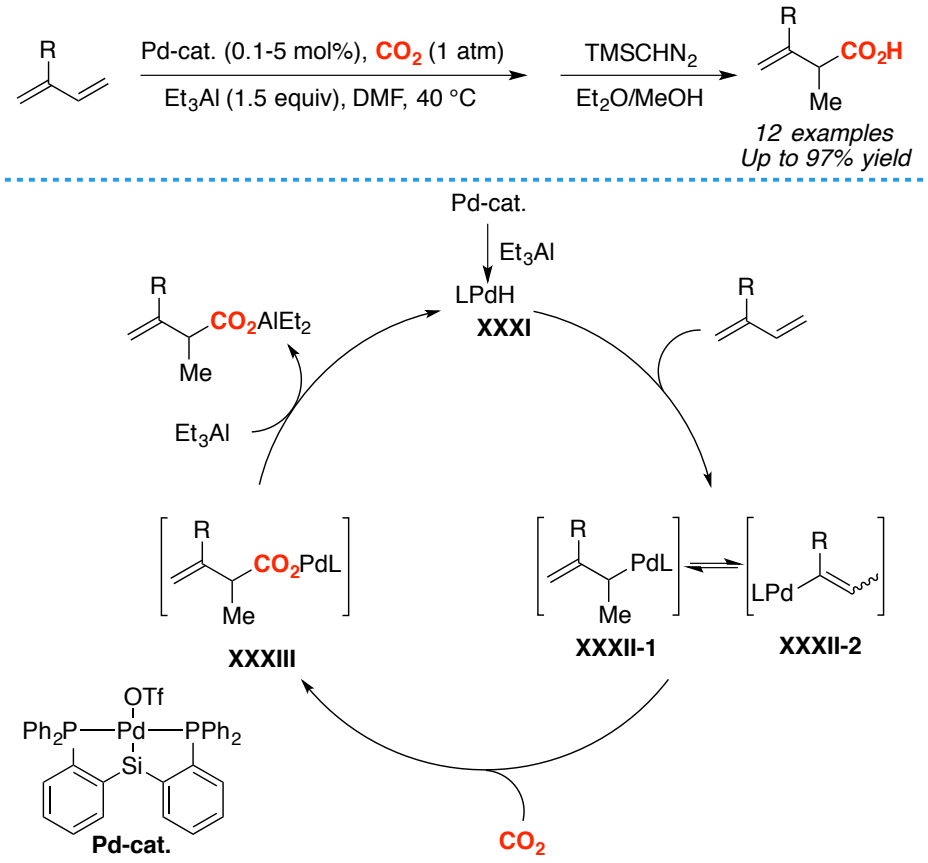

Scheme 1.37. Pd-catalyzed carboxylation of 1,3-diene and the proposed mechanism.

1.4.6 Transition Metal-catalyzed Carboxylation of Alkynes

Inspired by the ability of CO_2 to promote cycloaddition process, the Walther group studied the formation of pyrones via the incorporation of two alkyne units. The authors revealed that the use of phosphine ligands with relatively small cone angleswas potentially efficient. For example, the reaction of 3-hexyne with CO_2 (10 bar), $Ni(COD)_2$ and PEt_3 in a 1:1 mixture of THF/MeCN led to tetraethyl-2-pyrone in 96% yield. A mechanism involving the formation of five-membered nickelalactone **B** followed by insertion of another alkyne into the Ni-C bond was proposed (Scheme 1.38).

[49] Takaya, J.; Sasano, K.; Iwasawa, N. *Org. Lett.* **2011**, *13*, 1698.

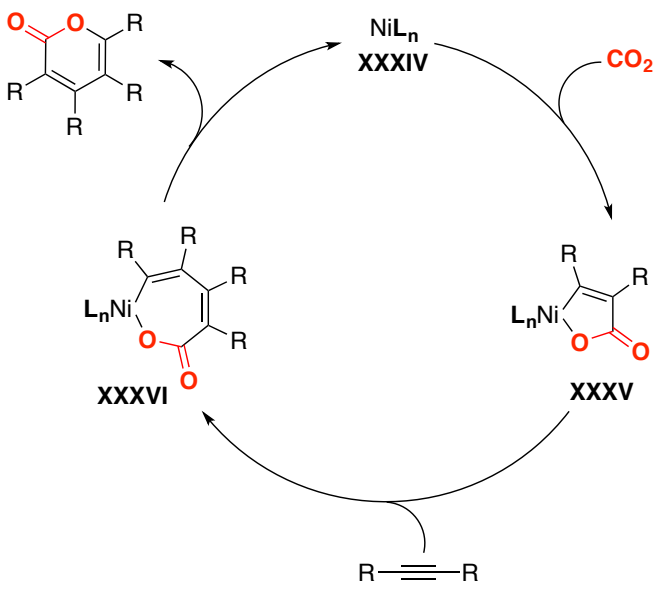

Scheme 1.38. Proposed mechanism.

Similarly to the work of Walther,[50] Tsuda[51] and Louie[52] described the carboxylation of diynes with CO_2 to synthesis pyrones in moderate to excellent yields (Scheme 1.39). This efficient [2 + 2 + 2] cycloaddition could be achieved when PCy_3 or IPr carbene was used as supporting ligand. Most likely, the use of such ligands prevent some of the side reactions due to their bulkiness. A similar mechanism to the one presented by the Walther group (Scheme 1.38) was proposed.

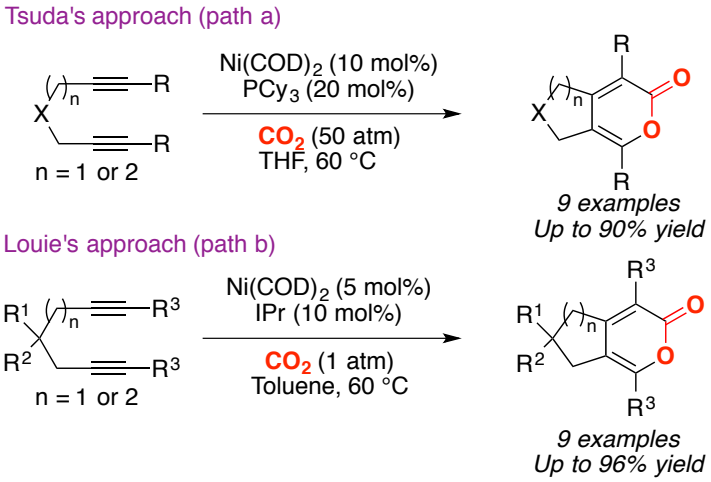

Scheme 1.39. Ni-catalyzed carboxylation of diynes.

[50] (a) Walther, D.; Schönberg, H.; Dinjus, E.; Sieler, J. *J. Organomet. Chem.* **1987**, *334*, 377. (b) Walther, D.; Bräunlich, G.; Kempe, R.; Sieler, J. *J. Organomet. Chem.* **1992**, *436*, 109.
[51] (a) Tsuda, T.; Morikawa, S.; Sumiya, R.; Saegusa, T. *J. Org. Chem.* **1988**, *53*, 3140. (b) Tsuda, T.; Morikawa, S.; Hasegawa, N.; Saegusa, T. *J. Org. Chem.* **1990**, *55*, 2978.
[52] Louie, J.; Gibby, J. E.; Farnworth, M. V.; Tekavec, T. N. *J. Am. Chem. Soc.* **2002**, *124*, 15188.

In 2011, Ma and co-workers reported the first nickel-catalyzed *syn*-hydrocarboxylation of alkynes with diethyl zinc and CO_2,[53] delivering the desired (*E*)-2,3-disubstituted acrylic acids in good to excellent yields with high regio- and stereoselectivities (Scheme 1.40).

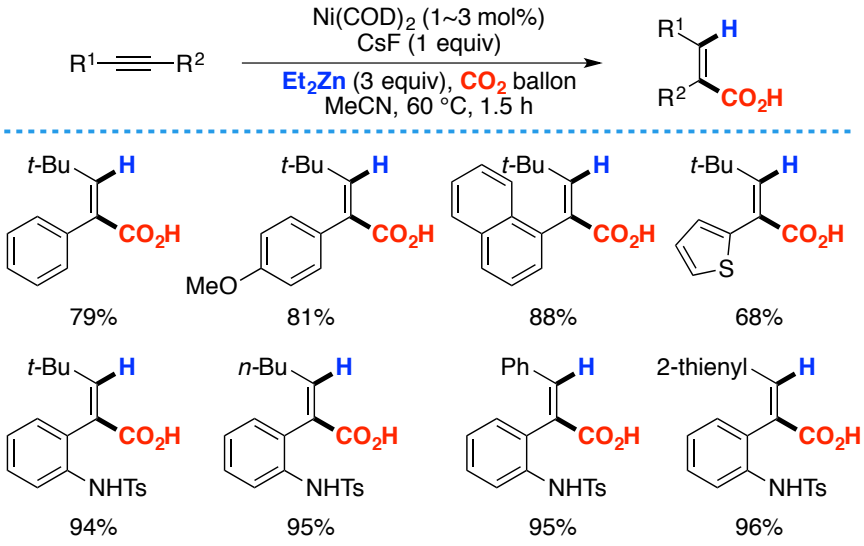

Scheme 1.40. Ni-catalyzed *syn*-hydrocarboxylation of alkynes.

The proposed mechanism involved two catalytic cycles involving Ni(0)Ln species, as shown in Scheme 1.41. In cycle 1, Ni-complex **XXXVII** initially reacts with the alkyne to generate nickelacyclopropene **XXXVIII**. Subsequent transmetallation and ethylene release results in the formation of intermediate **XXXIX**, setting the stage for a reductive elimination en route to **XLI** while regenerating catalyst **XXXVII**. In cycle 2, **XLI** reacts with the Aresta-type Ni-complex **XL** to deliver **XLII**. Followed by reductive elimination, thus producing a zinc carboxylated while recovering back **XXXVII**. However, no mechanistic studies were performed to correspond such hypothesis.

[53] Li, S.; Yuan, W.; Ma, S. *Angew. Chem. Int. Ed.* **2011**, *50*, 2578.

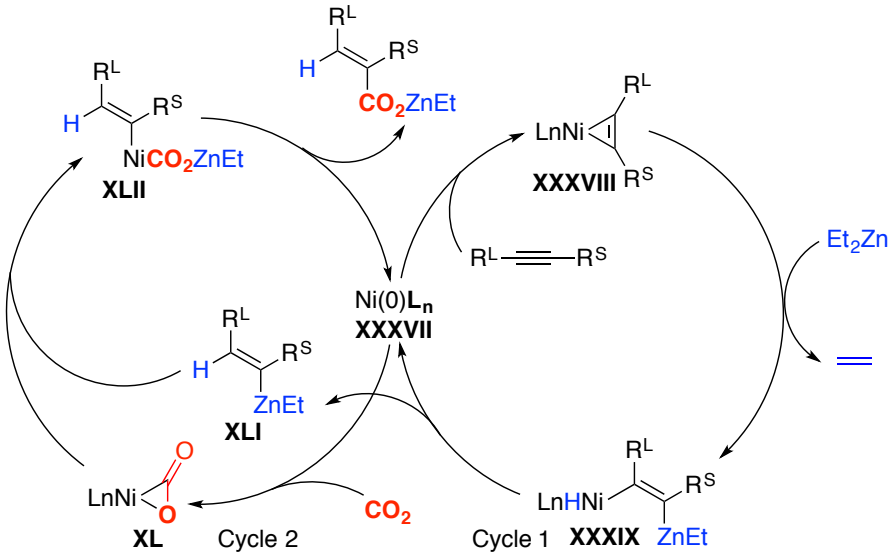

Scheme 1.41. Proposed mechanism. R^L = large group, R^S = small group.

Independently, the Tsuji group reported the Cu-catalyzed hydrocarboxylation of internal alkynes with CO_2 and hydrosilanes via a vinylcopper intermediate. The reactions were performed either in hexane or 1,4-dioxane in the presence of a catalytic amount of *N*-heterocyclic carbene-copper complex using $HSi(OEt)_3$ as a hydride source. The resulting acrylic acid analogues were isolated in moderate to excellent yields (Scheme 1.42).

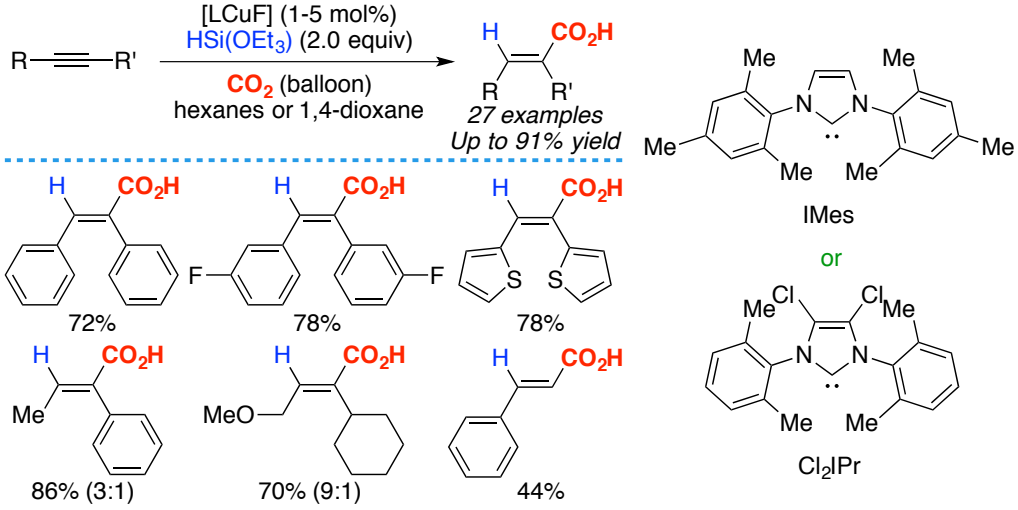

Scheme 1.42. Cu-catalyzed hydrocarboxylation of alkynes.

The authors proposed a catalytic cycle based on an *in situ* formed NHC-Cu(I) hydride species **XLIII**. *Syn*-addition of **XLIII** onto an alkyne produces vinylcopper intermediate **XLIV**, subsequent insertion and a final σ-bond metathesis with $HSi(OEt)_3$

to yield ester **XLV** and while regenerating **XLIII** (Scheme 1.43).[54]

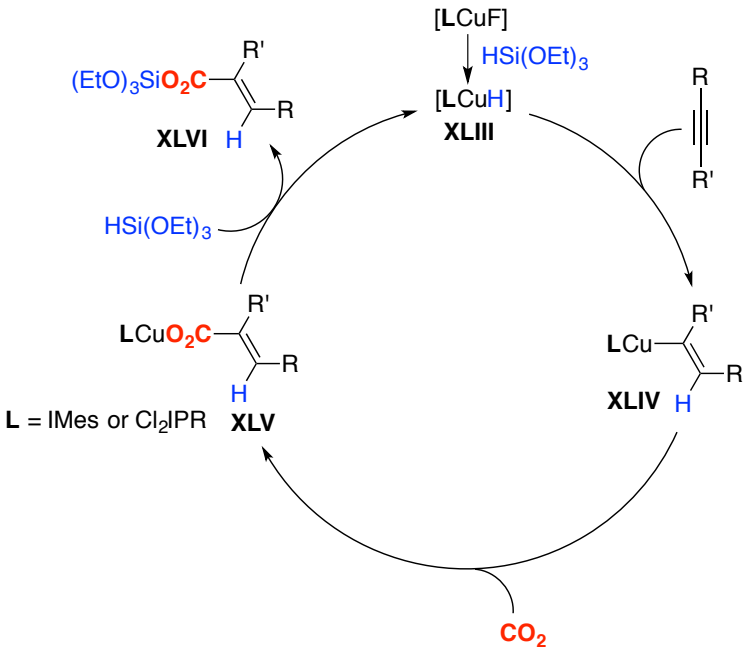

Scheme 1.43. Proposed mechanism.

In 2012, the same group developed a Cu-catalyzed silacarboxylation of internal alkynes with CO_2 and a silylborane reagent. The insertion of CO_2 selectively took place at the adjacent position of the aromatic ring, affording silalactones in moderate to high yields.[55] The authors suggested a possible catalytic cycle going via silyl complex **XLVII**, followed by *syn*-addition onto the alkyne to give intermediate **XLVIII**, which undergoes CO_2 insertion to provide corresponding copper carboxylate species **IL**. An intramolecular cyclization and metathesis generate the final product and regenerate the active Cu-complex **XLVII**.

[54] Fujihara, T.; Xu, T.; Semba, K.; Terao, J.; Tsuji, Y. *Angew. Chem. Int. Ed.* **2011**, *50*, 523.
[55] Fujihara, T.; Tani, Y.; Semba, K.; Terao, J.; Tsuji, Y. *Angew. Chem. Int. Ed.* **2012**, *51*, 11487.

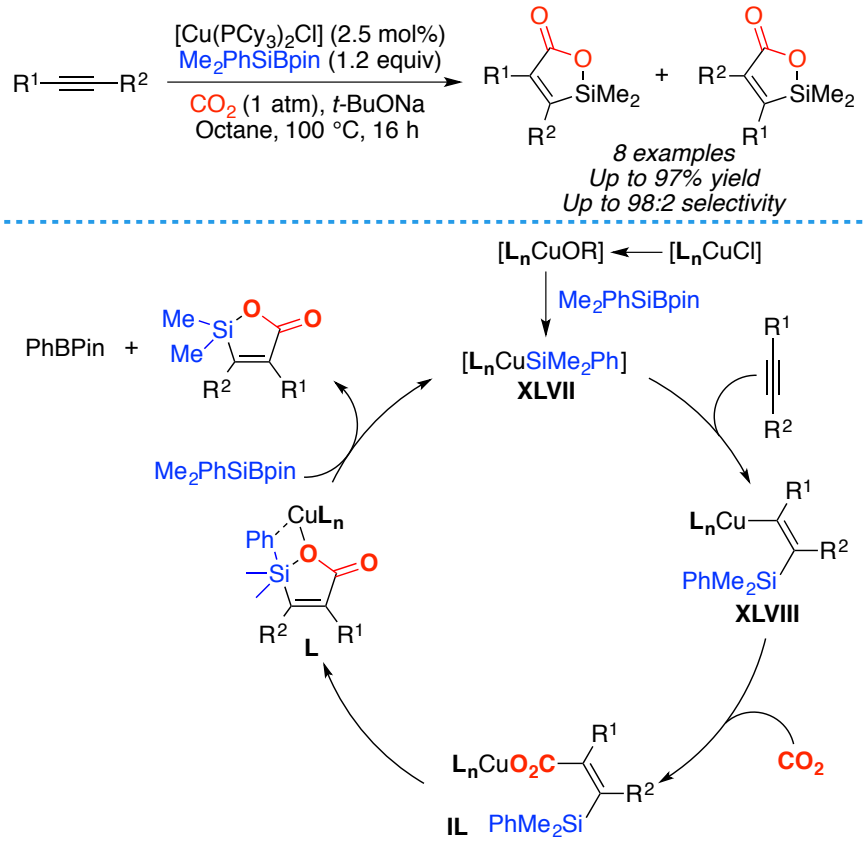

Scheme 1.44. Cu-catalyzed silacarboxylation of alkynes and the proposed mechanism.

In 2012, Hou and co-workers developed the first NHC-Cu complex catalyzed boracarboxylation reaction of alkynes with diborane and CO_2 (Scheme 1.45). This transformation furnished a novel family of α, β-unsaturated β-boralactone derivatives under mild conditions.[56] Diaryl alkynes and aryl, alkyl-disubstituted alkynes are suitable for this reaction and generate the corresponding β-boralactones in good yields with high regio- and stereoselectivities. Some crucial intermediates could be isolated and structurally characterized by X-ray analysis, thus offering significant insight into the mechanism. The reaction mechanism of this boracarboxylation reaction is similar to the silacarboxylation process described above in Scheme 1.44.

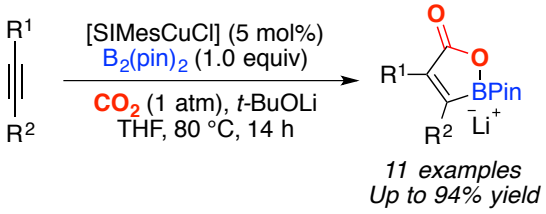

Scheme 1.45. Cu-catalyzed boracarboxylation of alkynes.

[56] Zhang, L.; Cheng, J.; Carry, B.; Hou, Z. *J. Am. Chem. Soc.* **2012**, *134*, 14314.

Subsequently, the Hou group described a Cu-catalyzed formal methylative and hydrogenative carboxylation event of various internal and terminal alkynes. The treatment of alkynes with aluminum reagents such as Me_3Al and *i*-Bu_2AlH in the presence of Sc-, Zr- and Ni-complexes generates corresponding vinylaluminum reagents. Subsequent carboxylation of the resulting alkenylaluminum species with CO_2 occurs in the presence of a *N*-heterocyclic carbene copper catalyst, generating the desired products in high yields. The regio- and stereoselectivity of the transformation is strongly dependent on the hydroalumination or methylalumination reaction, which mostly rely on the alkynes and catalysts employed, delivering *α,β*-unsaturated carboxylic acids via one pot process (Scheme 1.46).[57]

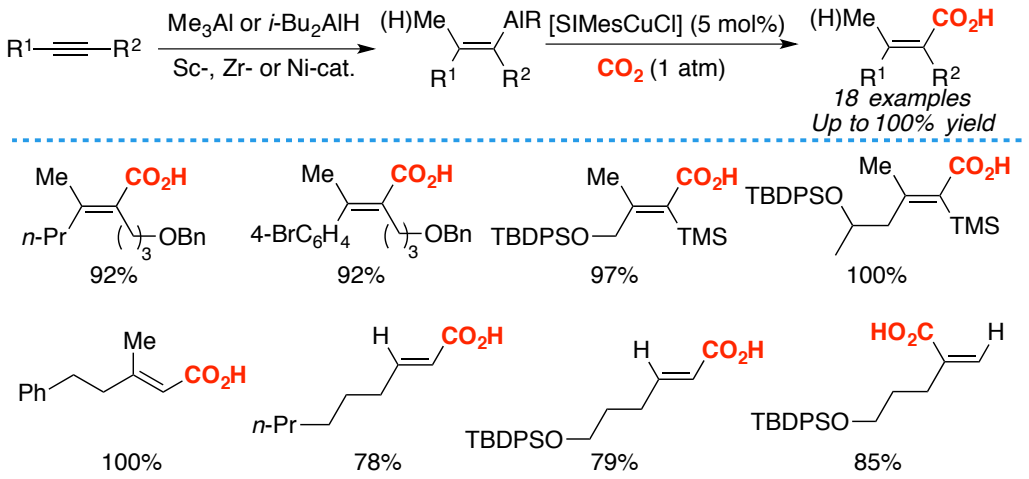

Scheme 1.46. Cu-catalyzed methylative and hydrogenative carboxylation of alkynes.

The Ma group reported a Cu-catalyzed *anti*-carbometallation/carboxylation event of 2-alkynyl anilines to synthesize various indolyl-3-carboxylic acids. Unfortunately, no mechanistic details were included that allowed for rationalizing the results shown in Scheme 1.47.

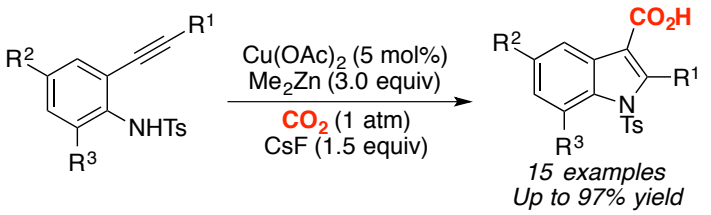

Scheme 1.47. Cu-catalyzed annulation-carboxylation of alkynes.

[57] Takimoto, M.; Hou, Z. *Chem. Eur. J.* **2013**, *19*, 11439.

1.4.7 Transition Metal-catalyzed Carboxylation of Allenes

In 2008, Iwasawa's group described the catalytic hydrocarboxylation of allenes with CO_2 as for their previous carboxylation of 1,3-dienes, a tridentate silyl pincer-type Pd-hydride species were employed as the catalyst, affording β, γ-unsaturated carboxylic acids in high yields and excellent regioselectivity. The transformation required the presence of Et_3Al or Et_2Zn as the reducing agents, thus generating the key Pd-hydride intimidate **LI** (Scheme 1.48).[58]

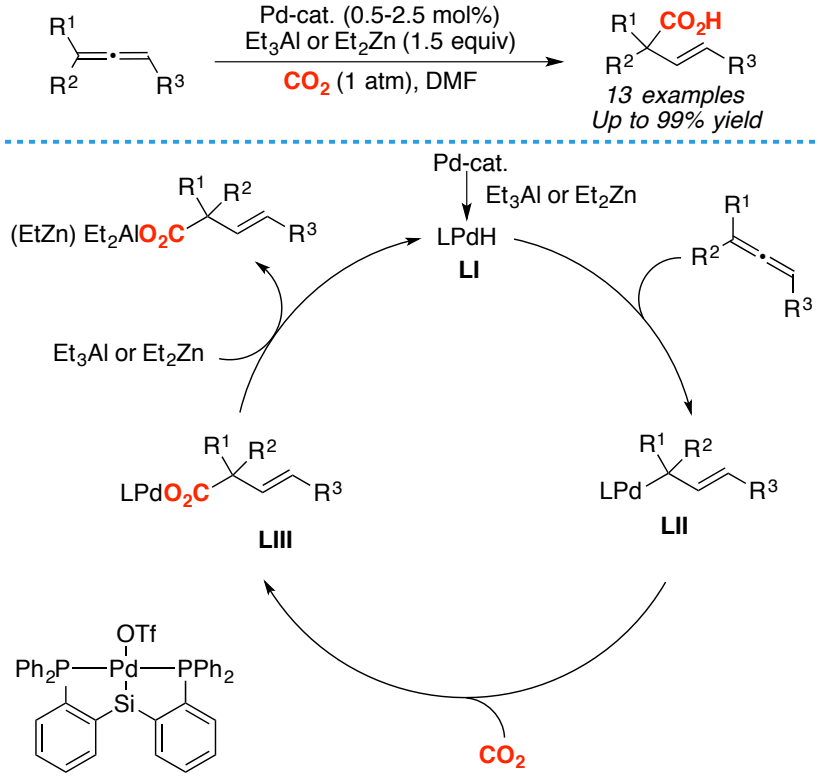

Scheme 1.48. Pd-catalyzed hydrocarboxylation of allenes and the proposed mechanism.

Recently, Tsuji's group reported a copper-catalyzed regiodivergent silacarboxylation of allenes with $PhMe_2Si$-BPin under atmospheric pressure of CO_2, in which the ligand dictated the selectivity pattern. While rac-Me-DuPhos affords the vinylsilanes, the introduction of PCy_3 leads to allylsilanes. Notably, the reactions could be carried out on a gram scale. However, the presented protocol is not suitable for allenes bearing an aryl substituent (Scheme 1.49).[59]

[58] Takaya, J.; Iwasawa, N. *J. Am. Chem. Soc.* **2008**, *130*, 15254.
[59] Tani, Y.; Fujihara, T.; Terao, J.; Tsuji, Y. *J. Am. Chem. Soc.* **2014**, *136*, 17706.

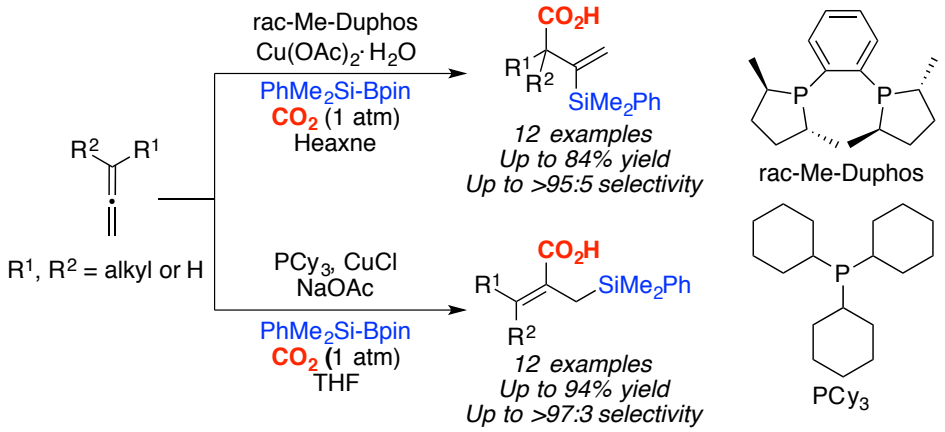

Scheme 1.49. Ligand-controlled regiodivergent Cu-catalyzed silacarboxylation of allenes.

The authors performed several control experiments in order to gain some insight into the reaction mechanism, suggesting that the regiodivergency occurs at the silylcupration stage. First, the silylcopper species **LIV** are generated *in situ* by treating Cu-precatalyst with $PhMe_2Si{-}Bpin$. While the use of *rac*-Me-DuPhos as the ligand results in the silylcupperation, which the Cu atom ends up at the terminal position, the employment of PCy_3 locate the Cu atom at the centeral C atom. Subsequent CO_2 insertion takes place, followed by σ-bond metathesis afforded the corresponding products (Scheme 1.50).

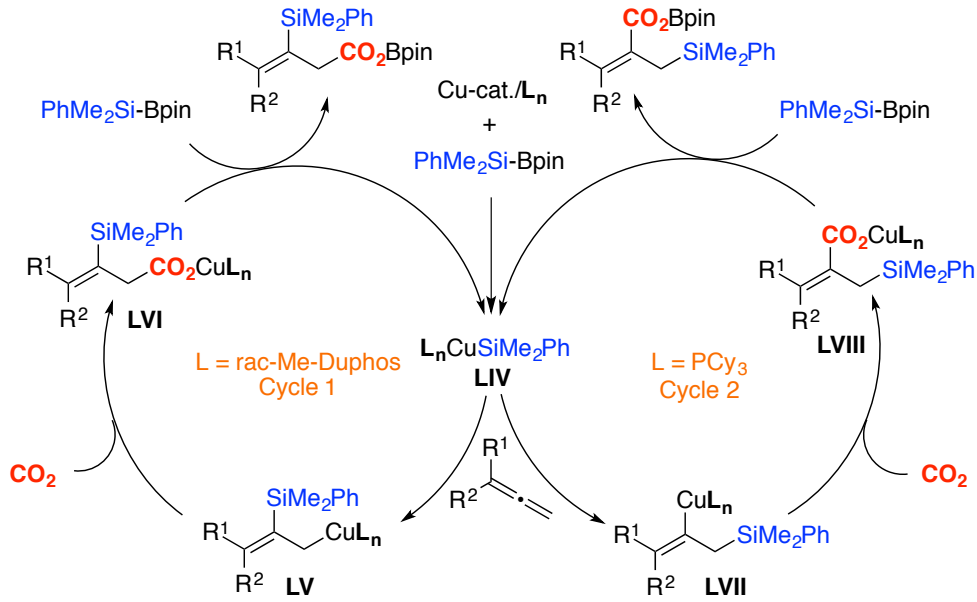

Scheme 1.50. Proposed mechanism.

1.4.8 Transition Metal-catalyzed C-H Carboxylation

1.4.8.1 Transition Metal-catalyzed C(sp)-H Carboxylation

In 1994, Inoue and co-workers demonstrated that simple CuBr could serve as catalysts for the C-H carboxylation of alkynes. The authors reported the synthesis of alkyl alkynoates using alkynes, CO_2 (1 atm), and alkyl halides catalyzed by CuBr (2 mol%) in polar aprotic solvents such as DMF, DMAc at 100 °C. They postulated that CuBr reacts firstly with the alkyne to give copper acetylide, followed by insertion of CO_2 into the Cu-C bond, and alkylation with an appropriate alkyl halides.[60] More recently, the research groups of Lu,[61] Kondo,[62] and Wang reported carboxylation of terminal acetylene. In Lu's work, a wide range of propiolic esters were delivered in good to excellent yields when IPrCuCl was used as precatalyst at high pressure of CO_2 (15 atm) in the presence of K_2CO_3 and various alkyl chlorides. In Kondo's system, CuI and PEt_3 were employed, producing the desired products. In 2013, Wang and co-workers obtained similar results when using a CuI catalyst system in the absence of ligand.[63] (Scheme 1.51).

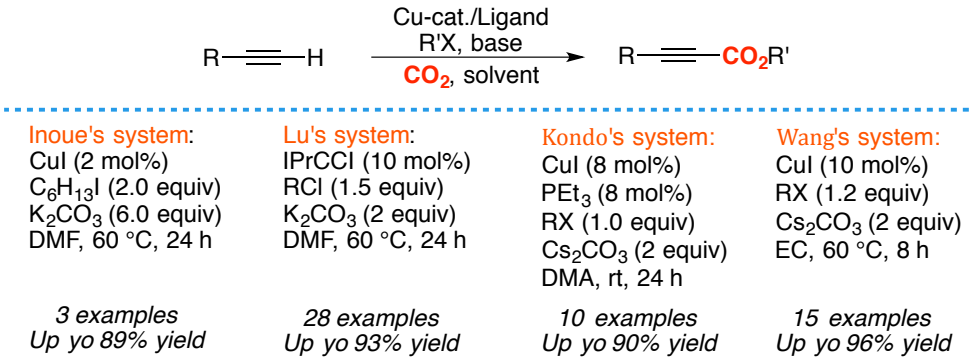

Scheme 1.51. Recent development in Cu-catalyzed C-H carboxylation/esterification of alkynes.

In 2010, the group of Gooßen published the synthesis of free propiolic acid with phenanthroline and phosphine coordinated Cu(I) catalyst,[64]generating propiolic acids in high yields. Independently, Zhang's group found that the polyNHC-Cu system could

[60] Fukue, Y.; Oi, S.; Inoue, Y. *J. Chem. Soc. Chem. Commun.* **1994**, 2091.
[61] Zhang, W. Z.; Li, W. J.; Zhang, X.; Zhou, H.; Lu, X. B. *Org. Lett.* **2010**, *12*, 4748.
[62] Inamoto, K.; Asano, N.; Kobayashi, K.; Yonemoto, M.; Kondo, Y. *Org. Biomol. Chem.* **2012**, *10*, 1514.
[63] Yu, B.; Diao, Z. F.; Guo, C. X.; Zhong, C. L.; He, L. N.; Zhao, Y. N.; Song, Q. W.; Liu, A. H.; Wang, J. Q. *Green Chem.* **2013**, *15*, 2401.
[64] Gooßen, L. J.; Rodríguez, N.; Manjolinho, F.; Lange, P. P. *Adv. Synth. Catal.* **2010**, *352*, 2913.

convert electron-deficient aryl alkynes towards the desired propiolic acids in high yields (Scheme 1.52). [65]

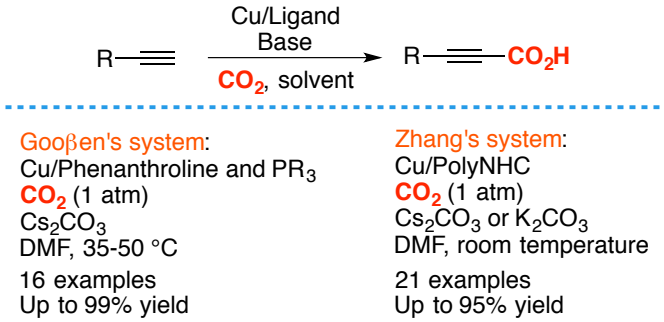

Scheme 1.52. Recent development in Cu-catalyzed C-H carboxylation of alkynes.

Besides the Cu-catalysts, silver salts have been used as catalysts for the C-H carboxylation of terminal alkynes to deliver propiolic acids. In 2011, the Lu group reported ligand-free AgI catalyzed C-H carboxylation of terminal alkynes with CO_2 (2 atm) in the presence of Cs_2CO_3 as base at 50 °C. This protocol exhibited a broad substrate scope including electron-deficient aryl alkynes. (Scheme 1.53).[66]

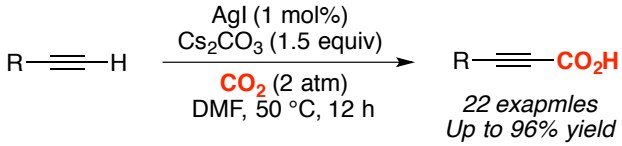

Scheme 1.53. Ag-catalyzed direct synthesis of propiolic acids.

1.4.8.2 Transition Metal-catalyzed C(sp^2)-H Carboxylation

Inspired by Fujiwara's report on the carboxylation of benzene,[67] Iwasawa described the first direct C(sp^2)-H arboxylation of arenes using Rh-catalysts and $AlMe_2(OMe)$ as reducing reagent in DMA at 70 °C under CO_2 (1 atm) atmosphere. The reaction was believed to preceed via C-H functionalization (**LX**), following by reductive elimination to release methane (**LXI**), subsequent CO_2 insertion affords rhodium carboxylated intermediate **LXII** and final transmetallation of the carboxylates with aluminum reagents gives aluminum carboxylates **LXIII** while liberating complex **LX** to restart the catalytic cycle (Scheme 1.54).[68]

---

[65] Yu, D.; Zhang, Y. *Proc. Natl. Acad. Sci.* **2010**, *107*, 20184.
[66] Zhang, X.; Zhang, W. Z.; Ren, X.; Zhang, L. L.; Lu, X. B. *Org. Lett.* **2011**, *13*, 2402.
[67] Sugimoto, H.; Kawata, I.; Taniguchi, H.; Fujiwara, Y. *J. Organomet. Chem.* **1984**, *266*, c44.
[68] Mizuno, H.; Takaya, J.; Iwasawa, N. *J. Am. Chem. Soc.* **2011**, *133*, 1251.

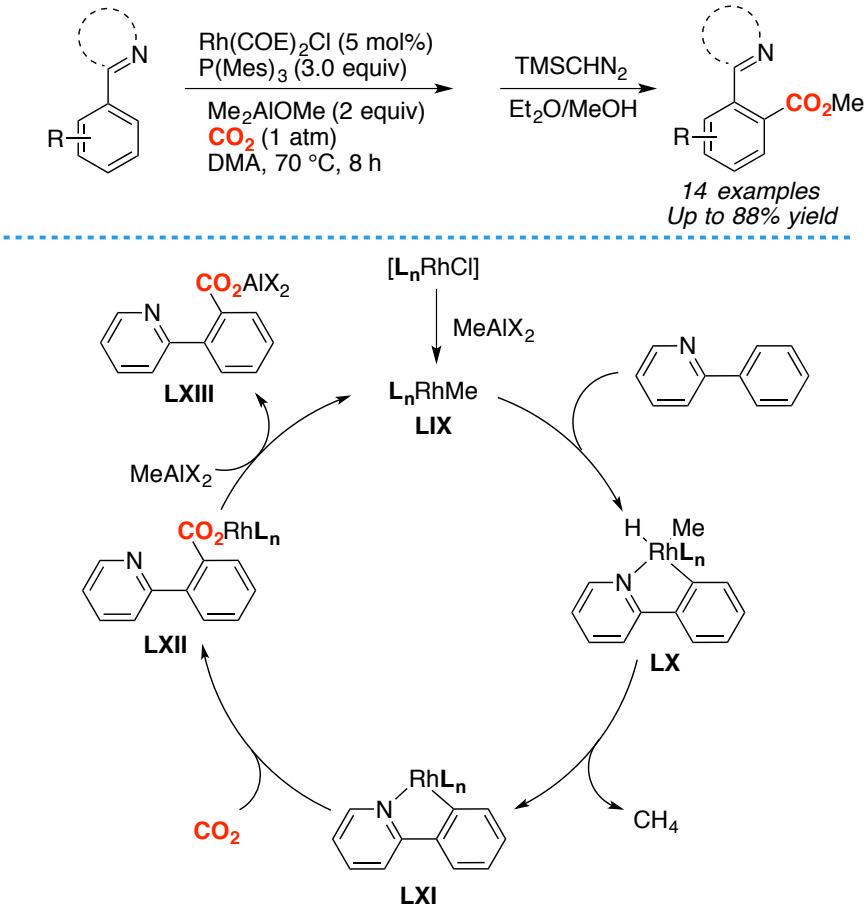

Scheme 1.54. Rh-catalyzed C(sp^2)-H carboxylation of arenes and the proposed mechanism.

While this work was limited to expensive Rh-catalysts and 2-prydine groups, the Iwasawa group published a Pd-catalyzed carboxylation of unactivated alkenyl C−H bond of 2-hydroxystyrenes.[69] The reaction is believed to undergo a six-membered alkenyl palladium intermediate **LXIV** that was confirmed by X-ray analysis. Subsequently, intermediate **LXIV** undergoes a CO_2 insertion to form palladium carboxylate intermediate **LXV**. The latter reacts with another molecule of 2-hydroxystyrene and the base to furnish coumarin with the release of the active catalyst. The lactone formation process was suggested to be an important factor in driving the catalytic cycle to completion (Scheme 1.55).

[69] Sasano, K.; Takaya, J.; Iwasawa, N. *J. Am. Chem. Soc.* **2013**, *135*, 10954.

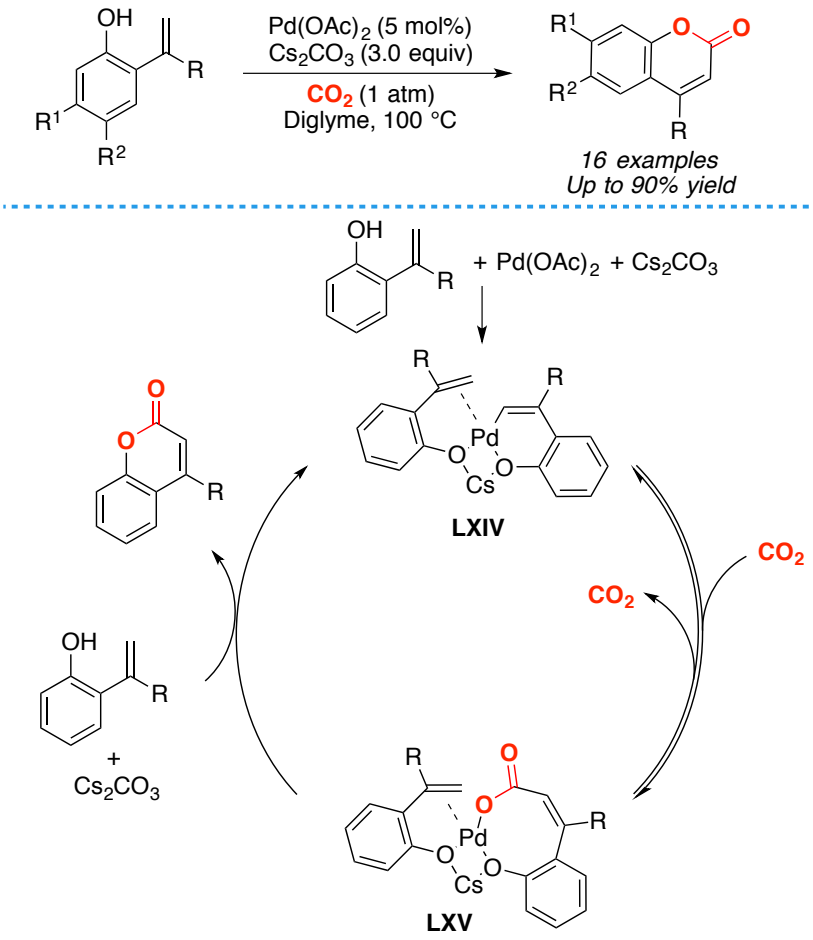

Scheme 1.55. Catalytic C(sp^2)-H carboxylation and the proposed mechanism.

In 2010, Nolan's group described the NHC-Au(I) hydroxide complexes could be used for the carboxylation of electron-poor arenes, in which the C-H carboxylation occurs at the most acidic C-H site. The impressive selectivity of this C-H carboxylation reaction can be rationalized with acid/base theory. The authors carried out mechanistic studies, the intermediates involved were isolated and characterized, that allowed them to build upon a rationale of these results (Scheme 1.56).[70]

[70] Boogaerts, I. I. F.; Nolan, S. P. *J. Am. Chem. Soc.* **2010**, *132*, 8858.

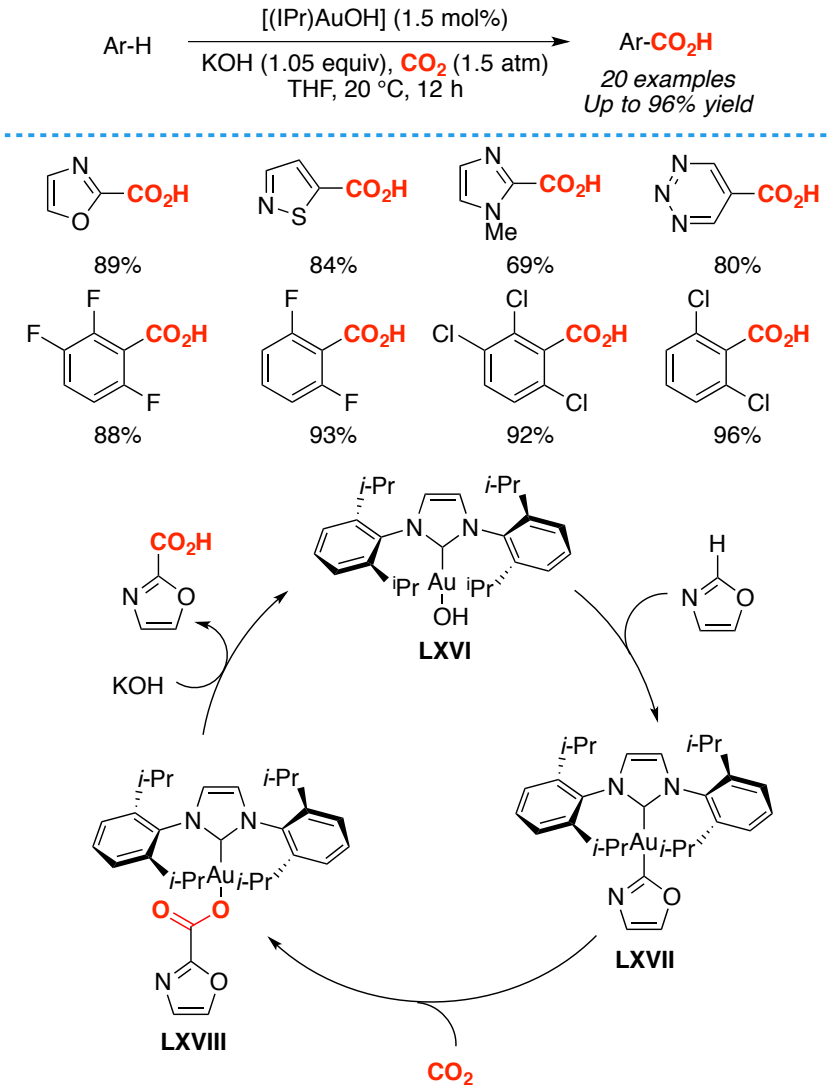

Scheme 1.56. Au-catalyzed C(sp^2)-H carboxylation and the proposed mechanism.

Shortly after, both the Nolan[71] and Hou's[72] groups published the Cu-catalyzed C(sp^2)-H carboxylation of heterocycles or polyfluorobenzenes with CO_2. The authors employed NHC-supported Cu-catalyst to prepare the corresponding acids in high yields. Once again, the isolation of reaction intermediates allowed the authors to propose a mechanism of this transformation.

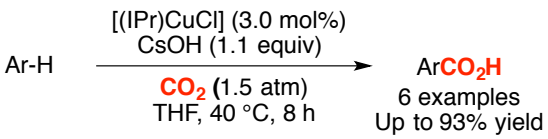

Scheme 1.57. Cu-catalyzed C(sp^2)-H carboxylation of active C-H bonds.

[71] Boogaerts, I. I. F.; Fortman, G. C.; Furst, M. R. L.; Cazin, C. S. J.; Nolan, S. P. *Angew. Chem. Int. Ed.* **2010**, *49*, 8674.
[72] Zhang, L.; Cheng, J.; Ohishi, T.; Hou, Z. *Angew. Chem. Int. Ed.* **2010**, *49*, 8670.

Recently, the Hou group reported the preparation of NHC–Cu complex **LXIX** bearing 1,2,3-triazol-5-ylidene ligand, and finding that it was an excellent precatalyst for C-H carboxylation reactions (Scheme 1.58), even with heterocycles with less acidic C-H bonds (benzothiazoles, pKa = 27.3, benzoxazole pKa = 24.8).[73]

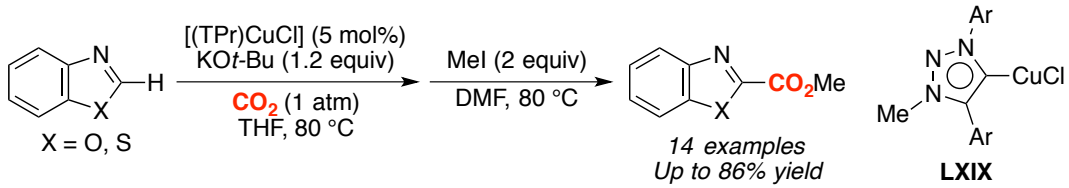

Scheme 1.58. Cu-catalyzed C(sp^2)-H carboxylation of heteroarenes.

More recently, the Iwasawa group published direct carboxylation of simple arenes under atmospheric pressure of CO_2 *via* a rhodium-catalyzed C–H bond activation without directing groups. Various arenes bearing electron-rich or deficient substituents, as well as heteroarenes, were directly converted into the desired acids. Although high turn over numbers could be achieved in this transformation, the products were obtained with poor regioselectivity (Scheme 1.59).[74]

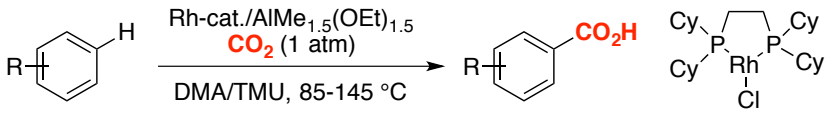

Scheme 1.59. Rh-catalyzed direct C(sp^2)-H carboxylation of simple arenes with CO_2.

[73] Inomata, H.; Ogata, K.; Fukuzawa, S.; Hou, Z. *Org. Lett.* **2012**, *14*, 3986.
[74] Suga, T.; Mizuno, H.; Takaya, J.; Iwasawa, N. *Chem. Commum.* **2014**, *50*, 14360.

Chapter 2: Ni-catalyzed Divergent Cyclization/ Carboxylation of Primary and Secondary Alkyl Halides with CO_2

2.1 Objectives

❖To develop a convenient transition metal-catalyzed reaction that affords tetra-substituted acrylic acid derivatives from simple starting materials.

❖To shed light on the mechanism by studying the effect of radical scavengers, by conducting stoichiometric reactions, and by studying the stereochemistry of the reaction.

2.2 Introduction to Distal Bond-Formation via Cascade Reactions

Catalytic reductive coupling reactions of organic halides have evolved from mere curiosities to robust tools that rapidly build up molecular complexity from simple precursors.[75] At present, this field of expertise remains essentially confined to bond-formation events at the initial site (Scheme 2.1, path a). Intriguingly, the ability to promote cascade reactions of unactivated alkyl electrophiles via multiple C−C bond formations (path b) has been virtually unexplored.[76,77] If successful, such protocols would offer a unique opportunity to increase our chemical collection by rapidly preparing carbocyclic skeletons while dealing with bond-formation events at distal sites.

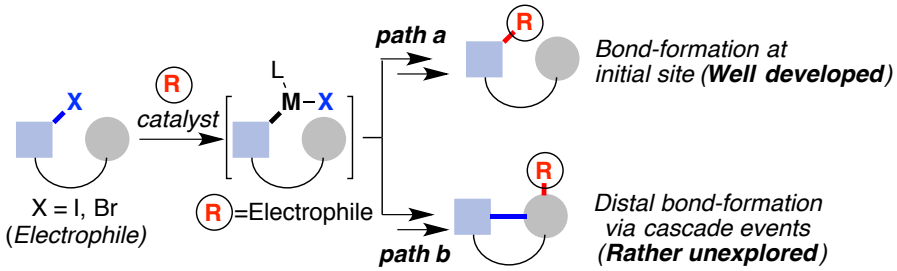

Scheme 2.1 Bond formation via electrophile couplings.

In 1968, the Rothman group reported the preparation of ethylidenecyclopentane through hydrolysis of a THF solution of Grignard reagent prepared from 7-chloro-2-heptyne. While the product could be obtained in excellent yields, it required harsh reaction conditions (heating at 100 °C for 6 days) (Scheme 2.2).[78]

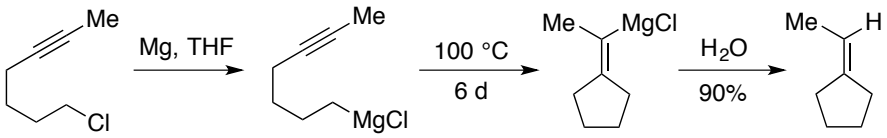

Scheme 2.2. Intramolecular cyclization of acetylenic Grignard reagents.

[75] For selected reviews: (a) Moragas, T.; Correa, A.; Martin, R. *Chem. Eur. J.* **2014**, *20*, 8242. (b) Tasker, S. Z.; Standley, E. A.; Jamison, T. F. *Nature* **2014**, *509*, 299. (c) Everson, D. A.; Weix, D. J. *J. Org. Chem.* **2014**, *79*, 4793. (d) Knappe, C. E. I.; Grupe, S.; Gärtner, D.; Corpet, M.; Gosmini, C.; Jacobi von Wangelin, A. *Chem. Eur. J.* **2014**, *20*, 6828. (e) Montgomery, J. Organonickel Chemistry. *In Organometallics in Synthesis;* Lipshutz, B. H., Ed.; John Wiley & Sons, Inc.; Hoboken, **2013**; pp 319-428.

[76] For an isolated example of a catalytic reductive cyclization: Zhao, C.; Jia, X.; Wang, X.; Gong, H. *J. Am. Chem. Soc.* **2014**, *136*, 17645.

[77] Durandetti, M.; Hardou, L.; Lhermet, R.; Rouen, M.; Maddaluno, J. *Chem. Eur. J.* **2011**, *17*, 12773.

[78] Richey Jr, H. G.; Rothman, A. M. *Tetrahedron Lett.* **1968**, *9*, 1457.

In 1989, Bailey and coworkers described a cyclization process through which primary 5-hexyn-1-yllithium, which may be generated in virtually quantitative yield by low-temperature lithium-iodine exchange, undergoes regiospecific 5-*exo*-dig cyclization via stereoselective *syn*-addition of the CH_2Li group to the alkyne moiety. The resulting vinyllithiums may be trapped with any variety of electrophiles to deliver functionalized cyclopentylidene-containing products.[79]

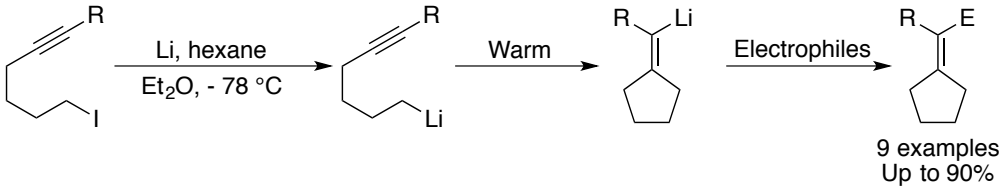

Scheme 2.3. Intramolecular cyclization of acetylenic lithium reagents.

Two years later, Rao and Knochel established a Cu-mediated distal C-C or C-H bond formation via a cascade event. The reaction was conducted at 25 °C for 1.5 h, delivering the corresponding coupled products in moderate yields.[80]

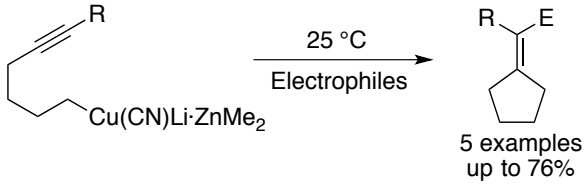

Scheme 2.4. Intramolecular cyclization of acetylenic lithium reagents.

Kambe and colleagues have developed a silver catalyzed carbomagnesiation of alkynes in the presence of a Grignard reagent. Applying this protocol to δ-haloalkylalkynes led to the formation of multiple substituted olefins. Although CO_2 could be coupled as electrophile in this procedure, only 23% of the cyclized acid was obtained when the corresponding alkyl bromide was used as starting material.[81]

[79] Bailey, W. F.; Ovaska, T. V.; Leipert, T. K. *Tetrahedron Lett.* **1989**, *30*, 3901.
[80] Rao, S. A.; Knochel, P. *J. Am. Chem. Soc.* **1991**, *113*, 5735.
[81] Kambe, N.; Moriwaki, Y.; Fujii, Y.; Iwasaki, T.; Terao, J. *Org. Lett.* **2011**, *13*, 4656.

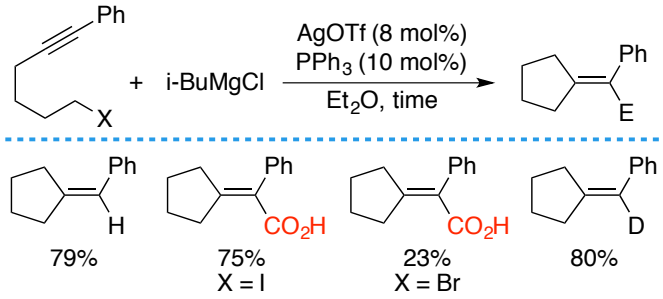

Scheme 2.5. Silver-catalyzed domino reaction.

2.3 Screening of the Reaction Conditions

In recent years, we and others have designed new catalytic techniques for reductive carboxylation of organic halides using CO_2.[9] Unlike the utilization of stoichiometric amounts of organometallic complexes,[10] many of these protocols can be conducted under mild conditions in the absence of sensitive reagents, thus representing a straightforward alternative for preparing carboxylic acids, privileged motifs in a myriad of pharmaceuticals.[82] At the outset of our investigations, however, it was unclear whether CO_2 could participate in cascade reductive coupling reactions via multiple bond-forming reactions.[83] Although we anticipated that reductive cascade processes based on the use of unactivated alkyl halides would be rather problematic,[84] we were attracted to the challenge.[85] Specifically, such a route would offer the unique opportunity to control β-hydride elimination pathways while resulting in carboxylated carbocyclic skeletons from simple precursors via distal catalytic CO_2 fixation.

We began our investigation by employing **2-1a** as our model substrate，and studied the effect of experimental parameters such as precatalysts, solvents, additives, ligands as well as reducing reagents.

Initially, we carried out a series of studies on the carboxylation of **2-1a** in the

[82] (a) Patai, S. The Chemistry of Acid Derivatives; Wiley: New York, 1992. (b) Goossen, L. J.; Rodríguez, N.; Goossen, K. *Angew. Chem. Int. Ed.* **2008**, *47*, 3100. (c) Maag, H. *Prodrugs of Carboxylic Acids*; Springer: New York, 2007.

[83] Fogg, D. E.; dos Santos, E. N. *Coord. Chem. Rev.* **2004**, *248*, 2365.

[84] (a) Kambe, N.; Iwasaki, T.; *Chem. Soc. Rev.* **2011**, *40*, 4937. (b) Jana, R.; Pathak, T. P.;Sigman, M. S. *Chem. Rev.* **2011**, *111*, 1417. (c) Rudolph, A.; Lautens, M. *Angew. Chem. Int. Ed.* **2009**, *48*, 2656.

[85] Selected nucleophile-electrophile regimes: (a) Venning, A. R. O.; Bohan, P. T.; Alexanian, E. J. *J. Am. Chem. Soc.* **2015**, *137*, 3731. (b) Cong, H.; Fu, G. C. *J. Am. Chem. Soc.* **2014**, *136*, 3788. (c) Monks, B. M.; Cook, S. P. *J. Am. Chem. Soc.* **2012**, *134*, 15297. (d) Bloome, K. S.; McMahen, R. L.; Alexanian, E. J. *J. Am. Chem. Soc.* **2011**, *133*, 20146. (e) Kim, H.; Lee, C. *Org. Lett.* **2011**, *13*, 2050. (f) Firmansjah, L.; Fu, G. C. *J. Am. Chem. Soc.* **2007**, *129*, 11340.

presence of different Pd-precatalysts with monodentate, bidentate or N-heterocyclic carbenes as ligand, Et_3Al as reducing agent in DMF under atmospheric pressure of CO_2 at room temperature overnight. As shown in Figure 2.2, combinations of Pd-precatalyst with different ligands did not generate even traces amount of the desired product.

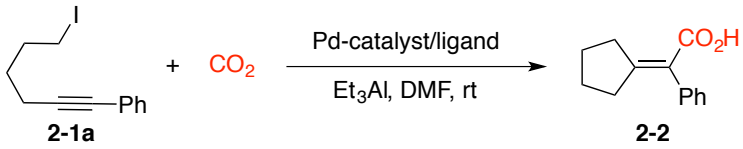

2-1a **2-2**

Entry	Catalyst	Ligand	Conversion (%)[b]	Yield (%)[c]
1	Pd_2dba_3	$PCy_3{\cdot}HBF_4$	2	0
2	$Pd(OAc)_2$	$PCy_3{\cdot}HBF_4$	36	0
3	$PdBr_2$	$PCy_3{\cdot}HBF_4$	42	0
4	IPrPd(allyl)Cl	IPr·HCl	100	0
5	$Pd(dppf)Cl_2$	dppf	0	0
6	$Pd(Ph_3)_2Cl_2$	PPh_3	0	0

[a] Reaction conditions: **2-1a** (0.3 mmol), Pd-cat. (10 mol%), ligand (20 mol%), Et_3Al (2.5 equiv), DMF (2 mL), rt, overnight. [b] HPLC conversions, determined by using naphthalene as internal standard. [c] HPLC yields, determined by using naphthalene as internal standard.

Table 2.1. Palladium precatalyst and ligand screening.[a]

Since the utilization of palladium catalysts did not give the target product, we moved on to screening of various Ni-precatalysts and different phosphine ligands. These have recently success in the related carboxylation reaction. A wide range of monodentate and bidentate phosphines was tested with $Ni(acac)_2$ under the indicated reaction conditions (Entries 1-10). However, no starting material was converted to the desired product. Although Ni-catalysts possessing ligands such as dppf or PCy_3 gave moderate conversions, no desired products were delivered.

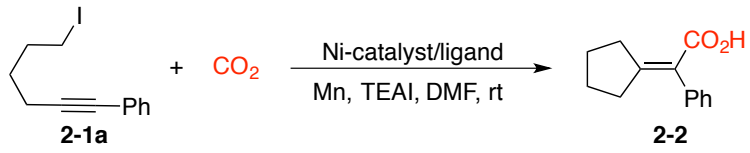

2-1a **2-2**

Entry	Catalyst	Ligand	Conversion (%)[b]	Yield (%)[c]
1	$Ni(acac)_2$	$PCp_3 \cdot HBF_4$	19	0
2	$Ni(acac)_2$	$PEt_3 \cdot HBF_4$	0	0
3	$Ni(acac)_2$	Ruphos	0	0
4	$Ni(acac)_2$	SPhos	0	0
5	$Ni(acac)_2$	XPhos	0	0
6	$Ni(acac)_2$	^{t}Bu-XPhos	0	0
7	$Ni(acac)_2$	^{t}Bu-DavePhos	0	0
8	$Ni(acac)_2$	JohnPhos	0	0
9	$Ni(acac)_2$	QPhos	0	0
10	$Ni(acac)_2$	$PCy_2(NM_2Ph)$	0	0
11	$Ni(dppf)Cl_2$	dppf	59	0
12	$Ni(dppb)Cl_2$	dppb	0	0
13	$Ni(PCy_3)_2Cl_2$	$PCy_3 \cdot HBF_4$	30	0

[a] Reaction conditions: **2-1a** (0.3 mmol), Ni-cat. (10 mol%), ligand (20 mol%), Mn (3.0 equiv),TEAI (2.0 equiv), DMF (2 mL), rt, overnight. [b] HPLC conversions, determined by using naphthalene as internal standard. [c] HPLC yields, determined by using naphthalene as internal standard.

Table 2.2. Phosphine ligand screening with Ni-catalysts.[a]

We then decided to fix the Ni-precatalyst ($NiCl_2 \cdot glyme$) and the ligand (2,9-Dimethyl-1,10-phenanthroline, neocuproine) to explore the effect of different solvents in our carboxylation event. To our delight, we observed cyclized acid in 35% HPLC yield in the presence of Mn (2.2 equiv) in DMF at room temperature (Table 2.3, Entry 1). Other solvents regardless their polarity, such as DEM, digylme, DMSO, benzene, $PhNO_2$, DMA, Dioxane, DCE, TCE, THF did not convert any starting material to product (Entries 3-13), indicating that our protocol has a significant solvent influence.

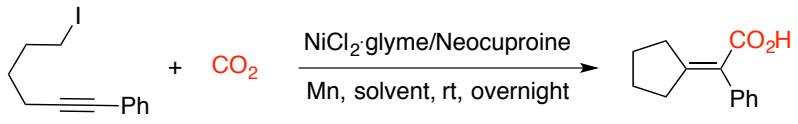

2-1a **2-2**

Entry	Catalyst	Solvent	Conversion (%)[b]	Yield (%)[c]
1	$NiCl_2$·glyme	DMF	100	33
2	$NiCl_2$·glyme	MeCN	0	0
3	$NiCl_2$·glyme	DME	0	0
4	$NiCl_2$·glyme	Diglyme	0	0
5	$NiCl_2$·glyme	DMSO	0	0
6	$NiCl_2$·glyme	benzene	0	0
7	$NiCl_2$·glyme	$PhNO_2$	0	0
8	$NiCl_2$·glyme	DMA	0	0
9	$NiCl_2$·glyme	Dioxane	0	0
10	$NiCl_2$·glyme	DCE	0	0
11	$NiCl_2$·glyme	TCE	0	0
12	$NiCl_2$·glyme	THF	0	0

[a] Reaction conditions: **2-1a** (0.3 mmol), Ni-cat. (10 mol%), neocuproine (20 mol%), Mn (2.2 equiv), DMF (2 mL), rt, overnight. [b] HPLC conversions, determined by using naphthalene as internal standard. [c] HPLC yields, determined by using naphthalene as internal standard.

Table 2.3. Solvent screening.[a]

With these results in hand, we decided to explore whether additives can influence the reaction outcome. As demonstrated in Table 2.4, additives such as AgF, ammonium salts, CsF, Cs_2CO_3, lithium bromide and lithium chloride were introduced with the expectation that these additives would either accelerate the reactivity or in the case of ammonium salts increase the solubility of CO_2 in DMF. However, the use of these additives suppressed the transformation immediately (Entries 1-5, 8-9 & 11). No significant changes were observed with the utilization of $MgBr_2$ or NaI. To our surprise, the use of $MgCl_2$ completely shut down the formation of the product.

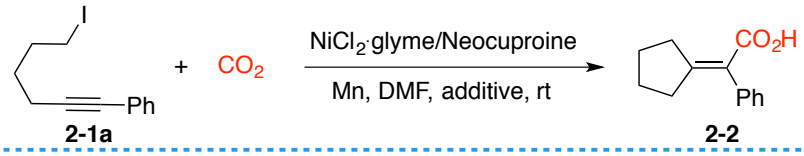

2-1a 2-2

Entry	Catalyst	Additive	Conversion (%)[b]	Yield (%)[c]
1	$NiCl_2$·glyme	AgF	100	0
2	$NiCl_2$·glyme	Et_4NBF_4	100	0
3	$NiCl_2$·glyme	Et_4NCl	100	0
4	$NiCl_2$·glyme	Et_4NBr	100	6
5	$NiCl_2$·glyme	CsF	100	0
6	$NiCl_2$·glyme	$MgBr_2$	100	28
7	$NiCl_2$·glyme	$MgCl_2$	100	0
8	$NiCl_2$·glyme	LiBr	100	0
9	$NiCl_2$·glyme	LiCl	100	0
10	$NiCl_2$·glyme	NaI	100	26
11	$NiCl_2$·glyme	Cs_2CO_3	100	0

[a] Reaction conditions: **2-1a** (0.3 mmol), Ni-cat. (10 mol%), neocuproine (20 mol%), Mn (2.2 equiv), additive (2.0 equiv), DMF (2 mL), rt, overnight. [b] HPLC conversions, determined by using naphthalene as internal standard. [c] HPLC yields, determined by using naphthalene as internal standard.

Table 2.4. Additive screening.[a]

Next, we screened N-containing ligands with the expectation of further improving the yield of our Ni-catalyzed carboxylation reaction. As summarized in Figure 2.6, monodentate ligand **L1** did not promote the reaction, as 0% conversion was detected. Bidentate ligands such as pyridine (**L2**), its derivative **L3**, **L7**, *i*-Pr-Box (**L9**) were tested as well. Although some level of conversion was observed in those cases, they did not afford the target product. As we expected, phenanthroline ligands bearing methyls at the α-position, like bathocuproine (**L8**), improved slightly the yield to 39% (*versus* **L7**). To our surprise, similar ligands such as **L5** and **L6** (without methyl groups at the ortho position) were not useful for the reaction, as either no product or only a trace amount was observed. The results above imply that methyl substituents on the phenanthroline backbone are critical for this transformation to occur.

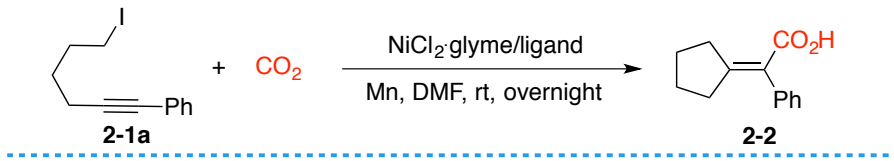

	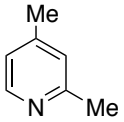 **L1**	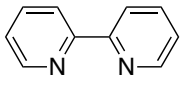 **L2**	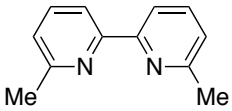 **L3**
Conversion (%)[b]	0	10	15
Yield (%)[c]	0	0	0
	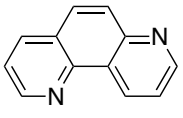 **L4**	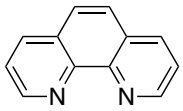 **L5**	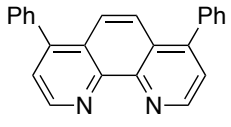 **L6**
Conversion (%)[b]	0	20	35
Yield (%)[c]	0	6	0
	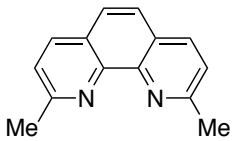 **L7**	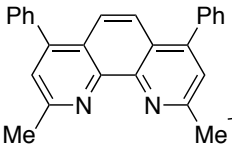 **L8**	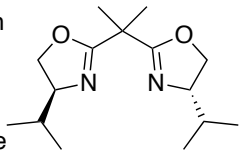 **L9**
Conversion (%)[b]	100	100	8
Yield (%)[c]	33	39	0

[a] Reaction conditions: 2-**1a** (0.3 mmol), Ni-cat. (10 mol%), ligand (20 mol%), Mn (2.2 equiv), DMF (2 mL), rt, overnight. [b] HPLC conversions, determined by using naphthalene as internal standard. [c] HPLC yields, determined by using naphthalene as internal standard.

Table 2.5. N-containing ligand screening.[a]

We also wondered whether the choice of precatalyst would have an influence on the reactivity of our process. Therefore, we turned our attention to the precatalyst effect. As depicted in Table 2.6, changing the counterion on the nickel source from chloride to bromide increased the yield to 63% (Figure 2.7 Entry 1 *vs* 2). Further modification of the Ni-catalyst to $NiBr_2$·diglyme gave us the highest yield, 72% (Entry 3). However, decreasing the catalyst loading to 5 mol% rendered less conversion of alkyl iodide **2-1a** to the final product, and only 57% of the cyclized acid was delivered (Entry 3). Surprisingly, the yield dropped dramatically to 24% when the reaction was conducted with 10 mol % of $Ni(COD)_2$ (Entry 5). Those results clearly indicated that the counterion of the Ni-catalyst plays an important role in the carboxylation reaction.

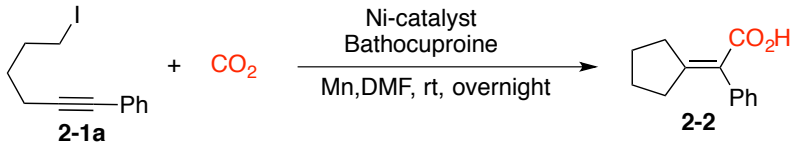

Entry	Catalyst	Conversion (%)[b]	Yield (%)[c]
1	$NiCl_2$·glyme	100	39
2	$NiBr_2$·glyme	100	63
3	$NiBr_2$·diglyme	100	72
4	$NiBr_2$·diglyme	100	57[d]
5	$Ni(COD)_2$	100	24

[a] Reaction conditions: **2-1a** (0.3 mmol), Ni-cat. (10 mol%), neocuproine (20 mol%), Mn (2.2 equiv), DMF (2 mL), rt, overnight. [b] HPLC conversions, determined by using naphthalene as internal standard. [c] HPLC yields, determined by using naphthalene as internal standard. [d] $NiBr_2$·diglyme (5 mol%).

Table 2.6. Nickel precatalyst screening.[a]

Encouraged by those findings, we next decided to test the impact of the type of halogen in our starting material. We were delighted to find out that when the reaction was performed with the corresponding alkyl bromide in the presence of 10 mol% of $NiBr_2$·diglyme, bathocuproine (**L8**) (20 mol%), Mn (2.2 equiv) under an atmospheric pressure of CO_2. We obtained the desired product in a higher yield (92%, 85% isolated yield), as shown Table 2.7, Entry 1. As anticipated, the lower proclivity of bromides (as compared to iodide) to undergo the carboxylation to minimize the formation of undesired byproducts and selectively delivers the corresponding acids. In addition to Mn, other reducing agents such as Al, In, Mg and Cu were also examined. While 20% of desired adduct was obtained when Al was employed instead of Mn, the rest of the metals did not generate any acid. changing the solvent to DMA or acetonitrile shut down the process. In line with our expectations, control experiments disclosed that all of the reaction parameters ($NiBr_2$·diglyme, **L8**, Mn, and DMF) were critical for success.

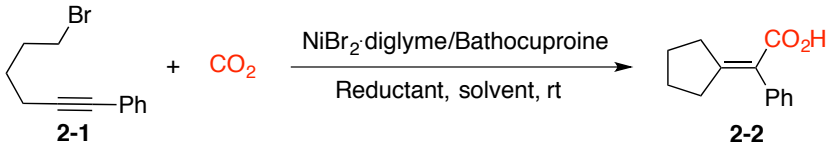

Entry	Reductant	Solvent	Conversion (%)[b]	Yield (%)[c]
1	Mn	DMF	100	92 (85[d])
2	Al	DMF	100	20
3	In	DMF	100	0
4	Mg	DMF	100	0
5	Cu	DMF	100	0
6	Mn	DMA	100	0
7	Mn	MeCN	100	3
8	Mn	DMF	100	0[e]

[a] Reaction conditions: **2-1** (0.3 mmol), Ni-cat. (10 mol%), neocuproine (20 mol%), Mn (2.2 equiv), DMF (2 mL), rt, overnight. [b] HPLC conversions, determined by using naphthalene as internal standard. [c] HPLC yields, determined by using naphthalene as internal standard. [d] Isolated yield. [e] Without catalyst and ligand.

Table 2.7. Reductant and solvent screening for **2-1**.[a]

In conclusion, the optimized conditions were found to be $NiBr_2$·diglyme (10 mol%) as precatalyst, bathocuproine as ligand (20 mol%), Mn (2.2 equiv) as reducing reagent in DMF under a CO_2 atmosphere (1 atm) at room temperature with stirring overnight.

2.4 Ni-catalyzed Divergent Cyclization/Carboxylation

2.4.1 Synthesis of Primary Alkyl Bromides

Having established the optimized reaction conditions, we then set out to survey the representative scope of this protocol by synthesizing a wide number of alkyl bromides. Various **2-1** analogues possessing electron-donating or electron- withdrawing groups on the phenyl ring were prepared in two steps. The first step was a Sonogashira coupling reaction, where the corresponding aryl iodides were treated with terminal alkynes in the presence of small amounts of Pd- and Cu-catalysts. The following Appel reaction replaced the hydroxyl group with a bromide in excellent yields (Table 2.8).

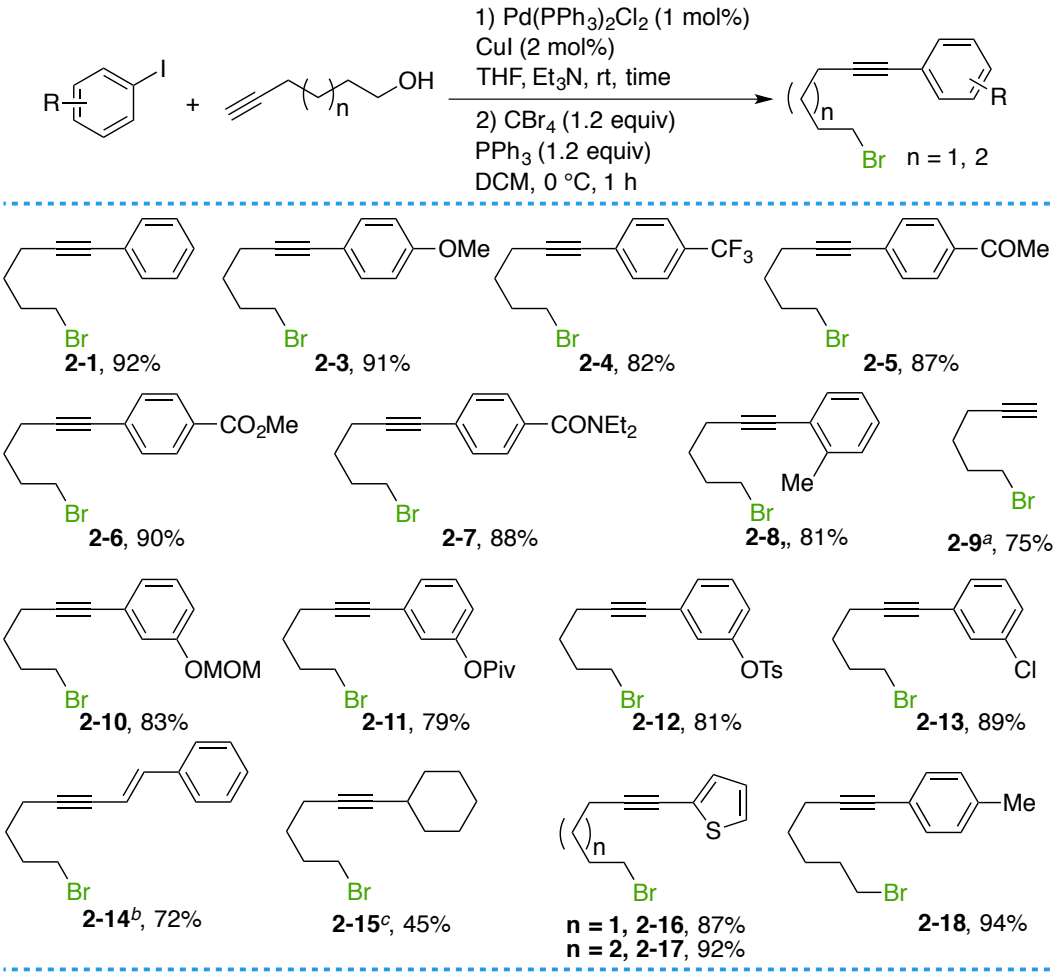

[a] **2-9** was synthesized from commerical availabe 5-hexyne-1-ol. [b] Starting from *trans*-β-bromostyrene. [c] **2-14** was prepared from cyclohexylacetylene and 1,4-dibromobutane. [d] All the given yields are overall yields.

Table 2.8. General route for preparing various alkyl bromides.[d]

Substrates **2-19** and **2-20** were synthesized in 4 steps as presented in Scheme 2.5. Esterification employing MeI as the alkylating reagent with K_2CO_3 as base in DMF, delivered the methyl ester in 95% isolated yield. The following Sonogashira coupling gave the alkyne-coupled product in 93% yield, which was reduced by $LiAlH_4$ (LAH) to produce the corresponding alcohols. The final Appel reaction generated the desired alkyl bromides in excellent yields.

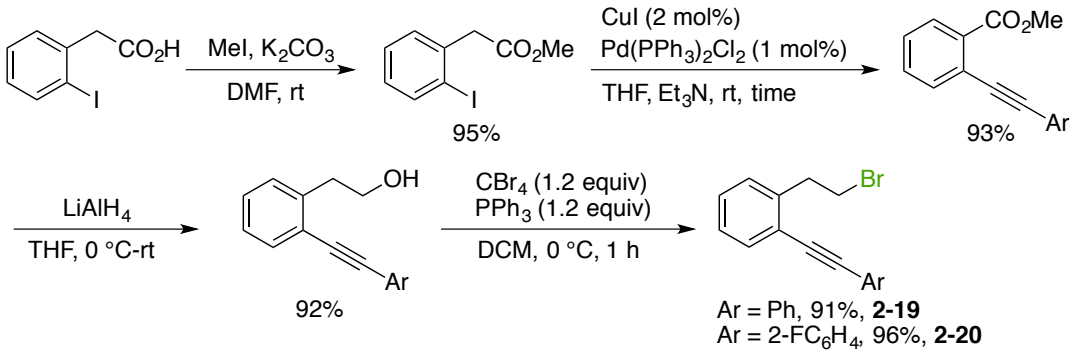

Scheme 2.6. General route for preparing alkyl bromides **2-19** and **2-20**.

2.4.2 Scope of Primary Alkyl Bromides

With the starting materials in hand, we next decided to investigate the scope of our Ni-catalyzed cyclization/carboxylation event. As depicted in Table 2.9, a wide range of products having electron-enrich, electron-neutral as well as electron-deficient substituents were delivered in moderate to high yields. Particularly noteworthy was the functional group tolerance of our protocol, as ketone (**2-23**), ethers (**2-21**, **2-28**), ester (**2-24**), amide (**2-25**) and heterocycle groups (**2-27**) were all perfectly accommodated. Undoubtedly, the exquisite chemoselectivity profile of our transformation represents a bonus compared with classical carbometalation techniques[86] based on the utilization of organolithium or Grignard reagents, among others. As shown for **2-26**, the inclusion of ortho substituents on the aromatic motif did not hamper the reaction. Interestingly, we found that the cyclization/carboxylation event could even be conducted in the presence of electrophilic partners that are suited for Ni-catalyzed reductive carboxylation reactions, such as aryl chloride (**2-31**), tosylate (**2-30**), or pivalate (**2-29**); notably, no traces of the corresponding benzoic acids derived from C−Cl or C−O bond cleavage were detected in the crude reaction mixtures, thus providing ample opportunities for further functionalization.

[86] Selected examples see: (a) Kambe, N.; Moriwaki, Y.; Fujii, Y.; Iwasaki, T.; Terao, J. *Org. Lett.* **2011**, *13*, 4656. (b) Rao, S. A.; Knochel, P. *J. Am. Chem. Soc.* **1991**, *113*, 5735. (c) Bailey, W. F.; Ovaska, T. V.; Leipert, T. K. *Tetrahedron Lett.* **1989**, *30*, 3901. (d) Bailey, W. F.; Ovaska, T. V. *J. Am. Chem. Soc.* **1983**, *115*, 3080. (e) Richey, H. G., J.; Rothman, A. M. *Tetrahedron Lett.* **1968**, *9*, 1457.

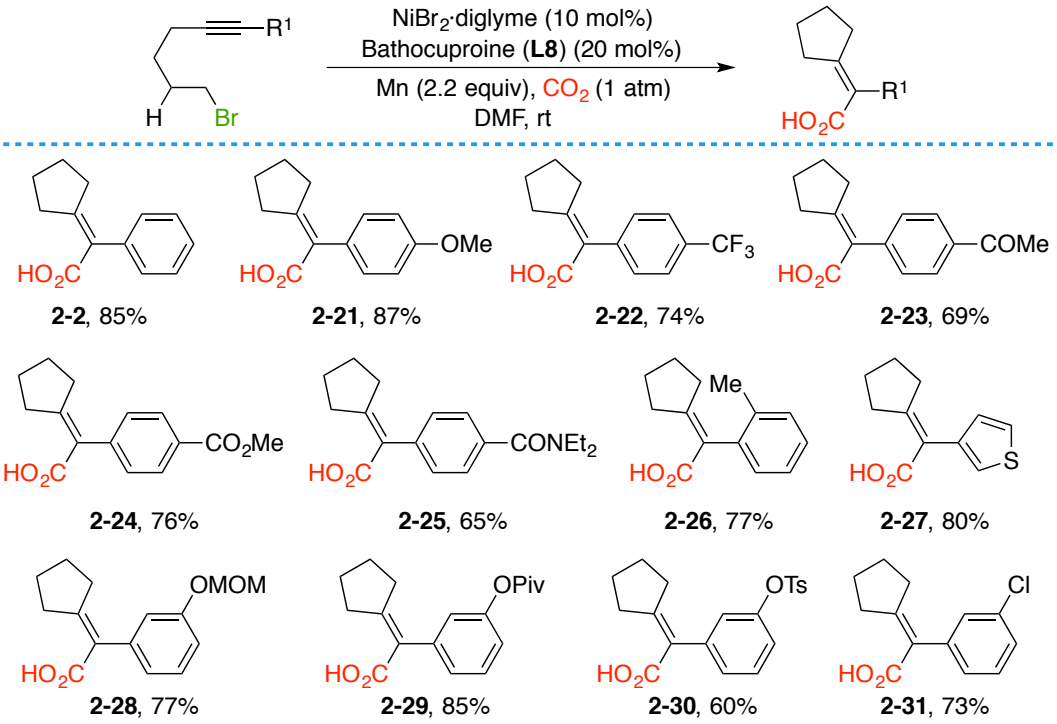

[a] Reaction conditions: Substrate (0.30 mmol), Ni-precatalyst (10 mol%), **L8** (20 mol%), Mn (2.2 equiv.), DMF (2 ml), CO_2 (1 atm) at rt overnight. [b] Isolated yield.

Table 2.9. Representative scope of primary alkyl bromides.[a,b]

While one might argue that such a protocol would essentially be restricted to five-membered rings or alkyne residues possessing aromatic motifs, the preparation of **2-33**, **2-34**, **2-35** and **2-36** clearly indicates otherwise. Strikingly, free alkynes posed no problems (**2-32**); such a finding is certainly remarkable in view of the proclivity of terminal alkynes to react via competitive trimerization pathways.[87] As anticipated from a classical *syn*-carbometalation reaction via an *in situ* generated alkyl nickel species,[98,88] we obtained **2-37** and **2-38** in excellent yields. The structure of **2-37** was unequivocally confirmed by X-ray crystallographic analysis (Table 2.10).

[87] (a) Galan, B. R.; Rovis, T. *Angew. Chem. Int. Ed.* **2009**, *48*, 2830. (b) Gandon, V.; Aubert, C.; Malacria, M. *Chem. Commun.* **2006**, 2209. (c) Chopade, P. R.; Louie, J. *Adv. Synth. Catal.* **2006,** *348*, 2307.

[88] (a) Hartwig, J. F. *Organotransition Metal Chemistry: From Bonding to Catalysis*; University Science Books: Mill Valley, CA, 2010; p 379. (b) Marek, I.; Minko, Y. In *Metal-Catalyzed Cross-Coupling Reactions and More*; de Meijere, A., Bräse, S., Oestreich, M., Eds.; Wiley-VCH: Weinheim, Germany, 2014; Chapter 10, pp 763−874.

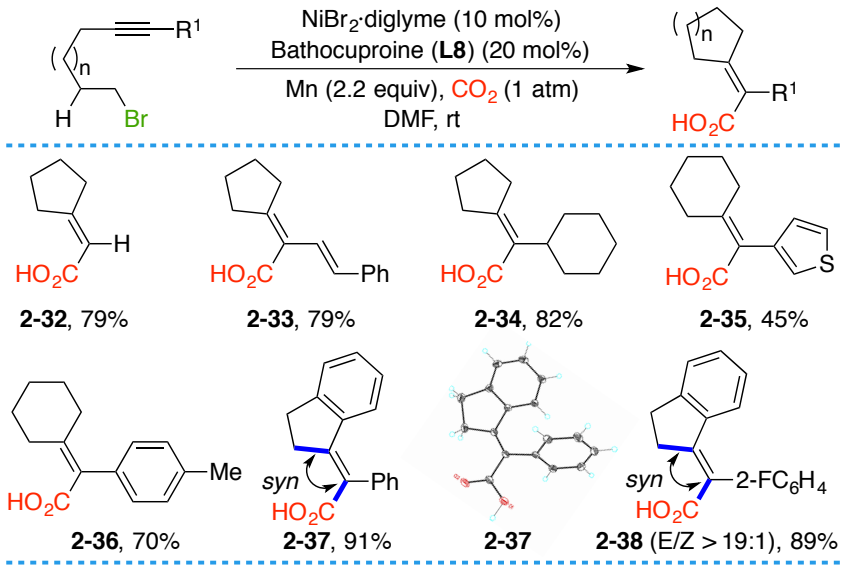

Table 2.10. Scope of primary alkyl bromides with different skeletons.[a,b]

2.4.3 Synthesis of Secondary Alkyl Bromides

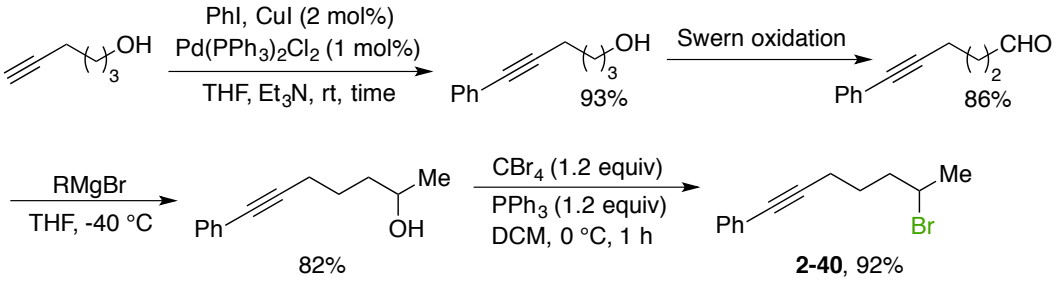

Scheme 2.7. General route for preparing secondary alkyl bromides.

Next, we focused our attention on a more challenging scenario dealing with unactivated secondary alkyl bromides.[89] Firstly, we decided to prepare a variety of secondary alkyl bromides containing different substituents. The four step synthetic route depicted in Scheme 2.7 was used. For example, starting from a Sonogashira coupling, 6-phenylhex-5-yn-1-ol was isolated in 93% yield. Swern oxidation to obtain an aldehyde was subsequently performed; then a Grignard reaction was used to generated the secondary alcohol. Finally, the introduction of bromide was performed by an Appel reaction with the combination of CBr_4 and PPh_3 in DCM at 0 °C. The prepared starting materials are presented in Figure 2.1.

[89] (a) Kambe, N.; Iwasaki, T.; Terao, J. *Chem. Soc. Rev.* **2011**, *40*, 4937. (b) Jana, R.; Pathak, T. P.; Sigman, M. S. *Chem. Rev.* **2011**, *111*, 1417. (c) Rudolph, A.; Lautens, M. *Angew. Chem. Int. Ed.* **2009**, *48*, 2656.

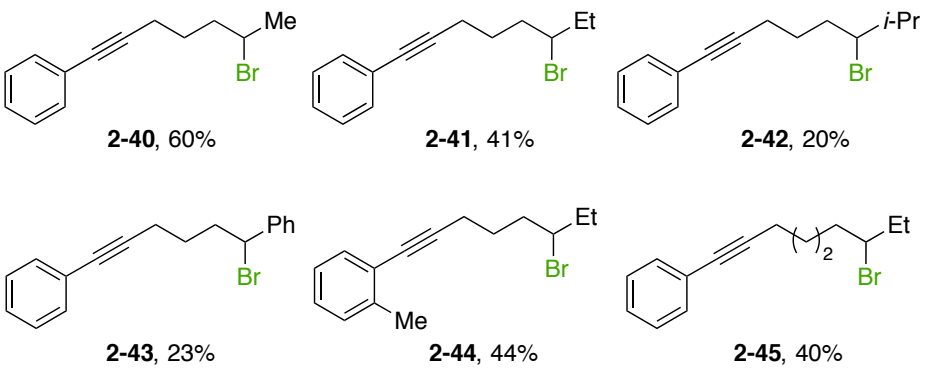

2-40, 60% **2-41**, 41% **2-42**, 20%

2-43, 23% **2-44**, 44% **2-45**, 40%

Figure 2.1. Prepared secondary alkyl bromides.

2.4.4 Scope of Secondary Alkyl Bromides

We were interested in the possibility of CO_2 incorporation into the prepared molecules. We anticipated that the ligand might have a profound influence on the reactivity as depicted in ligand screening for the primary alkyl bromides. Thus we decided to screen N-containing ligands for each substrate (From Figures 2-13 to 18).

Strikingly, the reaction of **2-40** using **L8** under optimized conditions resulted in an unexpected selectivity switch (**2-45**:**2-45'** = 3.3:1). In a formal sense, **2-45** can be derived from a rather elusive *anti*-carbometalation event.[90] Although **2-45** was fully characterized by NMR spectroscopic analysis, X-ray crystallography unambiguously identified the abnormal *anti*-selective motion. It is worth noting that the preparation of **2-45** represents the first reductive carboxylation that can be conducted with unactivated secondary alkyl electrophiles. Interestingly, the *anti*-selectivity could be enhanced by the choice of ligand. Specifically, we found that **L7** mostly afforded **2-45**, with only small amounts of **2-45'** being present in the crude mixtures (**2-45**:**2-45'** = 12.5:1). Other ligands such as **L9**-**L10** and **L12** were not suitable for our cyclization/carboxylation event (Table 2.11).

[90] Selected anti-carbometalation techniques: (a) Fressigné, C.; Girard, A.-L.; Durandetti, M.; Maddaluno, J. *Angew. Chem. Int. Ed.* **2008**, *47*, 891. (b) Simaan, S.; Marek, I. *Org. Lett.* **2007**, *9*, 2569. (c) Ma, S.; Negishi, E.-I. *J. Org. Chem*. **1997**, *62*, 784. (d) Lu, Z.; Ma, S. *J. Org. Chem*. **2006**, *71*, 2655.

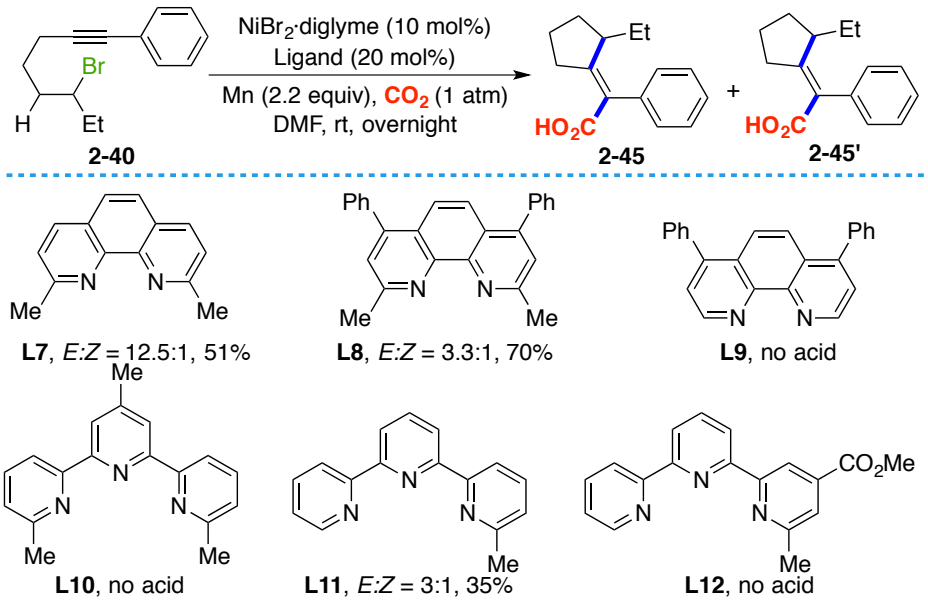

Table 2.11. Ligand screening for **2-40**.

As revealed in Figure 2.14，neocuproine (**L7**) is the best choice of ligand when **2-39** was used as substrate, giving us a 4:1 mixture of *E* and *Z* isomers in 86% isolated yield under the optimized conditions for primary alkyl bromides. The utilization of **L8** afforded inferior results. As expected, bathophenanthroline **L9** with no methyl substituents at the ortho positions did not afford acid. Beyond our expectation, terpyridine ligand **L11** yielded the desired product with the same ratio (*E*:*Z* = 4:1) as **L7**, although the yield dropped to 39%. The rest of the ligands (**L10** and **L12**) did not yield product.

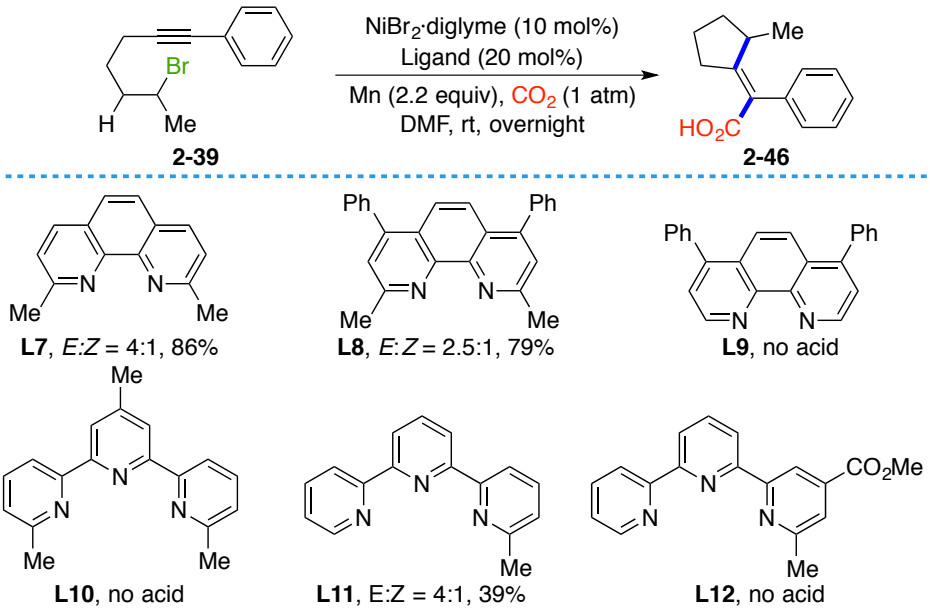

Table 2.12. Ligand screening for **2-39**.

Wondering whether we could achieve complete stereocontral of the reaction, we performed a ligand screening on a bulkier secondary halide (bearing a isopropyl group). As expected, with the use of **L7** we only observed one isomer **2-47** in 46% yield. **L8** and L**11** gave us product in 80% and 48% yields, respectively. However, the selectivity was not as good as with **L7**.

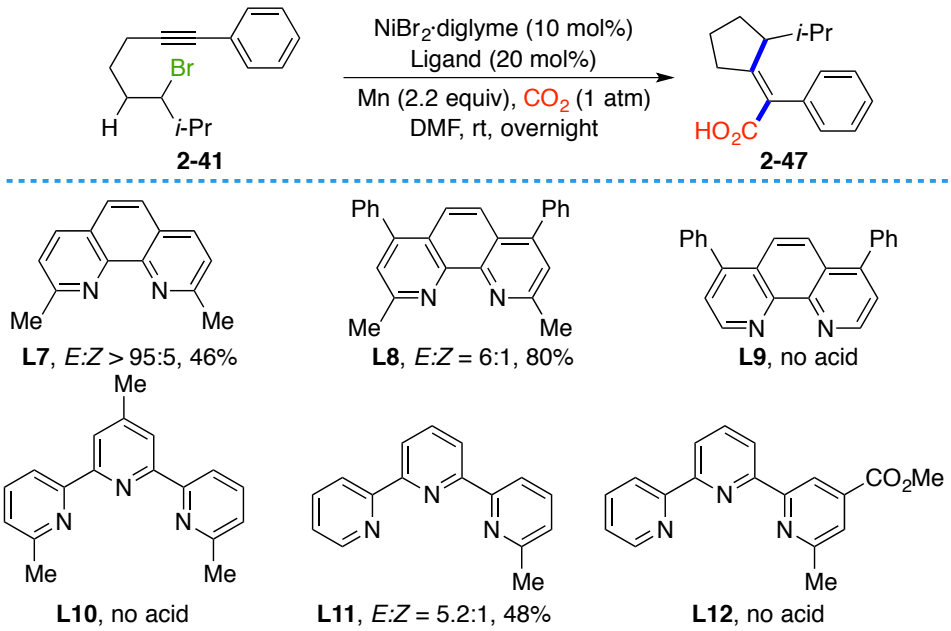

Table 2.13. Ligand screening for **2-41**.

A ligand assessment on alkyl bromide **2-42** was next performed. Again by using **L7** acid **2-48** was obtained in 64% yield with excellent stereocontral. While **2-48** was generated in similar yield with **L8**, the selectivity dropped dramatically to E:Z = 2.5:1. We did not obtained any aimed products by using ligands **L9**-**L12**.

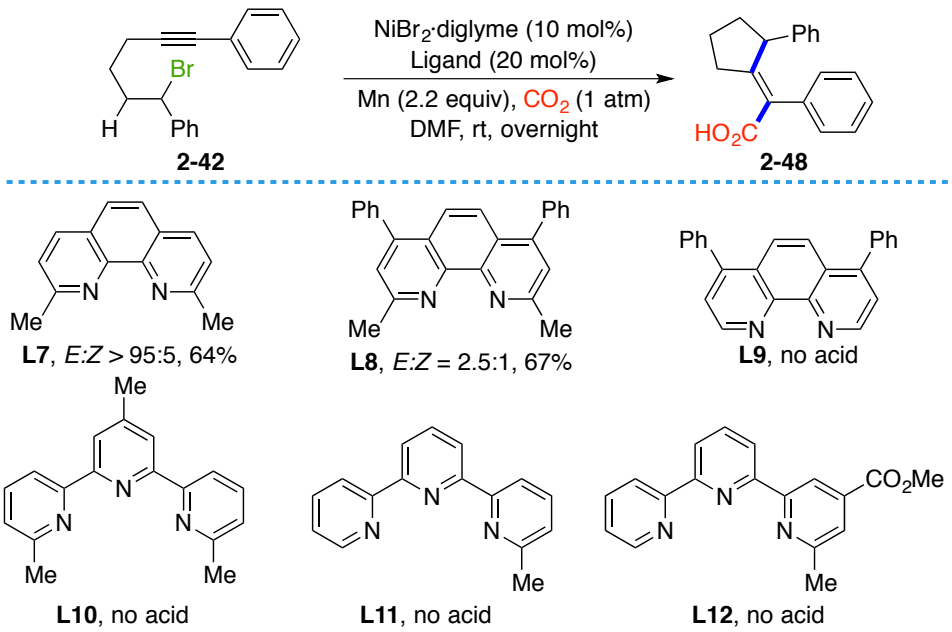

Table 2.14. Ligand screening for **2-42**.

Another successful example in our elusive anti-carbometalation system is **2-43**. Its reaction was conducted in the presence of **L8** and delivered the corresponding cyclized acid **2-49** in 53% isolated yield with excellent stereoselectivity. Beyond our understanding, **L7** did not yield the desired product, and neither did the rest of the phenanthroline and terpyridine ligands.

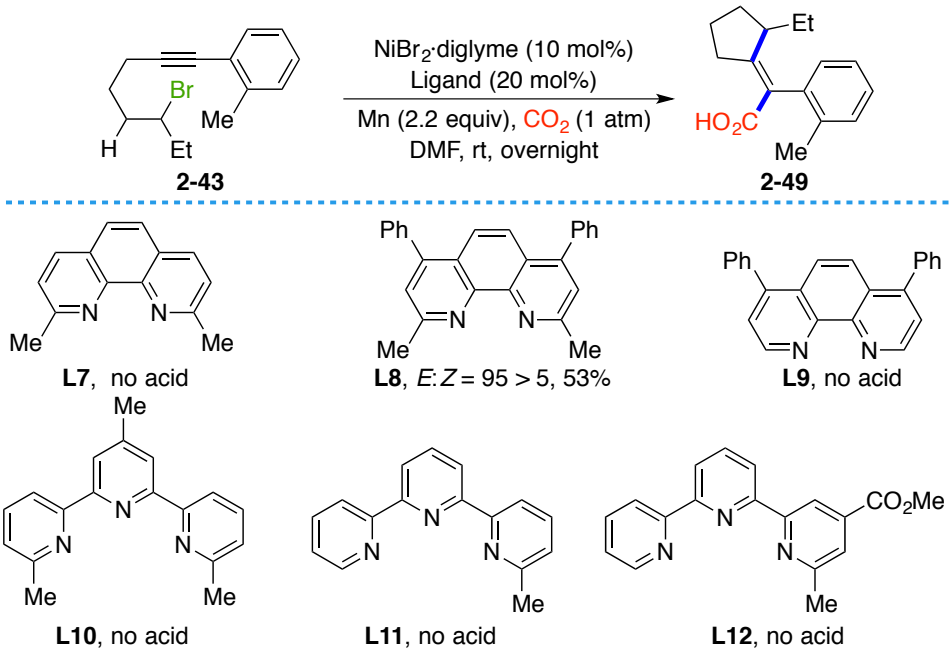

Table 2.15. Ligand screening for **2-43**.

As presented in Table 2.16, the reaction is not limited to the formation of 5-

membered rings, as we could obtain **2-50** in moderate yield (44%) by using **L9** as ligand. Interestingly, the *E*-isomer was selectively provided, and almost no *Z*-isomer was detected. Other ligands did not convert the starting material to the target acids, implying the importance of the ligand in reaction outcome.

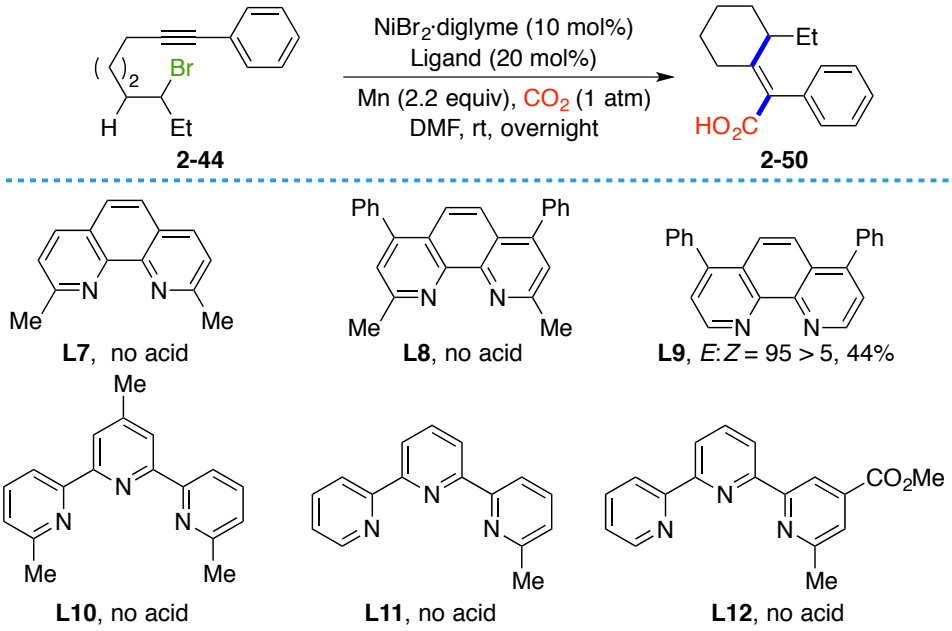

Table 2.16. Ligand screening for **2-44**.

In conclusion, a host of substituted secondary alkyl bromides could also be coupled in high yields and high *anti*-selectivities. Notably, six-membered carbocyclic skeletons could also be accommodated with excellent selectivity, albeit in lower yields (**2-50**). A simple comparison of **2-45** *vs* **2-46** and **2-47** clearly show that the *anti*-selectivity is favored with bulkier substituents on the side chain. A similar effect was found with *ortho*-substituted aromatic motifs (**2-48** *vs* **2-45**). Less counterintuitive was the observation that the ligand backbone exerted a profound influence on the selectivity pattern, with **L7** or **L9** providing the best *anti/syn* selectivities, thus showing the subtleties of our system.[19] Taken together, the data shown in Figures illustrate the prospective impact of our Ni-catalyzed reductive cyclization/carboxylation event from simple building blocks by promoting a *distal* CO_2 *fixation* while controlling the *syn/anti*-selectivity pattern of the cyclization event. The structure of **2-45** was confirmed by X-ray diffraction analysis (Table 2.17).

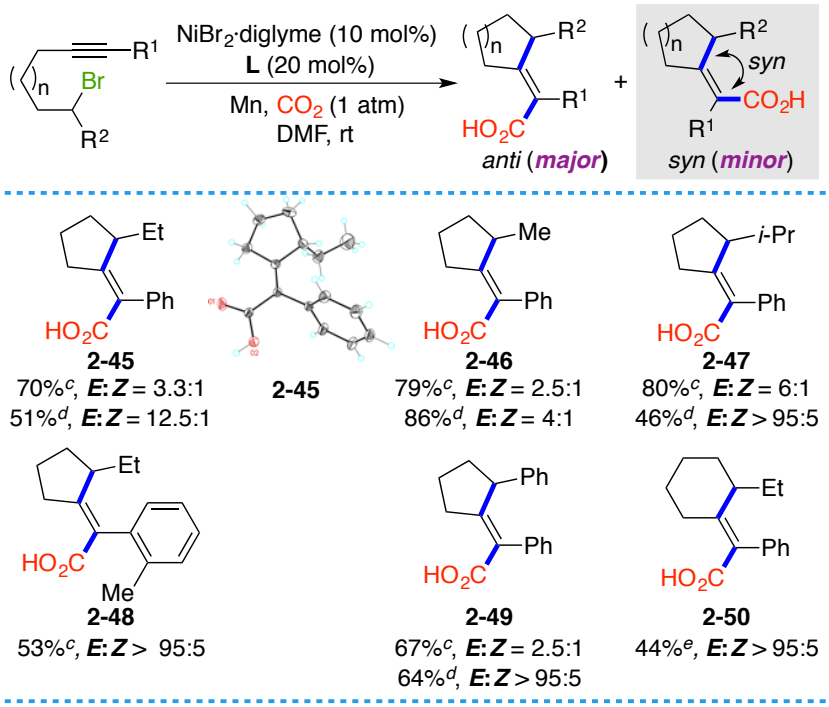

[a] Substrate (0.30 mmol), Ni-catalyst (10 mol%), **L** (20 mol%), Mn (2.2 equiv), DMF (2 mL), CO_2 (1 atm) at rt, overnight. [b] Isolated yields, average of at least two independent runs. [c] **L8** was used as ligand. [d] **L7** was used as ligand. [e] **L9** was used as ligand.

Table 2.17. Representative scope of secondary alkyl bromides.

2.4.5 Limitations of the Cyclization/Carboxylation Reactions

Besides the examples presented above, we found several limitations of our protocol for Ni-catalyzed divergent cyclization/carboxylation of unactivated primary and secondary alkyl halides with CO_2. Summarized in Figure 2.18 are the substrates that did not undergo carboxylation. The reaction of **2-51** with ligand **L7** or **L8** gave us a complex mixture, which we could not identify by NMR or GC-MS. We were attracted to prepare 2-cyclohexyli-deneacetic acid by conducting the reaction with **2-52** as starting material. Unfortunately, unlike **2-32**, we could not even obtain traces amount of the desired product with any of the ligands listed above. Surprisingly, the introduction of electron-donating (**2-53**) or electron-withdrawing (**2-54**) groups to the aromatic ring did not resulting the formation of the expected acid. The rest of the mass balance was accounted for by unreacted alkyl bromides or degradation to unidentifiable byproducts. No product was also observed when elongating the alkyl chain (**2-55**) or by employing a terminal alkyne (**2-56**). In the case of **2-57**, GC-MS analysis detected unreacted starting material and protonated product. We believed that **2-59** would

probably allow us to incorporate CO_2 into a tertiary alkyl bromide as it might be able to coordinate to a Ni(II) center, thus stabilizing the reaction intermediate, and accelerating the following triple bond insertion and CO_2 fixation steps. Although we could obtain full conversion, mixtures of acids were isolated in low yields regardless the ligand employed in this transformation.

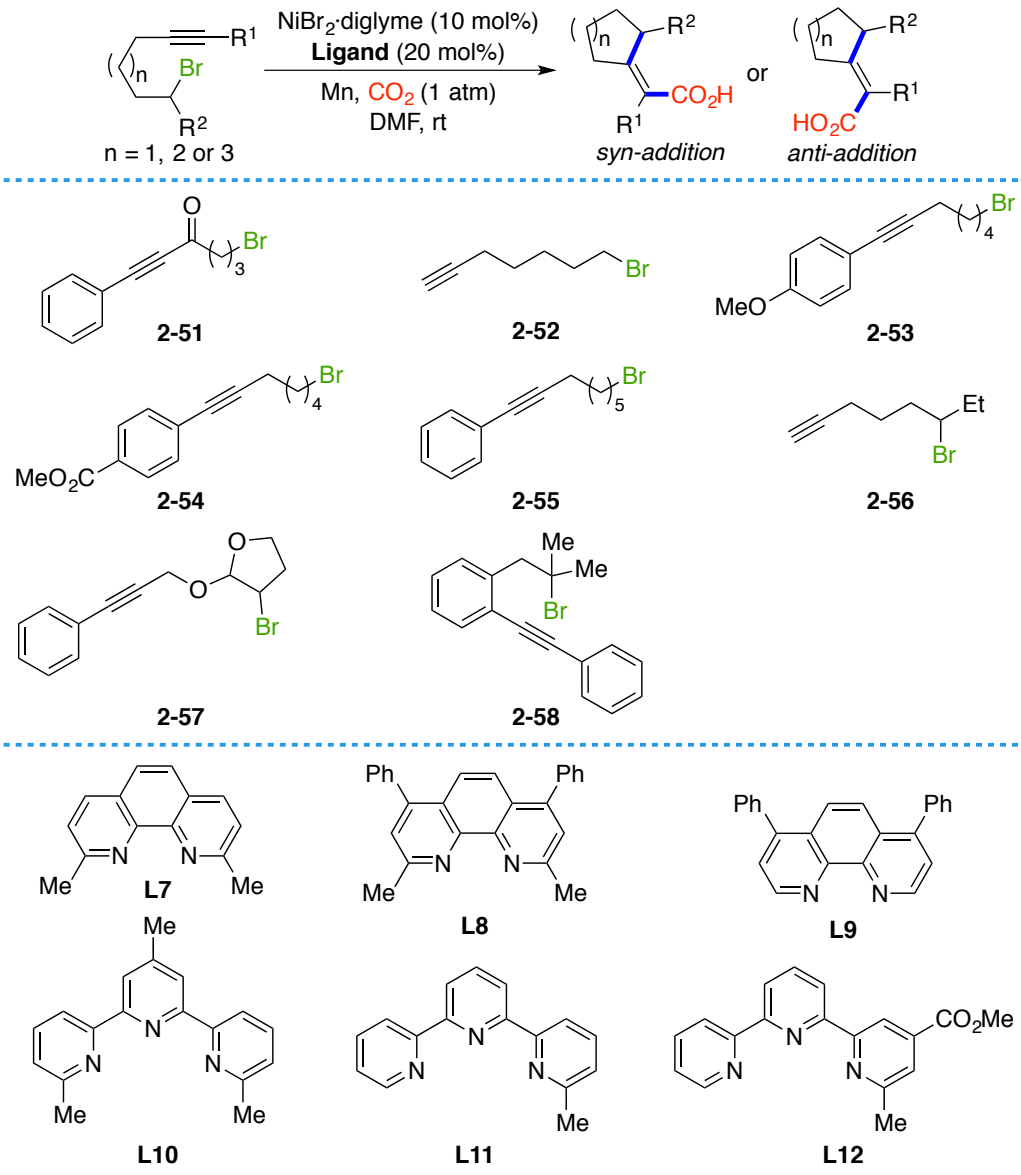

Scheme 2.8. Limitations of our cyclization/carboxylation protocol.

2.4.6 Mechanistic Studies

Once the scope of the reaction was studied, we next turned our attention to carry out several mechanistic studies of our Ni-catalyzed divergent cyclization/ carboxylation reaction. In this regard, studying the effect of radical scavengers, carrying out stoichiometric reactions, and studying the stereochemistry of the reaction would allow

us to gain precious information about the mechanism.

As described above, using either primary or secondary alkyl bromides with appropriate choice of ligand could enhance the selectivity to syn-addition or anti-addition acids. Thus indicating that these selectivity-switchable carboxylation protocols might undergo different mechanistic pathways.We firstly carried out a series of mechanistic studies using primary bromide substrates. We initiated this investigation by using **2-59** as substrate, and conducted the reaction with $NiBr_2$·diglyme (10 mol%) and **L8** (20 mol%). We envisioned that if the reaction goes via a radical pathway, we would allow obtain **2-61** or **2-62** because of its rapid cyclization rate. Nevertheless, we obtained small amounts of dimerization product **2-60**.

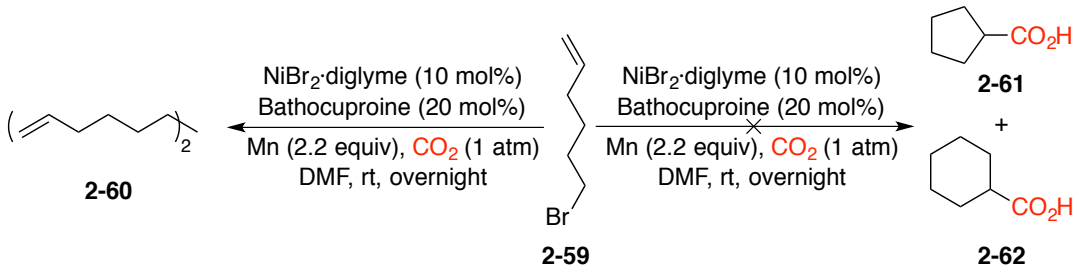

Scheme 2.9. Reaction of **2-59** under optimized condition.

In line with our hypothesis, radical scavengers such as TEMPO, BHT and 1,1-diphenylethane did not suppress the reaction under the above-mentioned reaction conditions, and in each case the corresponding acid was delivered in high yield. Although it is not a conclusive proof that the reaction is not radical, these results strongly suggests this so.

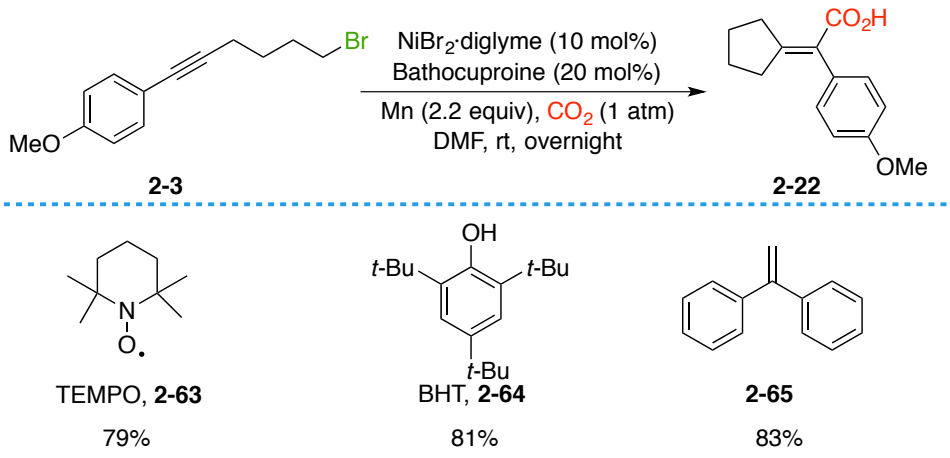

Scheme 2.10. The effect of radical scavengers for substrate **2-3**.

Inspired by these results, we were interested in studying the stereochemical course of this transformation so that we could gain more details about the mechanism. Following a six step synthetic procedure, we managed to synthesize deuterated primary alkyl bromide **2-73**. The initial step was the Pd- and Cu-catalyzed coupling reaction of **2-66** with **2-67**. The coupled product **2-68** then underwent desylilation by the combination of K_2CO_3 and MeOH to deliver phenyl acetylene **2-69**. Deuterated styrene **2-70** was obtained by simple hydroboration with 9-BBN and D-incorporation with AcOD. Treatment of **2-70** with $NaBD_4$ and H_2O_2 afforded desired primary alcohol **2-71**. Next, palladium-catalyzed alkyne installation of aryl bromide (**2-71**) led to the formation of intermediate **2-72**. Utilizing Appel conditions (CBr_4 and PPh_3 in DCM) completed the final step, generating the deuterated starting material **2-73**. We then conducted the carboxylation under our optimal reaction conditions. Careful ^1H NMR spectroscopic analysis revealed that the reaction exclusively afforded **7-74**, an observation that is consistent with a scenario consisting of an initial oxidative addition with inversion of configuration.[91] Such a labeling pattern differs from previous work where without pendant alkynes in the side chain. [92] This observation is consistent with the ability of alkynes to act as non-innocent auxiliary ligands.[93]

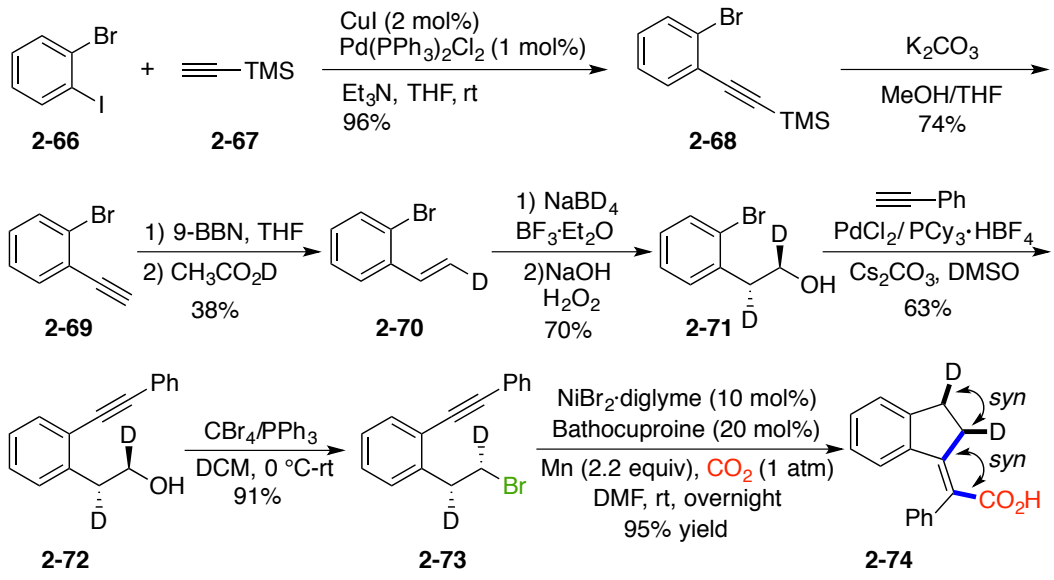

Scheme 2.11. The study of stereochemical course.

[91] For related isotopic-labeling studies with Pd catalysts see: (a) Netherton, M. R.; Fu, G. C. *Angew. Chem. Int. Ed.* **2002**, *41*, 3910. (b) Stokes, B. J.; Opra, S. M.; Sigman, M. S. *J. Am. Chem. Soc.* **2012**, *134*, 11408.
[92] Tsuji, Y.; Fujihara, T. *Chem. Commun.* **2012**, *48*, 9956.
[93] Cong, H.; Fu, G. C. *J. Am. Chem. Soc.* **2014**, *136*, 3788.

Next, we turned our attention to the reactivity of air-sensitive **2-75**, which is easily accessible simply by reacting $Ni(COD)_2$ with **L8** in THF.[94] Importantly, while no reaction took place upon exposure of **2-75** to **2-11** in the absence of Mn, the targeted cyclization/carboxylation product **2-29** was cleanly produced in the presence of the reducing agent. Although premature, we believe that these experiments tacitly suggest that the carboxylation event does not occur from an *in situ* generated Ni(II) species but rather from a putative Ni(I) reaction intermediate (Scheme 2.12).[95,96]

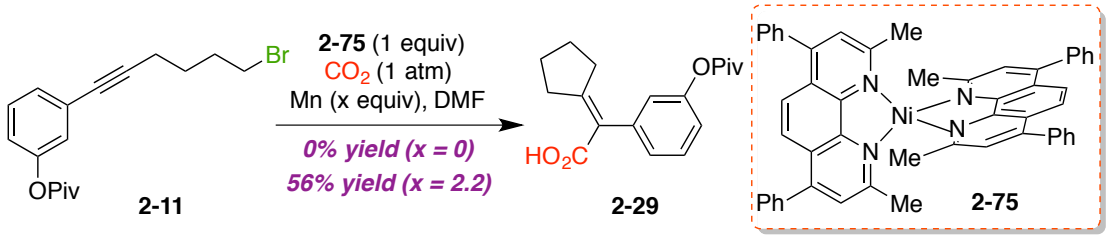

Scheme 2.12. Stoichiometric reactions of **2-11** with **2-75.**

Although a detailed mechanistic picture requires further investigations, we tentatively propose a catalytic cycle in analogy with previously developed Ni-catalyzed reductive carboxylation protocols. We believe the reaction begins with an initial Mn-assisted reduction of the Ni(II) precatalyst followed by oxidative addition into the corresponding $C(sp^3)$-Br bond. The triple bond insertion takes place to generate the *syn*-addition Ni(II)-complex **C**, and then the resulting Ni(II) intermediate **C** could be further reduced by Mn to yield a more nucleophilic Ni(I) species **D**, thus setting up the stage for a CO_2 insertion event. A final transmetallation with Mn would regenerate the active Ni(0)L species **A** and a manganese carboxylate. Isotope experiments are consistent with a scenario consisting of an initial oxidative addition with inversion of configuration.

---

[94] Powers, D. C.; Anderson, B. L.; Nocera, D. G. *J. Am. Chem. Soc.* **2013**, *135*, 18876.

[95] For the intermediacy of Ni species in odd oxidation states, see: (a) Laskowski, C. A.; Bungum, D. J.; Baldwin, S. M.; Del Ciello, S. A.; Iluc, V. M.; Hillhouse, G. L. *J. Am. Chem. Soc.* **2013**, *135*, 18272. (b) Breitenfeld, J.; Ruiz, J.; Wodrich, M. D.; Hu, X. *J. Am. Chem. Soc.* **2013**, *135*, 12004. (c) Biswas, S.; Weix, D. J. *J. Am. Chem. Soc.* **2013**, *135*, 16192. (d) Schley, N. D.; Fu, G. C. *J. Am. Chem. Soc.* **2014**, *136*, 16588. (e) Jones, G. D.; Martin, J. L.; McFarland, C.; Allen, O. R.; Hall, R. E.; Haley, A. D.; Brandon, R. J.; Konovalova, T.; Desrochers, P. J.; Pulay, P.; Vicic, D. A. *J. Am. Chem. Soc.* **2006**, *128*, 13175. (f) Ciszewski, J. T.; Mikhaylov, D. Y.; Holin, K. V.; Kadirov, M. K.; Budnikova, Y. H.; Sinyashin, O.; Vicic, D. A. *Inorg. Chem.* **2011**, *50*, 8630.

[96] Vinylnickel(I) species have been proposed to be generated from vinylnickel(II) by SET. For example, see ref 5c and: (a) Duñach, E.; Esteves, A. P.; Medeiros, M. J.; Olivero, S. *New J. Chem.* **2005**, *29*, 633. (b) Fujihara, T.; Horimoto, Y.; Mizoe, T.; Sayyed, F. B.; Tani, Y.; Terao, J.; Sakaki, S.; Tsuji, Y. *Org. Lett.* **2014**, *16*, 4960. (c) Nadal, M. L.; Bosch, J.; Vila, J. M.; Klein, G.; Ricart, S.; Moretó, J. M. *J. Am. Chem. Soc.* **2005**, *127,* 10476.

While either organometallic or radical pathways could explain these results, a mechanistic hypothesis based upon the involvement of organometallic process seems the more plausible avenue (Scheme 2.13).

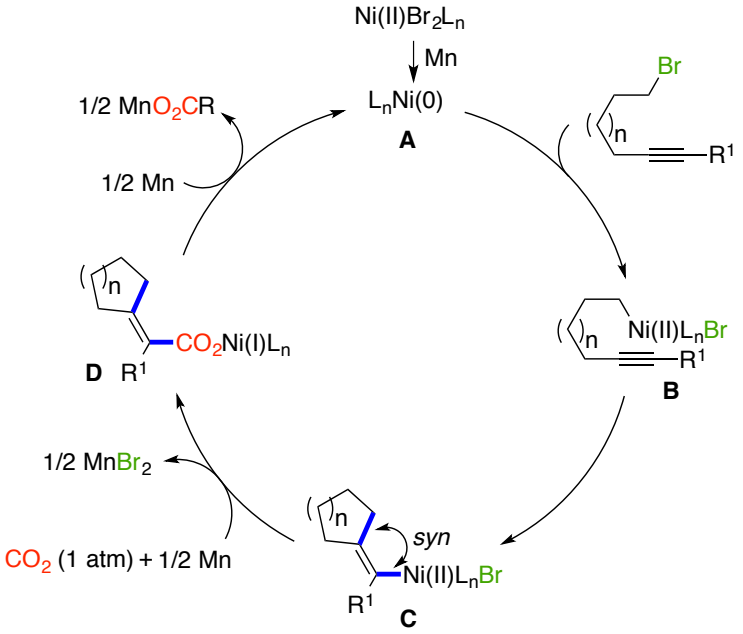

Scheme 2.13. A plausible mechanism for primary alkyl bromides.

We attempted to shed light on the mechanism of Ni-catalyzed cyclization/carboxylation of secondary alkyl bromides. Following the studies on primary alkyl bromides, we also performed the reactions with radical scavengers and the stoichiometric reaction with Ni(0)-complex **2-75**, to understand the rationale behind the *anti*-selectively carboxylation. As demonstrated in Figure 2.24, the reactions performed in the presence of TEMPO (**2-63**) and 1,1-diphenylethlene (**2-65**) did not give the desired acid.

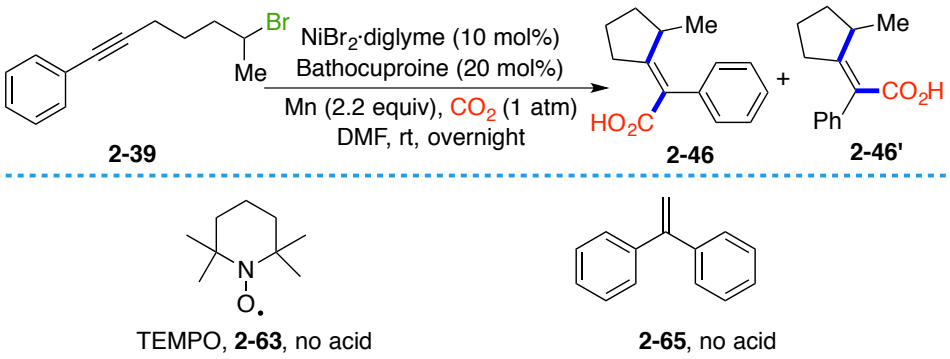

Scheme 2.14. The effect of radical scavengers for substrate **2-39**.

Remarkably, the treatment of **2-76** (*E*:*Z* = 2:1) with CO_2 under our optimized reaction

conditions gave us **2-77** as a single isomer in 22% isolated yield. This clearly demonstrated our hypothesis that the *anti*-selective carboxylation event probably happened via a vinylnickel species.

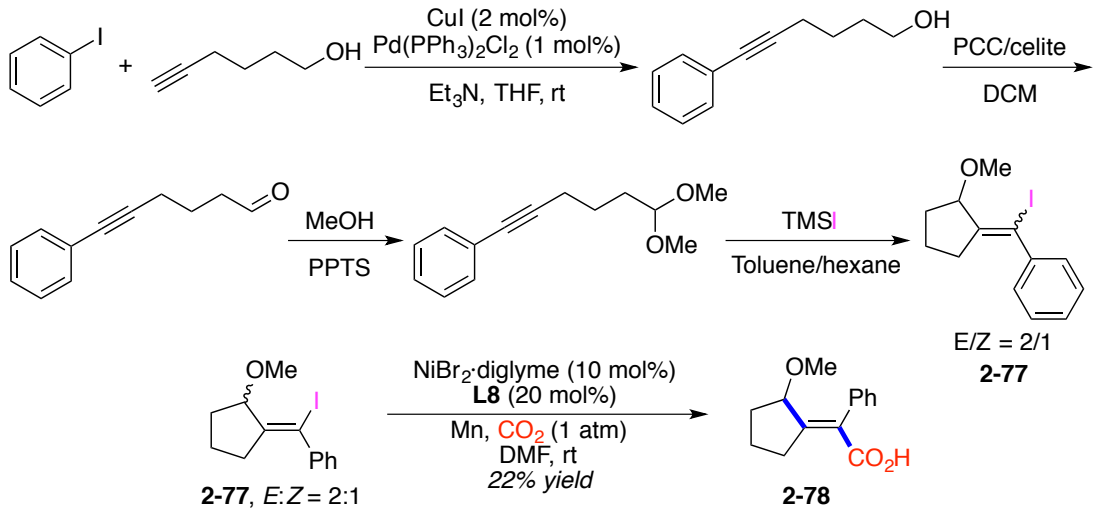

Scheme 2.15. Synthesis of **2-76** and its carboxylation reaction with CO_2.

As expected, while no reaction took place upon treatment of **2-39** with **2-75** without Mn, the desired cyclization/carboxylation products **2-47** and **2-47'** were generated in the presence of the reducing agent in 65% yield, indicating once again that a Ni(I) species is involved in the carboxylation event.

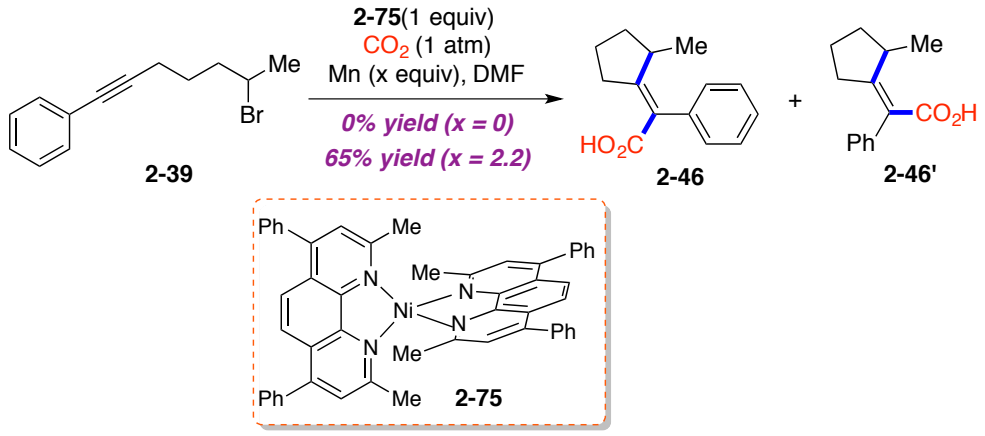

Scheme 2.16. Stoichiometric reactions of **2-39** with **2-75**.

While tentative, we would like to propose a catalytic cycle similar to that for previously developed Ni-catalyzed reductive carboxylations, but via a radical pathway instead. We believe the reaction originates from reduction of the Ni(II) precatalyst followed by formation a secondary alkyl radical **B** and a Ni(I)-complex. The following

radical cyclization with the alkyne moiety affords a vinyl radical species **E** which exists in equilibrium with **F** and **G**, and then radical species **F** rebinds quickly with the Ni(I)-complex because of less steric hindrance between **F** and Ni(I)LnBr, causing Ni(II) intermediate **C** that can be further reduced by Mn to deliver a more nucleophilic Ni(I) species **D**. This species allows the CO_2 insertion event to occur. Final reduction with Mn would regenerate the Ni(0)L species **A**, thereby closing the catalytic cycle.

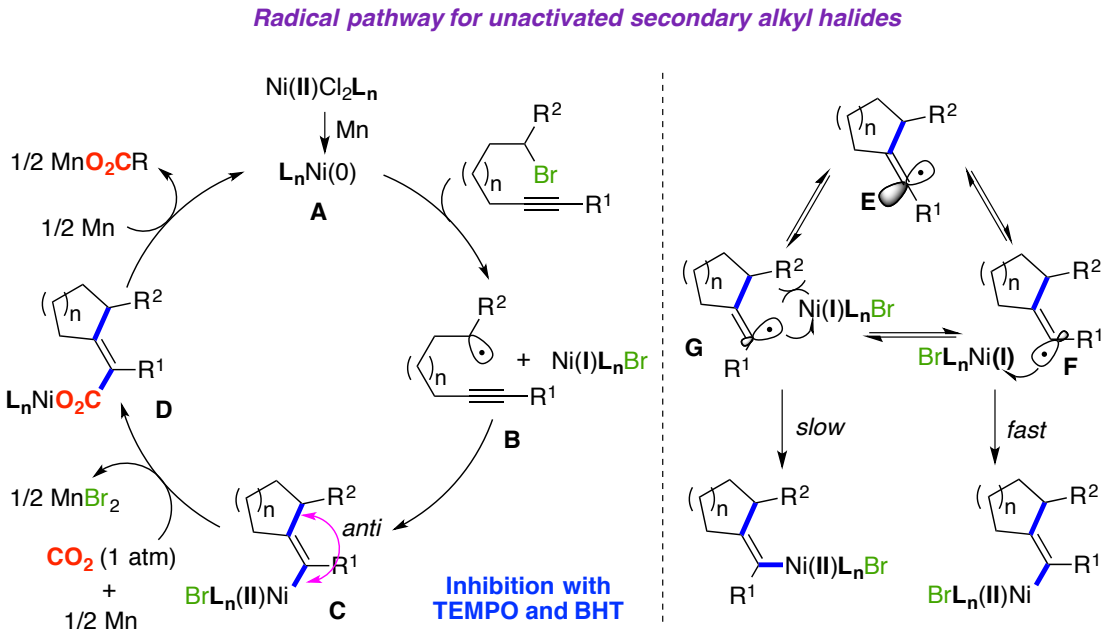

Scheme 2.17. A plausible mechanism for secondary alkyl bromides**.**

2.5 Conclusion

In conclusion, we have developed a mild, robust, and user-friendly Ni-catalyzed cascade reductive cyclization/carboxylation using CO_2 at atmospheric pressure in which the selectivity pattern is dictated by an appropriate substrate and/or ligand selection. The protocol represents a convenient way to access tri-substituted acrylic acid derivatives from simple starting materials and exhibits an excellent chemoselectivity profile and good functional group compatibility. Mechanistic studies showed that there might be different pathways operating for primary and secondary alkyl bromides.

2.6 Experimental Section

2.6.1 General Considerations

Reagents: All reactions were conducted in Schlenk tubes. L1-L6 were purchased from commercial sources and used as received. Anhydrous DMF was purchased from Acros and used as received. Mn powder was purchased from Aldrich and used as received. Nickel precatalysts were purchased from Strem Chemicals or Aldrich and used as received. Analytical methods: ^{1}H NMR, ^{13}C and ^{19}F NMR spectra and melting points (where applicable) are included for all compounds. ^{1}H and ^{13}C NMR spectra were recorded on a Bruker 400 MHz and a Bruker 500 MHz at 20 °C. All ^{1}H NMR spectra are reported in parts per million (ppm) downfield of TMS and were measured relative to the signals for $CHCl_3$ (7.26 ppm), and DMSO (2.50 ppm). All ^{13}C NMR spectra were reported in ppm relative to residual $CHCl_3$ (77.2 ppm), DMSO (39.5 ppm) and were obtained with 1H decoupling. Coupling constants, *J*, are reported in hertz. Melting points were measured using open glass capillaries in a Büchi B540 apparatus. Infrared spectra were recorded on a Bruker Tensor 27. Mass spectra were recorded on a Waters LCT Premier spectrometer. High Pressure Liquid Chromatographic (HPLC) analyses were performed on Agilent Technologies Model 1260 Infinity HPLC chromatography instrument equipped with Agilent Eclipse Plus C18 (3.5 um, 4.6 x 100 mm) column and UV detector. Flash chromatography was performed with EM Science silica gel 60 (230-400 mesh) and bromocresol was used as the TLC stain.

2.6.2 Data of Starting Materials

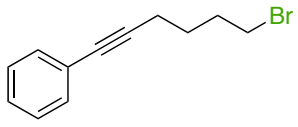

(6-bromohex-1-yn-1-yl)benzene (2-1): Yield, 92% over two steps. Colorless oil. The spectroscopic data correspond to those previously reported in the literature.[97] ^{1}H NMR (500 MHz, $CDCl_3$) δ 7.44-7.38 (m, 2H), 7.29 (dd, *J* = 5.1, 2.1 Hz, 3H), 3.48 (t, *J* = 6.7 Hz, 2H), 2.47 (t, *J* = 6.9 Hz, 2H), 2.5-2.4 (m, 2H), 1.87-1.67 (m, 2H) ppm. ^{13}C NMR (126 MHz, $CDCl_3$) δ 131.7, 128.4, 127.8, 123.9, 89.4, 81.4, 33.4, 31.9, 27.3, 18.8 ppm.

[97] Takanori I.; Reiko I.; Ryohei S.; Hitoshi K.; Jun T.; Nobuaki K. *J. Org. Chem.* **2014**, *79*, 8522.

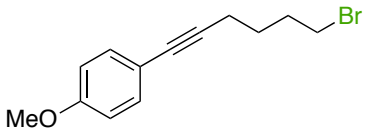

1-(6-Bromohex-1-yn-1-yl)-4-methoxybenzene (2-3): Yield, 91% over two steps. Colorless oil. The spectroscopic data correspond to those previously reported in the literature. [98] ^{1}H NMR (400 MHz, $CDCl_3$) δ 7.34 (d, *J* = 8.7 Hz, 2H), 6.82 (d, *J* = 8.7 Hz, 2H), 3.78 (s, 3H), 3.46 (t, *J* = 6.7 Hz, 2H), 2.44 (t, *J* = 7.0 Hz, 2H), 2.13-1.95 (m, 2H), 1.84-1.63 (m, 2H) ppm. ^{13}C NMR (101 MHz, $CDCl_3$) δ 159.2, 132.9, 116.0, 113.9, 87.7, 81.0, 55.3, 33.4, 31.9, 27.3, 18.7 ppm.

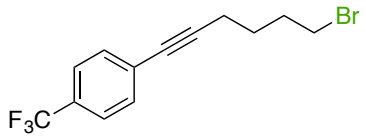

1-(6-Bromohex-1-yn-1-yl)-4-(trifluoromethyl)benzene (2-4): Yield, 82% over two steps. Colorless oil. ^{1}H NMR (400 MHz, $CDCl_3$) δ 7.54 (d, *J* = 8.4 Hz, 2H), 7.48 (d, *J* = 8.3 Hz, 2H), 3.47 (t, *J* = 6.6 Hz, 2H), 2.48 (t, *J* = 7.0 Hz, 2H), 2.12-1.98 (m, 2H), 1.88-1.66 (m, 2H) ppm. ^{13}C NMR (101 MHz, $CDCl_3$) δ 131.9, 129.6 (q, *J* = 32.6 Hz), 127.8, 125.3 (q, *J* = 3.8 Hz), 124.2 (q, *J* = 272.0 Hz), 92.2, 80.3, 33.2, 31.9, 27.1, 18.8 ppm. ^{19}F NMR (376 MHz, $CDCl_3$) δ 62.9 ppm. IR (neat, cm^{-1}): 2945, 1615, 1319, 1164, 1121, 1065. HRMS *calcd.* for ($C_{13}H_{12}BrF_3$-F): 285.0085, *found*: 285.0076.

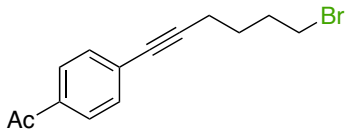

1-(4-(6-Bromohex-1-yn-1-yl)phenyl)ethanone (2-5): Yield, 87% over two steps. Colorless oil. ^{1}H NMR (400 MHz, $CDCl_3$) δ 7.82 (d, *J* = 8.0 Hz, 2H), 7.41 (d, *J* = 8.0 Hz, 2H), 3.42 (t, *J* = 6.6 Hz, 2H), 2.52 (s, 3H), 2.43 (t, *J* = 7.0 Hz, 2H), 2.09-1.89 (m, 2H), 1.82-1.67 (m, 2H) ppm. ^{13}C NMR (101 MHz, $CDCl_3$) δ 197.2, 135.8, 131.6, 128.7, 128.2, 93.1, 80.7, 33.2, 31.8, 27.0, 26.6, 18.8 ppm. IR (neat, cm^{-1}): 2948, 1678, 1600, 1260, 711, 592. HRMS *calcd.* for ($C_{14}H_{15}BrO$+Na): 301.0198, *found*: 301.0191.

[98] Chen, J.; Chen, C.; Chen, J.; Gao, H.; Qu, H. *Synlett* **2014**, *25*, 2721.

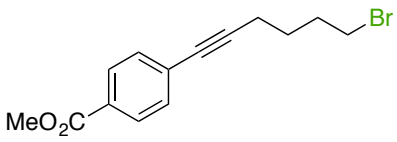

Methyl 4-(6-bromohex-1-yn-1-yl)benzoate (2-6): Yield, 90% over two steps. Colorless oil. ^{1}H NMR (400 MHz, $CDCl_3$) δ 7.92 (t, *J* = 8.3 Hz, 2H), 7.41 (t, *J* = 7.7 Hz, 2H), 3.86 (s, *J* = 11.8 Hz, 3H), 3.51-3.37 (m, 2H), 2.51-2.35 (m, 2H), 2.10-1.93 (m, 2H), 1.80-1.68 (m, 2H) ppm. ^{13}C NMR (101 MHz, $CDCl_3$) δ 166.6, 131.5, 129.5, 129.1, 128.6, 92.8, 80.8, 52.2, 33.2, 31.8, 27.0, 18.8 ppm. IR (neat, cm^{-1}): 2931, 2863, 1489, 1451, 754, 691. HRMS *calcd*. for ($C_{14}H_{15}BrO_2$+Na): 317.0148, *found*: 317.0153.

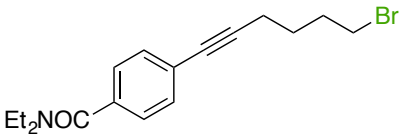

4-(6-Bromohex-1-yn-1-yl)-N,N-diethylbenzamide (2-7): Yield, 88% over two steps. Colorless oil. ^{1}H NMR (400 MHz, $CDCl_3$) δ 7.36 (d, *J* = 8.1 Hz, 2H), 7.24 (d, *J* = 8.1 Hz, 2H), 3.53-3.35 (m, 4H), 3.18 (s, 2H), 2.41 (t, *J* = 6.9 Hz, 2H), 2.05-1.89 (m, 2H), 1.81-1.61 (m, 2H), 1.11 (broad d, *J* = 50.5 Hz, 6H) ppm. ^{13}C NMR (101 MHz, $CDCl_3$) δ 170.7, 136.3, 131.5, 126.3, 124.7, 90.6, 80.7, 33.2, 31.8, 27.0, 18.6 ppm. IR (neat, cm^{-1}): 2970, 2934, 1625, 1424, 1286, 1094. HRMS *calcd*. for ($C_{17}H_{21}BrNO$+H): 336.0928, *found*: 336.0957.

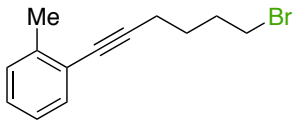

1-(6-Bromohex-1-yn-1-yl)-2-methylbenzene (2-8): Yield, 81% over two steps. Colorless oil. ^{1}H NMR (400 MHz, $CDCl_3$) δ 7.43 (td, *J* = 4.6, 1.8 Hz, 1H), 7.26-7.20 (m, 2H), 7.16 (td, *J* = 8.0, 3.7 Hz, 1H), 3.50 (t, *J* = 6.7 Hz, 2H), 2.54 (t, *J* = 6.9 Hz, 2H), 2.48 (d, *J* = 2.7 Hz, 3H), 2.20-2.00 (m, 2H), 1.91-1.71 (m, 2H) ppm. ^{13}C NMR (101 MHz, $CDCl_3$) δ 139.9, 131.9, 129.4, 127.7, 125.5, 123.6, 93.3, 80.2, 33.3, 31.9, 27.3, 20.9, 18.8 ppm. IR (neat, cm^{-1}): 2943, 1485, 1249, 755, 716, 561. HRMS *calcd*. for ($C_{13}H_{15}Br$+H): 251.0430 *found*: 251.0431.

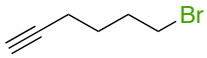

6-bromohex-1-yne (2-9): Yield, 75%. Colorless oil. The spectroscopic data correspond to those previously reported in the literature[99]. ^{1}H NMR (400 MHz, $CDCl_3$) δ 3.42 (t, *J* = 6.7 Hz, 2H), 2.23 (t, *J* = 8.0 Hz, 2H), 2.11-1.90 (m, 3H), 1.77-1.53 (m, 2H) ppm. ^{13}C NMR (101 MHz, $CDCl_3$) δ 83.7, 69.1, 33.3, 31.7, 27.0, 17.7 ppm.

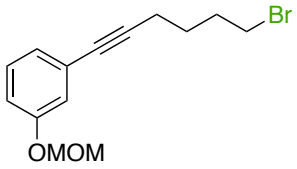

1-(6-bromohex-1-yn-1-yl)-3-(methoxymethoxy)benzene (2-10): Yield, 83% over three steps. Colorless oil. ^{1}H NMR (400 MHz, $CDCl_3$) δ 7.19 (t, *J* = 7.9 Hz, 1H), 7.09 (dd, *J* = 2.5, 1.4 Hz, 1H), 7.05 (dd, *J* = 7.6, 1.2 Hz, 1H), 6.96 (dd, *J* = 8.3, 2.6 Hz, 1H), 5.15 (s, 2H), 3.50-3.43 (m, 5H), 2.45 (t, *J* = 6.9 Hz, 2H), 2.13-1.96 (m, 2H), 1.85-1.67 (m, 2H) ppm. ^{13}C NMR (101 MHz, $CDCl_3$) δ 157.1, 129.4, 125.3, 124.9, 119.2, 116.2, 94.4, 89.4, 81.1, 56.1, 33.3, 31.9, 27.2, 18.7 ppm. IR (neat, cm^{-1}): 2947, 1573, 1482, 1149, 986, 784, 687. HRMS *calcd*. for ($C_{14}H_{17}BrO_2$+Na): 319.0304, *found*: 319.0311.

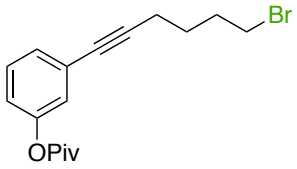

3-(6-bromohex-1-yn-1-yl)phenyl pivalate (2-11): Yield, 79% over three steps. Colorless oil. ^{1}H NMR (500 MHz, $CDCl_3$) δ 7.32-7.20 (m, 2H), 7.09 (t, *J* = 1.9 Hz, 1H), 6.98 (dd, *J* = 7.9, 2.4, 1.3 Hz), 3.47 (t, *J* = 6.6 Hz, 2H), 2.45 (t, *J* = 6.9 Hz, 2H), 2.04 (tt, *J* = 6.7 Hz, 2H), 1.75 (tt, *J* = 7.0 Hz, 2H), 1.35 (s, 9H) ppm. ^{13}C NMR (126 MHz, $CDCl_3$) δ 177.0, 151.0, 129.3, 129.0, 125.2, 124.8, 121.3, 90.2, 80.6, 39.2, 33.4, 31.9, 27.3, 26.7, 18.7 ppm. IR (neat, cm^{-1}): 2972, 1750, 1479, 1260, 1152, 1107, 778, 684. HRMS *calcd*. for ($C_{17}H_{21}BrO_2$+Na): 359.0617, *found*: 359.0613.

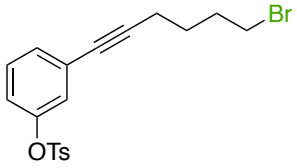

3-(6-bromohex-1-yn-1-yl)phenyl-4-methylbenzenesulfonate (2-12): Yield, 81% over three steps. Colorless oil. ^{1}H NMR (500 MHz, $CDCl_3$) δ 7.70 (d, *J* = 6.9 Hz, 2H),

[99] Sunaina, S.; Allan, C. O. *J. Org. Chem.* **1989**, *54*, 5064.

7.31 (d, J = 7.7 Hz, 2H), 7.25 (d, J = 7.7 Hz, 1H), 7.17 (t, J = 7.9 Hz, 1H), 7.07 (s, 1H), 6.85 (d, J = 9.0 Hz, 1H), 3.46 (t, J = 6.6 Hz, 2H), 2.51-2.35 (m, 5H), 2.01 (tt, J = 5.8 Hz, 2H), 1.74 (tt, J = 7.2 Hz, 2H) ppm. ^{13}C NMR (126 MHz, $CDCl_3$) δ 149.5, 145.6, 145.6, 132.4, 130.4, 129.9, 128.6, 125.6, 125.6, 121.8, 91.0, 80.0, 33.3, 31.9, 27.1, 21.9, 18.7 ppm. IR (neat, cm^{-1}): 2937, 1191, 1178, 1136, 1091, 882, 682, 546. HRMS *calcd*. for ($C_{19}H_{19}BrO_3S$+Na): 429.0130, *found*: 429.0127.

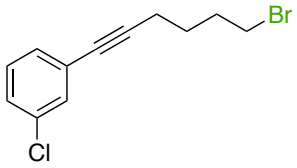

1-(6-bromohex-1-yn-1-yl)-3-chlorobenzene (2-13): Yield, 89% over two steps. Colorless oil. ^{1}H NMR (400 MHz, $CDCl_3$) δ 7.40-7.34 (m, 1H), 7.29-7.17 (m, 3H), 3.47 (t, J = 6.7 Hz, 2H), 2.45 (t, J = 6.9 Hz, 2H), 2.12-1.88 (m, 2H), 1.88-1.59 (m, 2H) ppm. ^{13}C NMR (75 MHz, $CDCl_3$) δ 134.2, 131.6, 129.8, 129.6, 128.1, 125.6, 90.8, 80.1, 33.3, 31.9, 27.1, 18.7 ppm. IR (neat, cm^{-1}): 2942, 1706, 1591, 1474, 782, 681. HRMS *calcd*. for ($C_{12}H_{12}BrCl$+H): 270.9884, *found*: 270.9879.

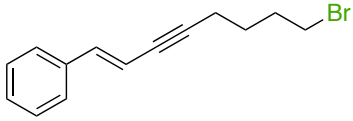

(*E*)-(8-bromooct-1-en-3-yn-1-yl)benzene (2-14): Yield, 72% over two steps. Colorless oil. ^{1}H NMR (400 MHz, $CDCl_3$) δ 7.43-7.22 (m, 5H), 6.88 (d, J = 16.3 Hz, 1H), 6.15 (dt, J = 16.3, 2.2 Hz, 1H), 3.47 (t, J = 6.7 Hz, 2H), 2.43 (td, J = 7.0, 2.2 Hz, 2H), 2.11-1.94 (m, 2H), 1.73 (tt, J = 7.0 Hz, 2H) ppm. ^{13}C NMR (101 MHz, $CDCl_3$) δ 140.5, 136.6, 128.8, 128.5, 126.2, 108.7, 91.9, 80.6, 33.4, 31.9, 27.3, 19.0 ppm. IR (neat, cm^{-1}): 2939, 1448, 1249, 951, 746, 690, 515. HRMS *calcd.* for ($C_{14}H_{15}Br$+H): 263.0430, *found*: 263.0435.

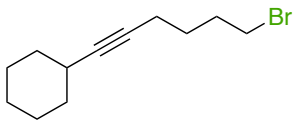

(6-Bromohex-1-yn-1-yl)cyclohexane (2-15): Yield, 45% over two steps. Colorless oil. ^{1}H NMR (400 MHz, $CDCl_3$) δ 3.41 (t, J = 6.8, 2 H), 2.35-2.23 (m, 1 H), 2.18 (t, J = 8.0 Hz, 2 H), 1.95 (p, J = 7.0 Hz, 2 H), 1.81-1.55 (m, 6 H), 1.54-1.41 (m, 1 H), 1.42-1.31 (m, 5 H) ppm. ^{13}C NMR (100 MHz, $CDCl_3$) δ 85.3, 78.9, 33.28, 33.26, 31.7, 29.0, 27.4,

25.9, 24.9, 17.8 ppm. IR (neat, cm^{-1}): 2926, 2852, 1447, 1250, 1233. HRMS *calcd*. for ($C_{12}H_{19}Br$+H): 243.0743, *found*: 243.0751.

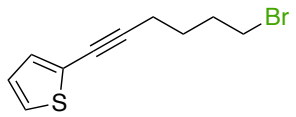

3-(6-Bromohex-1-yn-1-yl)thiophene (2-16): Yield, 87% over two steps. Colorless oil. ^{1}H NMR (400 MHz, $CDCl_3$) δ 7.36 (d, *J* = 1.7 Hz, 1 H), 7.26-7.21 (m, 1 H), 7.08 (d, *J* = 4.9 Hz, 1 H), 3.46 (t, *J* = 6.7 Hz, 2 H), 2.44 (t, *J* = 7.0 Hz, 2 H), 2.03 (tt, *J* = 7.0 Hz, 2 H), 1.75 (tt, *J* = 7.0 Hz, 2 H) ppm. ^{13}C NMR (100 MHz, $CDCl_3$) δ 129.8, 127.6, 125.0, 122.6, 88.7, 76.2, 33.2, 31.7, 27.0, 18.5 ppm. IR (neat, cm^{-1}): 3106, 2942, 1430, 1356, 1249, 1078. HRMS *calcd*. for ($C_{10}H_{11}BrS$+H): 242.9838, *found*: 242.9837.

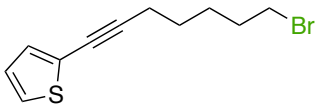

3-(7-bromohept-1-yn-1-yl)thiophene (2-17): Yield, 92% over two steps. Colorless oil. ^{1}H NMR (400 MHz, $CDCl_3$) δ 7.35 (dd, *J* = 3.0, 1.2 Hz, 1H), 7.23 (dd, *J* = 5.0, 3.0 Hz, 1H), 7.07 (dd, *J* = 5.0, 1.2 Hz, 1H), 3.43 (t, *J* = 6.8 Hz, 2H), 2.41 (t, *J* = 6.6 Hz, 2H), 1.91 (tt, *J* = 7.0 Hz, 2H), 1.69-1.56 (m, 4H) ppm. ^{13}C NMR (101 MHz, $CDCl_3$) δ 130.1, 127.8, 125.2, 123.0, 89.4, 76.1, 33.8, 32.5, 28.0, 27.6, 19.4 ppm. IR (neat, cm^{-1}): 2936, 1356, 857, 777, 626, 558. HRMS *calcd.* for ($C_{11}H_{13}BrS$+H): 256.9994, *found*: 256.9997.

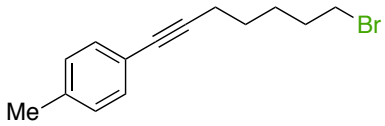

1-(7-bromohept-1-yn-1-yl)-4-methylbenzene (2-18): Yield, 94% over two steps. Colorless oil. ^{1}H NMR (500 MHz, $CDCl_3$) δ 7.28 (d, *J* = 8.1 Hz, 2H), 7.09 (d, *J* = 7.9 Hz, 2H), 3.43 (t, *J* = 6.8 Hz, 2H), 2.42 (t, *J* = 6.5 Hz, 2H), 2.33 (s, 3H), 1.92 (tt, *J* = 7.0 Hz, 2H), 1.70-1.57 (m, 4H) ppm. ^{13}C NMR (126 MHz, $CDCl_3$) δ 137.7, 131.6, 129.1, 121.0, 89.1, 81.1, 33.8, 32.5, 28.1, 27.6, 21.6, 19.5 ppm. IR (neat, cm^{-1}): 2937, 2860, 1509, 815, 525. HRMS *calcd.* for ($C_{14}H_{17}Br$+H): 265.0586, *found*: 265.0592.

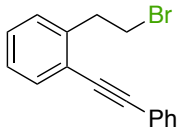

(6-bromooct-1-yn-1-yl)benzene (2-19): Yield, 74% over four steps. Colorless oil. ^{1}H NMR (400 MHz, $CDCl_3$) δ 7.42 -7.37 (m, 2H), 7.32-7.27 (m, 3H), 4.05 (tt, J = 8.6, 4.8 Hz, 1H), 2.46 (t, J = 6.9 Hz, 2H), 2.13-1.66 (m, 6H), 1.06 (t, J = 7.3 Hz, 3H) ppm. ^{13}C NMR (101 MHz, $CDCl_3$) δ 131.7, 128.4, 127.8, 124.0, 89.6, 81.3, 59.8, 37.9, 32.5, 26.9, 19.0, 12.3 ppm. IR (neat, cm^{-1}): 2966. 1489, 1441, 754, 690. HRMS *calcd.* for ($C_{14}H_{17}Br$+H): 265.0586, *found*: 265.0580.

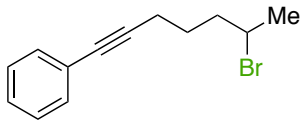

1-(2-bromoethyl)-2-(phenylethynyl)benzene (2-39): Yield, 60% over four steps. Colorless oil. ^{1}H NMR (400 MHz, $CDCl_3$) δ 7.67-7.54 (m, 3H), 7.44-7.36 (m, 3H), 7.34-7.24 (m, 3H), 3.73 (t, J = 7.8 Hz, 2H), 3.45 (t, J = 7.8 Hz, 2H) ppm. ^{13}C NMR (101 MHz, $CDCl_3$) δ 140.8, 132.5, 131.7, 129.6, 128.7, 128.6, 128.6, 127.2, 123.2, 123.0, 93.9, 87.4, 38.7, 32.0 ppm. IR (neat, cm-1): 1493, 1443, 1215, 751, 687. HRMS *calcd.* for ($C_{16}H_{13}Br$+H): 285.0273, *found*: 285.0274.

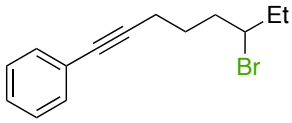

(6-bromohept-1-yn-1-yl)benzene (2-40): Yield, 41% over four steps. Colorless oil. ^{1}H NMR (400 MHz, $CDCl_3$) δ 7.44-7.36 (m, 2H), 7.32-7.21 (m, 3H), 4.30-4.10 (m, J = 6.6 Hz, 1H), 2.46 (t, J = 6.9 Hz, 2H), 2.10-1.93 (m, 2H), 1.94-1.65 (m, 5H) ppm. ^{13}C NMR (101 MHz, $CDCl_3$) δ 131.7, 128.4, 127.8, 124.0, 89.5, 81.3, 51.3, 40.3, 27.1, 26.7, 19.0 ppm. IR (neat, cm^{-1}): 2947, 2855, 1676, 1613, 1269, 1226, 846, 722. HRMS *calcd.* for ($C_{13}H_{15}Br$+H): 251.0430, *found*: 251.0428.

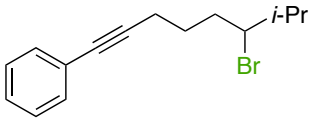

(6-bromo-7-methyloct-1-yn-1-yl)benzene (2-41): Yield, 20% over four steps.. ^{1}H NMR (400 MHz, $CDCl_3$) δ 7.49-7.35 (m, 1H), 7.28 (dd, J = 5.0, 2.0 Hz, 3H), 4.07 (dd, J = 7.0, 6.1 Hz, 1H), 2.46 (t, J = 6.8 Hz, 2H), 2.16-1.81 (m, 4H), 1.80-1.61 (m, 1H), 1.05 (d, J = 6.7 Hz, 3H), 1.01 (d, J = 6.6 Hz, 3H) ppm. ^{13}C NMR (101 MHz, $CDCl_3$) δ 131.7, 128.4, 127.8, 124.0, 89.6, 81.3, 66.3, 35.8, 34.8, 27.3, 21.1, 19.0, 18.4 ppm. IR

(neat, cm^{-1}): 2922, 1489, 1442, 754, 690, 525. HRMS *calcd.* for ($C_{15}H_{19}Br$+MeOH): 311.1005, *found*: 311.1004.

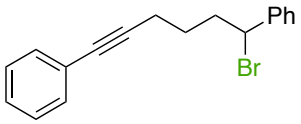

(6-bromohex-1-yne-1,6-diyl)dibenzene (2-42): Yield, 23% over four steps.Colorless solid. M.P. = 53-55 °C. ^{1}H NMR (400 MHz, $CDCl_3$) δ 7.15 (td, *J* = 7.2, 1.6 Hz, 2H), 7.11-7.05 (m, 6H), 6.95 (d, *J* = 7.1 Hz, 2H), 3.83-3.70 (m, 1H), 2.77 (td, *J* = 7.3, 2.1 Hz, 2H), 2.34-2.10 (m, 1H), 1.99-1.66 (m, 3H) ppm. ^{13}C NMR (101 MHz, $CDCl_3$) δ 148.2, 145.2, 140.7, 128.8, 128.2, 127.9, 127.8, 127.6, 125.9, 116.7, 50.6, 38.6, 37.7, 23.4 ppm. IR (neat, cm^{-1}): 2920, 2855, 1675, 1615, 1269, 1226, 846, 723. HRMS *calcd.* for ($C_{18}H_{17}Br$): 312.0508, *found*: 312.0512.

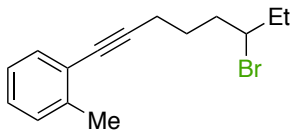

1-(6-bromooct-1-yn-1-yl)-2-methylbenzene (2-43): Yield, 44% over four steps. Colorless oil. ^{1}H NMR (400 MHz, $CDCl_3$) δ 7.36 (d, *J* = 7.4 Hz, 1H), 7.18 (d, *J* = 4.8 Hz, 2H), 7.15-7.06 (m, 1H), 4.05 (tt, *J* = 8.6, 4.8 Hz, 1H), 2.51 (t, *J* = 6.8 Hz, 2H), 2.42 (s, 3H), 2.15-1.68 (m, 6H), 1.07 (t, *J* = 7.3 Hz, 3H) ppm. ^{13}C NMR (101 MHz, $CDCl_3$) δ 140.1, 132.0, 129.5, 127.8, 125.6, 123.8, 93.5, 80.2, 59.8, 37.9, 32.5, 27.0, 21.0, 19.1, 12.3 ppm. IR (neat, cm^{-1}): 2936, 1485, 1455, 754. HRMS *calcd.* for ($C_{15}H_{19}Br$+H): 279.0743, *found*: 279.0736.

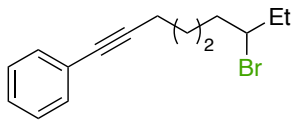

(7-bromonon-1-yn-1-yl)benzene (2-44): Yield, 40% over four steps. Colorless oil. ^{1}H NMR (400 MHz, $CDCl_3$) δ 7.49 – 7.34 (m, 2H), 7.31 – 7.24 (m, 3H), 4.01 (tt, *J* = 7.7, 5.0 Hz, 1H), 2.44 (t, *J* = 6.7 Hz, 2H), 2.07 – 1.44 (m, 8H), 1.05 (t, *J* = 7.3 Hz, 3H) ppm. ^{13}C NMR (101 MHz, $CDCl_3$) δ 131.7, 128.4, 127.7, 124.1, 90.0, 81.1, 60.4, 38.4, 32.4, 28.3, 27.1, 19.5, 12.3 ppm. IR (neat, cm^{-1}): 2937, 1489, 754, 690, 525. HRMS *calcd.* for ($C_{15}H_{19}Br$+H): 279.0743, *found*: 279.0730.

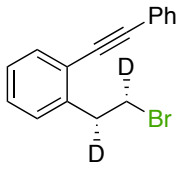

1-(phenylethynyl)-2-(2-bromo-1,2-diduteroethyl)benzene (2-73) [100]: Yield, 11% over six steps. Colorless oil. ^{1}H NMR (500 MHz, $CDCl_3$) δ 7.69-7.51 (m, 3H), 7.47-7.36 (m, 3H), 7.36-7.27 (m, 3H), 3.71 (d, J = 6.2 Hz, 1H), 3.43 (d, J = 6.3 Hz, 1H) ppm. ^{13}C NMR (126 MHz, $CDCl_3$) δ 140.8, 132.5, 131.7, 129.6, 128.7, 128.6, 128.6, 127.2, 123.2, 123.0, 93.9, 87.4, 38.3 (t, J = 20.2 Hz), 31.7 (t, J = 23.9 Hz) ppm. IR (neat, cm^{-1}): 1493, 1442, 751, 688, 522. HRMS *calcd.* for ($C_{16}H_{11}D_2Br$+H): 287.0399, *found*: 287.0396.

2.6.3 Selected Examples of NMR Spectra

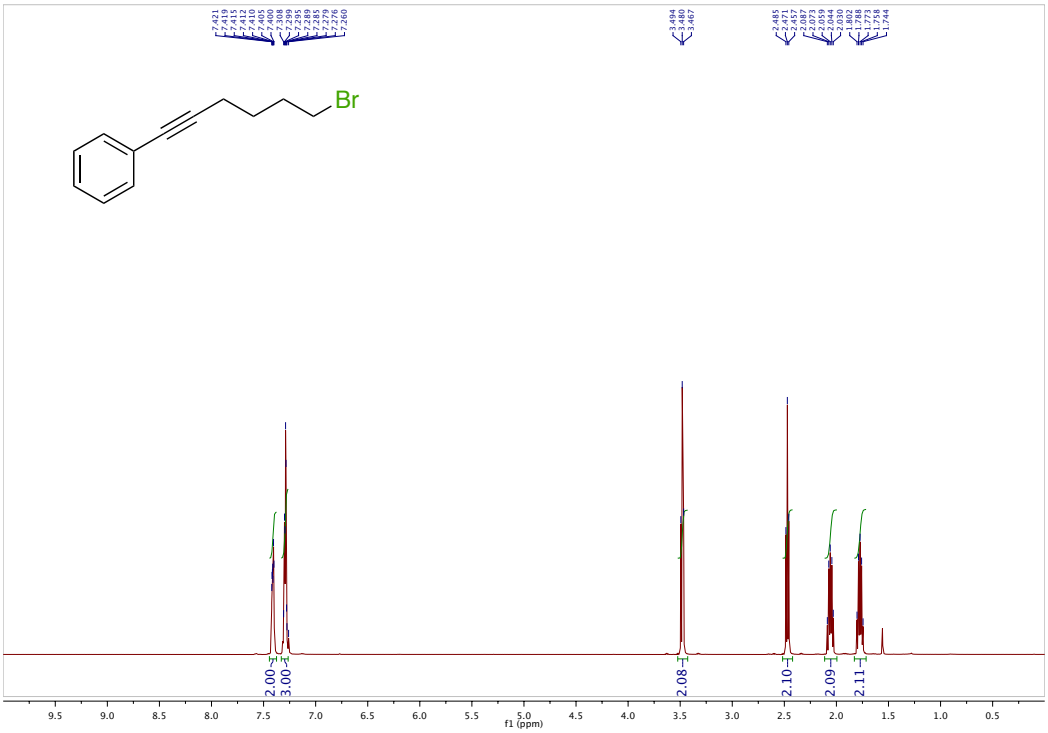

[100] (a) Netherton, M. R.; Fu, G. C. *Angew. Chem. Int. Ed.* **2002**, *41*, 3910. (b) Bissember, A. C.; Levina, A.; Fu, G. C. *J. Am. Chem. Soc.* **2012**, *134*, 14232. (c) Monks, B. M.; Cook, S. P. *J. Am. Chem. Soc.* **2012**, *134*, 15297.

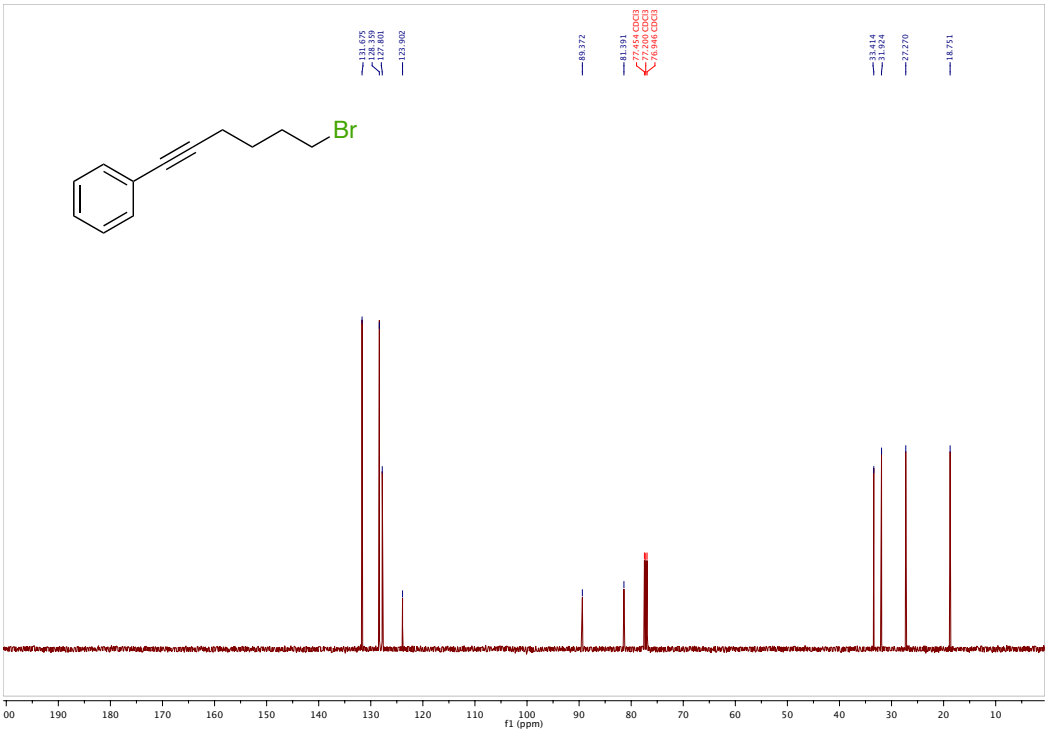
131.675
128.339
127.801
123.902
89.372
81.391
77.454 CDCl3
77.200 CDCl3
76.946 CDCl3
33.414
31.924
27.270
18.751
Br
f1 (ppm)

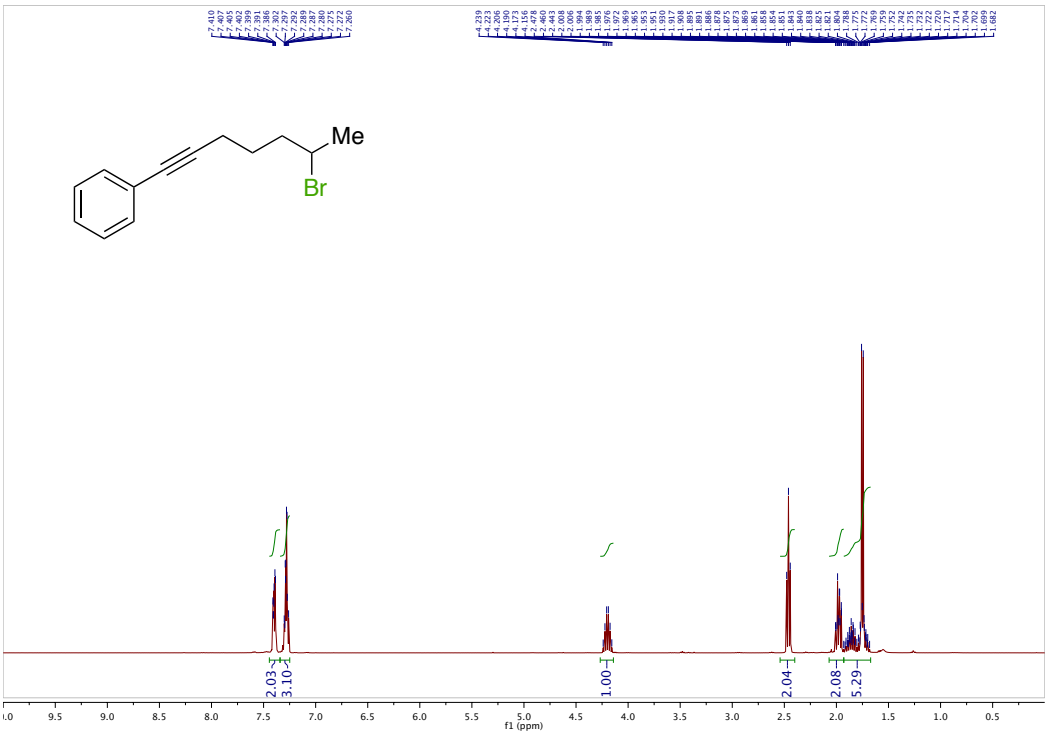
Me
Br
2.03
3.10
1.00
2.04
2.08
5.29
f1 (ppm)

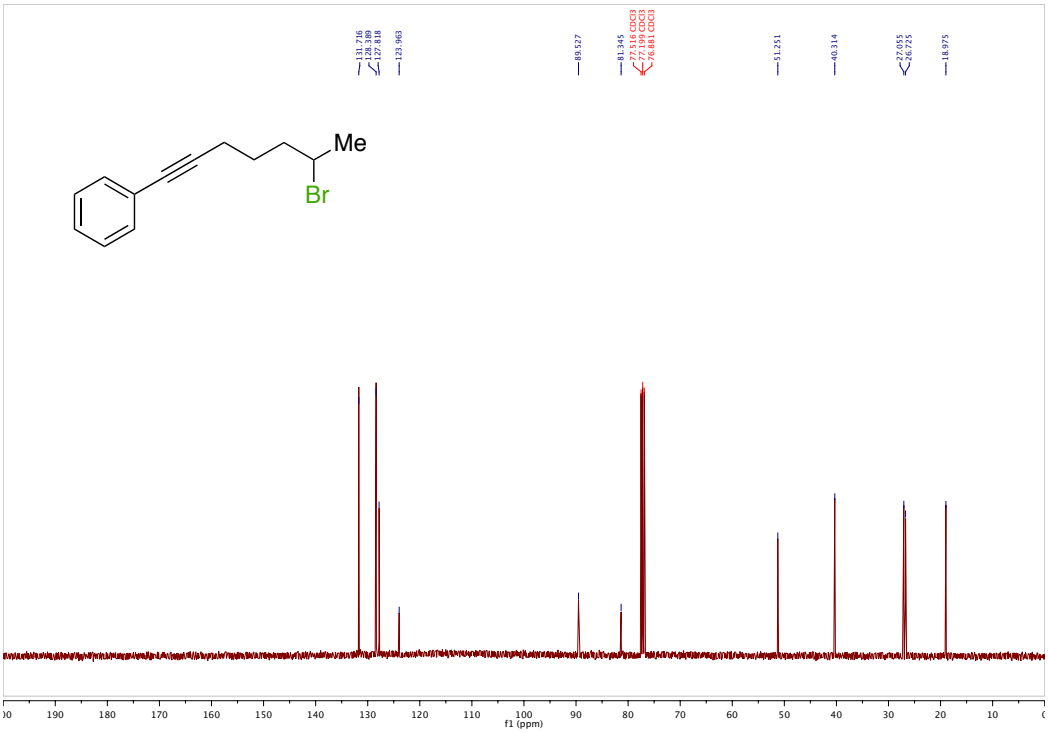
131.716
128.389
127.818
123.963
89.527
81.345
77.516 CDCl3
77.199 CDCl3
76.881 CDCl3
51.251
40.314
27.055
26.725
18.975
Me
Br
f1 (ppm)

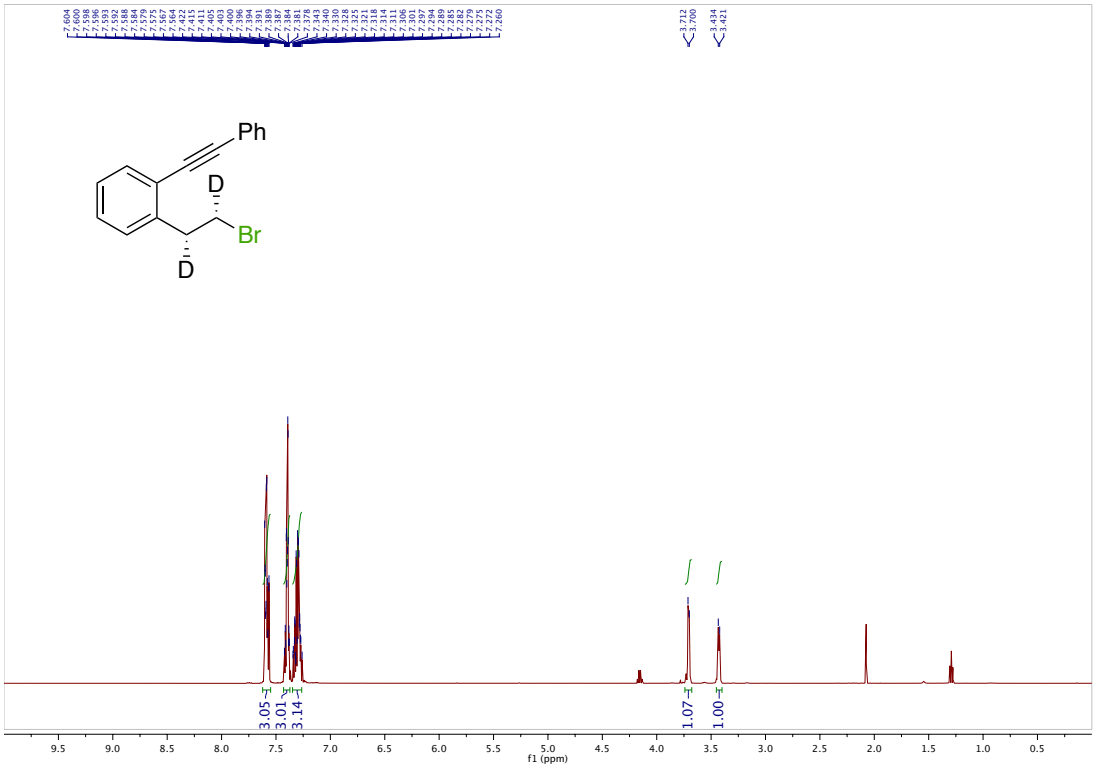
7.604
7.600
7.598
7.596
7.593
7.592
7.588
7.584
7.579
7.575
7.567
7.564
7.422
7.415
7.411
7.405
7.403
7.400
7.396
7.394
7.393
7.389
7.387
7.384
7.381
7.378
7.343
7.340
7.330
7.328
7.325
7.321
7.318
7.314
7.311
7.306
7.301
7.297
7.294
7.289
7.285
7.282
7.279
7.275
7.272
7.260
3.712
3.700
3.434
3.421
Ph
D
Br
D
3.05
3.01
3.14
1.07
1.00
f1 (ppm)

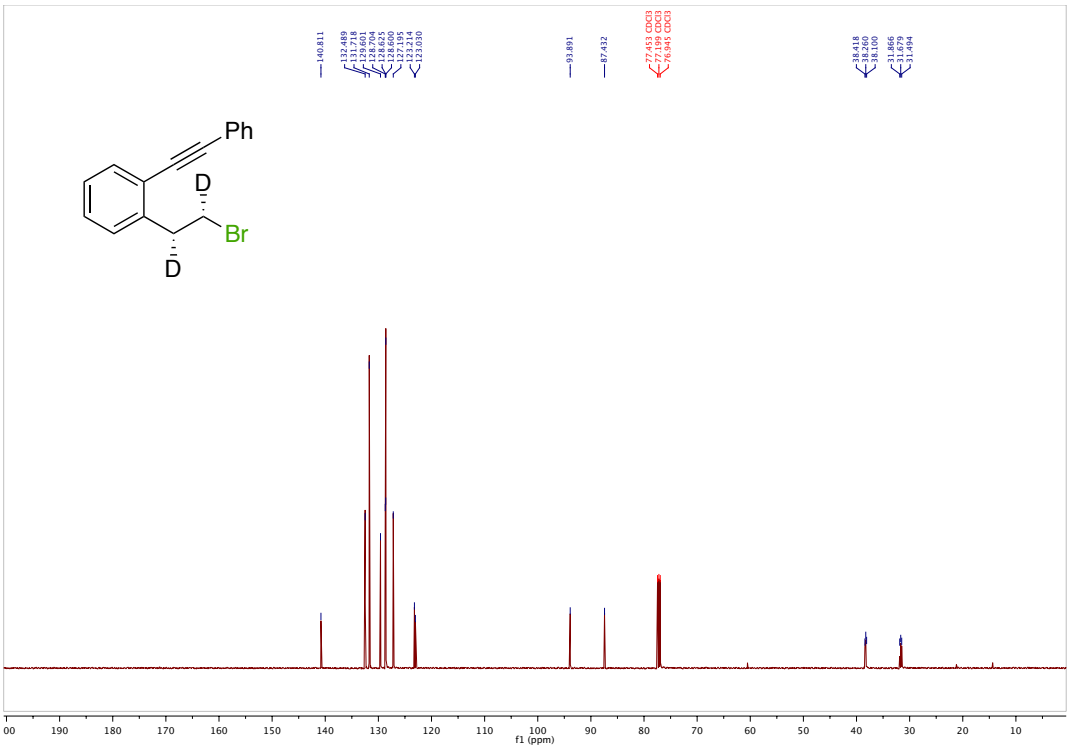

2.6.4 General Procedure for Divergent Cyclization/Carboxylation

General Procedure: A Schlenk tube containing a stirring bar was charged with $NiBr_2$·diglyme (10.6 mg, 0.03 mmol), bathocuproine (21.6 mg, 0.06 mmol) and Mn powder (37.0 mg, 0.66 mmol). The tube was then evacuated and back-filled with carbon dioxide. The bromide (0.3 mmol) and DMF (2 mL) were added under CO_2 flow. Once added, the Schleck tube was closed at atmospheric pressure of CO_2 (1atm) and stirred overnight. The mixture was quenched with 2M HCl and extracted with AcOEt. The combined organic layers were wished with brine and dried over anhydrous $MgSO_4$ and evaporated. The residue was purified by flash chromatography (hexane/Et_2O = 10/1 to 1/1).

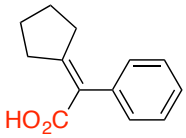

2-Cyclopentylidene-2-phenylacetic acid (2-2): Following the general procedure using **2-1** to provide **2-2** (51.5 mg, 85% yield) as a colorless solid. The spectroscopic data

correspond to those previously reported in the literature.[101] M.P. = 133-135 °C, (Lit. 132 °C). ^{1}H NMR (400 MHz, $CDCl_3$) δ 7.40-7.34 (m, 2 H), 7.29 (tt, *J* = 8.0 Hz, 2.0 Hz, 1H), 7.22-7.17 (m, 2H), 2.93 (t, *J* = 8.0 Hz, 2H), 2.23 (t, *J* = 8.0 Hz, 2H), 1.83-1.74 (m, 2H), 1.65-1.56 (m, 2H) ppm. ^{13}C NMR (100 MHz, $CDCl_3$) δ 172.7, 167.8, 138.7, 129.3, 128.1, 127.0, 125.1, 36.0, 34.5, 26.8, 25.7 ppm.

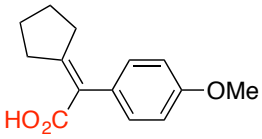

2-Cyclopentylidene-2-(4-methoxyphenyl)acetic acid (2-21): Following the general procedure using **2-3** to provide **2-21** (65.5 mg, 87% yield) as a colorless solid. M.P. = 153-154 °C. ^{1}H NMR (400 MHz, $CDCl_3$) δ 7.10 (dt, *J* = 10.0 Hz, 2.0 Hz, 2 H), 6.89 (dt, *J* = 10.0 Hz, 2.0 Hz, 2 H), 3.81 (s, 3H), 2.88 (t, *J* = 8.0 Hz, 2H), 2.22 (t, *J* = 8.0 Hz, 2H), 1.80-1.73 (m, 2H), 1.62-1.55 (m, 2H) ppm. ^{13}C NMR (100 MHz, $CDCl_3$) δ 172.9, 167.7, 156.4, 131.0, 130.4, 124.5, 113.8, 55.1, 36.0, 34.5, 26.8, 25.7 ppm. IR (neat, cm^{-1}): 2953, 1675, 1603, 1510, 1275, 1247, 1176, 1030. HRMS *calcd*. For ($C_{14}H_{16}O_3$-H): 231.1027, *found*: 231.1024.

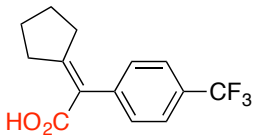

2-Cyclopentylidene-2-(4-(trifluoromethyl)phenyl)acetic acid (2-22): Following the general procedure using **2-4** to provide **2-22** (59.7 mg, 74% yield) as a colorless solid. M.P. = 173-175 °C. ^{1}H NMR (400 MHz, $CDCl_3$) δ 7.61 (d, *J* = 8.0 Hz, 2H), 7.30 (d, *J* = 8.0 Hz, 2H), 2.93 (t, *J* = 8.0 Hz, 2H), 2.19 (t, *J* = 8.0 Hz, 2H), 1.82-1.75 (m, 2H), 1.65-1.58 (m, 2H) ppm. ^{13}C NMR (100 MHz, $CDCl_3$) δ 172.1, 169.5, 142.3 (d, *J* = 1.0 Hz), 129.8, 129.2 (q, *J* = 32.3 Hz), 125.2 (q, *J* = 3.3 Hz), 124.2 (q, *J* = 270.3 Hz), 124.0, 36.2, 34.8, 26.7, 25.7 ppm. ^{19}F NMR (376 MHz, $CDCl_3$) δ 62.6 ppm. IR (neat, cm^{-1}): 2963, 1683, 1610, 1323, 1105, 1067. HRMS *calcd*. for ($C_{14}H_{13}F_3O_2$-H): 269.0795, *found*: 269.0794.

[101] Song, S.; Zhu, S.; Li, Y.; Zhou, Q. *Org. lett.* **2013**, *15*, 3722.

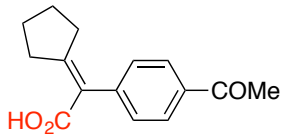

2-(4-Acetylphenyl)-2-cyclopentylideneacetic acid (2-23): Following the general procedure using **2-5** to provide **2-23** (50.4 mg, 69% yield) as a colorless solid. M.P. = 169-171 °C. ^{1}H NMR (400 MHz, $CDCl_3$) δ 7.98-7.91 (m, 2H), 7.32-7.23 (m, 2H), 2.92 (t, *J* = 7.4 Hz, 2H), 2.60 (s, 3H), 2.19 (t, *J* = 8.0 Hz, 2H), 1.77 (tt, *J* = 7.0 Hz, 2H), 1.61 (t, *J* = 7.1 Hz, 2H) ppm. ^{13}C NMR (100 MHz, $CDCl_3$) δ 197.8, 172.1, 169.0, 143.8, 135.7, 129.7, 128.3, 124.4, 36.0, 34.7, 26.6, 26.5, 25.7 ppm. IR (neat, cm-1): 2961, 2879, 1671, 1601, 1270, 1250, 958, 714, 596. HRMS *calcd*. for ($C_{15}H_{16}O_3$-H) 243.1027, *found*: 243.1024.

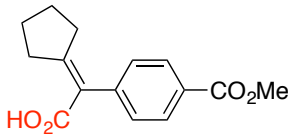

2-Cyclopentylidene-2-(4-(methoxycarbonyl)phenyl)acetic acid (2-24): Following the general procedure using **2-6** to provide **2-24** (59.3 mg, 76% yield) as a colorless solid. M.P. = 166-168 °C. ^{1}H NMR (400 MHz, $CDCl_3$) δ 8.02 (d, *J* = 7.7 Hz, 2H), 7.25 (d, *J* = 8.0 Hz, 2H), 3.91 (s, 3H), 2.92 (t, *J* = 6.0 Hz, 2H), 2.19 (t, *J* = 7.3 Hz, 2H), 1.77 (tt, *J* = 6.5 Hz, 2H), 1.60 (tt, *J* = 6.9 Hz, 2H). ^{13}C NMR (100 MHz, $CDCl_3$) δ 172.1, 168.9, 166.9, 143.6, 129.5, 128.7, 124.6, 124.5, 52.0, 36.0, 34.7, 26.6, 25.7 ppm. IR (neat, cm^{-1}): 2953, 2871, 1718, 1657, 1602, 1274, 1111, 733, 499. HRMS *calcd*. for ($C_{15}H_{16}O_4$-H) 259.0976, *found*: 259.0974.

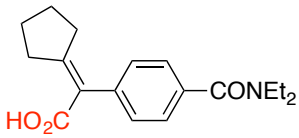

2-Cyclopentylidene-2-(4-(diethylcarbamoyl)phenyl)acetic acid (2-25): Following the general procedure using **2-7** to provide **2-25** (58.9 mg, 65% yield) as a colorless solid. M.P. = 116-118 °C. ^{1}H NMR (400 MHz, $CDCl_3$) δ 7.34 (dt, *J* = 8.0 Hz, 2.0 Hz, 2H), 7.17 (dt, *J* = 10.0 Hz, 1.0 Hz, 2H), 3.53 (bs, 2H), 3.29 (bs, 2H), 2.89 (t, *J* = 8.0 Hz, 2H), 2.17 (t, *J* = 6.9 Hz, 2H), 1.83-1.63 (m, *J* = 7.0 Hz, 2H), 1.65-1.51 (m, *J* = 6.7 Hz,

2H), 1.22 (bs, 3H), 1.12 (bs, 3H) ppm. ^{13}C NMR (100 MHz, $CDCl_3$) δ 172.0, 171.3, 167.7, 139.8, 135.4, 129.3, 126.2, 124.5, 43.3, 39.3, 35.9, 34.6, 26.7, 25.7, 14.2, 12.8 ppm. IR (neat, cm^{-1}): 2952, 2873, 1690, 1595, 1437, 1277, 1203, 1071. HRMS *calcd*. for ($C_{18}H_{23}NO_3$-H): 300.1605, *found*: 300.1604.

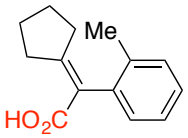

2-Cyclopentylidene-2-(o-tolyl)acetic acid (2-26): Following the general procedure using **2-8** to provide **2-26** (49.8 mg, 77% yield) as a colorless solid. M.P. = 144-146 °C. ^{1}H NMR (400 MHz, $CDCl_3$) δ 7.26-7.17 (m, 3H), 7.10-7.02 (m, 1H), 2.95 (t, *J* = 7.4 Hz, 2H), 2.23-1.92 (m, 5H), 1.87-1.67 (m, *J* = 7.0 Hz, 2H), 1.61 (tt, *J* = 7.3 Hz, 2H) ppm. ^{13}C NMR (100 MHz, $CDCl_3$) δ 172.4, 168.2, 138.2, 136.1, 129.9, 129.3, 127.4, 125.9, 124.3, 35.7, 34.2, 26.8, 25.5, 19.4 ppm. IR (neat, cm^{-1}): 2958, 2872, 1674, 1614, 1246, 737, 448. HRMS *calcd*. for ($C_{14}H_{16}O_2$-H): 215.1078, *found*: 215.1078

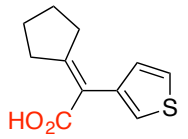

2-Cyclopentylidene-2-(thiophen-3-yl)acetic acid (2-27): Following the general procedure using **2-16** to provide **2-27** (50.2 mg, 80% yield) as a white solid. M.P. = 144-146 °C. ^{1}H NMR (400 MHz, $CDCl_3$) δ 7.29 (dd, *J* = 4.9, 2.9 Hz, 1H), 7.12 (dd, *J* = 3.0, 1.3 Hz, 1H), 7.00 (dd, *J* = 4.9, 1.3 Hz, 1H), 2.90 (t, *J* = 7.3 Hz, 2H), 2.35 (t, *J* = 7.2 Hz, 2H), 1.75-1.70 (m, 2H), 1.67-1.61 (m, 2H) ppm. ^{13}C NMR (100 MHz, $CDCl_3$) δ 172.7, 168.2, 138.1, 128.9, 124.4, 123.4, 119.9, 36.2, 34.7, 26.7, 25.7 ppm. IR (neat, cm^{-1}): 2956, 2871, 2804, 1659, 1603, 1412, 1279, 1238, 1203. HRMS *calcd.* for ($C_{11}H_{12}O_2S$-H) 207.0485, *found*: 207.0484

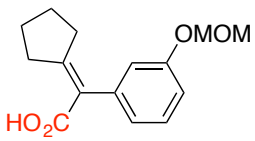

2-cyclopentylidene-2-(3-(methoxymethoxy)phenyl)acetic acid (2-28): Following the general procedure using **2-10** to provide **2-28** (60.5 mg, 85% yield) as a colorless solid.

M.P. = 95-98 °C. ^{1}H NMR (400 MHz, $CDCl_3$) δ 7.27 (t, *J* = 8.0 Hz, 1H), 6.97 (dd, *J* = 8.3, 2.6 Hz, 1H), 6.89-6.80 (m, 2H), 5.17 (s, 2H), 3.49 (s, 3H), 2.90 (t, *J* = 7.3 Hz, 2H), 2.24 (t, *J* = 7.1 Hz, 2H), 1.87-1.67 (m, 2H), 1.65-1.62 (m, 2H) ppm. ^{13}C NMR (101 MHz, $CDCl_3$) δ 172.6, 168.1, 157.3, 140.2, 129.3, 124.9, 123.1, 117.6, 114.9, 94.7, 56.2, 36.1, 34.7, 26.9, 25.9 ppm. IR (neat, cm^{-1}): 2958, 1661, 1249, 1150, 1024, 922, 787, 733. HRMS *calcd*. for ($C_{15}H_{18}O_4$-H): 261.1132, *found*: 261.1128.

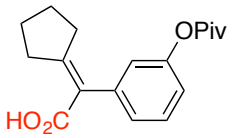

2-cyclopentylidene-2-(4-(pivaloyloxy)phenyl)acetic acid (2-29): Following the general procedure using **2-11** to provide **2-29** (76.7 mg, 77% yield) as a colorless solid. M.P. = 117-121 °C. ^{1}H NMR (400 MHz, $CDCl_3$) δ 7.35 (t, *J* = 7.9 Hz, 1H), 7.03 (dt, *J* = 7.7, 1.3 Hz, 1H), 7.00 (dd, *J* = 8.2, 2.4 Hz, 1H), 6.91 (dd, *J* = 2.3, 1.6 Hz, 1H), 2.90 (t, *J* = 7.3 Hz, 2H), 2.24 (t, *J* = 7.1 Hz, 2H), 1.87-1.67 (m, 2H), 1.70-1.55 (m, 2H), 1.36 s, 9H) ppm. ^{13}C NMR (101 MHz, $CDCl_3$) δ 177.1, 172.4, 169.0, 151.1, 140.1, 129.2, 126.7, 124.3, 122.7, 120.1, 39.2, 36.2, 34.8, 27.3, 27.3, 26.9, 25.9 ppm. IR (neat, cm^{-1}): 2962, 2872, 1750, 1679, 1249, 1111, 909, 728. HRMS *calcd*. for ($C_{18}H_{22}O_4$-H): 301.1445, *found*: 301.1444.

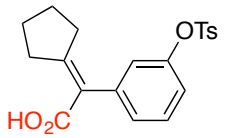

2-cyclopentylidene-2-(4-(tosyloxy)phenyl)acetic acid (2-30): Following the general procedure using **2-12** to provide **2-30** (67.0 mg, 60% yield) as a colorless solid. M.P. = 153-155 °C. ^{1}H NMR (400 MHz, $CDCl_3$) δ 7.67 (d, *J* = 8.3 Hz, 2H), 7.37-7.17 (m, 3H), 7.04 (dt, *J* = 7.7, 1.3 Hz, 1H), 6.99 (dd, *J* = 8.2, 2.4 Hz, 1H), 6.73 (dd, *J* = 2.4, 1.6 Hz, 1H), 2.87 (t, *J* = 7.3 Hz, 2H), 2.38 (s, 3H), 2.02 (t, *J* = 8.0 Hz, 2H), 1.85-1.66 (m, 2H), 1.67-1.49 (m, 2H) ppm. ^{13}C NMR (101 MHz, $CDCl_3$) δ 172.1, 169.3, 149.6, 145.4, 140.4, 132.4, 129.9, 129.5, 128.7, 128.3, 123.9, 123.6, 121.3, 36.2, 34.8, 26.8, 25.8, 21.8 ppm. IR (neat, cm^{-1}): 2954, 2681, 1680, 1622, 1369, 1251, 1178, 755, 547. HRMS *calcd*. for ($C_{20}H_{20}O_5$-H): 371.0959, *found*: 371.0956.

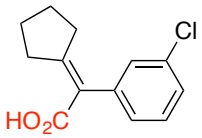

2-(4-chlorophenyl)-2-cyclopentylideneacetic acid (2-31): Following the general procedure using **2-13** to provide **2-31** (55.2mg, 77% yield) as a colorless solid. M.P. = 119-122 °C. ^{1}H NMR (400 MHz, $CDCl_3$) δ 7.34-7.24 (m, 2H), 7.21 – 7.19 (m, 1H), 7.10-7.06 (m, 1H), 2.93 (t, J = 7.4 Hz, 2H), 2.23 (t, J = 7.2 Hz, 2H), 1.70-1.64 (m, 2H), 1.63-1.51 (m, 2H) ppm. ^{13}C NMR (101 MHz, $CDCl_3$) δ 172.2, 169.3, 140.6, 134.1, 129.7, 129.7, 127.8, 127.4, 124.1, 36.3, 34.9, 26.9, 25.9 ppm. IR (neat, cm^{-1}): 2959, 2874, 1678, 1612, 1285, 1242, 714, 436. HRMS *calcd*. for ($C_{13}H_{13}O_2$-H): 235.0531, *found*: 235.0532.

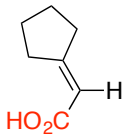

2-cyclopentylideneacetic acid (2-32): Following the general procedure using **2-9** to provide **2-32** (30.0 mg, 79% yield) as a colorless solid. The spectroscopic data correspond to those previously reported in the literature.[102] ^{1}H NMR (500 MHz, $CDCl_3$) δ 5.95-5.75 (m, 1H), 2.81 (t, J = 7.3 Hz, 2H), 2.50 (t, J = 7.2 Hz, 2H), 1.78 (t, J = 6.8 Hz, 2H), 1.70 (t, J = 7.3 Hz, 2H) ppm. ^{13}C NMR (126 MHz, $CDCl_3$) δ 172.7, 172.5, 111.5, 36.5, 33.2, 26.6, 25.6 ppm.

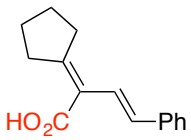

(*E*)-2-cyclopentylidene-4-phenylbut-3-enoic acid (2-33): Following the general procedure using **2-14** to provide **2-33** (54.5 mg, 79% yield) as a colorless solid. M.P. = 85-87 °C. ^{1}H NMR (400 MHz, $CDCl_3$) δ 7.52-7.43 (m, 2H), 7.38-7.30 (m, 2H), 7.26-7.21 (m, 1H), 2.82 (dd, J = 5.0, 3.6 Hz, 2H), 2.70-2.62 (m, 2H), 1.78 (tt, J = 3.6, 1.7 Hz, 4H) ppm. ^{13}C NMR (101 MHz, $CDCl_3$) δ 173.8, 162.2, 138.0, 131.1, 128.7, 127.6,

[102] Van der Veken, P.; Senten, K.; Kertesz, I.; Meester, I.; Anne-Marie L.; Marie-Berthe M.; Scharpe, S.; Haemers, A.; Augustyns, K. *J. Med. Chem.* **2005**, *48*, 1768.

126.5, 124.2, 123.0, 35.0, 34.2, 26.8, 26.0 ppm. IR (neat, cm^{-1}): 2955, 2872, 1677, 1252, 965, 748, 691. HRMS *calcd*. for ($C_{15}H_{16}O_2$+Na): 251.1043, *found*: 251.1053.

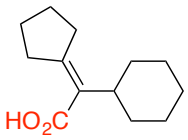

2-Cyclohexyl-2-cyclopentylideneacetic acid (2-34): Following the general procedure using **2-15** to provide **2-34** (51.3 mg, 82% yield) as a colorless solid. M.P. = 121-123 °C. ^{1}H NMR (400 MHz, $CDCl_3$) δ 2.62 (tt, *J* = 7.3, 2.2 Hz, 2H), 2.47-2.29 (m, 3H), 1.85-1.61 (m, 9H), 1.61-1.52 (m, 2H), 1.34-1.14 (m, 3H) ppm. ^{13}C NMR (100 MHz, $CDCl_3$) δ 174.9, 157.4, 128.7, 41.9, 34.1, 32.6, 30.2, 27.1, 26.7, 26.0, 25.7 ppm. IR (neat, cm^{-1}): 2918, 2848, 1656, 1604, 1418, 1324, 1279, 1233, 1189. HRMS *calcd*. for ($C_{13}H_{20}O_2$-H) 207.1391, *found*: 207.1391.

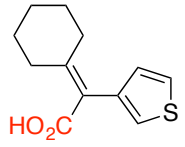

2-cyclohexylidene-2-(thiophen-3-yl)acetic acid (2-35): Following the general procedure using **2-17** to provide **2-35** (30.1 mg, 45% yield) as a colorless solid. M.P. = 120-123 °C. ^{1}H NMR (500 MHz, $CDCl_3$) δ 7.29 (dd, *J* = 4.9, 3.0 Hz, 1H), 7.10 (dd, *J* = 3.0, 1.2 Hz, 1H), 6.97 (dd, *J* = 4.9, 1.2 Hz, 1H), 2.76-2.59 (m, 2H), 2.27-2.12 (m, 2H), 1.76-1.69 (m, 2H), 1.67-1.51 (m, 4H) ppm. ^{13}C NMR (126 MHz, $CDCl_3$) δ 173.7, 156.0, 137.2, 129.4, 125.1, 123.8, 121.2, 33.4, 32.7, 28.6, 27.1, 26.5 ppm. IR (neat, cm^{-1}): 2920, 1675, 1615, 1269, 846, 723. HRMS *calcd*. for ($C_{12}H_{14}O_2S$-H): 221.0642, *found*: 221.0638.

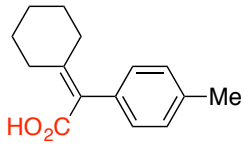

2-cyclohexylidene-2-(*p*-tolyl)acetic acid (2-36): Following the general procedure using **2-18** to provide **2-36** (48.4 mg, 70% yield) as a colorless solid. M.P. = 149-151 °C. ^{1}H NMR (500 MHz, $CDCl_3$) δ 7.17 (d, *J* = 7.8 Hz, 2H), 7.10 (d, *J* = 8.0 Hz, 2H), 2.77-2.66 (m, 2H), 2.37 (s, 3H), 2.13-2.01 (m, 2H), 1.76-1.71 (m, 2H), 1.66-1.52 (m, 4H)

ppm. ^{13}C NMR (126 MHz, $CDCl_3$) δ 174.6, 155.3, 137.0, 134.9, 129.7, 129.1, 126.4, 33.4, 32.6, 28.6, 28.6, 26.5, 21.4 ppm. IR (neat, cm^{-1}): 2931, 2851, 1677, 1620, 1278, 738, 418. HRMS *calcd*. for ($C_{15}H_{18}O_2$-H): 229.1234, *found*: 229.1234.

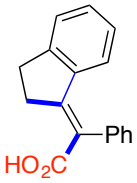

(*E*)-2-(2,3-dihydro-1H-inden-1-ylidene)-2-phenylacetic acid (2-37): Following the general procedure using **2-19** to provide **2-37** (30.0 mg, 79% yield) as a colorless solid. M.P. = 215-217 °C. ^{1}H NMR (500 MHz, DMSO-d_6) δ 7.40 (dd, J = 14.1, 7.1 Hz, 3H), 7.32 (d, J = 7.6 Hz, 1H), 7.17 (dd, J = 12.9, 7.0 Hz, 3H), 6.79 (t, J = 7.6 Hz, 1H), 5.97 (d, J = 8.0 Hz, 1H), 3.32-3.14 (m, 2H), 3.06-2.96 (m, 2H) ppm. ^{13}C NMR (126 MHz, DMSO) δ 169.1, 154.9, 150.4, 139.5, 139.0, 129.9, 129.6, 129.1, 127.6, 126.1, 126.0, 125.7, 33.1, 30.1 ppm. IR (neat, cm^{-1}): 3048, 2929, 2798, 1672, 1580, 1259, 752, 698, 454. HRMS *calcd*. for ($C_{19}H_{18}O_2$-H): 249.0921, *found*: 249.0923.

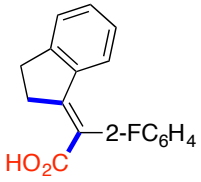

(*E*)-2-(2,3-dihydro-1H-inden-1-ylidene)-2-(2-fluorophenyl)acetic acid (2-38). Following the general procedure using **2-20** to provide **2-38** (**2-38**: **2-38'** > 19:1, 71.6 mg, 89% yield) as a colorless solid. M.P. = 207-209 °C. Spectra for the major product **2-38**: 1H NMR (400 MHz, $CDCl_3$) δ 7.48-7.41 (m, 2H), 7.36-7.29 (m, 1H), 7.26-7.17 (m, 3H), 6.89 (dd, J = 8.3, 7.2 Hz, 1H), 6.23 (d, J = 8.0 Hz, 1H), 3.81-3.31 (m, 2H), 3.21-2.76 (m, 2H) ppm. ^{13}C NMR (101 MHz, $CDCl_3$) δ 173.0, 162.8, 161.7, 159.3, 151.7, 139.6, 132.2 (d, J = 3.2 Hz), 130.7, 130.1 (d, J = 7.9 Hz), 126.5 (d, J = 2.5 Hz), 125.9 (d, J = 17.3 Hz), 125.6, 124.8 (d, J = 3.6 Hz), 117.5, 116.2 (d, J = 22.1 Hz), 34.1, 30.7 ppm. IR (neat, cm^{-1}): 2906, 1672, 1581, 1259, 753. HRMS *calcd.* For ($C_{17}H_{13}FO_2$-H): 267.0827, *found*: 267.0828.

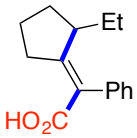

(*E*)-2-(2-ethylcyclopentylidene)-2-phenylacetic acid (2-45): Following the general procedure using **2-40** to provide **2-45** (35.0 mg, **2-45**:**2-45'** = 12.5:1, 51% yield) as a colorless solid. M.P. = 118-120 °C. Spectra for the major product **2-46**: ^{1}H NMR (500 MHz, $CDCl_3$) δ 7.30-7.36 (m, 2H), 7.32-7.20 (m, 1H), 7.23-7.13 (m, 2H), 3.04-2.78 (m, 2H), 2.56 (td, *J* = 7.4, 3.6 Hz, 1H), 1.86-1.51 (m, 4H), 1.11 (dt, *J* = 14.9, 7.5 Hz, 1H), 0.99 (dt, *J* = 17.1, 13.4 Hz, 1H), 0.58 (t, *J* = 7.4 Hz, 3H) ppm. ^{13}C NMR (126 MHz, $CDCl_3$) δ 173.0, 171.1, 138.4, 129.9, 128.2, 127.2, 125.5, 46.9, 34.0, 29.6, 25.2, 23.9, 12.1 ppm. IR (neat, cm^{-1}): 2957, 2871, 1676, 1661, 1614, 1282, 702. HRMS *calcd*. for ($C_{15}H_{18}O_2$-H): 229.1234, *found*: 229.1231.

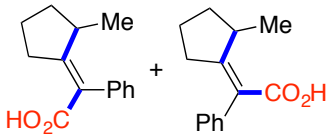

(*E*)-2-phenyl-2-(2-phenylcyclopentylidene)acetic acid (2-46): Following the general procedure using **2-39** to provide **2-46** (55.5 mg, **2-46**:**2-46'** = 4:1, 86% yield) as a colorless solid. M.P. = 114-116 °C. Spectra for the major product **2-46**: ^{1}H NMR (500 MHz, $CDCl_3$) δ 7.40-7.32 (m, 2H), 7.32-7.27 (m, 1H), 7.21-7.17 (m, 2H), 3.08-2.94 (m, 1H), 2.93-2.81 (m, 1H), 2.78-2.65 (m, 1H), 1.91-1.64 (m, 4H), 0.70 (d, *J* = 7.2 Hz, 3H) ppm. ^{13}C NMR (126 MHz, $CDCl_3$) δ 172.8, 171.9, 138.3, 129.9, 128.3, 127.2, 125.4, 40.0, 33.8, 27.1, 23.8, 18.7 ppm. IR (neat, cm^{-1}): 2959, 2869, 1676, 1660, 1614, 1283, 1247, 701. HRMS *calcd*. for ($C_{14}H_{16}O_2$-H): 215.1078, *found*: 215.1076.

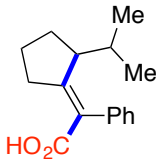

(*E*)-2-(2-isopropylcyclopentylidene)-2-phenylacetic acid (2-47): Following the general procedure using **2-41** to provide **2-47** (33.7 mg, **2-47**:**2-47'** > 95:5, 46% yield) as a colorless solid. M.P. = 174-177 °C. Spectra for the major product **2-47**: ^{1}H NMR (500 MHz, $CDCl_3$) δ 7.34 (t, *J* = 7.3 Hz, 2H), 7.32-7.26 (m, 1H), 7.22-7.14 (m, 2H),

3.13 (dd, J = 18.9, 7.0 Hz, 1H), 2.81-2.71 (m, 1H), 2.71-2.55 (m, 1H), 1.93-1.78 (m, 1H), 1.75-1.50 (m, 4H), 1.35 (dt, J = 13.6, 6.8 Hz, 1H), 0.62 (d, J = 6.8 Hz, 3H), 0.58 (d, J = 6.8 Hz, 3H) ppm. ^{13}C NMR (126 MHz, $CDCl_3$) δ 173.7, 169.6, 138.5, 129.7, 128.3, 127.3, 126.1, 50.6, 35.3, 28.5, 25.7, 24.7, 21.6, 17.2 ppm. IR (neat, cm^{-1}): 2957, 2869, 1672, 1609, 1270, 699. HRMS *calcd*. for ($C_{16}H_{20}O_2$-H): 243.1391, *found*: 243.1390.

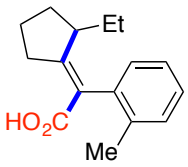

(*E*)-2-(2-ethylcyclopentylidene)-2-(o-tolyl)acetic acid (2-48): Following the general procedure using **2-42** to provide **2-48** (39.0 mg, **2-48**:**2-48'** > 95:5, 53% yield) as a colorless solid. M.P. = 137-139 °C. Spectra for the major product **2-48**: ^{1}H NMR (500 MHz, DMSO-d_6) δ 7.23-7.12 (m, 3H), 7.04 (d, J = 6.6 Hz, 1H), 2.82 (td, J = 7.4, 3.9 Hz, 2H), 2.10 (s, 3H), 1.82-1.41 (m, 7H), 0.52 (t, J = 7.4 Hz, 3H) ppm. ^{13}C NMR (126 MHz, DMSO-d_6) δ 168.3, 164.5, 139.4, 138.6, 129.7, 129.6, 127.0, 126.9, 125.8, 33.4, 30.3, 29.1, 26.8, 19.4, 19.1, 11.9 ppm. IR (neat, cm^{-1}): 2950, 2871, 1676, 1614, 1271, 1245, 728, 447. HRMS *calcd*. for ($C_{16}H_{20}O_2$-H): 243.1391, *found*: 243.1395.

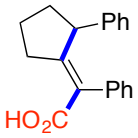

(*E*)-2-phenyl-2-(2-phenylcyclopentylidene)acetic acid (2-49): Following the general procedure using **2-43** to provide **2-49** (53.7 mg, **2-49**:**2-49'** > 95:5, 64% yield) as a colorless solid. M.P. = 153-155 °C. Spectra for the major product **5e**: ^{1}H NMR (500 MHz, $CDCl_3$) δ 7.17-7.00 (m, 6H), 6.93-6.69 (m, 4H), 3.72 (dd, J = 7.6, 5.1 Hz, 1H), 3.23 (dt, J = 19.7, 7.0 Hz, 1H), 3.15-2.97 (m, 1H), 2.19-2.00 (m, 1H), 1.98-1.86 (m, 1H), 1.86-1.58 (m, 2H) ppm. ^{13}C NMR (126 MHz, $CDCl_3$) δ 173.0, 169.2, 145.1, 137.8, 129.4, 128.1, 127.8, 127.6, 126.9, 125.7, 52.1, 36.4, 35.7, 24.7 ppm. IR (neat, cm^{-1}): 2955, 1674, 1658, 1278, 1248, 694. HRMS *calcd*. for ($C_{19}H_{18}O_2$-H): 277.1234, *found*: 277.1234.

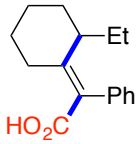

(*E*)-2-(2-ethylcyclohexylidene)-2-phenylacetic acid (2-50): Following the general procedure using **2-44** to provide **2-50** (33.3 mg, **2-50**:**2-50'** > 95:5, 44% yield) as a colorless solid. M.P. = 139-141 °C. Spectra for the major product **2-50**: ^{1}H NMR (400 MHz, $CDCl_3$) δ 7.38-7.31 (m, 2H), 7.30-7.27 (m, 1H), 7.21-7.14 (m, 2H), 3.23 (d, *J* = 13.0 Hz, 1H), 2.28 (dt, *J* = 10.8, 5.9 Hz, 1H), 2.13 (td, *J* = 13.5, 4.5 Hz, 1H), 1.93-1.87 (m, 1H), 1.75-1.33 (m, 7H), 0.69 (t, *J* = 7.4 Hz, 3H) ppm. ^{13}C NMR (101 MHz, $CDCl_3$) δ 173.6, 157.8, 137.8, 129.6, 128.6, 128.2, 127.1, 40.8, 31.5, 28.7, 27.3, 24.5, 20.6, 11.9 ppm. IR (neat, cm^{-1}): 2931, 2852, 1671, 1609, 1225, 701, 429. HRMS *calcd*. for ($C_{16}H_{20}O_2$-H): 243.1391, *found*: 243.1388.

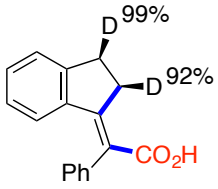

(*E*)-2-(2,3-didutero-2,3-dihydro-1*H*-inden-1-ylidene)-2-phenylacetic acid (2-74): Following the general procedure using **2-73** to provide 2-**74** (65.2 mg, 86% yield) as a colorless solid. M.P. = 217-219 °C. ^{1}H NMR (500 MHz, $CDCl_3$) δ 7.52-7.39 (m, 3H), 7.34-7.25 (m, 3H), 7.20 (td, *J* = 7.4, 1.1 Hz, 1H), 6.83 (dd, *J* = 8.2, 7.2 Hz, 1H), 6.13 (d, *J* = 8.1 Hz, 1H), 3.42 (d, *J* = 8.8 Hz, 1H), 3.05 (d, *J* = 8.2 Hz, 1H) ppm. ^{13}C NMR (126 MHz, $CDCl_3$) δ 173.6, 160.7, 151.3, 139.9, 138.4, 130.3, 130.0, 129.3, 127.9, 127.3, 126.3, 125.5, 124.3, 34.51 (t, *J* = 20.9 Hz), 30.30 (t, *J* = 19.7 Hz) ppm. IR (neat, cm^{-1}): 3048, 2932, 2796, 1650, 1576, 1443, 1261, 937, 721. HRMS *calcd.* for ($C_{15}H_{19}Br$+H): 279.0743, *found*: 279.0730.

2.6.5 Selected Examples of NMR Spectra

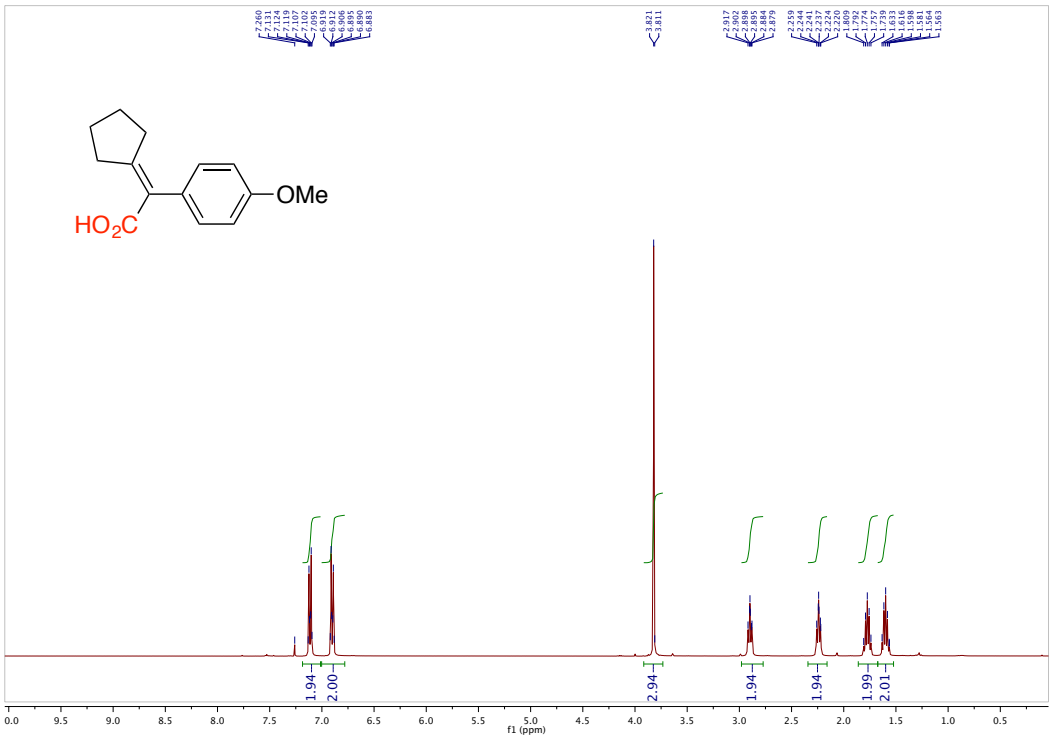

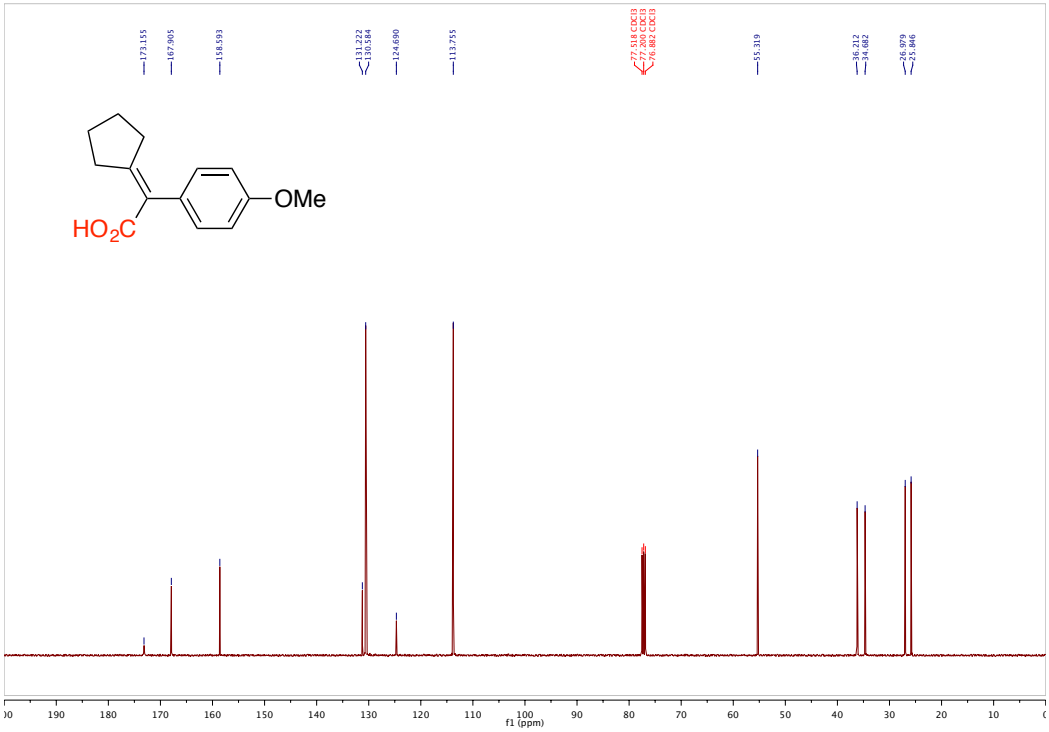

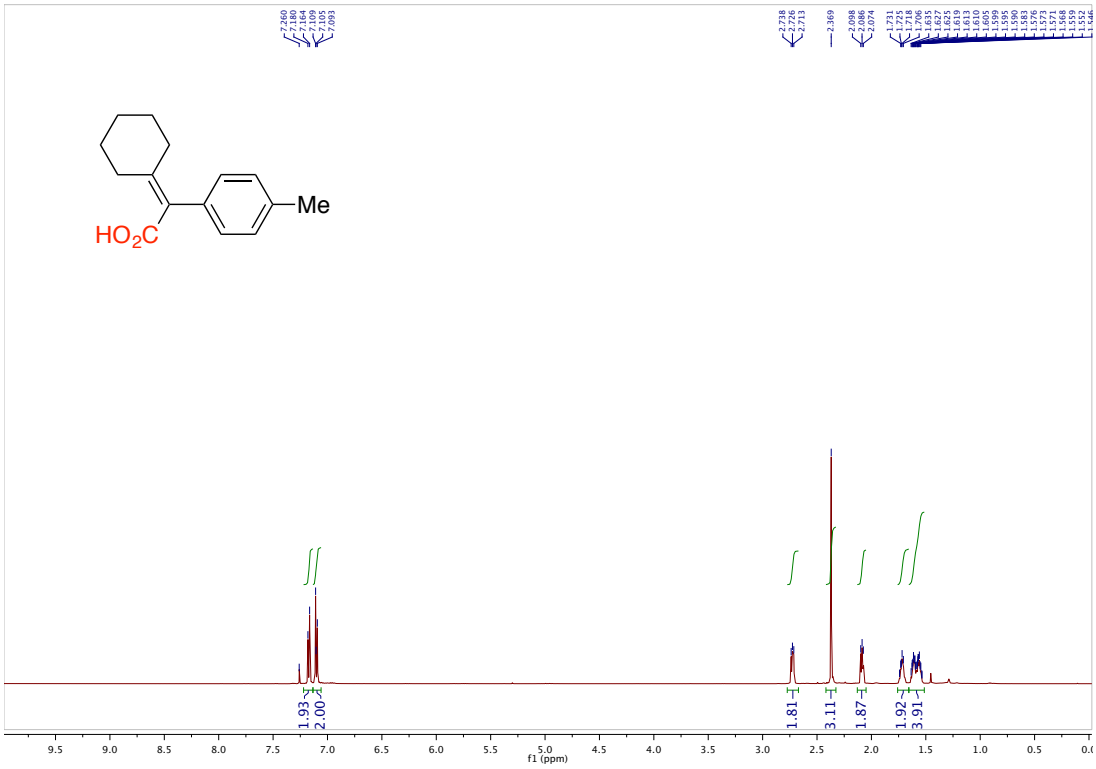
Me
HO2C
f1 (ppm)

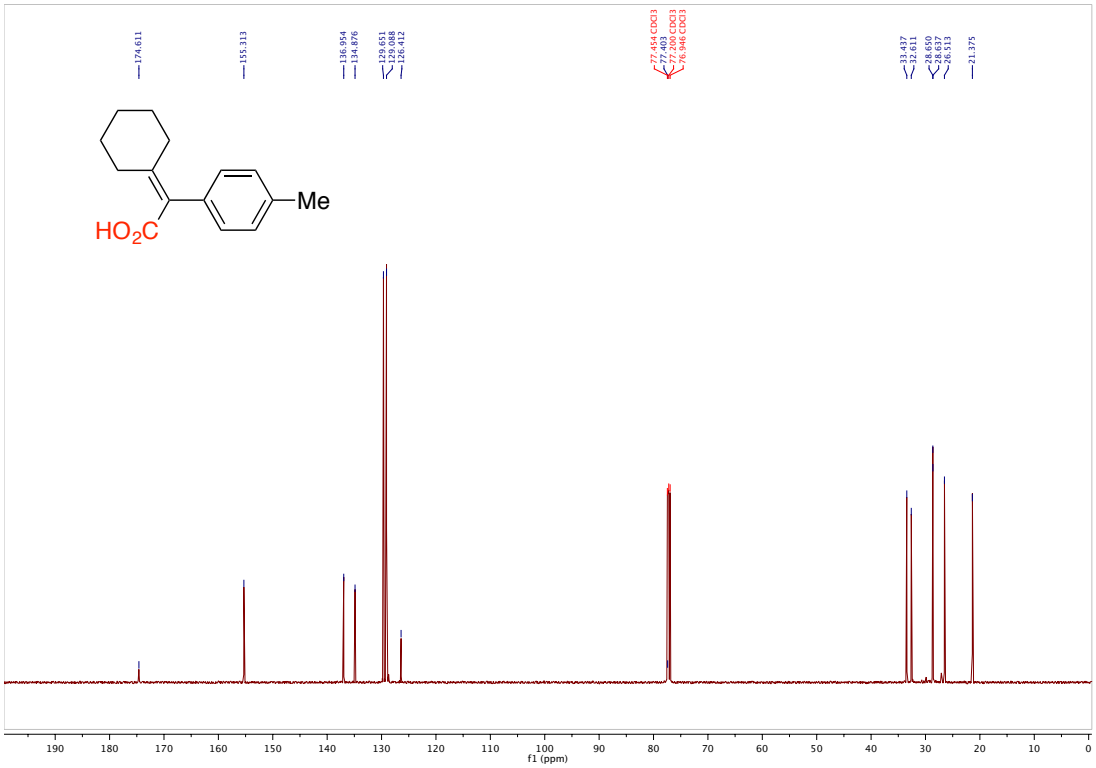
Me
HO2C
f1 (ppm)

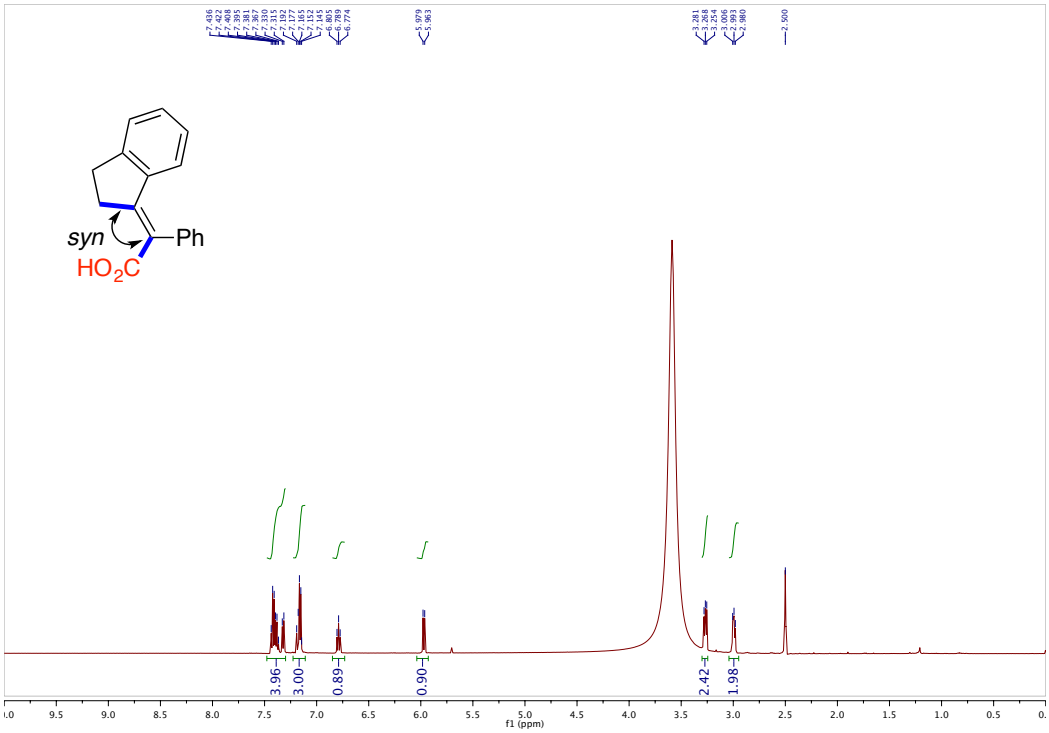
syn
Ph
HO2C
3.96
3.00
0.89
0.90
2.42
1.98
f1 (ppm)

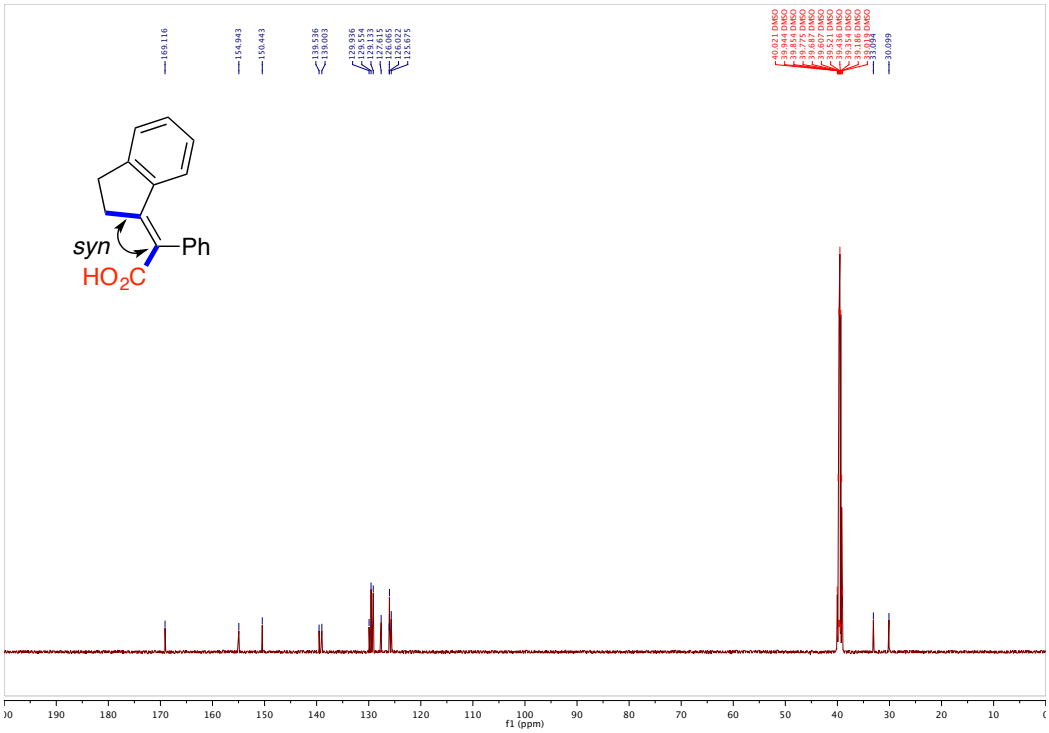
syn
Ph
HO2C
f1 (ppm)

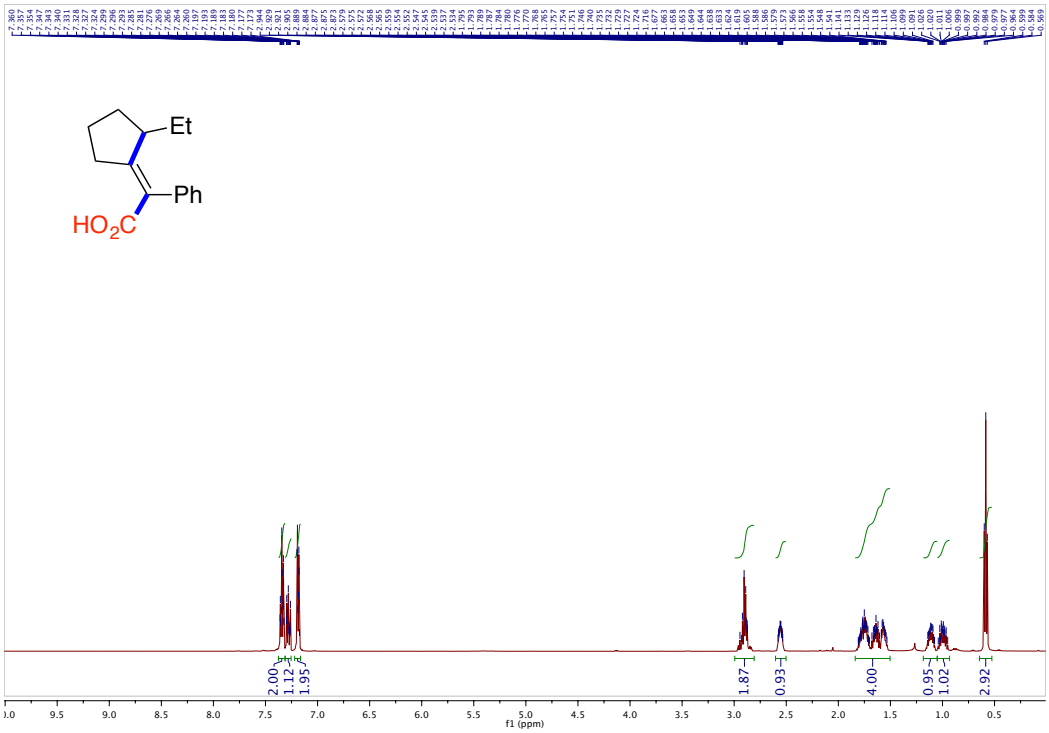
Et
Ph
HO2C
2.00
1.12
1.95
1.87
0.93
4.00
0.95
1.02
2.92
f1 (ppm)

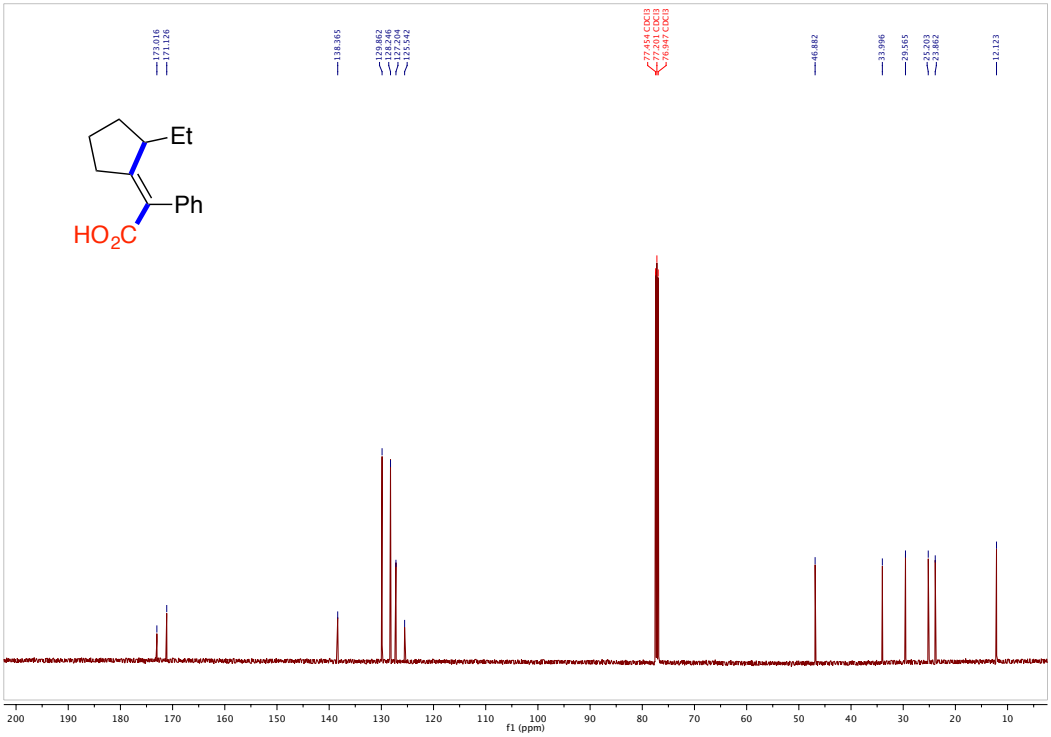
Et
Ph
HO2C
f1 (ppm)

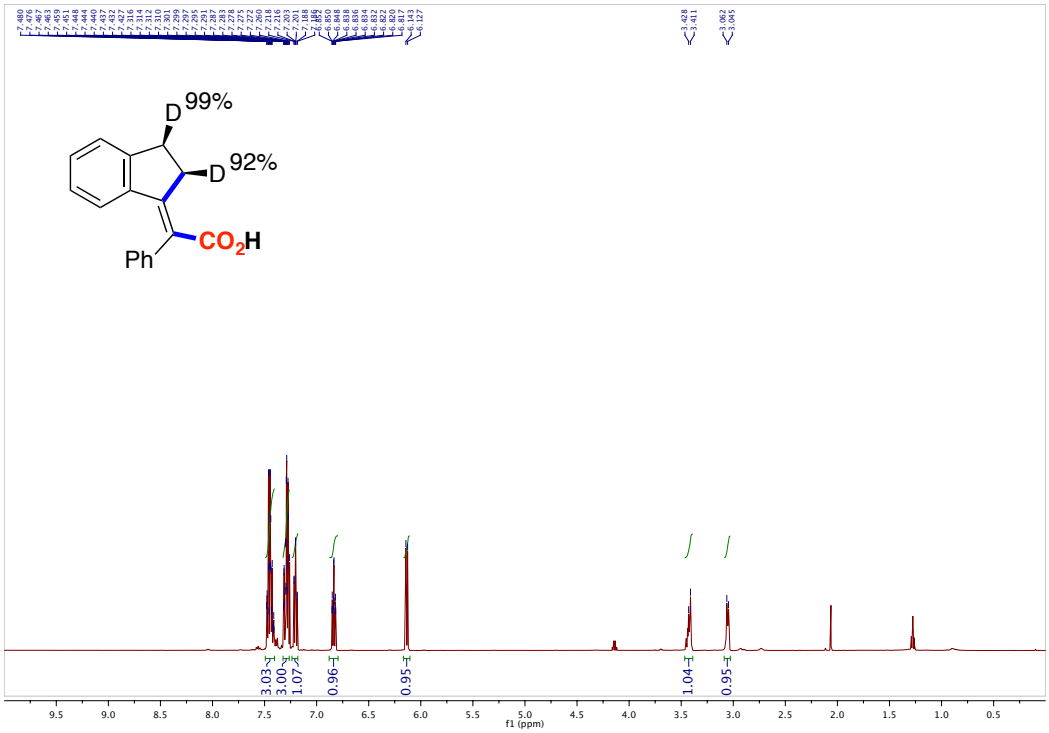
D 99%
D 92%
CO2H
Ph
3.03
3.00
1.07
0.96
0.95
1.04
0.95
f1 (ppm)

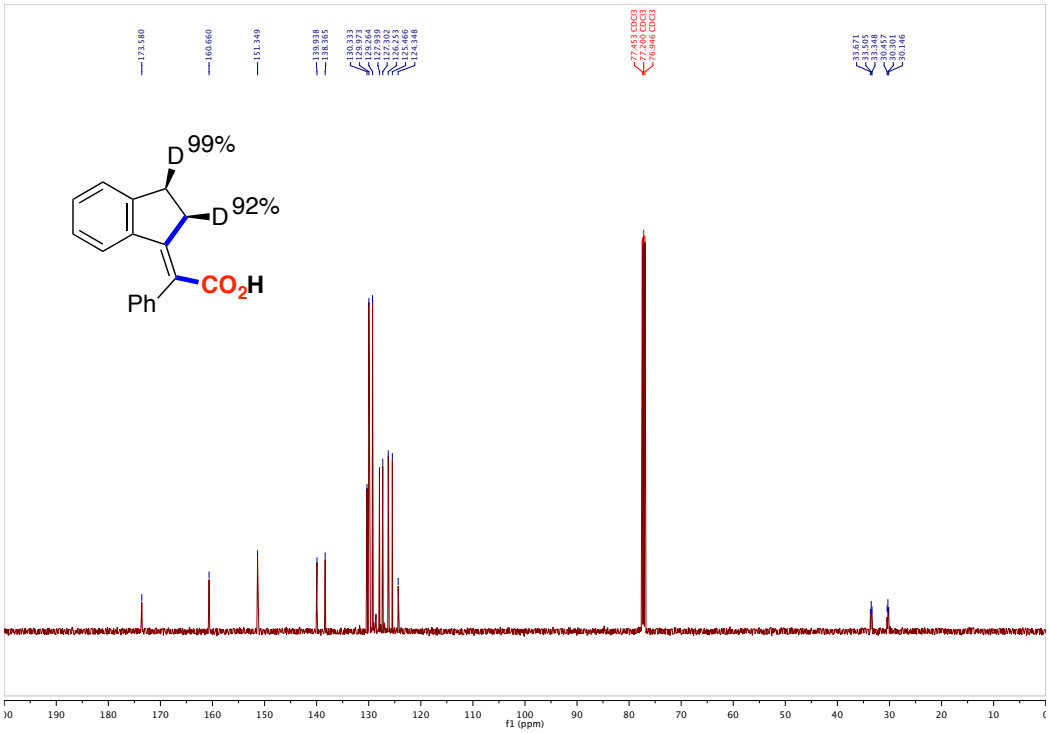
D 99%
D 92%
CO2H
Ph
f1 (ppm)

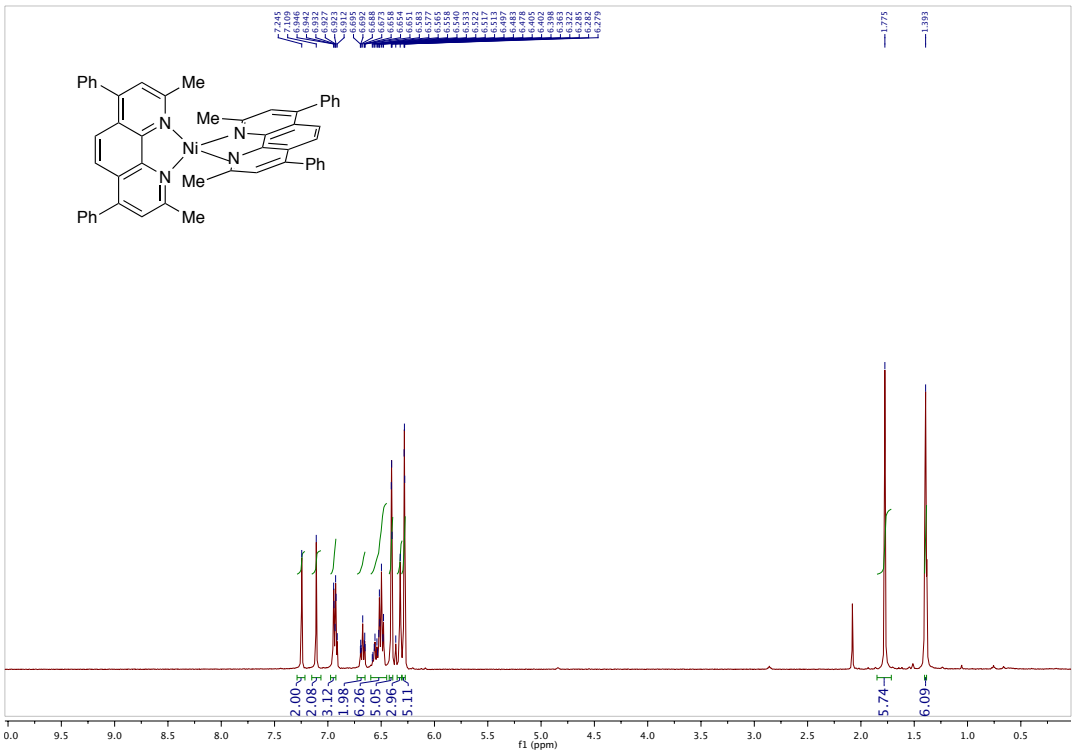
Ph
Me
N
Ni
N
Me
Ph
Me
N
N
Ph
Ph
Me
2.00
2.08
3.12
1.98
6.26
5.05
2.96
5.11
5.74
6.09
f1 (ppm)

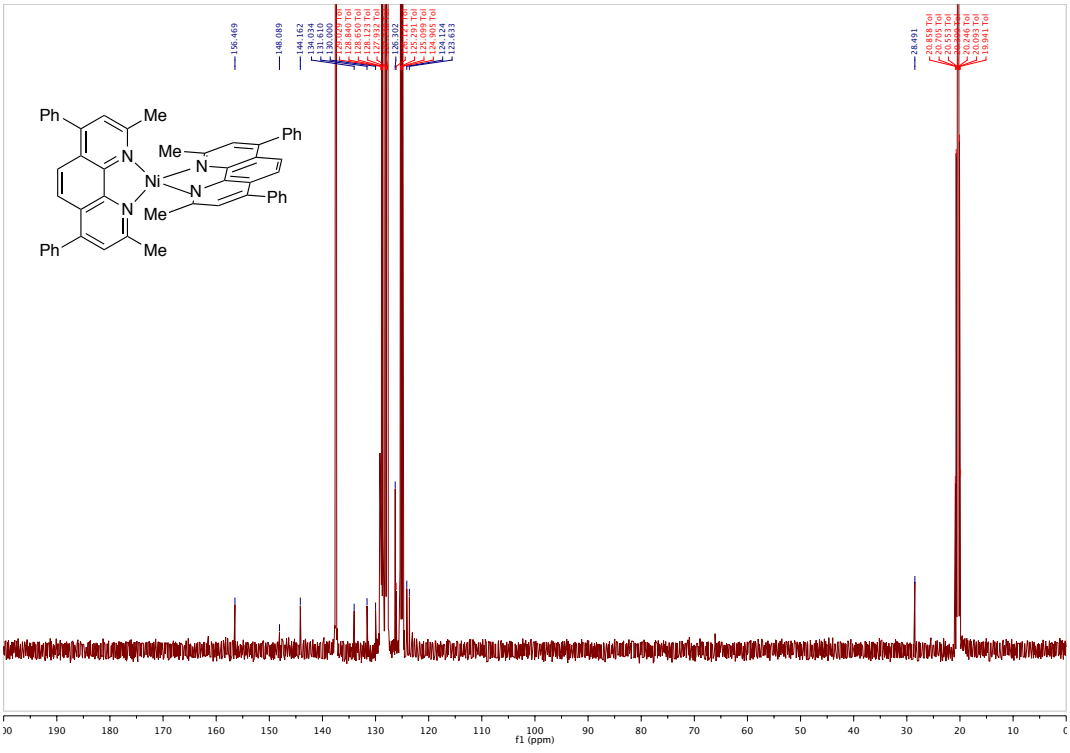
Ph
Me
N
Ni
N
Me
Ph
Me
N
N
Ph
Ph
Me
f1 (ppm)

2.6.6 X-Ray Crystallographic Data for 2-37 and 2-46

X-Ray Crystallography of 2-37

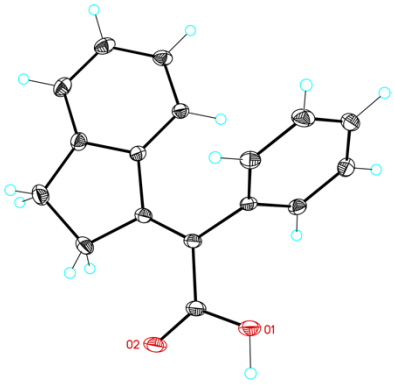

Table 1. Crystal data and structure refinement for **2-37**

Identification code	**2-37**
Empirical formula	C17 H14 O2
Formula weight	250.28
Temperature	100(2) K
Wavelength	0.71073 Å
Crystal system	Triclinic
Space group	P-1
Unit cell dimensions	a = 5.6858(12)Å a= 91.607(5)°.
	b = 7.8358(17)Å b = 95.157(4)°.
	c = 14.314(3)Å g = 90.745(5)°.
Volume	634.8(2) Å3
Z	2
Density (calculated)	1.309 Mg/m3
Absorption coefficient	0.085 mm-1
F(000)	264
Crystal size	0.25 x 0.25 x 0.03 mm3
Theta range for data collection	2.601 to 35.771°.
Index ranges	-9<=h<=8,-6<=k<=12,-23<=l<=22
Reflections collected	9944
Independent reflections	5433[R(int) = 0.0248]
Completeness to theta =35.771°	91.9%

Absorption correction	Empirical
Max. and min. transmission	0.997 and 0.811
Refinement method	Full-matrix least-squares on F2
Data / restraints / parameters	5433/ 0/ 174
Goodness-of-fit on F2	1.046
Final R indices [I>2sigma(I)]	R1 = 0.0505, wR2 = 0.1326
R indices (all data)	R1 = 0.0716, wR2 = 0.1468
Largest diff. peak and hole	0.607 and -0.225 e.Å-3

Table 2. Bond lengths [Å] and angles [°] for **2-37**.

Bond lengths----

O1-C17	1.3254(12)
O2-C17	1.2372(11)
C1-C10	1.3600(13)
C1-C9	1.4823(12)
C1-C2	1.5223(13)
C2-C3	1.5443(15)
C3-C4	1.5053(14)
C4-C5	1.3968(14)
C4-C9	1.4065(13)
C5-C6	1.3909(15)
C6-C7	1.3980(15)
C7-C8	1.3915(13)
C8-C9	1.4041(13)
C10-C17	1.4782(12)
C10-C11	1.4919(12)
C11-C16	1.3949(14)
C11-C12	1.3974(12)
C12-C13	1.3984(13)
C13-C14	1.3868(16)
C14-C15	1.3927(14)
C15-C16	1.3911(13)

Angles----------

C10-C1-C9 126.46(8)

C10-C1-C2 127.14(8)

C9-C1-C2 106.37(8)

C1-C2-C3 105.84(7)

C4-C3-C2 104.12(8)

C5-C4-C9 120.82(9)

C5-C4-C3 127.97(9)

C9-C4-C3 111.21(8)

C6-C5-C4 118.70(9)

C5-C6-C7 120.75(9)

C8-C7-C6 120.77(9)

C7-C8-C9 118.92(9)

C8-C9-C4 119.80(8)

C8-C9-C1 130.69(8)

C4-C9-C1 109.47(8)

C1-C10-C17 121.38(8)

C1-C10-C11 121.62(7)

C17-C10-C11 116.96(8)

C16-C11-C12 119.22(8)

C16-C11-C10 120.20(8)

C12-C11-C10 120.44(8)

C11-C12-C13 119.98(9)

C14-C13-C12 120.24(9)

C13-C14-C15 119.96(9)

C16-C15-C14 119.85(10)

C15-C16-C11 120.62(8)

O2-C17-O1 122.13(8)

O2-C17-C10 124.21(9)

O1-C17-C10 113.64(8)

Table 3. Torsion angles [°] for **2-37**.

C10-C1-C2-C3	160.46(10)
C9-C1-C2-C3	-17.48(11)
C1-C2-C3-C4	15.23(11)
C2-C3-C4-C5	172.24(10)
C2-C3-C4-C9	-7.69(12)
C9-C4-C5-C6	2.57(15)
C3-C4-C5-C6	-177.35(10)
C4-C5-C6-C7	1.87(15)
C5-C6-C7-C8	-3.65(15)
C6-C7-C8-C9	0.91(14)
C7-C8-C9-C4	3.48(13)
C7-C8-C9-C1	-179.05(9)
C5-C4-C9-C8	-5.28(14)
C3-C4-C9-C8	174.65(8)
C5-C4-C9-C1	176.75(9)
C3-C4-C9-C1	-3.31(11)
C10-C1-C9-C8	17.54(16)
C2-C1-C9-C8	-164.51(9)
C10-C1-C9-C4	-164.79(10)
C2-C1-C9-C4	13.16(10)
C9-C1-C10-C17	-174.57(9)
C2-C1-C10-C17	7.89(16)
C9-C1-C10-C11	3.17(15)
C2-C1-C10-C11	-174.37(9)
C1-C10-C11-C16	-102.50(11)
C17-C10-C11-C16	75.33(11)
C1-C10-C11-C12	73.18(12)
C17-C10-C11-C12	-108.99(10)
C16-C11-C12-C13	2.64(14)
C10-C11-C12-C13	-173.09(8)
C11-C12-C13-C14	0.77(15)

C12-C13-C14-C15 -2.94(15)

C13-C14-C15-C16 1.69(15)

C14-C15-C16-C11 1.76(15)

C12-C11-C16-C15 -3.91(14)

C10-C11-C16-C15 171.83(8)

C1-C10-C17-O2 2.41(16)

C11-C10-C17-O2 -175.43(10)

C1-C10-C17-O1 -179.10(9)

C11-C10-C17-O1 3.06(13)

X-Ray Crystallography of 2-46

Table 1. Crystal data and structure refinement for **2-46**.

Identification code	**2-46**
Empirical formula	C15 H18 O2
Formula weight	230.29
Temperature	100(2) K
Wavelength	0.71073 Å
Crystal system	Monoclinic
Space group	P2(1)/n
Unit cell dimensions	a = 14.6838(19)Å a= 90°.
	b = 5.5897(7)Å b = 106.256(3)°.
	c = 16.502(2)Å g = 90°.

Volume 1300.3(3) Å3

Z 4

Density (calculated) 1.176 Mg/m3

Absorption coefficient 0.077 mm-1

F(000) 496

Crystal size 0.04 x 0.01 x 0.001 mm3

Theta range for data collection 2.186 to 33.790°.

Index ranges -22<=h<=17,-8<=k<=5,-23<=l<=22

Reflections collected 14737

Independent reflections 4851[R(int) = 0.0438]

Completeness to theta =33.790° 92.7%

Absorption correction Empirical

Max. and min. transmission 1.000 and 0.942

Refinement method Full-matrix least-squares on F2

Data / restraints / parameters 4851/ 0/ 156

Goodness-of-fit on F2 1.026

Final R indices [I>2sigma(I)] R1 = 0.0468, wR2 = 0.1341

R indices (all data) R1 = 0.0551, wR2 = 0.1421

Largest diff. peak and hole 0.458 and -0.195 e.Å-3

Table 2. Bond lengths [Å] and angles [°] for **2-46**.

Bond lengths----

C1-O1 1.2413(9)

C1-O2 1.3021(10)

C1-C2 1.4766(10)

C2-C3 1.3506(11)

C2-C10 1.4945(10)

C3-C7 1.5169(11)

C3-C4 1.5178(10)

C4-C5 1.5382(12)

C5-C6 1.5323(14)

C6-C7 1.5395(13)

C7-C8 1.5410(14)

C8-C9 1.5226(17)

C10-C11 1.3949(11)

C10-C15 1.3960(10)

C11-C12 1.3957(11)

C12-C13 1.3862(13)

C13-C14 1.3877(13)

C14-C15 1.3902(11)

Angles----------

O1-C1-O2 122.12(7)

O1-C1-C2 123.05(7)

O2-C1-C2 114.83(6)

C3-C2-C1 121.04(6)

C3-C2-C10 122.79(6)

C1-C2-C10 116.15(6)

C2-C3-C7 123.02(7)

C2-C3-C4 128.11(7)

C7-C3-C4 108.86(6)

C3-C4-C5 105.30(6)

C6-C5-C4 103.97(7)

C5-C6-C7 103.67(7)

C3-C7-C6 103.23(7)

C3-C7-C8 110.53(7)

C6-C7-C8 112.76(8)

C9-C8-C7 111.97(12)

C11-C10-C15 118.66(7)

C11-C10-C2 121.15(7)

C15-C10-C2 120.16(7)

C10-C11-C12 120.54(7)

C13-C12-C11 120.08(8)

C12-C13-C14 119.90(7)

C13-C14-C15 120.00(8)

C14-C15-C10 120.82(7)

Table 3. Torsion angles [°] for **2-46**.

O1-C1-C2-C3	-2.19(13)
O2-C1-C2-C3	177.34(8)
O1-C1-C2-C10	179.42(8)
O2-C1-C2-C10	-1.05(10)
C1-C2-C3-C7	-176.92(7)
C10-C2-C3-C7	1.36(12)
C1-C2-C3-C4	3.62(12)
C10-C2-C3-C4	-178.10(7)
C2-C3-C4-C5	-177.93(8)
C7-C3-C4-C5	2.55(9)
C3-C4-C5-C6	-25.05(9)
C4-C5-C6-C7	38.08(9)
C2-C3-C7-C6	-158.79(8)
C4-C3-C7-C6	20.76(9)
C2-C3-C7-C8	80.39(10)
C4-C3-C7-C8	-100.06(8)
C5-C6-C7-C3	-36.09(9)
C5-C6-C7-C8	83.20(9)
C3-C7-C8-C9	-169.97(10)
C6-C7-C8-C9	75.06(12)
C3-C2-C10-C11	79.69(10)
C1-C2-C10-C11	-101.95(9)
C3-C2-C10-C15	-102.34(9)
C1-C2-C10-C15	76.02(10)
C15-C10-C11-C12	0.19(12)
C2-C10-C11-C12	178.19(8)
C10-C11-C12-C13	0.15(14)
C11-C12-C13-C14	-0.50(14)
C12-C13-C14-C15	0.51(14)

C13-C14-C15-C10 -0.17(14)

C11-C10-C15-C14 -0.18(13)

C2-C10-C15-C14 -178.20(8)

Chapter 3: Ni-catalyzed Regioselective Hydrocarboxylation of Alkynes with CO_2 Using Simple Alcohols as Proton Sources

3.1 Objectives

❖To develop a mild and user-friendly Ni-catalyzed regioselective hydrocarboxylation of alkynes with CO_2 (1 atm) using simple and unconventional proton sources, which was not accessible by a traditional way, affording quick access to tri-substituted acrylic acid derivatives from simple starting materials.

❖To gain insights into the underlying mechanism by studying the effect of radical scavengers, stoichiometric reactions, isotopic experiments as well as kinetic isotope effects.

3.2 Introduction to the Hydrocarboxylation of Alkynes with CO_2

The recent years have witnessed tremendous progress within the cross-coupling arena, invariably leading to new knowledge in catalytic design.[103] Unfortunately, site selectivity is oftentimes sacrificed at the expense of discovering new reactivity.[104] Indeed, the ability to switch the outcome of catalytic endeavors in a rational and predictable manner still remains a formidable challenge. Undoubtedly, such a selectivity switch scenario represents a unique opportunity to increase our ever-growing chemical repertoire and improve the flexibility in synthetic design.

As shown in chapter 1, the utilization of carbon dioxide (CO_2) as an abundant and inexpensive C1-synthon has gained considerable momentum in catalytic reductive events,[105] holding promise for defining new paradigms en route to carboxylic acids, which are privileged motifs in a myriad of pharmaceuticals.[106] Intriguingly, a limited number of catalytic carboxylation protocols of alkynes with CO_2 have been described. Among these, hydrocarboxylation reactions are particularly appealing, providing rapid access to industrially relevant acrylic acids.[107] In 2011, Tsuji and Ma independently reported an elegant hydrocarboxylation of alkynes with air-sensitive and pyrophoric Et_2Zn (Scheme 3.1, *path a*) or pre-formed silanes (*path b*) as hydride sources. A close inspection of these procedures indicates that CO_2 insertion preferentially occurs adjacent to aromatic or directing groups;[66,69] furthermore, low selectivity profiles were found for sterically unbiased substrates. While we anticipated that altering such selectivity pattern might be rather problematic, we were attracted to the challenge of providing approaches for retrosynthetic analysis while leading to previously

[103] Diederich, F.; de Meijere, A., Eds. *Metal-Catalyzed Cross-Coupling Reactions*; Wiley-VCH: Weinheim, 2004**.**

[104] For selected reviews: (a) Mahatthananchai, J.; Dumas, A. M.; Bode, J. W. *Angew. Chem. Int. Ed.* **2012**, *51*, 10954. (b) Afagh, N. A.; Yudin, A. K. *Angew. Chem. Int. Ed.* **2010**, *49*, 262. (c) Neufeldt, S. R.; Sanford, M. S. *Acc. Chem. Res.* **2012**, *45*, 936.

[105] Selected reviews: (a) Moragas, T.; Correa, A.; Martin, R. *Chem. Eur. –J.* **2014**, *20*, 8242. (b) Tasker, S. Z.; Standley, E. A.; Jamison, T. F. *Nature* **2014**, *509*, 299. (c) Everson, D. A.; Weix, D. J. *J. Org. Chem.* **2014**, *79*, 4793. (d) Knappe, C. E. I.; Grupe, S.; Gärtner, D.; Corpet, M.; Gosmini, C.; Jacobi von Wangelin, A. *Chem. Eur. J.* **2014**, *20*, 6828. (e) Montgomery, J. *Organonickel Chemistry. Organometallics in Synthesis*; Ed. John Wiley & Sons, Inc.; Hoboken, 2013.

[106] For selected examples: (a) Patai, S. *The Chemistry of Acid Derivatives*; Wiley: New York, 1992. (b) Gooßen, L. J.; Rodríguez, N.; Gooßen, K. *Angew. Chem. Int. Ed.* **2008**, *47*, 3100. (c) Maag, H. *Prodrugs of Carboxylic Acids*; Springer: New York, 2007.

[107] Wittcoff, H. A.; Reuben, B. G.; Plotkin, J. S. *Industrial Organic Chemicals;* Ed.; John Wiley & Sons, Inc.; Hoboken, 2012.

inaccessible building blocks. In line with our studies in CO_2, we envisaged develop an exceedingly practical and user-friendly hydrocarboxylation of alkynes that obviates the need for air-sensitive or organometallic reagents (*path c*).

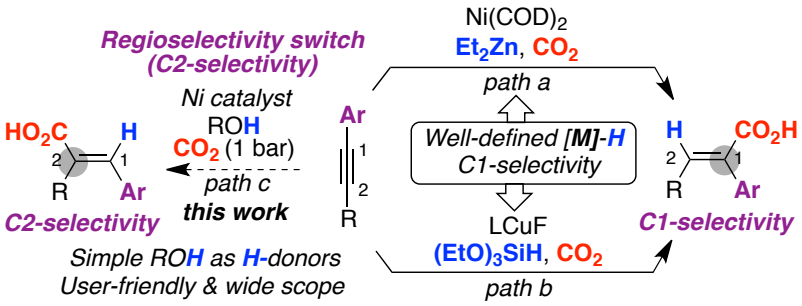

Scheme 3.1. Hydrocarboxylation of Alkynes with CO_2.

3.3 Screening of the Reaction Conditions

We started our investigation by performing a carboxylation reaction with diphenylacetylene **3-1** in the presence of $NiCl_2$·glyme as precatalyst, isopropanol **3-2** as proton source, bathocuproine (**L8**) as ligand, Mn as reducing reagent under atmospheric pressure of CO_2 in DMF at room temperature overnight. To our delight, we found the desired product **3-3** formed in 85% isolated yield under this mild condition.

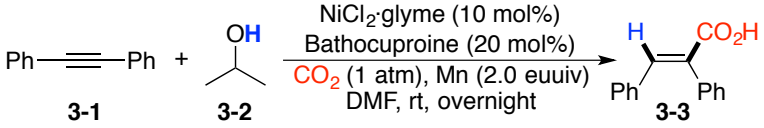

Scheme 3.2. Ni-catalyzed reductive carboxylation of **3-1** with CO_2.

Encouraged by this finding, we decided to employ **3-1** as our model substrate to study our Ni-catalyzed hydrocarboxylation protocol. We studied the effect of several experimental parameters such as nickel precatalysts, ligands, catalyst loading, temperature, the amount of reductant, the ratio of metal to ligand, the amount of proton source and additives, among other factors. The first parameter we examined was Ni-precatalysts as summarized in Table 3.1. In general, NiX_2 (X = halide) could initiate this transformation, delivering **3-3** in acceptable to good yields (Entries 1, and 2- 6). However, other precatalyst such as $Ni(acac)_2$ did not have any effect as no conversion was observed under the given conditions.

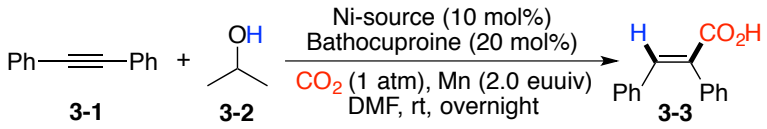

Entry	Ni-source	Conversion (%)[b]	Yield (%)[c]
1	$NiCl_2$·glyme	100	85
2	$NiBr_2$·diglyme	100	72
3	NiI_2	78	35
4	$NiBr_2$	92	66
5	$NiCl_2$	100	74

[a] Reaction condition: **3-1** (0.25 mmol), **3-2** (0.5 mmol), Ni-cat. (10 mol%), ligand (20 mol%), Mn (2.0 equiv), DMF (1 mL), rt, overnight. [b] HPLC conversions, determined by using naphthalene as internal standard. [c] HPLC yields, determined by using naphthalene as internal standard.

Table 3.1. Screening of nickel precatalysts.[a]

The screening of ligands showed us that only **L3** and **L7** (Table 3.2, Entries 3 & 7), which bear methyl groups at the *ortho*-positions, were beneficial for our hydrocarboxylation protocol, affording the final acids in 75% and 66%, respectively. On the other hand, the rest of the monodentate and bidentate N-containing ligands were tested, such as bipyridine (**L2**) and phenanthrolines (**L8** *vs* **L5**, **L6**) were not suitable (Entries 1-2, 4-6 & 9), once again demonstrating the importance of alkyl substituents at the *ortho*-position of the coordinating nitrogen.

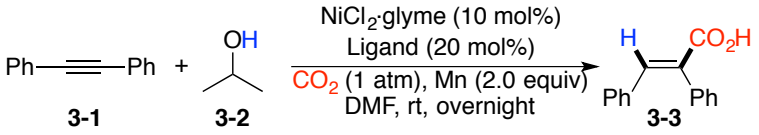

3-1 **3-2** **3-3**

Entry	Ligand	Conversion. (%)[b]	Yield (%)[c]
1	**L1**	0	0
2	**L2**	0	0
3	**L3**	98	75
4	**L4**	0	0
5	**L5**	0	0
6	**L6**	0	0
7	**L7**	88	66
8	**L9**	0	0

[a]Reaction condition: **3-1** (0.25 mmol), **3-2** (0.5 mmol), $NiCl_2$·glyme. (10 mol%), ligand (20 mol%), Mn (2.0 equiv), DMF (1 mL), rt, overnight. [b]HPLC conversions, determined by using naphthalene as internal standard. [c]HPLC yields, determined by using naphthalene as internal standard.

Table 3.2. Screening of ligands.[a]

We also wondered, whether we could lower the catalyst loading. We were glad to find that the reaction proceeded smoothly using 5 mol% Ni-precatalyst, giving 73% of conversion and 72% of HPLC yield. However, further decreasing the loading to 2.5% led to reduced conversion and yield. The reaction almost did not take place when 1 mol% $NiCl_2$·glyme was employed in the process. It is worth noting that we could improve the yield to 94% by running the reaction at an elevated temperature of 60 °C (Table 3.3, Entry 5).

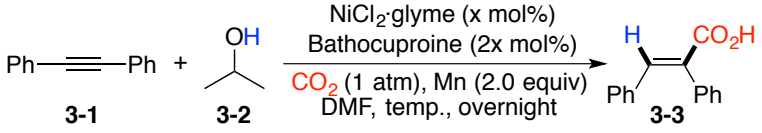

3-1 3-2 3-3

Entry	Loading (mol%)	Temp. (°C)	Conervsion (%)[b]	Yield (%)[c]
1	5	rt	73	72
2	2.5	rt	42	42
3	1	rt	5	3
4	5	50	98	88
5	5	60	99	94

[a]Reaction condition: **3-1** (0.25 mmol), **3-2** (0.5 mmol), $NiCl_2$·glyme. (x mol%), ligand (2x mol%), Mn (2.0 equiv), DMF (1 mL), overnight. [b]HPLC conversions, determined by using naphthalene as internal standard. [c]HPLC yields, determined by using naphthalene as internal standard.

Table 3.3. Screening of catalyst loading and temperature.[a]

Next, we turned our attention to prolong the reaction time to 36 h with 5 mol% and 2.5 mol% catalyst loadings. As anticipated, we could obtain quantitative HPLC yield and 94% isolated yield when 5 mol% Ni-precatalyst was used at 60 °C (Table 3.4, Entry 1). We were delight to obtain 85% of the desired acid even with 2.5% nickel (Entry 2). Afterwards, we decided to explore whether the amount of Mn could exert an influence in the reaction outcomes. As shown in Figure 3.4, the reductant could be reduced to 1.5 equivalents without an erosion of the yield, allowing for the isolation of 94% of acid after acidic workup (Entry 3). However, a further decrease of Mn led to inferior yields.

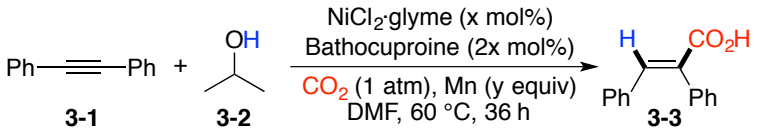

3-1 3-2 3-3

Entry	Loading (mol%)	Mn (equiv)	Conv. (%)[b]	Yield (%)[c]
1	5	2.0	100	99 (94[d])
2	2.5	2.0	100	85
3	5	1.5	100	99 (94[d])
4	5	1.2	100	88

[a] Reaction condition: **3-1** (0.25 mmol), **3-2** (0.5 mmol), $NiCl_2$·glyme. (x mol%), ligand (2x mol%), Mn (y equiv), DMF (1 mL), 60 °C, 36 h. [b] HPLC conversions, determined by using naphthalene as internal standard. [c] HPLC yields, determined by using naphthalene as internal standard. [d] Isolated yield.

Table 3.4. Screening of catalyst loading and Mn amount.[a]

The effect of the metal to ligand ratio was studied next (Table 3.5). We were glad to observe that decreasing the ratio to 1:1.2 gave the product without any loss in the yield (Entry 2). The use of lower amounts of ligand caused erosion of the yield, and a 15% decrease was observed when employing a 1:1 ratio (Entry 4).

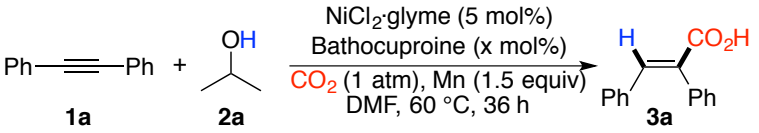

1a 2a 3a

Entry	Ligand (mol%)	Conversion. (%)[b]	Yield (%)[c]
1	9	100	99 (94[d])
2	6	100	99 (94[d])
3	5.5	100	96 (92[d])
4	5	100	84

[a] Reaction condition: 1a (0.25 mmol), 2a (0.5 mmol), $NiCl_2$·glyme. (5 mol%), ligand (x mol%), Mn (1.5 equiv), DMF (1 mL), 60 °C, 36 h. [b] HPLC conversions, determined by using naphthalene as internal standard. [c] HPLC yields, determined by using naphthalene as internal standard. [d] Isolated yield.

Table 3.5. Screening of ratio of metal to ligand.[a]

Later, we were interested in decreasing the amount of proton source. As expected, 1.5 equivalents of *i*-PrOH afforded the same level of reactivity (Table 3.6, Entry 1). Lower amounts of *i*-PrOH were insufficient for retaining the excellent yields (Entries

2 & 3).

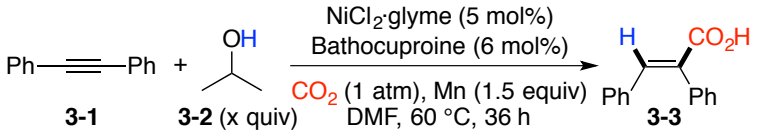

3-1 **3-2** (x quiv) **3-3**

Entry	**2a** (equiv)	Conversion. (%)[b]	Yield (%)[c]
1	1.5	100	99 (94[d])
2	1.2	100	88
3	1.0	100	83

[a]Reaction condition: **3-1** (0.25 mmol), **3-2** (x mmol), $NiCl_2$·glyme. (5 mol%), ligand (6 mol%), Mn (1.5 equiv), DMF (1 mL), 60 °C, 36 h. [b]HPLC conversions, determined by using naphthalene as internal standard.[c]HPLC yields, determined by using naphthalene as internal standard.[d]Isolated yield.

Table 3.6. Screening of stoichiometry.[a]

The next factor that we investigated was the effect of different proton sources. In general, several alcohols such as MeOH, EtOH, BnOH, phenol and HFIP gave full conversion and delivered the corresponding acids in moderate yields. Although the reaction with *t*-BuOH did not convert all of the starting material to the desired product (38%), we detected comparable yield.

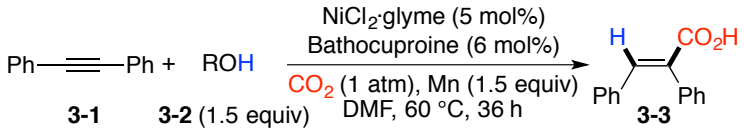

3-1 **3-2** (1.5 equiv) **3-3**

Entry	Alcohol	Conversion. (%)[b]	Yield (%)[c]
1	MeOH instead of *i*-PrOH	100	47
2	EtOH instead of *i*-PrOH	100	52
3	*t*-BuOH instead of *i*-PrOH	38	37
4	BnOH instead of *i*-PrOH	100	37
5	Phenol instead of *i*-PrOH	100	45
6	1,1,1,3,3,3-hexfluoroisopropanol (HFIP) instead of *i*-PrOH	100	50

[a]Reaction condition: **3-1** (0.25 mmol), **3-2** (0.375 mmol), $NiCl_2$·glyme. (5 mol%), ligand (6 mol%), Mn (1.5 equiv), DMF (1 mL), 60 °C, 36 h. [b]HPLC conversions, determined by using naphthalene as internal standard. [c]HPLC yields, determined by using naphthalene as internal standard.

Table 3.7. The effect of proton sources.[a]

As summarized in Table 3.8, control experiments indicated that all reaction parameters were essential for the reaction to occur. The reactions conducted without catalyst, ligand, reducing reagent or proton source did not give any acids or only trace amounts were detected (Entries 1-4). Changing the solvent to DMA led to a dramatic reduction of yield to 36%. Inferior results were likewise obtained when DMSO was used (Entries 5-6). Interestingly, worse results were found with other catalysts or reducing agent combinations, thus showing the subtleties of our protocol (Entries 7-8). As we anticipated, conducting the reaction in the presence of a radical scavenger such as BHT did not stop the hydrocarboxylation protocol, thus indicating that our catalytic process probably does not proceed *via* a radical pathway (Entry 9).

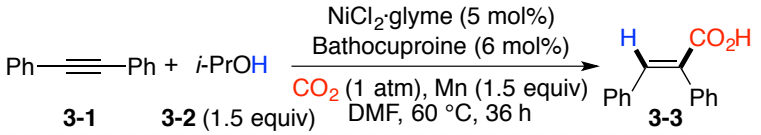

Entry	Deviation	Conversion. (%)[b]	Yield (%)[c]
1	No Ni-catalyst	0	0
2	No ligand	0	0
3	No Mn	6	trace
4	No *i*-PrOH	0	0
5	DMA as the solvent	41	36
6	DMSO as the solvent	75	66
7	$Ni(COD)_2$ as catalyst	88	78
8	Zn as reducing agent	32	20
9	BHT (1 equiv) as additive	100	74

[a]Reaction condition: **3-1** (0.25 mmol), **3-2** (0.375 mmol), $NiCl_2$·glyme. (5 mol%), ligand (6 mol%), Mn (1.5 equiv), DMF (1 mL), 60 °C, 36 h. [b]HPLC conversions, determined by using naphthalene as internal standard. [c]HPLC yields, determined by using naphthalene as internal standard.

Table 3.8. Deviation from the standard condition.[a]

In conclusion, after scrupulous evaluation of all reaction parameters, we found the optimized reaction conditions consisting of $NiCl_2$·glyme (5 mol%), **L8** (6 mol%), Mn as reducing agent (1.5 equiv), *i*-PrOH (**3-2**, 1.5 equiv) as proton donor in DMF at 60 °C for 36 h delivered **3-3** in 94% isolated yield. It is worth noting that the anti-addition

product was not detected in the crude mixtures. As detailed in the ligands screening section, the efficiency was found to be dependent on the nature of the ligand backbone.

3.4 Ni-catalyzed Regioselective Hydrocarboxylation of Alkynes

3.4.1 Synthesis of Starting Materials

With the optimized reaction condition in hand, we set out to study the scope of our carboxylation protocol and thus prepared a wide range of alkynes. A variety of starting materials possessing different substituents on phenyl ring were prepared by Sonogashira coupling reactions. Accordingly, the reaction of the corresponding aryl iodides with terminal alkynes in the presence of small amount of palladium- and copper-catalyst delivered the targeted substrates in excellent yields (Scheme 3.3).

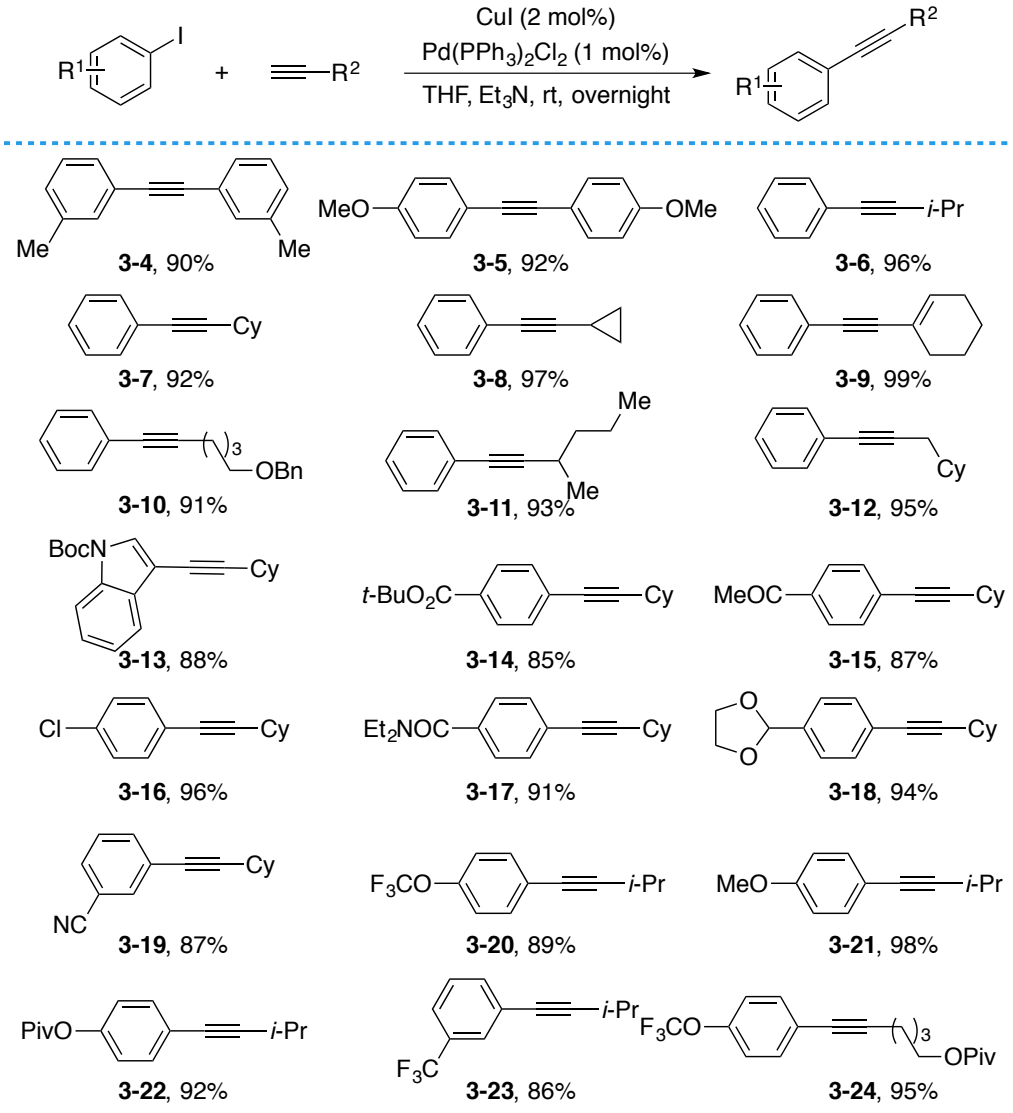

Scheme 3.3. General synthetic route for preparing various alkynes.

3.4.2 Scope of the Hydrocarboxylation Reactions

We next moved to study the scope of our catalytic hydrocarboxylation reaction of alkynes. As detailed in Table 3.9, we first investigated the symmetric substrates. Gratifyingly, the coupling of symmetrical alkynes posed no problems. It is particularly noteworthy was the example of **3-3**, as it was prepared in gram scale in excellent yield under the optimized conditions. The structure of the acid was univocally confirmed by X-ray crystallography of **3-3**. Besides the symmetric alkynes, a number of asymmetric alkynes possessing different alkyl substituents moiety reacted to generate the corresponding acids in good to excellent yields. It is worth noting that **3-24** and **3-25** were obtained in 87% combined isolated yield with the regioselectivity of 4:1 when *i*-PrOH was employed as the proton source. To our delight, we could obtain **3-24** as single isomer in 85% isolated yield when the reaction was performed with *t*-BuOH (**3-33**) as the proton source. Remarkably, such an *exquisite regioselectivity profile* was found for a wide variety of unsymmetrical alkynes, even without significant steric bias (from **3-25** to **3-32**). As shown, CO_2 insertion occurs predominantly *distal* to the aromatic site. These results are certainly noteworthy taking into consideration the opposite selectivity pattern or the significantly lower regioselectivity observed in previous hydrocarboxylation methodologies for sterically unbiased unsymmetrical alkynes.[66,69] Strikingly, the nature of the alcohol exerted a profound influence on site-selectivity for unsymmetrical substrates. While a system based on *i*-PrOH (**3-2**) resulted in low regioselectivities, the utilization of *t*-BuOH (**3-33**) dramatically improved the selectivity pattern, delivering single regioisomers in virtually all cases analyzed, albeit with a remarkable exception (**3-28**). At present, we do not have an explanation for such distinctive selectivity pattern depending on the substrate utilized.

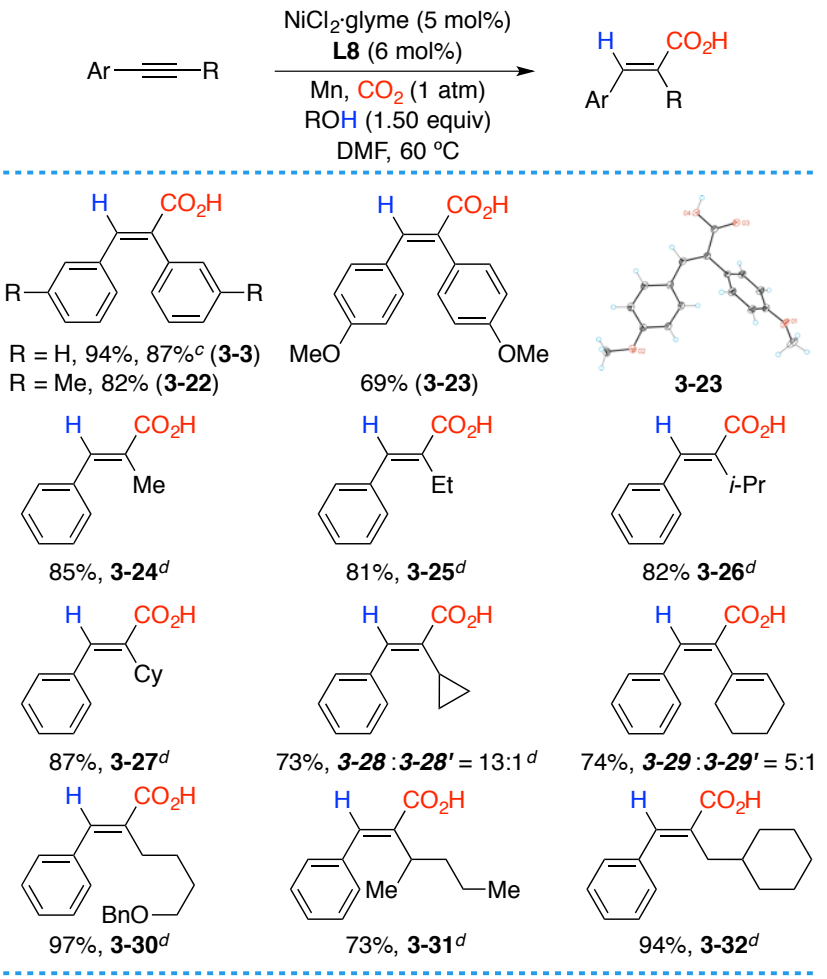

[a] Alkyne (0.5 mmol), **3-2** (0.75 mmol), $NiCl_2$·glyme (5 mol%), ligand (6 mol%), Mn (0.75 mmol), DMF (2 mL) at 60 °C, 36 h. [b] Isolated yields, average of at least two independent runs. [c] **3-3** (1.10 g). [d] *t*-BuOH (**3-33**) was used instead of **3-2**.

Table 3.9. Scope of alkynes.

Afterwards, we turned our attention to explore the scope of the aromatic moiety. As shown in Figure 3.12, our protocol exhibited a remarkable chemoselectivity profile, different substrates containing a carbamate (**3-34**), esters (**3-35, 3-43** & **3-45**), a ketone (**3-36**), an amide (**3-37**), an acetal (**3-38**), a nitrogen-containing heterocycle (**3-34**) as well as nitriles (**3-40**) were perfectly tolerated. As evident from careful NMR spectroscopic analysis, CO_2 insertion took place predominantly *distal* to the aromatic site. Such observation was univocally confirmed by X-ray crystallography of **3-42**. However, care must be taken when generalizing this since single regioisomers were found for **3-39** and **3-40** by using *i*-PrOH (**3-2**), thus showing the subtleties of our system.

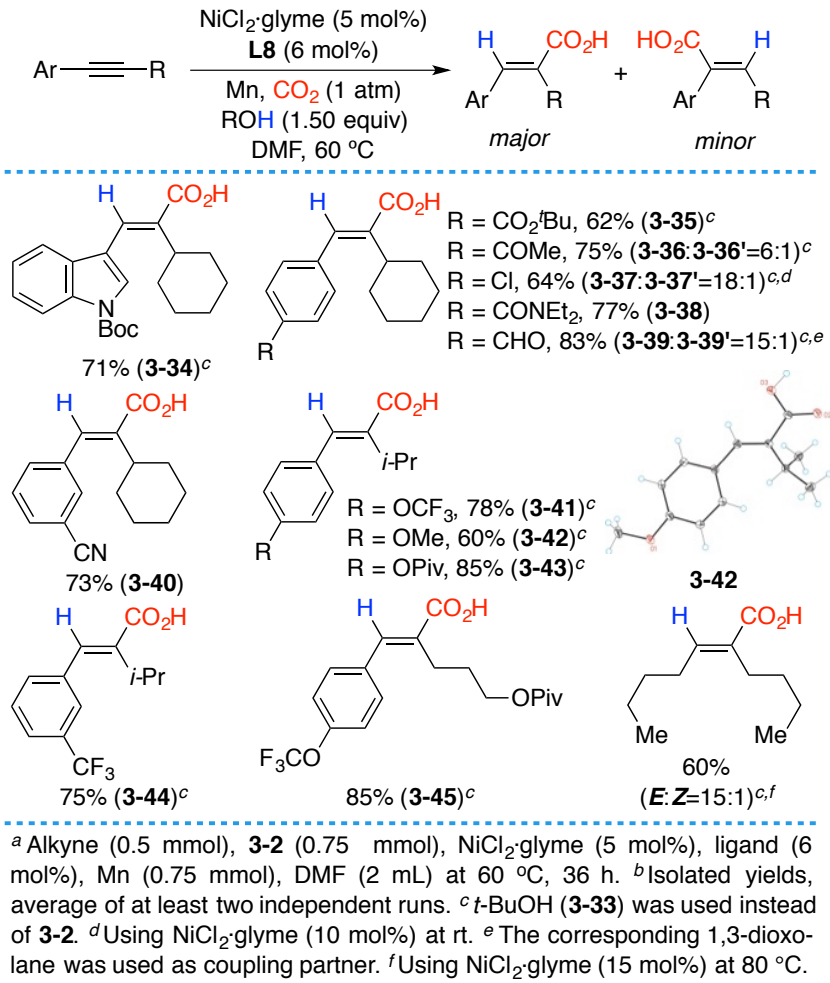

[a] Alkyne (0.5 mmol), **3-2** (0.75 mmol), $NiCl_2$·glyme (5 mol%), ligand (6 mol%), Mn (0.75 mmol), DMF (2 mL) at 60 °C, 36 h. [b] Isolated yields, average of at least two independent runs. [c] *t*-BuOH (**3-33**) was used instead of **3-2**. [d] Using $NiCl_2$·glyme (10 mol%) at rt. [e] The corresponding 1,3-dioxolane was used as coupling partner. [f] Using $NiCl_2$·glyme (15 mol%) at 80 °C.

Table 3.10. Functional group compatibility.

Although tentative, we believe these results reinforce the notion that the alcohol utilized is not a mere spectator and that interacts with the putative reaction intermediates. Interestingly, no carboxylation occurred at electrophilic sites amenable to Ni-catalyzed cross-coupling reactions such as aryl chlorides or aryl pivalates, thus providing an additional handle for further manipulation. Notably, the reaction proceeded equally well with internal alkynes possessing aliphatic motifs at both ends (**3-46**). Taken together, we believe the results in Figure 3.12 clearly illustrate the prospective impact of our methodology and demonstrate that our exceedingly practical Ni-catalyzed regioselective hydrocarboxylation protocol might pave the way for future reductive CO_2 fixation techniques into organic matter.

3.4.3 Mechanistic studies

Having studied the scope of the transformation, we next turned our attention towards gaining some insights on the mechanism of our Ni-catalyzed regioselective hydrocarboxylation reaction. In this regard, the effect of radical scavengers, as well as, the results of stoichiometric reactions were studied and isotope-labeling studies were performed as they would allow us to gain precious information about the mechanism.

Although an in-depth mechanistic discussion should await further investigations, the utilization of alcohols as hydrogen donors exhibits features reminiscent of a number of elegant hydrogen-borrowing strategies reported in the literature.[108] In order to shed light on the mechanism, we decided to gather indirect evidence by studying the reactivity of **3-2D$_1$** and **3-2D$_2$** (Scheme 3.4). While **3-2D$_1$** reacted at a significantly lower rate than **3-2D$_2$**, **3-2D$_1$** was exclusively observed with a protocol based on **3-2D$_1$** (Scheme 3.4, top right). Importantly, **3-47** was fully recovered en route to **3-3** with not even traces of benzophenone detected in the crude mixtures (Figure 3.13, top left). We also performed a reaction with **3-1** under our optimized condition in DMF-d_7, so that we could gain information whether the proton originated from the solvent. As expected, no deuterium content could be found after acid hydrolysis. Overall, the results depicted in Figure 3.13 reinforce the notion that a hydrogen-borrowing strategy does not come into play and suggest that the alcohol might act with dual roles, both as proton source and a reagent that interacts with reaction intermediates within the catalytic cycle.[109]

[108] For selected reviews: (a) Ketcham, J. M.; Shin, I.; Montgomery, T. P.; Krische, M. J. *Angew. Chem. Int. Ed.* **2014**, *53*, 9142. (b) Moran, J.; Krische, M. J. *Pure Appl. Chem.* **2012**, *84*, 1729. (c) Obora, Y.; Ishii, Y. *Synlett* **2011**, 30. (d) Bower, J. F.; Krische, M. J. *Top. Organomet. Chem.* **2011**, *43*, 107. (e) Dobereiner, G. E.; Crabtree, R. H. *Chem. Rev.* **2010**, *110*, 681. (f) Guillena, G.; Ramón, D. J.; Yus, M. *Chem. Rev.* **2010**, *110*, 1611. (g) Hamid, M. H. S. A.; Slatford, P. A.; Williams, J. M. J. *Adv. Synth. Catal.* **2007**, *349*, 1555.

[109] Nakai, K.; Yoshida, Y.; Kurahashi, T.; Matsubara, S. *J. Am. Chem. Soc.* **2014**, *136*, 7797.

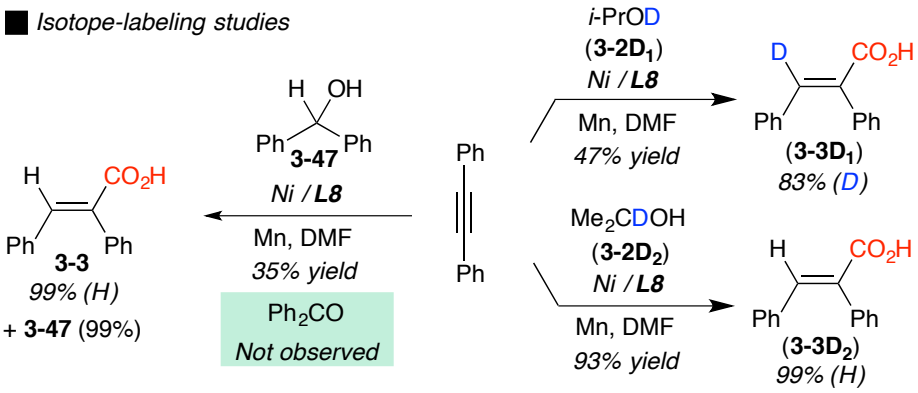

Scheme 3.4. Isotope-labeling studies.

Interestingly, we observed a k_H/k_D = 1.1 when comparing the initial rates for the reactions of **3-1** with **3-2** and **3-2D$_1$** (Figure 3.14), indicating the O-H bond cleavage is not the rate-determine step.

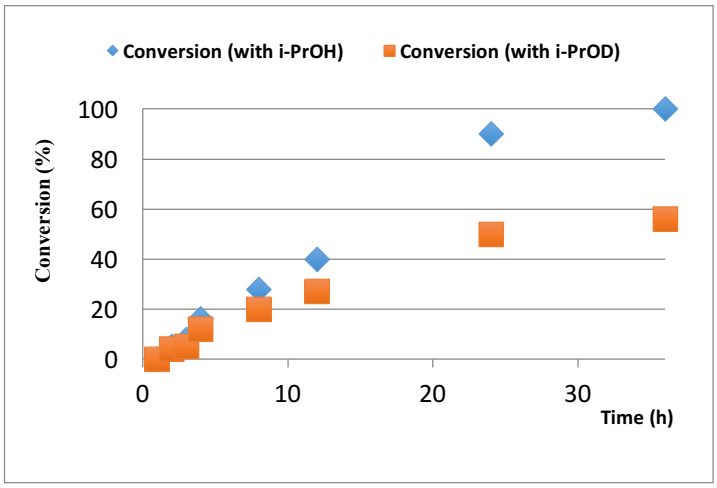

Figure 3.1. K_H/K_D studies.

Next, we set out to explore the reactivity of **3-48**[110] or Ni(COD)$_2$/**L8** with **3-1** and **3-2** in a stoichiometric fashion followed by DCl workup. As shown in Scheme 3.5, we found that **3-3** was invariably formed regardless of whether Mn was present or not. Although tentative, we believe these results rule out the intermediacy of Ni(I) intermediates and support a scenario based on Ni(II) species.

[110] (a) Wang, X.; Liu, Y.; Martin, R. *J. Am. Chem. Soc.* **2015**, *137*, 6476. (b) Powers, D. C.; Anderson, B. L.; Nocera, D. G. *J. Am. Chem. Soc.* **2013**, *135*, 18876.

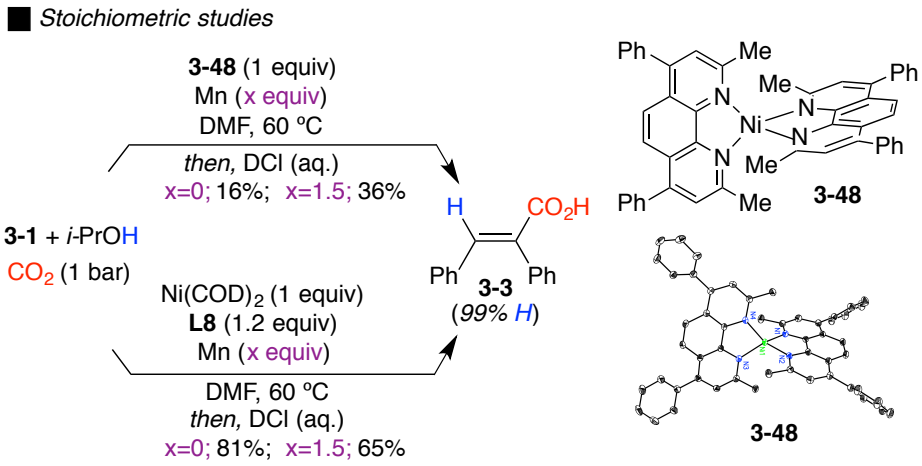

Scheme 3.5 Stoichiometric studies.

The regioselectivity profile shown in Table 3.10 do not match the inherent propensity of metal hydride complexes to undergo *syn*-addition across the alkyne motif with the incoming hydride located at the most sterically hindered position.[111] Although tentative, we support a mechanistic scenario consisting of the intermediacy of nickelalactones (**C** and **C'**)[112] that are likely in equilibrium *via* **B** formed by a reversible CO_2 extrusion (Scheme 3.6). We propose that **C** reacts preferentially with the alcohol donor in order to avoid the clash with the alkyl substituent on the alkyne terminus of **C'**. Thus the protonolysis of the C–Ni(II) bond would generate **D** that precedes a reduction event, which affords manganese carboxylate while regenerating the circulating Ni(0)$\mathbf{L_n}$ species.[113]

[111] (a) Trost, B. M.; Ball, Z. T. *Synthesis* **2005**, *6*, 853. (b) Andersson, P. G.; Munslow, I. J. *Modern Reduction Methods;* Ed. Wiley-VCH, 2008. (c) See also ref. 8d or ref. 10 for examples dealing with CO_2 or CO as coupling partner.

[112] (a) Fischer, R.; Langer, J.; Malassa, A.; Walther, D.; Görls, H.; Vaughan, G. *Chem. Commun.* **2006**, 2510. (b) Hoberg, H.; Peres, Y.; Krüger, C.; Tsay, Y. H. *Angew. Chem., Int. Ed.* **1987**, *26*, 771. (c) Hoberg, H.; Schäfer, H.; Burkhardt, G.; Krüger, C.; Rmao, M. J. *J. Organomet. Chem.* **1984**, *266*, 203. (d) Hoberg, H.; Schäfer, D. *J. Organomet. Chem.* **1983**, *251*, C51. (d) Burkhardt, G.; Hoberg, H. *Angew. Chem. Int. Ed.* **1982**, *21*, 76.

[113] Although radical intermediates might also account for the observed reactivity, we found no significant inhibition in the presence of BHT or related radical scavengers.

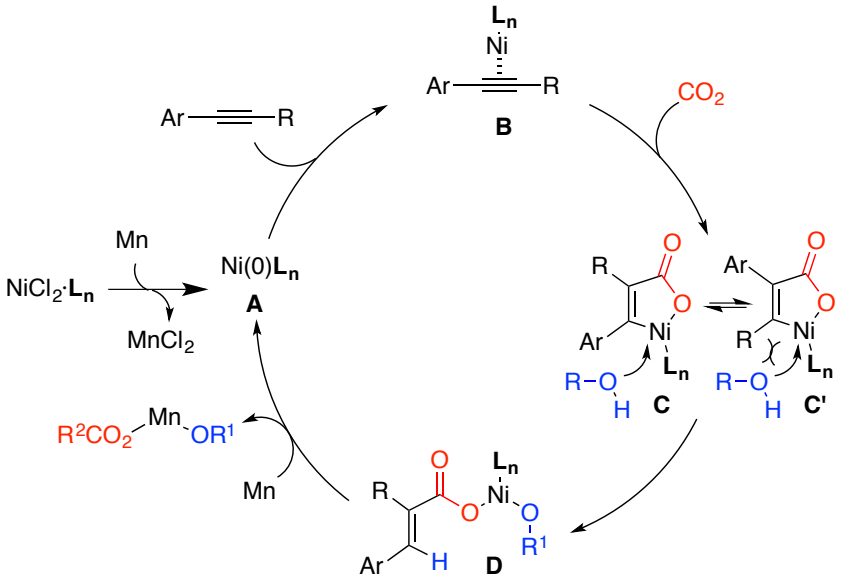

Scheme 3.6. Mechanistic Rationale.

3.4.4 Limitations of the Hydrocarboxylation Reactions

As shown in Scheme 3.7, we also observed limitations of our Ni-catalyzed reductive hydrocarboxylation protocol. The reactions that employed substrates from **3-49** to **3-52** delivered mixtures of acids under optimized reaction conditions, which could be identified. In case of **3-55**, we observed the desired product and desilylation products as a mixture in low yields. We did not observe any conversion when **3-56** was used in this reaction, we suggest that the bulky TIPS substituent suppressed the reaction.

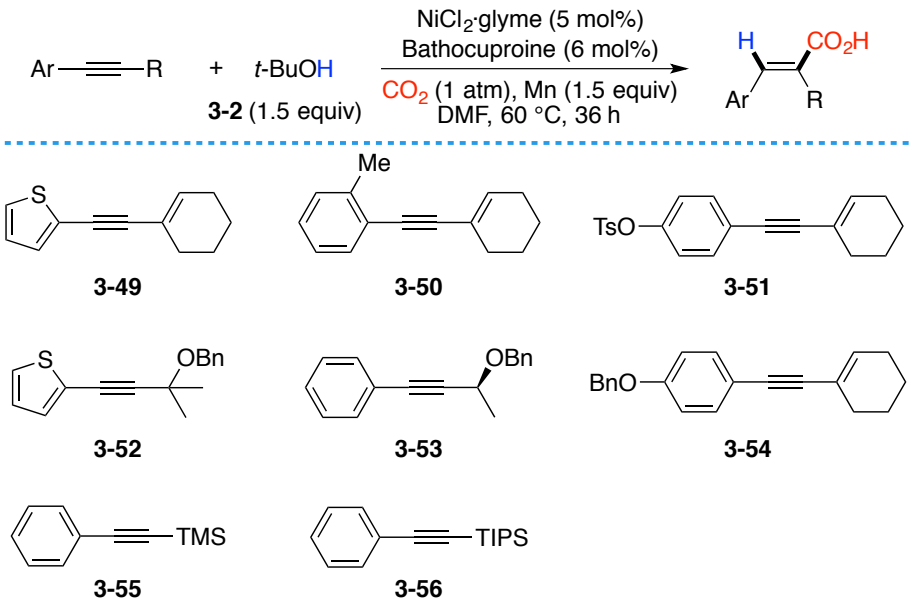

Scheme 3.7. Limitations of the Hydrocarboxylation.

3.5 Conclusion

In summary, we have described a novel, mild and user-friendly Ni-catalyzed hydrocarboxylation of alkynes at atmospheric pressure of CO_2 that occurs with an exquisite regioselectivity profile using commercially available and inexpensive alcohols as proton sources. This protocol is distinguished by its excellent functional group tolerance. We anticipate this study will find widespread use.

3.6 Experimental Section

3.6.1 General Considerations

Reagents: All reactions were conducted in Schlenk tubes. $NiCl_2$·glyme was purchased from Strem. All other Nickel catalysts, Ligands and Mn were purchased from Aldrich or Strem. Bathocuproine (**L8**) was purchased from TCI. Anhydrous DMF was purchased from Acros and used as received. Analytical methods: ^{1}H NMR and ^{13}C NMR spectra and melting points (where applicable) are included for all compounds. ^{1}H and ^{13}C NMR spectra were recorded on a Bruker 400 MHz and a Bruker 500 MHz at 20 °C. All ^{1}H NMR spectra are reported in parts per million (ppm) downfield of TMS and were measured relative to the signals for $CHCl_3$ (7.26 ppm), DMSO (2.50 ppm). All ^{13}C NMR spectra were reported in ppm relative to residual $CHCl_3$ (77.2 ppm), DMSO (39,5 ppm) and were obtained with 1H decoupling. Coupling constants, *J*, are reported in Hertz. Melting points were measured using open glass capillaries in a Büchi B540 apparatus. Infrared spectra were recorded on a Bruker Tensor 27. Mass spectra were recorded on a Waters LCT Premier spectrometer. Gas chromatographic analyses were performed on Hewlett-Packard 6890 gas chromatography instrument with a FID detector using 25m x 0.20 mm capillary column with cross-linked methyl siloxane as the stationary phase. High Pressure Liquid Chromatographic (HPLC) analyses were performed on Agilent Technologies Model 1260 Infinity HPLC chromatography instrument equipped with Agilent Eclipse Plus C18 (3.5 um, 4.6 x 100 mm) column and UV/V is detector. Flash chromatography was performed with EM Science silica gel 60 (230-400 mesh) and using bromocresol as TLC stain. The yields reported in table 2 refer to isolated yields and represent an average of at least two independent runs. The procedures described in this section are representative.

3.6.2 General Procedure and Data

General procedure: A Schlenk tube containing a stirring bar was charged with acetylene (0.50 mmol), **L8** (10.8 mg, 0.03 mmol), Mn powder (41.2 mg, 0.75 mmol) and $NiCl_2$·glyme (5.5 mg, 0.025 mmol). The tube was then evacuated and back-filled with CO_2 three times. *i*-PrOH (57.4 µL, 0.75 mmol) and DMF (2 mL) were then added by syringe under a CO_2 flow. Once added, the Schlenk tube was closed at atmospheric pressure of CO_2 (1atm) and stirred for 36 h at 60 °C. The mixture was quenched with

HCl (2M) and extracted with DCM. The combined organic layers were washed with brine and dried over anhydrous $MgSO_4$ and concentrated under reduced pressure. The residue was purified by flash chromatography (hexanes/ethyl acetate = 10/1 to 1/1).

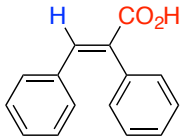

(*E*)-2,3-diphenylacrylic acid (3-3): Following the general procedure using **3-1** to afford **3-3** (105.4 mg, 95% yield) as a colorless solid. The spectroscopic data correspond to those previously reported in the literature.[69] M.P. = 170-171 °C. ^{1}H NMR (400 MHz, $CDCl_3$) δ 7.96 (s, 1H), 7.43 – 7.34 (m, 3H), 7.29-7.20 (m, 3H), 7.20-7.12 (m, 2H), 7.10-7.05 (m, 2H) ppm. ^{13}C NMR (101 MHz, $CDCl_3$) δ 173.2, 142.6, 135.5, 134.5, 131.8, 131.0, 130.0, 129.7, 128.9, 128.4, 128.2 ppm.

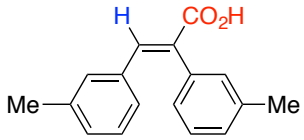

(*E*)-2,3-di-*m*-tolylacrylic acid (3b): Following the general procedure using **3-4** to afford **3-22** (103.4 mg, 84% yield) as a colorless solid. The spectroscopic data correspond to those previously reported in the literature.[69] M.P. = 151-153 °C. ^{1}H NMR (500 MHz, $CDCl_3$) δ 7.91 (s, 1H), 7.28 (t, J = 7.6 Hz, 1H), 7.19 (d, J = 7.6 Hz, 1H), 7.10-6.99 (m, 4H), 6.94 (s, 1H), 6.90-6.83 (m, 1H), 2.36 (s, 3H), 2.21 (s, 3H) ppm. ^{13}C NMR (126 MHz, $CDCl_3$) δ 173.6, 142.6, 138.5, 138.0, 135.5, 134.4, 132.1, 131.7, 130.5, 130.4, 128.9, 128.7, 128.3, 128.0, 126.9, 21.6, 21.4 ppm.

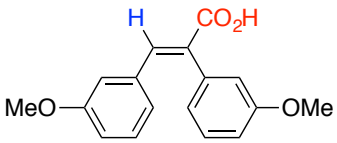

(*E*)-2,3-bis(4-methoxyphenyl)acrylic acid (3-23): Following the general procedure using **3-5** to afford **3-23** (98.1 mg, 70% yield) as a colorless solid. The spectroscopic data correspond to those previously reported in the literature.[69] M.P. = 208-211 °C. ^{1}H NMR (300 MHz, $CDCl_3$) δ 7.88 (s, 1H), 7.18 (d, J = 8.8 Hz, 2H), 7.06 (d, J = 8.8 Hz, 2H), 6.93 (d, J = 8.8 Hz, 2H), 6.71 (d, J = 8.8 Hz, 2H), 3.85 (s, 3H), 3.77 (s, 3H) ppm.

^{13}C NMR (75 MHz, $CDCl_3$) δ 173.5, 160.7, 159.4, 142.2, 132.8, 131.2, 128.8, 128.0, 127.3, 114.5, 113.9, 55.4 (2C) ppm.

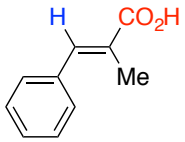

(*E*)-2-methyl-3-phenylacrylic acid (3-24): Following the general procedure using **prop-1-yn-1-ylbenzene** and *t*-BuOH (**3-33**) to afford **3-24** (68.9 mg, 85% yield) as a colorless solid. The spectroscopic data correspond to those previously reported in the literature.[69] M.P. = 78-80 °C. ^{1}H NMR (500 MHz, $CDCl_3$) δ 7.89 (s, 1H), 7.54-7.40 (m, 4H), 7.40-7.33 (m, 1H), 2.19 (d, J = 1.5 Hz, 3H) ppm. ^{13}C NMR (126 MHz, $CDCl_3$) δ 174.8, 141.3, 135.7, 130.0, 128.9, 128.6, 127.7, 13.9 ppm.

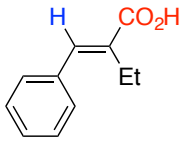

(*E*)-2-benzylidenebutanoic acid (3-25): Following the general procedure using **but-1-yn-1-ylbenzene** and *t*-BuOH (**3-33**) to afford **3-25** (71.4 mg, 84% yield) as a colorless solid. The spectroscopic data correspond to those previously reported in the literature.[114] M.P. = 98-100 °C. ^{1}H NMR (500 MHz, $CDCl_3$) δ 7.83 (s, 1H), 7.50-7.40 (m, 4H), 7.40-7.30 (m, 1H), 2.60 (q, J = 7.4 Hz, 2H), 1.25 (t, J = 7.4 Hz, 3H) ppm. ^{13}C NMR (126 MHz, $CDCl_3$) δ 174.4, 141.0, 135.6, 134.1, 129.6, 128.9, 128.7, 20.7, 13.9 ppm.

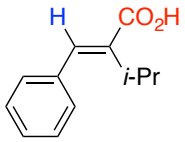

(*E*)-2-benzylidene-3-methylbutanoic acid (3-26): Following the general procedure using **3-6** and *t*-BuOH (**3-33**) to afford **3-26** (78.0 mg, 83% yield) as a colorless solid. M.P. = 111-113 °C. ^{1}H NMR (500 MHz, $CDCl_3$) δ 7.76 (s, 1H), 7.44-7.39 (m, 2H), 7.37-7.32 (m, 3H), 3.21 (m, 1H), 1.30 (d, J = 7.0 Hz, 6H) ppm. ^{13}C NMR (126 MHz, $CDCl_3$) δ 173.8, 140.6, 138.4, 135.9, 129.1, 128.6, 128.4, 27.6, 21.3 ppm. IR (neat, cm$^-$

[114] Zargarian, D.; Alper, H. *Organometallics* **1993**, *12*, 712.

[1]): 2956, 1671, 1418, 1258, 692. HRMS *calcd.* for ($C_{12}H_{14}O_2$-H): 189.0921, *found*: 189.0927.

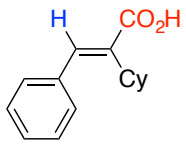

(*E*)-2-cyclohexyl-3-phenylacrylic acid (3-27): Following the general procedure using **3-7** and *t*-BuOH (**3-33**) to afford **3-27** (100.2 mg, 89% yield) as a colorless solid. The spectroscopic data correspond to those previously reported in the literature.[115] M.P. = 184-186 °C. ^{1}H NMR (500 MHz, $CDCl_3$) δ 7.74 (s, 1H), 7.41 (dd, *J* = 8.1, 6.7 Hz, 2H), 7.37-7.30 (m, 3H), 2.81 (tt, *J* = 12.0, 3.3 Hz, 1H), 2.18-1.90 (m, 2H), 1.77 (m, 2H), 1.70-1.55 (m, 3H), 1.39-1.12 (m, 3H) ppm. ^{13}C NMR (126 MHz, $CDCl_3$) δ 173.6, 140.7, 137.7, 136.0, 129.2, 128.6, 128.5, 38.6, 30.8, 26.8, 26.0 ppm.

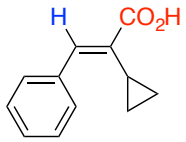

(*E*)-2-cyclopropyl-3-phenylacrylic acid (3-28): Following the general procedure using **3-8** and *t*-BuOH (**3-33**) to afford **3-28** (68.7 mg, **3-28:3-28´** = 13:1, 75% yield) as a colorless solid. M.P. = 54-55 °C. Spectroscopic data for the major isomer (**3-28**): ^{1}H NMR (500 MHz, $CDCl_3$) δ 7.85 (d, *J* = 2.0 Hz, 1H), 7.63 (d, *J* = 6.9 Hz, 2H), 7.47-7.40 (m, 2H), 7.41-7.33 (m, 1H), 1.80-1.74 (m, 1H), 1.00-0.86 (m, 2H), 0.52-0.49 (dt, *J* = 6.1, 4.5 Hz, 2H) ppm. ^{13}C NMR (126 MHz, $CDCl_3$) δ 174.4, 142.6, 135.0, 132.5, 130.7, 129.0, 128.2, 10.0, 9.3 ppm. IR (neat, cm^{-1}): 3005, 1669, 609, 273, 774, 690. HRMS *calcd*. for ($C_{12}H_{12}O_2$-H): 187.0765, *found*: 187.0763.

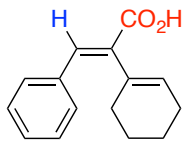

(*E*)-2-(cyclohex-1-en-1-yl)-3-phenylacrylic acid (3-29): Following the general procedure using **3-9** to afford **3-29** (84.4 mg, **3-29**: **3-29´** = 5:1, 76% yield) as a colorless solid. M.P. = 81-82 °C. Spectroscopic data for the major isomer (**3-29**): ^{1}H NMR (500

[115] Kowalski, C. J.; Sakdarat, S. *J. Org. Chem.* **1990**, *55*, 1977.

MHz, $CDCl_3$) δ 7.67 (s, 1H), 7.64-7.58 (m, 2H), 7.40-7.30 (m, 3H), 5.67 (dt, *J* = 3.8, 2.0 Hz, 1H), 2.25-2.16 (m, 2H), 2.12 (d, *J* = 3.7 Hz, 2H), 1.84-1.73 (m, 2H), 1.70 (dt, *J* = 8.4, 2.5 Hz, 2H) ppm. ^{13}C NMR (126 MHz, $CDCl_3$) δ 173.8, 140.6, 135.1, 134.4, 133.2, 130.6, 129.5, 128.7, 128.5, 28.1, 25.6, 22.9, 21.9 ppm. IR (neat, cm^{-1}): 2931, 1670, 1414, 1258, 918, 688. HRMS *calcd*. for ($C_{15}H_{16}O_2$-H): 227.1078, *found*: 227.1075.

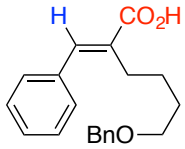

(*E*)-2-benzylidene-6-(benzyloxy)hexanoic acid (3-30): Following the general procedure using **3-10** and *t*-BuOH (**3-33**) to afford **33-30** (150.5 mg, 99% yield) as a colorless solid. M.P. = 65-67 °C. ^{1}H NMR (500 MHz, $CDCl_3$) δ 7.90 (s, 1H), 7.64-7.31 (m, 10H), 4.58 (s, 2H), 3.66-3.44 (m, 2H), 2.66 (t, *J* = 7.3 Hz, 2H), 1.79 (m, 4H) ppm. ^{13}C NMR (126 MHz, $CDCl_3$) δ 174.2, 141.3, 138.6, 135.5, 132.7, 129.5, 128.8, 128.7, 128.4, 127.7, 127.6, 73.0, 70.0, 29.8, 27.1, 25.8 ppm. IR (neat, cm^{-1}): 2938, 2851, 1673, 1615, 1262, 728, 694. HRMS *calcd*. for ($C_{20}H_{22}O_3$-H): 309.1496, *found*: 309.1502.

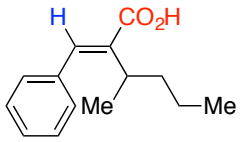

(*E*)-2-benzylidene-3-methylhexanoic acid (3-31): Following the general procedure using **3-11** and *t*-BuOH (**3-33**) to afford **3-31** (80.7 mg, 77% yield) as a colorless solid. The spectroscopic data correspond to those previously reported in the literature.[69] M.P. = 72-54 °C. ^{1}H NMR (400 MHz, $CDCl_3$) δ 7.83 (s, 1H), 7.48-7.37 (m, 2H), 7.37-7.29 (m, 3H), 3.03 (m, 1H), 1.87-1.67 (m, 1H), 1.59-1.45 (m, 1H), 1.31 (d, *J* = 7.0 Hz, 3H), 1.28-1.11 (m, 2H), 0.81 (t, *J* = 7.3 Hz, 3H) ppm. ^{13}C NMR (101 MHz, $CDCl_3$) δ 173.7, 141.3, 137.3, 135.9, 128.9, 128.4, 128.2, 37.0, 32.5, 21.2, 19.4, 14.1 ppm.

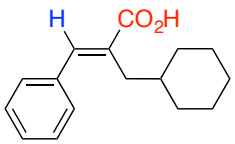

(*E*)-2-(cyclohexylmethyl)-3-phenylacrylic acid (3-32): Following the general

procedure using **3-12** and *t*-BuOH (**3-33**) to afford **3-32** (114.9 mg, 95% yield) as a colorless solid. M.P. = 105-107 °C. ^{1}H NMR (500 MHz, $CDCl_3$) δ 7.88 (s, 1H), 7.50-7.38 (m, 4H), 7.38-7.32 (m, 1H), 2.54 (d, J = 7.1 Hz, 2H), 1.85-1.55 (m, 6H), 1.30-1.05 (m, 3H), 1.07-0.78 (m, 2H) ppm. ^{13}C NMR (126 MHz, $CDCl_3$) δ 175.1, 141.9, 135.9, 132.0, 129.7, 128.7, 128.6, 37.9, 34.3, 33.4, 26.6, 26.5 ppm. IR (neat, cm^{-1}): 2921, 2848, 1663, 1446, 1262, 1217, 686. HRMS *calcd*. for ($C_{16}H_{20}O_2$-H): 243.1391, *found*: 243.1385.

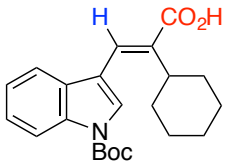

(*E*)-3-(1-(*tert*-butoxycarbonyl)-1*H*-indol-3-yl)-2-cyclohexylacrylic acid (3-34): Following the general procedure using **3-13** and *t*-BuOH (**3-33**) to afford **3-34** (131.2 mg, 73% yield) as a colorless solid. M.P. = 188 – 191 °C. ^{1}H NMR (400 MHz, $CDCl_3$) δ 8.17 (d, J = 8.4 Hz, 1H), 7.84 (s, 1H), 7.78 (d, J = 1.1 Hz, 1H), 7.70 (d, J = 7.8 Hz, 1H), 7.39 (dd, J = 8.4, 1.3 Hz, 1H), 7.35-7.29 (m, 1H), 2.94 (tt, J = 12.1, 3.2 Hz, 1H), 2.19-2.02 (m, 2H), 1.95-1.79 (m, 2H), 1.75-1.68 (m, 12H), 1.38-1.32 (m, 3H) ppm. ^{13}C NMR (101 MHz, $CDCl_3$) δ 173.5, 149.6, 137.1, 135.1, 130.5, 130.1, 125.6, 125.3, 123.4, 119.2, 115.7, 115.4, 84.6, 40.1, 30.5, 28.4, 27.0, 26.2 ppm. IR (neat, cm^{-1}): 2927, 1729, 1669, 1451, 1372, 1144, 743. HRMS *calcd*. for ($C_{22}H_{27}NO_4$-H): 368.1867, *found*: 368.1865.

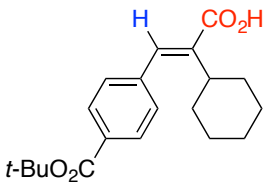

(*E*)-3-(4-(*tert*-butoxycarbonyl)phenyl)-2-cyclohexylacrylic acid (3-35): Following the general procedure using **3-14** and *t*-BuOH (**3-33**) to afford **3-35** (102.4 mg, 66% yield) as a colorless solid. M.P. = 149-151 °C. ^{1}H NMR (400 MHz, $CDCl_3$) δ 8.02 (d, J = 8.3 Hz, 2H), 7.72 (s, 1H), 7.34 (d, J = 8.3 Hz, 2H), 2.72 (tt, J = 12.0, 3.3 Hz, 1H), 2.07 – 1.91 (m, 2H), 1.82-1.69 (m, 2H), 1.61 (m, 12H), 1.30-1.12 (m, 3H) ppm. ^{13}C NMR (101 MHz, $CDCl_3$) δ 173.4, 165.5, 140.1, 139.6, 139.2, 131.8, 129.7, 128.9, 81.5, 38.9, 30.8, 28.4, 26.7, 25.9 ppm. IR (neat, cm^{-1}): 2927, 1713, 1678, 1292, 1161, 1115.

HRMS *calcd*. for ($C_{20}H_{26}O_4$-H): 329.1758, *found*: 329.1760.

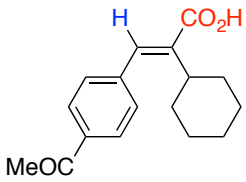

(*E*)-3-(4-acetylphenyl)-2-cyclohexylacrylic acid (3-36): Following the general procedure using **3-15** and *t*-BuOH (**3-33**) to afford **33-36** (102.1 mg, 75% yield; **33-36:33-36'**=6:1) as a colorless solid. **33-36** could be isolated in pure form by column chromatography: M.P. = 156-158 °C. Spectroscopic data for the major isomer (**33-36**): ^{1}H NMR (400 MHz, $CDCl_3$) δ 7.99 (d, *J* = 8.3 Hz, 2H), 7.71 (s, 1H), 7.39 (d, *J* = 8.3 Hz, 2H), 2.79-2.66 (m, 1H), 2.63 (s, 3H), 2.08-1.91 (m, 2H), 1.87-1.69 (m, 2H), 1.69-1.55 (m, 3H), 1.32-1.10 (m, 3H) ppm. ^{13}C NMR (101 MHz, $CDCl_3$) δ 197.8, 173.4, 140.7, 139.6, 139.2, 136.6, 129.2, 128.6, 38.9, 30.8, 26.8, 26.7, 25.9 ppm. IR (neat, cm^{-1}): 2924, 2850, 1668, 1602, 1258, 821. HRMS *calcd*. for ($C_{17}H_{20}O_3$-H): 271.1340, *found*: 271.1340.

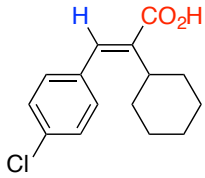

(*E*)-3-(4-chlorophenyl)-2-cyclohexylacrylic acid (3-37): Following the general procedure using **3-16** and *t*-BuOH (**3-33**) to afford **3-37** (68.7 mg, 76% yield; **3-37: 3-37'**=18:1) as a colorless solid. Spectroscopic data for the major isomer (**3-37**): M.P. = 122-123 °C. ^{1}H NMR (400 MHz, $CDCl_3$) δ 7.68 (s, 1H), 7.40 (d, *J* = 8.2 Hz, 2H), 7.27 (d, *J* = 8.2 Hz, 2H), 2.75 (t, *J* = 12.0 Hz, 1H), 2.08-1.98 (m, 2H), 1.79 (d, *J* = 11.2 Hz, 2H), 1.65 (m, 3H), 1.35-1.18 (m, 3H) ppm. ^{13}C NMR (101 MHz, $CDCl_3$) δ 173.7, 139.3, 138.4, 134.4, 134.3, 130.5, 128.9, 38.7, 30.8, 26.8, 26.0 ppm. IR (neat, cm-1): 2925, 2852, 1673, 1238, 816. HRMS *calcd*. for ($C_{15}H_{16}ClO_2$-H): 263.0844, *found*: 263.0838.

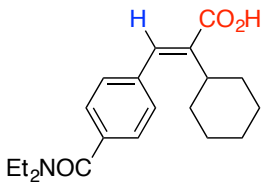

(*E*)-2-cyclohexyl-3-(4-(diethylcarbamoyl)phenyl)acrylic acid (3-38): Following the general procedure using **3-17** to afford **3-38** (126.8 mg, 78% yield) as a colorless solid. M.P. = 149-151 °C. ^{1}H NMR (500 MHz, $CDCl_3$) δ 7.66 (s, 1H), 7.41 (d, *J* = 8.1 Hz, 2H), 7.32 (d, *J* = 8.1 Hz, 2H), 3.57 (brs, 2H), 3.30 (brs, 2H), 2.74 (tt, *J* = 12.0, 3.3 Hz, 1H), 2.08-1.92 (m, 2H), 1.83-1.68 (m, 2H), 1.69-1.51 (m, 3H), 1.39-0.97 (m, 9H) ppm. ^{13}C NMR (126 MHz, $CDCl_3$) δ 173.0, 171.1, 139.2, 138.9, 136.9, 136.9, 129.2, 126.6, 43.6, 39.6, 38.7, 30.8, 26.7, 25.9, 14.4, 13.0 ppm. IR (neat, cm^{-1}): 2925, 1697, 1589, 1209, 839, 765. HRMS *calcd*. for ($C_{20}H_{27}NO_3$-H): 328.1918, *found*: 328.1915.

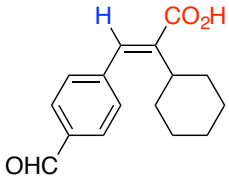

(*E*)-2-cyclohexyl-3-(4-formylphenyl)acrylic acid (3-39): Following the general procedure using **3-18** and *t*-BuOH (**3-33**) to afford **3-39** (107.2 mg, 85% yield over two steps; **3-39: 3-39´**=15:1) as a colorless solid. Spectroscopic data for the major isomer (**3-39**): M.P. = 177-178 °C. ^{1}H NMR (400 MHz, $CDCl_3$) δ 10.04 (s, 1H), 7.92 (d, *J* = 8.2 Hz, 2H), 7.72 (s, 1H), 7.46 (d, *J* = 8.1 Hz, 2H), 2.84-2.57 (m, 1H), 2.16-1.90 (m, 2H), 1.82-1.69 (m, 2H), 1.69-1.39 (m, 3H), 1.37-0.90 (m, 3H) ppm. ^{13}C NMR (101 MHz, $CDCl_3$) δ 191.9, 173.4, 142.1, 140.0, 139.0, 135.9, 130.0, 129.6, 39.0, 30.8, 26.7, 25.9 ppm. IR (neat, cm^{-1}): 2930, 2848, 1698, 1667, 1598, 1199, 835, 666. HRMS *calcd*. for ($C_{16}H_{18}O_3$-H): 257.1183, *found*: 257.1181.

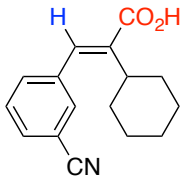

(*E*)-3-(3-cyanophenyl)-2-cyclohexylacrylic acid (3-40): Following the general procedure using **3-19** to afford **3-40** (93.2 mg, 73% yield) as a colorless solid. M.P. = 159-161 °C. ^{1}H NMR (500 MHz, $CDCl_3$) δ 7.71-7.61 (m, 2H), 7.56 (s, 1H), 7.54-7.49 (m, 2H), 2.62 (tt, *J* = 12.0, 3.3 Hz, 1H), 2.03-1.92 (m, 2H), 1.82-1.73 (m, 2H), 1.66 (dt, *J* = 10.3, 3.0 Hz, 1H), 1.64-1.54 (m, 2H), 1.35-1.07 (m, 3H) ppm. ^{13}C NMR (126 MHz, $CDCl_3$) δ 173.2, 140.1, 137.7, 137.2, 133.2, 132.4, 131.8, 129.5, 118.6, 113.0, 38.9,

30.8, 26.6, 25.8 ppm. IR (neat, cm^{-1}): 2926, 2856, 2233, 1677, 1265, 919, 797. HRMS *calcd*. for ($C_{16}H_{17}NO_2$-H): 254.1187, *found*: 254.1190.

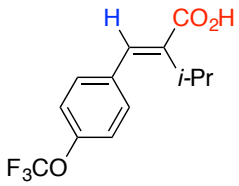

(*E*)-3-methyl-2-(4-(trifluoromethoxy)benzylidene)butanoic acid (3-41): Following the general procedure using **3-20** and *t*-BuOH (**3-33**) to afford **3-41** (107 mg, 80% yield) as a colorless solid. M.P. = 82-84 °C. ^{1}H NMR (500 MHz, $CDCl_3$) δ 7.73 (s, 1H), 7.38 (d, *J* = 8.3 Hz, 2H), 7.28 (d, *J* = 8.3 Hz, 2H), 3.17 (m, 1H), 1.33 (d, *J* = 7.0 Hz, 6H) ppm. ^{13}C NMR (126 MHz, $CDCl_3$) δ 173.8, 149.1, 139.2, 139.0, 134.4, 130.6, 120.63 (q, *J* = 257.6 Hz), 121.0, 27.7, 23.8. ^{19}F NMR (376 MHz, $CDCl_3$) δ -57.90 ppm. IR (neat, cm^{-1}): 2963, 1676, 1247, 1203, 1159. HRMS *calcd*. for ($C_{13}H_{13}F_3O_3$-H): 273.0744, *found*: 273.0747.

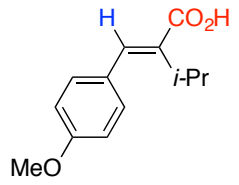

(*E*)-2-(4-methoxybenzylidene)-3-methylbutanoic acid (3-42): Following the general procedure using **3-21** and *t*-BuOH (**3-33**) to afford **3-42** (66.3 mg, 63% yield) as a colorless solid. M.P. = 125-127 °C. ^{1}H NMR (500 MHz, $CDCl_3$) δ 7.69 (s, 1H), 7.32 (d, *J* = 8.7 Hz, 2H), 6.94 (d, *J* = 8.7 Hz, 2H), 3.84 (s, 3H), 3.25 (m, 1H), 1.30 (d, *J* = 6.9 Hz, 6H) ppm. ^{13}C NMR (126 MHz, $CDCl_3$) δ 173.9, 159.9, 140.2, 136.6, 131.0, 128.3, 114.1, 55.5, 27.5, 21.2 ppm. IR (neat, cm^{-1}): 2957, 1665, 1602, 1509, 1247, 1169, 829. HRMS *calcd*. for ($C_{13}H_{16}O_3$-H): 219.1027, *found*: 219.1023.

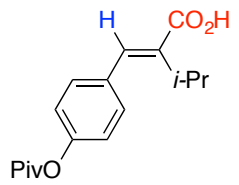

(*E*)-3-methyl-2-(4-(pivaloyloxy)benzylidene)butanoic acid (3-43): Following the general procedure using **3-22** and *t*-BuOH (**3-33**) to afford **33-43** (123.4 mg, 79%

yield) as a colorless solid. M.P. = 165-167 °C. ^{1}H NMR (500 MHz, $CDCl_3$) δ 7.70 (s, 1H), 7.33 (d, *J* = 8.5 Hz, 2H), 7.10 (d, *J* = 8.5 Hz, 2H), 3.17 (m, 1H), 1.37 (s, 9H), 1.28 (d, *J* = 7.0 Hz, 6H) ppm. ^{13}C NMR (126 MHz, $CDCl_3$) δ 177.2, 173.2, 151.1, 139.6, 138.5, 133.3, 130.3, 121.8, 39.3, 27.6, 27.3, 21.2 ppm. IR (neat, cm^{-1}): 2963, 1752, 1683, 1262, 1166, 1109. HRMS *calcd*. for ($C_{17}H_{22}O_4$-H): 289.1445, *found*: 289.1446.

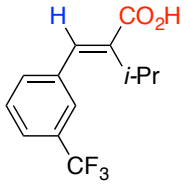

(*E*)-3-methyl-2-(3-(trifluoromethyl)benzylidene)butanoic acid (3-44): Following the general procedure using **3-23** and *t*-BuOH (**3-33**) to afford **33-44** (96.8 mg, 75% yield) as a colorless solid. M.P. = 107-109 °C. ^{1}H NMR (500 MHz, $CDCl_3$) δ 7.74 (s, 1H), 7.61 (d, *J* = 7.6 Hz, 1H), 7.58 (s, 1H), 7.56-7.52 (m, 1H), 7.51 (d, *J* = 7.7 Hz, 1H), 3.10 (m, 1H), 1.31 (d, *J* = 7.0 Hz, 6H) ppm. ^{13}C NMR (126 MHz, $CDCl_3$) δ 173.6, 140.1, 138.7, 136.7, 132.2, 131.2 (q, *J* = 32.4 Hz), 129.2, 131.2 (q, *J* = 272.3 Hz), 125.8 (q, *J* = 3.8 Hz), 125.1 (q, *J* = 3.8 Hz), 27.8, 21.2. ^{19}F NMR (376 MHz, $CDCl_3$) δ -62.94 ppm. IR (neat, cm^{-1}): 2968, 1680, 1329, 1286, 1120, 805, 700. HRMS *calcd*. for ($C_{13}H_{13}F_3O_2$-H): 257.0795, *found*: 257.0801.

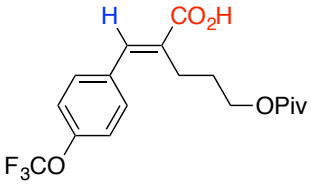

(*E*)-5-(pivaloyloxy)-2-(4-(trifluoromethoxy)benzylidene)pentanoic acid (3-45): Following the general procedure using **3-24** and *t*-BuOH (**3-33**) to afford **3-45** (162.9 mg, 87% yield) as a colorless solid. M.P. = 78-79 °C. ^{1}H NMR (400 MHz, $CDCl_3$) δ 7.84 (s, 1H), 7.45 (d, *J* = 8.3 Hz, 2H), 7.27 (d, *J* = 8.3 Hz, 2H), 4.15 (t, *J* = 6.1 Hz, 2H), 2.73-2.53 (m, 2H), 2.03-1.87 (m, 2H), 1.20 (s, 9H) ppm. ^{13}C NMR (101 MHz, $CDCl_3$) δ 178.8, 173.6, 149.5 (q, *J* = 1.8 Hz), 140.4, 134.0, 132.5, 131.0, 121.1, 120.6 (q, *J* = 257.8 Hz), 64.2, 38.9, 28.3, 27.3, 24.2. ^{19}F NMR (376 MHz, $CDCl_3$) δ -57.91 ppm. IR (neat, cm^{-1}): 2974, 1726, 1686, 1246, 1150, 849. HRMS *calcd*. for ($C_{18}H_{21}F_3O_5$-H): 373.1268, *found*: 373.1265.

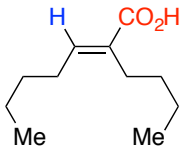

(*E*)-2-butylhept-2-enoic acid (3-46): Following the general procedure using **dec-5-yne** and *t*-BuOH (**3-33**) to afford **3-46** (55.3 mg, 60% yield) as a colorless solid. The spectroscopic data correspond to those previously reported in the literature.[116] ^{1}H NMR (400 MHz, $CDCl_3$) δ 6.90 (t, *J* = 7.5 Hz, 1H), 2.32-2.26 (m, 2H), 2.19-2.23 (m, 2H), 1.70-1.25 (m, 8H), 0.86 – 0.94 (m, 6H) ppm. ^{13}C NMR (101 MHz, $CDCl_3$) δ 174.1, 145.7, 132.0, 31.7, 31.1, 28.6, 26.4, 22.9, 22.7, 14.1 (2C) ppm.

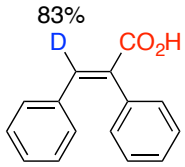

(*E*)-3-D-2,3-diphenylacrylic acid (3-3D$_1$): Following the general procedure using **3-1** to afford **3-3D$_1$** (52.9 mg, 47% yield) as a colorless solid. M.P. = 166-168 °C. ^{1}H NMR (500 MHz, $CDCl_3$) δ 7.96 (s, 0.17H), 7.46-7.34 (m, 3H), 7.26 (s, 3H), 7.17 (dd, *J* = 8.3, 1.4 Hz, 2H), 7.12-7.01 (m, 2H) ppm. ^{13}C NMR (126 MHz, $CDCl_3$) δ 173.0, 142.6, 135.5, 134.4, 131.7, 131.0, 130.0, 129.7, 128.9, 128.5, 128.2 ppm. IR (neat, cm^{-1}): 1671, 1424, 1330, 1259, 695. HRMS *calcd*. for ($C_{15}H_{11}DO_2$-H): 224.0827, *found*: 224.0827.

[116] Back, T. G.; Minksztym, K. *Chem. Commun.* **1997**, 1759.

3.6.3 Selected Examples of NMR Spectra

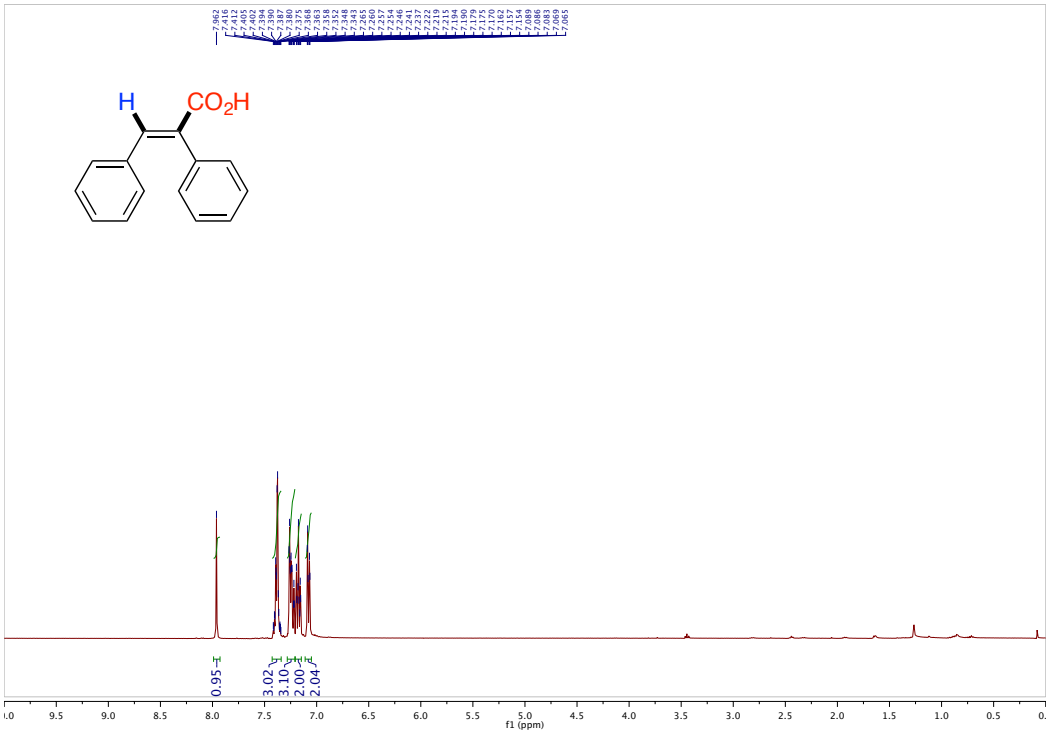

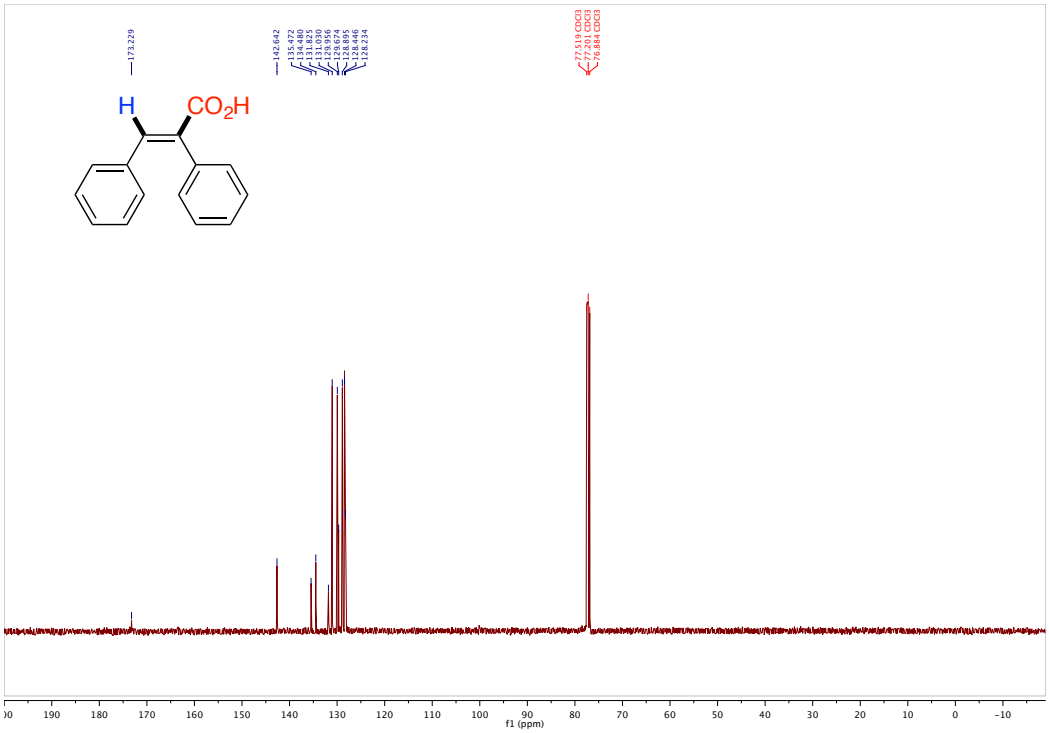

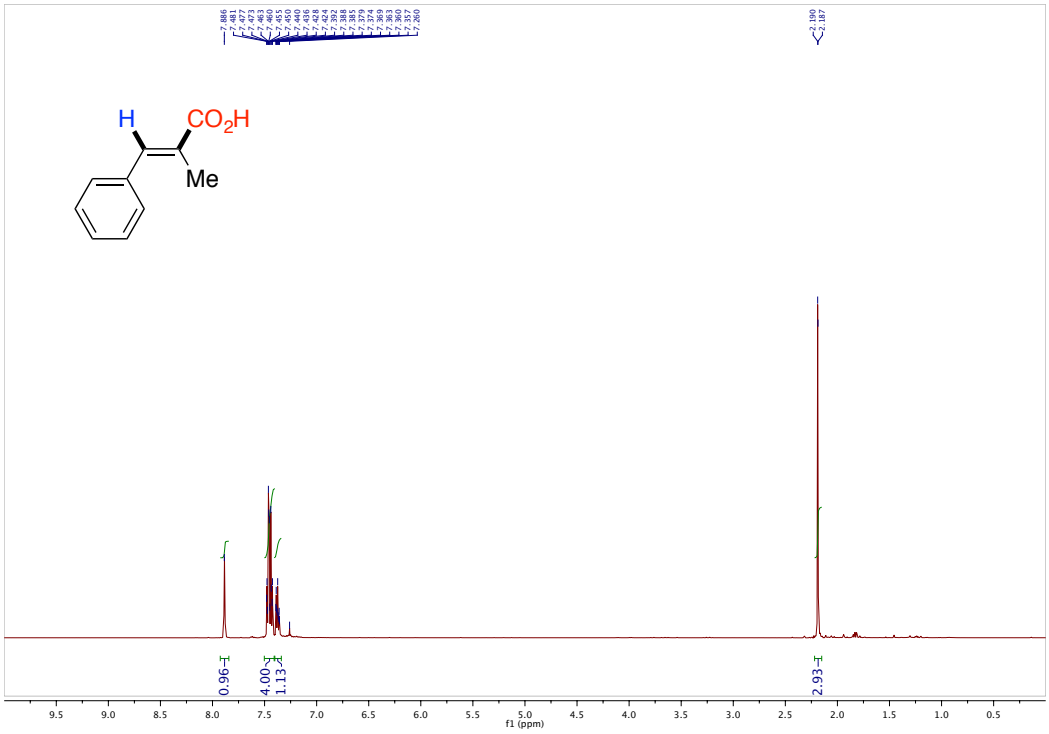
H
CO2H
Me
0.96
4.00
1.13
2.93
f1 (ppm)

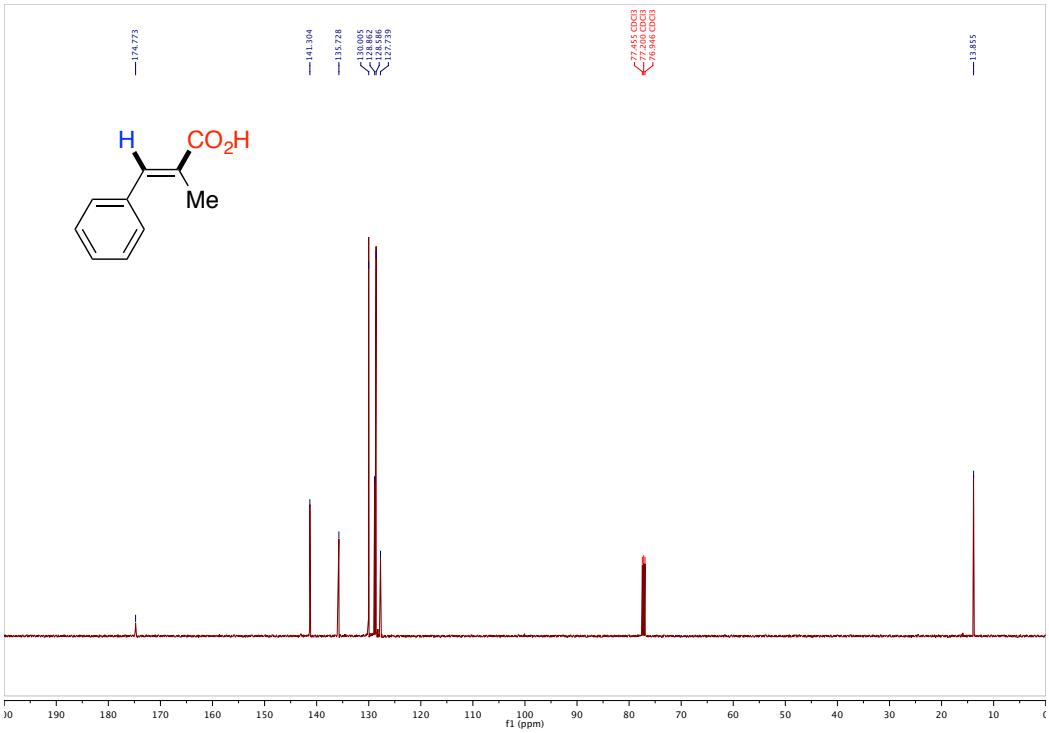
174.773
141.304
135.728
130.005
128.862
128.586
127.239
77.455 CDCl3
77.000 CDCl3
76.546 CDCl3
13.855
H
CO2H
Me
f1 (ppm)

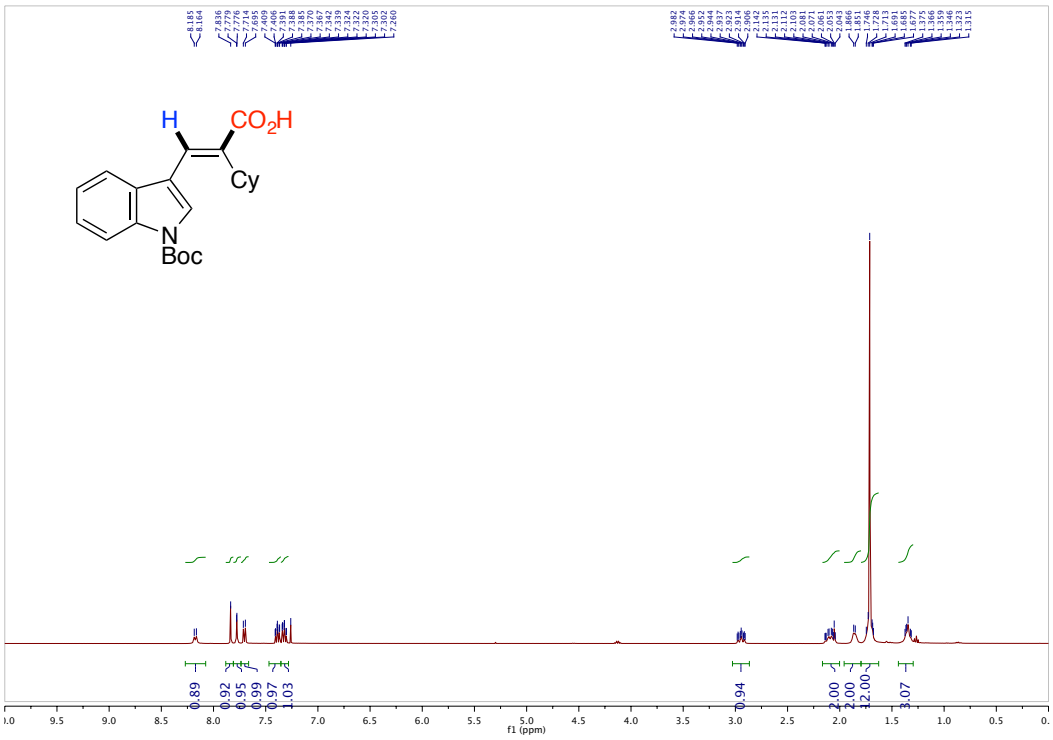
H
CO2H
Cy
N
Boc
f1 (ppm)

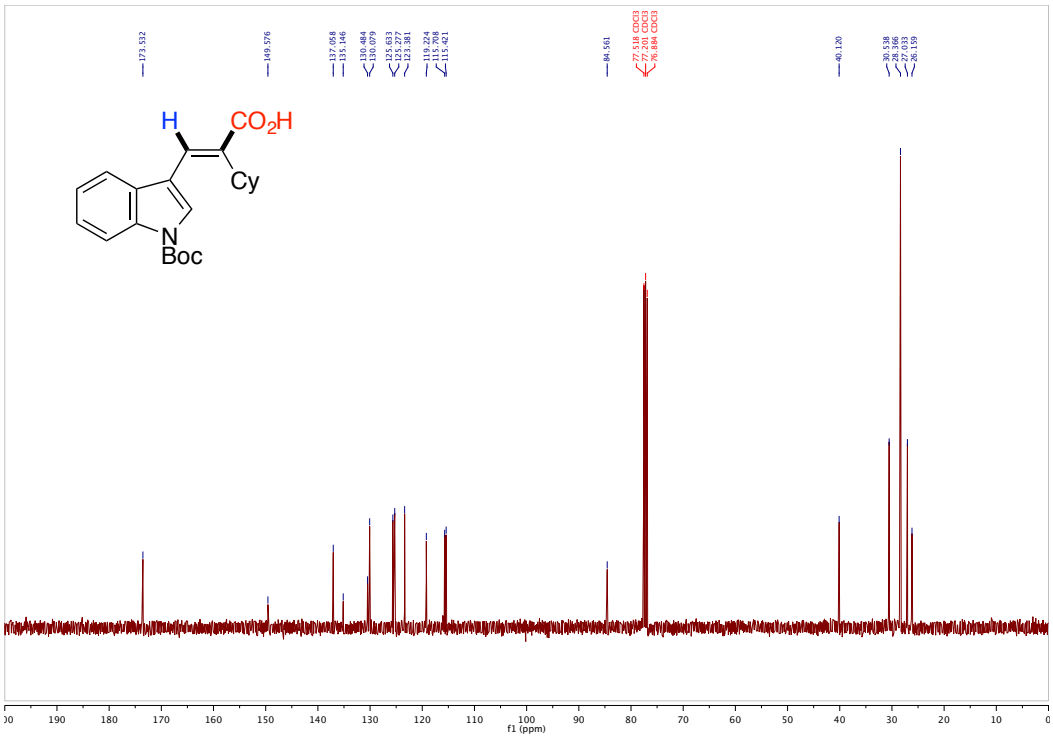
H
CO2H
Cy
N
Boc
f1 (ppm)

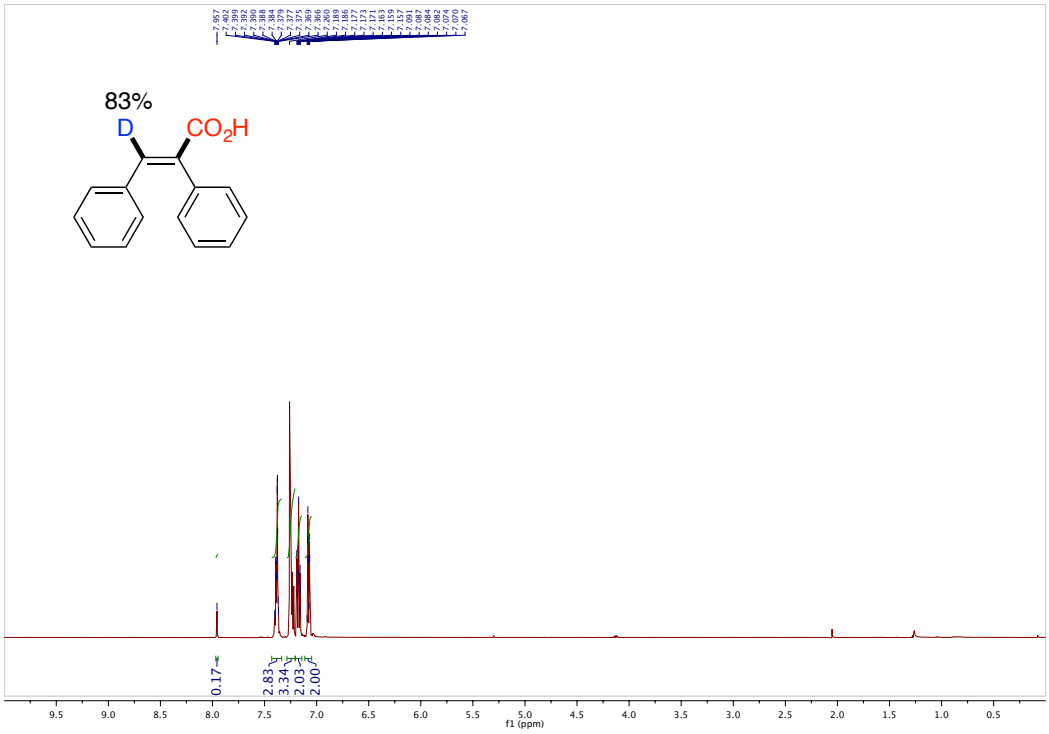
83%
D
CO2H
0.17
2.83
3.34
2.03
2.00
f1 (ppm)

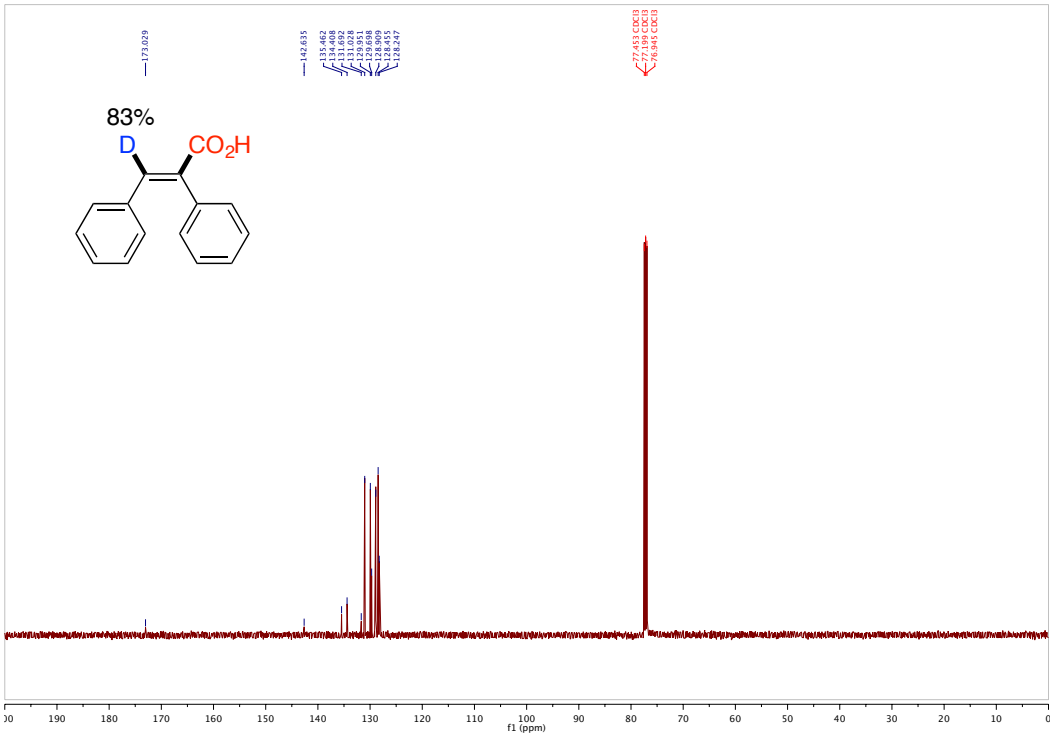
83%
D
CO2H
f1 (ppm)

3.6.4 Mechanistic Studies

(1) Reaction of 3-1 with different secondary alcohols.

→ Reaction with 3-2D$_2$

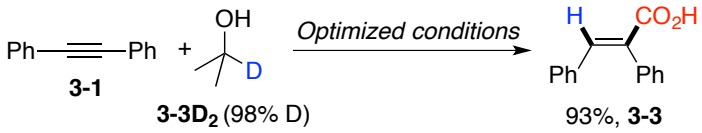

Following the general procedure using **3-1** and **3-2D$_2$** to afford **3-3** (104.3 mg, 93% yield) as a white solid.

→ Reaction with 3-2D$_1$

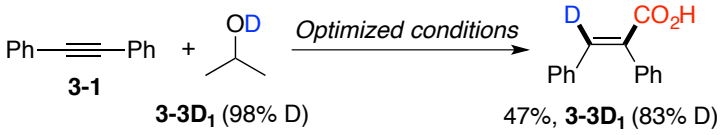

Following the general procedure using **3-1** and **3-2D$_1$** to afford **3-3D$_1$** (52.7 mg, 47% yield) as a white solid. The D-content was determined by H NMR analysis.

→ Reaction with 3-47

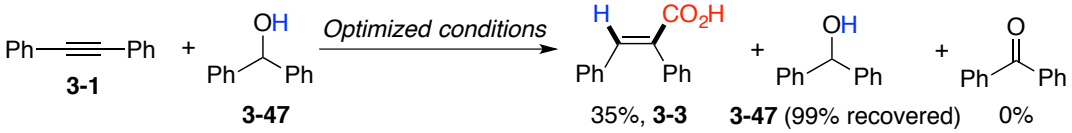

Following the general procedure using **3-1** and **3-47** to afford **3-3** (39.3 mg, 35% yield) as a white solid.

(2) Reaction rate of 3-2 *vs* 3-2D$_1$.

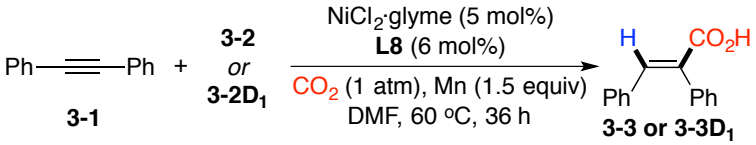

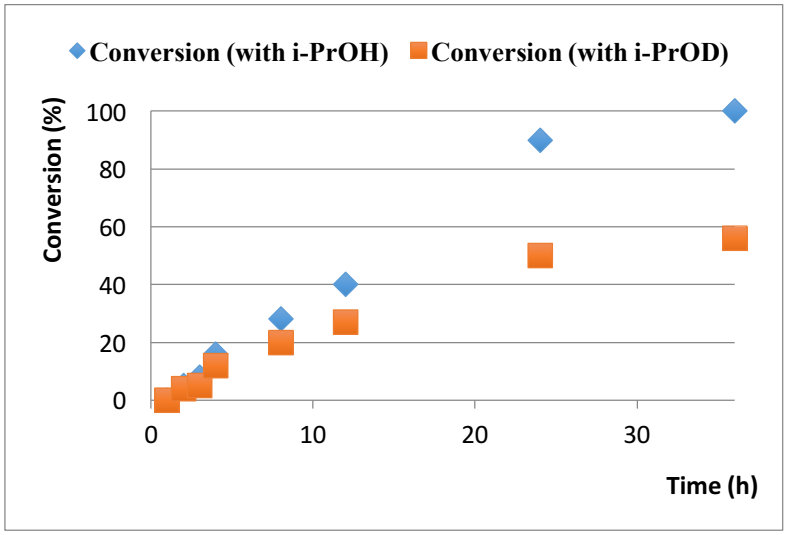

Following the general procedure, the yields were measured by HPLC using naphthalene as internal standard. The results clearly indicate that **3-2** reacts at a significant higher rate than **3-2D$_1$**. Taking into consideration initial rates (<30% conversion), the k_H/k_D was found to be 1.14.

(3) Stoichiometric experiments

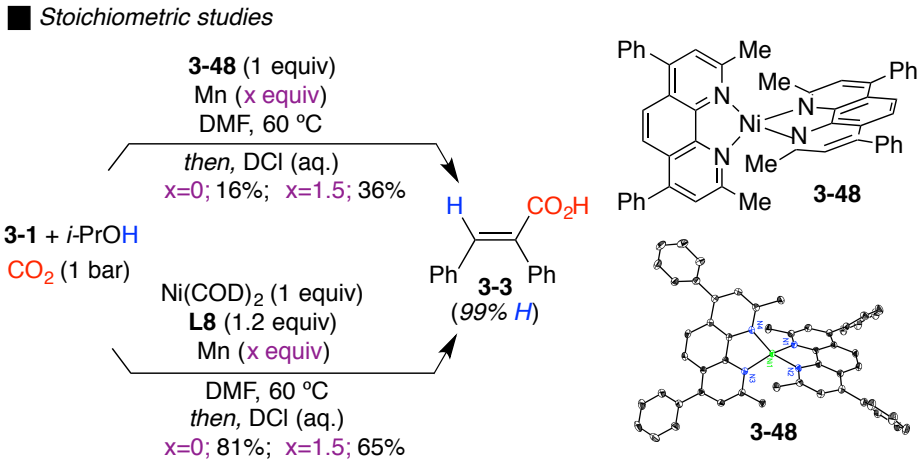

→ Reaction with complex-3-48

A Schlenk tube containing a stirring bar was charged with diphenylacetylene (44.6 mg, 0.25 mmol), complex-3-48 (194.9 mg, 0.25 mmol) inside of glovebox. The tube was then evacuated and back-filled with CO_2 three times. *i*-PrOH (28.7 μL, 0.375 mmol) and DMF (2 mL) were then added by syringe under a CO_2 flow. Once added, the Schlenk tube was closed at atmospheric pressure of CO_2 (1atm) and stirred for 36 h at 60°C. The mixture was quenched with DCl (2M) and extracted with DCM. The

combined organic layers were washed with brine and dried over anhydrous $MgSO_4$ and evaporated. The residue was purified by flash chromatography (hexanes/ethyl acetate = 10/1 to 1/1).

a) Following the above procedure, Mn (20.6 mg, 0.375 mmol) was used, **3a** was obtained in 36% isolated yield as a white solid.

b) Following the above procedure, no Mn (20.6 mg, 0.375 mmol) was used, **3a** was obtained in 16% isolated yield as a white solid.

→ **Reaction with $Ni(COD)_2$**

A Schlenk tube containing a stirring bar was charged with diphenylacetylene (44.6 mg, 0.25 mmol), bathocuproine (108 mg, 0.30 mmol) and $Ni(COD)_2$ (69 mg, 0.25 mmol) inside of glovebox. The tube was then evacuated and back-filled with CO_2 three times. *i*-PrOH (28.7 µL, 0.375 mmol) and DMF (2 mL) were then added by syringe under a CO_2 flow. Once added, the Schlenk tube was closed at atmospheric pressure of CO_2 (1atm) and stirred for 36 h at 60 °C. The mixture was quenched with DCl (2M) and extracted with DCM. The combined organic layers were washed with brine and dried over anhydrous $MgSO_4$ and evaporated. The residue was purified by flash chromatography (hexanes/ethyl acetate = 10/1 to 1/1).

a) Following the above procedure, Mn (20.6 mg, 0.375 mmol) was used, **3a** was obtained in 65% isolated yield as a white solid.

b) Following the above procedure, no Mn (20.6 mg, 0.375 mmol) was used, **3a** was obtained in 81% isolated yield as a white solid

3.6.5 X-Ray crystallographic data for 3-3, 3-23 and 3-42

X-Ray crystallographic data of 3-3

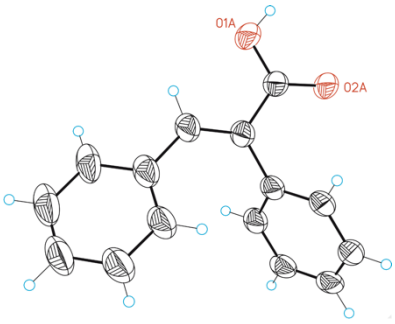

Table 1. Crystal data and structure refinement for **3-3**.

Identification code	**3-3**
Empirical formula	C15.50 H13 O2.17
Formula weight	233.92
Temperature	100(2) K
Wavelength	0.71073 Å
Crystal system	Triclinic
Space group	P-1
Unit cell dimensions	a = 5.8667(11)Å α = 119.655(10)°.
	b = 38.923(6)Å β = 92.878(9)°.
	c = 38.924(6)Å γ = 92.933(9)°.
Volume	7685(2) Å3
Z	24
Density (calculated)	1.213 Mg/m3
Absorption coefficient	0.080 mm-1
F(000)	2960
Crystal size	0.20 x 0.20 x 0.20 mm3
Theta range for data collection	2.418 to 25.373°.
Index ranges	-5<=h<=7,-46<=k<=33,-40<=l<=46
Reflections collected	37942
Independent reflections	24861[R(int) = 0.0455]
Completeness to theta =25.373°	98.4%

Absorption correction Multi-scan

Max. and min. transmission 0.998 and 0.768

Refinement method Full-matrix least-squares on F2

Data / restraints / parameters 24861/ 1889/ 2528

Goodness-of-fit on F2 1.024

Final R indices [I>2sigma(I)] R1 = 0.0797, wR2 = 0.1670

R indices (all data) R1 = 0.1739, wR2 = 0.2075

Largest diff. peak and hole 0.383 and -0.396 e.Å-3

Table 2. Bond lengths [Å] and angles [°] for **3-3**.

Bond lengths----

O1A-C1A 1.326(6)

O2A-C1A 1.228(6)

C1A-C2A 1.469(7)

C2A-C9A 1.339(6)

C2A-C3A 1.482(6)

C3A-C4A 1.390(6)

C3A-C8A 1.401(7)

C4A-C5A 1.380(6)

C5A-C6A 1.372(7)

C6A-C7A 1.375(6)

C7A-C8A 1.381(6)

C9A-C10A 1.455(8)

C10A-C15A 1.390(7)

C10A-C11A 1.400(9)

C11A-C12A 1.389(7)

C12A-C13A 1.396(9)

C13A-C14A 1.362(11)

C14A-C15A 1.384(9)

O1X-C1X 1.326(6)

O2X-C1X 1.231(7)

C1X-C2X 1.468(8)
C2X-C9X 1.339(7)
C2X-C3X 1.484(7)
C3X-C4X 1.390(7)
C3X-C8X 1.400(7)
C4X-C5X 1.380(7)
C5X-C6X 1.372(8)
C6X-C7X 1.375(7)
C7X-C8X 1.381(7)
C9X-C10X 1.457(8)
C10X-C15X 1.391(8)
C10X-C11X 1.401(9)
C11X-C12X 1.388(8)
C12X-C13X 1.396(10)
C13X-C14X 1.361(12)
C14X-C15X 1.384(10)
O1B-C1B 1.236(5)
O2B-C1B 1.315(4)
C1B-C2B 1.466(6)
C2B-C9B 1.337(6)
C2B-C3B 1.501(5)
C3B-C8B 1.372(6)
C3B-C4B 1.395(5)
C4B-C5B 1.381(6)
C5B-C6B 1.371(6)
C6B-C7B 1.382(6)
C7B-C8B 1.380(5)
C9B-C10B 1.446(6)
C10B-C15B 1.397(6)
C10B-C11B 1.406(6)
C11B-C12B 1.375(6)
C12B-C13B 1.402(6)
C13B-C14B 1.370(6)

C14B-C15B 1.366(7)
O1C-C1C 1.304(5)
O2C-C1C 1.224(5)
C1C-C2C 1.494(5)
C2C-C9C 1.332(5)
C2C-C3C 1.481(5)
C3C-C4C 1.378(5)
C3C-C8C 1.397(6)
C4C-C5C 1.380(6)
C5C-C6C 1.372(6)
C6C-C7C 1.382(6)
C7C-C8C 1.369(6)
C9C-C10C 1.481(5)
C10C-C11C 1.387(6)
C10C-C15C 1.398(6)
C11C-C12C 1.389(6)
C12C-C13C 1.377(7)
C13C-C14C 1.355(7)
C14C-C15C 1.410(6)
O1D-C1D 1.216(5)
O2D-C1D 1.320(4)
C1D-C2D 1.481(6)
C2D-C9D 1.335(5)
C2D-C3D 1.490(5)
C3D-C4D 1.384(5)
C3D-C8D 1.391(5)
C4D-C5D 1.381(5)
C5D-C6D 1.375(6)
C6D-C7D 1.379(6)
C7D-C8D 1.380(5)
C9D-C10D 1.466(6)
C10D-C11D 1.391(6)
C10D-C15D 1.398(6)

C11D-C12D 1.414(7)
C12D-C13D 1.371(7)
C13D-C14D 1.365(6)
C14D-C15D 1.387(6)
O1E-C1E 1.308(5)
O2E-C1E 1.236(5)
C1E-C2E 1.480(6)
C2E-C9E 1.338(6)
C2E-C3E 1.496(5)
C3E-C8E 1.385(5)
C3E-C4E 1.394(6)
C4E-C5E 1.375(6)
C5E-C6E 1.382(6)
C6E-C7E 1.385(6)
C7E-C8E 1.384(5)
C9E-C10E 1.462(6)
C10E-C11E 1.392(6)
C10E-C15E 1.393(6)
C11E-C12E 1.372(7)
C12E-C13E 1.374(7)
C13E-C14E 1.387(6)
C14E-C15E 1.383(6)
O1F-C1F 1.229(6)
O2F-C1F 1.329(5)
C1F-C2F 1.456(7)
C2F-C9F 1.330(7)
C2F-C3F 1.499(6)
C3F-C4F 1.385(6)
C3F-C8F 1.388(6)
C4F-C5F 1.388(6)
C5F-C6F 1.378(7)
C6F-C7F 1.367(7)
C7F-C8F 1.379(6)

C9F-C10F 1.451(8)
C10F-C11F 1.398(7)
C10F-C15F 1.402(8)
C11F-C12F 1.394(9)
C12F-C13F 1.392(10)
C13F-C14F 1.378(9)
C14F-C15F 1.391(8)
O1Y-C1Y 1.231(7)
O2Y-C1Y 1.327(6)
C1Y-C2Y 1.456(8)
C2Y-C9Y 1.328(8)
C2Y-C3Y 1.499(6)
C3Y-C4Y 1.385(7)
C3Y-C8Y 1.388(7)
C4Y-C5Y 1.386(7)
C5Y-C6Y 1.378(8)
C6Y-C7Y 1.368(7)
C7Y-C8Y 1.383(7)
C9Y-C10Y 1.453(9)
C10Y-C11Y 1.398(8)
C10Y-C15Y 1.404(9)
C11Y-C12Y 1.396(10)
C12Y-C13Y 1.394(11)
C13Y-C14Y 1.378(9)
C14Y-C15Y 1.392(9)
O1G-C1G 1.222(5)
O2G-C1G 1.320(5)
C1G-C2G 1.479(5)
C2G-C9G 1.339(5)
C2G-C3G 1.483(5)
C3G-C4G 1.383(6)
C3G-C8G 1.400(5)
C4G-C5G 1.378(6)

C5G-C6G 1.389(6)
C6G-C7G 1.364(6)
C7G-C8G 1.375(6)
C9G-C10G 1.468(6)
C10G-C11G 1.396(6)
C10G-C15G 1.407(6)
C11G-C12G 1.391(6)
C12G-C13G 1.368(7)
C13G-C14G 1.366(7)
C14G-C15G 1.400(6)
O1H-C1H 1.322(4)
C1H-O2H 1.233(4)
C1H-C2H 1.469(5)
C2H-C9H 1.346(5)
C2H-C3H 1.486(5)
C3H-C8H 1.386(5)
C3H-C4H 1.392(5)
C4H-C5H 1.393(6)
C5H-C6H 1.362(6)
C6H-C7H 1.376(6)
C7H-C8H 1.388(5)
C9H-C10H 1.465(5)
C10H-C11H 1.389(5)
C10H-C15H 1.404(5)
C11H-C12H 1.369(6)
C12H-C13H 1.383(6)
C13H-C14H 1.390(6)
C14H-C15H 1.372(6)
O1I-C1I 1.229(4)
O2I-C1I 1.323(4)
C1I-C2I 1.468(6)
C2I-C9I 1.339(5)
C2I-C3I 1.495(5)

C3I-C8I	1.385(5)
C3I-C4I	1.387(5)
C4I-C5I	1.378(5)
C5I-C6I	1.377(6)
C6I-C7I	1.379(6)
C7I-C8I	1.385(5)
C9I-C10I	1.466(6)
C10I-C11I	1.390(6)
C10I-C15I	1.395(5)
C11I-C12I	1.372(6)
C12I-C13I	1.380(6)
C13I-C14I	1.374(6)
C14I-C15I	1.389(6)
O1J-C1J	1.230(5)
O2J-C1J	1.313(4)
C1J-C2J	1.474(5)
C2J-C9J	1.352(5)
C2J-C3J	1.483(5)
C3J-C8J	1.391(6)
C3J-C4J	1.391(5)
C4J-C5J	1.394(5)
C5J-C6J	1.371(6)
C6J-C7J	1.371(6)
C7J-C8J	1.382(6)
C9J-C10J	1.465(5)
C10J-C11J	1.392(6)
C10J-C15J	1.392(5)
C11J-C12J	1.382(6)
C12J-C13J	1.377(6)
C13J-C14J	1.375(6)
C14J-C15J	1.385(6)
O1K-C1K	1.327(5)
O2K-C1K	1.228(6)

C1K-C2K 1.459(7)
C2K-C9K 1.348(7)
C2K-C3K 1.494(6)
C3K-C4K 1.381(6)
C3K-C8K 1.394(6)
C4K-C5K 1.377(6)
C5K-C6K 1.372(7)
C6K-C7K 1.366(7)
C7K-C8K 1.391(6)
C9K-C10K 1.444(8)
C10K-C15K 1.402(8)
C10K-C11K 1.410(7)
C11K-C12K 1.378(9)
C12K-C13K 1.380(10)
C13K-C14K 1.401(9)
C14K-C15K 1.378(8)
O1K'-C1K' 1.326(6)
O2K'-C1K' 1.231(7)
C1K'-C2K' 1.460(8)
C2K'-C9K' 1.346(7)
C2K'-C3K' 1.495(7)
C3K'-C4K' 1.380(7)
C3K'-C8K' 1.393(7)
C4K'-C5K' 1.380(7)
C5K'-C6K' 1.372(7)
C6K'-C7K' 1.365(8)
C7K'-C8K' 1.388(7)
C9K'-C10' 1.444(8)
C10'-C15' 1.402(9)
C10'-C11' 1.410(8)
C11'-C12' 1.379(10)
C12'-C13' 1.382(10)
C13'-C14' 1.399(9)

C14'-C15' 1.378(8)
O1L-C1L 1.233(5)
O2L-C1L 1.315(5)
C1L-C2L 1.479(6)
C2L-C9L 1.340(6)
C2L-C3L 1.499(5)
C3L-C8L 1.381(5)
C3L-C4L 1.392(5)
C4L-C5L 1.395(5)
C5L-C6L 1.375(6)
C6L-C7L 1.378(6)
C7L-C8L 1.379(5)
C9L-C10L 1.453(6)
C10L-C11L 1.393(6)
C10L-C15L 1.397(6)
C11L-C12L 1.385(6)
C12L-C13L 1.392(6)
C13L-C14L 1.370(7)
C14L-C15L 1.381(7)
O1S-C1S 1.226(6)
C1S-C3S 1.469(5)
C1S-C2S 1.502(5)
O1S'-C1S' 1.184(8)
C1S'-C2S' 1.513(5)
C1S'-C3S' 1.513(5)
O1T-C1T 1.239(7)
C1T-C3T 1.442(6)
C1T-C2T 1.498(7)
O1U-C1U 1.238(7)
C1U-C3U 1.444(6)
C1U-C2U 1.498(7)
O1V-C1V 1.234(8)
C1V-C3V 1.450(7)

C1V-C2V 1.498(7)
O1V'-C1V' 1.236(8)
C1V'-C3V' 1.452(7)
C1V'-C2V' 1.499(7)

Angles----------
O2A-C1A-O1A 121.1(6)
O2A-C1A-C2A 122.5(5)
O1A-C1A-C2A 116.3(5)
C9A-C2A-C1A 118.8(5)
C9A-C2A-C3A 126.2(5)
C1A-C2A-C3A 114.9(4)
C4A-C3A-C8A 118.5(5)
C4A-C3A-C2A 119.4(5)
C8A-C3A-C2A 122.0(5)
C5A-C4A-C3A 121.2(5)
C6A-C5A-C4A 119.4(5)
C5A-C6A-C7A 120.7(5)
C6A-C7A-C8A 120.4(5)
C7A-C8A-C3A 119.9(5)
C2A-C9A-C10A 128.6(5)
C15A-C10A-C11A 118.0(6)
C15A-C10A-C9A 119.9(7)
C11A-C10A-C9A 122.1(5)
C12A-C11A-C10A 121.0(6)
C11A-C12A-C13A 119.3(8)
C14A-C13A-C12A 120.1(7)
C13A-C14A-C15A 120.7(7)
C14A-C15A-C10A 120.9(8)
O2X-C1X-O1X 120.5(8)
O2X-C1X-C2X 122.4(7)
O1X-C1X-C2X 117.1(7)
C9X-C2X-C1X 119.6(6)

C9X-C2X-C3X 125.7(7)
C1X-C2X-C3X 114.6(7)
C4X-C3X-C8X 118.8(6)
C4X-C3X-C2X 119.4(7)
C8X-C3X-C2X 121.8(7)
C5X-C4X-C3X 121.3(7)
C6X-C5X-C4X 119.0(7)
C5X-C6X-C7X 121.0(7)
C6X-C7X-C8X 120.4(7)
C7X-C8X-C3X 119.5(7)
C2X-C9X-C10X 128.1(8)
C15X-C10X-C11X 117.9(7)
C15X-C10X-C9X 120.0(8)
C11X-C10X-C9X 122.1(7)
C12X-C11X-C10X 121.2(8)
C11X-C12X-C13X 119.2(9)
C14X-C13X-C12X 120.0(8)
C13X-C14X-C15X 120.8(8)
C14X-C15X-C10X 120.8(9)
O1B-C1B-O2B 121.5(4)
O1B-C1B-C2B 122.8(4)
O2B-C1B-C2B 115.7(4)
C9B-C2B-C1B 119.9(4)
C9B-C2B-C3B 125.1(4)
C1B-C2B-C3B 114.9(4)
C8B-C3B-C4B 119.0(4)
C8B-C3B-C2B 119.6(3)
C4B-C3B-C2B 121.2(4)
C5B-C4B-C3B 120.0(4)
C6B-C5B-C4B 120.6(4)
C5B-C6B-C7B 119.6(4)
C8B-C7B-C6B 120.0(4)
C3B-C8B-C7B 120.9(4)

C2B-C9B-C10B 129.7(4)
C15B-C10B-C11B 116.9(5)
C15B-C10B-C9B 120.1(4)
C11B-C10B-C9B 122.8(4)
C12B-C11B-C10B 121.4(4)
C11B-C12B-C13B 119.8(5)
C14B-C13B-C12B 119.2(5)
C15B-C14B-C13B 120.9(5)
C14B-C15B-C10B 121.7(5)
O2C-C1C-O1C 123.4(4)
O2C-C1C-C2C 120.5(4)
O1C-C1C-C2C 116.0(4)
C9C-C2C-C3C 126.0(4)
C9C-C2C-C1C 119.3(4)
C3C-C2C-C1C 114.7(3)
C4C-C3C-C8C 118.6(4)
C4C-C3C-C2C 119.0(4)
C8C-C3C-C2C 122.2(4)
C3C-C4C-C5C 120.7(4)
C6C-C5C-C4C 120.5(5)
C5C-C6C-C7C 119.2(5)
C8C-C7C-C6C 120.8(4)
C7C-C8C-C3C 120.3(4)
C2C-C9C-C10C 127.9(4)
C11C-C10C-C15C 119.0(4)
C11C-C10C-C9C 122.0(4)
C15C-C10C-C9C 118.8(4)
C10C-C11C-C12C 120.8(5)
C13C-C12C-C11C 119.9(5)
C14C-C13C-C12C 120.4(5)
C13C-C14C-C15C 120.9(5)
C10C-C15C-C14C 118.9(5)
O1D-C1D-O2D 122.7(4)

O1D-C1D-C2D 121.9(4)
O2D-C1D-C2D 115.3(4)
C9D-C2D-C1D 120.3(4)
C9D-C2D-C3D 125.7(4)
C1D-C2D-C3D 113.9(4)
C4D-C3D-C8D 118.6(4)
C4D-C3D-C2D 122.4(4)
C8D-C3D-C2D 118.9(4)
C5D-C4D-C3D 120.6(4)
C6D-C5D-C4D 120.5(4)
C5D-C6D-C7D 119.4(4)
C6D-C7D-C8D 120.4(4)
C7D-C8D-C3D 120.5(4)
C2D-C9D-C10D 128.4(4)
C11D-C10D-C15D 118.2(4)
C11D-C10D-C9D 119.7(4)
C15D-C10D-C9D 122.1(4)
C10D-C11D-C12D 119.5(5)
C13D-C12D-C11D 120.5(5)
C14D-C13D-C12D 120.5(5)
C13D-C14D-C15D 119.7(5)
C14D-C15D-C10D 121.6(5)
O2E-C1E-O1E 123.1(4)
O2E-C1E-C2E 121.4(4)
O1E-C1E-C2E 115.5(4)
C9E-C2E-C1E 118.9(4)
C9E-C2E-C3E 126.2(4)
C1E-C2E-C3E 114.9(4)
C8E-C3E-C4E 119.3(4)
C8E-C3E-C2E 118.9(4)
C4E-C3E-C2E 121.7(4)
C5E-C4E-C3E 120.0(4)
C4E-C5E-C6E 121.4(4)

C5E-C6E-C7E 118.3(4)
C8E-C7E-C6E 121.2(4)
C7E-C8E-C3E 119.8(4)
C2E-C9E-C10E 128.8(4)
C11E-C10E-C15E 118.9(4)
C11E-C10E-C9E118.6(4)
C15E-C10E-C9E122.4(4)
C12E-C11E-C10E 120.3(5)
C11E-C12E-C13E 121.1(5)
C12E-C13E-C14E 119.1(5)
C15E-C14E-C13E 120.4(5)
C14E-C15E-C10E 120.1(4)
O1F-C1F-O2F 120.7(6)
O1F-C1F-C2F 123.1(5)
O2F-C1F-C2F 116.3(5)
C9F-C2F-C1F 119.3(5)
C9F-C2F-C3F 125.7(5)
C1F-C2F-C3F 114.8(5)
C4F-C3F-C8F 119.1(4)
C4F-C3F-C2F 122.5(4)
C8F-C3F-C2F 118.4(4)
C3F-C4F-C5F 119.9(5)
C6F-C5F-C4F 120.4(5)
C7F-C6F-C5F 119.7(5)
C6F-C7F-C8F 120.7(5)
C7F-C8F-C3F 120.2(5)
C2F-C9F-C10F 129.0(5)
C11F-C10F-C15F 118.5(6)
C11F-C10F-C9F 119.2(6)
C15F-C10F-C9F 122.2(5)
C12F-C11F-C10F 119.4(7)
C13F-C12F-C11F 121.2(7)
C14F-C13F-C12F 119.9(7)

C13F-C14F-C15F 119.2(8)
C14F-C15F-C10F 121.7(6)
O1Y-C1Y-O2Y 120.6(8)
O1Y-C1Y-C2Y 122.9(7)
O2Y-C1Y-C2Y 116.4(7)
C9Y-C2Y-C1Y 120.2(6)
C9Y-C2Y-C3Y 125.9(7)
C1Y-C2Y-C3Y 113.8(6)
C4Y-C3Y-C8Y 120.0(6)
C4Y-C3Y-C2Y 121.1(6)
C8Y-C3Y-C2Y 118.8(6)
C3Y-C4Y-C5Y 119.7(7)
C6Y-C5Y-C4Y 119.7(7)
C7Y-C6Y-C5Y 120.1(7)
C6Y-C7Y-C8Y 120.6(7)
C7Y-C8Y-C3Y 119.1(7)
C2Y-C9Y-C10Y 128.5(7)
C11Y-C10Y-C15Y 118.7(8)
C11Y-C10Y-C9Y 119.6(8)
C15Y-C10Y-C9Y 121.5(7)
C12Y-C11Y-C10Y 119.0(8)
C13Y-C12Y-C11Y 120.8(8)
C14Y-C13Y-C12Y 120.4(9)
C13Y-C14Y-C15Y 118.6(9)
C14Y-C15Y-C10Y 121.9(7)
O1G-C1G-O2G 121.8(4)
O1G-C1G-C2G 122.3(4)
O2G-C1G-C2G 115.9(4)
C9G-C2G-C1G 120.4(4)
C9G-C2G-C3G 125.6(4)
C1G-C2G-C3G 114.1(3)
C4G-C3G-C8G 118.3(4)
C4G-C3G-C2G 119.2(4)

C8G-C3G-C2G 122.2(4)
C5G-C4G-C3G 121.4(4)
C4G-C5G-C6G 119.5(5)
C7G-C6G-C5G 119.5(4)
C6G-C7G-C8G 121.4(4)
C7G-C8G-C3G 119.9(4)
C2G-C9G-C10G 128.2(4)
C11G-C10G-C15G 118.2(4)
C11G-C10G-C9G 122.2(4)
C15G-C10G-C9G 119.5(4)
C12G-C11G-C10G 120.7(4)
C13G-C12G-C11G 120.5(5)
C14G-C13G-C12G 120.0(5)
C13G-C14G-C15G 121.1(5)
C14G-C15G-C10G 119.5(5)
O2H-C1H-O1H 121.8(4)
O2H-C1H-C2H 122.7(4)
O1H-C1H-C2H 115.5(3)
C9H-C2H-C1H 119.3(4)
C9H-C2H-C3H 124.8(4)
C1H-C2H-C3H 115.8(3)
C8H-C3H-C4H 119.3(4)
C8H-C3H-C2H 119.2(3)
C4H-C3H-C2H 121.5(4)
C3H-C4H-C5H 119.2(4)
C6H-C5H-C4H 121.0(4)
C5H-C6H-C7H 120.2(4)
C6H-C7H-C8H 119.8(4)
C3H-C8H-C7H 120.5(4)
C2H-C9H-C10H 128.4(4)
C11H-C10H-C15H 117.7(4)
C11H-C10H-C9H 118.6(4)
C15H-C10H-C9H 123.6(4)

C12H-C11H-C10H 121.6(4)
C11H-C12H-C13H 120.5(4)
C12H-C13H-C14H 118.7(4)
C15H-C14H-C13H 121.0(4)
C14H-C15H-C10H 120.4(4)
O1I-C1I-O2I 121.6(4)
O1I-C1I-C2I122.9(4)
O2I-C1I-C2I115.5(4)
C9I-C2I-C1I119.2(4)
C9I-C2I-C3I125.5(4)
C1I-C2I-C3I115.3(3)
C8I-C3I-C4I119.1(4)
C8I-C3I-C2I122.1(4)
C4I-C3I-C2I118.8(4)
C5I-C4I-C3I119.8(4)
C6I-C5I-C4I120.9(4)
C5I-C6I-C7I119.8(4)
C6I-C7I-C8I119.7(4)
C7I-C8I-C3I120.7(4)
C2I-C9I-C10I 128.3(4)
C11I-C10I-C15I 118.5(4)
C11I-C10I-C9I 118.1(4)
C15I-C10I-C9I 123.3(4)
C12I-C11I-C10I 121.3(4)
C11I-C12I-C13I 120.0(5)
C14I-C13I-C12I 119.7(5)
C13I-C14I-C15I 120.8(5)
C14I-C15I-C10I 119.7(4)
O1J-C1J-O2J 122.4(4)
O1J-C1J-C2J 122.1(4)
O2J-C1J-C2J 115.5(4)
C9J-C2J-C1J 118.8(4)
C9J-C2J-C3J 125.2(4)

C1J-C2J-C3J 116.0(3)
C8J-C3J-C4J 119.2(4)
C8J-C3J-C2J 122.2(4)
C4J-C3J-C2J 118.6(4)
C3J-C4J-C5J 119.8(4)
C6J-C5J-C4J 120.2(4)
C5J-C6J-C7J 120.4(4)
C6J-C7J-C8J 120.3(4)
C7J-C8J-C3J 120.2(4)
C2J-C9J-C10J 128.1(4)
C11J-C10J-C15J 118.7(4)
C11J-C10J-C9J 117.9(4)
C15J-C10J-C9J 123.3(4)
C12J-C11J-C10J 121.1(4)
C13J-C12J-C11J 119.1(5)
C14J-C13J-C12J 120.7(4)
C13J-C14J-C15J 120.3(5)
C14J-C15J-C10J 119.9(4)
O2K-C1K-O1K 121.6(5)
O2K-C1K-C2K 122.4(5)
O1K-C1K-C2K 116.0(5)
C9K-C2K-C1K 119.3(5)
C9K-C2K-C3K 125.1(5)
C1K-C2K-C3K 115.4(4)
C4K-C3K-C8K 118.9(5)
C4K-C3K-C2K 119.0(4)
C8K-C3K-C2K 122.0(5)
C5K-C4K-C3K 121.6(5)
C6K-C5K-C4K 119.4(5)
C7K-C6K-C5K 119.9(5)
C6K-C7K-C8K 121.5(5)
C7K-C8K-C3K 118.7(5)
C2K-C9K-C10K 128.5(5)

C15K-C10K-C11K 117.8(6)
C15K-C10K-C9K 123.2(5)
C11K-C10K-C9K 118.8(6)
C12K-C11K-C10K 120.0(7)
C11K-C12K-C13K 121.8(6)
C12K-C13K-C14K 118.8(7)
C15K-C14K-C13K 120.0(7)
C14K-C15K-C10K 121.6(6)
O2K'-C1K'-O1K' 120.9(8)
O2K'-C1K'-C2K' 122.6(7)
O1K'-C1K'-C2K' 116.3(7)
C9K'-C2K'-C1K' 120.8(6)
C9K'-C2K'-C3K' 125.2(7)
C1K'-C2K'-C3K' 114.0(6)
C4K'-C3K'-C8K' 119.6(6)
C4K'-C3K'-C2K' 119.9(6)
C8K'-C3K'-C2K' 120.4(6)
C3K'-C4K'-C5K' 120.9(6)
C6K'-C5K'-C4K' 119.3(7)
C7K'-C6K'-C5K' 120.5(7)
C6K'-C7K'-C8K' 121.0(7)
C7K'-C8K'-C3K' 118.7(7)
C2K'-C9K'-C10' 127.9(7)
C15'-C10'-C11' 117.9(7)
C15'-C10'-C9K' 123.0(7)
C11'-C10'-C9K' 118.9(8)
C12'-C11'-C10' 119.9(8)
C11'-C12'-C13' 121.5(8)
C12'-C13'-C14' 119.1(8)
C15'-C14'-C13' 119.8(8)
C14'-C15'-C10' 121.6(7)
O1L-C1L-O2L 122.5(4)
O1L-C1L-C2L 122.1(4)

O2L-C1L-C2L 115.3(4)
C9L-C2L-C1L 119.3(4)
C9L-C2L-C3L 126.2(4)
C1L-C2L-C3L 114.5(4)
C8L-C3L-C4L 119.4(4)
C8L-C3L-C2L 122.4(4)
C4L-C3L-C2L 118.0(4)
C3L-C4L-C5L 119.5(4)
C6L-C5L-C4L 120.4(4)
C5L-C6L-C7L 120.0(4)
C6L-C7L-C8L 120.2(4)
C7L-C8L-C3L 120.6(4)
C2L-C9L-C10L 128.9(4)
C11L-C10L-C15L 118.1(5)
C11L-C10L-C9L122.6(4)
C15L-C10L-C9L119.1(4)
C12L-C11L-C10L 121.0(5)
C11L-C12L-C13L 119.9(5)
C14L-C13L-C12L 119.4(5)
C13L-C14L-C15L 121.0(5)
C14L-C15L-C10L 120.5(5)
O1S-C1S-C3S 121.4(6)
O1S-C1S-C2S 124.9(7)
C3S-C1S-C2S 113.6(6)
O1S'-C1S'-C2S' 123.2(8)
O1S'-C1S'-C3S' 122.6(8)
C2S'-C1S'-C3S' 114.2(7)
O1T-C1T-C3T 119.5(8)
O1T-C1T-C2T 128.5(9)
C3T-C1T-C2T 111.6(8)
O1U-C1U-C3U 119.8(8)
O1U-C1U-C2U 128.4(9)
C3U-C1U-C2U 111.6(8)

O1V-C1V-C3V 120.3(9)
O1V-C1V-C2V 127.9(10)
C3V-C1V-C2V 111.8(8)
O1V'-C1V'-C3V' 119.6(10)
O1V'-C1V'-C2V' 127.0(11)
C3V'-C1V'-C2V' 111.2(9)

Table 3. Torsion angles [°] for **3-1**.

O2A_a-C1A_a-C2A_a-C9A_a 172.3(9)
O1A-C1A-C2A-C9A -7.8(11)
O2A-C1A-C2A-C3A -10.2(11)
O1A-C1A-C2A-C3A 169.6(7)
C9A-C2A-C3A-C4A 64.8(9)
C1A-C2A-C3A-C4A -112.4(7)
C9A-C2A-C3A-C8A -120.1(8)
C1A-C2A-C3A-C8A 62.7(8)
C8A-C3A-C4A-C5A 0.1(9)
C2A-C3A-C4A-C5A 175.4(6)
C3A-C4A-C5A-C6A -0.5(9)
C4A-C5A-C6A-C7A 0.5(10)
C5A-C6A-C7A-C8A -0.2(10)
C6A-C7A-C8A-C3A -0.2(9)
C4A-C3A-C8A-C7A 0.2(9)
C2A-C3A-C8A-C7A -174.9(6)
C1A-C2A-C9A-C10A -174.1(7)
C3A-C2A-C9A-C10A 8.8(12)
C2A-C9A-C10A-C15A -152.6(7)
C2A-C9A-C10A-C11A 31.1(11)
C15A-C10A-C11A-C12A 0.1(11)
C9A-C10A-C11A-C12A 176.5(7)
C10A-C11A-C12A-C13A 2.5(12)

C11A-C12A-C13A-C14A -2.4(12)
C12A-C13A-C14A-C15A -0.2(12)
C13A-C14A-C15A-C10A 2.9(11)
C11A-C10A-C15A-C14A -2.8(10)
C9A-C10A-C15A-C14A -179.3(6)
O2X-C1X-C2X-C9X 170(2)
O1X-C1X-C2X-C9X -8(3)
O2X-C1X-C2X-C3X -13(3)
O1X-C1X-C2X-C3X 168.8(17)
C9X-C2X-C3X-C4X 66(2)
C1X-C2X-C3X-C4X -111.0(17)
C9X-C2X-C3X-C8X -115.5(18)
C1X-C2X-C3X-C8X 68(2)
C8X-C3X-C4X-C5X -2(2)
C2X-C3X-C4X-C5X 176.9(13)
C3X-C4X-C5X-C6X 1(2)
C4X-C5X-C6X-C7X 0(2)
C5X-C6X-C7X-C8X 1(2)
C6X-C7X-C8X-C3X -2(2)
C4X-C3X-C8X-C7X 2(2)
C2X-C3X-C8X-C7X -176.5(13)
C1X-C2X-C9X-C10X -170.2(17)
C3X-C2X-C9X-C10X 13(3)
C2X-C9X-C10X-C15X -149.7(17)
C2X-C9X-C10X-C11X 32(3)
C15X-C10X-C11X-C12X -1(2)
C9X-C10X-C11X-C12X 178.1(14)
C10X-C11X-C12X-C13X 0(2)
C11X-C12X-C13X-C14X 2(2)
C12X-C13X-C14X-C15X -4(3)
C13X-C14X-C15X-C10X 3(3)
C11X-C10X-C15X-C14X -1(2)
C9X-C10X-C15X-C14X 180.0(15)

O1B-C1B-C2B-C9B 171.3(4)
O2B-C1B-C2B-C9B -7.1(6)
O1B-C1B-C2B-C3B -11.5(6)
O2B-C1B-C2B-C3B 170.0(4)
C9B-C2B-C3B-C8B 65.0(6)
C1B-C2B-C3B-C8B -112.0(5)
C9B-C2B-C3B-C4B -120.8(5)
C1B-C2B-C3B-C4B 62.2(5)
C8B-C3B-C4B-C5B -0.3(6)
C2B-C3B-C4B-C5B -174.5(4)
C3B-C4B-C5B-C6B 0.6(7)
C4B-C5B-C6B-C7B -0.9(7)
C5B-C6B-C7B-C8B 0.9(7)
C4B-C3B-C8B-C7B 0.3(7)
C2B-C3B-C8B-C7B 174.6(4)
C6B-C7B-C8B-C3B -0.6(7)
C1B-C2B-C9B-C10B -172.9(4)
C3B-C2B-C9B-C10B 10.2(8)
C2B-C9B-C10B-C15B -152.0(5)
C2B-C9B-C10B-C11B 32.0(7)
C15B-C10B-C11B-C12B 0.5(7)
C9B-C10B-C11B-C12B 176.6(4)
C10B-C11B-C12B-C13B 0.5(7)
C11B-C12B-C13B-C14B 0.1(7)
C12B-C13B-C14B-C15B -1.6(8)
C13B-C14B-C15B-C10B 2.6(8)
C11B-C10B-C15B-C14B -2.0(7)
C9B-C10B-C15B-C14B -178.3(5)
O2C-C1C-C2C-C9C -171.0(4)
O1C-C1C-C2C-C9C 8.3(6)
O2C-C1C-C2C-C3C 10.3(6)
O1C-C1C-C2C-C3C -170.4(4)
C9C-C2C-C3C-C4C -67.3(6)

C1C-C2C-C3C-C4C 111.3(4)
C9C-C2C-C3C-C8C 117.6(5)
C1C-C2C-C3C-C8C -63.8(5)
C8C-C3C-C4C-C5C 0.8(6)
C2C-C3C-C4C-C5C -174.5(3)
C3C-C4C-C5C-C6C 0.0(6)
C4C-C5C-C6C-C7C -1.1(6)
C5C-C6C-C7C-C8C 1.4(6)
C6C-C7C-C8C-C3C -0.6(6)
C4C-C3C-C8C-C7C -0.5(5)
C2C-C3C-C8C-C7C 174.6(3)
C3C-C2C-C9C-C10C -8.6(7)
C1C-C2C-C9C-C10C 172.8(4)
C2C-C9C-C10C-C11C -34.2(7)
C2C-C9C-C10C-C15C 150.2(5)
C15C-C10C-C11C-C12C -1.7(7)
C9C-C10C-C11C-C12C -177.3(4)
C10C-C11C-C12C-C13C -0.2(7)
C11C-C12C-C13C-C14C 0.6(8)
C12C-C13C-C14C-C15C 0.9(8)
C11C-C10C-C15C-C14C 3.2(7)
C9C-C10C-C15C-C14C 178.9(4)
C13C-C14C-C15C-C10C -2.8(7)
O1D-C1D-C2D-C9D 171.4(4)
O2D-C1D-C2D-C9D -8.3(6)
O1D-C1D-C2D-C3D -10.2(6)
O2D-C1D-C2D-C3D 170.1(4)
C9D-C2D-C3D-C4D -117.9(5)
C1D-C2D-C3D-C4D 63.8(5)
C9D-C2D-C3D-C8D 66.9(6)
C1D-C2D-C3D-C8D -111.4(4)
C8D-C3D-C4D-C5D 1.0(6)
C2D-C3D-C4D-C5D -174.2(4)

C3D-C4D-C5D-C6D -0.4(7)

C4D-C5D-C6D-C7D -0.4(7)

C5D-C6D-C7D-C8D 0.5(7)

C6D-C7D-C8D-C3D 0.2(7)

C4D-C3D-C8D-C7D -0.9(6)

C2D-C3D-C8D-C7D 174.5(4)

C1D-C2D-C9D-C10D -173.0(4)

C3D-C2D-C9D-C10D 8.9(8)

C2D-C9D-C10D-C11D -150.4(5)

C2D-C9D-C10D-C15D 33.4(7)

C15D-C10D-C11D-C12D -2.5(7)

C9D-C10D-C11D-C12D -178.9(4)

C10D-C11D-C12D-C13D 2.7(7)

C11D-C12D-C13D-C14D -1.2(8)

C12D-C13D-C14D-C15D -0.4(8)

C13D-C14D-C15D-C10D 0.5(7)

C11D-C10D-C15D-C14D 1.0(7)

C9D-C10D-C15D-C14D 177.3(4)

O2E-C1E-C2E-C9E -171.6(4)

O1E-C1E-C2E-C9E 8.7(6)

O2E-C1E-C2E-C3E 10.2(6)

O1E-C1E-C2E-C3E -169.6(4)

C9E-C2E-C3E-C8E -65.3(6)

C1E-C2E-C3E-C8E 112.8(4)

C9E-C2E-C3E-C4E 119.8(5)

C1E-C2E-C3E-C4E -62.1(5)

C8E-C3E-C4E-C5E 0.0(6)

C2E-C3E-C4E-C5E 174.8(4)

C3E-C4E-C5E-C6E -0.8(6)

C4E-C5E-C6E-C7E 1.3(6)

C5E-C6E-C7E-C8E -1.1(6)

C6E-C7E-C8E-C3E 0.3(6)

C4E-C3E-C8E-C7E 0.3(6)

C2E-C3E-C8E-C7E -174.7(4)
C1E-C2E-C9E-C10E 172.9(4)
C3E-C2E-C9E-C10E -9.1(8)
C2E-C9E-C10E-C11E 151.4(5)
C2E-C9E-C10E-C15E -32.7(7)
C15E-C10E-C11E-C12E 2.1(7)
C9E-C10E-C11E-C12E 178.1(4)
C10E-C11E-C12E-C13E -3.0(7)
C11E-C12E-C13E-C14E 1.7(8)
C12E-C13E-C14E-C15E 0.3(7)
C13E-C14E-C15E-C10E -1.1(7)
C11E-C10E-C15E-C14E -0.1(6)
C9E-C10E-C15E-C14E -175.9(4)
O1F-C1F-C2F-C9F -172.8(8)
O2F-C1F-C2F-C9F 6.0(10)
O1F-C1F-C2F-C3F 12.3(11)
O2F-C1F-C2F-C3F -169.0(6)
C9F-C2F-C3F-C4F 120.7(8)
C1F-C2F-C3F-C4F -64.7(8)
C9F-C2F-C3F-C8F -62.4(9)
C1F-C2F-C3F-C8F 112.2(7)
C8F-C3F-C4F-C5F 0.3(10)
C2F-C3F-C4F-C5F 177.2(7)
C3F-C4F-C5F-C6F -1.7(12)
C4F-C5F-C6F-C7F 2.4(13)
C5F-C6F-C7F-C8F -1.8(12)
C6F-C7F-C8F-C3F 0.5(11)
C4F-C3F-C8F-C7F 0.3(10)
C2F-C3F-C8F-C7F -176.8(6)
C1F-C2F-C9F-C10F 174.5(7)
C3F-C2F-C9F-C10F -11.2(11)
C2F-C9F-C10F-C11F 153.3(7)
C2F-C9F-C10F-C15F -29.8(11)

C15F-C10F-C11F-C12F 1.3(10)
C9F-C10F-C11F-C12F 178.3(6)
C10F-C11F-C12F-C13F -0.7(11)
C11F-C12F-C13F-C14F -1.8(12)
C12F-C13F-C14F-C15F 3.8(13)
C13F-C14F-C15F-C10F -3.2(12)
C11F-C10F-C15F-C14F 0.7(11)
C9F-C10F-C15F-C14F -176.2(7)
O1Y-C1Y-C2Y-C9Y -168.2(19)
O2Y-C1Y-C2Y-C9Y 10(2)
O1Y-C1Y-C2Y-C3Y 9(2)
O2Y-C1Y-C2Y-C3Y -172.1(15)
C9Y-C2Y-C3Y-C4Y 113.0(17)
C1Y-C2Y-C3Y-C4Y -64.5(18)
C9Y-C2Y-C3Y-C8Y -69(2)
C1Y-C2Y-C3Y-C8Y 113.4(16)
C8Y-C3Y-C4Y-C5Y -6(2)
C2Y-C3Y-C4Y-C5Y 171.7(15)
C3Y-C4Y-C5Y-C6Y 8(3)
C4Y-C5Y-C6Y-C7Y -9(3)
C5Y-C6Y-C7Y-C8Y 8(3)
C6Y-C7Y-C8Y-C3Y -6(3)
C4Y-C3Y-C8Y-C7Y 5(2)
C2Y-C3Y-C8Y-C7Y -172.4(14)
C1Y-C2Y-C9Y-C10Y 172.3(14)
C3Y-C2Y-C9Y-C10Y -5(2)
C2Y-C9Y-C10Y-C11Y 146.5(16)
C2Y-C9Y-C10Y-C15Y -38(2)
C15Y-C10Y-C11Y-C12Y 5(2)
C9Y-C10Y-C11Y-C12Y -178.9(14)
C10Y-C11Y-C12Y-C13Y -9(2)
C11Y-C12Y-C13Y-C14Y 9(2)
C12Y-C13Y-C14Y-C15Y -4(2)

C13Y-C14Y-C15Y-C10Y 0(2)
C11Y-C10Y-C15Y-C14Y -1(2)
C9Y-C10Y-C15Y-C14Y -176.4(13)
O1G-C1G-C2G-C9G -171.3(4)
O2G-C1G-C2G-C9G 7.8(6)
O1G-C1G-C2G-C3G 10.5(6)
O2G-C1G-C2G-C3G -170.5(4)
C9G-C2G-C3G-C4G -67.2(6)
C1G-C2G-C3G-C4G 110.9(4)
C9G-C2G-C3G-C8G 118.4(5)
C1G-C2G-C3G-C8G -63.5(5)
C8G-C3G-C4G-C5G 0.7(6)
C2G-C3G-C4G-C5G -173.9(4)
C3G-C4G-C5G-C6G -0.9(6)
C4G-C5G-C6G-C7G -0.2(7)
C5G-C6G-C7G-C8G 1.4(7)
C6G-C7G-C8G-C3G -1.6(6)
C4G-C3G-C8G-C7G 0.5(6)
C2G-C3G-C8G-C7G 175.0(4)
C1G-C2G-C9G-C10G 172.8(4)
C3G-C2G-C9G-C10G -9.2(8)
C2G-C9G-C10G-C11G -33.4(7)
C2G-C9G-C10G-C15G 150.6(5)
C15G-C10G-C11G-C12G -1.2(7)
C9G-C10G-C11G-C12G -177.2(4)
C10G-C11G-C12G-C13G -0.6(8)
C11G-C12G-C13G-C14G 0.5(9)
C12G-C13G-C14G-C15G 1.4(9)
C13G-C14G-C15G-C10G -3.2(8)
C11G-C10G-C15G-C14G 3.0(7)
C9G-C10G-C15G-C14G 179.2(4)
O2H-C1H-C2H-C9H 170.8(4)
O1H-C1H-C2H-C9H -8.2(6)

O2H-C1H-C2H-C3H -10.8(6)
O1H-C1H-C2H-C3H 170.2(3)
C9H-C2H-C3H-C8H 65.0(6)
C1H-C2H-C3H-C8H -113.3(4)
C9H-C2H-C3H-C4H -117.4(5)
C1H-C2H-C3H-C4H 64.3(5)
C8H-C3H-C4H-C5H -1.5(6)
C2H-C3H-C4H-C5H -179.0(4)
C3H-C4H-C5H-C6H 1.4(6)
C4H-C5H-C6H-C7H -0.4(7)
C5H-C6H-C7H-C8H -0.5(7)
C4H-C3H-C8H-C7H 0.7(6)
C2H-C3H-C8H-C7H 178.2(4)
C6H-C7H-C8H-C3H 0.3(6)
C1H-C2H-C9H-C10H -174.9(4)
C3H-C2H-C9H-C10H 6.9(7)
C2H-C9H-C10H-C11H -154.5(4)
C2H-C9H-C10H-C15H 29.3(7)
C15H-C10H-C11H-C12H -2.6(6)
C9H-C10H-C11H-C12H -179.0(4)
C10H-C11H-C12H-C13H 1.8(7)
C11H-C12H-C13H-C14H 0.3(8)
C12H-C13H-C14H-C15H -1.5(8)
C13H-C14H-C15H-C10H 0.7(7)
C11H-C10H-C15H-C14H 1.3(6)
C9H-C10H-C15H-C14H 177.6(4)
O1I-C1I-C2I-C9I 170.8(4)
O2I-C1I-C2I-C9I -8.5(6)
O1I-C1I-C2I-C3I -10.8(6)
O2I-C1I-C2I-C3I 169.9(3)
C9I-C2I-C3I-C8I-116.8(5)
C1I-C2I-C3I-C8I64.9(5)
C9I-C2I-C3I-C4I64.0(5)

C1I-C2I-C3I-C4I-114.3(4)

C8I-C3I-C4I-C5I-0.9(6)

C2I-C3I-C4I-C5I178.3(4)

C3I-C4I-C5I-C6I1.5(6)

C4I-C5I-C6I-C7I-0.7(7)

C5I-C6I-C7I-C8I-0.5(7)

C6I-C7I-C8I-C3I1.0(7)

C4I-C3I-C8I-C7I-0.3(6)

C2I-C3I-C8I-C7I-179.5(4)

C1I-C2I-C9I-C10I -174.4(4)

C3I-C2I-C9I-C10I 7.4(7)

C2I-C9I-C10I-C11I -154.9(4)

C2I-C9I-C10I-C15I 28.5(7)

C15I-C10I-C11I-C12I -2.8(6)

C9I-C10I-C11I-C12I -179.6(4)

C10I-C11I-C12I-C13I 2.4(7)

C11I-C12I-C13I-C14I -0.2(7)

C12I-C13I-C14I-C15I -1.4(7)

C13I-C14I-C15I-C10I 0.8(7)

C11I-C10I-C15I-C14I 1.2(6)

C9I-C10I-C15I-C14I 177.8(4)

O1J-C1J-C2J-C9J 170.7(4)

O2J-C1J-C2J-C9J -8.2(6)

O1J-C1J-C2J-C3J -10.6(6)

O2J-C1J-C2J-C3J 170.4(3)

C9J-C2J-C3J-C8J -117.0(5)

C1J-C2J-C3J-C8J 64.4(5)

C9J-C2J-C3J-C4J 64.9(5)

C1J-C2J-C3J-C4J -113.7(4)

C8J-C3J-C4J-C5J -0.1(5)

C2J-C3J-C4J-C5J 178.1(3)

C3J-C4J-C5J-C6J 0.7(6)

C4J-C5J-C6J-C7J -0.5(6)

C5J-C6J-C7J-C8J -0.4(6)
C6J-C7J-C8J-C3J 1.1(6)
C4J-C3J-C8J-C7J -0.8(5)
C2J-C3J-C8J-C7J -178.9(4)
C1J-C2J-C9J-C10J -174.7(4)
C3J-C2J-C9J-C10J 6.8(7)
C2J-C9J-C10J-C11J -154.6(4)
C2J-C9J-C10J-C15J 29.3(6)
C15J-C10J-C11J-C12J -3.3(6)
C9J-C10J-C11J-C12J -179.6(4)
C10J-C11J-C12J-C13J 2.9(7)
C11J-C12J-C13J-C14J -1.3(7)
C12J-C13J-C14J-C15J 0.0(7)
C13J-C14J-C15J-C10J -0.4(7)
C11J-C10J-C15J-C14J 2.0(6)
C9J-C10J-C15J-C14J 178.1(4)
O2K-C1K-C2K-C9K -172.7(7)
O1K-C1K-C2K-C9K 6.8(9)
O2K-C1K-C2K-C3K 11.8(10)
O1K-C1K-C2K-C3K -168.7(6)
C9K-C2K-C3K-C4K -63.6(9)
C1K-C2K-C3K-C4K 111.6(7)
C9K-C2K-C3K-C8K 120.6(7)
C1K-C2K-C3K-C8K -64.1(8)
C8K-C3K-C4K-C5K 0.0(9)
C2K-C3K-C4K-C5K -175.9(6)
C3K-C4K-C5K-C6K 1.0(10)
C4K-C5K-C6K-C7K -2.1(10)
C5K-C6K-C7K-C8K 2.3(11)
C6K-C7K-C8K-C3K -1.3(10)
C4K-C3K-C8K-C7K 0.1(9)
C2K-C3K-C8K-C7K 175.9(6)
C1K-C2K-C9K-C10K 174.0(6)

C3K-C2K-C9K-C10K -10.9(11)
C2K-C9K-C10K-C15K -30.7(11)
C2K-C9K-C10K-C11K 153.2(7)
C15K-C10K-C11K-C12K 2.7(10)
C9K-C10K-C11K-C12K 179.0(7)
C10K-C11K-C12K-C13K -1.9(12)
C11K-C12K-C13K-C14K -0.7(13)
C12K-C13K-C14K-C15K 2.6(12)
C13K-C14K-C15K-C10K -1.8(12)
C11K-C10K-C15K-C14K -0.9(11)
C9K-C10K-C15K-C14K -177.0(7)
O2K'-C1K'-C2K'-C9K' -166.7(17)
O1K'-C1K'-C2K'-C9K' 8(2)
O2K'-C1K'-C2K'-C3K' 11(2)
O1K'-C1K'-C2K'-C3K' -174.2(13)
C9K'-C2K'-C3K'-C4K' -70.3(19)
C1K'-C2K'-C3K'-C4K' 111.9(15)
C9K'-C2K'-C3K'-C8K' 113.3(16)
C1K'-C2K'-C3K'-C8K' -64.6(17)
C8K'-C3K'-C4K'-C5K' 2(2)
C2K'-C3K'-C4K'-C5K' -174.0(12)
C3K'-C4K'-C5K'-C6K' -3(2)
C4K'-C5K'-C6K'-C7K' 3(2)
C5K'-C6K'-C7K'-C8K' -2(3)
C6K'-C7K'-C8K'-C3K' 2(2)
C4K'-C3K'-C8K'-C7K' -2(2)
C2K'-C3K'-C8K'-C7K' 174.5(12)
C1K'-C2K'-C9K'-C10' 172.3(14)
C3K'-C2K'-C9K'-C10' -5(2)
C2K'-C9K'-C10'-C15' -38(2)
C2K'-C9K'-C10'-C11' 147.1(15)
C15'-C10'-C11'-C12' 4(2)
C9K'-C10'-C11'-C12' 178.9(14)

C10'-C11'-C12'-C13' -6(2)
C11'-C12'-C13'-C14' 4(2)
C12'-C13'-C14'-C15' 0(2)
C13'-C14'-C15'-C10' -2(2)
C11'-C10'-C15'-C14' 0(2)
C9K'-C10'-C15'-C14' -175.1(14)
O1L-C1L-C2L-C9L -172.0(4)
O2L-C1L-C2L-C9L 7.2(6)
O1L-C1L-C2L-C3L 10.4(6)
O2L-C1L-C2L-C3L -170.3(4)
C9L-C2L-C3L-C8L 120.3(5)
C1L-C2L-C3L-C8L -62.3(6)
C9L-C2L-C3L-C4L -64.6(6)
C1L-C2L-C3L-C4L 112.8(5)
C8L-C3L-C4L-C5L 0.7(7)
C2L-C3L-C4L-C5L -174.6(4)
C3L-C4L-C5L-C6L -0.2(7)
C4L-C5L-C6L-C7L -1.1(7)
C5L-C6L-C7L-C8L 1.8(7)
C6L-C7L-C8L-C3L -1.2(7)
C4L-C3L-C8L-C7L 0.0(7)
C2L-C3L-C8L-C7L 175.0(4)
C1L-C2L-C9L-C10L 173.1(4)
C3L-C2L-C9L-C10L -9.6(8)
C2L-C9L-C10L-C11L -31.9(7)
C2L-C9L-C10L-C15L 152.3(5)
C15L-C10L-C11L-C12L 0.2(6)
C9L-C10L-C11L-C12L -175.7(4)
C10L-C11L-C12L-C13L -1.7(6)
C11L-C12L-C13L-C14L 1.1(7)
C12L-C13L-C14L-C15L 1.1(7)
C13L-C14L-C15L-C10L -2.7(7)
C11L-C10L-C15L-C14L 2.0(6)

C9L-C10L-C15L-C14L 178.0(4)

X-Ray crystallographic data of **3-23**

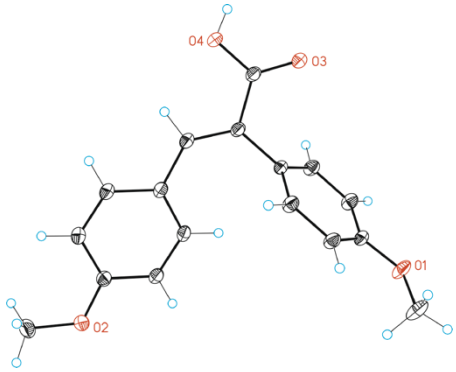

Table 1. Crystal data and structure refinement for **3-23**.

Identification code	**3-23**
Empirical formula	C17 H16 O4
Formula weight	284.30
Temperature	100(2) K
Wavelength	0.71073 Å
Crystal system	Triclinic
Space group	P-1
Unit cell dimensions	a = 5.8239(4)Å a= 84.6047(18)°.
	b = 9.0597(6)Å b = 84.7115(18)°.
	c = 13.9214(8)Å g = 79.8913(19)°.
Volume	717.78(8) Å3
Z	2
Density (calculated)	1.315 Mg/m3
Absorption coefficient	0.093 mm-1
F(000)	300
Crystal size	0.40 x 0.005 x 0.005 mm3
Theta range for data collection	2.291 to 32.609°.
Index ranges	-7<=h<=8,-12<=k<=13,-14<=l<=21
Reflections collected	11300
Independent reflections	4668[R(int) = 0.0210]

Completeness to theta =32.609° 89.1%

Absorption correction Empirical

Max. and min. transmission 1.000 and 0.921

Refinement method Full-matrix least-squares on F2

Data / restraints / parameters 4668/ 0/ 192

Goodness-of-fit on F2 1.036

Final R indices [I>2sigma(I)] R1 = 0.0449, wR2 = 0.1207

R indices (all data) R1 = 0.0550, wR2 = 0.1285

Largest diff. peak and hole 0.587 and -0.235 e.Å-3

Table 2. Bond lengths [Å] and angles [°] for **3-23**.

Bond lengths----

O1-C4 1.3673(12)

O1-C15 1.4253(15)

O2-C12 1.3574(13)

O2-C17 1.4337(14)

O3-C16 1.2308(13)

O4-C16 1.3225(12)

C1-C2 1.3904(14)

C1-C6 1.3985(14)

C1-C7 1.4890(13)

C2-C3 1.3943(14)

C3-C4 1.3923(15)

C4-C5 1.3954(15)

C5-C6 1.3864(14)

C7-C8 1.3570(14)

C7-C16 1.4812(14)

C8-C9 1.4608(15)

C9-C14 1.4005(14)

C9-C10 1.4090(14)

C10-C11 1.3808(15)

C11-C12 1.4041(15)

C12-C13 1.3943(15)
C13-C14 1.3912(15)

Angles----------
C4-O1-C15 117.05(9)
C12-O2-C17 117.51(9)
C2-C1-C6 118.13(9)
C2-C1-C7 120.17(9)
C6-C1-C7 121.70(9)
C1-C2-C3 121.67(9)
C4-C3-C2 119.40(9)
O1-C4-C3 124.49(9)
O1-C4-C5 115.86(9)
C3-C4-C5 119.64(9)
C6-C5-C4 120.23(9)
C5-C6-C1 120.93(9)
C8-C7-C16 117.85(9)
C8-C7-C1 126.23(9)
C16-C7-C1 115.88(9)
C7-C8-C9 130.56(9)
C14-C9-C10 117.32(10)
C14-C9-C8 117.61(9)
C10-C9-C8 124.96(9)
C11-C10-C9 120.71(10)
C10-C11-C12 120.99(10)
O2-C12-C13 125.17(10)
O2-C12-C11 115.62(9)
C13-C12-C11 119.21(10)
C14-C13-C12 119.16(10)
C13-C14-C9 122.51(10)
O3-C16-O4 122.19(9)
O3-C16-C7 121.77(9)
O4-C16-C7 116.04(9)

Table 3. Torsion angles [°] for **3-23**.

C6-C1-C2-C3	-0.34(16)
C7-C1-C2-C3	-179.28(10)
C1-C2-C3-C4	0.02(17)
C15-O1-C4-C3	0.11(17)
C15-O1-C4-C5	178.94(11)
C2-C3-C4-O1	178.58(10)
C2-C3-C4-C5	-0.22(17)
O1-C4-C5-C6	-178.15(10)
C3-C4-C5-C6	0.74(17)
C4-C5-C6-C1	-1.08(17)
C2-C1-C6-C5	0.86(16)
C7-C1-C6-C5	179.79(10)
C2-C1-C7-C8	-64.04(15)
C6-C1-C7-C8	117.05(12)
C2-C1-C7-C16	113.71(11)
C6-C1-C7-C16	-65.20(13)
C16-C7-C8-C9	176.34(10)
C1-C7-C8-C9	-5.95(18)
C7-C8-C9-C14	169.24(11)
C7-C8-C9-C10	-14.61(18)
C14-C9-C10-C11	-2.32(16)
C8-C9-C10-C11	-178.48(10)
C9-C10-C11-C12	-0.23(17)
C17-O2-C12-C13	-2.55(16)
C17-O2-C12-C11	177.86(10)
C10-C11-C12-O2	-177.68(10)
C10-C11-C12-C13	2.70(16)
O2-C12-C13-C14	177.90(10)
C11-C12-C13-C14	-2.52(16)

C12-C13-C14-C9 -0.09(17)

C10-C9-C14-C13 2.50(16)

C8-C9-C14-C13 178.95(10)

C8-C7-C16-O3 177.50(10)

C1-C7-C16-O3 -0.44(15)

C8-C7-C16-O4 -2.29(14)

C1-C7-C16-O4 179.76(9)

X-Ray crystallographic data of **3-42**

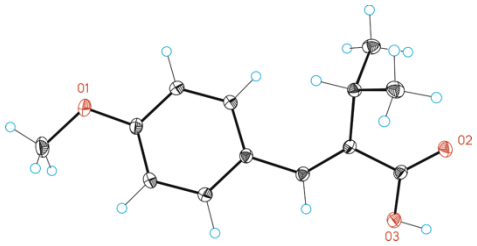

Table 1. Crystal data and structure refinement for **3-42**.

Identification code **3-42**

Empirical formula C13 H16 O3

Formula weight 220.26

Temperature 100(2) K

Wavelength 0.71073 Å

Crystal system Monoclinic

Space group P2(1)/n

Unit cell dimensions a = 5.2457(13)Å a= 90°.

b = 20.488(5)Å b = 93.965(5)°.

c = 10.644(3)Å g = 90°.

Volume 1141.3(5) Å3

Z 4

Density (calculated) 1.282 Mg/m3

Absorption coefficient 0.090 mm-1

F(000) 472

Crystal size 0.40 x 0.30 x 0.30 mm3

Theta range for data collection 2.763 to 29.662°.

Index ranges -7<=h<=7,-28<=k<=28,-14<=l<=11

Reflections collected 11376

Independent reflections 3193[R(int) = 0.0279]

Completeness to theta =29.662° 98.799995%

Absorption correction Empirical

Max. and min. transmission 0.973 and 0.748

Refinement method Full-matrix least-squares on F2

Data / restraints / parameters 3193/ 0/ 209

Goodness-of-fit on F2 1.058

Final R indices [I>2sigma(I)] R1 = 0.0363, wR2 = 0.0983

R indices (all data) R1 = 0.0412, wR2 = 0.1000

Largest diff. peak and hole 0.381 and -0.247 e.Å-3

Table 2. Bond lengths [Å] and angles [°] for **3-42**.

Bond lengths----

C1-C6 1.3987(12)

C1-C2 1.4046(12)

C1-C8 1.4665(12)

C2-C3 1.3818(12)

C3-C4 1.3974(13)

C4-O1 1.3620(11)

C4-C5 1.3908(13)

C5-C6 1.3941(12)

C7-O1 1.4305(12)

C8-C9 1.3494(12)

C9-C13 1.4864(12)

C9-C10 1.5144(13)

C10-C12 1.5327(13)

C10-C11 1.5340(12)

C13-O2 1.2279(11)

C13-O3 1.3239(11)

Angles----------

C6-C1-C2 117.62(8)

C6-C1-C8 118.82(8)

C2-C1-C8 123.38(8)

C3-C2-C1 121.03(8)

C2-C3-C4 120.40(8)

O1-C4-C5 124.65(8)

O1-C4-C3 115.57(8)

C5-C4-C3 119.77(8)

C4-C5-C6 119.27(8)

C5-C6-C1 121.87(8)

C9-C8-C1 129.15(8)

C8-C9-C13 117.28(8)

C8-C9-C10 125.18(8)

C13-C9-C10 117.55(7)

C9-C10-C12 113.33(7)

C9-C10-C11 111.62(7)

C12-C10-C11 111.64(7)

O2-C13-O3 122.14(8)

O2-C13-C9 122.45(8)

O3-C13-C9 115.37(8)

C4-O1-C7 117.22(8)

Table 3. Torsion angles [°] for **3-42**.

C6-C1-C2-C3 2.23(13)

C8-C1-C2-C3 177.19(8)

C1-C2-C3-C4 -0.62(14)

C2-C3-C4-O1 -179.62(8)

C2-C3-C4-C5 -0.78(14)
O1-C4-C5-C6 179.22(8)
C3-C4-C5-C6 0.49(14)
C4-C5-C6-C1 1.22(14)
C2-C1-C6-C5 -2.54(13)
C8-C1-C6-C5 -177.74(8)
C6-C1-C8-C9 -152.83(9)
C2-C1-C8-C9 32.27(14)
C1-C8-C9-C13 -170.30(8)
C1-C8-C9-C10 9.16(15)
C8-C9-C10-C12 -111.97(10)
C13-C9-C10-C12 67.49(10)
C8-C9-C10-C11 120.95(9)
C13-C9-C10-C11 -59.60(10)
C8-C9-C13-O2 173.66(9)
C10-C9-C13-O2 -5.84(13)
C8-C9-C13-O3 -4.01(12)
C10-C9-C13-O3 176.49(7)
C5-C4-O1-C7 -9.90(13)
C3-C4-O1-C7 168.88(8)

Chapter 4: Ni-catalyzed Regioselective Hydroamidation of Alkynes with Isocyanates

4.1 Objectives

❖To develop a mild and user-friendly Ni-catalyzed regioselective hydroamidation of alkynes with isocyanates using simply available, inexpensive hydride sources, giving access to tri-substituted acrylic acid derivatives, which are not readily available by traditional means, from simple starting materials.

❖To gain mechanistic information by studying the effects of radical scavengers, and conducting stoichiometric reactions, as well as isotope- labelling experiments.

4.2 Introduction to Hydroamidation of Alkynes

Amides are often encountered as key structural units in the skeletons of natural products or pharmaceutically active compounds such as Januvia, Vyvanse, Atenolol, and others.[117] Selective formation of amides is a long-standing task for chemists.[118] Traditional methods involve condensation of carboxylic acids and their derivatives with amines in the presence of activating reagents.[119] Recently, several interesting catalytic methods have been published such as oxidative coupling of α-bromo nitroalkanes with amines,[120] hydrocarbamoylation of alkenes/alkynes,[121] transamidation reactions,[122] and acylation of amine surrogates.[123] Nevertheless, most of these protocols suffer from several disadvantages, such as generation of undesired products, harsh conditions or/and limited substrate scope. The recent years have witnessed a significant progress within the area of transition-metal catalyzed amidation arena of unsaturated bonds, thus leading to a continuous expansion of our knowledge about such catalytic transformations.[124, 125] However, the highly selective hydroamidation reaction of alkynes is rather unexplored. Irrefutably, the ability to control selectivity of catalytic events in a reasonable and predictable fashion still remains an impressive challenge. Such a methodology would offer a unique prospect to increase our ever-growing chemical knowledge and expand the flexibility in synthetic design. The utilization of isocyanate (RNCO) as synthon has gained significant momentum in catalytic events, holding promise for describing new paradigms en route to amides, central motifs in

[117] Humphrey, J. M.; Chamberlin, A. R. *Chem. Rev.* **1997**, *97*, 2243. (b) Bode, J. W. *Curr. Opin. Drug Discovery Dev.* **2006**, *9*, 765. (c) Cupido, T.; Tulla-Puche, J.; Spengler, J.; Albericio, F. *Curr. Opin. Drug Discovery Dev.* **2007**, *10*, 768.

[118] Pattabiraman, V. R.; Bode, J. W. *Nature* **2011**, *480*, 471.

[119] (a) Montalbetti, C. A. G. N.; Falque, V. *Tetrahedron* **2005**, *61*, 10827. (b) Han, S. Y.; Kim, Y. A. *Tetrahedron* **2004**, *60*, 2447. (c) Valeur, E.; Bradley, M. *Chem. Soc. Rev.* **2009**, *38*, 606.

[120] Shen, B.; Makley, D. M.; Johnston, J. N. *Nature* **2010**, *465*,1027.

[121] (a) Tsuji, Y.; Yoshii, S.; Ohsumi, T.; Kondo, T.; Watanabe, Y. *J. Organomet. Chem.* **1987**, *331*, 379. (b) Kobayashi, Y.; Kamisaki, H.; Yanada, K.; Yanada, R.; Takemoto, Y. *Tetrahedron Lett.* **2005**, *46*, 7549. (c) Nakao, Y.; Idei, H.; Kanyiva, K. S.; Hiyama, T. *J. Am. Chem. Soc.* **2009**, *131*, 5070. (d) Fujihara, T.; Katafuchi, Y.; Iwai, T.; Terao, J.; Tsuji, Y. *J. Am. Chem. Soc.* **2010**, *132*, 2094. (e) Miyazaki, Y.; Nakao, Y.; Hiyama, T. *Chem. Lett.* **2012**, *41*, 298. (f) Li, B.; Park, Y.; Chang, S. *J. Am. Chem. Soc.* **2013**, *136*, 1125.

[122] Stephenson, N. A.; Gellman, S. H.; Stahl, S. S. *J. Am. Chem. Soc.* **2009**, *131*, 10003.

[123] (a) Shangguan, N.; Katukojvala, S.; Greenberg, R.; Williams, L. J. *J. Am. Chem. Soc.* **2003**, *125*, 7754. (b) Li, X.; Danishefsky, S. J. *J. Am. Chem. Soc.* **2008**, *130*, 5446. (c) Rao, Y.; Li, X.; Danishefsky, S. J. *J. Am. Chem. Soc.* **2009**, *131*, 12924.

[124] Huang, L.; Arndt, M.; Gooßen, K.; Heydt, H.; Gooßen, L. J. *Chem. Rev.* **2015**, *115*, 2596.

[125] Correa, A.; Martin, R. *J. Am. Chem. Soc.* **2014**, *136*, 7253.

numerous pharmaceuticals.[126] To our surprise, the reductive hydroamidation of alkynes with isocyanates was rather unexplored. We envisioned that we might be able to achieve this protocol in the presence of appropriate hydride sources to provide a C1 functionalized product (Scheme 4.1, path a *vs* path b). In line with our research towards reductive carboxylation and amidation reactions, we were attracted to the challenge of providing new knowledge in this field.

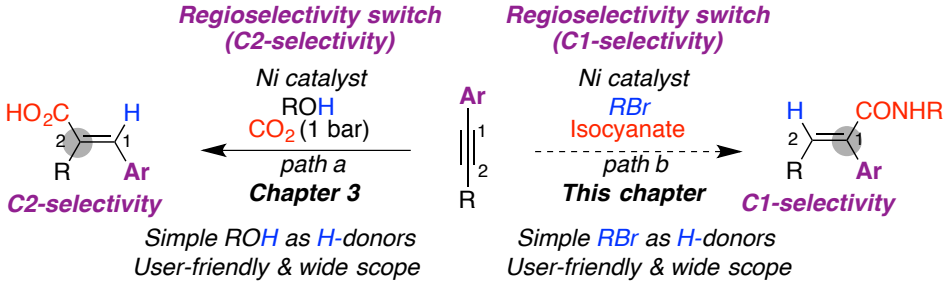

Scheme 4.1. Ni-catalyzed regioselectivity-controllable carboxylation and amidation.

4.3 Screening of the Reaction Conditions

We initiated our investigation by performing an amidation reaction with diphenylacetylene **3-1** in the presence of $NiBr_2$·diglyme (10 mol%) as precatalyst, *t*-BuNCO (**4-2**, 1.5 equiv), 1-bromobutane (**4-3**, 1.5 equiv) as proton source, bathocuproine (**L8**) (20 mol%) as ligand, Mn (2.0 equiv) as reducing reagent under an atmosphere of argon in DMF at room temperature overnight. To our delight, we could obtain our desired product **4-4** in 55% isolated yield under these mild conditions.

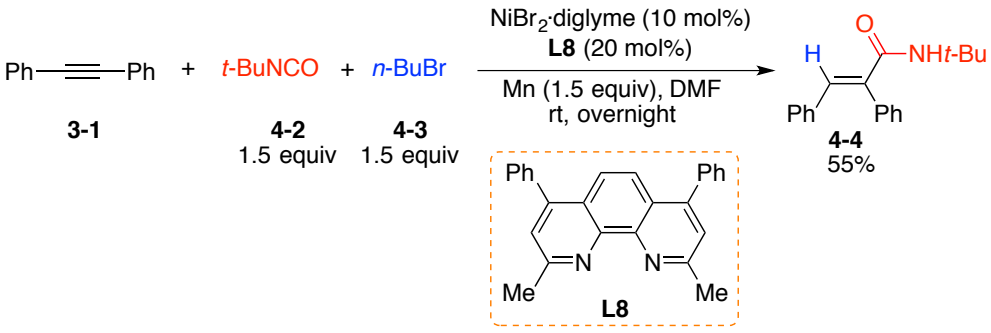

Scheme 4.2. Ni-catalyzed reductive hydroamidation.

Encouraged by this finding, we decided to employ **3-1** as our model substrate to develop our Ni-catalyzed regioselective hydroamidation of alkynes with isocyanates. We studied the effect of several experimental parameters such as nickel precatalysts,

[126] (a) Shi, X. Y.; Liu, K. Y.; Fan, J.; Dong, X. F.; Wei, J.-F.; Li, C.-J. *Chem. Eur. J.* **2015**, *21*, 1900. Li, J.; (b) Ackermann, L. *Angew. Chem. Int. Ed.* **2015**, *54*, 8551.

ligands, catalyst loading, temperature, the amount of reductant, the ratio of metal to ligand, the amount of hydride source, additives as well as other factors.

Inspired by our pervious carboxylation and amidation methodologies, we anticipated that the ligand might have a profound influence on the reactivity of **3-1**. We decided to began our research by surveying the ligand effect. Unlike the carboxylation events (Figure 4.1), bipyridine-type ligands bearing ortho alkyl substitutes were found to be suitable for this process, **L3** and **L16** delivered the desired product in moderate yields. However, other bipyridines did not promote this reaction or not to the final amide (**L12-L15**). As expected, phenanthroline derivatives **L7** and **L18** are applicable to this approach, although moderate yields were observed. Further screening showed that *tert*-pyridines, no matter whether the ligands possess methyl groups at ortho position or not, were not efficient for promoting this reaction. Since those ligands generated no product (**L21**-**L23**) or in low yields (**L10**, **L11** and **L20**). Therefore, we decided to employ **L8** as ligand to study other reaction parameters, since we could obtain the best yield (*vs* conversion)

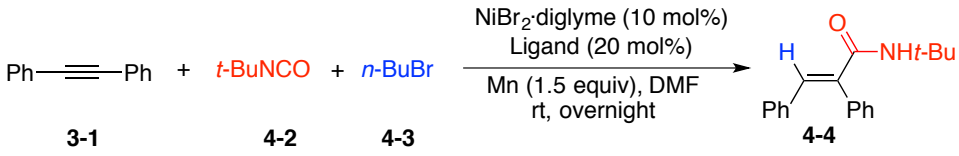

3-1 **4-2** **4-3** **4-4**

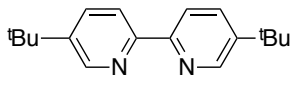

L12

Conversion (%)	0
yield (%)	0

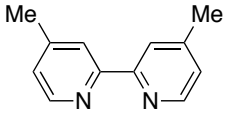

L13

	0
	0

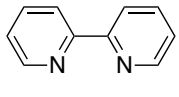

L2

	66
	8

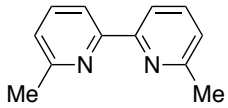

L3

Conversion (%)	94
yield (%)	64

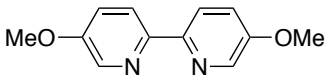

L14

	0
	0

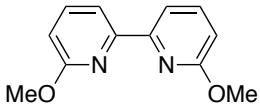

L15

	100
	0

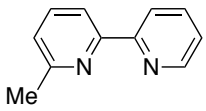

L16

Conversion (%)	100
yield (%)	44

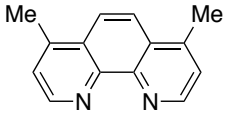

L17

	67
	14

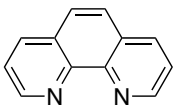

L5

	0
	0

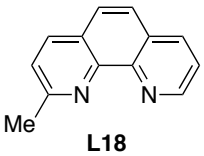

L18

	87
	31

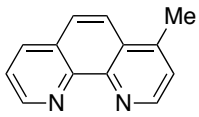

L19

Conversion (%)	34
yield (%)	trace

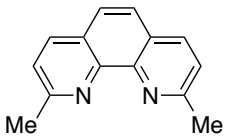

L7

	94
	57

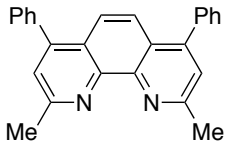

L8

	79
	55

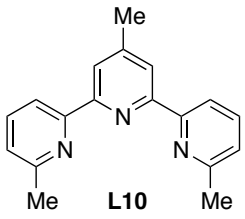

L10

Conversion (%)	92
yield (%)	18

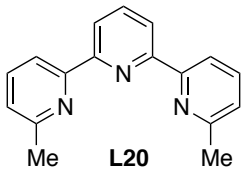

L20

	73
	5

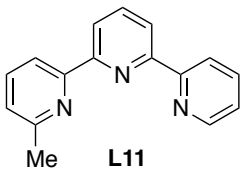

L11

	43
	12

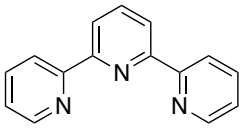

L21

Conversion (%)	54
yield (%)	trace

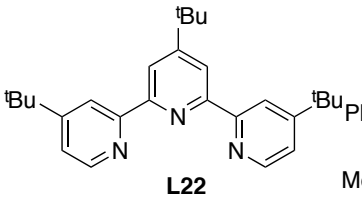

L22

	84
	trace

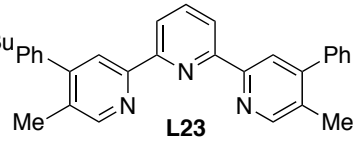

L23

	0
	0

[a] Reaction conditions: **3-1** (0.25 mmol), **4-2** (0.375 mmol), **4-3** (0.375 mmol), $NiBr_2$·diglyme (10 mol%), ligand (20 mol%), Mn (0.375 mmol), DMF (1 mL) at rt, overnight. [b] HPLC conversions and yields using naphthalene as internal standard.

Table 4.1. Ligand screening for hydroamidation of alkynes.

We next turned our attention to examine the effect of the hydride source effect. While the use of EtBr afforded a similar yield (54%) of amide, *n*-PrBr produced the targeted product in lower yield (Figure 4.2, Entries 1 and 2). To our delight, conducting the reaction was conducted in the presence of *i*-PrBr led to an increase of the yield (Entry 3).

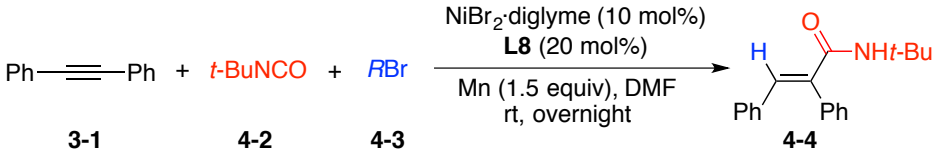

Entry	RBr	Conversion (%)[b]	Yield (%)[b]
1	EtBr	100	54
2	*n*-PrBr	100	44
3	*i*-PrBr	100	74

[a] Reaction conditions: **3-1** (0.25 mmol), **4-2** (0.375 mmol), **RBr** (0.375 mmol), $NiBr_2$·diglyme (10 mol%), **L8** (20 mol%), Mn (0.375 mmol), DMF (1 mL) at rt, overnight. [b] HPLC conversion and yields by using naphthalene as internal standard.

Table 4.2. Hydride source screening for hydroamidation of alkynes.

With those results in hand, we decided to explore whether solvent influence the reaction outcome. As shown in Figure 4.3, only polar solvents yielded the desired product, and NMP turned out to be the best choice of solvent (Entries 1, 3 and 4). The other less polar or non-polar solvents did not support the reaction as no amide could be detected.

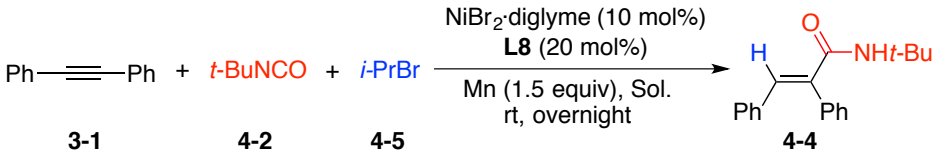

3-1 **4-2** **4-5** **4-4**

Entry	Solvent	Conversion (%)[b]	Yield (%)[b]
1	DMF	100	74
2	$PhCF_3$	0	0
3	DMA	58	54
4	NMP	100	86
5	THF	0	0
6	DCM	0	0
7	PhCl	0	0
8	Dioxane	0	0

[a] Reaction conditions: **3-1** (0.25 mmol), **4-2** (0.375 mmol), **4-5** (0.375 mmol), $NiBr_2$·diglyme (10 mol%), **L8** (20 mol%), Mn (0.375 mmol), Sol. (1 mL) at rt, overnight. [b] HPLC conversion and yields by using naphthalene as internal standard.

Table 4.3. Solvent screening for hydroamidation.

We also wondered whether the reaction temperature would have an influence on the reactivity of our process. Therefore, we turned our attention to temperature screening. Surprisingly, the yield dramatically dropped to 44% when the reaction was performed at 40 °C, and further increasing the reaction temperature led to much lower yields (Figure 4.4, Entries 2-4). The temperature screening demonstrated that our process is sensitive to the temperature and established room temperature as the optimum for our process.

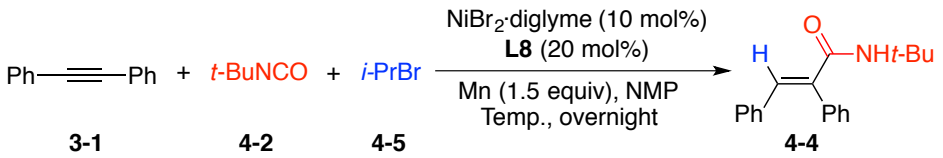

3-1 **4-2** **4-5** **4-4**

Entry	Temperature	Conversion (%)[b]	Yield (%)[b]
1	rt	100	86
2	40 °C	90	44
3	50 °C	73	15
4	60 °C	21	12

[a] Reaction conditions: **3-1** (0.25 mmol), **4-2** (0.375 mmol), **4-5** (0.375 mmol), $NiBr_2$·diglyme (10 mol%), **L8** (20 mol%), Mn (0.375 mmol), NMP (1 mL), overnight. [b] HPLC conversion and yields by using naphthalene as internal standard.

Table 4.4. Temperature screening for hydroamidation.

We next decided to explore the impact of the Ni-catalyst. The precatalyst bearing halides promoted our hydroamidation reaction, and high yields were obtained (Figure 4.5, Entries 1-3). However, no conversion was observed when $Ni(acac)_2$ was used in this protocol. It is worth to note that, $Ni(COD)_2$ resulted in moderate conversion and yield. We believed that the presence of COD-ligand suppressed the reaction by slowing down the ligand exchange rate.

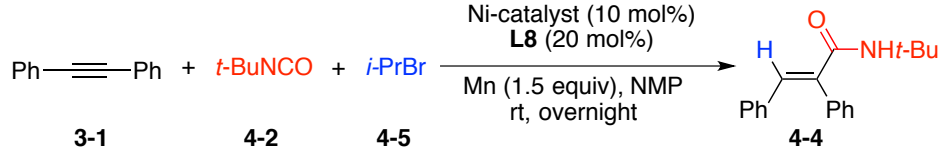

3-1 **4-2** **4-5** **4-4**

Entry	Ni-catalyst	Conversion (%)[b]	Yield (%)[b]
1	$NiCl_2$·glyme	100	86
2	$NiBr_2$	87	81
3	$NiBr_2$·glyme	100	84
4	$Ni(acac)_2$	0	0
5	$Ni(COD)_2$	57	48

[a] Reaction conditions: **3-1** (0.25 mmol), **4-2** (0.375 mmol), **4-5** (0.375 mmol), Ni-catalyst (10 mol%), **L8** (20 mol%), Mn (0.375 mmol), NMP (1 mL) at rt, overnight. [b] HPLC conversion and yields by using naphthalene as internal standard.

Table 4.5. Ni-catalyst screening for hydroamidation.

Next, we screened the isocyanate loading with the expectation to further improve the yield of our Ni-catalyzed hydroamidation, using $NiBr_2$·diglyme as the precatalyst and NMP as the solvent of selection. However, increasing or decreasing the amount of **4-2** all led to the erosion of yield, as summarized in Figure 4.6. Thus, 1.5 equivalent of **4-2** was still the best choice.

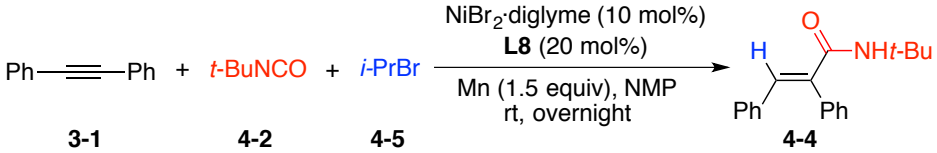

3-1 **4-2** **4-5** **4-4**

Entry	**4-2** (x equiv)	Conversion (%)[b]	Yield (%)[b]
1	1.0	100	67
2	1.2	100	77
3	1.8	100	80
4	2.0	100	80

[a] Reaction conditions: **3-1** (0.25 mmol), **4-2** (x mmol), **4-5** (0.375 mmol), $NiBr_2$·diglyme (10 mol%), **L8** (20 mol%), Mn (0.375 mmol), NMP (1 mL) at rt, overnight. [b] HPLC conversion and yields by using naphthalene as internal standard.

Table 4.6. **4-2** loading screening for hydroamidation.

The screening of hydride source loading is summarized in Figure 4.7. As shown, we could obtain almost quantitative yield of **4-4** when 1.3 equivalents of *i*-PrBr were employed in our hydroamidation protocol (Entry 2). Further lowering down the amount of hydride source to 1.1 equivalents resulted in a reduction of the yield by 26%, and 70% of desire of product was obtained. Not surprisingly, increasing the amount of **4-5** was not helpful for improving yield (Entries 3-4).

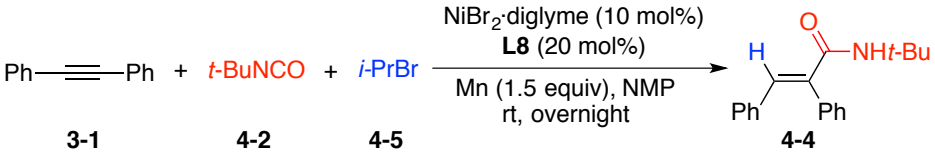

3-1 **4-2** **4-5** **4-4**

Entry	***i*-PrBr** (x equiv)	Conversion (%)[b]	Yield (%)[b]
1	1.1	89	70
2	1.3	100	96
3	1.8	100	83
4	2.2	100	70

[a] Reaction conditions: **3-1** (0.25 mmol), **4-2** (0.375 mmol), **4-5** (x mmol), $NiBr_2$·diglyme (10 mol%), **L8** (20 mol%), Mn (0.375 mmol), NMP (1 mL) at rt, overnight. [b] HPLC conversion and yields by using naphthalene as internal standard.

Table 4.7. **4-5** loading screening for hydroamidation.

We also investigated the effect of the reducing agent loading. Interestingly, lower yields were observed when decreased or increased amounts of Mn were used. The use of a large excess of reductant caused a significant loss of catalytic efficiency, and only 52% of the desired were produced (Entry 4).

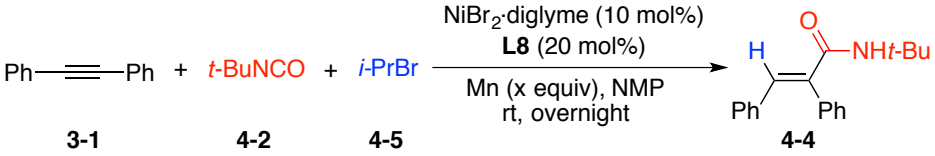

3-1 **4-2** **4-5** **4-4**

Entry	Mn (equiv)	Conversion (%)[b]	Yield (%)[b]
1	1.2	100	82
2	1.6	100	80
3	2.0	100	81
4	2.5	100	52

[a] Reaction conditions: **3-1** (0.25 mmol), **4-2** (0.375 mmol), **4-5** (0.325 mmol), $NiBr_2$·diglyme (10 mol%), **L8** (20 mol%), Mn (x mmol), NMP (1 mL) at rt, overnight. [b] HPLC conversion and yields by using naphthalene as internal standard.

Table 4.8. Mn loading screening for hydroamidation.

The last parameter for this hydroamidation transformation we surveyed was the catalyst loading. Unfortunately, all the effects have been made to decrease catalyst loading were unsuccessful. As summarized in Figure 4.9, although good yields were detected with 5 mol% of Ni-catalyst, the results were significantly worse than the best

previous result (Figure 4.7, Entry 2). Further lowering the catalyst loading to 2.5 mol% caused a dramatic erosion of the yield to 32% or 44% (Entries 3-4). We also performed the reaction with 1 mol% of Ni-catalyst with prolonged reaction time. However, we did not obtain satisfying results.

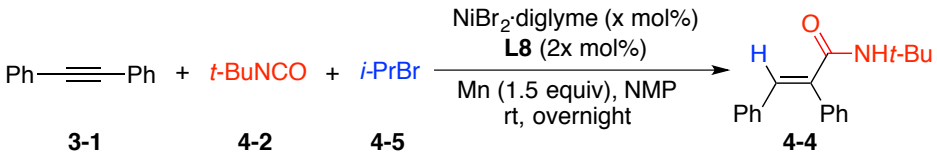

3-1 **4-2** **4-5** **4-4**

Entry	$NiBr_2$·diglyme (mol%)	Time (h)	Conversion (%)[b]	Yield (%)[b]
1	5.0	10	80	74
2	5.0	16	84	78
3	2.5	10	33	32
4	2.5	24	56	44
3	1.0	24	25	24
4	1.0	48	38	30

[a] Reaction conditions: **3-1** (0.25 mmol), **4-2** (0.375 mmol), **4-5** (0.325 mmol), $NiBr_2$·diglyme (x mol%), **L8** (2x mol%), Mn (1.5 mmol), NMP (1 mL) at rt, overnight. [b] HPLC conversion and yields by using naphthalene as internal standard.

Table 4.9. Catalyst loading screening for hydroamidation.

In summary, the optimized conditions found consisted of $NiBr_2$·diglyme (10 mol%) as precatalyst, bathocuproine as ligand (20 mol%), Mn (1.5 equiv) as reducing agent, *i*-PrBr (1.5 equiv) as hydride source and isocyanate (1.5 equiv) in NMP at room temperature overnight. As expected, control experiments indicated that all reaction parameters were essential for the reaction to occur.

4.4 Ni-catalyzed Regioselective Hydroamidation of Alkynes

4.4.1 Synthesis of Starting Materials

Having established the optimized reaction conditions, we set out to survey the scope of this protocol by synthesizing a wide number of alkynes. As presented in Figure **4.10**, various symmetric and asymmetric alkynes bearing electron-withdrawing or electron-donating substituents were prepared by classical Sonogashira coupling.

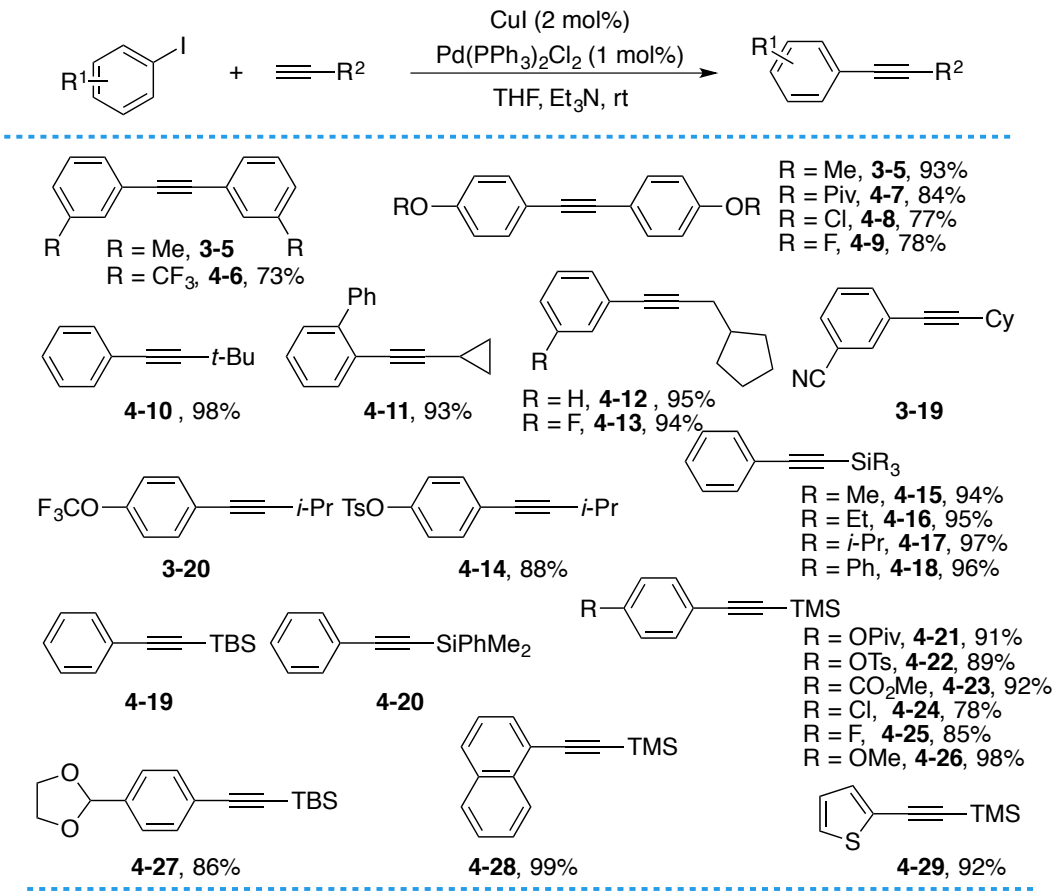

Scheme 4.3. Substrates for hydroamidation.

4.4.2 Scope of the Hydroamidation Reactions

Having the substrates in hand, we began to explore the scope of our Ni-catalyzed reductive hydroamidation reactions. As expected, the coupling of symmetrical alkynes posed no problem, the desired amides were obtained in good to excellent yields. Notably, electrophiles that have been used in other Ni-catalyzed coupling reactions such as aryl chlorides and pivalates are well tolerated (**4-31**, **4-32**), therefore leaving the potential for further manipulation of the reaction products. Other isocyanates with *c*-Pent-, *i*-Pr- and Cy- substituents could be incorporated into alkyne moieties as well, delivering the targeted products (from **4-36** to **4-38**) in excellent yields. We next investigated unsymmetric substrates bearing alkyl substituent. Remarkably, an attractive regioselectivity and stereoselectivity profile was found for a wide range of asymmetrical alkynes, even for the substrate without significant steric biased. As observed from careful NMR spectroscopic analysis,[13] amidation took place mainly on the aromatic site. This observation was univocally confirmed by X-ray crystallography of **5f**. Good functional group compatibility was demonstrated as shown in Figure 4.11,

substitutes such as -OCF_3, -OTs, -CN, and -OPiv were perfectly accommodated. These results are certainly noteworthy as they highlight the genuine potential of our protocol.

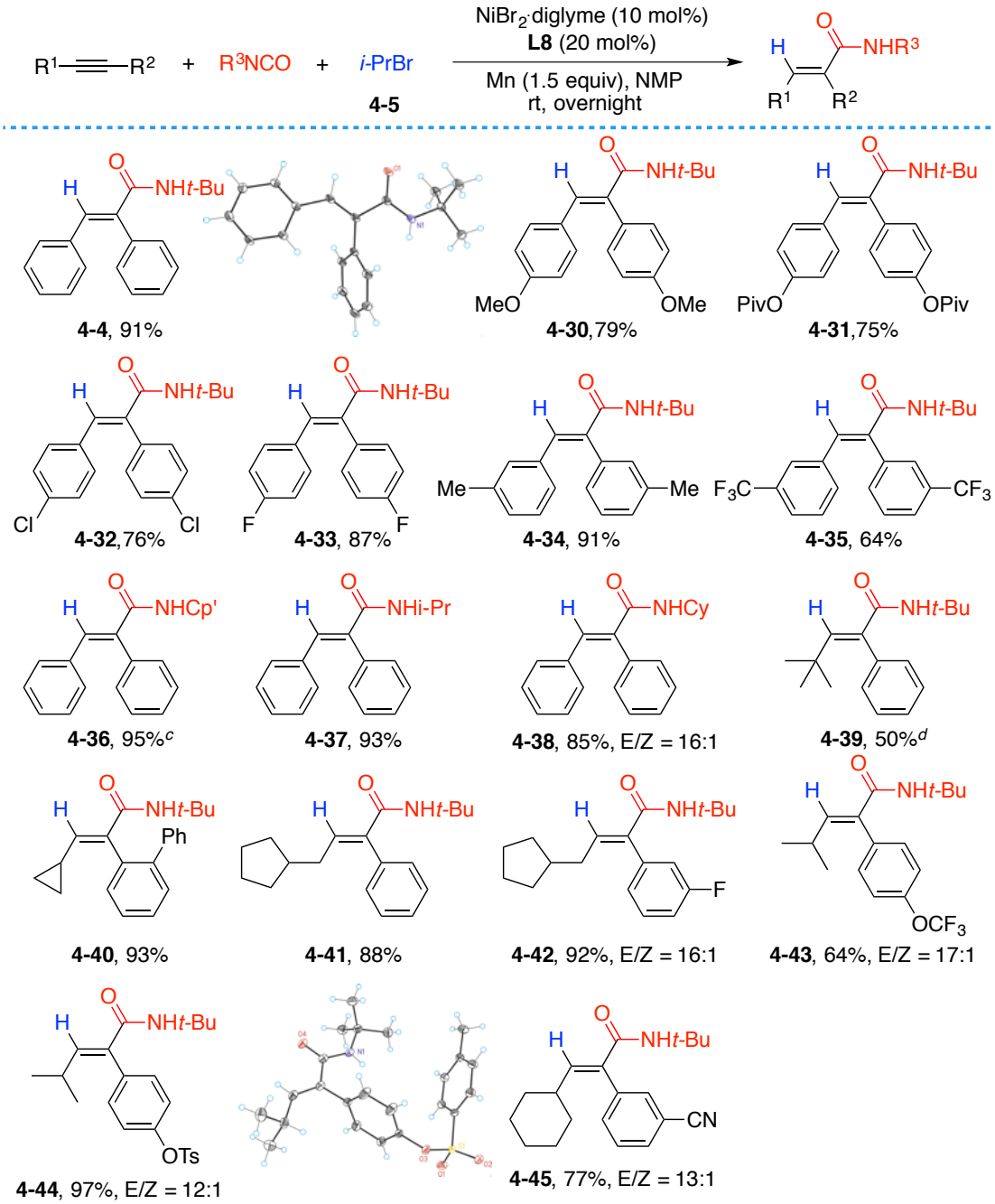

[a] Reaction conditions: **Substrate** (0.5 mmol), **isocyanate** (0.75 mmol), **4-5** (0.65 mmol), $NiBr_2$·diglyme (10 mol%), **L8** (20 mol%), Mn (1.5 mmol), NMP (2 mL) at rt, overnight. [b] Isolated yield, average of at least two independent runs. [c] Cp' = cyclopentyl. [d] 35 °C, 3d.

Table 4.10. Ni-catalyzed reductive hydroamidation.

Silane-containing compounds are of considerable important due to their widespread utilization in industry and academic laboratories.[127] Thus, we turned our attention to

[127] (a) I. Fleming, J. Dunoguès, R. Smithers, in *Organic Reactions*, A. S. Kende, Ed. (John Wiley &

test the reactivity of trimethyl(phenylethynyl)silane under our optimized conditions (Table 4-11). To our delight, **4-46** could be obtained as single isomer in excellent yield. Promoted by this intriguing finding, we explored the influence of the nature of the silane substituent on the reactivity and selectivity. Notably, this regio- and stereoselectivity methodology is suitable for a wide variety of silane-substituted alkynes, generating the corresponding products in moderate to excellent yields (**4-46** to **4-51**). Moreover, our protocol exhibited a remarkable functional group compatibility and chemoselectivity profile as shown, as a host of products containing an ester (**4-52**), halides (**4-55**, **4-56**), an acetal (**4-58**) and a thio-containing heterocycle (**4-60**) were conveniently obtained. Therefore, providing products with an additional handle for further manipulation. Notably, other isocyanates were applicable for our approach as well. While one might argue that such a protocol would essentially be restricted to aliphatic isocyanates the preparation of **4-61** clearly indicates otherwise. Remarkably, the reaction could be executed on a gram scale, delivering **4-4** and **4-46** in 80% and 73% isolated yield, respectively. Taken together, these results clearly demonstrate that our practical Ni-catalyzed regioselective hydroamidation protocol might pave the way to future techniques for the reductive incorporation of isocyanates into organic molecules. These results are certainly noteworthy taking into consideration the opposite selectivity pattern in our previous hydrocarboxylation protocol (Chapter 3) for unsymmetrical alkynes.

Sons, 1989), vol. 2, pp. 57. 11. T. Y. Luh, S. T. Liu, in *The Chemistry of Organic Silicon Compounds*, Y. A. Z. Rappoport, Ed. (Wiley, vol. 2, Chichester, 2003), pp. 1793.

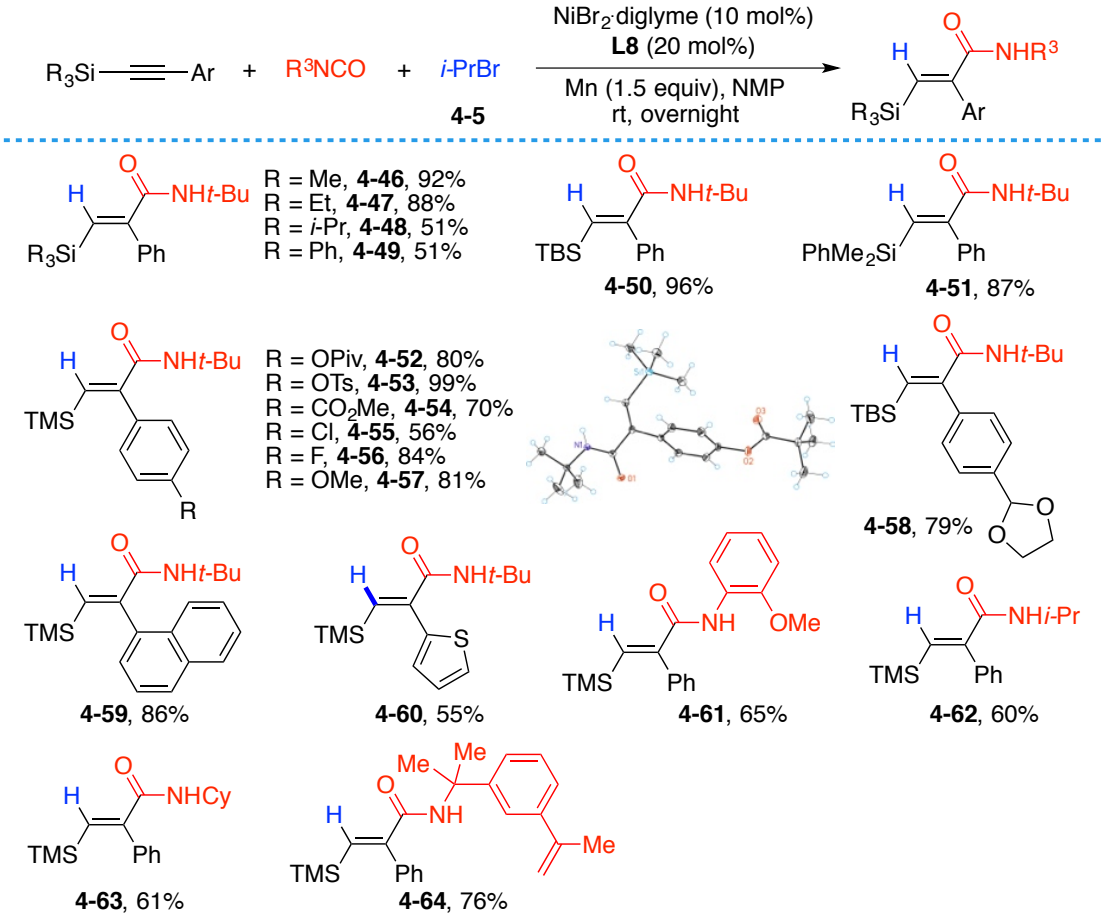

[a] Reaction conditions: **Substrate** (0.5 mmol), **isocyanate** (0.75 mmol), **4-5** (0.65 mmol), $NiBr_2$·diglyme (10 mol%), **L8** (20 mol%), Mn (1.5 mmol), NMP (2 mL) at rt, overnight. [b] Isolated yield, average of at least two independent runs.

Table 4.11. Ni-catalyzed reductive hydroamidation.

4.4.3 Mechanistic Studies

Having investigated the scope of the reaction, we next turned our attention to mechanistic studies on our Ni-catalyzed regioselective hydroamidation reaction. In this regard, we anticipated that the effect of radical scavengers, and conducting stoichiometric reactions as well as isotope-labelling experiments would allow us to gain precious information about the mechanism.

Following up on our Ni-catalyzed reductive protocol, we propose a mechanism as shown in Figure 4.13. We hypothesize that our hydroamidation process might undergo a catalytic cycle that involves a *β*-hydride elimination step. We believe that the reaction is initiated by the reduction of Ni(II) precatalyst to Ni(0) species **A** in the presence of Mn, followed by [Ni-H] formation with *i*-PrBr to afford intermediate **B**. Next, Ni(II) species **B** reacts with the alkyne to provide intermediate **C** that is subsequently reduced

to Ni(I) species **D** by Mn. Isocyanate fixation then occurs to yield intermediate **E**, and a final transmetallation/reduction with Mn would regenerate the active Ni(0)L species **A**, while at the same time liberating **F** that upon hydrolytic workup delivers the corresponding amide.

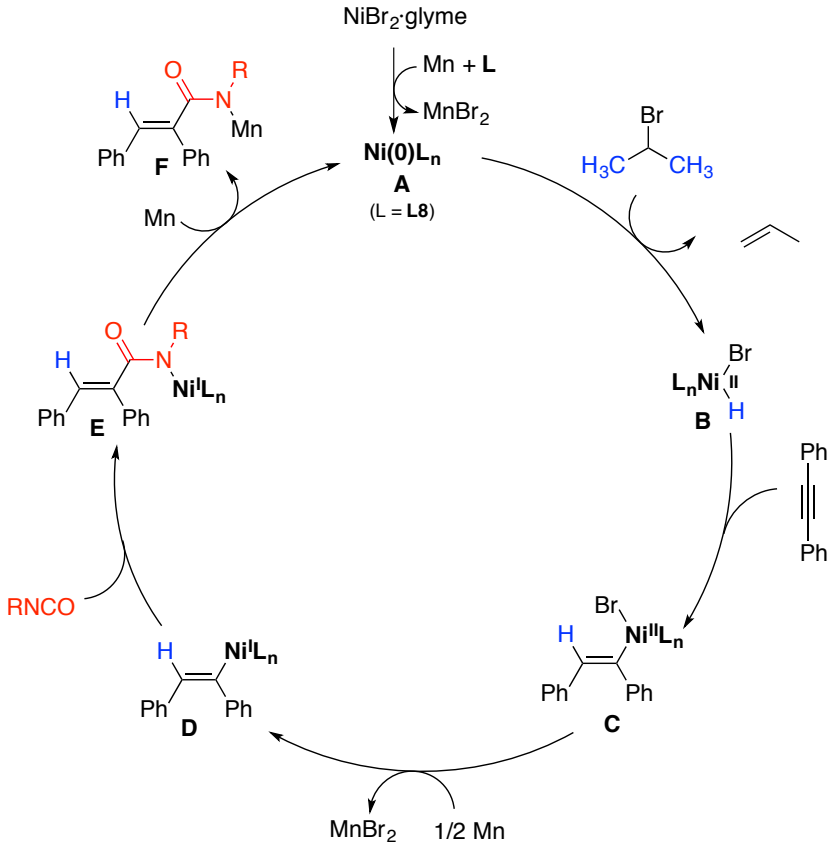

Scheme 4.4. Plausible mechanism.

Interestingly, radical scavengers such as TEMPO and BHT did suppress the reaction under the optimized reaction conditions. We could not obtain the corresponding amide in both cases, as presented in Figure 4.13. Although this is not a conclusive proof that the reactions undergo a radical pathway, it strongly suggests so.

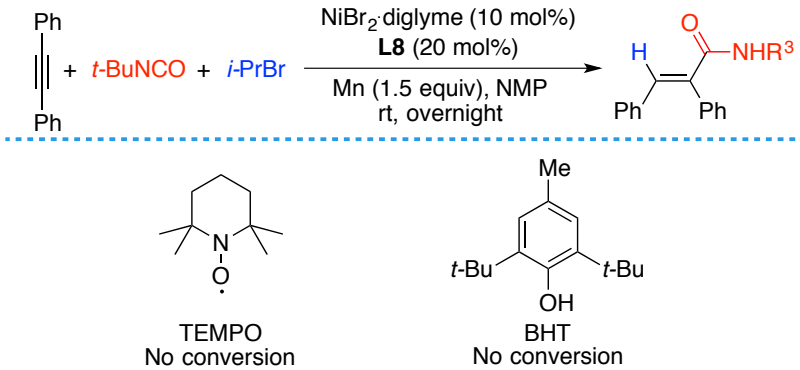

Scheme 4.5. Radical scavenger effect for substrate **3-1**.

Next, we carried out stoichiometric studies in the presence of **3-1** as starting material. We found that the hydride source is critical for the reaction to occur (Figure 4.14, left side *vs* right side), only trace amounts of the desired product were generated without *i*-PrBr. Those results indicate that this protocol might not proceed a nickelalactam intermediate. To our surprise, we obtained the desired amide in 41% isolated yield in the absence of Mn (top, left). The presence of Mn improves the reactivity and the yield increased to 74% (bottom, left). These results suggest another mechanism might come into play in this transformation as compared the one proposed in Scheme 4.4.

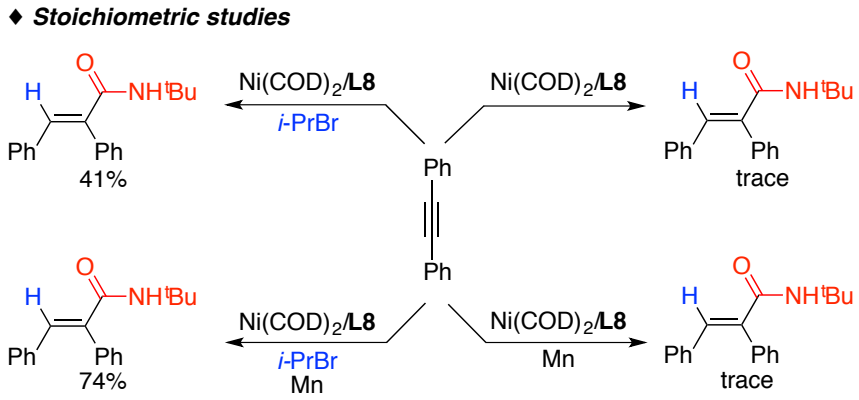

Scheme 4.6. Stoichiometric studies.

The isotope-labelling experiments showed that a β-hydride elimination step occurs, as we did not observe any D-incorporation within the final product when **4-66** was employed as hydride source. In contrast, when **4-65** was used, we found 75% of D-incorporation within product **4-67**.

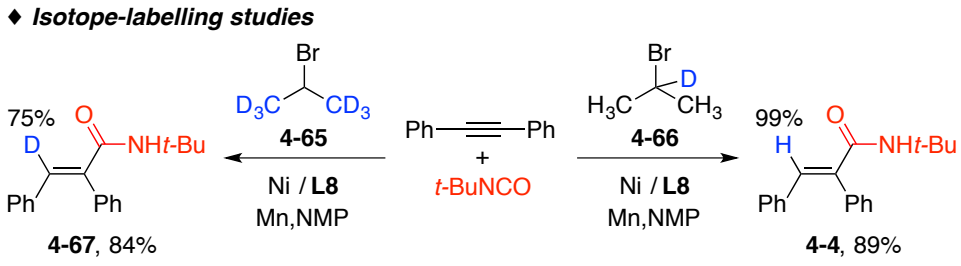

Scheme 4.7. Isotope-labelling studies.

Taking these results into consideration, we suggest that another mechanism involving the hydrometalation of isocyanate comes into play (Scheme 4.8). In this mechanism, we believe that the initial step is the formation of the Ni(0) species **A** in the presence of Mn, followed by [Ni-H] formation with *i*-PrBr to afford intermediate **B**. Subsequently, Ni(II) species **B** reacts with isocyanate to generate intermediate **G**,

followed by carbometalation with alkyne to deliver the Ni(II) species **H**. A final reduction with Mn would regenerate the active Ni(0)L species **A**, while liberating **I** that upon hydrolytic workup delivers the corresponding amide. At present, we cannot rule out one of these mechanisms based on our mechanistic studies.

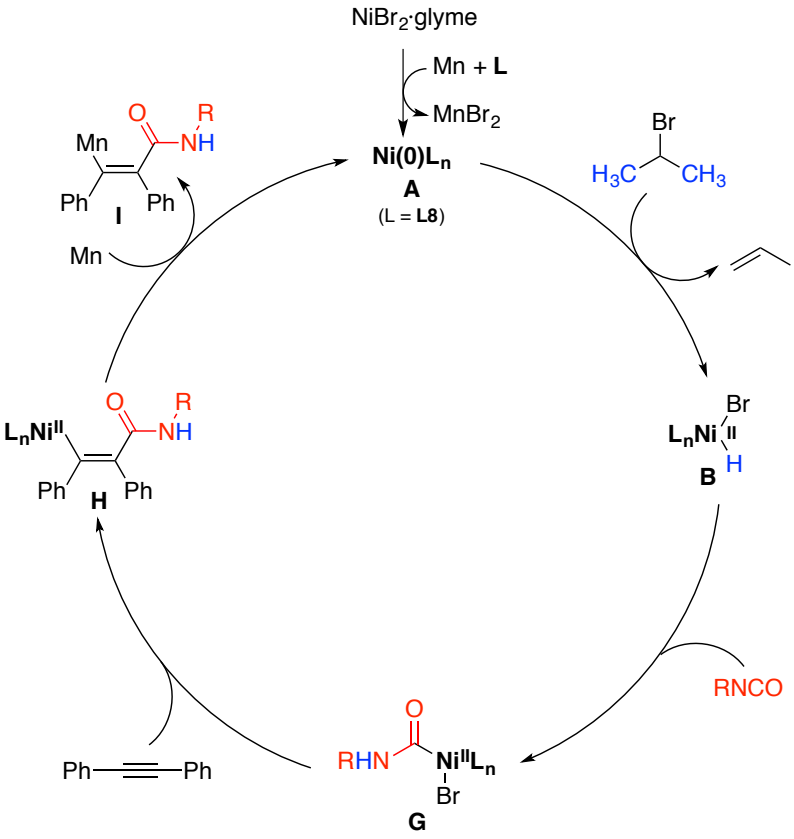

Scheme 4.8. Another plausible mechanism.

4.4.4 Limitations of the Hydroamidation Reactions

Besides the examples presented above, we found several limitations of our protocol for the Ni-catalyzed regioselective hydroamidation of alkynes with isocyanates as summarized in Table 4-12. The substrate **4-49** that bears a pyridine did not deliver even a trace of the desired product. Although **4-50** afforded the corresponding amide in high selectivity, the yield was moderate. We obtained the desired products with **4-51**, **3-13**, **4-57**, and **3-17**. However, in these cases the selectivity was not good. A ketone group was not tolerated in this transformation, as it was reduced to the corresponding alcohol (**4-52**). Low conversion was found in cases of **4-55** and **4-56** as starting material. We wondered whether the electronic properties on the aryl ring would influence the selectivity, the results of using **4-57** and **4-58** as starting material indicated that no significant influence is exerted, as one to one mixture of regioisomers. The internal

alkyl acetylene **4-59** generated a mixture of regio- and stereoisomers. All efforts made towards the use of terminal alkynes were unsuccessful and no desired products were observed in any case. Besides the alkynes, we also observed limitations in the scope of isocyanates. Most aryl substituted isocyanates studied were not suitable for amidation reactions and either low yields or no conversion were observed. The same trend was found in case of primary alkyl substituted isocyanates.

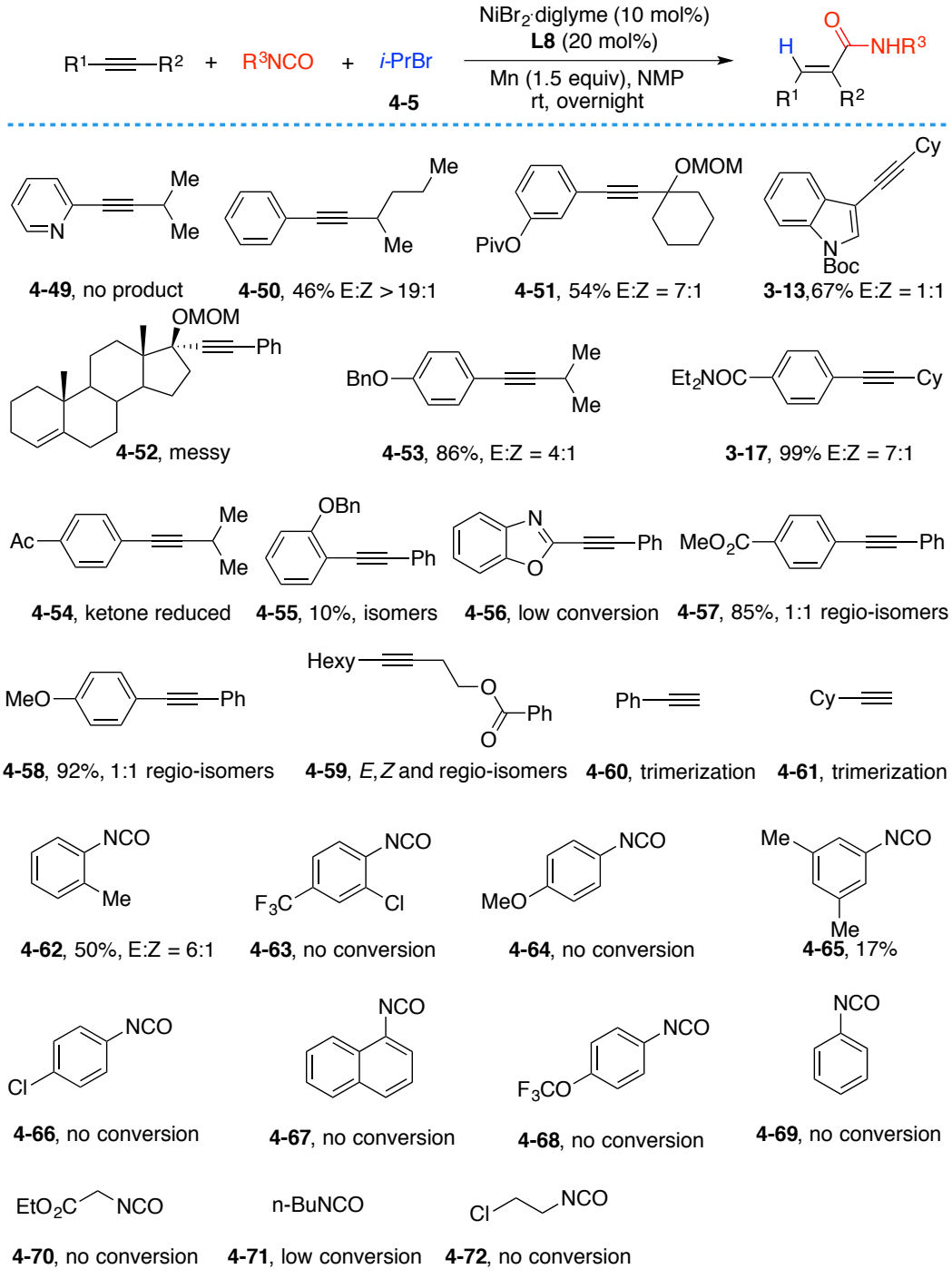

Table 4.12. Limitation of the hydroamidation.

4.5 Conclusion

In conclusion, we have developed a mild, robust, and user-friendly Ni-catalyzed reductive hydroamidation of alkynes using isocyanates that occurs with an exquisite regioselectivity profile using commercially available and inexpensive alkyl bromides as hydride sources. This protocol is distinguished by its excellent functional group tolerance and excellent selectivity. We anticipate this study will find widespread use, leading to new knowledge in metal-catalyzed reductive reactions. Mechanistic studies have shown that this approach might occur through two catalytic cycles that involve *β*-hydride elimination.

4.6 Experimental Section

4.6.1 General Considerations

Reagents: All reactions were conducted in Schlenk tubes. $NiBr_2$·diglyme was purchased from Aldrich. All other Nickel catalysts, ligands and Mn were purchased from Aldrich or Strem. Bathocuproine (**L8**) was purchased from TCI. Anhydrous NMP was purchased from Acros and used as received. Analytical methods: ^{1}H NMR and ^{13}C NMR spectra and melting points (where applicable) are included for all compounds. ^{1}H and ^{13}C NMR spectra were recorded on a Bruker 400 MHz and a Bruker 500 MHz at 20 °C. All ^{1}H NMR spectra are reported in parts per million (ppm) downfield of TMS and were measured relative to the signals for $CHCl_3$ (7.26 ppm). All ^{13}C NMR spectra were reported in ppm relative to residual $CHCl_3$ (77.20 ppm) and were obtained with 1H decoupling. Coupling constants, *J*, are reported in hertz. Melting points were measured using open glass capillaries in a Büchi B540 apparatus. Infrared spectra were recorded on a Bruker Tensor 27. Mass spectra were recorded on a Waters LCT Premier spectrometer. Gas chromatographic analyses were performed on Hewlett-Packard 6890 gas chromatography instrument with a FID detector using 25m x 0.20 mm capillary column with cross-linked methyl siloxane as the stationary phase. High Pressure Liquid Chromatographic (HPLC) analyses were performed on Agilent Technologies Model 1260 Infinity HPLC chromatography instrument equipped with Agilent Eclipse Plus C18 (3.5 um, 4.6 x 100 mm) column and UV/V is detector. Flash chromatography was performed with EM Science silica gel 60 (230-400 mesh) and using bromocresol as TLC stain.

4.6.2 General Procedure and Data

General procedure: An oven-dried Schlenk tube containing a stirring bar was charged with acetylene (0.50 mmol), **L5** (36 mg, 0.1 mmol), Mn powder (41.2 mg, 0.75 mmol) and $NiBr_2$·diglyme (18 mg, 0.05 mmol). The tube was then evacuated and back-filled with argon three times. *i*-PrBr (71.2 μL, 0.65 mmol), RNCO (0.75 mmol) and NMP (2 mL) were then added by syringe. Once added, the reaction mixture was stirred overnight at room temperature. The mixture was quenched with HCl (5% aq) and extracted with ethyl acetate three times. The combined organic layers were washed with brine and dried over anhydrous $MgSO_4$ and concentrated under reduced pressure. The residue was purified by flash chromatography (hexanes/ethyl acetate = 30/1 to 10/1).

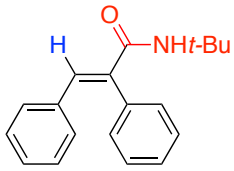

(*E*)-N-(*tert*-butyl)-2,3-diphenylacrylamide (4-4). Following the general procedure using **3-1** to afford **4-4** (127.1 mg, 91% yield) as a colorless solid. M.P. = 92-94 ºC. ^{1}H NMR (500 MHz, $CDCl_3$) δ 7.80 (s, 1H), 7.49-7.36 (m, 3H), 7.27-7.21 (m, 2H), 7.18-7.08 (m, 3H), 7.00-6.93 (m, 2H), 5.34 (s, 1H), 1.31 (s, 9H) ppm. ^{13}C NMR (126 MHz, $CDCl_3$) δ 166.5, 136.7, 136.3, 135.8, 135.3, 130.4, 130.0, 129.6, 128.5, 128.4, 128.2, 51.6, 28.8 ppm. IR (neat, cm^{-1}): 3411, 2974, 1666, 1614, 1500, 1199, 781, 692. HRMS *calcd.* for ($C_{19}H_{21}NO$+H): 280.1696, *found:* 280.1689.

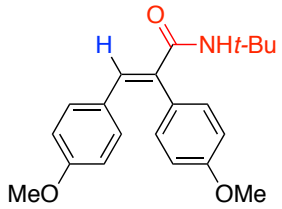

(*E*)-N-(*tert*-butyl)-2,3-bis(4-methoxyphenyl)acrylamide (4-30). Following the general procedure using **3-5** to afford **3-30** (134.0 mg, 79% yield) as a colorless solid. M.P. = 134 - 136 ºC. ^{1}H NMR (400 MHz, $CDCl_3$) δ 7.72 (s, 1H), 7.17-7.12 (m, 2H), 7.03-6.89 (m, 4H), 6.71-6.62 (m, 2H), 5.36 (s, 1H), 3.87 (s, 3H), 3.73 (s, 3H), 1.31 (s, 9H). ^{13}C NMR (75 MHz, $CDCl_3$) δ 167.0, 159.6, 159.5, 135.7, 132.9, 131.9, 131.2, 128.7, 128.0, 115.0, 113.6, 55.3, 55.2, 51.3, 28.7. IR (neat, cm^{-1}): 3415, 2968, 1670, 1603, 1504, 1246, 1172, 1020, 830. HRMS *calcd.* for ($C_{21}H_{25}NO_3$+H): 340.1907, *found:* 340.1904.

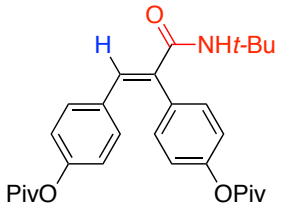

(*E*)-N-(*tert*-butyl)-2,3-bis(pivaloyloxyphenyl)acrylamide (4-31). Following the general procedure using **4-7** to afford **4-31** (180.8 mg, 75% yield) as a colorless solid. M.P. = 145-147 ºC. ^{1}H NMR (400 MHz, $CDCl_3$) δ 7.79 (s, 1H), 7.27 (d, J = 8.7 Hz, 2H), 7.16 (d, J = 8.7 Hz, 2H), 7.04-6.98 (m, 2H), 6.88 (d, J = 8.7 Hz, 2H), 5.36 (s, 1H), 1.41 (s, 9H), 1.34 (s, 9H), 1.32 (s, 9H). ^{13}C NMR (101 MHz, $CDCl_3$) δ 176.9, 176.8,

166.1, 151.2, 151.0, 135.7, 134.7, 133.5, 132.4, 131.3, 130.9, 122.8, 121.3, 51.5, 39.2, 39.1, 28.7, 27.1 (2C). IR (neat, cm^{-1}): 3432, 2973, 1747, 1674, 1501, 1270, 1196, 1164, 1106, 894. HRMS *calcd.* for ($C_{29}H_{37}NO_5$+H): 480.2744, *found:* 480.2745.

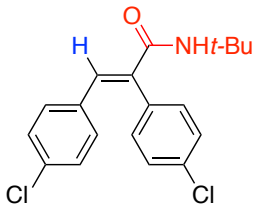

(*E*)-N-(*tert*-butyl)-2,3-bis(4-chlorophenyl)acrylamide (4-32). Following the general procedure using **4-8** to afford **4-32** (132.2 mg, 76% yield) as a colorless solid. M.P. = 124-125 ºC. ^{1}H NMR (300 MHz, $CDCl_3$) δ 7.72 (s, 1H), 7.41 (d, *J* = 8.0 Hz, 2H), 7.08 (m, 4H), 6.88 (d, *J* = 8.5 Hz, 2H), 5.28 (s, 1H), 1.32 (s, 9H). ^{13}C NMR (126 MHz, $CDCl_3$) δ 158.7, 128.5, 128.3, 127.8, 127.6, 127.5, 126.4, 124.4, 124.3, 123.0, 121.6, 44.7, 21.7. IR (neat, cm^{-1}): 3420, 2965, 1668, 1618, 1503, 1271, 1095, 1010, 824, 743. HRMS *calcd.* for ($C_{19}H_{19}Cl_2NO$+Na): 370.0741, *found:* 370.0736.

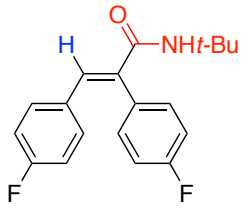

(*E*)-N-(*tert*-butyl)-2,3-bis(4-fluorophenyl)acrylamide (4-33). Following the general procedure using **4-9** to afford **4-33** (137.3 mg, 87% yield) as a colorless solid. M.P. = 109 - 111 ºC. ^{1}H NMR (400 MHz, $CDCl_3$) δ 7.74 (s, 1H), 7.24-7.08 (m, 3H), 6.98-6.87 (m, 2H), 6.83 (dd, *J* = 8.9, 2.0 Hz, 2H), 5.27 (s, 1H), 1.31 (s, 9H) ppm. ^{13}C NMR (101 MHz, $CDCl_3$) δ 166.2, 164.0 (d, *J* = 19.6 Hz), 161.5 (d, *J* = 20.7 Hz), 135.6, 134.5, 132.3 (d, *J* = 3.7 Hz), 132.1 (d, *J* = 8.2 Hz), 131.9 (d, *J* = 8.1 Hz), 131.3 (d, *J* = 3.4 Hz), 117.0 (d, *J* = 21.5 Hz), 115.5 (d, *J* = 21.5 Hz), 51.7, 28.8 ppm. ^{19}F NMR (376 MHz, $CDCl_3$) δ -112.0, -112.5 ppm. IR (neat, cm^{-1}): 3424, 2966, 1670, 1496, 1222, 1157, 837. 808. HRMS *calcd.* for ($C_{19}H_{19}F_2NO$+Na): 338.1327, *found:* 338.1318.

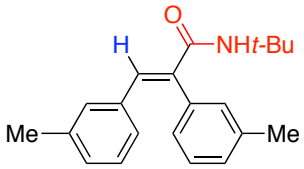

(*E*)-*N*-(*tert*-butyl)-2,3-di-*m*-tolylacrylamide (4-34). Following the general procedure using **3-5** to afford **4-34** (139.8 mg, 91% yield) as a colorless solid. M.P. = 115-116 ºC. ^{1}H NMR (500 MHz, $CDCl_3$) δ 7.77 (s, 1H), 7.33 (td, *J* = 7.4, 1.0 Hz, 1H), 7.24-7.20 (m, 1H), 7.10-6.94 (m, 4H), 6.84 (dt, *J* = 1.7, 0.8 Hz, 1H), 6.78-6.73 (m, 1H), 5.42 (s, 1H), 2.37 (s, 3H), 2.18 (s, 3H), 1.34 (s, 9H). IR (neat, cm^{-1}): 3270, 2958, 1633, 1613, 1537, 1450, 1314, 1222, 1091, 921. 783. HRMS *calcd.* for ($C_{21}H_{25}NO$+Na): 330.1834, *found:* 330.1840.

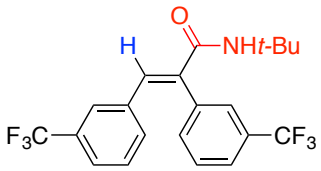

(*E*)-N-(*tert*-butyl)-2,3-bis(3-(trifluoromethyl)phenyl)acrylamide (4-35). Following the general procedure using **4-6** to afford **4-35** (133.2 mg, 64% yield) as a colorless solid. M.P. = 64-65 ºC. ^{1}H NMR (400 MHz, $CDCl_3$) δ 7.79 (s, 1H), 7.69 (d, *J* = 7.9 Hz, 1H), 7.58 (t, *J* = 7.8 Hz, 1H), 7.49 (s, 1H), 7.46-7.38 (m, 2H), 7.28 (dd, *J* = 9.7, 5.9 Hz, 1H), 7.14 (d, *J* = 7.8 Hz, 1H), 7.08 (s, 1H), 5.32 (s, 1H), 1.34 (s, 9H). ^{13}C NMR (101 MHz, $CDCl_3$) δ 165.2, 136.7, 136.6, 135.5, 135.4, 133.2 (2C), 132.1 (q, *J* = 32.7 Hz), 130.7 (q, *J* = 33.5 Hz), 130.2, 128.9, 126.7 (q, *J* = 3.7 Hz), 126.4 (q, *J* = 3.9 Hz), 125.5 (q, *J* = 3.8 Hz), 125.1 (q, *J* = 3.7 Hz), 123.6 (2C, q, *J* = 273 Hz), 51.9, 28.6. ^{19}F NMR (376 MHz, $CDCl_3$) δ -55.7, -56.1. IR (neat, cm^{-1}): 3275, 2971, 1638, 1548, 1322, 1118, 1072, 912, 698. HRMS *calcd.* for ($C_{21}H_{20}F_6NO$+H): 416.1444, *found:* 416.1438.

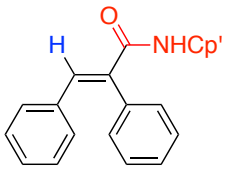

(*E*)-N-cyclopentyl-2,3-diphenylacrylamide (4-36). Following the general procedure using **3-1** to afford **4-36** (138.4 mg, 95% yield) as a colorless solid. M.P. = 84-86 ºC. ^{1}H NMR (400 MHz, $CDCl_3$) δ 7.83 (s, 1H), 7.59-7.31 (m, 3H), 7.25-7.20 (m, 2H), 7.15 - 7.06 (m, 3H), 7.00 - 6.92 (m, 2H), 5.40 (d, *J* = 7.7 Hz, 1H), 4.32-4.23 (m, 1H), 2.15-1.79 (m, 2H), 1.58 - 1.50 (m, 4H), 1.37-1.08 (m, 2H) ppm. ^{13}C NMR (101 MHz, $CDCl_3$) δ 166.7, 136.8, 136.4, 135.2, 134.7, 130.3, 129.9, 129.6, 128.5, 128.5, 128.2, 51.8, 33.1, 23.7. IR (neat, cm^{-1}): 3422, 2961, 1667, 1618, 1495, 1205, 692. HRMS *calcd.* for ($C_{20}H_{21}NO$+H): 292.1696, *found:* 292.1688.

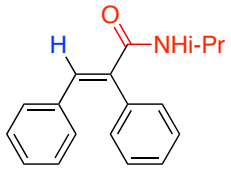

(*E*)-N-*iso*propyl-2,3-diphenylacrylamide (4-37). Following the general procedure using **3-1** to afford **4-37** (123.4 mg, 93% yield) as a colorless solid. M.P. = 82-84 ºC. ^{1}H NMR (400 MHz, $CDCl_3$) δ 7.83 (s, 1H), 7.55-7.32 (m, 3H), 7.25-7.19 (m, 2H), 7.19-7.03 (m, 3H), 7.03-6.82 (m, 2H), 5.28 (d, *J* = 7.8 Hz, 1H), 4.16 (m, 6.5 Hz, 1H), 1.07 (d, *J* = 6.6 Hz, 6H) ppm. ^{13}C NMR (101 MHz, $CDCl_3$) δ 166.3, 136.9, 136.3, 135.2, 134.8, 130.3, 129.9, 129.6, 128.5, 128.5, 128.2, 42.0, 22.7 ppm. IR (neat, cm^{-1}): 3304, 2970, 1649, 1510, 690. HRMS *calcd.* for ($C_{18}H_{19}NO$+H): 266.1539, *found:* 266.1535.

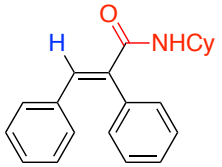

(*E*)-N-cyclohexyl-2,3-diphenylacrylamide (4-38). Following the general procedure using **3-1** to afford **4-38** (129.8 mg, **4-38**:**3-38' = 10:1**, 85% yield) as a colorless solid. M.P. = 104 - 106 ºC. Spectroscopic data for the major isomer (**3j**): ^{1}H NMR (400 MHz, $CDCl_3$) δ 7.82 (s, 1H), 7.60-7.32 (m, 3H), 7.25-7.20 (m, 2H), 7.17-7.02 (m, 3H), 7.02-6.71 (m, 2H), 5.35 (d, J = 8.2 Hz, 1H), 3.92-3.83 (m 1H), 1.84 (dt, *J* = 12.6, 4.3 Hz, 2H), 1.59-1.51 (m, 3H), 1.47-1.27 (m, 2H), 1.18-0.87 (m, 3H) ppm. ^{13}C NMR (101 MHz, $CDCl_3$) δ 166.1, 136.8, 136.4, 135.2, 134.8, 130.3, 129.9, 129.6, 128.5, 128.4, 128.2, 48.6, 32.8, 25.6, 24.7 ppm. IR (neat, cm^{-1}): 3423, 2929, 2854, 1664, 1618, 1496, 1203, 709, 692. HRMS *calcd.* for ($C_{21}H_{23}NO$+H): 306.1852, *found:* 306.1838.

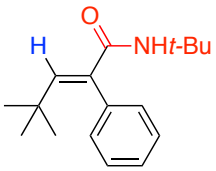

(*E*)-N-(*tert*-butyl)-4,4-dimethyl-2-phenylpent-2-enamide (4-39). Following the general procedure using **4-10** to afford **4-39** (65.5 mg, 50% yield) as a colorless solid. M.P. = 99-100 ºC. ^{1}H NMR (300 MHz, $CDCl_3$) δ 7.39-7.31 (m, 3H), 7.21-7.13 (m, 2H), 7.01 (s, 1H), 5.06 (s, 1H), 1.22 (s, 9H), 0.88 (s, 9H). ^{13}C NMR (75 MHz, $CDCl_3$) δ 166.8, 148.5, 136.9, 133.5, 130.3, 128.4, 127.9, 51.1, 33.7, 30.5, 28.6. IR (neat, cm^{-1}):

3293, 2960, 1621, 1533, 1452, 1358, 1306, 1219, 1157, 708. HRMS *calcd.* for ($C_{17}H_{26}NO+H$): 260.2009, *found:* 260.2005.

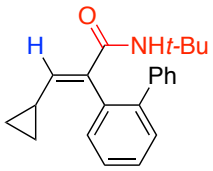

(*E*)-2-([1,1'-biphenyl]-2-yl)-N-(*tert*-butyl)-3-cyclopropylacrylamide (4-40). Following the general procedure using **4-11** to afford **4-40** (129.8 mg, 85% yield) as a white solid. M.P. = 104-106 ºC. ^{1}H NMR (300 MHz, $CDCl_3$) δ 7.52-7.26 (m, 9H), 6.27 (d, *J* = 10.9 Hz, 1H), 4.98 (s, 1H), 1.38-1.19 (m, 1H), 1.04 (s, 9H), 0.90-0.77 (m, 1H), 0.77-0.59 (m, 1H), 0.59-0.40 (m, 1H) ppm. ^{13}C NMR (101 MHz, $CDCl_3$) δ 165.0, 146.0, 142.0, 140.8, 134.5, 134.1, 132.2, 130.5, 129.0, 128.7, 128.3, 127.9, 127.4, 50.9, 28.5, 12.5, 8.3, 8.2 ppm. IR (neat, cm^{-1}): 3424, 2965, 1666, 1621, 1505, 743, 703, 499. HRMS *calcd.* for ($C_{22}H_{25}NO+H$): 320.2009, *found:* 320.1999.

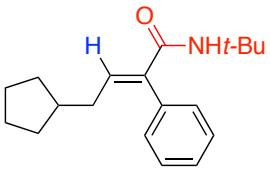

(*E*)-N-(*tert*-butyl)-4-cyclopentyl-2-phenylbut-2-enamide (4-41). Following the general procedure using **4-12** to afford **4-41** (131.3 mg, 92% yield) as a colorless solid. M.P. = 61-62 ºC. ^{1}H NMR (400 MHz, $CDCl_3$) δ 7.59-7.28 (m, 3H), 7.20-7.06 (m, 2H), 6.98 (t, J = 7.5 Hz, 1H), 5.14 (s, 1H), 1.99-1.90 (m, 2H), 1.91-1.80 (m, 1H), 1.76-1.66 (m, 2H), 1.55-1.41 (m, 4H), 1.26 (s, 9H), 1.11-0.96 (m, 2H) ppm. ^{13}C NMR (101 MHz, $CDCl_3$) δ 166.3, 139.8, 136.8, 136.5, 130.0, 128.9, 128.0, 51.3, 39.9, 35.4, 32.5, 29.0, 25.1 ppm. IR (neat, cm^{-1}): 3295, 2948, 2865, 1619, 1531, 1222, 700. HRMS *calcd.* for ($C_{19}H_{27}NO+Na$): 308.1985, *found:* 308.1980.

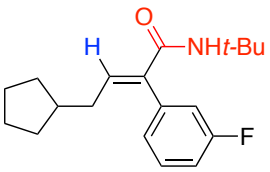

(*E*)-N-(*tert*-butyl)-4-cyclopentyl-2-(3-fluorophenyl)but-2-enamide (4-42). Following the general procedure using **1m** to afford **4-42** (133.3 mg, **4-42**:**4-42' = 16:1** 88% yield) as a colorless solid. M.P. = 74-76 ºC. Spectroscopic data for the major isomer (**3m**): ^{1}H NMR (400 MHz, $CDCl_3$) δ 7.51-7.33 (m, 1H), 7.06 (td, *J* = 8.5, 2.7,

1H), 7.02-6.92 (m, 2H), 6.88 (dd, *J* = 9.4, 2.6, 1H), 5.10 (s, 1H), 1.99-1.94 (m, 1H) 1.93-1.79 (m, 2H), 1.79-1.66 (m, 2H), 1.59-1.44 (m, 4H), 1.29 (s, 9H), 1.11-0.95 (m, 2H) ppm. ^{13}C NMR (101 MHz, $CDCl_3$) δ 165.7, 162.9 (d, *J* = 247.6 Hz), 140.6, 138.8 (d, *J* = 7.5 Hz), 135.8, 130.6 (d, *J* = 8.5 Hz), 125.7 (d, *J* = 3.1 Hz), 117.0 (d, *J* = 21.2 Hz), 115.1 (d, *J* = 21.0 Hz), 51.5, 39.8, 35.4, 32.6, 28.9, 25.1 ppm. ^{19}F NMR (376 MHz, $CDCl_3$) δ -112.09 ppm. IR (neat, cm^{-1}): 3281, 2957, 2865, 1624, 1539, 1223, 740, 678. HRMS *calcd.* for ($C_{19}H_{26}FNO$+H): 304.2071, *found:* 304.2063.

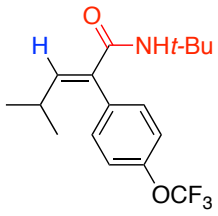

(*E*)-N-(*tert*-butyl)-4-methyl-2-(4-(trifluoromethoxy)phenyl)pent-2-enamide (4-43). Following the general procedure using **3-20** to afford **4-43** (105.4 mg, **4-43**:**4-43' = 17:1**, 64% yield) as a colorless solid. M.P. = 66 – 69 ºC. Spectroscopic data for the major isomer (**3o**): ^{1}H NMR (400 MHz, $CDCl_3$) δ 7.35-7.14 (m, 4H), 6.73 (d, *J* = 10.6 Hz, 1H), 5.07 (s, 1H), 2.22-2.13 (m, 1H), 1.29 (s, 9H), 0.96 (d, J = 6.6 Hz, 6H) ppm. ^{13}C NMR (101 MHz, $CDCl_3$) δ 166.0, 149.0 (q, *J* = 1.7 Hz), 147.2, 135.1, 133.5, 131.3, 121.7, 120.6 (q, *J* = 257.4 Hz), 51.5, 28.8, 28.6, 22.4 ppm. ^{19}F NMR (376 MHz, $CDCl_3$) δ -57.90 ppm. IR (neat, cm^{-1}): 3296, 2960, 1612, 1534, 1250, 1159. HRMS *calcd.* for ($C_{17}H_{22}F_3NO$+Na): 352.1495, *found:* 352.1491.

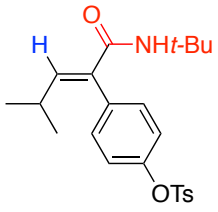

(*E*)-4-(1-(*tert*-butylamino)-4-methyl-1-oxopent-2-en-2-yl)phenyl 4-methylbenzene sulfonate (**4-44**). Following the general procedure using **4-14** to afford **4-44** (207.8 mg, **4-44**:**4-44' = 12:1**, 97% yield) as a colorless solid. M.P. = 123-125 ºC. Spectroscopic data for the major isomer (**3p**): ^{1}H NMR (400 MHz, $CDCl_3$) δ 7.65 (d, *J* = 8.3 Hz, 2H), 7.25 (d, *J* = 7.9 Hz, 2H), 7.08-7.02 (m, 2H), 7.02-6.94 (m, 2H), 6.63 (d, *J* = 10.5 Hz, 1H), 4.95 (s, 1H), 2.38 (s, 3H), 2.17-1.86 (m, 1H), 1.21 (s, 9H), 0.87 (d, *J* = 6.6 Hz, 6H) ppm. ^{13}C NMR (101 MHz, $CDCl_3$) δ 165.8, 149.2, 146.9, 145.6, 135.3, 133.4, 132.2, 130.9, 129.8, 128.5, 122.7, 51.3, 28.6, 28.4, 22.3, 21.7 ppm. IR

(neat, cm^{-1}): 3423, 2965, 1668, 1497, 1361, 1153, 858, 549. HRMS *calcd.* for ($C_{23}H_{30}NO_4S$+Na): 416.1890, *found:* 416.1891.

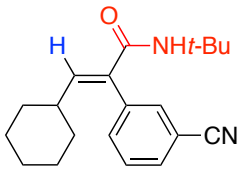

(*E*)-N-(*tert*-butyl)-2-(4-cyanophenyl)-3-cyclohexylacrylamide (4-45). Following the general procedure using **3-19** to afford **4-44** (119.5 mg, **4-45**:**4-45' = 12:1**, 77% yield) as a colorless solid. M.P. = 115-117 ºC. Spectroscopic data for the major isomer (**3q**): ^{1}H NMR (500 MHz, $CDCl_3$) δ 7.62 (d, *J* = 7.7, 1H), 7.51 (t, *J* = 7.7, 1H), 7.43 (s, 1H), 7.39 (d, *J* = 7.7 Hz, 1H), 6.66 (d, *J* = 10.5 Hz, 1H), 5.01 (s, 1H), 1.84-1.69 (m, 1H), 1.65-1.44 (m, 5H), 1.25 (s, 9H), 1.18-0.92 (m, 5H) ppm. ^{13}C NMR (126 MHz, $CDCl_3$) δ 165.6, 146.0, 137.8, 134.1, 133.4, 132.9, 131.6, 129.7, 118.4, 113.0, 51.6, 38.2, 32.2, 29.7, 28.8, 25.2 ppm. IR (neat, cm^{-1}): 3304, 2926, 2229, 1619 1536, 1447, 1220, 800, 681. HRMS *calcd.* for ($C_{20}H_{26}N_2O$+Na): 333.1937, *found:* 333.1930.

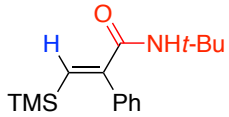

(*E*)-N-(*tert*-butyl)-2-phenyl-3-(trimethylsilyl)acrylamide (4-46). Following the general procedure using **4-15** to afford **4-46** (127.0 mg, 92% yield) as a colorless solid. M.P. = 104– 106 ºC. ^{1}H NMR (300 MHz, $CDCl_3$) δ 7.50-7.29 (m, 3H), 7.24-7.09 (m, 3H), 5.30 (s, 1H), 1.25 (s, 9H), -0.19 (s, 9H) ppm. ^{13}C NMR (101 MHz, $CDCl_3$) δ 165.6, 150.7, 139.8, 138.8, 129.6, 128.6, 128.3, 51.4, 28.7, -0.6 ppm. IR (neat, cm^{-1}): 3293, 2973, 1636, 1537, 836, 697. HRMS *calcd.* for ($C_{16}H_{25}NOSi$+Na): 298.1598, *found:* 298.1597.

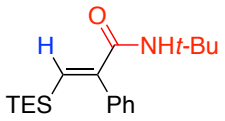

(*E*)-N-(*tert*-butyl)-2-phenyl-3-(triethylsilyl)acrylamide (4-47). Following the general procedure using **4-16** to afford **4-47** (139.7 mg, 88% yield) as a colorless solid. M.P. = 50 – 52 ºC. ^{1}H NMR (400 MHz, $CDCl_3$) δ 7.35-7.33 (m, 3H), 7.22-7.15 (m, 2H), 7.13 (s, 1H), 5.27 (s, 1H), 1.25 (s, 9H), 0.79 (t, *J* = 7.9 Hz, 9H), 0.28 (q, *J* = 7.9 Hz, 6H) ppm. ^{13}C NMR (101 MHz, $CDCl_3$) δ 165.4, 151.3, 139.0, 137.2, 129.4, 128.5, 128.3, 51.4, 28.7, 7.5, 3.9 ppm. IR (neat, cm^{-1}) 3279, 2952, 2875, 1636, 1533, 1285, 1224, 839, 699. HRMS *calcd.* for ($C_{19}H_{31}NOSi$+H): 318.2248, *found:* 318.2244.

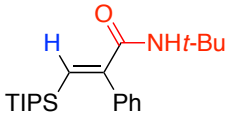

(*E*)-N-(*tert*-butyl)-2-phenyl-3-(triisopropylsilyl)acrylamide (4-48). Following the general procedure using **4-17** to afford **4-48** (91.7 mg, 51% yield) as colorless oil. ^{1}H NMR (300 MHz, $CDCl_3$) δ 7.34-7.28 (m, 3H), 7.25-7.19 (m, 2H), 7.15 (s, 1H), 5.20 (s, 1H), 1.23 (s, 9H), 0.90 (d, *J* = 6.4 Hz, 18H), 0.85-0.72 (m, 3H). ^{13}C NMR (75 MHz, $CDCl_3$) δ 165.5, 150.9, 139.2, 135.7, 129.4, 128.2, 51.2, 28.6, 18.9, 11.8. IR (neat, cm^{-1}): 3426, 2942, 2865, 1671, 1505, 1452, 1263, 1210, 999, 881, 706. HRMS *calcd.* for ($C_{22}H_{37}NOSi$+H): 360.2717, *found:* 360.2717.

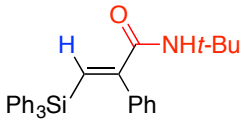

(*E*)-N-(*tert*-butyl)-2-phenyl-3-(triphenylsilyl)acrylamide (4-49). Following the general procedure using **4-18** to afford **4-49** (119.1 mg, 51% yield) as a colorless solid. M.P. = 145-147 ºC. ^{1}H NMR (400 MHz, $CDCl_3$) δ 7.84 (s, 1H), 7.49-7.36 (m, 6H), 7.37-7.28 (m, 3H), 7.26-7.18 (m, 6H), 7.08-6.98 (m, 1H), 6.98-6.79 (m, 4H), 5.36 (s, 1H), 1.30 (s, 9H) ppm. ^{13}C NMR (101 MHz, $CDCl_3$) δ 165.5, 154.1, 137.1, 135.9, 134.4, 133.2, 129.4, 129.3, 128.1, 128.0, 127.8, 51.5, 28.7 ppm. IR (neat, cm^{-1}) 3412, 3066, 2971, 1665, 1506, 1105, 697, 501. HRMS *calcd.* for ($C_{31}H_{31}NOSi$+H): 462.2248, *found:* 462.2249.

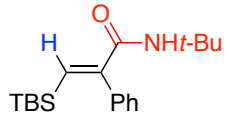

(*E*)-*N*-(*tert*-butyl)-3-(*tert*-butyldimethylsilyl)-2-phenylacrylamide (4-50). Following the general procedure using **4-19** to afford **4-50** (152.0 mg, 96% yield) as colorless oil. ^{1}H NMR (400 MHz, $CDCl_3$) δ 7.40-7.31 (m, 3H), 7.24 (s, 1H), 7.22-7.10 (m, 2H), 5.25 (s, 1H), 1.24 (s, 9H), 0.86 (s, 9H), -0.38 (s, 6H) ppm. ^{13}C NMR (101 MHz, $CDCl_3$) δ 165.4, 151.4, 138.9, 136.9, 129.7, 128.5, 128.3, 51.4, 28.7, 26.7, 16.9, -5.3 ppm. IR (neat, cm^{-1}) 3424, 2954, 2928, 2856, 1671, 1506, 1263, 824, 703. HRMS *calcd.* for ($C_{19}H_{31}NOSi$+H): 318.2248, *found:* 318.2249.

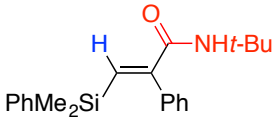

(*E*)-N-(*tert*-butyl)-3-(dimethyl(phenyl)silyl)-2-phenylacrylamide (4-51). Following the general procedure using **4-20** to afford **4-51** (147.3 mg, 87% yield) as a colorless

oil. ^{1}H NMR (500 MHz, $CDCl_3$) δ 7.38-7.36 (m, 2H), 7.32 (s, 1H), 7.31-7.23 (m, 6H), 7.13-7.06 (m, 2H), 5.32 (s, 1H), 1.26 (s, 9H), 0.04 (s, 6H). ^{13}C NMR (126 MHz, $CDCl_3$) δ 165.2, 151.5, 138.3, 138.2, 137.4, 133.6, 129.3, 128.8, 128.3, 128.2, 127.6, 51.3, 28.5, -2.2. IR (neat, cm^{-1}): 3422, 2963, 1669, 1505, 1263, 1212, 1112, 816, 698. HRMS *calcd.* for ($C_{21}H_{27}NOSi$+H): 338.1935, *found:* 338.1935.

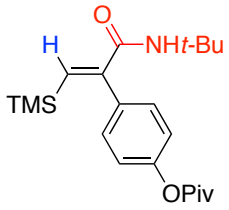

(*E*)-4-(3-(*tert*-butylamino)-3-oxo-1-(trimethylsilyl)prop-1-en-2-yl)phenyl pivalate (4-52). Following the general procedure using **4-21** to afford **4-52** (150.0 mg, 80% yield) as a colorless solid. M.P. = 121-122 ºC. ^{1}H NMR (400 MHz, $CDCl_3$) δ 7.18 (d, *J* = 8.4 Hz, 2H), 7.12 (s, 1H), 7.05 (d, *J* = 8.5 Hz, 2H), 5.28 (s, 1H), 1.33 (s, 9H), 1.24 (s, 9H), -0.18 (s, 9H) ppm. ^{13}C NMR (101 MHz, $CDCl_3$) δ 177.0, 165.4, 151.2, 149.8, 140.4, 136.0, 130.5, 121.8, 51.5, 39.2, 28.6, 27.2, -0.6 ppm. IR (neat, cm^{-1}) 3367, 2965, 1749, 1632, 1526, 1197, 1115, 860, 833. HRMS *calcd.* for ($C_{21}H_{33}NOSi$+H): 376.2302, *found:* 376.2314.

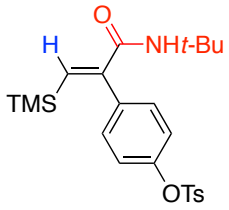

(*E*)-4-(3-(*tert*-butylamino)-3-oxo-1-(trimethylsilyl)prop-1-en-2-yl)phenyl-4-methylbenzenesulfonate (4-53). Following the general procedure using **4-22** to afford **4-53** (222.0 mg, 99% yield) as a colorless solid. M.P. = 143-145 ºC. ^{1}H NMR (400 MHz, $CDCl_3$) δ 7.66 (d, *J* = 8.4 Hz, 2H), 7.26 (d, *J* = 8.0 Hz, 2H), 7.11 (d, *J* = 8.5 Hz, 2H), 7.06 (s, 1H), 6.99 (d, *J* = 8.5 Hz, 2H), 5.15 (s, 1H), 2.41 (s, 3H), 1.24 (s, 9H), -0.21 (s, 9H) ppm. ^{13}C NMR (101 MHz, $CDCl_3$) δ 165.2, 149.6, 149.5, 145.7, 140.5, 137.8, 132.0, 130.8, 129.9, 128.7, 122.6, 51.6, 28.6, 21.8, -0.6 ppm. IR (neat, cm^{-1}) 3347, 2975, 1524, 1373, 1149, 866, 552. HRMS *calcd.* for ($C_{23}H_{31}NO_4SSi$+H): 446.1816, *found:* 446.1814

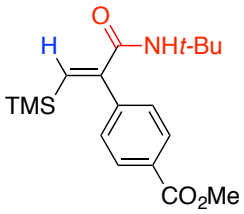

(E)-methyl-4-(3-(*tert*-butylamino)-3-oxo-1-(trimethylsilyl)prop-1-en-2-yl)benzoate (4-54). Following the general procedure using **4-23** to afford **4-54** (116.8 mg, 70% yield) as a colorless solid. M.P. = 97-99 ºC. ^{1}H NMR (400 MHz, $CDCl_3$) δ 8.04 (d, *J* = 8.3 Hz, 2H), 7.29 (d, *J* = 8.3 Hz, 2H), 7.14 (s, 1H), 5.17 (s, 1H), 3.92 (s, 3H), 1.25 (s, 9H), -0.18 (s, 9H) ppm. ^{13}C NMR (101 MHz, $CDCl_3$) δ 166.7, 165.0, 149.9, 143.8, 140.6, 130.1, 129.8, 129.7, 52.4, 51.7, 28.7, -0.6 ppm. IR (neat, cm^{-1}) 3114, 2968, 1725, 1636, 1525, 1273, 831, 710. HRMS *calcd.* for ($C_{18}H_{27}NO_3Si$+Na): 356.1652, *found:* 356.1641.

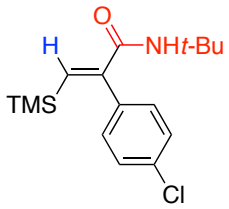

(*E*)-N-(*tert*-butyl)-2-(4-chlorophenyl)-3-(trimethylsilyl)acrylamide (4-55). Following the general procedure using **4-24** to afford **4-55**(92.4 mg, 60% yield) as a colorless solid. M.P. = 128-129 ºC. ^{1}H NMR (500 MHz, $CDCl_3$) δ 7.33 (d, *J* = 8.3 Hz, 2H), 7.13 (d, *J* = 8.4 Hz, 2H), 7.09 (s, 1H), 5.22 (s, 1H), 1.26 (s, 9H), -0.18 (s, 9H) ppm. ^{13}C NMR (126 MHz, $CDCl_3$) δ 165.3, 149.6, 140.5, 137.2, 134.4, 130.9, 128.8, 51.6, 28.7, -0.6 ppm. IR (neat, cm^{-1}) 3297, 2972, 1637, 1602, 1535, 1784, 1287, 1222, 1089, 867. HRMS *calcd.* for ($C_{16}H_{24}ClNOSi$+H): 310.1388, *found:* 310.1392.

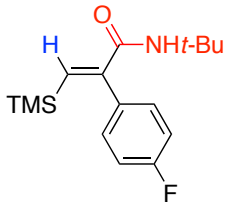

(*E*)-N-(*tert*-butyl)-2-(4-fluorophenyl)-3-(trimethylsilyl)acrylamide (4-56). Following the general proce- dure using **4-25** to afford **4-56** (123.2 mg, 84% yield) as a colorless solid. M.P. = 98-99 ºC. ^{1}H NMR (300 MHz, $CDCl_3$) δ 7.43-7.33 (m, 2H), 7.27 (s, 1H), 7.18-7.13 (m, 2H), 5.32 (s, 1H), 1.34 (s, 9H), -0.10 (s, 9H). ^{13}C NMR (75 MHz, $CDCl_3$) δ 165.4, 164.2, 161.0, 149.6, 140.2, 134.6, 134.5, 131.2, 131.1, 115.7,

115.4, 51.4, 28.6, -0.7. ^{19}F NMR (376 MHz, $CDCl_3$) δ -105.8 (tt, J = 8.6, 5.4 Hz). IR (neat, cm^{-1}): 3296, 2968, 1634, 1605, 1539, 1505, 1290, 1218, 1157, 838. HRMS *calcd.* for ($C_{16}H_{24}FNOSi$+Na): 316.1509, *found:* 316.1503.

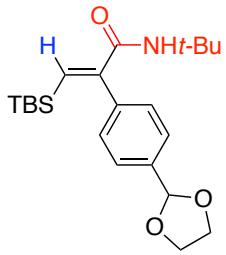

(*E*)-2-(4-(1,3-dioxolan-2-yl)phenyl)-*N*-(*tert*-butyl)-3-(*tert*-butyldimethylsilyl acrylamide (4-58). Following the general procedure using **4-27** to afford **4-58** (153.9 mg, 79% yield) as a colorless oil. ^{1}H NMR (300 MHz, $CDCl_3$) δ 7.46 (d, J = 8.0 Hz, 1H), 7.22 (s, 1H), 7.19 (d, J = 7.9 Hz, 2H), 5.78 (s, 1H), 5.20 (s, 1H), 4.15 – 3.98 (m, 4H), 1.22 (s, 9H), 0.83 (s, 9H), -0.41 (s, 6H). ^{13}C NMR (101 MHz, $CDCl_3$) δ 164.9, 150.8, 139.6, 137.7, 137.3, 129.5, 126.5, 103.3, 65.2, 51.2, 28.5, 26.4, 16.6, -5.5. IR (neat, cm^{-1}): 3423, 2954, 2928, 2883, 2856, 1669, 1504, 1453, 1265, 1212, 1081, 825. HRMS *calcd.* for ($C_{22}H_{35}NOSi$+H): 390.2459, *found:* 390.2454.

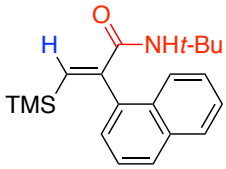

(*E*)-N-(*tert*-butyl)-2-(naphthalen-1-yl)-3-(trimethylsilyl)acrylamide (4-59). Following the general procedure using **4-28** to afford **4-59** (140.3 mg, 86% yield) as a colorless solid. M.P. = 137-138 ºC. ^{1}H NMR (400 MHz, $CDCl_3$) δ 7.88-7.82 (m, 2H), 7.79-7.75 (m, 1H), 7.51-7.42 (m, 4H), 7.32 (dd, J = 7.0, 1.2 Hz, 1H), 5.21 (s, 1H), 1.14 (s, 9H), -0.35 (s, 9H). ^{13}C NMR (75 MHz, $CDCl_3$) δ 165.1, 148.8, 141.7, 135.8, 133.4, 132.2, 128.8, 128.2, 127.6, 126.5, 126.3, 125.6, 125.1, 51.1, 28.3, -1.2. IR (neat, cm^{-1}): 3299, 2962, 1636, 1525, 1449, 1285, 1246, 1225, 839, 774. HRMS *calcd.* for ($C_{20}H_{27}NOSi$+H): 326.1935, *found:* 326.1937.

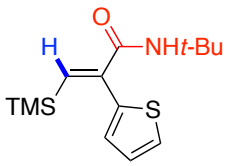

(*Z*)-N-(*tert*-butyl)-2-(thiophen-2-yl)-3-(trimethylsilyl)acrylamide (4-60). Following the general procedure using **4-29** to afford **4-60** (77.1 mg, 55% yield) as a colorless

solid. M.P. = 101-102 ºC. ^{1}H NMR (400 MHz, $CDCl_3$) δ 7.38 (dd, *J* = 5.1, 1.2 Hz, 1H), 7.28 (s, 1H), 7.05 (dd, *J* = 5.1, 3.5 Hz, 1H), 6.95 (dd, *J* = 3.5, 1.2 Hz, 1H), 5.70 (s, 1H), 1.32 (s, 9H), -0.06 (s, 9H). ^{13}C NMR (101 MHz, $CDCl_3$) δ 165.0, 143.8, 143.0, 138.9, 128.5, 127.0, 126.8, 51.4, 28.5, -0.9. IR (neat, cm^{-1}): 3315, 2961, 1638, 1534, 1454, 1287, 1220, 830, 695. HRMS *calcd.* for ($C_{19}H_{19}F_2NO$+Na): 338.1327, *found:* 338.1318.

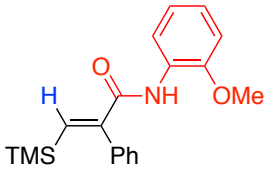

(*E*)-N-(2-methoxyphenyl)-2-phenyl-3-(trimethylsilyl)acrylamide (4-61). Following the general procedure using **4-30** to afford **4-61** (106.3 mg, 65% yield) as colorless oil. ^{1}H NMR (400 MHz, $CDCl_3$) δ 8.46 (dd, *J* = 7.7, 2.0 Hz, 1H), 8.00 (s, 1H), 7.49-7.38 (m, 3H), 7.36 (s, 1H), 7.34-7.28 (m, 2H), 7.01-6.91 (m, 2H), 6.75 (dd, *J* = 7.8, 1.7 Hz, 1H), 3.58 (s, 3H), -0.11 (s, 9H) ppm. ^{13}C NMR (101 MHz, $CDCl_3$) δ 163.8, 150.2, 148.3, 141.7, 138.2, 129.9, 128.6, 128.5, 128.0, 123.9, 121.3, 119.5, 110.1, 55.8, -0.6 ppm. IR (neat, cm^{-1}) 3391, 2954, 1673, 1520, 1459, 1247, 833, 745, 703. HRMS *calcd.* for ($C_{19}H_{24}NO_2Si$+H): 326.1571, *found:* 326.1569.

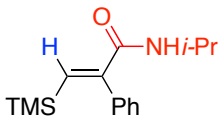

(*E*)-N-isopropyl-2-phenyl-3-(trimethylsilyl)acrylamide (4-62). Following the general procedure using **4-31** to afford **4-62** (78.4 mg, 60% yield) as a colorless solid. M.P. = 105 – 107 ºC. ^{1}H NMR (500 MHz, $CDCl_3$) δ 7.58-7.34 (m, 3H), 7.26-7.05 (m, 3H), 5.26 (s, 1H), 4.14-4.07 (m, 6.6 Hz, 1H), 1.07 (d, *J* = 6.6 Hz, 6H), -0.15 (s, 9H) ppm. ^{13}C NMR (126 MHz, $CDCl_3$) δ 165.4, 149.7, 140.7, 138.6, 129.7, 128.6, 128.4, 42.1, 22.7, -0.6 ppm. IR (neat, cm^{-1}) 3274, 2974, 1626, 1581, 1543, 1244, 835, 694. HRMS *calcd.* for ($C_{15}H_{23}NOSi$+H): 262.1622, *found:* 262.1616.

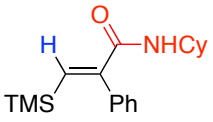

(*E*)-N-cyclohexyl-2-phenyl-3-(trimethylsilyl)acrylamide (4-63). Following the general procedure using **4-32** to afford **4-63** (91.6 mg, 61% yield) as a colorless solid. M.P. = 108-109 ºC. ^{1}H NMR (500 MHz, $CDCl_3$) δ 7.42-7.33 (m, 3H), 7.23-7.16 (m, 3H), 5.30 (s, 1H), 3.79 (td, *J* = 10.3, 8.0 Hz, 1H), 1.89-1.67 (m, 2H), 1.61-1.47 (m, 3H),

1.39-1.27 (m, 2H), 1.16-0.88 (m, 3H), -0.18 (s, 9H) ppm. ^{13}C NMR (126 MHz, $CDCl_3$) δ 165.3, 149.8, 140.6, 138.6, 129.6, 128.6, 128.4, 48.7, 32.8, 25.6, 24.7, -0.6 ppm. IR (neat, cm^{-1}) 3268, 2933, 2854, 1627, 1533, 1242, 861, 836, 696. HRMS *calcd.* for ($C_{18}H_{27}NOSi$+H): 302.1935, *found:* 302.1942.

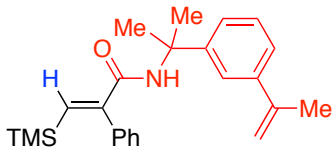

(E)-2-phenyl-N-(2-(3-(prop-1-en-2-yl)phenyl)propan-2-yl)-3-(trimethylsilyl) acrylamide (4-64). Following the general procedure using **4-33** to afford **4-64** (91.6 mg, 61% yield) as a colorless solid. M.P. = 86-87 ºC. ^{1}H NMR (500 MHz, $CDCl_3$) δ 7.48-7.33 (m, 4H), 7.33-7.23 (m, 4H), 7.23-7.13 (m, 2H), 5.82 (s, 1H), 5.31 (dd, *J* = 1.6, 0.8 Hz, 1H), 5.08 (t, *J* = 1.5 Hz, 1H), 2.13 (dd, *J* = 1.5, 0.8 Hz, 3H), 1.65 (s, 6H), -0.15 (s, 9H) ppm. ^{13}C NMR (126 MHz, $CDCl_3$) δ 165.0, 150.0, 146.6, 143.3, 141.2, 140.3, 138.5, 129.3, 128.5, 128.2, 128.1, 123.8, 123.5, 121.5, 112.3, 56.1, 28.7, 21.8, -0.9 ppm. IR (neat, cm^{-1}) 3279, 2954, 1639, 1525, 1244, 860, 832, 696. HRMS *calcd.* for ($C_{24}H_{31}NOSi$+Na): 400.2067, *found:* 400.2076.

(1) Isotope-labelling studies.

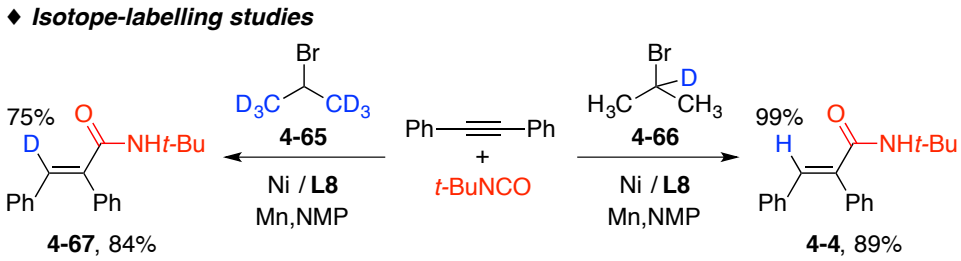

➔ **Reaction with 4-65**

Following the general procedure using **3-1** and **4-65** to afford **3-47** (84% yield, 75% D-content) as a colorless solid. D-content was determined by H NMR analysis.

➔ **Reaction with 4-66**

Following the general procedure using **3-1** and **4-66** to afford **4-4** (89% yield, 0% D-content) as a colorless solid.

(2) Stoichiometric experiments

♦ ***Stoichiometric studies***

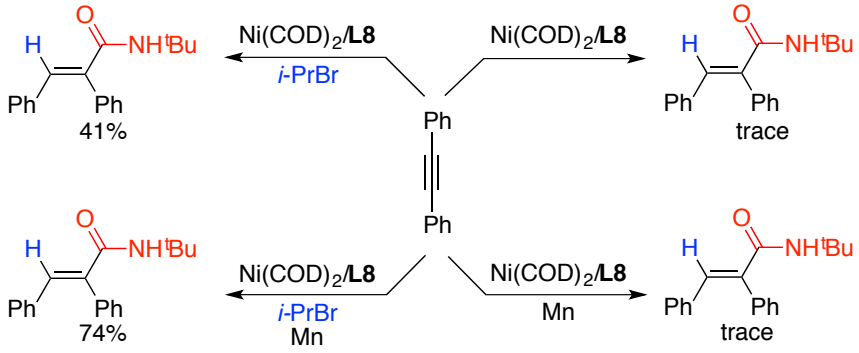

A Schlenk tube containing a stirring bar was charged with diphenylacetylene (44.6 mg, 0.25 mmol), bathocuproine (180 mg, 0.50 mmol) and $Ni(COD)_2$ (69 mg, 0.25 mmol) inside the glovebox. The tube was extracted from the glovebox and added *i*-PrBr (28.7 μL, 0.375 mmol), *t*-BuNCO (0.375, 42.8 μL) and NMP (1 mL) were added by syringe under an argon atmosphere. Once added, the Schlenk tube was sealed with parafilm and stirred overnight at room temperature. The mixture was quenched with HCl (5%) and extracted with DCM. The combined organic layers were washed with brine and dried over anhydrous $MgSO_4$ and concentrated under reduced pressure. The residue was purified by flash chromatography (hexanes/ethyl acetate = 10/1).

c) Following the above procedure, no Mn (20.6 mg, 0.375 mmol) was used, **4-4** was obtained in 41% isolated yield as a colorless solid (top, left one).

d) Following the above procedure, no Mn (20.6 mg, 0.375 mmol) was used, without *i*-PrBr, **4-4** was not generated (top, right one).

e) Following the above procedure, Mn (20.6 mg, 0.375 mmol) was used, **4-4** was obtained in 74% isolated yield as a colorless solid (bottom, left one).

f) Following the above procedure, Mn (20.6 mg, 0.375 mmol) was used, without *i*-PrBr, **4-4** was not generated (bottom, right one).

4.6.3 Selected Examples of NMR Spectra

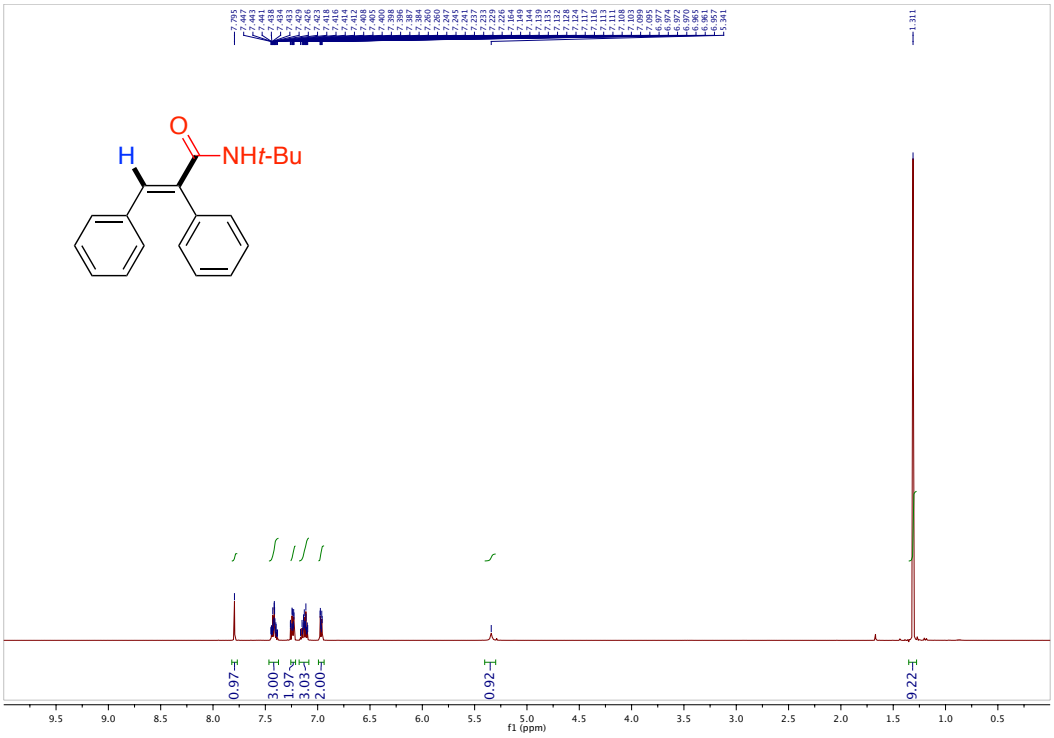

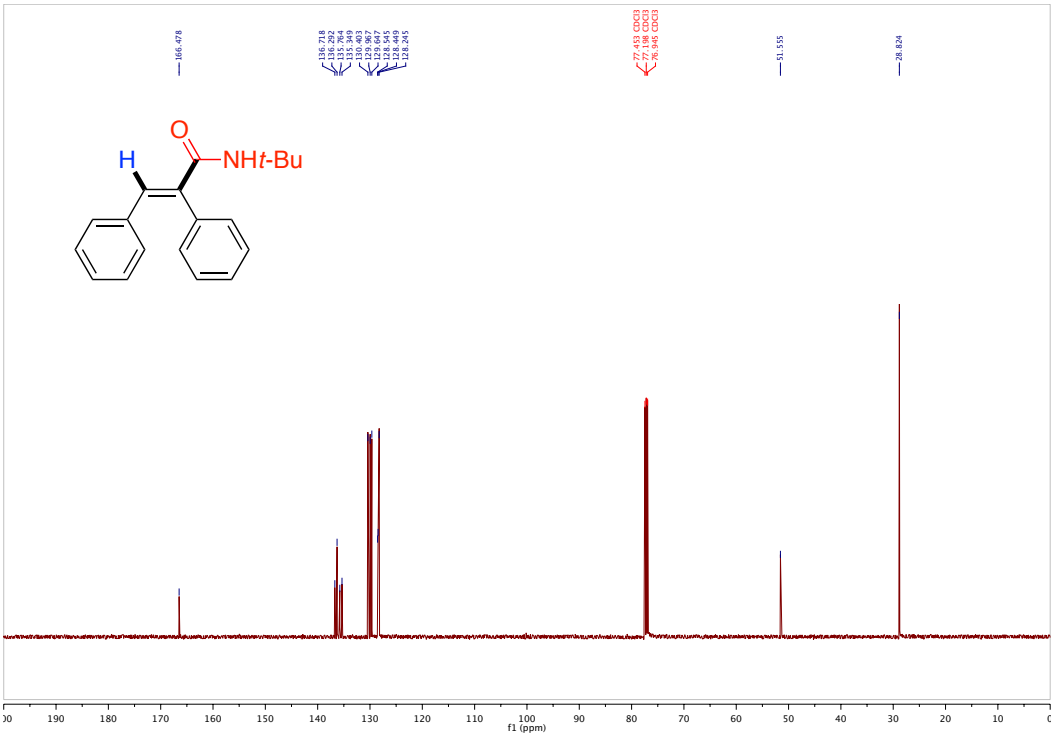

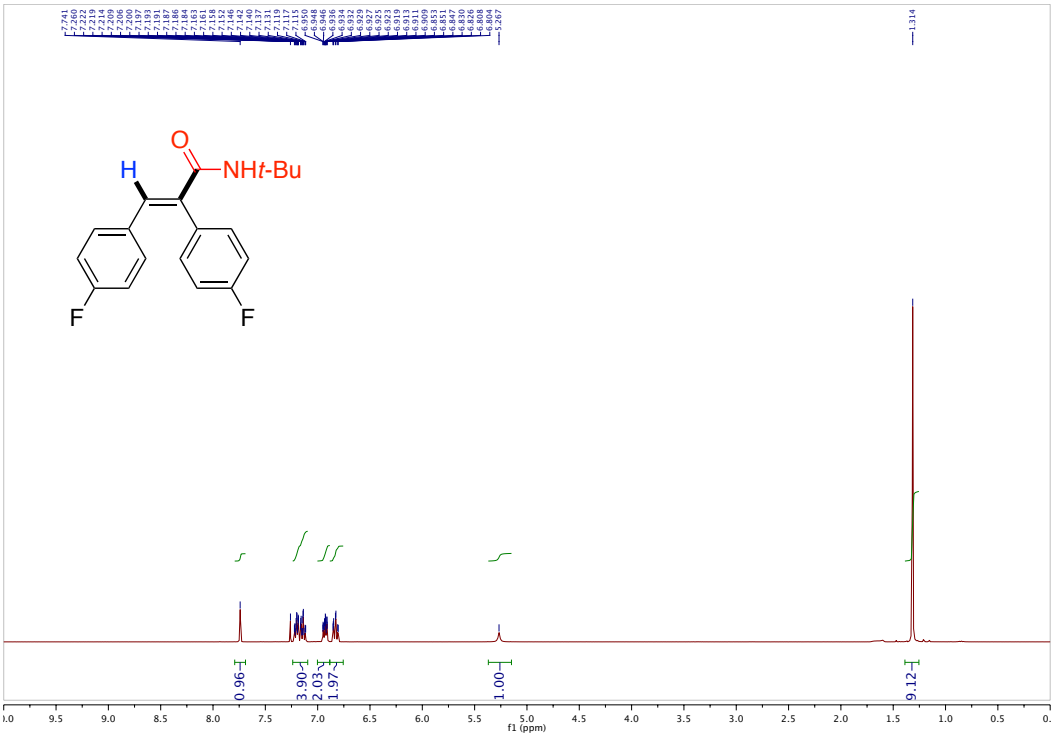
O
H
NHt-Bu
F
F
0.96
3.90
2.03
1.97
1.00
9.12
f1 (ppm)

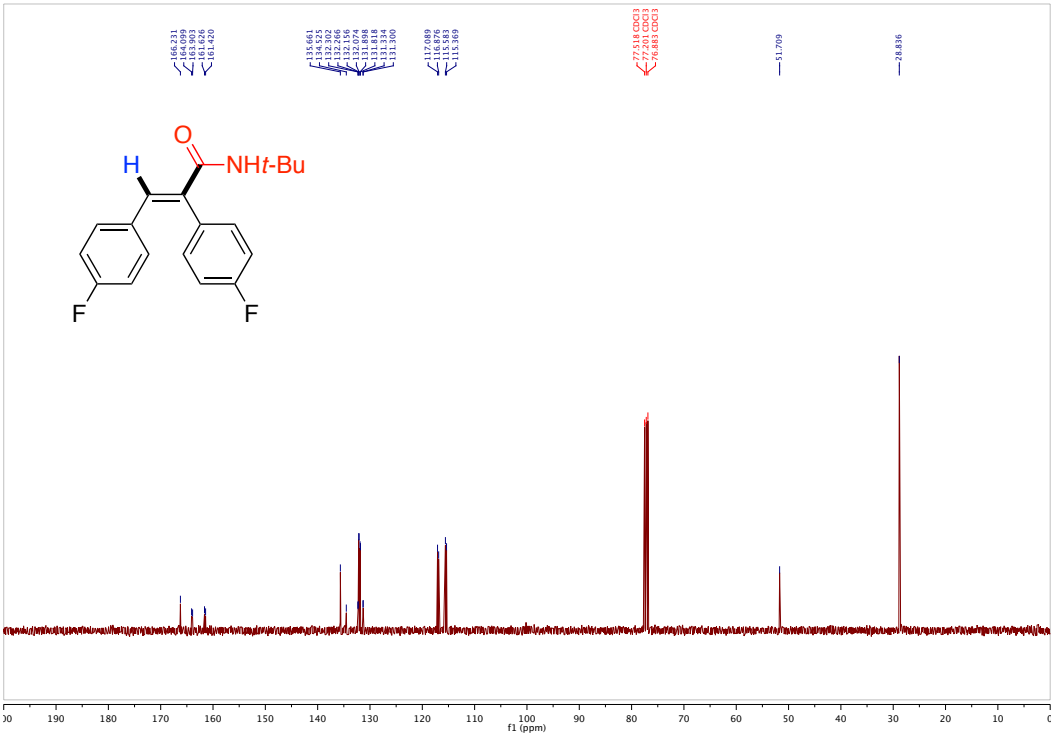
O
H
NHt-Bu
F
F
f1 (ppm)

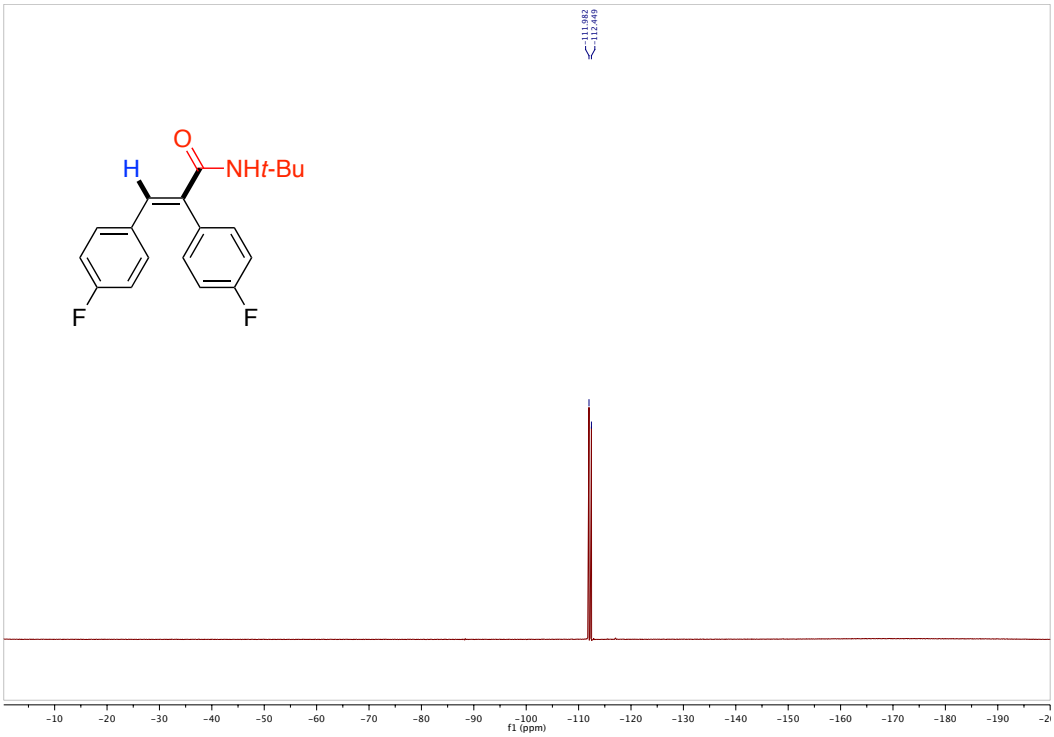
O
H
NHt-Bu
F
F
f1 (ppm)

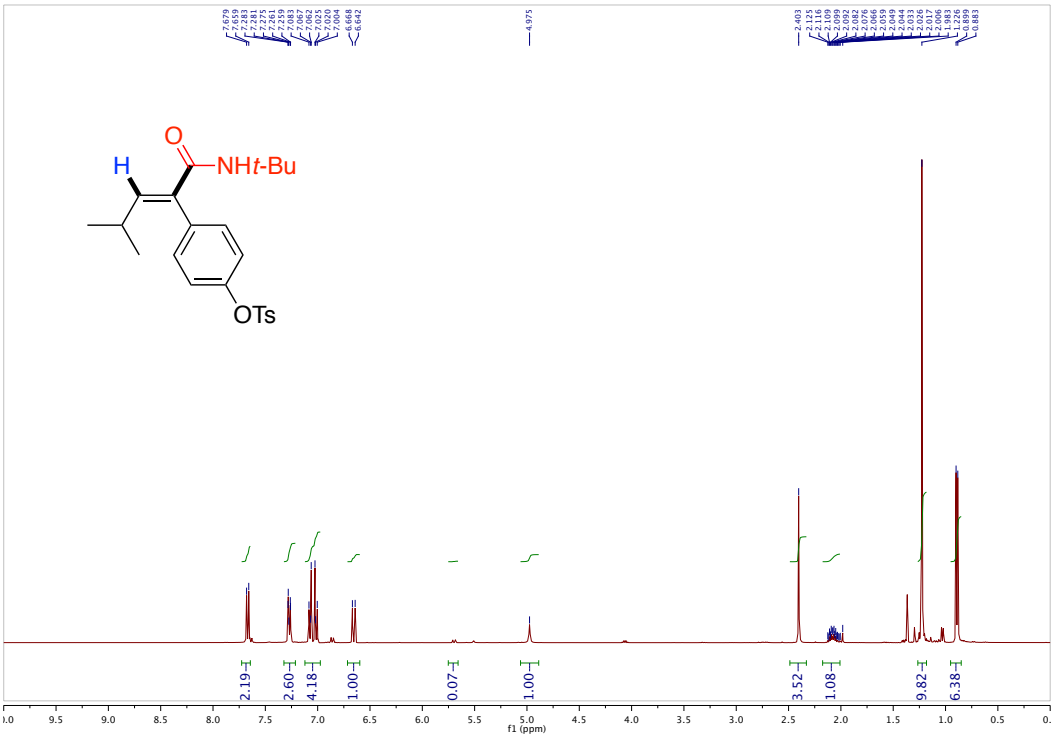
O
H
NHt-Bu
OTs
2.19
2.60
4.18
1.00
0.07
1.00
3.52
1.08
9.82
6.38
f1 (ppm)

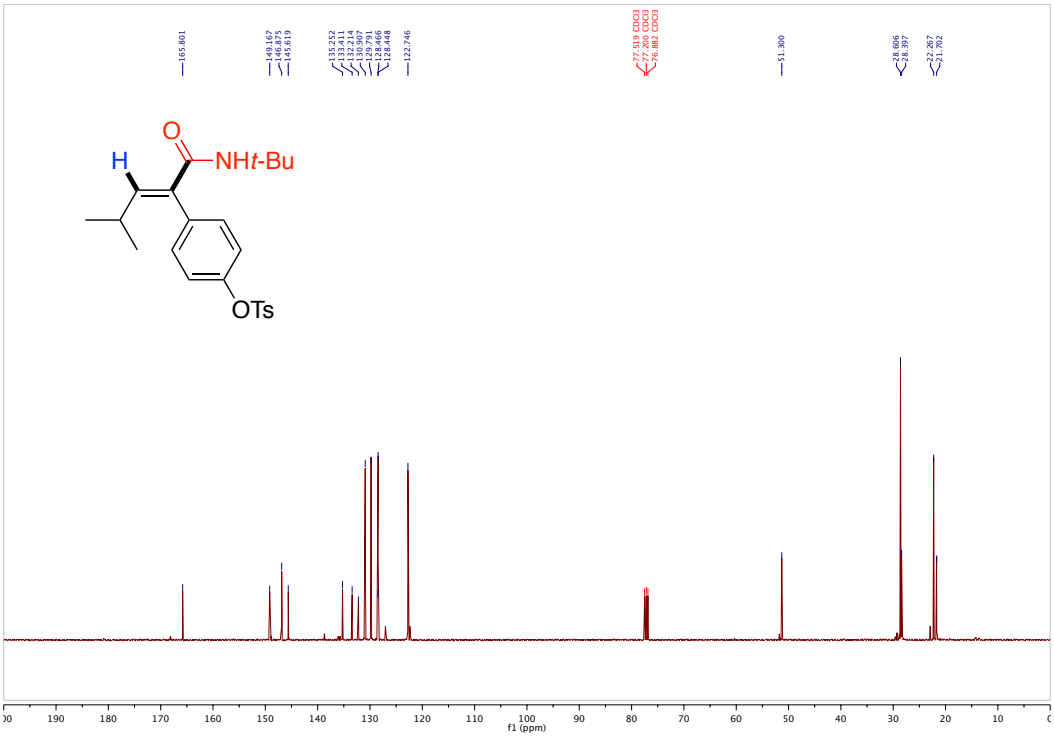
O
H
NHt-Bu
OTs
f1 (ppm)

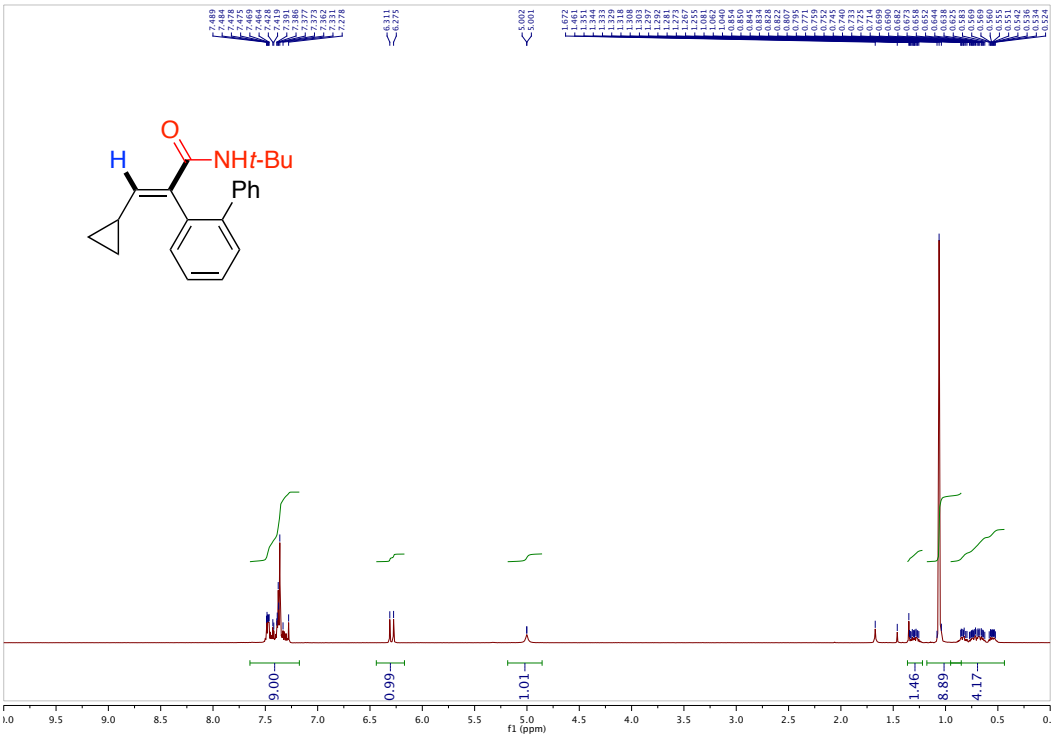
O
H
NHt-Bu
Ph
9.00
0.99
1.01
1.46
8.89
4.17
f1 (ppm)

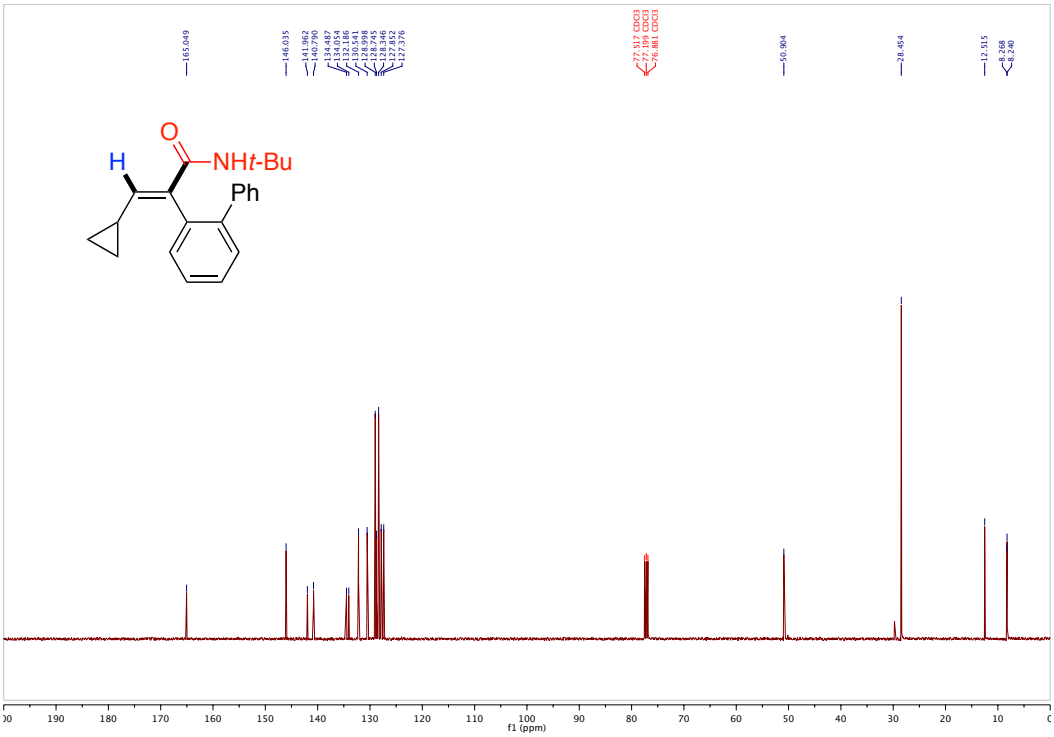
O
H
NHt-Bu
Ph
f1 (ppm)

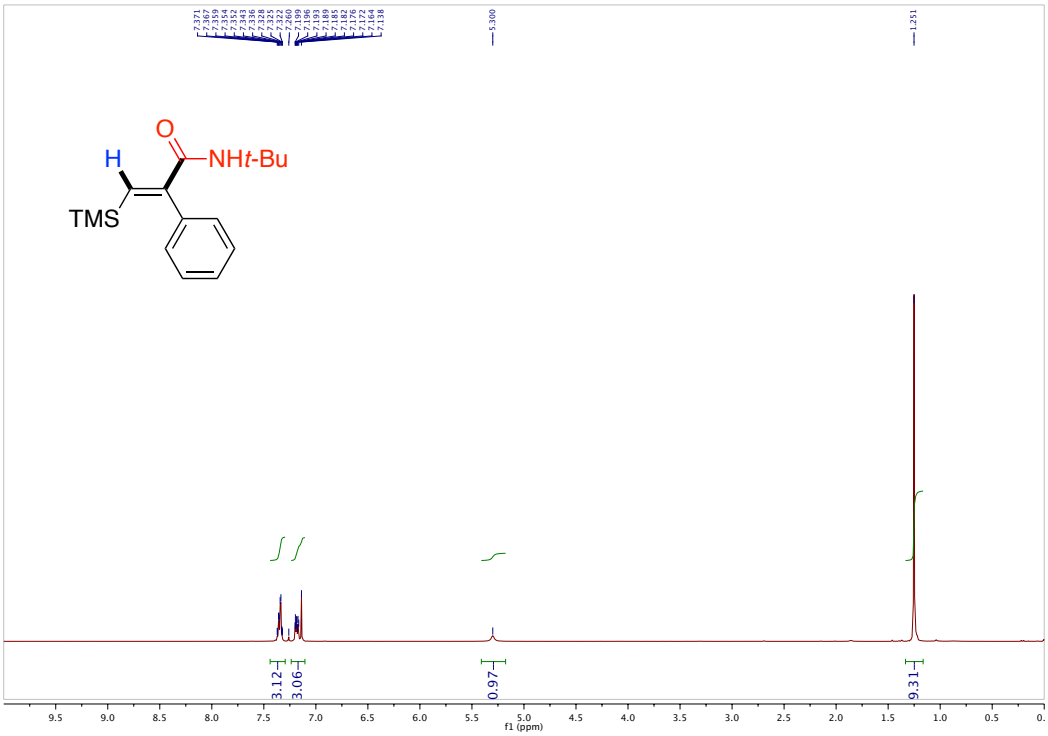
O
H
NHt-Bu
TMS
3.12
3.06
0.97
9.31
f1 (ppm)

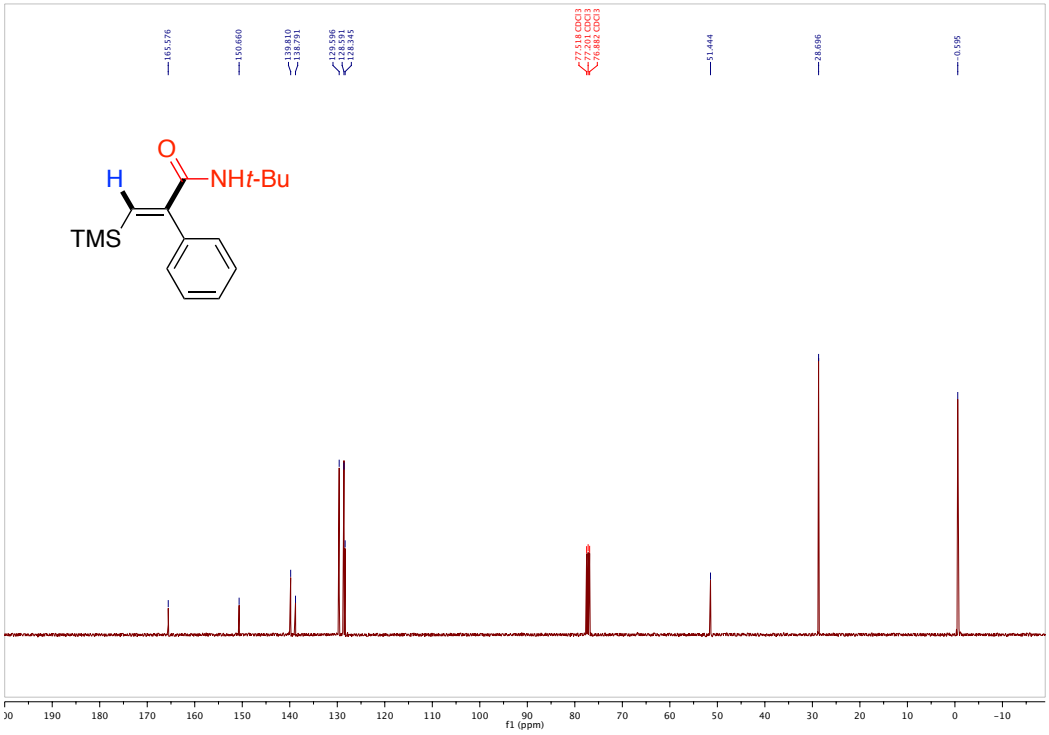
165.576
150.660
139.810
138.791
129.596
128.591
128.345
77.518 CDCl3
77.200 CDCl3
76.882 CDCl3
51.444
28.696
0.595
O
H
NHt-Bu
TMS
f1 (ppm)

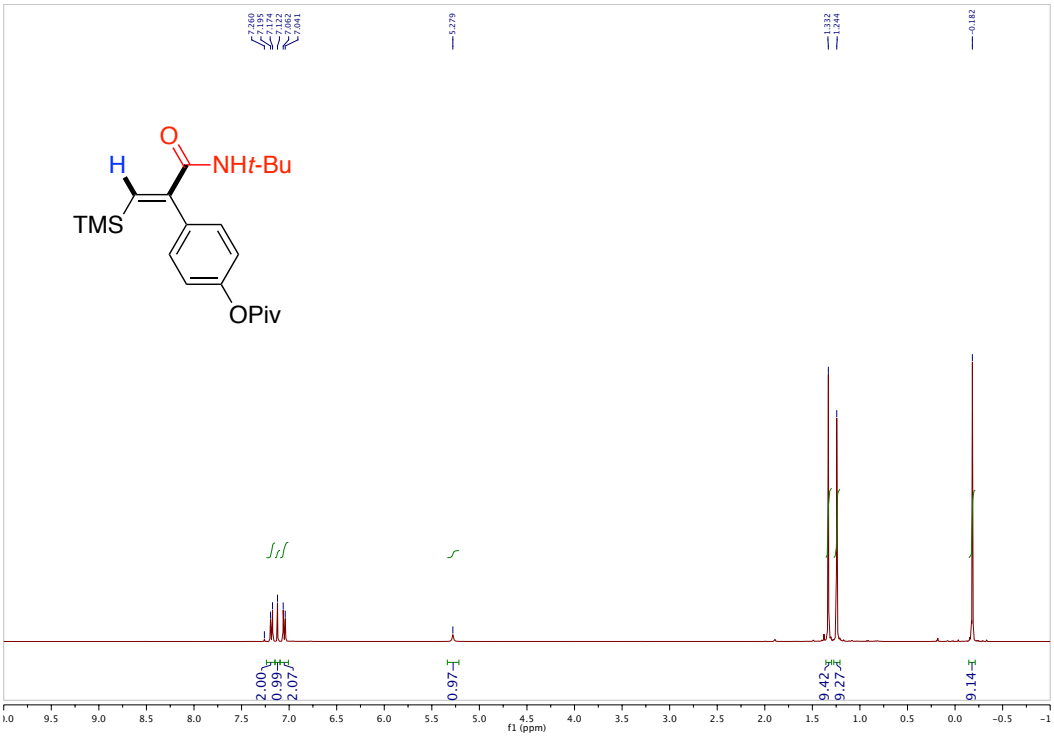
7.360
7.195
7.174
7.122
7.062
7.041
5.279
1.332
1.244
0.182
O
H
NHt-Bu
TMS
OPiv
2.00
0.99
2.07
0.97
9.42
9.27
9.14
f1 (ppm)

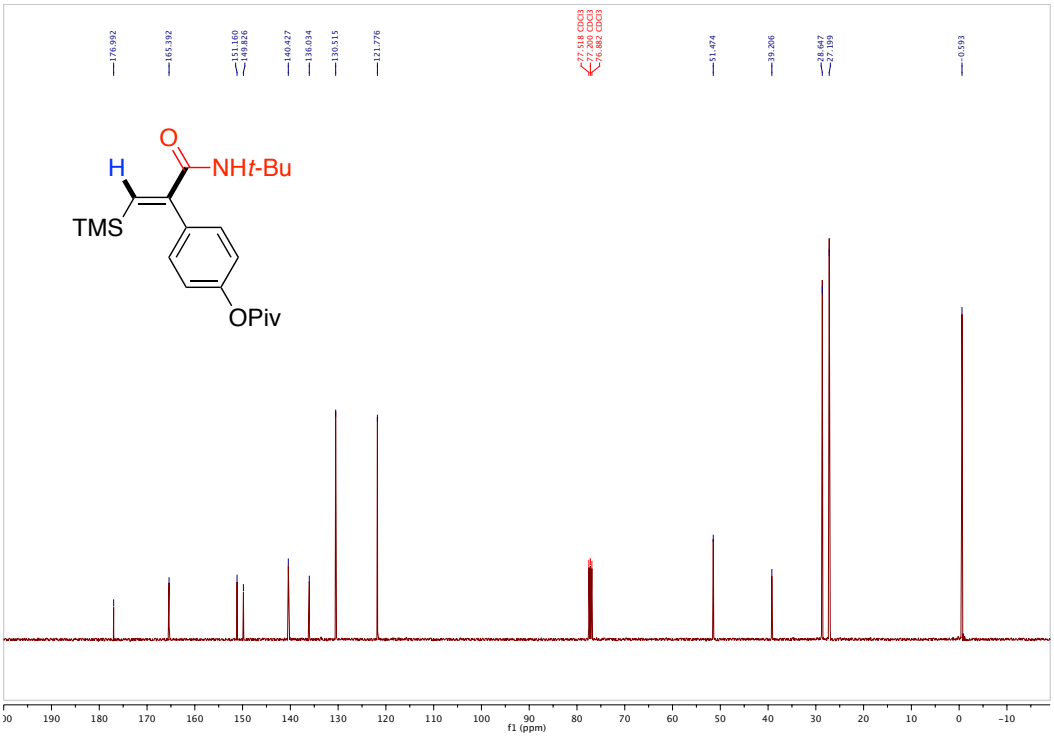

4.6.4 X-Ray Crystallographic Data for 4-4, 4-44 and 4-52

Crystal data for 4-4

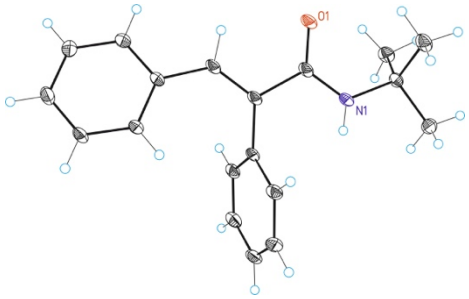

Table 1. Crystal data and structure refinement for **4-4**.

Identification code	**4-4**	
Empirical formula	C19 H21 N O	
Formula weight	279.37	
Temperature	100(2) K	
Wavelength	0.71073 Å	
Crystal system	Monoclinic	
Space group	Cc	
Unit cell dimensions	a = 5.827(3)Å	= 90°.
	b = 18.141(6)Å	= 98.777(9)°.

	c = 14.817(6)Å = 90°.
Volume	1547.9(11) Å^3
Z	4
Density (calculated)	1.199 Mg/m^3
Absorption coefficient	0.073 mm^{-1}
F(000)	600
Crystal size	0.25 x 0.20 x 0.10 mm^3
Theta range for data collection	2.245 to 32.118°.
Index ranges	-8<=h<=8,-26<=k<=26,-22<=l<=22
Reflections collected	10678
Independent reflections	4997[R(int) = 0.0647]
Completeness to theta =32.118°	99.7%
Absorption correction	Empirical
Max. and min. transmission	0.993 and 0.764
Refinement method	Full-matrix least-squares on F^2
Data / restraints / parameters	4997/ 2/ 193
Goodness-of-fit on F^2	1.027
Final R indices [I>2sigma(I)]	R1 = 0.0565, wR2 = 0.1429
R indices (all data)	R1 = 0.0596, wR2 = 0.1442
Flack parameter	x =-1.0(10)
Largest diff. peak and hole	0.632 and -0.300 e.Å^{-3}

Table 2. Bond lengths [Å] and angles [°] for **4-4**.

Bond lengths----	
C1-C2	1.347(3)
C1-C9	1.491(3)
C1-C15	1.521(3)
C2-C3	1.468(3)
C3-C8	1.403(3)

C3-C4	1.407(3)
C4-C5	1.396(3)
C5-C6	1.390(3)
C6-C7	1.396(3)
C7-C8	1.391(3)
C9-C14	1.399(3)
C9-C10	1.405(3)
C10-C11	1.398(3)
C11-C12	1.388(4)
C12-C13	1.395(4)
C13-C14	1.394(3)
C15-O1	1.236(3)
C15-N1	1.352(3)
C16-N1	1.483(3)
C16-C17	1.528(3)
C16-C18	1.535(3)
C16-C19	1.535(3)

Angles----------

C2-C1-C9	125.59(18)
C2-C1-C15	114.67(17)
C9-C1-C15	119.52(17)
C1-C2-C3	130.69(19)
C8-C3-C4	118.45(19)
C8-C3-C2	116.83(18)
C4-C3-C2	124.67(19)
C5-C4-C3	120.2(2)
C6-C5-C4	120.43(19)
C5-C6-C7	120.0(2)
C8-C7-C6	119.6(2)
C7-C8-C3	121.16(19)
C14-C9-C10	118.52(19)
C14-C9-C1	120.07(19)
C10-C9-C1	121.34(19)

C11-C10-C9	120.2(2)
C12-C11-C10	120.5(2)
C11-C12-C13	119.8(2)
C14-C13-C12	119.7(2)
C13-C14-C9	121.2(2)
O1-C15-N1	123.08(19)
O1-C15-C1	121.06(19)
N1-C15-C1	115.86(17)
N1-C16-C17	106.34(17)
N1-C16-C18	111.35(18)
C17-C16-C18	109.18(19)
N1-C16-C19	108.85(18)
C17-C16-C19	109.91(19)
C18-C16-C19	111.11(18)
C15-N1-C16	124.73(17)

Table 3. Torsion angles [°] for **4-4**.

C9-C1-C2-C3	5.9(4)
C15-C1-C2-C3	-179.6(2)
C1-C2-C3-C8	-154.6(2)
C1-C2-C3-C4	28.1(4)
C8-C3-C4-C5	1.1(3)
C2-C3-C4-C5	178.3(2)
C3-C4-C5-C6	1.4(4)
C4-C5-C6-C7	-2.1(4)
C5-C6-C7-C8	0.3(4)
C6-C7-C8-C3	2.2(4)
C4-C3-C8-C7	-2.9(3)
C2-C3-C8-C7	179.6(2)
C2-C1-C9-C14	68.1(3)
C15-C1-C9-C14	-106.0(2)
C2-C1-C9-C10	-115.0(2)

C15-C1-C9-C10	70.8(3)
C14-C9-C10-C11	0.1(3)
C1-C9-C10-C11	-176.87(19)
C9-C10-C11-C12	1.4(3)
C10-C11-C12-C13	-1.8(3)
C11-C12-C13-C14	0.8(3)
C12-C13-C14-C9	0.7(3)
C10-C9-C14-C13	-1.1(3)
C1-C9-C14-C13	175.84(19)
C2-C1-C15-O1	2.6(3)
C9-C1-C15-O1	177.4(2)
C2-C1-C15-N1	-176.62(19)
C9-C1-C15-N1	-1.8(3)
O1-C15-N1-C16	-9.2(4)
C1-C15-N1-C16	170.03(19)
C17-C16-N1-C15	176.8(2)
C18-C16-N1-C15	57.9(3)
C19-C16-N1-C15	-64.9(3)

Crystal data for 4-44

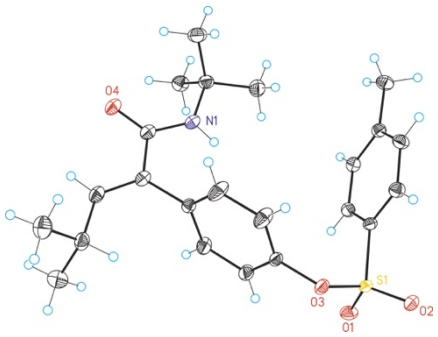

Table 1. Crystal data and structure refinement for **4-44**.

Identification code	XW-7-24DP21n
Empirical formula	C23 H29 N O4 S
Formula weight	415.53
Temperature	100(2) K

Wavelength	0.71073 Å
Crystal system	Monoclinic
Space group	P2(1)/n
Unit cell dimensions	a = 9.6344(10)Å = 90°. b = 9.5419(12)Å = 101.317(4)°. c = 24.422(3)Å = 90°.
Volume	2201.4(4) $Å^3$
Z	4
Density (calculated)	1.254 Mg/m^3
Absorption coefficient	0.175 mm^{-1}
F(000)	888
Crystal size	0.10 x 0.20 x 0.30 mm^3
Theta range for data collection	3.264 to 28.298°.
Index ranges	-12<=h<=8,-12<=k<=12,-32<=l<=24
Reflections collected	17729
Independent reflections	4807[R(int) = 0.0260]
Completeness to theta =28.298°	89.0%
Absorption correction	Multi-scan
Max. and min. transmission	0.966 and 0.743
Refinement method	Full-matrix least-squares on F^2
Data / restraints / parameters	4807/ 0/ 272
Goodness-of-fit on F^2	1.048
Final R indices [I>2sigma(I)]	R1 = 0.0327, wR2 = 0.0857
R indices (all data)	R1 = 0.0356, wR2 = 0.0871
Largest diff. peak and hole	0.364 and -0.402 $e.Å^{-3}$

Table 2. Bond lengths [Å] and angles [°] for **4-44**.

Bond lengths----	
C1-C6	1.3862(17)

C1-C2	1.3918(16)
C1-S1	1.7517(12)
C2-C3	1.3870(17)
C3-C4	1.3956(18)
C4-C5	1.3930(16)
C4-C7	1.5046(16)
C5-C6	1.3880(17)
C8-C13	1.3752(17)
C8-C9	1.3769(16)
C8-O3	1.4154(13)
C9-C10	1.3877(17)
C10-C11	1.3875(17)
C11-C12	1.3906(15)
C11-C14	1.4976(15)
C12-C13	1.3940(16)
C14-C15	1.3371(18)
C14-C19	1.5100(17)
C15-C16	1.4968(18)
C16-C18	1.5301(18)
C16-C17	1.5320(18)
C19-O4	1.2330(14)
C19-N1	1.3486(17)
C20-N1	1.4798(17)
C20-C23	1.5267(17)
C20-C21	1.5270(18)
C20-C22	1.5339(16)
O1-S1	1.4252(9)
O2-S1	1.4269(9)
O3-S1	1.6033(9)

Angles----------

C6-C1-C2	121.56(11)
C6-C1-S1	119.42(9)
C2-C1-S1	119.02(9)

C3-C2-C1	118.79(11)
C2-C3-C4	120.84(11)
C5-C4-C3	118.98(11)
C5-C4-C7	120.38(11)
C3-C4-C7	120.63(11)
C6-C5-C4	121.06(11)
C1-C6-C5	118.72(10)
C13-C8-C9	121.98(11)
C13-C8-O3	122.00(10)
C9-C8-O3	115.98(10)
C8-C9-C10	118.53(11)
C11-C10-C9	121.64(11)
C10-C11-C12	118.00(10)
C10-C11-C14	121.02(10)
C12-C11-C14	120.97(10)
C11-C12-C13	121.41(11)
C8-C13-C12	118.43(10)
C15-C14-C11	122.04(11)
C15-C14-C19	118.26(10)
C11-C14-C19	119.67(11)
C14-C15-C16	126.57(11)
C15-C16-C18	111.09(11)
C15-C16-C17	109.39(11)
C18-C16-C17	110.05(11)
O4-C19-N1	123.25(12)
O4-C19-C14	121.61(11)
N1-C19-C14	115.13(10)
N1-C20-C23	110.35(10)
N1-C20-C21	105.68(10)
C23-C20-C21	109.66(11)
N1-C20-C22	109.88(11)
C23-C20-C22	110.80(10)
C21-C20-C22	110.36(11)
C19-N1-C20	126.75(10)

C8-O3-S1	118.79(8)
O1-S1-O2	119.73(5)
O1-S1-O3	109.07(5)
O2-S1-O3	103.19(5)
O1-S1-C1	109.42(6)
O2-S1-C1	110.26(5)
O3-S1-C1	103.85(5)

Table 3. Torsion angles [°] for **4-44**.

C6-C1-C2-C3	-1.41(18)
S1-C1-C2-C3	178.60(9)
C1-C2-C3-C4	-0.66(18)
C2-C3-C4-C5	1.86(18)
C2-C3-C4-C7	-177.41(11)
C3-C4-C5-C6	-1.04(18)
C7-C4-C5-C6	178.24(11)
C2-C1-C6-C5	2.21(17)
S1-C1-C6-C5	-177.80(9)
C4-C5-C6-C1	-0.96(17)
C13-C8-C9-C10	-0.3(2)
O3-C8-C9-C10	-178.05(13)
C8-C9-C10-C11	0.2(2)
C9-C10-C11-C12	-0.2(2)
C9-C10-C11-C14	178.94(13)
C10-C11-C12-C13	0.4(2)
C14-C11-C12-C13	-178.81(12)
C9-C8-C13-C12	0.5(2)
O3-C8-C13-C12	178.03(11)
C11-C12-C13-C8	-0.5(2)
C10-C11-C14-C15	-99.37(16)
C12-C11-C14-C15	79.78(16)
C10-C11-C14-C19	78.96(16)

C12-C11-C14-C19	-101.89(14)
C11-C14-C15-C16	2.06(19)
C19-C14-C15-C16	-176.30(11)
C14-C15-C16-C18	-113.78(14)
C14-C15-C16-C17	124.54(13)
C15-C14-C19-O4	7.22(17)
C11-C14-C19-O4	-171.18(11)
C15-C14-C19-N1	-173.40(11)
C11-C14-C19-N1	8.20(15)
O4-C19-N1-C20	0.32(19)
C14-C19-N1-C20	-179.05(10)
C23-C20-N1-C19	-60.19(15)
C21-C20-N1-C19	-178.67(11)
C22-C20-N1-C19	62.27(15)
C13-C8-O3-S1	64.74(14)
C9-C8-O3-S1	-117.55(11)
C8-O3-S1-O1	-69.22(9)
C8-O3-S1-O2	162.46(8)
C8-O3-S1-C1	47.37(9)
C6-C1-S1-O1	14.35(11)
C2-C1-S1-O1	-165.66(9)
C6-C1-S1-O2	148.03(9)
C2-C1-S1-O2	-31.98(11)
C6-C1-S1-O3	-102.00(10)
C2-C1-S1-O3	77.99(10)

Crystal data for 4-52

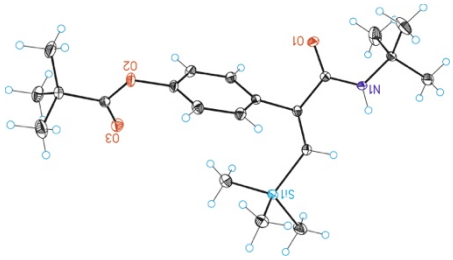

Table 1. Crystal data and structure refinement for **4-52.**

Identification code	**4-52**
Empirical formula	C21 H33 N O3 Si
Formula weight	375.57
Temperature	100(2) K
Wavelength	0.71073 Å
Crystal system	Monoclinic
Space group	P2(1)/c
Unit cell dimensions	a =
10.0373(8)Å	a= 90°.
	b =
20.8698(17)Å	b = 91.723(2)°.
	c =
10.3716(8)Å	g = 90°.
Volume	2171.6(3) Å3
Z	4
Density (calculated)	1.149 Mg/m3
Absorption coefficient	0.127 mm-1
F(000)	816
Crystal size	0.50 x 0.40 x 0.20 mm3
Theta range for data collection	2.194 to 27.471°.
Index ranges	-12<=h<=13,-27<=k<=27,-13<=l<=13
Reflections collected	40741
Independent reflections	4966[R(int) = 0.0260]
Completeness to theta =27.471°	99.8%
Absorption correction	Multi-scan
Max. and min. transmission	0.975 and 0.75
Refinement method	Full-matrix least-squares on F2
Data / restraints / parameters	4966/ 0/ 244
Goodness-of-fit on F2	1.064
Final R indices [I>2sigma(I)]	R1 = 0.0310, wR2 = 0.0844
R indices (all data)	R1 = 0.0341, wR2 = 0.0862
Largest diff. peak and hole	0.368 and -0.211 e.Å-3

Table 2. Bond lengths [Å] and angles [°] for **4-52.**.

Bond lengths----	
C1-C2	1.3436(13)
C1-Si1	1.8835(10)
C2-C8	1.4951(13)
C2-C3	1.5191(13)
C3-O1	1.2368(12)
C3-N1	1.3452(12)
C4-C7	1.5225(14)
C5-C7	1.5250(15)
C6-C7	1.5261(14)
C7-N1	1.4827(12)
C8-C13	1.3961(13)
C8-C9	1.3987(14)
C9-C10	1.3902(14)
C10-C11	1.3860(14)
C11-C12	1.3813(15)
C11-O2	1.4123(11)
C12-C13	1.3953(13)
C14-O3	1.1991(12)
C14-O2	1.3659(12)
C14-C15	1.5273(13)
C15-C16	1.5249(14)
C15-C17	1.5299(14)
C15-C18	1.5380(15)
C19-Si1	1.8735(11)
C20-Si1	1.8708(11)
C21-Si1	1.8691(11)
Angles----------	
C2-C1-Si1	129.13(7)
C1-C2-C8	120.35(8)
C1-C2-C3	123.94(8)

C8-C2-C3	115.64(8)
O1-C3-N1	122.59(9)
O1-C3-C2	119.60(8)
N1-C3-C2	117.81(8)
N1-C7-C4	110.56(8)
N1-C7-C5	110.24(8)
C4-C7-C5	110.93(10)
N1-C7-C6	106.90(8)
C4-C7-C6	109.23(9)
C5-C7-C6	108.89(9)
C13-C8-C9	118.68(9)
C13-C8-C2	119.59(8)
C9-C8-C2	121.55(9)
C10-C9-C8	120.74(9)
C11-C10-C9	119.01(9)
C12-C11-C10	121.75(9)
C12-C11-O2	118.13(9)
C10-C11-O2	120.08(9)
C11-C12-C13	118.65(9)
C12-C13-C8	121.04(9)
O3-C14-O2	122.65(9)
O3-C14-C15	125.01(9)
O2-C14-C15	112.28(8)
C16-C15-C14	112.65(8)
C16-C15-C17	109.91(9)
C14-C15-C17	108.38(8)
C16-C15-C18	110.30(9)
C14-C15-C18	106.16(8)
C17-C15-C18	109.33(9)
C3-N1-C7	124.50(8)
C14-O2-C11	116.21(7)
C21-Si1-C20	108.91(5)
C21-Si1-C19	109.14(6)
C20-Si1-C19	109.78(5)

C21-Si1-C1	104.26(5)
C20-Si1-C1	113.28(5)
C19-Si1-C1	111.26(5)

Table 3. Torsion angles [°] for **4-52.**

Si1-C1-C2-C8	11.72(14)
Si1-C1-C2-C3	-165.04(7)
C1-C2-C3-O1	173.66(9)
C8-C2-C3-O1	-3.24(12)
C1-C2-C3-N1	-5.34(14)
C8-C2-C3-N1	177.77(8)
C1-C2-C8-C13	60.06(13)
C3-C2-C8-C13	-122.93(9)
C1-C2-C8-C9	-115.03(11)
C3-C2-C8-C9	61.98(12)
C13-C8-C9-C10	-3.53(14)
C2-C8-C9-C10	171.60(9)
C8-C9-C10-C11	1.00(15)
C9-C10-C11-C12	2.00(15)
C9-C10-C11-O2	179.55(9)
C10-C11-C12-C13	-2.35(15)
O2-C11-C12-C13	-179.95(8)
C11-C12-C13-C8	-0.30(15)
C9-C8-C13-C12	3.18(14)
C2-C8-C13-C12	-172.05(9)
O3-C14-C15-C16	-159.09(10)
O2-C14-C15-C16	23.61(12)
O3-C14-C15-C17	-37.26(13)
O2-C14-C15-C17	145.45(9)
O3-C14-C15-C18	80.09(12)
O2-C14-C15-C18	-97.20(10)
O1-C3-N1-C7	-0.71(15)
C2-C3-N1-C7	178.25(8)

C4-C7-N1-C3	60.07(13)
C5-C7-N1-C3	-62.94(13)
C6-C7-N1-C3	178.85(9)
O3-C14-O2-C11	2.85(14)
C15-C14-O2-C11	-179.78(8)
C12-C11-O2-C14	-110.75(10)
C10-C11-O2-C14	71.61(12)
C2-C1-Si1-C21	155.35(10)
C2-C1-Si1-C20	-86.40(10)
C2-C1-Si1-C19	37.85(11)

Chapter 5: Mild ArI-catalyzed C(sp^2)-H or C(sp^3)-H Functionalization/C-O Formation: An Intriguing Catalyst-controlled Selectivity Switch

5.1 Objectives

❖To develop a mild and operationally simple I(III)-catalyzed *site*-selective C(sp^2)-H or C(sp^3)-H bond functionalization/C-O bond formation protocol in order to access pharmaceutically interesting benzopyranones.

❖To gain the mechanistic information about the cascade rearrangement/C-O bond formation event by studying the effect of different I(III) reagents and concentration effects.

5.2 General Introduction

Chatt and Davidson published the first example of a C-H activation reaction from a modern organometallic perspective in 1965.[128] This protocol involved the insertion of a Ru-atom into the C-H bond of naphthalene. In the last few decades, the field of carbon hydrogen (C-H) bond functionalization, especially the transition metal catalyzed C-H functionalization, has achieved tremendous progress, and greatly improved our ever-growing chemical knowledge, thus opening up the potential to develop novel chemical technologies that would benefit our synthetic chemistry in practical ways.

In general, C-H bond functionalization has two fundamental challenges: The first one is the inert nature of most C-H bonds. The second challenge is achieving selective functionalization of C-H bond(s) in molecules that contain diverse C-H bonds. The recent research carried out by many groups has demonstrated that transition metals including Pd, Rh, Ru, Co, Ir, Cu and others can react with C-H bonds to afford C-M species. They can rapidly be converted to C-X (X = halogens, S, O, N…) bonds due to the high reactivity of the resulting C-M bonds. While several strategies have been developed to address the selectivity issue, the most common one involves the utilization of substrates possessing a directing group that can bind to the catalyst, and thus selectively functionalize the C-H bond. However, these methods are still suffering from harsh reaction condition. Additionally, the toxicity and high cost of some of the transition metal salts greatly restrict the applications on a larger scale process. As global demand and prices for chemicals and noble metals continue to rise, chemists are being challenged to devise new reactivity under metal-free conditions. To such end, the use of well-defined I(III) reagents has recently gained considerable momentum.[129]

In 1969，Musher established the term of “hypervalent” for the molecules with elements of groups 15-18 containing more than 8 electrons in their valence shell.[130] Iodine is most commonly found in monovalent compounds with -1 as oxidation state.

---

[128] Chatt, J.; Davidson, J. M. *J. Chem. Soc.* **1965**, 843.

[129] For a selection of reviews dealing with the use of hypervalent iodine (III) reagents: (a) Samanta, R.; Matcha, K.; Antonchick, A. P. *Eur. J. Org. Chem.* **2013**, 5769. (b) Yusubov, M. S.; Maskaev, A. V.; Zhdankin, V. V. *ARKIVOC* **2011**, *1*, 370. (c) Uyanik, M.; Ishihara, K. *Chem. Commun.* **2009**, 2086. (d) Zhdankin, V. V.; Stang, P. J. *Chem. Rev.* **2008**, *108*, 5299. (e) Ochiai, M. *Chem. Rec.* **2007**, *7*, 12. (f) In *Topics in Current Chemistry*; Wirth, T., Ed.; Springer: Berlin, 2003; Vol. 224. (g) Wirth, T. *Angew. Chem. Int. Ed.* **2005**, *44*, 3656. (h) Tohma, H.; Kita, Y. *Adv. Synth. Catal*. **2004**, *346*, 111.

[130] Musher, J. I. *Angew. Chem. Int. Ed.* **1969**, *8*, 54.

It also forms stable polycoordinate, hypervalent compounds, since it is the largest, most polarizable, and most electropositive element in-group 17. In 1886, the first hypervalent organic iodine compound ($PhICl_2$) was prepared by Willgerodt.[131] Although its oxidizing properties were known since late 19th century, the chemistry of hypervalent iodine compound has only experienced a rapid development in the past several decades. This growing interest in iodine chemistry is mainly due to its particular properties: (1) Reactivity is similar to the heavy metal reagents such as Hg(III), Tl(III), Pb(IV) but associated with lower toxicity and environmental issues; (2) Mild reaction conditions and easy handling of hypervalent iodine compounds; (3) Commercial availability of key precursors such as $PhI(OAc)_2$.

Differing from the Martin-Arduengo definition, the IUPAC designates most common hypervalent aryl iodide compounds (III or V) as aryl-λ^3-iodane [$ArIL_2$ (L = heteroatom)] and aryl-λ^5-iodane ($ArIL_4$), respectively. As shown in Figure 4.1 (left), while the two ligands of $ArIL_2$ are located in the apical position, the aryl group and two pairs of electron are accommodated in the equatorial positions. The aryl substituent is bound to iodine by a two electron covalent bond with 5 sp^2 hybridization, bonding in $ArIL_2$ uses the nonhybridized 5p orbital of iodine in the linear L-I-L bond. Such a linear three-center four-electron (3c-4e) bond is highly polarized and is longer and weaker compared to a regular covalent bond. This is termed "hypervalent" and the presence of this bond in λ^3-iodanes is responsible for their high electrophilic reactivity. Onium salts refer to a tetrahedral geometry with an octet in the valence shell of a positively charged atom and are not hypervalent compounds.[140]

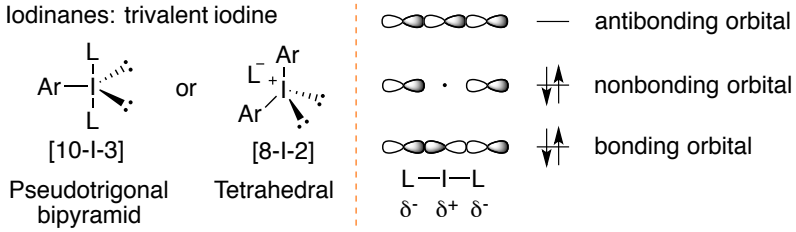

Figure 5.1. Trivalent iodine.

Although most of hypervalent compounds were originally prepared for replacing toxic heavy-metal oxidants such as Pb(IV), TI(III) or Hg(II) species. In recent years,

[131] Willgerodt, C. *J. Prakt. Chem.* **1886**, *33*, 154.

they have been used in wide range of synthetic protocols such as α-functionalization of carbonyl compounds, oxidative rearrangements, heterocycle synthesis, C-H functionalization as well as cyclization.[140] Representative hypervalent iodine(III) compounds are summarized in Figure 5.2.

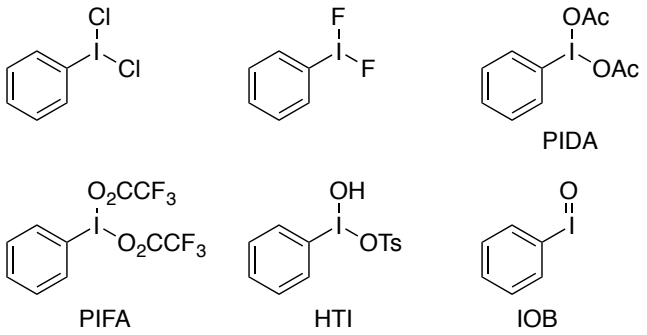

Figure 5.2. Representative aryl iodine(III) reagents.

In general, typical mechanisms in hypervalent iodine chemistry involve two steps as shown in Figure 5.3:[140] (1) Ligand exchange, the strong electrophilicity of the iodine making it susceptible to nucleophilic attack, which can theoretically proceed through either an associative or dissociative pathway. (2) Reductive elimination. The favorable reduction of the hypervalent iodine to normal valence by reductive elimination of iodobenzene is the key for its reactivity.

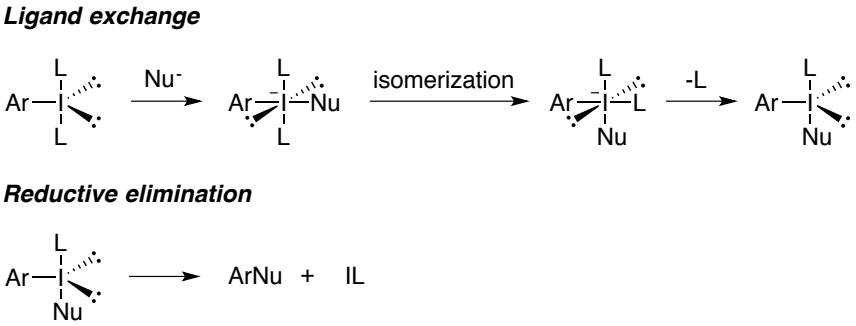

Figure 5.3. General mechanisms in hypervalent iodine chemistry.

5.2.1 Iodine(III) Reagent Mediated C-H Functionalization

In recent years, iodine(III) reagents have been widely used in C-H functionalization protocols, since they are less toxic, relatively stable and readily available. In 1994, Abramovitch published a $C_6F_5I(O_2CCF_3)_2$ promoted oxidative C–O bond-forming event for the synthesis of cularine alkaloids (Figure 5.4).[132] The authors believed that

[132] de Sousa, J. D. F.; Rodrigues, J. A. R.; Abramovitch, R. A. *J. Am. Chem. Soc.* **1994**, *116*, 9745.

the reaction proceeded *via* an aryloxenium ion that could be immediately trapped by an electron-rich arene. The final product was obtained in high yield (87%) through fast aromatization.

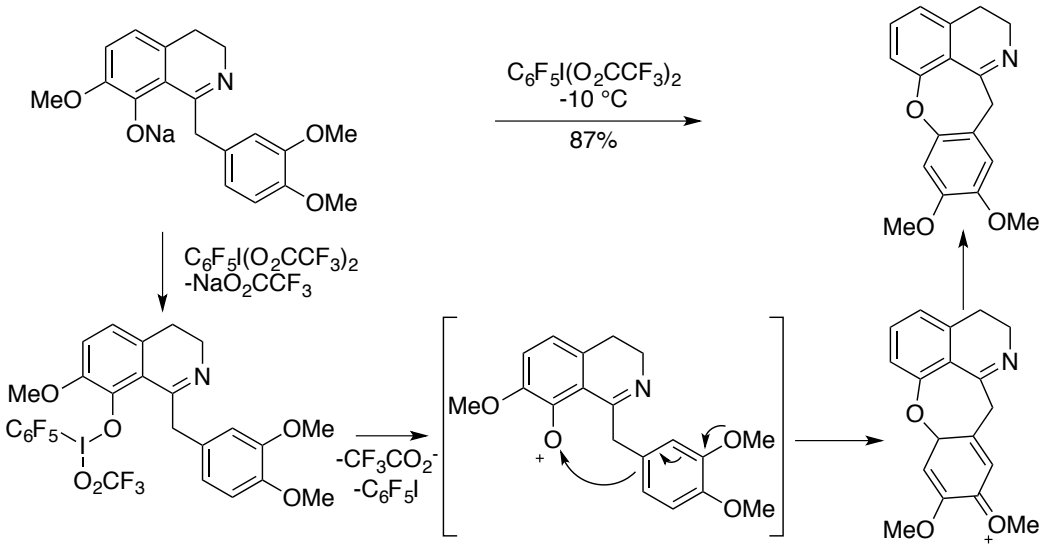

Scheme 5.1. $C_6F_5I(O_2CCF_3)_2$ mediated C-O bond formation.

In 1996, Yokoyama [and] coworkers reported a PIDA mediated intramolecular C-O bond formation reaction of alcohols for the synthesis of chromane derivatives. In their approach, a W-lamp was crucial for the reactions to occur.[133] The research group proposed a mechanism involves radical species, as shown in Figure 5.5.[134] Initial ligand exchange between (Diacetoxyiodo)benzene (PIDA) and alcohol, followed by reaction with iodine gives hypoiodite specie. Subsequent, light-mediated cleavage of the weak I–O bond affords an alkoxy radical, which then reacts with a phenyl ring, followed by an oxidative aromatization to generate the cyclized product. In their approach, however, aldehydes were obtained in some cases when a more reactive reagent such as PIFA was employed.

[133] Muraki, T.; Togo, H.; Yokoyama, M. *Tetrahedron Lett.* **1996**, *37*, 2441.
[134] Togo, H.; Muraki, T.; Hoshina, Y.; Yamaguchi, K.; Yokoyama, M. *J. Chem. Soc. Perkin Trans. 1* **1997**, 787.

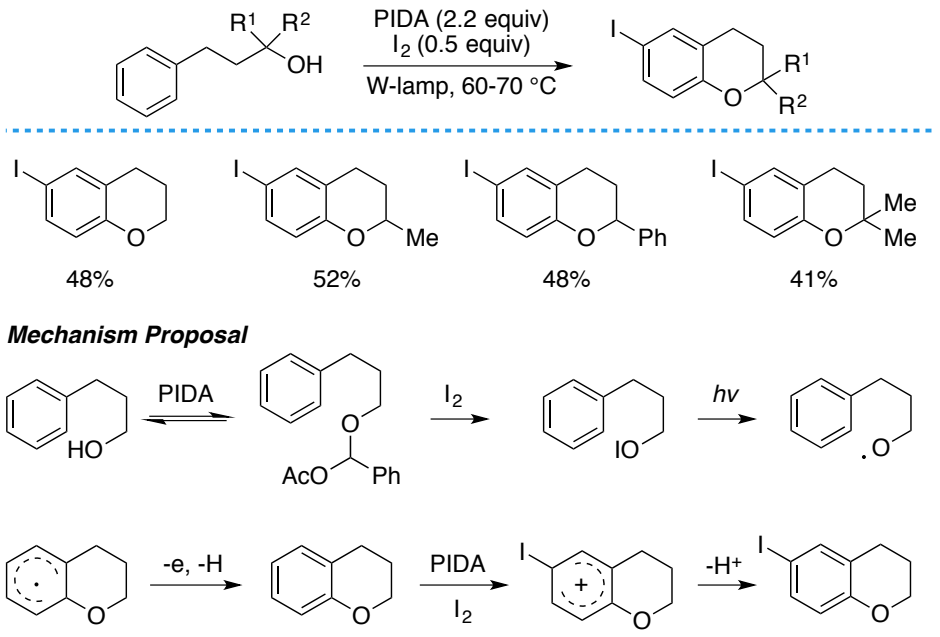

Scheme 5.2. PIDA mediated C-O bond formation.

Later, Kita's group developed a similar protocol en route to chromanes in the presence of a stoichiometric oxidant.[135] The desired products were isolated in moderate yields, and only a six-membered ring was achievable. The authors believed that this reaction proceeds through a different pathway from the above. Nucleophilic attack of a hydroxy group on the aromatic cation radical in the presence of PIFA and a solid acid additive could be operative.

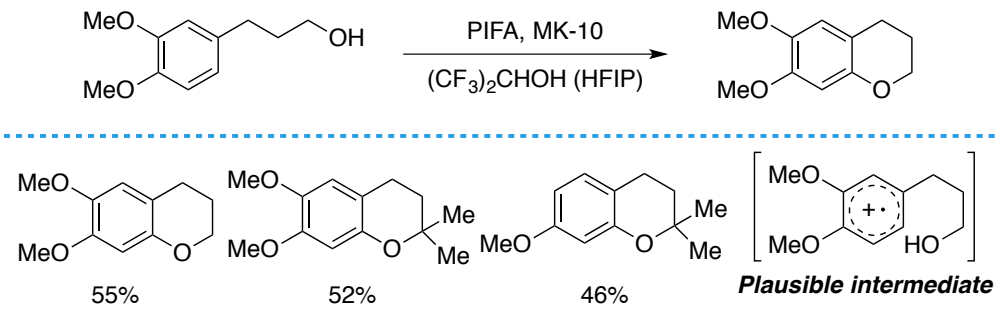

Scheme 5.3. PIFA mediated C-O bond formation.

The Yu group developed a metal-free intramolecular oxidative C–O bond formation event of electron-rich N-phenylbenzamides to synthesize benzoxazoles.[136] A wide range of desired products was obtained in the presence of stoichiometric amounts of

[135] Hamamoto, H.; Hata, K.; Nambu, H.; Shiozaki, Y.; Tohma, H.; Kita, Y. *Tetrahedron Lett.* **2004**, *45*, 2293.
[136] Yu, Z.; Ma, L.; Yu, W. *Synlett* **2012**, *23*, 1534.

PIFA. The authors proposed that TMSOTf serves as Lewis acid to activate the iodine(III) reagent. The researchers suggested two possible mechanisms. The first one involves the intermediacy of a nitrenium ion. On the other hand, the formation of a radical cation, and subsequent attack of the carbonyl oxygen was proposed in the as a second plausible mechanism.

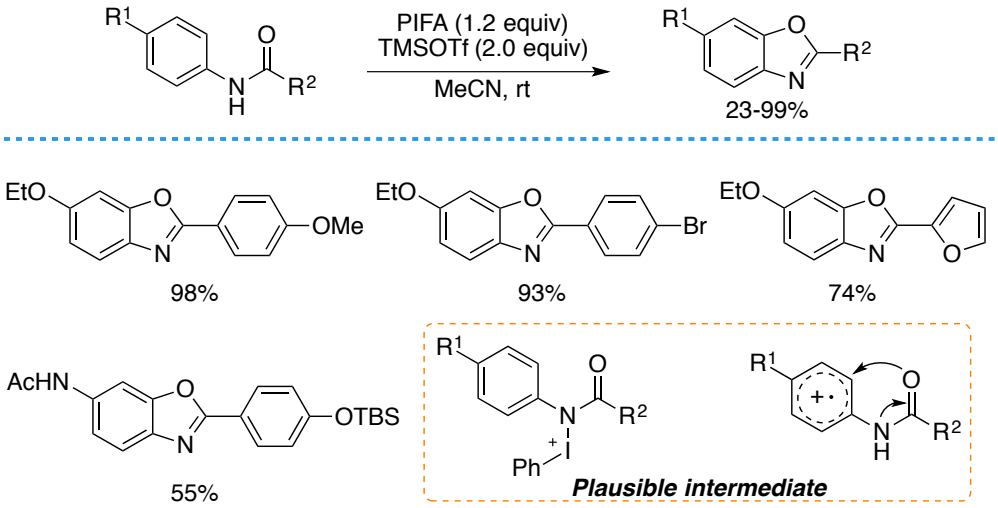

Scheme 5.4. PIFA mediated C-O bond formation.

In the same year, the Zhao group reported a PIDA promoted metal-free cyclization protocol to construct functionalized oxazoles. A wide range of desired products was synthesized in moderate to good yields from easily available enamides. Notably, oxaprozin and its derivatives were prepared with this reported method.[137]

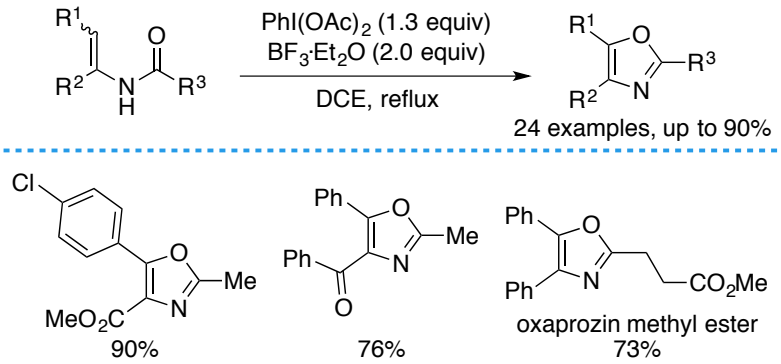

Scheme 5.5. PIDA mediated C-O bond formation.

Apart from the C(sp^2)-O bond formation, hypervalent iodine(III) reagents were used in the protocols of C(sp^3)-O bond formation. In 1997, the Yokoyama group described

[137] Zheng, Y.; Li, X.; Ren, C.; Zhang, D.; Du, Y.; Zhao, K. *J. Org. Chem.* **2012**, *77*, 10353.

the synthesis of lactones and iodinated lactones by using the combination of iodine and different hypervalent iodine reagents.[138] The authors proposed a similar oxygen-centered radical intermediate as shown in Figure 5.5. The abstraction of a hydrogen atom was then suggested to generate a carbon-centered radical, followed by an iodination to provide benzyl iodide. A final ring-closing process would then deliver the desired lactone moieties.

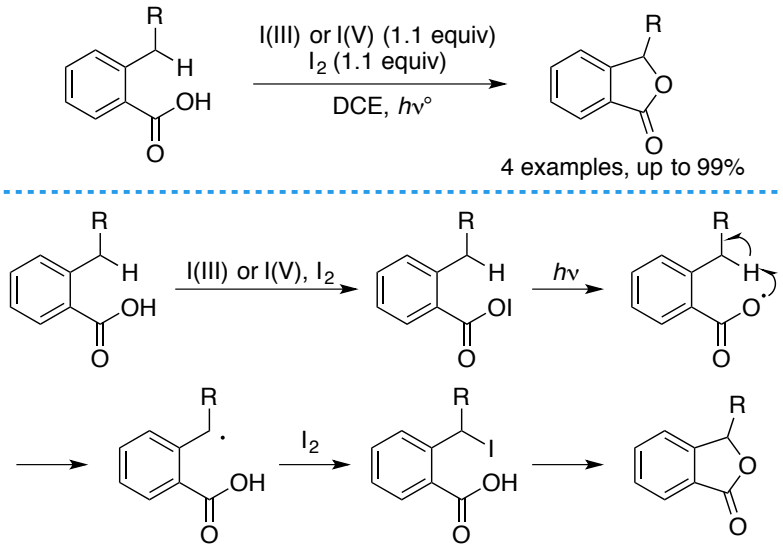

Scheme 5.6. Iodine(III) or iodine(V) mediated C(sp^3)-O bond formation.

Hypervalent iodine reagents have been utilized in intermolecular C-H functionalization/C-O bond formation approaches. In 2002， Kikugaw's group developed a hydroxylation of substituted anilides in the presence of stoichiometric amounts of PIFA.[139] The hydroxylation preferentially occurred in the *para*-position of electron-rich anilides, and various substituted products were prepared in moderate to good yields.

[138] Muraki, T.; Togo, H.; Yokoyama, M. *J. Chem. Soc. Perkin Trans. 1* **1999**, 1713.
[139] Itoh, N.; Sakamoto, T.; Miyazawa, E.; Kikugawa, Y. *J. Org. Chem.* **2002**, *67*, 7424.

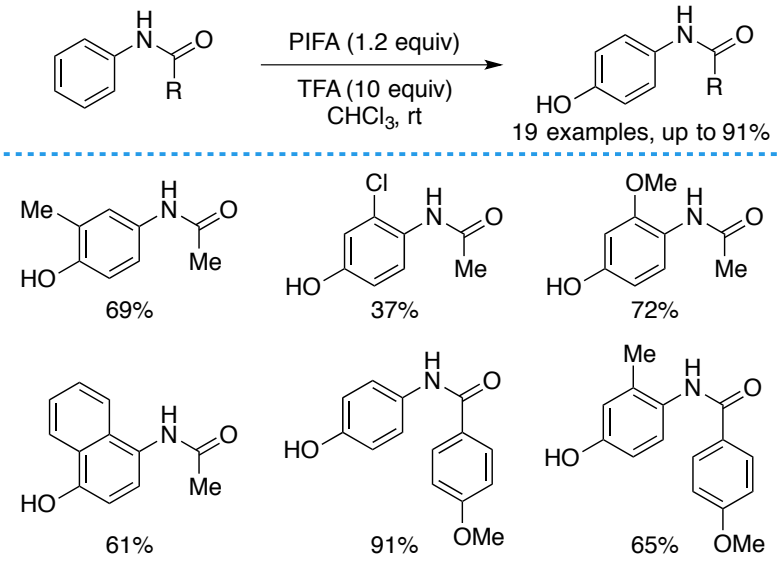

Scheme 5.7. PIFA mediated intermolecular C-O bond formation.

Later，the research group of Gu reported a direct acetoxylation, tosyloxylation and estherification of arylanilides using combinations with PIFA, $BF_3 \cdot OEt_2$ and appropriate oxygen nucleophiles.[140,141] Such transformations preferentially occurred at the *para*-position to the amide, affording the corresponding functionalized anilides. Those modified protocols unlike Kikugawa's hydroxylation also allowed to form C–O bonds in electron-deficient arylanilides. Interestingly, the C–O bond was formed at the *meta*-position when the *para*-position of the arene was blocked by a substituent. In all the electrophilic C-O bond formation processes, a mechanism as been proposed, consisting of generation of a nitrenium cation by the reaction between the amide and PIFA, followed by nucleophilic trapping of the charge-delocalized arene.

[140] Liu, H.; Wang, X.; Gu, Y. *Org. Biomol. Chem.* **2011**, *9*, 1614.
[141] Liu, H.; Xie, Y.; Gu, Y. *Tetrahedron Lett.* **2011**, *52*, 4324.

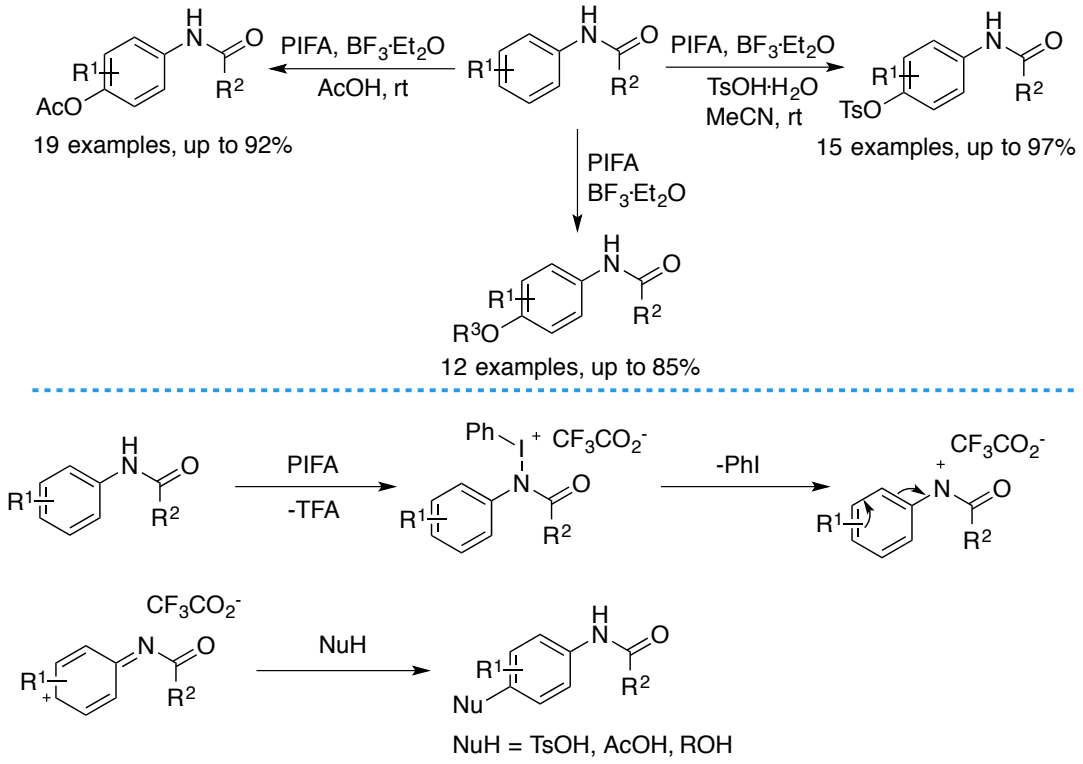

Scheme 5.8. PIFA mediated intermolecular C-O bond formation.

In 2012, the group of Zhao described the synthesis of oxazoles from carboxylic acids enamines in the presence of PhIO as oxidant.[142] Various enamines underwent β-acyloxylation with carboxylic acids to give *β*-acyloxy enamines. Subsequent cyclization by heating to reflux in acetic acid afforded the corresponding oxazoles. The authors proposed an *in situ* generated $PhI(O_2CR)_2$ could account for the observed acyloxylation.

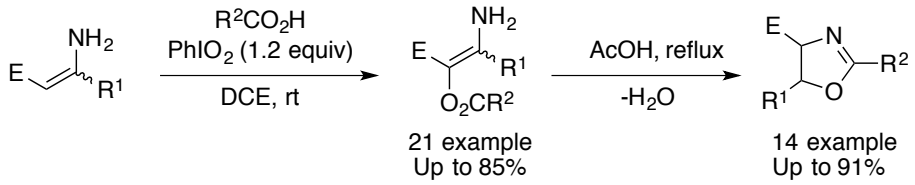

Scheme 5.9. PhIO mediated oxazoles formation.

Hypervalent iodine reagents were applied for the construction of esters from aldehydes as well. In 2006, Karade and coworkers developed a simple and mild new procedure for the facile direct oxidative methyl esterification of aldehydes using molecular iodine in combination with PIDA. The authors speculated that the oxidative

[142] Liu, X.; Cheng, R.; Zhao, F.; Zhang-Negrerie, D.; Du, Y.; Zhao, K. *Org. Lett.* **2012**, *14*, 5480.

esterification was induced by an *in situ* generated iodonium ion.[143]

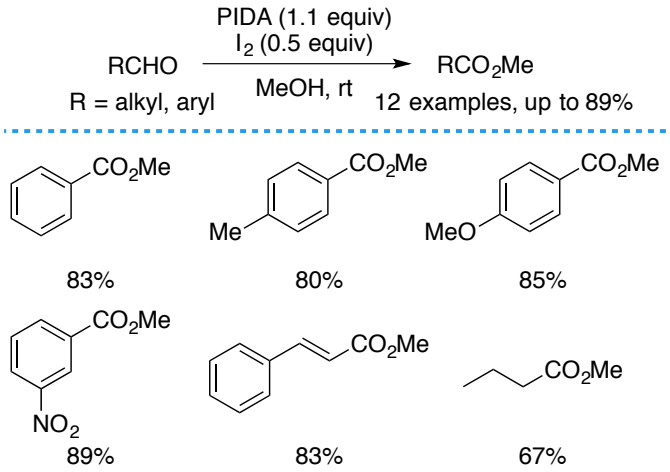

Scheme 5.10. PIDA mediated esterification of aldehydes.

In 2009, Liang and co-workers developed a selective functionalization of C(sp^3)–H bonds protocol with hypervalent iodine reagents.[144] Upon treatment with PIDA, a wide number of piperidine derivatives underwent direct diacetoxylation of the α- and β-C(sp^3)-H bonds adjacent to nitrogen to generate the desired products in moderate yields.

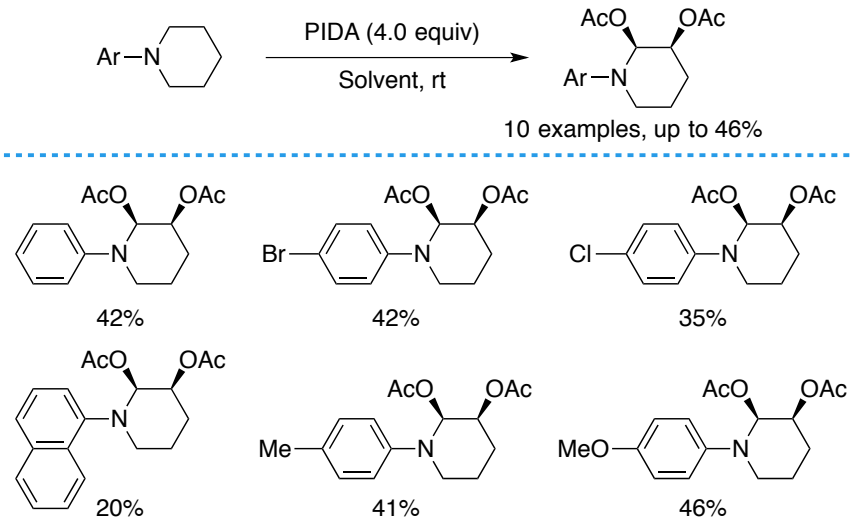

Scheme 5.11. PIDA mediated diacetoxylation of C(sp^3)-H bonds.

Mechanistically, the authors proposed a tertiary amine could initially be oxidized to form an imine, and then isomerize to afford enamine. Subsequent electrophilic addition of PIDA could result in the targeted product.

[143] Karade, N. N.; Budhewar, V. H.; Katkar, A. N.; Tiwari, G. B. *ARKIVOC* **2006**, *11*, 162.
[144] Shu, X.-Z.; Xia, X.-F.; Yang, Y.-F.; Ji, K.-G.; Liu, X.-Y.; Liang, Y.-M. *J. Org. Chem.* **2009**, *74*, 7464.

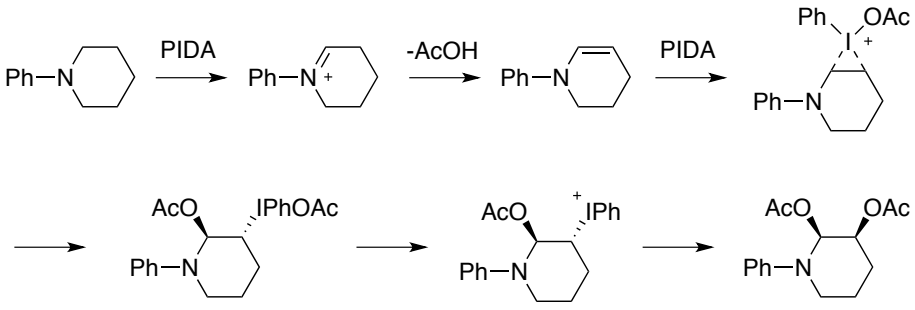

Scheme 5.12. Proposed mechanism PIDA mediated diacetoxylation of C(sp^3)-H bonds.

In 2005, Kita's group reported the first example of an iodine(III) reagent-catalyzed cascade cyclization/C-O bond formation by using *m*-CPBA as co-oxidant.[145] This catalytic event was distinguished by advantages such as short reaction time, high catalytic efficiency, and no need for the preparation of hypervalent iodine(III) reagents.

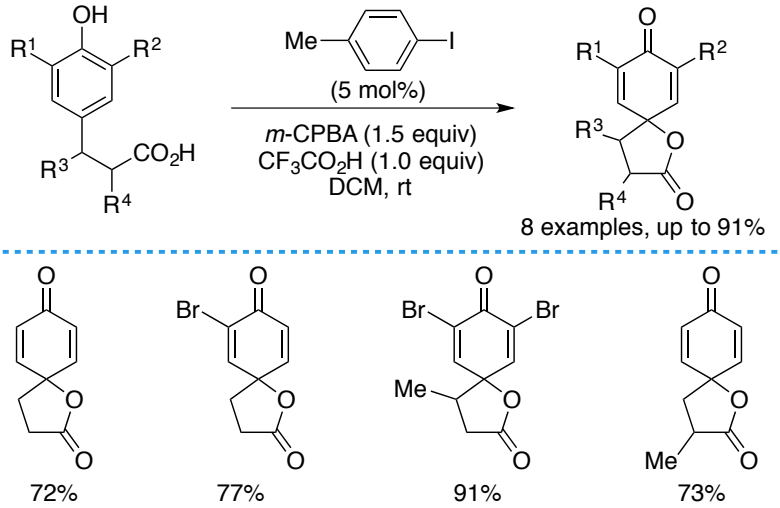

Scheme 5.13. Aryl iodide-catalyzed C-O bond formation.

The authors proposed a mechanism for this cyclization event. The cycle initiates with the generation of an active iodine(III) species A. Next, the intermediate A converts the phenol derivative into the desired product alongside the formation of 4-iodotoluene, which could regenerate A in the presence of *m*-CPBA.

[145] Dohi, T.; Maruyama, A.; Yoshimura, M.; Morimoto, K.; Tohma, H.; Kita, Y. *Angew. Chem. Int. Ed.* **2005**, *44*, 6193.

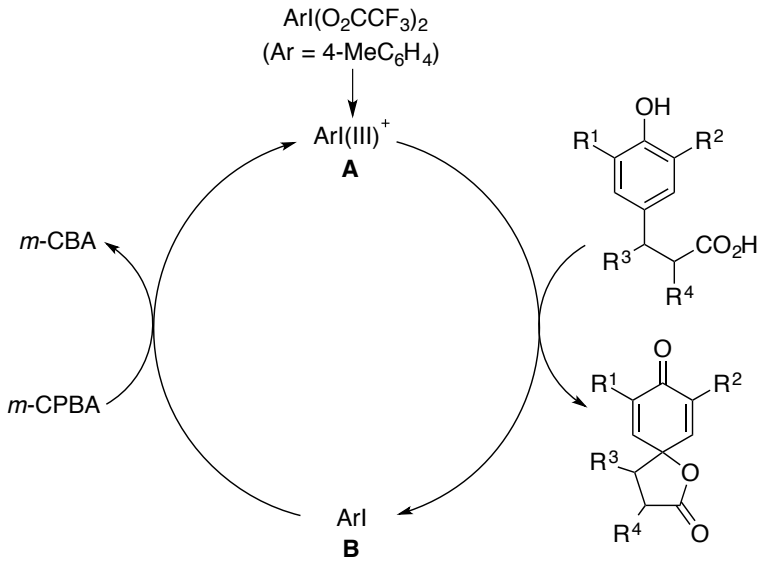

Scheme 5.14. Plausible mechanism.

In the same year, Ochiai's group reported an iodobenzene-catalyzed *α*-acetoxylation of ketones with *in situ* generated PIDA as catalytic oxidant.[146] *m*-CPBA serves as a terminal oxidant in this protocol. Good functional group compatibility was observed and various α-acetoxy ketones were obtained. The authors found that when the reaction was conducted in the absence of catalytic amount of iodobenzene, at the Baeyer-Villiger oxidation of a ketone took place. Notably, water and $BF_3 \cdot Et_2O$ are crucial for this α-acetoxylation to occur. The authors proposed a similar mechanism as shown in Figure 5.13.

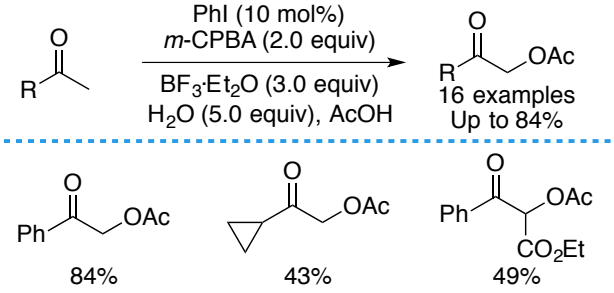

Scheme 5.15. ArI catalyzed *α*-acetoxylation of ketones.

Asymmetric transformations with hypervalent iodine also gained attention in the last years. Although tremendous efforts have been made towards achieving high enantioselectivities in hypervalent iodine chemistry, only a limited number of

[146] Ochiai, M.; Takeuchi, Y.; Katayama, T.; Sueda, T.; Miyamoto, K. *J. Am. Chem. Soc.* **2005**, *127*, 12244.

successful cases were reported.[147] In 2013, Kita and coworkers developed a series of spirobiindane-based chiral hypervalent iodine compounds and used them in the oxidative dearomatizing-spirolactonization of naphthols. The authors demonstrated that the enantioselectivity could be dramatically improved by inducing substituents at the *ortho*-position of iodine atom.[148]

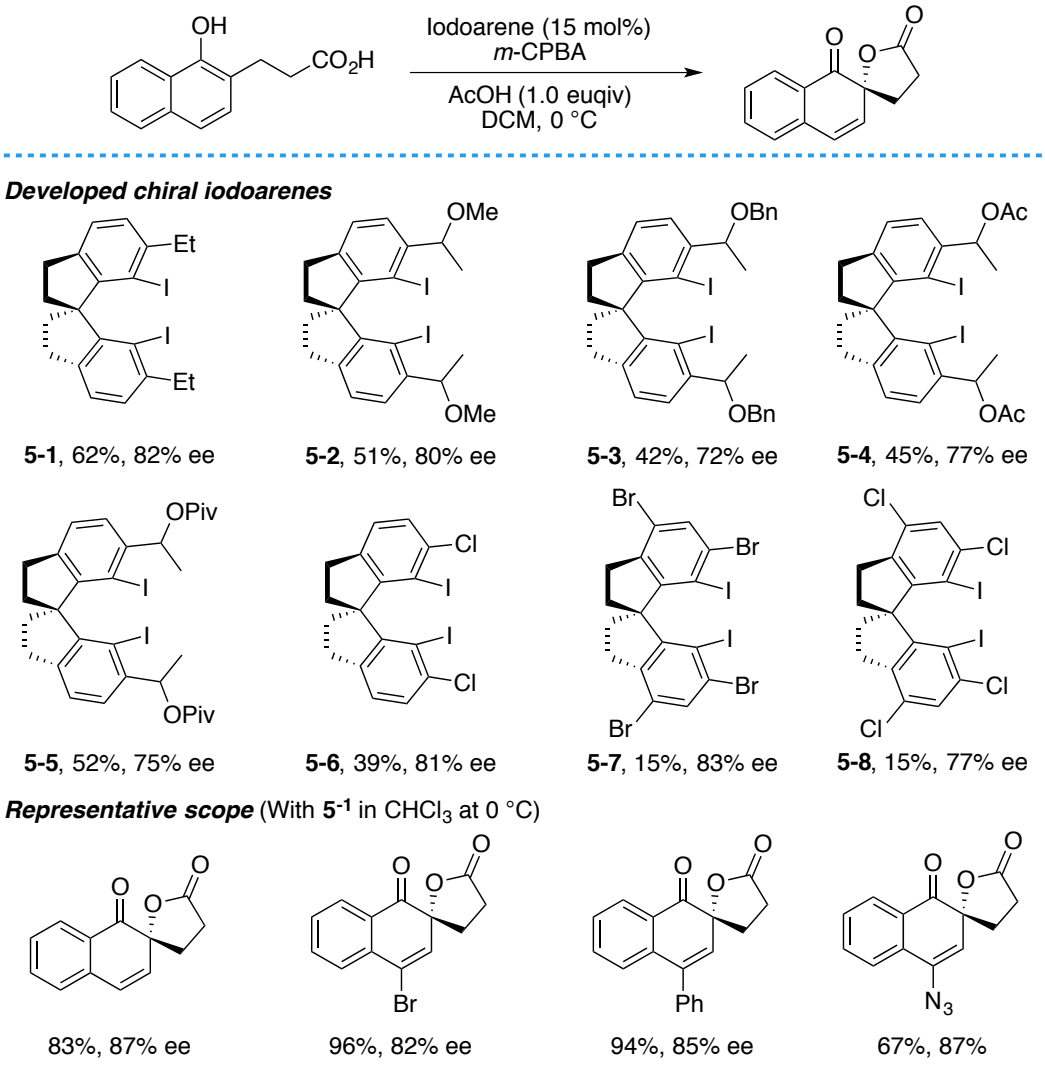

Table 5.1. ArI-catalyzed asymmetric dearomatizing spirolactonization of naphthols.

5.2.2 Current Methods for the Synthesis of Benzo[c]chromenone

Benzo[c]chrom-6-ones are privileged scaffolds in natural products and compounds with biological activities such as alternariol, graphislactone, gilvocarcin as well as

[147] Liang, H.; Ciufolini, M. A. *Angew. Chem. Int. Ed.* **2011**, *50*, 11849.

[148] Dohi, T.; Takenaga, N.; Nakae, T.; Toyoda, Y.; Yamasaki, M.; Shiro, M.; Fujioka, H.; Maruyama, A.; Kita, Y. *J. Am. Chem. Soc.* **2013**, *135*, 4558.

ellagic acid. [149] Recently, the preparation of benzo[c]chrom-6-ones has gained inscreasing attention due to their attractive biological properties, as shown in Figure 5.16.

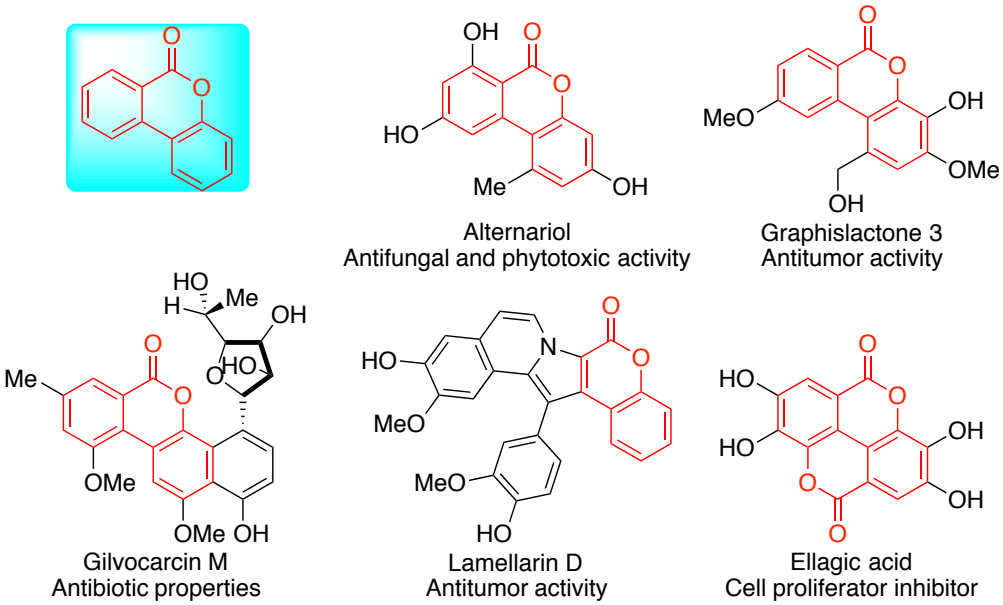

Figure 5.4. Representative benzo[c]chrom-6-ones containing compounds.

Traditional approaches for the synthesis of benzo[c]chrom-6-ones are based on the cyclization of carboxylic acids and alcohols. However, these methodologies have the drawback of multistep synthetic operations to incorporate the targeted functional groups prior the lactionization event.[150,151] Alternatively, several groups described the synthesis of benzo[c]chrom-6-ones by Suzuki-Miyaura coupling reactions.[152] Those methods display good chemoselectivity profiles for a wide variety of boronic acids and coupling partners. However, those protocols suffer from several disadvantages, such as the generation of stoichiometric amounts of halogen waste and harsh reaction

[149] (a) Plisson, F.; Conte, M.; Khalil, Z.; Huang, X. C.; Piggott, A. M.; Capon, R. J. *ChemMedChem* **2012**, *7*, 983. (b) Garino,C.; Bihel, F.; Pietrancosta, N.; Laras, Y.; Quelever, I.; Woo, I.; Klein, P.; Bain, J.; Boucher, J.; Kraus, J. *Bioorg. Med. Chem. Lett.* **2005**, *15*, 135. (c) Yoganathan, K.; Rossant, C.; Huang, Y.; Butler, M. S.; Buss, A. D. *J. Nat. Prod.* **2003**, *66*, 1116.

[150] Hamann, L. G.; Higuchi, R. I.; Zhi, L.; Edwards, J. P.; Wang, X.-N.; Marschke, K. B.; Kong, J. W.; Farmer, L. J.; Jones, T. K. *J. Med. Chem.* **1998**, *41*, 623.

[151] Parenty, A.; Moreau, X.; Campagne, J. M. *Chem. Rev.* **2006**, *106*, 911.

[152] (a) Alo, B. I.; Kandil, A.; Patil, P. A.; Sharp, M. J.; Siddiqui, M. A.; Snieckus, V.; Josephy, P. D. *J. Org. Chem.* **1991**, *56*, 3763. (b) Zhou, Q. J.; Worm, K.; Dolle, R. E. *J. Org. Chem.* **2004**, *69*, 5147. (c) Kemperman, G. J.; Ter Horst, B.; Van de Goor, D.; Roeters, T.; Bergwerff, J.; Van der Eem, R.; Basten, J. *Eur. J. Org. Chem* **2006**, *2006*, 3169. (d) Kemperman, G. J.; Ter Horst, B.; Van de Goor, D.; Roeters, T.; Bergwerff, J.; Van der Eem, R.; Basten, J. *Eur. J. Org. Chem* **2006**, *2006*, 3169. (e) Vishnumurthy, K.; Makriyannis, A. *J. Comb. Chem* **2010**, *12*, 664.

conditions.

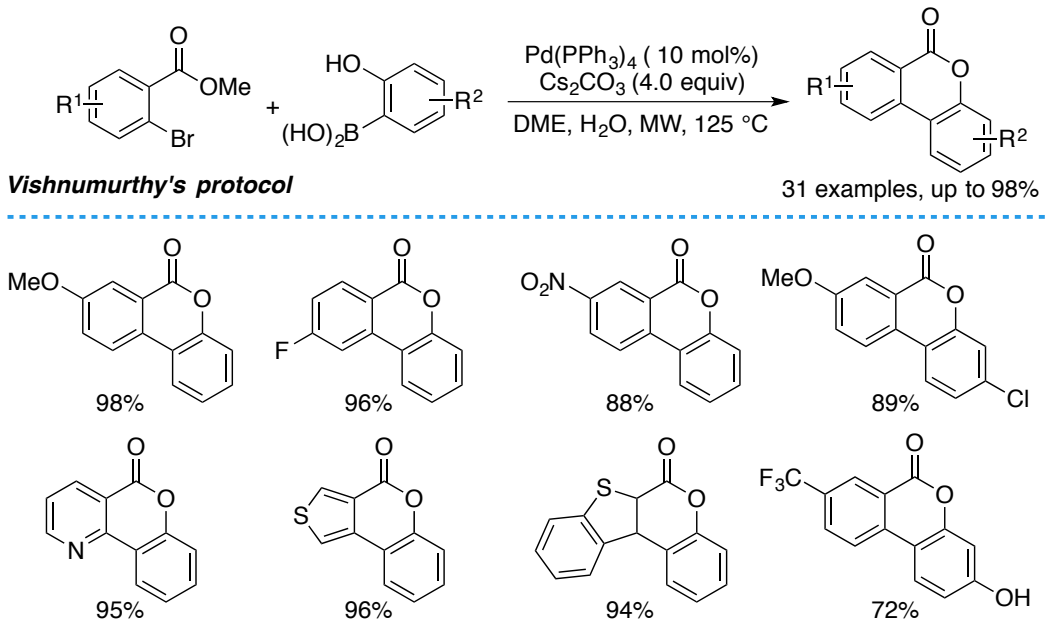

Scheme 5.16. Benzo[c]chrom-6-one synthesis by Suzuki-Miyaura coupling reactions.

In 2011, Deng and co-workers realized a highly selective palladium/copper-cocatalyzed tandem decarboxylative cross-coupling/cyclization sequence to prepare dibenzopyranones. This approach represents an efficient method to prepare a variety of substituted dibenzopyranones.[153]

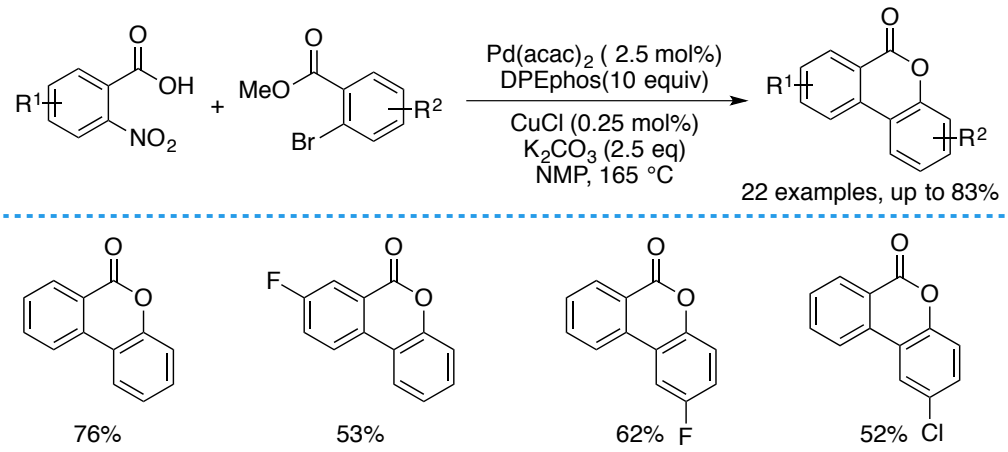

Scheme 5.17. Benzo[c]chrom-6-ones synthesis by decarboxylative cross-coupling reactions.

Recently, chemists realized the construction of benzo[c]chrom-6-ones via transition-metal-catalyzed C-H functionalization strategies. In 2013, our group reported a Cu-

[153] Luo, J.; Lu, Y.; Liu, S.; Liu, J.; Deng, G.-J. *Adv. Synth. Catal.* **2011**, *353*, 2604.

catalyzed tandem remote C-H functionalization/ C-O bond formation reaction en route to benzo[c]chrom-6-one derivatives.[154] The procedure is distinguished by its mild reaction conditions and wide functional group tolerance utilizing simple and cheap Cu catalysts. Thus becoming a user-friendly and operationally simple protocol for C(sp^2)-H functionalization. Moreover, the treatment of benzolactones with LiOH in MeOH could deliver hydroxylated arenes in good to excellent yields.

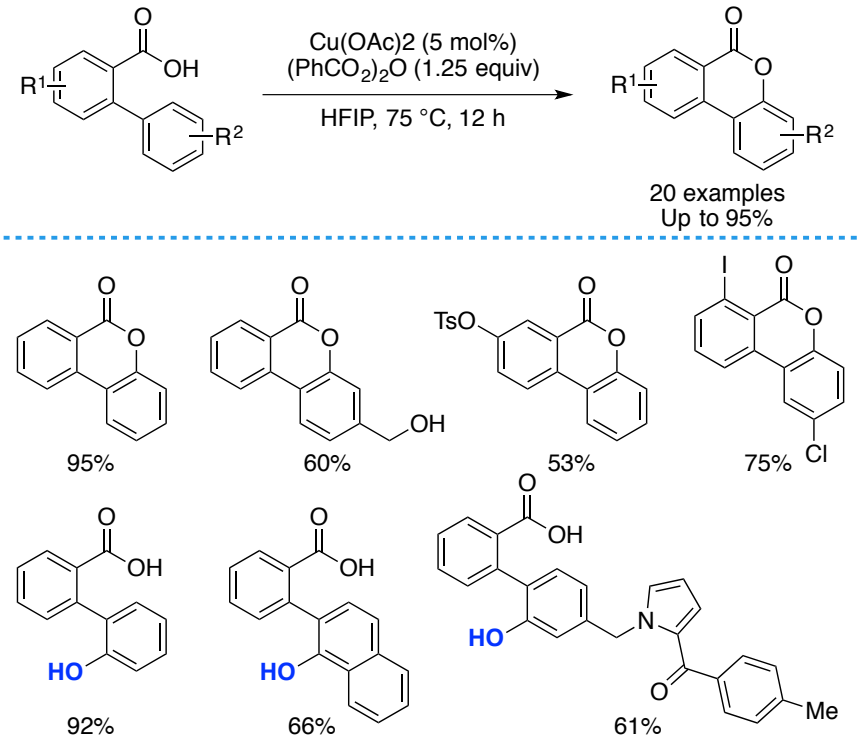

Scheme 5.18. Cu-catalyzed C-H functionalization/cyclization.

In the same year, the research group of Wang described an analogous transformation in the presence of Pd-catalyst.[155] The protocol displayed good functional group compatibility and a wide range of targeted products were generated. The authors demonstrated the potential of this new methodology by carrying out a total synthesis of the natural product cannabinol using the newly developed C-H activation/C-O cyclization reaction as key steps. Mechanistically, the authors found no significant kinetic isotope effect through isotope-labelling studies and suggested C-H activation was not the rate-determining step. Based on their mechanistic studies, the researchers proposed that this process proceeds through a Pd(II)/Pd(IV) catalytic cycle.

[154] Gallardo-Donaire, J.; Martin, R. *J. Am. Chem. Soc.* **2013**, *135*, 9350.
[155] Li, Y.; Ding, Y.-J.; Wang, J.-Y.; Su, Y.-M.; Wang, X.-S. *Org. Lett.* **2013**, *15*, 2574.

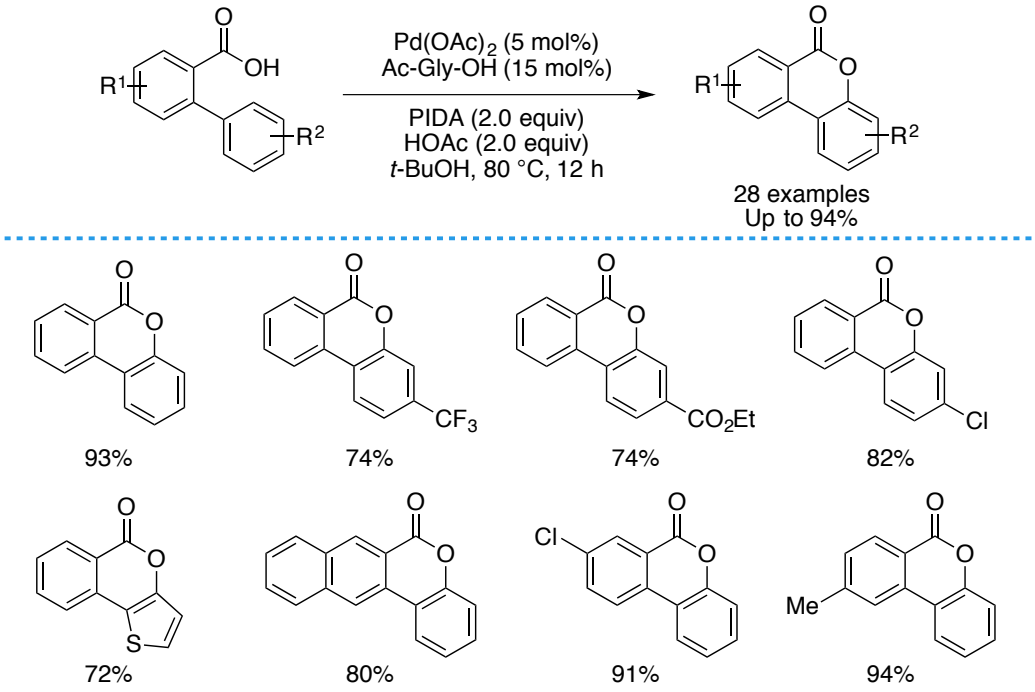

Scheme 5.19. Pd-catalyzed C-H functionalization/cyclization.

Almost simultaneously, Gevorgyan and coworkers published a similar Cu-catalyzed intramolecular C-H/O-H oxidative coupling of carboxylic acids with unactivated C(sp^2)-H bond en route to a variety of valuable lactone-containing molecules.[156] It's worth noting that the authors also developed a more general and practical method for the synthesis of the desired products, as shown in Figure 5.21. The $K_2S_2O_8$-mediated oxygenation event has a wide substrate scope, cyclization products bearing electron-neutral, -donating and -withdrawing substituents were prepared. The authors proposed a SET pathway for their transformation.

[156] Wang, Y.; Gulevich, A. V.; Gevorgyan, V. *Chem. Eur. J.* **2013**, *19*, 15836.

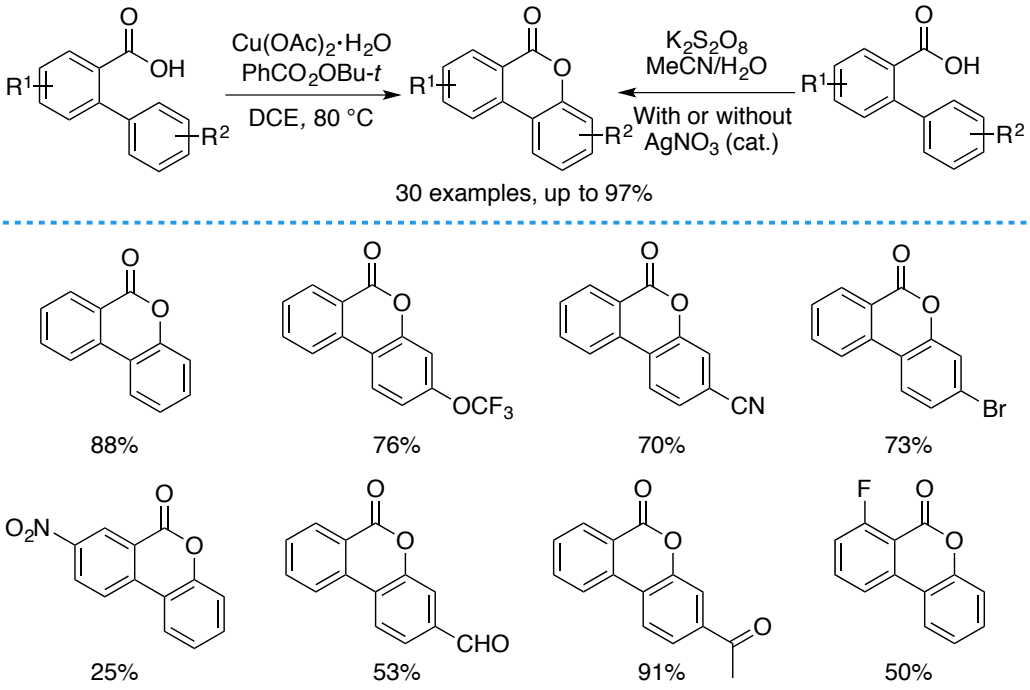

Scheme 5.20. Cu-catalyzed and $K_2S_2O_8$-promoted C-H functionalization/cyclization.

5.3 Reaction Condition Screening for ArI-catalyzed C(sp^2)-H Functionalization

Although tremendous progress has been made, the existing methods are suffering from several disadvantages such as using transition metals as catalysts, stoichiometric amounts of toxic oxidants, UV irradiation as well as harsh reaction conditions, which potentially restricts the industrial applications. At the outset of our investigations, a C-H functionalization assisted by carboxylic acids and ArI catalysts en route to benzolactones did not have any literature precedents.[157] We hypothesized that it is promising to develop a general, practical, and environmentally benign C-H functionalization/ C-O bond formation of 2-arylbenzoic acids with hypervalent iodine reagents.

We began our investigation by exploring the reactivity of **5-9** with stoichiometric amounts of PIFA, and we studied the effect of several experimental parameters such as solvents, concentration, amount of PIFA, as well as reaction time.

Initially, we investigated the effect of different solvents in our cyclization event. To our delight, we could observe the desired product **5-10** in 75% yield by employing 1,1,1,3,3,3-hexfluoroisoproanol (HFIP) as solvent (Figure 5-22, Entry 8). While

[157] Uyanik, M.; Suzuki, D.; Yasui, T.; Ishihara, K. *Angew. Chem. Int. Ed.* **2011**, *50*, 5331.

CF_3CO_2H and THF afforded lactone in inferior yields, we did not detect the targeted product when the reactions were conducted in AcOH, $CHCl_3$, MeCN, C_6F_6 as well as CF_3CH_2OH.

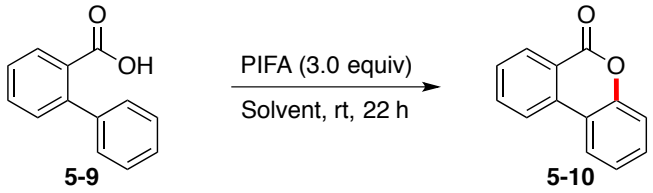

5-9 **5-10**

Entry	Solvent	Conversion[a]	Yield[b]
1	CH_3CO_2H	< 1%	No product
2	$CHCl_3$	< 1%	No product
3	MeCN	5%	No product
4	C_6F_6	25%	No product
5	CF_3CH_2OH	41%	No product
6	THF	100%	51%
7	CF_3CO_2H	100%	64%
8	HFIP	100%	75%

[a] HPLC conversion by using naphthalene as internal standard. [b] HPLC yield by using naphthalene as internal standard.

Table 5.2. The effect of solvent.

Encouraged by these findings, we next turned our attention to the influence of the concentration of starting material and the equivalents of PIFA onto the C(sp^2)-H functionalization. As shown in Figure 5.23, while using 2.5 equivalents of PIFA delivered **5-10** in 95% yield at a concentration of 0.5 mol/L, decreasing or increasing the amount of PIFA led to the erosion of yields. The protocol had a same tendency when the reactions were conducted at the concentration of 0.33 mol/L as at the concentration of 0.5 mmol. We found that using 2.5 equivalents of PIFA, being the ideal amount of hypervalent reagent, led to the generation of the cyclized lactone in 98% yield (Figure 5.23, Entry 7).

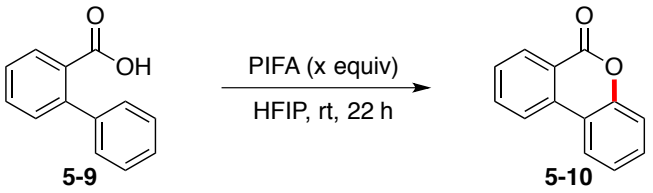

5-9 5-10

Entry	Concentration	PIFA	Conversion[a]	Yield[b]
1	0.5 mol/mL	1.5	100%	82%
2	0.5 mol/mL	2.0	100%	89%
3	0.5 mol/mL	2.5	100%	95%
4	0.5 mol/mL	3.0	100%	87%
5	0.33 mol/mL	1.5	100%	81%
6	0.33 mol/mL	2.0	100%	86%
7	0.33 mol/mL	2.5	100%	98%
8	0.33 mol/mL	3.0	100%	88%

[a] HPLC conversion by using naphthalene as internal standard. [b] HPLC yield by using naphthalene as internal standard.

Table 5.3. Concentration effect and the equivalents of PIFA.

Next, we wondered whether we could decrease the reaction time, however, the reduced reaction times resulted in lower yields (Figure 5.24).

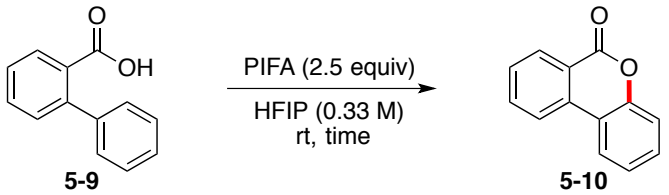

5-9 5-10

Entry	Time (h)	Conversion[a]	Yield[b]
1	1.0	22%	6%
2	2.0	32%	14%
3	8.0	100%	67%
4	16.0	100%	89%

[a] HPLC conversion by using naphthalene as internal standard. [b] HPLC yield by using naphthalene as internal standard.

Table 5.4. Influence of reaction time.

Inspired by those encouraging results and the pioneering work of Kita's and Ochiai's,[156,157] we envisioned to realize this transformation with a catalytic amount of aryl iodide and in the presence of a terminal oxidant. Indeed, we found promising

results when using catalytic amounts of iodobenzene and peracetic acid as the oxidant at room temperature. We could observe the desired benzolactone in some solvents such as DCM, DCE, toluene, $PhCF_3$, PhCl, and $CHCl_3$, although in low yields (from 4% to 7%). HFIP was found to be the best selection of solvent, and 14% of final product was detected (Figure 5.25).

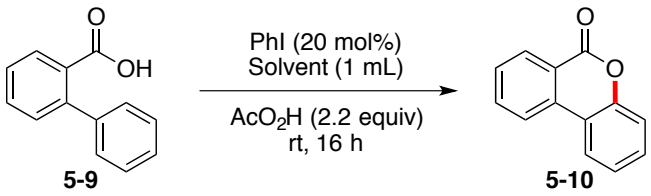

5-9 **5-10**

Entry	Solvent	Conversion[b]	Yield[c]
1	DCM	17%	4%
2	toluene	18%	7%
3	MeCN	17%	1%
4	t-BuOH	0%	--
5	CF_3CH_2OH	20%	5%
6	acetone	12%	trace
7	HFIP	25%	14%
8	dioxane	0%	--
9	$PhCF_3$	6%	5%
10	PhOMe	14%	0%
11	PhCl	21%	7%
12	DCE	11%	4%
13	$CHCl_3$	28%	5%

[a] Reaction conditions: **5-9** (0.2 mmol), PhI (20 mol%), AcO_2H (2.2 equiv),rt, 16 h. [b] HPLC conversion by using naphthalene as internal standard.[c] HPLC yield by using naphthalene as internal standard.

Table 5.5. Influence of solvent.

We anticipated that the nature of the aryl iodide fragment would play a critical role for the success. As shown in Figure 5.26, this was indeed the case and electron-deficient catalysts provided low conversions to **5-10** (**5-12, 5-21**). Interestingly, the presence of halides in *para*-position had a positive effect (**5-14**, **5-15**, **5-16**). In sharp contrast to the use of **5-13**, the inclusion of *para*-alkyl substituents had a dramatic influence on

reactivity (**5-17**), indicating that electronic effects might not be the only factor coming into play. Indeed, **5-17** allowed us to obtain the desired product in 85% yield in open air at room temperature. Strikingly, *ortho*- or *meta*-alkyl substituents had a detrimental effect, thus showing the subtleties of our system (**5-18, 5-19**). At present, we do not have an explanation for this marked difference in reactivity.

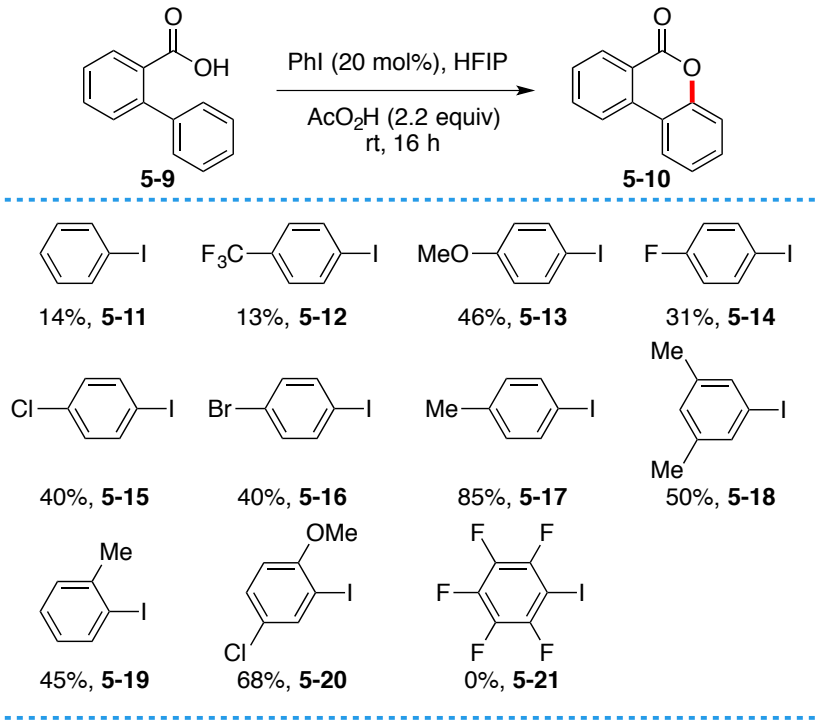

[a] Reaction conditions: **5-9** (0.2 mmol), PhI (20 mol%), HFIP (1 mL), AcO_2H (2.2 equiv),rt, 16 h. [b] HPLC conversion by using naphthalene as internal standard. [c] HPLC yield by using naphthalene as internal standard.

Table 5.6. The catalyst effect.

With those results in hand, we next screened different oxidants. Surprisingly, inorganic oxidants such as $NaIO_4$, Oxone, and $K_2S_2O_8$ did not generate the final product (Figure 2.27, Entries 1-3). We also learned that *t*-BuO_2H and H_2O_2 were not applicable for our cyclization protocol (Entries 4, 6). On the other hand, the utilization of *m*-CPBA delivered **5-10** in 29% yield.

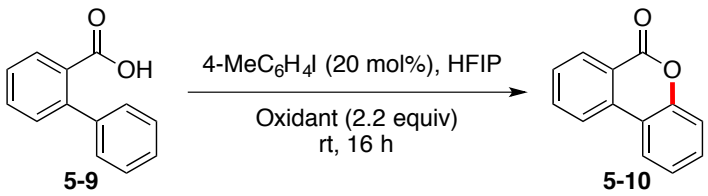

Entry	Oxidant	Conversion[b]	Yield[c]
1	$NaIO_4$	0%	--
2	OXONE	0%	--
3	$K_2S_2O_8$	0%	--
4	*t*-BuO_2H	0%	--
5	*m*-CPBA	38%	29%
6	H_2O_2	0%	--

[a] Reaction conditions: **5-9** (0.2 mmol), **5-17** (20 mol%), HFIP (1 mL), oxidant (2.2 equiv),rt, 16 h. [b] HPLC conversion by using naphthalene as internal standard. [c] HPLC yield by using naphthalene as internal standard.

Table 5.7. The oxidant effect.

The screening of oxidant loading showed that the choice of 2.2 equivalents of AcO_2H is critical for obtaining good yield. Either increasing or decreasing the amount of oxidant led to lower yields.

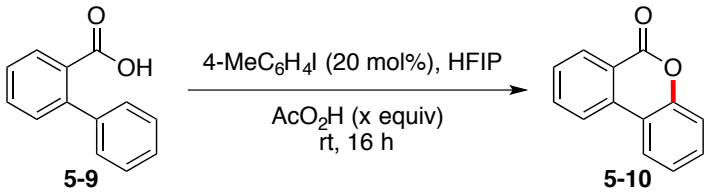

Entry	AcO_2H	Conversion[b]	Yield[c]
1	1.5 equiv	64%	60%
2	2.2 equiv	93%	85%
3	3.0 equiv	100%	81%

[a] Reaction conditions: **5-9** (0.2 mmol), **5-17** (20 mol%), HFIP (1 mL), AcO_2H (x equiv),rt, 16 h. [b] HPLC conversion by using naphthalene as internal standard. [c] HPLC yield by using naphthalene as internal standard.

Table 5.8. Influence of oxidant loading.

To our delight, we could improve the yield by adjusting the concentration of the reaction and 93% of **5-10** were obtained when the reaction was conducted at a 0.1 M the concentration (Figure 5.29, Entry 6). However, increasing the concentration led to

the decrease of yield (Entries 1-5). We also tried to lower the catalyst loading, however, dramatically decreased yields were observed when 10 mol% or 15 mol% of **5-17** were employed in our C(sp^2)-H cyclization protocol (Entries 7-8).

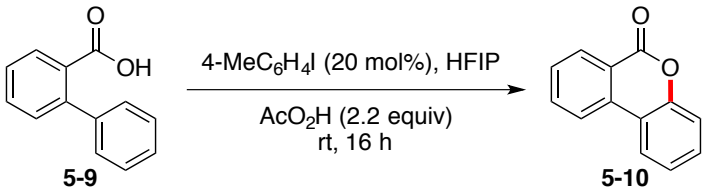

5-9 **5-10**

Entry	Concentration	Conversion[b]	Yield[c]
1	1 mmol/mL	7%	5%
2	0.5 mmol/mL	53%	46%
3	0.33 mmol/mL	81%	67%
4	0.25 mmol/mL	86%	75%
5	0.125 mmol/mL	100%	89%
6	0.1 mmol/mL	100%	93%
7	0.1 mmol/mL	53%	46%[d]
8	0.1 mmol/mL	81%	67%[e]
9	0.1 mmol/mL	100%	97%[f]

[a] Reaction conditions: **5-9** (0.2 mmol), **5-17** (20 mol%), HFIP (1 mL), AcO_2H (2.2 equiv), r t, 16 h. [b] HPLC conversion by using naphthalene as internal standard. [c] HPLC yield by using naphthalene as internal standard. [d] 10 mol% of **5-17** were used. [e] 15 mol% of **5-17** were used. [f] Isolated yield.

Table 5.9. Influence of concentration and catalyst loading.

As a conclusion, we found our optimized reaction conditions after investigating several experimental parameters. The reaction performed in the presence of **5-17** (20 mol%) as catalyst, AcO_2H (2.2 equiv) as oxidant in HFIP at room temperature led to the desired benzolactone in nearly quantitative yield (97%). The reactions were conducted open to air, a remarkable finding that constitutes an additional bonus when compared with metal-catalyzed protocols for similar means.

5.4 Scope of the ArI-catalyzed C(sp^2)-H Functionalization/C-O Bond Formation

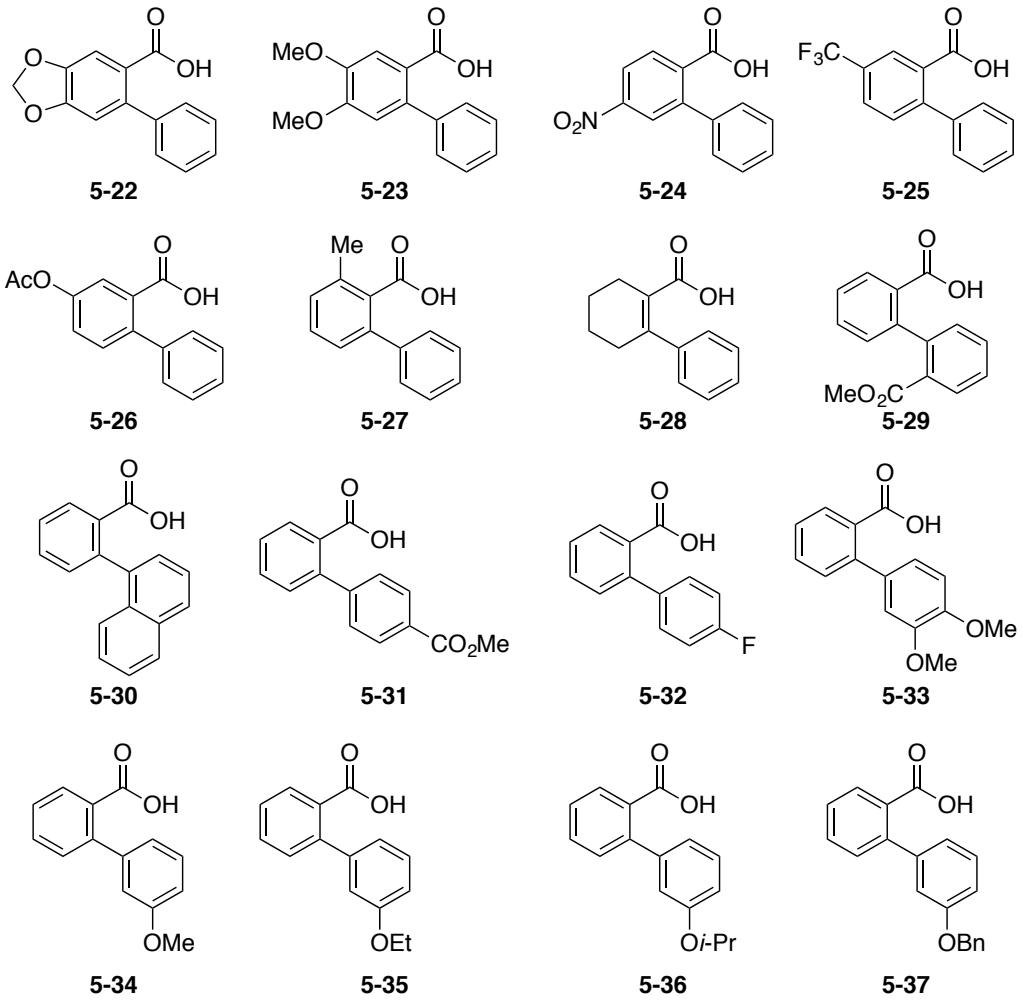

Figure 5.5. Starting materials for the C(sp^2)-H functionalization.

With a family of benzoic acids in hand (from our previous project[165]), we set out to explore the preparative scope of our aryliodide-catalyzed C(sp^2)–H functionalization/C–O bond formation. As shown in Figure 5.31, the outcome was largely insensitive to changes in the electronic nature of the substrates. The excellent chemoselectivity profile was particularly noteworthy as acetals (**5-40**), nitro groups (**5-42**), esters (**5-44**, **5-47** and **5-49**) and aryl fluorides (**5-50**), were well accommodated. Under these conditions, non-aromatic carboxylic acids (**5-46**) or substrates prone to C(sp^3)–H functionalization (**5-45**) posed no problems. To put these results into perspective, we observed little conversion, if any, of **5-22, 5-23** or substrates bearing electron-withdrawing groups such as **5-25, 5-26**, **5-29** and **5-31** under previously developed Cu-catalyzed conditions.[165] Interestingly, **5-48**, **5-49**, **5-50**, and **5-51** were

isolated as *single regioisomers*, with **5-50** being unambiguously characterized by X-ray analyses. These results are rather important taking into consideration that Cu-catalyzed oxidative protocols provide regioisomeric mixtures of these compounds.

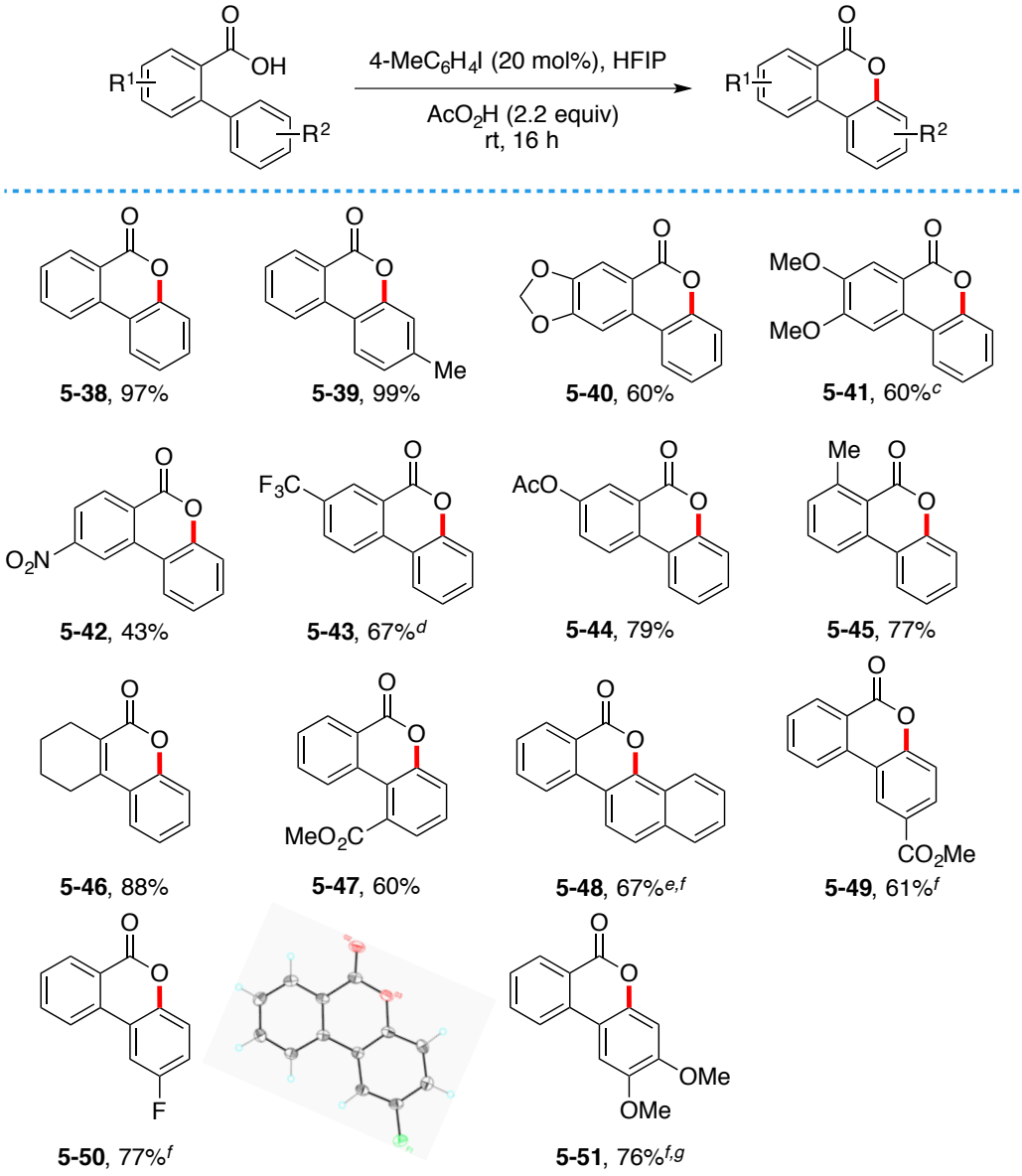

[a] Conditions: Starting material (0.20 mmol), **5-17** (20 mol%), AcO_2H (2.20 equiv), HFIP (1 mL) at rt for 16 h, open to air. [b] Isolated yields, average of two independent runs. [c] **5-20** (20 mol%). [d] AcO_2H (4.40 equiv), 80 °C. [e] AcO_2H (1.10 equiv). [f] A single regioisomer was observed. [g] PIFA (1.0 equiv).

Table 5.10. Representative substrate scope of C(sp^2)-H functionalization.

5.5 Reaction Condition Screening for ArI-catalyzed C(sp^3)-H Functionalization

A closer look into the literature data indicates that harsh reaction conditions are typically required to prepare benzolactones via metal-catalyzed C(sp^3)-H bond

functionalization using carboxylic acids as weakly coordinating directing group. In 2006, Chang and coworkers reported a Pt-catalyzed C(sp^3)-H activation/C-O bond formation process to synthesize benzolactones.[158] As illustrated in Scheme 5.21, the reactions were conducted under harsh conditions and the products were isolated in moderate yields.

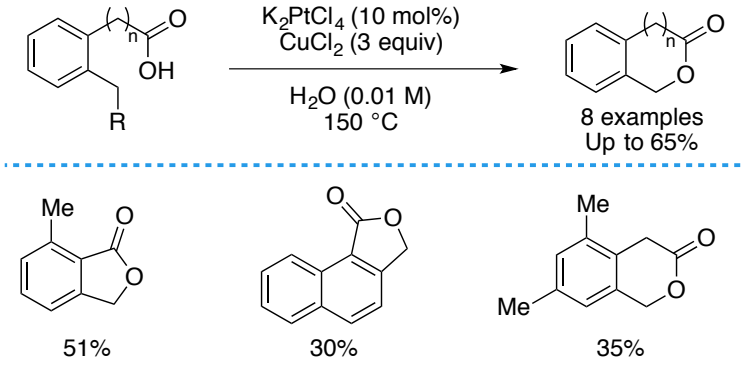

Scheme 5.21. Pt-catalyzed C(sp^3)-H functionalization.

Later, our group described a similar transformation in the presence of Pd as catalyst, a direct and operationally simple protocol to prepare benzolactones with various functional groups and a diverse set of substitution patterns.[159] The authors also conducted isotope-labelling experiments. The authors did not observe a significant kinetic isotope effect in the competitive reaction, indicating that the C(sp^3)-H bond cleavage might not be the rate-determining step. The researchers support the hypothesis that the C(sp^3)-O bond forming reductive elimination is rate-limiting in the C-O bond formation protocol.

[158] Lee, J. M.; Chang, S. *Tetrahedron Lett.* **2006**, *47*, 1375.
[159] Novák, P.; Correa, A.; Gallardo-Donaire, J.; Martin, R. *Angew. Chem. Int. Ed.* **2011**, *50*, 12236.

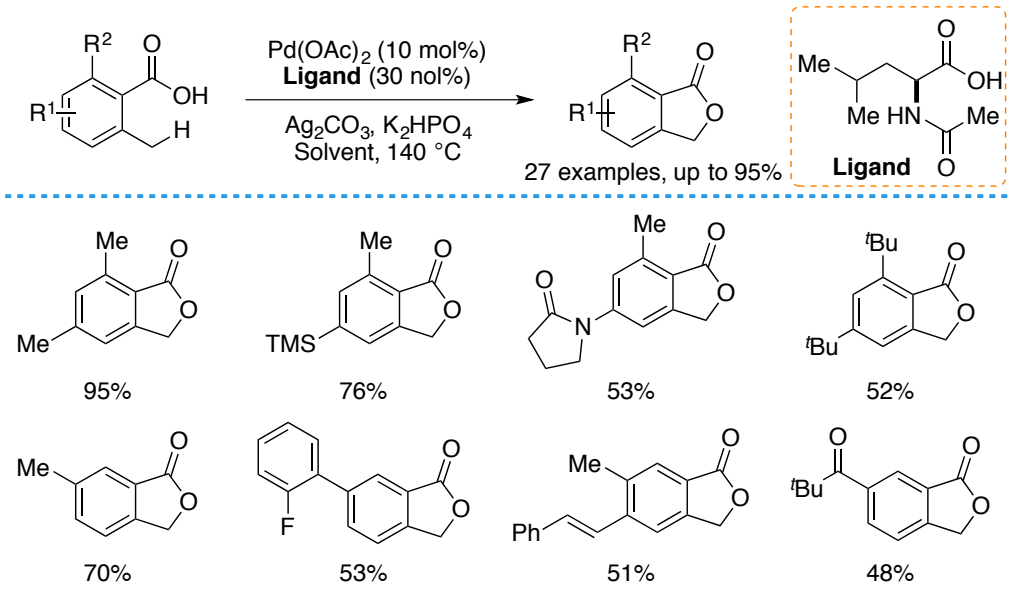

Scheme 5.22. Pd-catalyzed C(sp^3)-H functionalization.

Challenged by these findings, we wondered whether the mild protocol in Figure 5.31 could be adapted to a more challenging C(sp^3)-H functionalization scenario.[160] We envisioned that the catalyst would have a profound influence onto the reactivity. Therefore, we decided to start our studies on the C(sp^3)-H functionalization by screening the ArI-catalyst. Indeed, the best choice of catalyst **5-17** for Figure 5.31 did not yield the desired product at room temperature in 24 h (Figure 5.33, Entry 1). To our delight, we could achieve a yield of 50% by performing the reaction at 80 °C (Entry 2). Catalyst **5-16** turned out to be the best catalyst amongst the other species studied, and a comparable yield of final product as with **5-17** was obtained when 68% of starting material were consumed (Entry 3). Further catalyst screening showed that catalysts **5-11** and **5-14** led to minor reduction of the yield (Entries 4-5) and the use of **5-12**, **5-13** and **5-18** resulted in a dramatically decrease of the yields (Entries 6-8).

[160] For selected reviews on C(sp^3)–H functionalization, see: (a) Li, H.; Li, B. J.; Shi, Z. J. *Catal. Sci. Technol.* **2011**, *1*, 191. (b) Jazzar, R.; Hitce, J.; Renaudat, A.; Sofack- Kreutzer, J.; Baudoin, O. *Chem. - Eur. J.* **2010**, *16*, 2654.

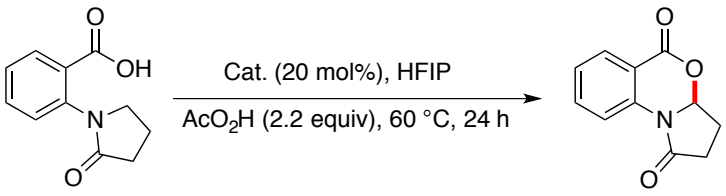

5-52 **5-53**

Entry	Catalyst	Conversion[b]	Yield[c]
1[d]	**5-17**	22%	21%
2[e]	**5-17**	90%	50%
3	**5-16**	68%	50%
4	**5-14**	73%	48%
5	**5-11**	67%	47%
6	**5-18**	32%	18%
7	**5-13**	27%	6%
8	**5-12**	30%	7%

[a] Reaction conditions: **5-52** (0.2 mmol), Cat. (20 mol%), HFIP (2 mL), AcO_2H (2.2 equiv), 60 °C, 24 h. [b] HPLC conversion by using naphthalene as internal standard. [c] HPLC yield by using naphthalene as internal standard. [d] At rt. [e] At 80 °C.

Table 5.11. Catalyst screening for C(sp^3)-H functionalization.

Next, we turned our attention to the effect of the oxidant loading. We anticipated that increasing the amount of peracetic acid would enhance the conversion, since the access oxidant might be able to oxidize the amide to corresponding pyrrol-1-ium, thus, accelerating the reactivity of the starting material. As depicted in Figure 5.33, we could achieve 65% of yield when 4 equivalents of AcO_2H were used (Entry 2). However, furthering increasing the loading of oxidant led to inferior yields (Entries 3-5). Unlike HFIP, other solvents are not applicable for this transformation (Entries 6-15). While relatively high yield was observed when the reaction was conducted in CF_3CH_2OH, no product or low yield was detected with other solvents such as THF, DCM, DMF etc.

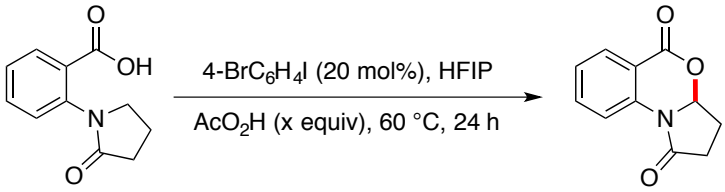

5-52 **5-53**

Entry	AcO_2H	Solvent	Conversion[b]	Yield[c]
1	3.0 equiv	HFIP	84%	63%
2	4.0 equiv	HFIP	91%	65%
3	5.0 equiv	HFIP	95%	60%
4	6.0 equiv	HFIP	89%	48%
5	8.0 equiv	HFIP	86%	39%
6	4.0 equiv	THF	4%	--
7	4.0 equiv	DCM	27%	11%
8	4.0 equiv	DCE	11%	4%
9	4.0 equiv	DMF	4%	--
10	4.0 equiv	Et_2O	0%	--
11	4.0 equiv	$CHCl_3$	15%	7%
12	4.0 equiv	Pr^iOH	6%	--
13	4.0 equiv	MeCN	18%	7%
14	4.0 equiv	CF_3CO_2H	0%	--
15	4.0 equiv	CF_3CH_2OH	37%	23%

[a] Reaction conditions: **5-52** (0.2 mmol), **5-16** (20 mol%), HFIP (2 mL), AcO_2H (x equiv), 60 °C, 24 h. [b] HPLC conversion by using naphthalene as internal standard. [c] HPLC yield by using naphthalene as internal standard.

Table 5.12. AcO_2H loading and solvent screening for C(sp^3)-H functionalization.

Encouraged by these findings, we were attracted to survey the influence of reaction concentration. High concentrated catalytic systems were not suitable for this transformation, dramatically dropped yields were detected (Figure 5.35, Entries 1-2). Interestingly, a concentration of 0.13 mmol/mL turned out to be the best choice and the yield could be improved slightly to 68% (Entry 5).

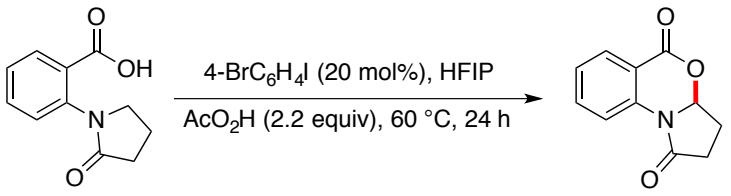

5-52 **5-53**

Entry	Concentration	Conversion[b]	Yield[c]
1	0.40 mmol/mL	50%	32%
2	0.33 mmol/mL	53%	29%
3	0.25 mmol/mL	76%	52%
4	0.20 mmol/mL	79%	60%
5	0.13 mmol/mL	86%	68%
6	0.08 mmol/mL	89%	68%

[a] Reaction conditions: **5-52** (0.2 mmol), **5-16** (20 mol%), HFIP (x mL), AcO_2H (4.0 equiv), 60 °C, 24 h. [b] HPLC conversion by using naphthalene as internal standard. [c] HPLC yield by using naphthalene as internal standard.

Table 5.13. Concentration screening for C(sp^3)-H functionalization.

We also wondered whether the temperature has a profound influence on the reactivity. Therefore, we performed our ArI-catalyzed C(sp^3)-H functionalization/C-O bond formation reactions at different temperatures (Figure 5.35). Notably, while we observed the desired product in 70% yield when the reaction was performed at 40 °C, we found that 77% of the starting material were converted (Entry 4). We envisioned that prolonging the reaction time would allow us to improve the yield. As anticipated, we obtained the cyclized product in 81% yield (Entry 5), when the reaction time was increased to 36h. Conducting the reaction at room temperature significantly lowered the reactivity (Entry 6). Finally, the blank experiments demonstrated that ArI and AcO_2H were crucial for the process to occur.

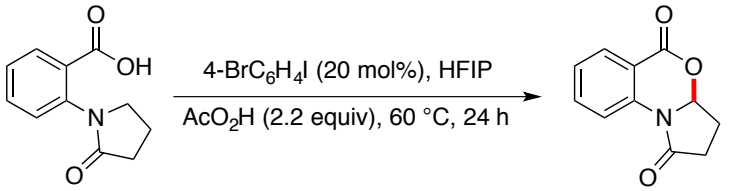

5-52 **5-53**

Entry	Temperature	Conversion[b]	Yield[c]
1	80 °C	82%	57%
2	60 °C	86%	68%
3	50 °C	75%	60%
4	40 °C	77%	70%
5[d]	40 °C	95%	81%
6	RT	11%	10%
7[e]	40 °C	32%	3%
8[f]	40 °C	0%	--

[a] Reaction conditions: **5-52** (0.2 mmol), **5-16** (20 mol%), HFIP (x mL), AcO_2H (4.0 equiv), 60 °C, 24 h. [b] HPLC conversion by using naphthalene as internal standard. [c] HPLC yield by using naphthalene as internal standard. [d] 36 h. [e] Without **5-16**. [f] Without AcO_2H

Table 5.14. Temperature screening and blanks experiments for C(sp^3)-H functionalization.

In summary, we found the optimized reaction conditions for our ArI-catalyzed C(sp^3)-H functionalization/C-O bond formation protocol after a thorough investigation of experimental parameter. When the reaction was performed in the presence of **5-16** (20 mol%) as catalyst, AcO_2H (4.0 equiv) as oxidant in HFIP at 40 °C for 36h, we could obtain the desired benzolactone in 81% yield. Remarkably, all the reactions were conducted open to air, demonstrating the operational simplicity of this protocol.

5.6 Scope of the ArI-catalyzed C(sp^3)-H Functionalization/C-O Bond Formation

Having established the optimized reaction conditions, we then set out to survey the scope of this protocol by synthesizing a wide number of starting materials. The benzoic acids **5-53** and **5-58** were prepared via a two-step synthetic route as shown in Scheme 5.3. Cu-catalyzed C-N bond formation of **5-54** and **5-55** delivered **5-56** (**5-57**) in moderate yield, which underwent a hydrolysis with LiOH in MeOH, THF and H_2O to

generate the desired substrate **5-53** (**5-58**) in good yield.[161,165]

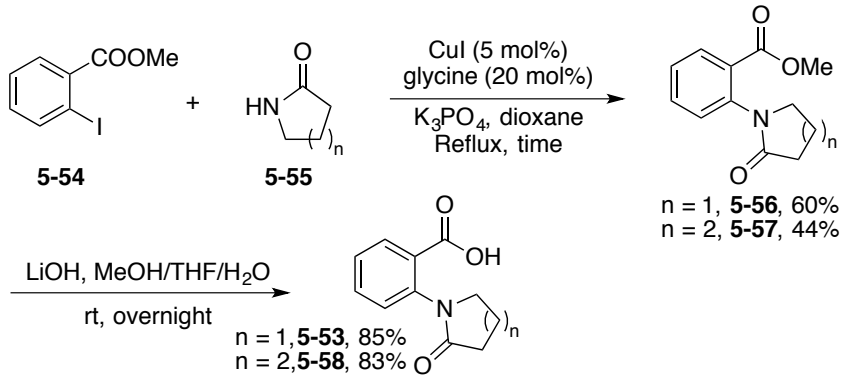

Scheme 5.23. Synthetic routes for **5-53** and **5-58**.

The benzoic acid derivatives from **5-59** to **5-66** were synthesized via a synthetic route as shown in Scheme 5.4. First, 2-amino methyl benzoic acid was reacted with 4-chlorobutanoyl chloride to generate amide **5-59**, which could undergo cyclization promoted by NaH to afford intermediate **5-60**. The final hydrolysis with KOH generated the targeted substrate.[162]

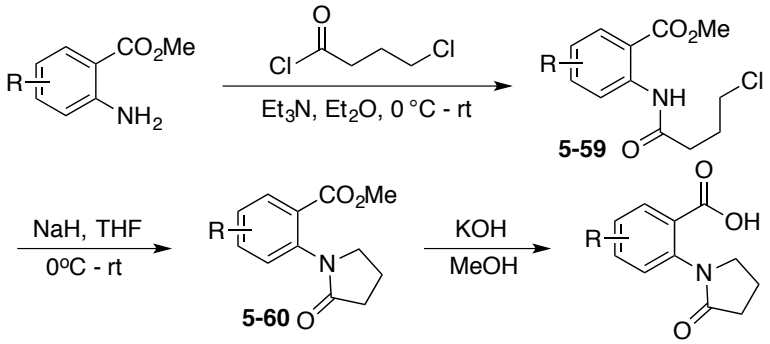

Scheme 5.24. Synthetic routes for **5-53** analogies.

As show in Figure 5.36, a variety of substrates bearing electron-withdrawing or electron-donating substituent were prepared in moderate to good yields via the method illustrated above.

[161] Deng, W.; Wang, Y. F.; Zou, Y.; Liu, L.; Guo, Q. X. *Tetrahedron Lett.* **2004**, *45*, 2311.
[162] Bassoli, A.; Borgonovo, G.; Busnelli, G.; Morini, G. *Eur. J. Org. Chem.* **2006**, 1656.

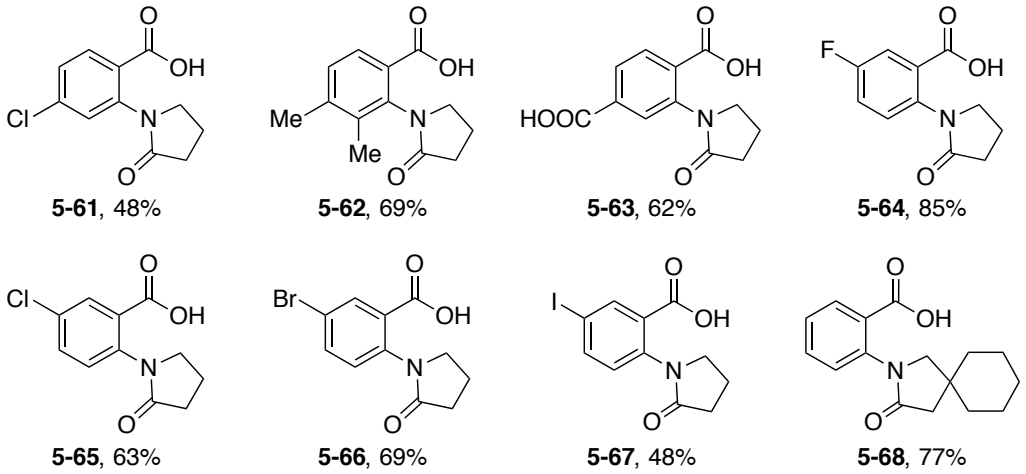

Figure 5.6. Prepared substrates.

Finally, we prepared substrate **5-73** through a modified synthetic route. Aniline **5-69** reacts with isocyanate to generate urea **5-70**, which can undergo cyclization to yield imidazolidin-2-one in high yield. The following methylation and nucleophilic carboxylation with CO_2 allowed us to obtain the final product.

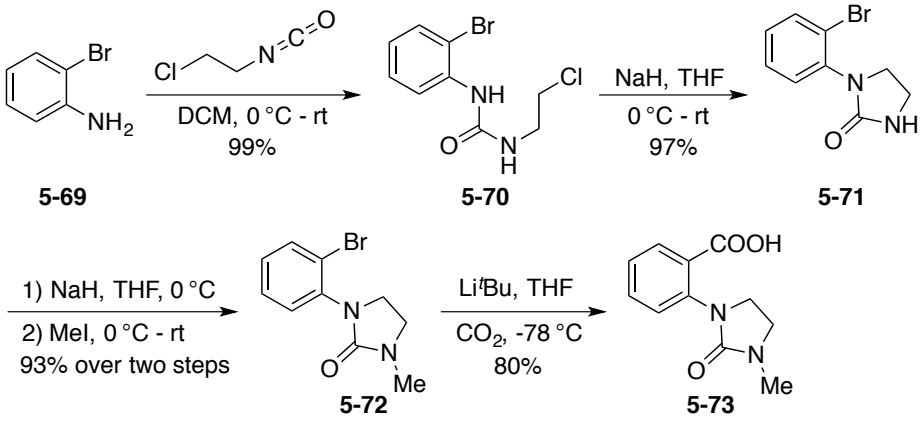

Scheme 5.25. Synthetic routes for **5-73**.

Having a wide range of substrates in hand, we then turned our attention to the scope of our C(sp^3)-H functionalization/C-O bond formation approach. As it becomes evident from the results in Figure 5.37, the method tolerates a variety of substitution patterns without significantly influencing the reaction outcome. Interestingly, remote carboxylic acids (**5-77**) or aryl halide entities were tolerated (**5-75** and from **5-78** to **5-81**), leaving ample opportunities for subsequent manipulation via common cross-coupling techniques. The successful preparation of **5-83**, **5-84** and **5-85** indicates that five-membered rings other than pyrrolidinone can be used without significant erosion in yield. Similarly, pyrido-benzoxazinones (**5-82**) are also within reach, albeit in lower

yields. We found that **5-85** was obtained as a single diastereoisomer, whose stereochemistry was confirmed by X-ray crystallographic analysis. Taken together, we believe the results in Figure 5.37 improve significantly on the practicality of methods aimed at promoting a catalytic C(sp^3)-H functionalization/C-O bond formation with carboxylic acids as weak directing groups en route to benzolactones.

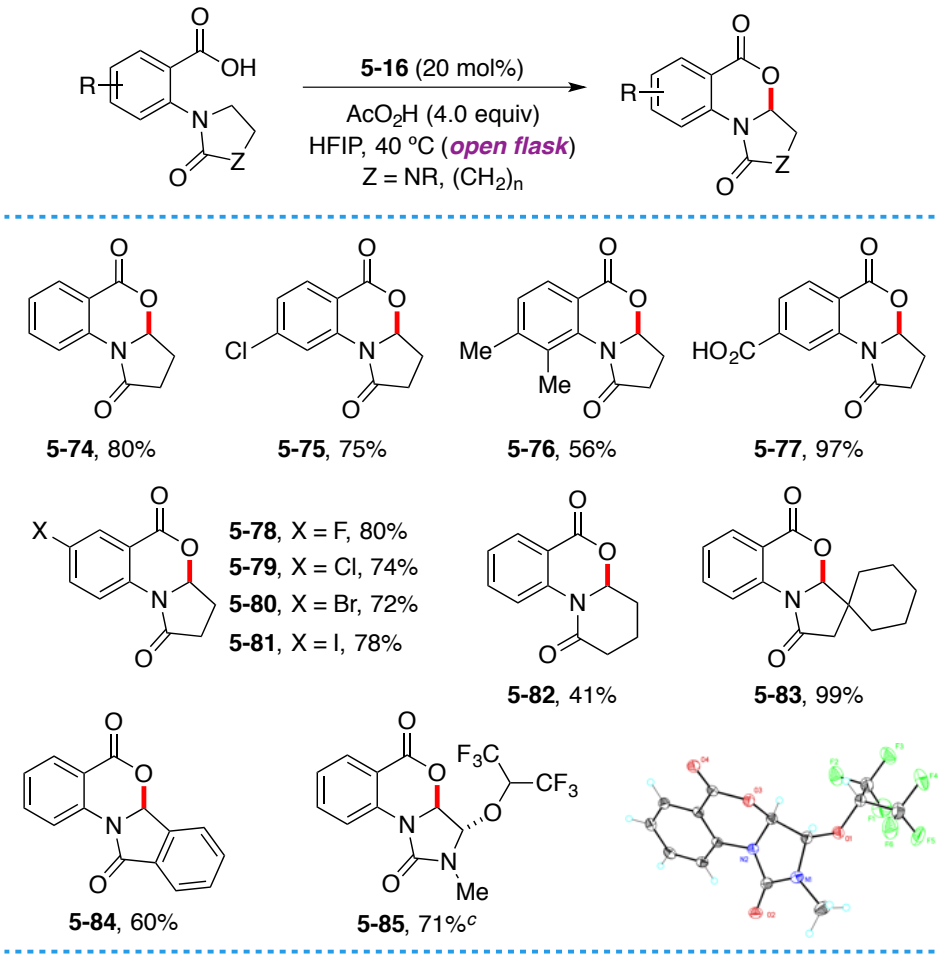

[a] Reaction conditions: **Substrate** (0.2 mmol), **5-16** (20 mol%), HFIP (2 mL), AcO_2H (4.0 equiv), at 40 °C, 24 h, open to air. [b] Isolated yields, average of two independent runs. [c] PIFA (2.5 equiv).

Table 5.15. Substrate scope of C(sp^3)-H functionalization/C-O bond formation.

5.7 Catalyst-controlled Selectivity Switch in the C(sp^2)-H Functionalization

The observed influence of the ArI backbone suggests that site-selectivity could be accomplished under appropriate conditions. As shown in Scheme 2, we found an unprecedented catalyst-controlled selectivity switch when using **5-34** as substrate. Although not yet fully optimized, we found that the use of **5-20** as catalyst resulted in 37% yield of the expected **5-86** together with a minor regioisomer that was initially

assigned as **5-86''**; a careful NMR spectroscopical analysis, however, revealed that our assignment was premature and the minor regioisomer turned out to be **5-86'**, a species not expected through a simple selectivity between the two *ortho*- C-H sites. Intriguingly, structurally the related catalyst **5-16** resulted in a selectivity switch, delivering predominantly **5-86'** in 70% yield. This result might suggest that an incipient positive charge is developed on the electron-rich aromatic ring, thus triggering a [1,2]-aryl shift. The assignment of both **5-86** and **5-86'** was univocally established by X-ray analysis.

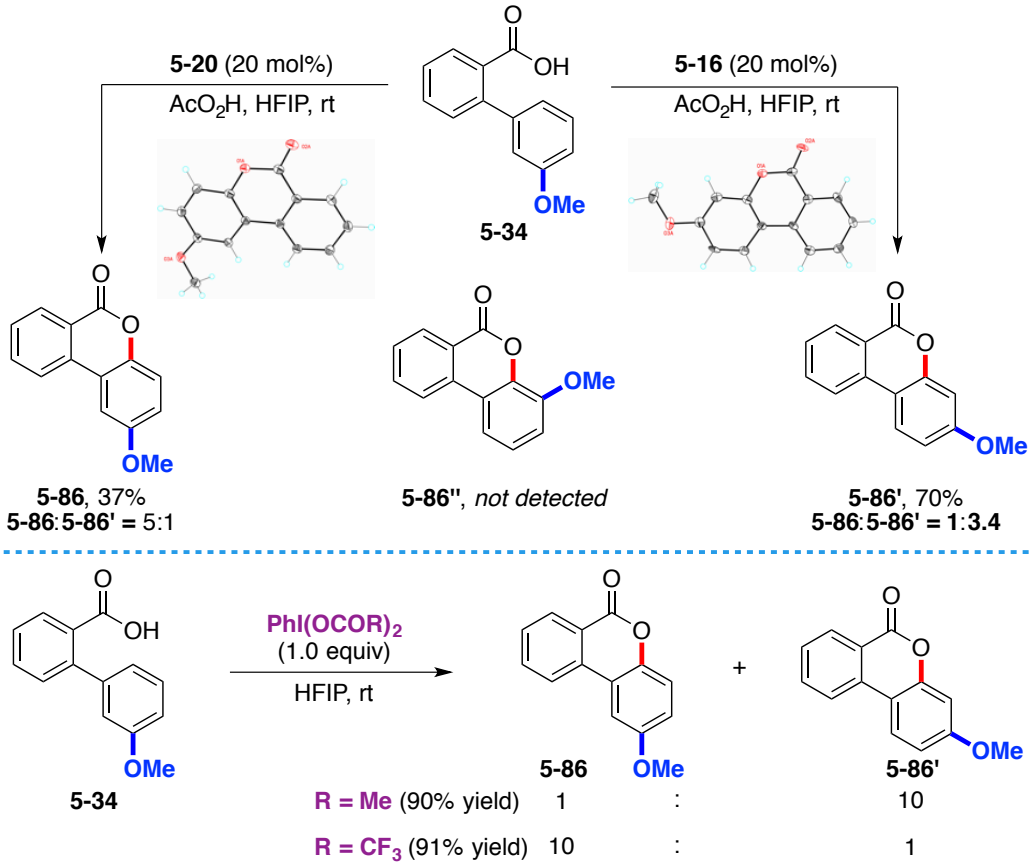

Scheme 5.26. Selectivity switch dictated by the ArI motif.

Interestingly, while PIFA cleanly delivered **5-86**, an opposite selectivity pattern was observed with PIDA (**5-86'**), hence confirming that seemingly trivial modifications have a profound impact on the reaction outcome (Scheme 5.6, bottom). We next wondered whether the nature of the *in situ* generated iodine(III) reagent exerts an influence on the selectivity. We initiated mechanistic studies by synthesizing iodine(III) reagent **5-87** with PIDA and **5-34** (Scheme 5.7).

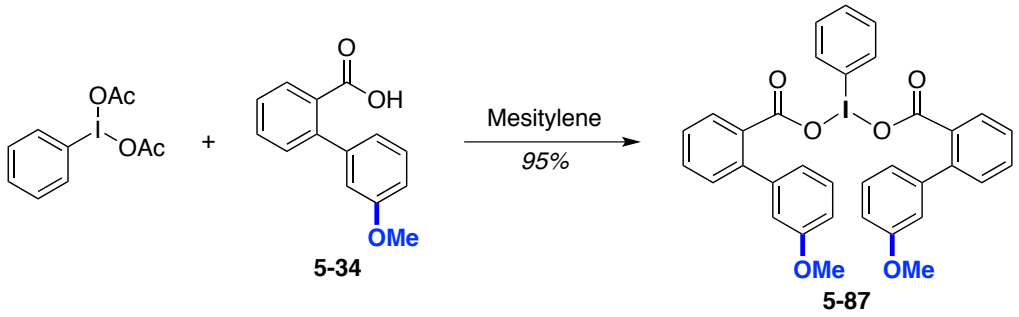

Scheme 5.27. Syntheses of **5-87**.

Having **5-87** in hand, we wondered if we could gain detailed information about the selectivity switching event by investigating its reactivity with or without additives, as presented in Figure 5.38. Remarkably, we could obtain the best selectivity by performing the reaction without additives (**5-86**:**5-86'** = **1**:**17**). While we observed a slight erosion of selectivity with AcOH as additive and almost no selectivity was detected when CF_3CO_2H was employed. It is worth noting that around 50% of starting material were recovered in both cases (Entries b and c). No surprisingly, AcO_2H offered the final product with 3.3:1 selectivity.

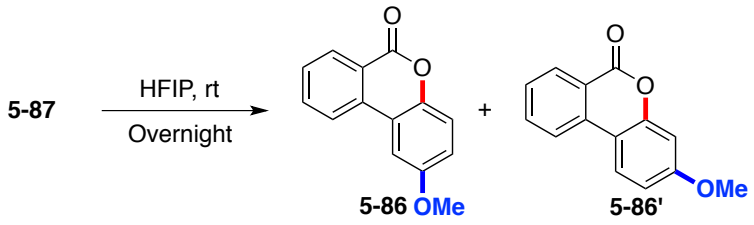

a. Without additive. 44%, **5-86**:**5-86'** = 1:17.

b. AcOH (2 equiv) as additive. 44%, **5-86**:**5-86'** = 1/16. 53% of **5-34** was recovered.

c. CF_3CO_2H (2 equiv) as additive.49%, **5-86**:**5-86'** = 1.2/1, 50% of **5-34** was recovered.

d. AcO_2H (2 equiv, 35% in $MeCO_2H$) as additive. 73%,**5-86**:**5-86'** = 1/3.3.

Scheme 5.28. Reactivity of **5-87** with or without additives.

Taking all the results into consideration, a ligand exchange process might occur. Although a detailed mechanistic picture requires further investigations，we believe that intermediate **5-88** is the true catalyst in our catalytic system and that the RO-moiety plays an important role in the selectivity switching process.

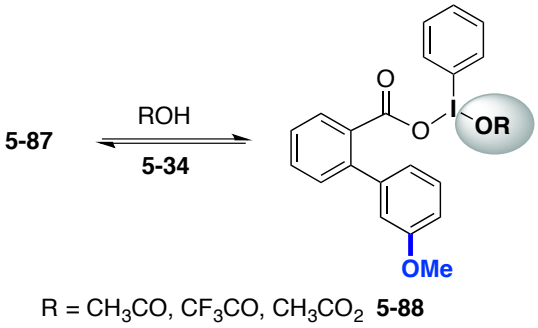

Scheme 5.29. Plausible ligand exchange process.

The role of the AcO_2H was nicely illustrated by careful analysis of the **5-86'**:**5-86** ratio as a function of time when using catalytic amounts of **5-16** (Figure 5.39), clearly evidencing that the concentration of AcO_2H had a profound influence on the **5-86'**:**5-86** ratio. We speculated that AcO_2H might not be a mere spectator and that it could be assuming dual roles, both as an oxidant and as a modulator at the I(III) center.

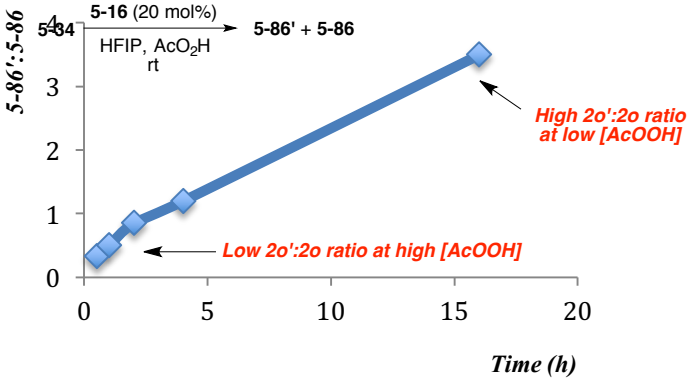

Figure 5.7 Plot of selectivity as a function of time.

Next, we focused our attention on unraveling whether the ArI exerts an influence onto the selectivity switch by studying the reaction of **5-34** with I(III) reagents derived from **5-16** and **5-20**. Interestingly, we found that both **5-89** and **5-90** provided preferentially **5-86'** (Figure, Entries 1 and 5), with **5-89** displaying a slightly better selectivity profile (Entry 1 *vs* Entry 5). It is worth note that the addition of AcO_2H to the reaction that was performed with **5-89** led to worse selectivity and the ratio of **5-86**:**5-86'** dropped significantly (Entries 2 and 3). On the other hand, we observed a selectivity switch when AcO_2H was employed in the reaction that was conducted with **5-90** (Entry 6). We believed those results demonstrate that the Ar moiety of the iodine(III) reagent is also critical for controlling selectivity. Moreover, this selectivity switch was applicable for analogies of **5-34**, and **5-91'**, **5-92'**, and **5-93'** were prepared

in good selectivity.

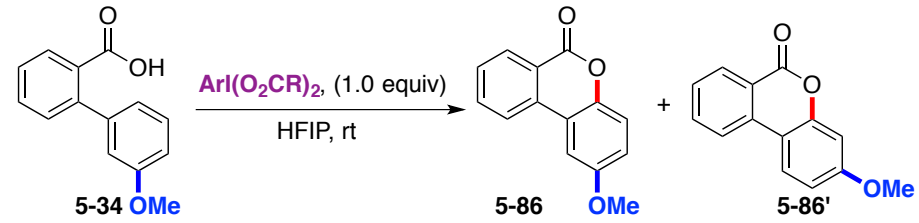

Entry	ArI reagent	Additives (x equiv)	Yield (%)	5-86:5-86'
1	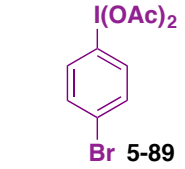	none	83	**1:13.6**
2		AcOOH (0.50)	75	**1:5**
3		AcOOH (2.0)	69	**1:1.2**
4	**5-16** (20 mol%)	AcOOH (2.0)	74	**1:3.4**
5	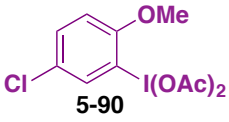	none	75	**1:10**
6		AcOOH (2.0)	50	**3:1**
7	**5-20** (20 mol%)	AcOOH (2.0)	37	**5:1**

*With **5-89***

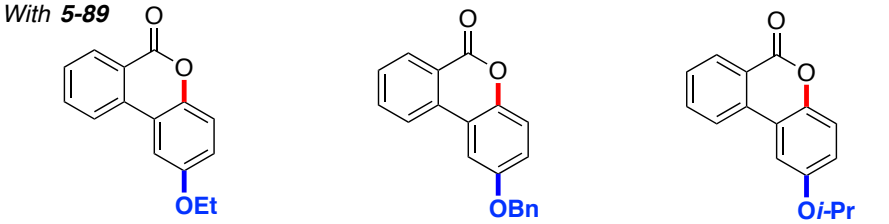

81%, **5-91**:**5-91'** = 1:6.7

80%, **5-92**:**5-92'** = 1:10

76%, **5-93**:**5-93'** = 1:4

Table 5.16. Selectivity profile with I(III) reagents.

Overall, we believe that these results support the intermediacy of a species like **5-95** species within the catalytic cycle, thus revealing an intimate interplay between the ArI motif and non-innocent additives.

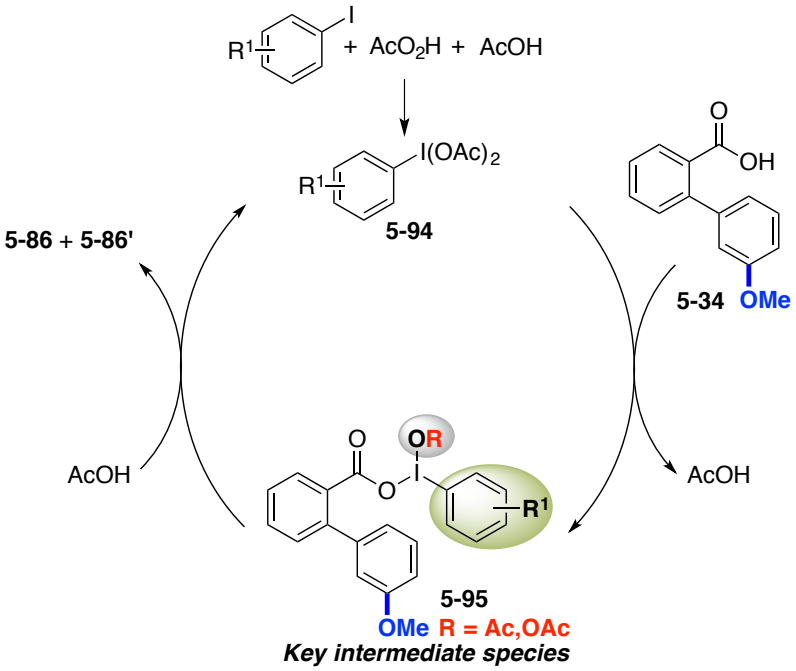

Scheme 5.30. Mechanistic proposal

In light of these results, we wondered whether a related selectivity switch could be applied in other motifs. Gratifyingly, we found that **5-96** followed a distinctive pattern when using **5-16** or **5-17** (Figure 5.42). While one might have anticipated that **5-96** would trigger a C(sp^2)–H functionalization (**5-98**), this was not the case and **5-53** or **5-97** were obtained, an assumption that was confirmed by X-ray analysis.

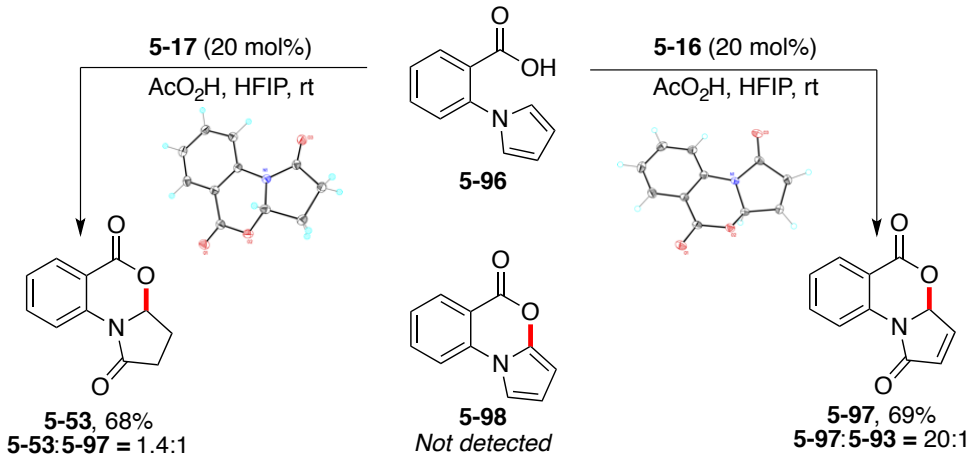

Scheme 5.31. Selectivity Switch for **5-96**.

5.8 Limitations of ArI-catalyzed C-H Functionalization

Besides the examples presented in Table 5.10, we found several limitations of the protocol for ArI-catalyzed C(sp^2)-H functionalization/C-O bond formation as

summarized in Table 5.17. In the case of **5-102**, we obtained a mixture of lactones. Low yields were observed when the substrate of **5-102**, **5-103**, and **5-104** were employed. Other analogies such as from **5-99** to **5-111** did not delivered the corresponding products. We also tried the cyclization lactones formation with alkyl substituted carboxylic acid and C(sp^3)-H functionalization (from **5-116** to **5-122**), however, we did not even traces of product.

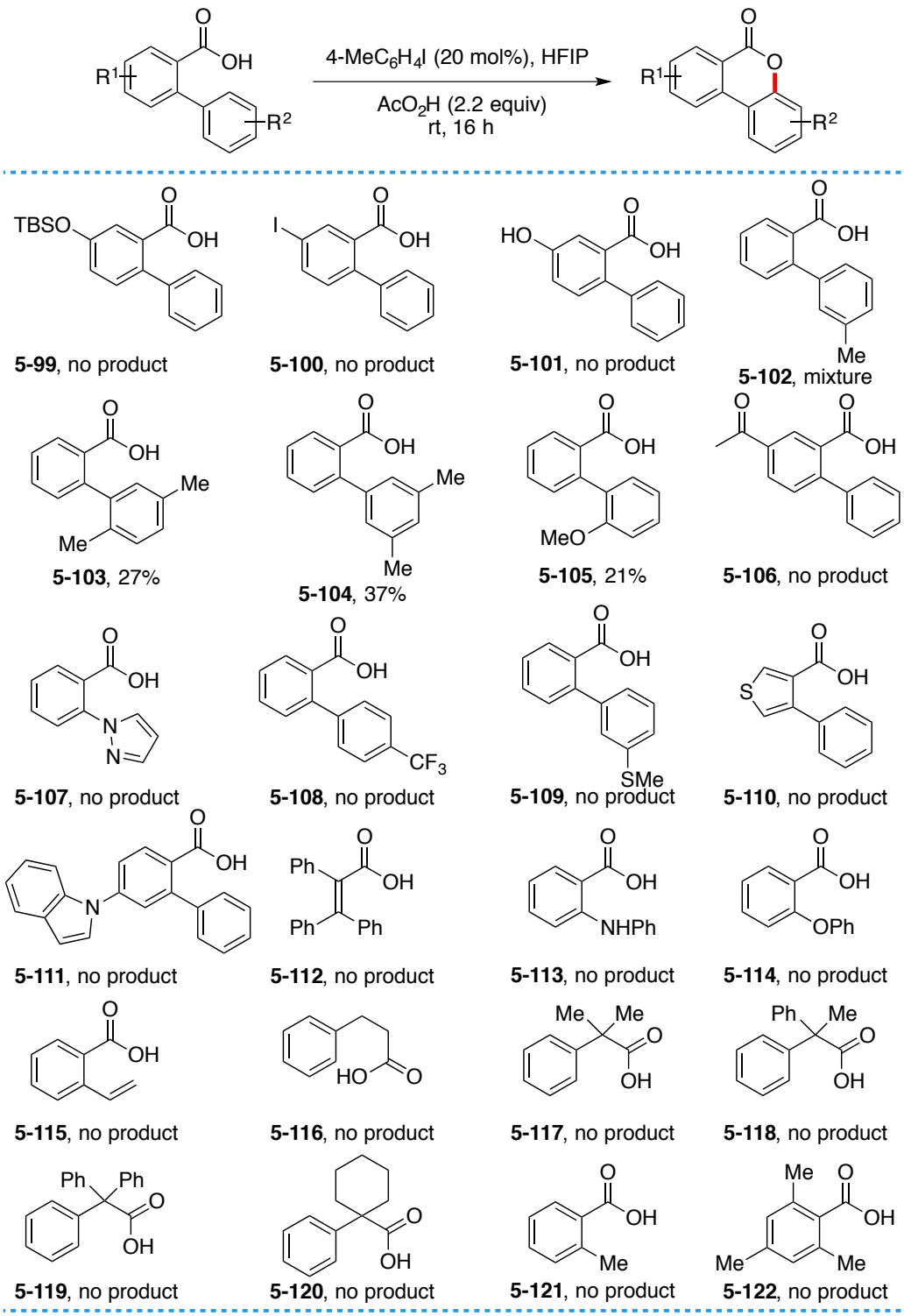

Table 5.17. Limitations of C(sp^2)-H functionalization.

We also found several limitations of ArI-catalyzed C(sp^2)-H functionalization/ C-O bond formation reactions, as shown in Table 5.18. We did not observe when the substrates bearing a 4-membered or 7-membere lactam was used. To our surprise, α-methyl substituent adjacent to nitrogen suppress the reactivity, no desired cyclized

product was obtained (**5-125**). The reactions did not occur when **5-126**, **5-127**, **5-128**, and **5-129** were employed as starting materials, probably the substrates were too electron-poor or too electron-rich. The substrates bearing an acyclic amide such as 5-129, 5-130 were not suitable for this transformation.

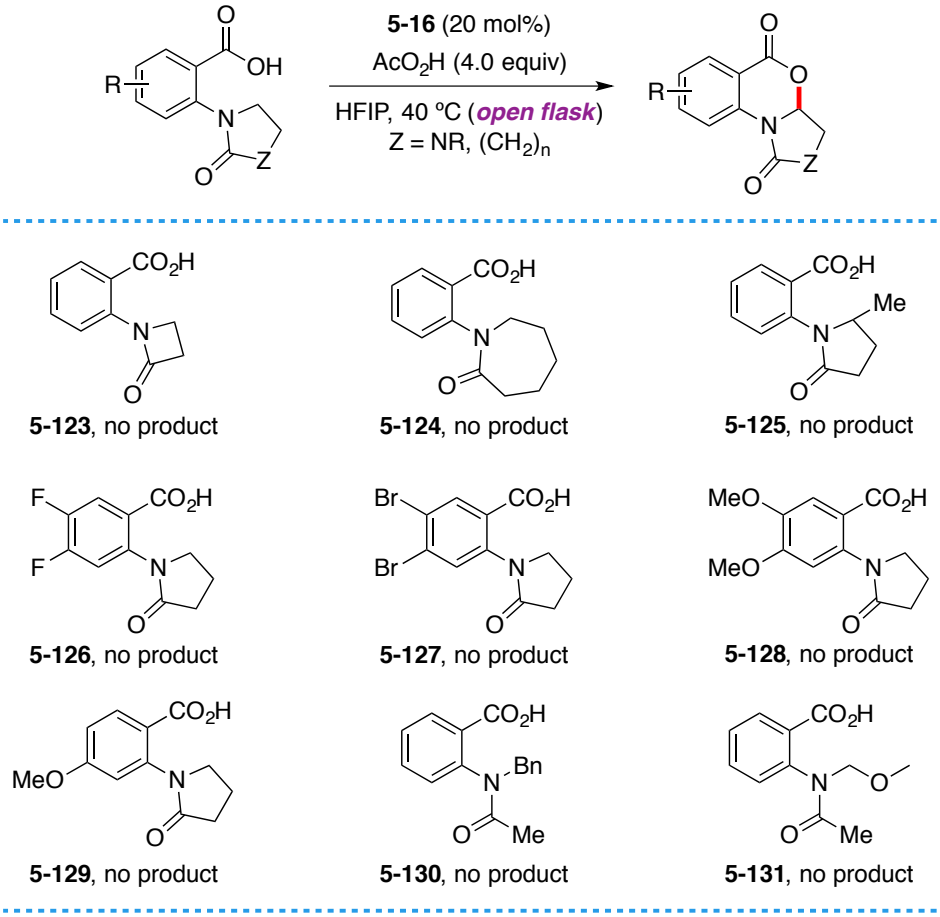

Table 5.17. Limitations of C(sp^3)-H functionalization.

5.9 Conclusion

In summary, we have developed C(sp^2)-H and C(sp^3)-H functionalization/C–O bond-formation reactions catalyzed by *in situ* generated hypervalent I(III) reagents. The reactions occur under mild conditions and with an exquisite and intriguing selectivity profiles depending on the catalyst employed. This new air-insensitive method represents a cheap, practical, and a powerful alternative to related metal-catalyzed protocols.

5.10 Experimental Section

5.10.1 General Considerations

Reagents: All reactions were set up in Schlenk tubes, open to air. All of the commercially available reagents were used without any further purification. Catalyst from **5-11** to **5-21** were purchased from commercial sources and used as received. AcO_2H was purchased from Acros. 1,1,1,3,3,3-hexafluoro- 2-propanol (HFIP) was purchased from Fluorochem, and used as received. 4-bromo(diacetoxyiodo)benzene (**5-89**) was prepared according to literature procedures. Analytical methods: ^{1}H NMR and ^{13}C NMR spectra and melting points (where applicable) are included for all compounds. ^{1}H and ^{13}C NMR spectra were recorded on a Bruker 300 MHz, a Bruker 400 MHz and a Bruker 500 M Hz at 20 °C. All ^{1}H NMR spectra are reported in parts per million (ppm) downfield of TMS and were measured relative to the signals for $CHCl_3$ (7.26 ppm), DMSO (2.50 ppm), CD_3OD (3.31 ppm). All ^{13}C NMR spectra were reported in ppm relative to residual $CHCl_3$ (77.20 ppm) DMSO (39.52 ppm), CD_3OD (49.00 ppm) and were obtained with ^{1}H decoupling. Coupling constants, *J*, are reported in Hertz. Melting points were measured using open glass capillaries in a Büchi B540 apparatus. Infrared spectra were recorded on a Bruker Tensor 27. Mass spectra were recorded on a Waters LCT Premier spectrometer. High Pressure Liquid Chromatographic (HPLC) analyses were performed on Agilent Technologies Model 1260 Infinity HPLC chromatography instrument equipped with Agilent Eclipse Plus C18 (3.5 um, 4.6 x 100 mm) column and UV/V is detector. Flash chromatography was performed with EM Science silica gel 60 (230-400 mesh) and using bromocresol as TLC stain. The yields reported in Figure 5.31 and 5.37 refer to isolated yields and represent an average of at least two independent runs. The procedures described in this section are representative.

5.10.2 Data of C(sp^2)–H Functionalization/C–O Bond Formation

General Procedure A: A Schlenk tube containing a stirring bar was charged with the corresponding benzoic acid (0.20 mmol), 4-methyliodobezene (**5-17**; 8.7 mg, 0.04 mmol, 20 mol%), HFIP (2 mL) and AcO_2H (83.2 µL, 2.20 equiv, 35% in AcOH). The reaction mixture was then stirred at room temperature for 16 h. The solvents were removed under reduced pressure and the crude was purified by column chromatography on silica gel (eluting with hexanes/ethyl acetate mixtures).

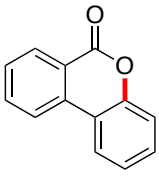

6*H*-benzo[*c*]chromen-6-one (5-10): Following the general procedure, **5-9** was used. Colorless solid. Yield: 38.0 mg, 97%. The spectroscopic data correspond to those previously reported in the literature.[163] ^{1}H NMR (500 MHz, $CDCl_3$) δ 8.33 (dd, *J* = 7.9, 0.9 Hz, 1H), 8.04 (d, *J* = 8.1 Hz, 1H), 7.98 (dd, *J* = 7.9, 1.4 Hz, 1H), 7.77 (dd, *J* = 8.1, 7.3 Hz, 1H), 7.53 (dd, *J* = 8.1, 7.3 Hz, 1H), 7.43 (dd, *J* = 8.5, 7.1 Hz, 1H), 7.33 – 7.26 (m, 2H) ppm. ^{13}C NMR (126 MHz, $CDCl_3$) δ 161.0, 151.1, 134.7, 1345.6, 130.4, 130.3, 128.7, 124.4, 122.6, 121.5, 121.1, 117.9, 117.6 ppm.

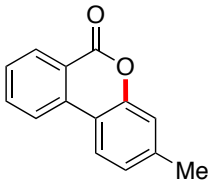

3-methyl-6*H*-benzo[*c*]chromen-6-one (5-39): Following the general procedure, **4'-methyl- [1,1'-biphenyl]-2-carboxylic acid** was used. Colorless solid. Yield: 41.6 mg, 99%. The spectroscopic data correspond to those previously reported in the literature.[2] ^{1}H NMR (500 MHz, $CDCl_3$) δ 8.35 (dd, *J* = 8.0, 1.0 Hz, 1H), 8.04 (dd, *J* = 8.0, 1.0 Hz, 1H), 7.89 (d, *J* = 7.9 Hz, 1H), 7.78 (dd, *J* = 8.2, 7.2 Hz, 1H), 7.52 (dd, *J* = 8.1, 7.3 Hz, 1H), 7.14-7.09 (m, 2H), 2.43 (s, 3H) ppm. ^{13}C NMR (126 MHz, $CDCl_3$) δ 161.5, 151.4, 141.4, 135.1, 134.9, 130.6, 128.5, 125.8, 122.6, 121.6, 121.0, 118.0, 115.5, 21.6 ppm.

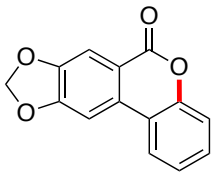

6*H*-[1,3]dioxolo[4',5':4,5]benzo[1,2-*c*]chromen-6-one (5-40): Following the general procedure, **5-22** was used. Colorless solid. 28.8 mg, Yield: 60%. The spectroscopic data correspond to those previously reported in the literature.[164] ^{1}H NMR (400 MHz, $CDCl_3$)

[163] Gallardo-Donaire, J.; Martin, R. *J. Am. Chem. Soc.* **2013**, *135*, 9350.
[164] Lee, T. H.; Jayakumar, J.; Cheng, C, H.; Chuang, S. C. *Chem. Commun.* **2013**, *49*, 11797.

δ 7.86 (d, *J* = 7.9 Hz, 1H), 7.70 (s, 1H), 7.43 (d, *J* = 15.4 Hz, 1H), 7.43 (s, 1H), 7.33 (d, *J* = 16.9 Hz, 1H), 7.29 (d, *J* = 17.6 Hz, 1H), 6.14 (s, 2H) ppm. ^{13}C NMR (101 MHz, $CDCl_3$) δ 160.6, 154.0, 150.7, 148.8, 132.1, 129.8, 124.4, 122.3, 118.1, 117.6, 116.1, 108.4, 102.4, 100.7 ppm.

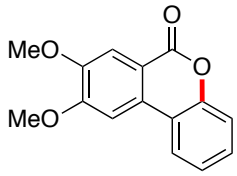

8,9-dimethoxy-6*H*-benzo[*c*]chromen-6-one (5-41): Following the general procedure, using **5-23**, and **5-21** as the catalyst. Colorless solid. Yield: 30.8 mg, 60%. The spectroscopic data correspond to those previously reported in the literature.[165] ^{1}H NMR (400 MHz, $CDCl_3$) δ 7.94 (d, *J* = 7.9 Hz, 1H), 7.74 (s, 1H), 7.44 (d, *J* = 15.4 Hz, 1H), 7.43 (s, 1H), 7.35 (d, *J* = 16.0 Hz, 1H), 7.31 (d, *J* = 15.0 Hz, 1H), 4.09 (s, 3H), 4.00 (s, 3H) ppm. ^{13}C NMR (101 MHz, $CDCl_3$) δ 161.0, 155.1, 151.0, 150.1, 129.9, 129.5, 124.3, 122.1, 118.1, 117.7, 114.5, 110.5, 102.7, 56.3 ppm.

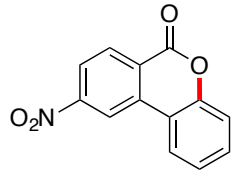

9-nitro-6*H*-benzo[*c*]chromen-6-one (5-42): Following the general procedure A, **5-24** was used. Colorless solid. Yield: 20.7 mg, 43%. The spectroscopic data correspond to those previously reported in the literature.[166] ^{1}H NMR (400 MHz, $CDCl_3$) δ 8.97 (d, *J* = 2.2 Hz, 1H), 8.60 (d, *J* = 8.7 Hz, 1H), 8.36 (dd, *J* = 8.8, 2.3 Hz, 1H), 8.16 (dd, *J* = 8.4, 1.5 Hz, 1H), 7.67-7.55 (m, 1H), 7.52-7.38 (m, 2H) ppm. ^{13}C NMR (101 MHz, $CDCl_3$) δ 159.6, 152.0, 151.8, 136.6, 132.8, 132.3, 125.6, 125.5, 123.5, 122.9, 118.32, 117.5, 116.9 ppm.

[176] Singha, R.; Roy, S.; Nandi, S.; Ray, P.; Ray, J. K. *Tetrahedron Lett.* **2013**, *54*, 657.
[166] Wang, Y.; Gulevich, A. V.; Gevorgyan, V. *Chem. Eur. J.* **2013**, *19*, 15836.

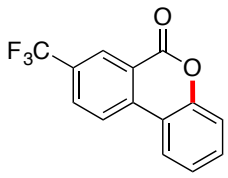

8-(trifluoromethyl)-6*H*-benzo[*c*]chromen-6-one (5-43): Following the general procedure, **5-25** was used with AcO_2H (4.4 equiv) at 80 ºC for 24 h. Colorless solid. Yield: 35.4 mg, 67%. The spectroscopic data correspond to those previously reported in the literature.[167] H NMR (400 MHz, $CDCl_3$) δ 8.65-8.60 (m, 1H), 8.21 (d, *J* = 8.4 Hz, 1H), 8.05 (dd, *J* = 7.9, 1.5 Hz, 1H), 8.01 (dd, *J* = 8.5, 2.0 Hz, 1H), 7.54 (dd, *J* = 8.2, 7.4 Hz, 1H), 7.40-7.33 (m, 2H) ppm. ^{13}C NMR (126 MHz, $CDCl_3$) δ 160.1, 151.8, 137.8, 132.0, 131.1 (q, *J* = 33.9 Hz), 131.4-131.1 (m), 128.1 (q, *J* = 4.1 Hz), 123.5 (q, *J* = 272.7Hz), 125.2, 123.4, 122.8, 121.6, 118.15, 117.0 ppm. ^{19}F NMR (471 MHz, $CDCl_3$) δ -62.91 ppm.

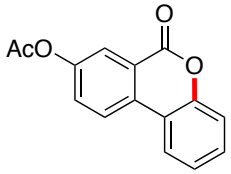

6-oxo-6*H*-benzo[*c*]chromen-8-yl acetate (5-44): Following the general procedure, **5-26** was used. Colorless solid. Yield: 30.0 mg, 59%. The spectroscopic data correspond to those previously reported in the literature. ^{1}H NMR (500 MHz, $CDCl_3$) δ 8.10 – 8.05 (m, 2H), 7.96 (dd, *J* = 7.8, 1.5 Hz, 1H), 7.55 (dd, *J* = 8.7, 2.6 Hz, 1H), 7.45 (dd, *J* = 8.5, 7.2 Hz, 1H), 7.34-7.27 (m, 2H), 2.35 (s, 3H) ppm. ^{13}C NMR (126 MHz, $CDCl_3$) δ 169.1, 160.5, 151.1, 150.9, 132.6, 130.6, 129.0, 124.9, 123.4, 122.9, 122.8, 122.5, 117.9, 117.6, 21.2 ppm.

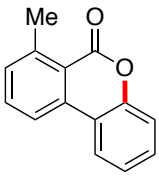

7-methyl-6*H*-benzo[*c*]chromen-6-one (5-45): Following the general procedure, **5-27** was used. Colorless solid. Yield: 31.1 mg, 77%. The spectroscopic data correspond to

[167] Li, Y.; Ding, Y. J.; Wang, J. Y.; Su, Y. M.; Wang, X. S. *Org. Lett.* **2013**, *15*, 2574.

those previously reported in the literature. ^{1}H NMR (400 MHz, $CDCl_3$) δ 7.95 (dd, *J* = 8.0, 1.5 Hz, 1H), 7.91 (d, *J* = 8.1 Hz, 1H), 7.58 (t, *J* = 7.8 Hz, 1H), 7.38 (dd, *J* = 8.5, 7.1 Hz, 1H), 7.30 (dt, *J* = 7.5, 0.9 Hz, 1H), 7.27-7.18 (m, 2H), 2.80 (s, 3H) ppm. ^{13}C NMR (101 MHz, $CDCl_3$) δ 160.6, 151.4, 144.5, 136.2, 134.1, 132.3, 130.4, 124.4, 123.2, 119.9, 119.9, 118.4, 117.4, 24.0 ppm.

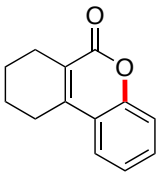

7,8,9,10-tetrahydro-6*H*-benzo[*c*]chromen-6-one (5-46): Following the general procedure, **5-28** was used for 60 h. Colorless solid. Yield: 35.2 mg, 88%. The spectroscopic data correspond to those previously reported in the literature. ^{1}H NMR (300 MHz, $CDCl_3$) δ 7.39 (dd, *J* = 7.9, 1.5 Hz, 1H), 7.28 (dd, *J* = 8.6, 7.1 Hz, 1H), 7.16 – 7.05 (m, 2H), 2.62 (tt, *J* = 6.1, 2.1 Hz, 2H), 2.42 (dt, *J* = 5.9, 4.0 Hz, 2H), 1.68 (m, 4H) ppm. ^{13}C NMR (126 MHz, $CDCl_3$) δ 161.8, 152.1, 147.1, 130.3, 124.1, 123.9, 123.3, 120.3, 116.8, 25.3, 24.2, 21.7, 21.5 ppm.

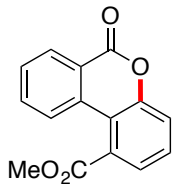

Methyl 6-oxo-6*H*-benzo[*c*]chromene-1-carboxylate (5-47): Following the general procedure, **5-29** was used. Colorless solid. Yield: 20.3 mg, 40%. M.P = 150.0-151.2 °C ^{1}H NMR (400 MHz, $CDCl_3$) δ 8.38 (dd, *J* = 7.9, 1.4 Hz, 1H), 8.20 (dd, *J* = 8.0, 1.6 Hz, 1H), 8.10 (d, *J* = 8.1 Hz, 1H), 7.93 (dd, *J* = 7.7, 1.6 Hz, 1H), 7.83 (dd, *J* = 8.1, 7.3 Hz, 1H), 7.59 (dd, *J* = 7.8, 7.3, Hz, 1H), 7.36 (t, *J* = 7.8 Hz, 1H), 4.00 (s, 3H) ppm. ^{13}C NMR (101 MHz, $CDCl_3$) δ 165.6, 160.0, 149.7, 135.1, 134.2, 132.4, 130.7, 129.5, 126.7, 124.0, 122.0, 121.3, 121.1, 119.0, 52.9 ppm. IR (neat, cm^{-1}): 1740, 1705, 1283, 1050, 718. HRMS *calcd.* for ($C_{15}H_{10}O_4$+1): 255.0652, *found* 255.0651.

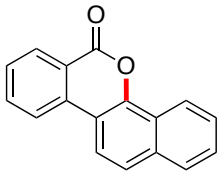

6*H*-dibenzo[*c*,*h*]chromen-6-one (5-48): Following the general procedure, **5-30** was used. *A single regioisomer was obtained.* Colorless solid. Yield: 33.0 mg, 67%. The spectroscopic data correspond to those previously reported in the literature. ^{1}H NMR (400 MHz, $CDCl_3$) δ 8.54 (d, *J* = 8.2 Hz, 1H), 8.43 (d, *J* = 8.2 Hz, 1H), 8.14 (d, *J* = 8.1 Hz, 1H), 8.00 (d, *J* = 8.8 Hz, 1H), 7.87-7.80 (m, 2H), 7.72 (d, *J* = 8.7 Hz, 1H), 7.64-7.54 (m, 3H) ppm. ^{13}C NMR (101 MHz, $CDCl_3$) δ 161.3, 147.4, 135.5, 135.1, 134.4, 130.7, 128.7, 128.0, 127.8, 127.2, 124.6, 124.0, 122.4, 122.1, 121.3, 119.3, 113.1 ppm.

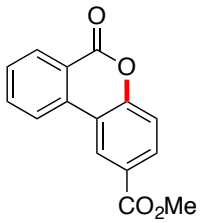

Methyl 6-oxo-6*H*-benzo[*c*]chromene-2-carboxylate (5-49): Following the general procedure, **5-31** was used. *A single regioisomer was obtained* Colorless solid. Yield: 31.0 mg, 61%. The spectroscopic data correspond to those previously reported in the literature.[5] ^{1}H NMR (400 MHz, $CDCl_3$) δ 8.76 (d, *J* = 2.0 Hz, 1H), 8.39 (dd, *J* = 8.0, 1.5 Hz, 1H), 8.21 (dd, *J* = 8.1, 1.1 Hz, 1H), 8.12 (dd, *J* = 8.6, 2.0 Hz, 1H), 7.86 (dd, *J* = 8.1, 7.3 Hz, 1H), 7.62 (dd. *J* = 7.9, 7.3 Hz, 1H), 7.39 (dd, *J* = 8.7, 0.4 Hz, 1H), 3.97 (s, 3H) ppm. ^{13}C NMR (101 MHz, $CDCl_3$) δ 166.2, 160.6, 154.3, 135.3, 134.2, 131.6, 130.8, 129.7, 126.7, 125.2, 122.2, 121.3, 118.2, 118.1, 52.6 ppm.

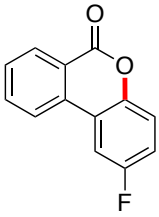

2-fluoro-6*H*-benzo[*c*]chromen-6-one (5-50): Following the general procedure A, **5-32** was used. *A single regioisomer was obtained*. Colorless solid. Yield: 33.0 mg, 77%. The spectroscopic data correspond to those previously reported in the literature.[5] ^{1}H

NMR (400 MHz, $CDCl_3$) δ 8.39 (d, J = 7.9 Hz, 1H), 8.00 (d, J = 8.2 Hz, 1H), 7.83 (dd, J = 8.1, 7.3 Hz, 1H), 7.68 (dd, J = 9.1, 2.9 Hz, 1H), 7.61 (dd, J = 8.2, 7.4 Hz, 1H), 7.32 (dd, J = 9.0, 4.7 Hz, 1H), 7.17 (dd, J = 9.0, 7.7 Hz, 1H) ppm. ^{13}C NMR (101 MHz, $CDCl_3$) δ 160.9, 159.4 (d, J = 244.4 Hz), 147.5 (d, J = 3.0 Hz), 135.1, 134.0 (d, J = 2.0 Hz), 130.8, 129.7, 122.0, 121.4, 119.4 (d, J = 9.1 Hz), 119.4 (d, J = 9.1 Hz), 117.8 (d, J = 24.0 Hz), 108.9 (d, J = 25.3 Hz) ppm. ^{19}F NMR (376 MHz, $CDCl_3$) δ -117.26 (td, J = 8.5, 4.7 Hz) ppm.

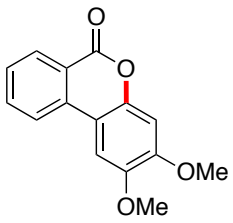

2,3-dimethoxy-6*H*-benzo[*c*]chromen-6-one (5-51): Following the general procedure, but using **5-33** and PIFA (1.0 equiv), under argon. *A single regioisomer was obtained*. Colorless solid. Yield: 39.0 mg, 76%. The spectroscopic data correspond to those previously reported in the literature.[2] ^{1}H NMR (500 MHz, $CDCl_3$) δ 8.23 (d, J = 7.9 Hz, 1H), 7.82 (d, J = 8.0 Hz, 1H), 7.69 (dd, J = 8.1, 7.2 Hz, 1H), 7.40 (dd, J = 8.1, 7.2 Hz, 1H), 7.24 (s, 1H), 6.70 (s, 1H), 3.93 (s, 3H), 3.87 (s, 3H) ppm. ^{13}C NMR (126 MHz, $CDCl_3$) δ 161.5, 151.4, 146.4, 146.2, 135.0, 134.7, 130.5, 127.6, 121.0, 120.1, 109.9, 103.8, 100.7, 56.4, 56.2 ppm.

5.10.3 Data of C(sp^3)–H Functionalization/ C–O Bond Formation

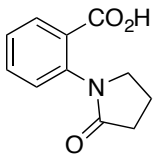

2-(2-oxoprrolidin-1-yl)benzoic acid (5-52): Colorless solid. The spectroscopic data correspond to those previously reported in the literature.[168] ^{1}H NMR (400 MHz, DMSO-d_6) δ 7.79 (dd, J = 7.8, 1.6 Hz, 1H), 7.59 (td, J = 7.7, 1.6 Hz, 1H), 7.41 – 7.30 (m, 2H), 3.76 (t, J = 6.9 Hz, 2H), 2.33 (t, J = 8.0 Hz, 2H), 2.09 (t, J = 7.8, 7.4 Hz, 2H) ppm. ^{13}C NMR (101 MHz, DMSO-d_6) δ 174.2, 167.3, 138.3, 132.5, 130.4, 129.4, 127.1,

[168] Giri, R.; Lam, J. K.; Yu J. Q. *J. Am. Chem. Soc.* **2010**, *132*, 686.

126.9, 50.4, 31.3, 18.6 ppm.

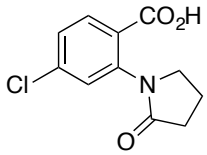

4-chloro-2-(2-oxopyrrolidin-1-yl)benzoic acid (5-61): Colorless solid. M.P. = 216.4–217.9 °C. ^{1}H NMR (500 MHz, DMSO-d_6) δ 7.78 (d, J = 8.4 Hz, 1H), 7.51 (d, J = 2.1 Hz, 1H), 7.44 (dd, J = 8.4, 2.1 Hz, 1H), 3.79 (t, J = 6.9 Hz, 2H), 2.34 (t, J = 8.0 Hz, 2H), 2.09 (t, J = 7.4 Hz, 2H) ppm. ^{13}C NMR (126 MHz, DMSO-d_6) δ 174.1, 166.5, 139.6, 136.4, 131.9, 128.1, 126.7, 126.6, 50.0, 31.1, 18.5 ppm. IR (neat, cm^{-1}): 1706, 1625, 1261, 1106, 802. HRMS *calcd.* for ($C_{11}H_{10}ClNO_3$-1): 238.0276, *found* 238.0274.

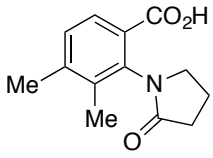

3,4-dimethyl-2-(2-oxopyrrolidin-1-yl)benzoic acid (5-62): Colorless solid. M. P. = 245.8–247.2 °C. ^{1}H NMR (500 MHz, DMSO-d_6) δ 7.64 (d, J = 7.9 Hz, 1H), 7.25 (d, J = 7.9 Hz, 1H), 3.62-3.50 (m, 2H), 2.37 (dd, J = 16.3, 8.8 Hz, 1H), 2.30 (s, 3H), 2.29-2.21 (m, 1H), 2.19-2.09 (m, 2H), 2.08 (s, 3H) ppm. ^{13}C NMR (126 MHz, DMSO-d_6) δ 174.7, 167.1, 142.4, 137.3, 136.1, 128.8, 128.3, 127.3, 49.6, 30.8, 20.4, 18.9, 13.6 ppm. IR (neat, cm^{-1}): 1707, 1628, 1230, 751, 510. HRMS *calcd.* for ($C_{13}H_{15}NO_3$-1): 232.0979, *found* 232.0978.

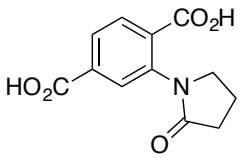

2-(2-oxopyrrolidin-1-yl)terephthalic acid (5-63): Colorless solid. M.P. = 274.2-276.3 °C. ^{1}H NMR (400 MHz, DMSO-d_6) δ 7.90 (dd, J = 8.1, 1.5 Hz, 1H), 7.88-7.85 (m, 2H), 3.81 (t, J = 6.9 Hz, 2H), 2.35 (t, J = 8.0 Hz, 2H), 2.10 (t, J = 7.8, 7.3 Hz, 2H) ppm. ^{13}C NMR (101 MHz, DMSO-d_6) δ 174.3, 166.9, 166.3, 138.3, 134.3, 133.2, 130.6, 127.4, 127.3, 50.1, 31.2, 18.6 ppm. IR (neat, cm^{-1}): 1722, 1690, 1633, 1302, 1213, 759. HRMS *calcd.* for ($C_{12}H_{11}NO_5$-1): 248.0564, *found* 248.0573.

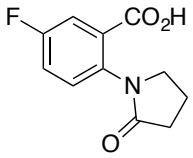

5-fluoro-2-(2-oxopyrrolidin-1-yl)benzoic acid (5-64): Colorless solid. M.P. = 173.0-173.9 °C. ^{1}H NMR (400 MHz, DMSO-d_6) δ 7.55 (dd, J = 9.1, 2.9 Hz, 1H), 7.50-7.39 (m, 2H), 3.74 (t, J = 6.9 Hz, 2H), 2.32 (t, J = 8.0 Hz, 2H), 2.09 (t, J = 7.8, 7.4 Hz, 2H) ppm. ^{13}C NMR (101 MHz, DMSO-d_6) δ 174.3, 166.1 (d, J = 2.2 Hz), 159.9 (d, J = 245.0 Hz), 134.6 (d, J = 3.0 Hz), 131.3 (d, J = 7.4 Hz), 129.6 (d, J = 8.2 Hz), 119.3 (d, J = 22.3 Hz), 116.8 (d, J = 24.1 Hz), 50.3, 31.1, 18.5 ppm. ^{19}F NMR (376 MHz, DMSO-d_6) δ -114.7 (td, J = 8.5, 5.3 Hz) ppm. IR (neat, cm^{-1}): 1711, 1613, 1240, 1163, 529. HRMS *calcd.* for ($C_{11}H_{10}FNO_3$-1): 222.0572, *found* 222.0573.

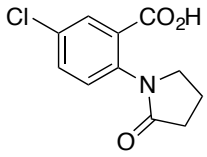

5-chloro-2-(2-oxopyrrolidin-1-yl)benzoic acid (5-65): Colorless solid. M. P. = 171.3-173.8 °C. ^{1}H NMR (400 MHz, DMSO-d_6) δ 7.74 (d, J = 2.6 Hz, 1H), 7.66 (dd, J = 8.5, 2.6 Hz, 1H), 7.40 (d, J = 8.5 Hz, 1H), 3.76 (t, J = 6.9 Hz, 2H), 2.34 (t, J = 8.0 Hz, 2H), 2.09 (t, J = 7.3 Hz, 2H) ppm. ^{13}C NMR (101 MHz, DMSO-d_6) δ 174.6, 166.5, 137.4, 132.5, 131.5, 131.2, 130.2, 129.1, 50.4, 31.6, 18.9 ppm. IR (neat, cm^{-1}): 1715, 1629, 1216, 850, 538. HRMS *calcd.* for ($C_{11}H_{10}ClNO_3$-1): 238.0276, *found* 238.0283.

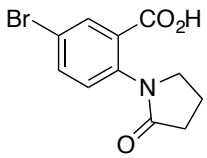

5-bromo-2-(2-oxopyrrolidin-1-yl)benzoic acid (5-66): Colorless solid. M.P. = 213.0-215.9 °C. ^{1}H NMR (400 MHz, DMSO-d_6) δ 7.86 (d, J = 2.4 Hz, 1H), 7.77 (dd, J = 8.5, 2.4 Hz, 1H), 7.32 (d, J = 8.5 Hz, 1H), 3.75 (t, J = 6.9 Hz, 2H), 2.32 (t, J = 8.0 Hz, 2H), 2.08 (t, J = 7.6 Hz, 2H) ppm. ^{13}C NMR (101 MHz, DMSO-d_6) δ 174.5, 166.2, 137.5, 135.2, 132.8, 131.4, 129.1, 119.1, 50.2, 31.3, 18.6 ppm. IR (neat, cm^{-1}): 1713, 1625, 1214, 1123, 893. HRMS *calcd.* for ($C_{11}H_{10}BrNO_3$-1): 281.9771, *found* 281.9763.

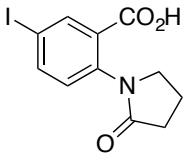

5-iodo-2-(2-oxopyrrolidin-1-yl)benzoic acid (5-67): Colorless solid. M. P. = 254.8-257.2 °C. ^{1}H NMR (400 MHz, DMSO-d_6) δ 8.04 (d, J = 2.1 Hz, 1H), 7.93 (dd, J = 8.4, 2.2 Hz, 1H), 7.17 (d, J = 8.3 Hz, 1H), 3.75 (t, J = 6.9 Hz, 2H), 2.33 (t, J = 8.0 Hz, 2H), 2.08 (t, J = 7.3 Hz, 2H) ppm. ^{13}C NMR (101 MHz, DMSO-d_6) δ 174.1, 165.9, 140.8, 138.4, 137.8, 131.2, 128.8, 91.4, 49.9, 31.2, 18.4 ppm. IR (neat, cm^{-1}): 1712, 1619, 1486, 1210, 849. HRMS *calcd.* for ($C_{11}H_{10}INO_3$-1): 329.9633, *found* 329.9621.

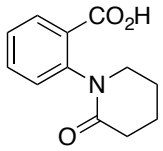

2-(2-oxopiperidin-1-yl)benzoic acid (5-58): Colorless solid. M. P. = 193.6-197.6 °C. ^{1}H NMR (500 MHz, $CDCl_3$) δ 7.99 (dd, J = 7.8, 1.6 Hz, 1H), 7.57 (td, J = 7.7, 1.6 Hz, 1H), 7.37 (td, J = 7.7, 1.1 Hz, 1H), 7.22 (dd, J = 8.0, 1.2 Hz, 1H), 3.63 (s, 2H), 2.61 (d, J = 55.2 Hz, 2H), 1.95 (s, 4H) ppm. ^{13}C NMR (126 MHz, $CDCl_3$) δ 172.4, 168.3, 143.1, 133.7, 131.9, 128.8, 128.5, 127.9, 52.3, 32.7, 23.4, 21.1 ppm. IR (neat, cm^{-1}): 1697, 1598, 1566, 1229, 769. HRMS *calcd.* for ($C_{12}H_{13}NO_3$-1): 218.0823, *found* 218.0828.

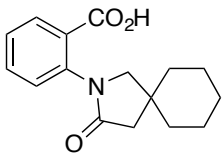

2-(3-oxo-2-azaspiro[4.5]decan-2-yl)benzoic acid (5-68): Colorless solid. M. P. = 152.7-154.6°C. ^{1}H NMR (400 MHz, DMSO-d_6) δ 7.74 (dd, J = 7.8, 1.6 Hz, 1H), 7.57 (td, J = 7.7, 1.6 Hz, 1H), 7.38-7.29 (m, 2H), 3.57 (s, 2H), 2.23 (s, 2H), 1.66-1.33 (m, 10H) ppm. ^{13}C NMR (101 MHz, DMSO-d_6) δ 172.8, 167.4, 137.8, 132.2, 130.1, 129.3, 126.4, 126.0, 60.6, 44.0, 36.3, 36.0, 25.4, 22.4 ppm. IR (neat, cm^{-1}): 1722, 1658, 1235, 1122, 766. HRMS *calcd.* for ($C_{16}H_{19}NO_3$-1): 272.1292, *found* 272.1291.

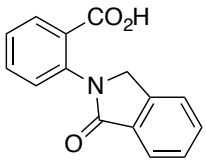

2-(1-oxoisoindolin-2-yl)benzoic acid (5-100). Colorless solid. Yield: 45%. The spectroscopic data correspond to those previously reported in the literature.[169] ^{1}H NMR (400 MHz, DMSO-d_6) δ 7.86 (dd, J = 7.8, 1.6 Hz, 1H), 7.75 (dd, J = 7.7, 1.0 Hz, 1H), 7.71-7.64 (m, 3H), 7.61-7.51 (m, 2H), 7.47 (td, J = 7.6, 1.3 Hz, 1H), 4.92 (s, 2H) ppm. ^{13}C NMR (101 MHz, DMSO-d_6) δ 167.2, 142.1, 137.4, 132.5, 132.0, 131.9, 130.4, 129.8, 128.1, 127.8, 127.2, 123.5, 123.2, 52.5 ppm.

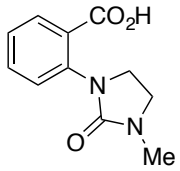

2-(3-methyl-2-oxoimidazolidin-1-yl)benzoic acid (5-73): Colorless solid. M.P. = 199.2-201.3 °C. ^{1}H NMR (500 MHz, DMSO-d_6) δ 7.68 (dd, J = 7.8, 1.7 Hz, 1H), 7.52 (dd, J = 7.7, 1.7 Hz, 1H), 7.37 – 7.19 (m, 2H), 3.78 (dd, J = 8.9, 6.7 Hz, 2H), 3.42 (dd, J = 8.9, 6.7 Hz, 2H), 2.72 (s, 3H) ppm. ^{13}C NMR (126 MHz, DMSO-d_6) δ 167.8, 158.5, 138.9, 131.8, 130.0, 129.0, 125.2, 125.0, 44.6, 44.4, 31.1 ppm. IR (neat, cm^{-1}): 2919, 1721, 1641, 1227, 1120, 796. HRMS *calcd.* for ($C_{11}H_{12}BrN_2O_3$-1): 219.0775, *found* 219.0773.

General procedure B for the I6-catalyzed C(sp^3)-H functionalization/C-O bond-formation (Figure 5.37). A Schlenk tube containing a stirring bar was charged with the corresponding benzoic acid (0.20 mmol), 4-bromoiodobezene (**5-16;** 11.4 mg, 0.04 mmol, 20 mol%), HFIP (1.5 mL) and AcO_2H (4.0 equiv, 35% in AcOH). The reaction mixture was then stirred at 40 ºC for 36 h. The solvents were concentrated under reduced pressure and the crude was purified by column chromatography on silica gel (eluting with hexanes/ethyl acetate/dichloromethane mixtures).

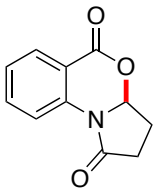

3,3a-dihydro-1*H*-benzo[*d*]pyrrolo[2,1-*b*][1,3]oxazine-1,5(2*H*)-dione (5-53): Following the general procedure B, **5-52** was used. Colorless solid. Yield: 32.5 mg,

[169] Chen, Y.; Li, H.; Cai, S. L. *Chem. Commun.* **2009**, 5392.

80%. The spectroscopic data correspond to those previously reported in the literature.[170] ^{1}H NMR (400 MHz, $CDCl_3$) δ 8.09 (dd, *J* = 7.9, 1.5 Hz, 1H), 8.05 (dd, *J* = 8.1, 1.1 Hz, 1H), 7.67 (dd, *J* = 8.2, 7.4 Hz, 1H), 7.33 (td, *J* = 7.7, 1.1 Hz, 1H), 5.94 (dd, *J* = 6.4, 3.6 Hz, 1H), 2.88-2.73 (m, 1H), 2.73-2.55 (m, 2H), 2.49-2.34 (m, 1H) ppm. ^{13}C NMR (101 MHz, $CDCl_3$) δ 171.9, 162.5, 137.8, 135.6, 130.9, 126.1, 120.1, 116.8, 87.6, 29.6, 24.4 ppm.

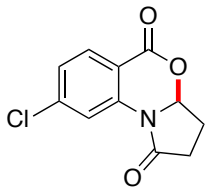

8-chloro-3,3a-dihydro-1*H*-benzo[*d*]pyrrolo[2,1-*b*][1,3]oxazine-1,5(2*H*)-dione (5-75): Following the general procedure B, **5-61** was used. Colorless solid. M. P. = 182.6–185.0 °C. Yield: 35.6 mg, 75%. ^{1}H NMR (500 MHz, $CDCl_3$) δ 8.11 (d, *J* = 2.0 Hz, 1H), 8.01 (d, *J* = 8.4 Hz, 1H), 7.30 (dd, *J* = 8.4, 2.0 Hz, 1H), 5.92 (dd, *J* = 6.6, 4.0 Hz, 1H), 2.85-2.75 (m, 1H), 2.71-2.61 (m, 2H), 2.46-2.36 (m, 1H) ppm. ^{13}C NMR (126 MHz, $CDCl_3$) δ 171.7, 161.8, 142.2, 138.5, 132.1, 126.6, 120.1, 114.8, 87.5, 29.5, 24.4 ppm. IR (neat, cm^{-1}): 1744, 1698, 1437, 1205, 1047, 777. HRMS *calcd.* for ($C_{11}H_8NO_3$+1): 238.0265, *found* 238.0260.

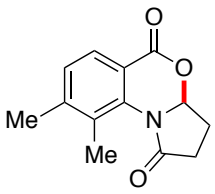

8,9-dimethyl-3,3a-dihydro-1*H*-benzo[*d*]pyrrolo[2,1-*b*][1,3]oxazine-1,5(2*H*)-dione (5-76): Following the general procedure, **5-62** was used. Colorless solid. M. P. = 140.7–142.5 °C. Yield: 25.9 mg, 56%. ^{1}H NMR (500 MHz, $CDCl_3$) δ 7.85 (d, *J* = 7.9 Hz, 1H), 7.23 (d, *J* = 7.9 Hz, 1H), 5.90 (dd, *J* = 5.7, 0.7 Hz, 1H), 2.80 (dd, *J* = 17.9, 9.7 Hz, 1H), 2.67 (dd, *J* = 17.9, 9.8 Hz, 1H), 2.61-2.45 (m, 2H), 2.39 (s, 3H), 2.23 (s, 3H) ppm. ^{13}C NMR (126 MHz, $CDCl_3$) δ 174.2, 163.4, 146.3, 136.7, 132.3, 129.2, 127.9, 118.3, 89.5, 28.7, 24.7, 21.2, 15.7 ppm. IR (neat, cm^{-1}): 1714, 1284, 1105, 976, 849. HRMS *calcd.* for ($C_{13}H_{13}NO_3$+Na): 254.0788, *found* 254.0786.

[170] Franck, R. W.; Auercach, J. *J. Org. Chem.* **1971**, *36*, 31.

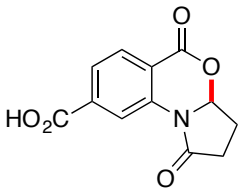

1,5-dioxo-2,3,3a,5-tetrahydro-1*H*-benzo[*d*]pyrrolo[2,1-*b*][1,3]oxazine-8-carboxylic acid (5-77): Following the general procedure, **5-63** was used. Colorless solid. M. P. = 248.2-250.3 °C. Yield: 47.9 mg, 97%. ^{1}H NMR (500 MHz, CD_3OD) δ 8.66 (s, 1H), 8.13 (d, *J* = 8.2 Hz, 1H), 7.95 (d, *J* = 7.9 Hz, 1H), 6.10 (dd, *J* = 6.3, 4.0 Hz, 1H), 2.83-2.63 (m, 3H), 2.34 (ddt, *J* = 12.7, 10.5, 5.3 Hz, 1H) ppm. ^{13}C NMR (126 MHz, CD_3OD) δ 174.2, 168.0, 163.6, 139.2, 138.3, 131.6, 127.3, 121.9, 121.0, 89.5, 30.3, 25.1 ppm. IR (neat, cm^{-1}): 1655, 1611, 1440, 1208, 753. HRMS *calcd.* for ($C_{12}H_9NO_5$-1): 246.0408, *found* 246.0408.

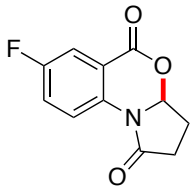

7-fluoro-3,3a-dihydro-1*H*-benzo[*d*]pyrrolo[2,1-*b*][1,3]oxazine-1,5(2*H*)-dione (5-78): Following the general procedure, **5-64** was used. Colorless solid. M. P. = 137.2-139.3 °C. Yield: 35.4 mg, 80%. ^{1}H NMR (400 MHz, $CDCl_3$) δ 8.04 (dd, *J* = 9.0, 4.6 Hz, 1H), 7.76 (dd, *J* = 8.1, 3.0 Hz, 1H), 7.38 (dd, *J* = 9.0, 7.9 Hz, 1H), 5.95-5.92 (m, 1H), 2.86-2.74 (m, 1H), 2.73-2.58 (m, 2H), 2.50-2.34 (m, 1H) ppm. ^{13}C NMR (101 MHz, $CDCl_3$) δ 171.8, 161.5 (d, *J* = 2.6 Hz), 160.0 (d, *J* = 248.0 Hz), 134.1 (d, *J* = 2.7 Hz), 123.0 (d, *J* = 23.3 Hz), 122.3 (d, *J* = 7.6 Hz), 118.5 (d, *J* = 7.7 Hz), 117.0 (d, *J* = 24.4 Hz), 87.9, 29.4, 24.3 ppm. ^{19}F NMR (376 MHz, $CDCl_3$) δ -113.6 (td, *J* = 8.0, 4.6 Hz) ppm. IR (neat, cm^{-1}): 1711, 1495, 1402, 1218, 887. HRMS *calcd.* for ($C_{11}H_8FNO_3$+1): 222.0561, *found* 222.0565.

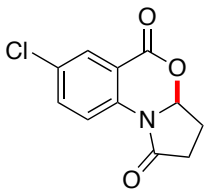

7-chloro-3,3a-dihydro-1*H*-benzo[*d*]pyrrolo[2,1-*b*][1,3]oxazine-1,5(2*H*)-dione (5-

79): Following the general procedure, **5-65** was used. Colorless solid. M. P. = 137.2-139.3 °C. Yield: 35.2 mg, 74%. ^{1}H NMR (400 MHz, $CDCl_3$) δ 8.07 (dd, *J* = 2.5, 0.4 Hz, 1H), 8.04 (dd, *J* = 8.8, 0.4 Hz, 1H), 7.63 (dd, *J* = 8.7, 2.5 Hz, 1H), 5.95-5.90 (m, 1H), 2.87-2.74 (m, 1H), 2.75-2.59 (m, 2H), 2.49-2.36 (m, 1H) ppm. ^{13}C NMR (101 MHz, $CDCl_3$) δ 171.7, 161.4, 136.3, 135.7, 131.8, 130.5, 121.6, 118.0, 87.6, 29.5, 24.4 ppm. IR (neat, cm^{-1}): 1742, 1716, 1480, 1388, 1202, 842. HRMS *calcd.* for ($C_{11}H_8ClNO_3$+1): 238.0265, *found* 238.0264.

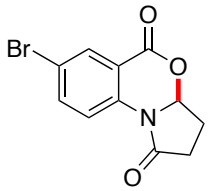

7-bromo-3,3a-dihydro-1*H*-benzo[*d*]pyrrolo[2,1-*b*][1,3]oxazine-1,5(2*H*)-dione (5-80): Following the general procedure, **5-66** was used. Colorless solid. M. P. = 134.2–135.9 °C. Yield: 40.6 mg, 72%. ^{1}H NMR (400 MHz, $CDCl_3$) δ 8.19 (d, *J* = 2.3 Hz, 1H), 7.95 (d, *J* = 8.7 Hz, 1H), 7.75 (dd, *J* = 8.7, 2.3 Hz, 1H), 5.96-5.86 (m, 1H), 2.87-2.72 (m, 1H), 2.72-2.59 (m, 2H), 2.48-2.33 (m, 1H) ppm. ^{13}C NMR (101 MHz, $CDCl_3$) δ 171.7, 161.2, 138.4, 136.7, 133.4, 121.7, 119.1, 118.1, 87.5, 29.5, 24.3 ppm. IR (neat, cm^{-1}): 1711, 1479, 1396, 1201, 842, 526. HRMS *calcd.* for ($C_{11}H_8BrNO_3$+Na): 303.9580, *found* 303.9580.

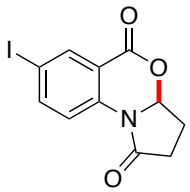

7-iodo-3,3a-dihydro-1*H*-benzo[*d*]pyrrolo[2,1-*b*][1,3]oxazine-1,5(2*H*)-dione (5-81): Following the general procedure B, but using **5-67** and PIFA (2.50 equiv), under argon. Colorless solid. M. P. = 175.1-177.3 °C. Yield: 51.3 mg, 78%. ^{1}H NMR (500 MHz, $CDCl_3$) δ 8.41 (d, *J* = 2.1 Hz, 1H), 7.95 (dd, *J* = 8.6, 2.1 Hz, 1H), 7.84 (d, *J* = 8.6 Hz, 1H), 5.91 (dd, *J* = 5.8, 3.8 Hz, 1H), 2.85-2.72 (m, 1H), 2.72-2.59 (m, 2H), 2.46-2.34 (m, 1H) ppm. ^{13}C NMR (126 MHz, $CDCl_3$) δ 171.7, 161.0, 144.2, 139.5, 137.3, 121.7, 118.2, 89.4, 87.5, 29.5, 24.4 ppm. IR (neat, cm^{-1}): 1742, 1702, 1476, 1395, 1207, 838, 523. HRMS *calcd.* for ($C_{11}H_8INO_3$+Na): 351.9441, *found* 351.9442.

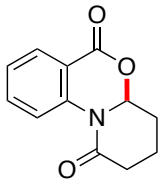

2,3,4,4a-tetrahydrobenzo[*d*]pyrido[2,1-*b*][1,3]oxazine-1,6-dione (5-82): Following the general procedure B, **5-58** was used at 60 °C. Colorless solid. M. P. = 180.2–182.3 °C. Yield: 18.0 mg, 41%. ^{1}H NMR (500 MHz, $CDCl_3$) δ 8.07 (dd, *J* = 7.8, 1.6 Hz, 1H), 7.85 (dd, *J* = 8.2, 1.2 Hz, 1H), 7.62 (dd, *J* = 8.3, 7.4 Hz, 1H), 7.34 (td, *J* = 7.7, 1.1 Hz, 1H), 5.66 – 5.60 (m, 1H), 2.70-2.54 (m, 2H), 2.32 (dd, *J* = 12.6, 5.7 Hz, 1H), 2.26-2.11 (m, 2H), 2.00-1.85 (m, 1H) ppm. ^{13}C NMR (126 MHz, $CDCl_3$) δ 169.2, 163.7, 141.5, 134.3, 130.3, 126.4, 124.3, 119.6, 85.8, 33.5, 27.9, 16.9 ppm. IR (neat, cm^{-1}): 1721, 1674, 1299, 1233, 773. HRMS *calcd.* for ($C_{12}H_{11}NO_3$+Na): 240.0631, *found* 240.0632.

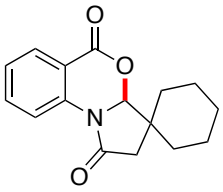

Spiro[benzo[*d*]pyrrolo[2,1-*b*][1,3]oxazine-3,1'-cyclohexane]-1,5(2*H*,3a*H*)-dione (5-83): Following the general procedure B, **5-68** was used. Colorless solid. M. P. = 138.6–141.1 °C. Yield: 53.7 mg, 99%. ^{1}H NMR (400 MHz, $CDCl_3$) δ 8.08 (dd, *J* = 7.9, 1.5 Hz, 1H), 8.03 (dd, *J* = 8.2, 1.1 Hz, 1H), 7.65 (dd, *J* = 8.1, 7.4 Hz, 1H), 7.31 (td, *J* = 7.7, 1.1 Hz, 1H), 5.49 (s, 1H), 2.67 (d, *J* = 17.6 Hz, 1H), 2.50 (d, *J* = 17.6 Hz, 1H), 1.89 (dd, *J* = 13.8, 10.3 Hz, 1H), 1.79-1.53 (m, 5H), 1.43 (m, 3H) ppm. ^{13}C NMR (101 MHz, $CDCl_3$) δ 171.7, 162.6, 138.1, 135.6, 130.8, 125.8, 120.3, 116.9, 93.7, 42.6, 39.9, 36.1, 30.7, 25.5, 22.8, 22.6 ppm. IR (neat, cm^{-1}): 1707, 1481, 1399, 1213, 755, 536. HRMS *calcd.* for ($C_{16}H_{17}NO_3$+Na): 294.1101, *found* 294.1098.

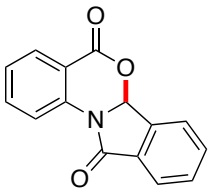

5*H*-benzo[4,5][1,3]oxazino[2,3-*a*]isoindole-5,11(6a*H*)-dione (5-84): Following the general procedure B, **5-100** was used. Colorless solid. Yield: 30.1mg, 60%. The

spectroscopic data correspond to those previously reported in the literature.[171] ^{1}H NMR (500 MHz, $CDCl_3$) δ 8.17 (d, *J* = 8.2 Hz, 1H), 8.15 (d, *J* = 7.9 Hz, 1H), 7.97 (dt, *J* = 7.5, 1.0 Hz, 1H), 7.78 (dt, *J* = 7.5, 1.3 Hz, 1H), 7.73 (td, *J* = 7.6, 1.2 Hz, 2H), 7.66 (td, *J* = 7.4, 1.2 Hz, 1H), 7.34 (td, *J* = 7.7, 1.1 Hz, 1H), 6.66 (s, 1H) ppm. ^{13}C NMR (126 MHz, $CDCl_3$) δ 164.7, 162.8, 139.0, 138.2, 136.1, 133.9, 131.9, 131.5, 131.3, 125.6, 124.9, 124.3, 119.8, 115.3, 84.9 ppm.

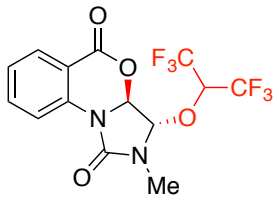

3-((1,1,1,3,3,3-hexafluoropropan-2-yl)oxy)-2-methyl-3,3a-dihydro-1*H*-benzo[*d*]imidazo[5,1-*b*][1,3]oxazine-1,5(2*H*)-dione (5-85): Following the general procedure B, **5-73** was used with PIFA (2.50 equiv), under argon. Colorless solid. Yield: 54.6 mg, 71%. M. P. = 152.1-154.0 °C. ^{1}H NMR (500 MHz, $CDCl_3$) δ 8.07 (dd, *J* = 7.9, 1.4 Hz, 1H), 7.75-7.68 (m, 2H), 7.34 (dd, *J* = 7.9, 7.0 Hz, 1H), 5.81 (s, 1H), 5.26 (s, 1H), 4.58-4.53 (m, *J* = 5.7 Hz, 1H), 3.06 (s, 3H) ppm ^{13}C NMR (126 MHz, $CDCl_3$) δ 160.6, 153.4, 137.2, 136.0, 130.7, 125.9, 121.6, 116.8, 93.8, 86.1, 74.6 (p, *J* = 33.4 Hz), 28.0 ppm. ^{19}F NMR (376 MHz, $CDCl_3$) δ -73.5 (q, *J* = 8.8 Hz), -73.7 (q, *J* = 8.9 Hz) ppm. IR (neat, cm^{-1}): 1725, 1192, 1101, 757, 686. HRMS *calcd.* for ($C_{14}H_{10}F_6NO_4$+Na): 407.0437, *found* 407.0445.

5.10.4 ArI-catalyzed Site-selectivity Switching

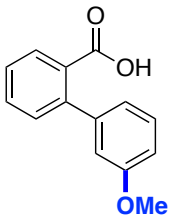

3'-methoxy-[1,1'-biphenyl]-2-carboxylic acid (5-34). Colorless solid. The spectroscopic data correspond to those previously reported in the literature.[165] ^{1}H NMR (500 MHz, $CDCl_3$) δ 7.95 (dt, *J* = 7.8, 1.7 Hz, 1H), 7.56 (td, *J* = 7.6, 1.5 Hz, 1H), 7.43

[171] Gromachevskaya, E. V.; Finko, A. V.; Butin, A. V.; Pushkareva, K. S.; Strelkov, V. D.; Isakova1, L. I.; Krapivin, G. D. *Chem. Hetero.Comp.* **2013**, *49,* 1331.

(dt, *J* = 7.6, 1.4 Hz, 1H), 7.39 (dt, *J* = 7.7, 1.6 Hz, 1H), 7.30 (td, *J* = 8.4 Hz, 1.5 Hz, 1H), 6.97-6.88 (m, 3H) ppm. ^{13}C NMR (126 MHz, $CDCl_3$) δ 173.8, 159.4, 143.2, 142.5, 132.2, 131.2, 130.7, 129.6, 129.2, 127.4, 121.2, 114.3, 113.2, 55.4 ppm.

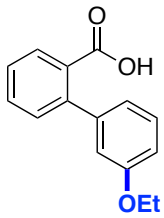

3'-ethoxy-[1,1'-biphenyl]-2-carboxylic acid (5-101). Colorless solid. M. P. = 90.5–93.0 °C. ^{1}H NMR (400 MHz, $CDCl_3$) δ 7.95 (d, *J* = 7.8 Hz, 1H), 7.56 (d, *J* = 7.6 Hz, 1H), 7.43 (d, *J* = 7.6 Hz, 1H), 7.39 (d, *J* = 7.6 Hz, 1H), 7.34-7.25 (m, 1H), 6.96-6.86 (m, 2H), 4.07 (q, *J* = 7.0 Hz, 2H), 1.43 (t, *J* = 7.0 Hz, 3H) ppm. ^{13}C NMR (101 MHz, $CDCl_3$) δ 173.8, 158.8, 143.3, 142.5, 132.2, 131.2, 130.7, 129.6, 129.2, 127.4, 121.1, 114.9, 113.8, 63.6, 15.0 ppm. IR (neat, cm^{-1}): 2970, 1679, 1297, 1215, 1052, 789, 746. HRMS *calcd.* for ($C_{15}H_{14}O_3$-1): 241.0870, *found* 241.0867.

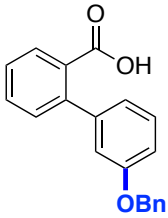

3'-(benzyloxy)-[1,1'-biphenyl]-2-carboxylic acid (5-102). Colorless solid. The spectro-scopic data correspond to those previously reported in the literature.[165] ^{1}H NMR (400 MHz, $CDCl_3$) δ 7.95 (dd, *J* = 7.8, 1.3 Hz, 1H), 7.56 (td, *J* = 7.6, 1.4 Hz, 1H), 7.47-7.27 (m, 9H), 7.02-6.92 (m, 3H), 5.08 (s, 2H) ppm. ^{13}C NMR (101 MHz, $CDCl_3$) δ 173.5, 158.7, 143.2, 142.6, 137.1, 132.2, 131.2, 130.8, 129.5, 129.3, 128.7, 128.1, 127.7, 127.5, 121.5, 115.3, 114.1, 70.2 ppm.

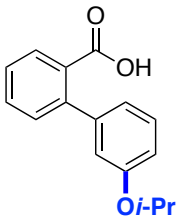

3'-isopropoxy-[1,1'-biphenyl]-2-carboxylic acid (5-103). Purple oil. ^{1}H NMR (400 MHz, $CDCl_3$) δ 7.92 (dd, *J* = 7.8, 1.4 Hz, 1H), 7.55 (td, *J* = 7.6, 1.4 Hz, 1H), 7.42 (td, *J* = 7.6, 1.3 Hz, 1H), 7.38 (dd, *J* = 7.7, 1.2 Hz, 1H), 7.27 (td, *J* = 7.6, 1.0 Hz, 1H), 6.98-6.80 (m, 3H), 4.55 (hept, *J* = 6.1 Hz, 1H), 1.33 (d, *J* = 6.0 Hz, 6H) ppm. ^{13}C NMR (101 MHz, $CDCl_3$) δ 173.2, 157.7, 143.3, 142.5, 132.1, 131.2, 130.7, 129.6, 129.3, 127.4, 121.0, 116.3, 115.4, 70.1, 22.2 ppm. IR (neat, cm^{-1}): 2978, 1676, 1586, 1291, 1209, 1116, 749. HRMS *calcd.* for ($C_{15}H_{16}O_3$-1): 255.1027, *found* 255.1027.

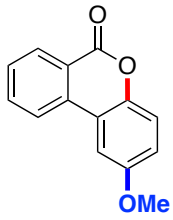

3-methoxy-6*H*-benzo[*c*]chromen-6-one (5-86): Following the general procedure A, **5-21** and **5-34** were used (37%, **5-86**:**5-86'**=5:1). Colorless solid. The spectroscopic data correspond to those previously reported in the literature.[165] ^{1}H NMR (400 MHz, $CDCl_3$) δ 8.40 (d, *J* = 7.9 Hz, 1H), 8.06 (d, *J* = 8.1 Hz, 1H), 7.82 (dd, *J* = 8.1, 7.3 Hz, 1H), 7.58 (dd, *J* = 7.9, 7.3 Hz, 1H), 7.48 (d, *J* = 2.9 Hz, 1H), 7.29 (d, *J* = 9.0 Hz, 1H), 7.04 (dd, *J* = 9.0, 2.9 Hz, 1H) 3.90 (s, 3H) ppm. ^{13}C NMR (101 MHz, $CDCl_3$) δ 161.5, 156.5, 145.8, 134.9, 134.8, 130.8, 129.1, 121.9, 121.5, 118.9, 118.7, 117.3, 106.5, 56.0 ppm.

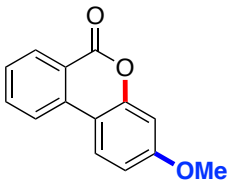

2-methoxy-6*H*-benzo[*c*]chromen-6-one (5-86'): Following the general procedure A, several aryl iodide catalysts were utilized (20 mol%). The results are summarized in the following table:

Entry	*ArI catalyst*	Yield (%)	**5-86:5-86'**
1	**5-11**	56	**1:1.2**
2	**5-12**	69	**1:1.8**
3	**5-13**	22	**1:1.1**
4	**5-16**	70	**1:3.4**
5	**5-17**	67	**1:1.7**
6	**5-21**	37	**5:1**

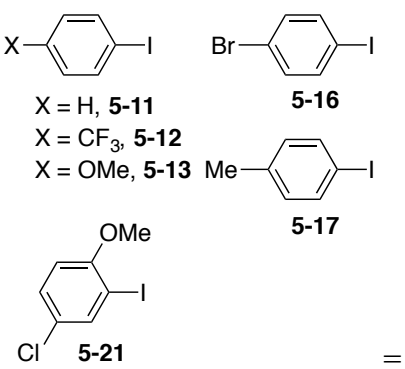

Spectroscopical data for **5-86':** Colorless solid. The spectroscopic data correspond to those previously reported in the literature.[6] ^{1}H NMR (400 MHz, $CDCl_3$) δ 8.36 (d, *J* = 8.0 Hz, 1H), 8.01 (d, *J* = 8.1 Hz, 1H), 7.95 (d, *J* = 8.8 Hz, 1H), 7.79 (dd, *J* = 8.1, 7.3 Hz, 1H), 7.51 (dd, *J* = 7.9, 7.2, 1.1 Hz, 1H), 6.92 (dd, *J* = 8.8, 2.6 Hz, 1H), 6.88 (d, *J* = 2.5 Hz, 1H), 3.89 (s, 3H) ppm. ^{13}C NMR (101 MHz, $CDCl_3$) δ 161.7, 152.8, 135.4, 135.0, 130.8, 127.9, 124.0, 121.3, 120.2, 112.7, 111.4, 101.8, 55.9 ppm.

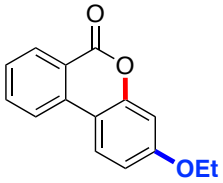

3-ethoxy-6*H*-benzo[*c*]chromen-6-one (5-91'). Following the general procedure A, **101** and **5-89** were used in HFIP at rt, providing 81% yield (**5-91**:**5-91'**=1:6.7). Colorless solid. The spectroscopic data of major product **5-91'** is the following: M. P. = 105.5-106.3 °C. ^{1}H NMR (400 MHz, $CDCl_3$) δ 8.33 (dd, *J* = 8.0 Hz, 1H), 7.97 (d, *J* = 8.2 Hz, 1H), 7.90 (d, *J* = 8.8 Hz, 1H), 7.76 (dd, *J* = 8.1, 7.3 Hz, 1H), 7.48 (dd, *J* = 8.2, 7.2 Hz, 1H), 6.88 (dd, *J* = 8.8, 2.5 Hz, 1H), 6.82 (d, *J* = 2.5 Hz, 1H), 4.09 (q, *J* = 7.0 Hz, 2H), 1.46 (t, *J* = 7.0 Hz, 3H) ppm. ^{13}C NMR (101 MHz, $CDCl_3$) δ 161.7, 152.7, 135.4, 135.0, 130.8, 129.0, 127.8, 123.9, 121.8, 120.1, 112.9, 111.1, 102.2, 64.2, 14.8 ppm. IR (neat, cm^{-1}): 1716, 1605, 1453, 1261, 1174, 1034, 762. HRMS *calcd.* for ($C_{15}H_{12}O_3$+1): 241.0859, *found* 241.0864.

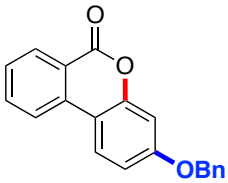

3-(benzyloxy)-6*H*-benzo[*c*]chromen-6-one (5-92'). Following the general procedure A, **102** and **5-89** were used in HFIP at rt, providing 80% yield (**5-91**:**5-91'** =1:10). Colorless solid. The spectroscopic data of major product **5-91'** is the following: M. P. = 107.6–109.8 °C. ^{1}H NMR (400 MHz, $CDCl_3$) δ 8.33 (dd, *J* = 8.0, 1.4 Hz, 1H), 7.96 (d, *J* = 8.3 Hz, 0H), 7.91 (d, *J* = 8.8 Hz, 1H), 7.79-7.73 (m, 1H), 7.53-7.32 (m, 8H), 6.97 (dd, *J* = 8.8, 2.6 Hz, 1H), 6.91 (d, *J* = 2.5 Hz, 1H), 5.12 (s, 2H) ppm. ^{13}C NMR (101 MHz, $CDCl_3$) δ 161.6, 160.7, 152.6, 136.2, 135.2, 135.0, 130.6, 128.9, 128.4, 127.9, 127.7, 123.9, 121.2, 120.1, 113.2, 111.5, 102.8, 70.6 ppm. IR (neat, cm^{-1}): 1728, 1605, 1446, 1266, 1176, 1099, 762. HRMS *calcd.* for ($C_{20}H_{14}O_3$+1): 325.0835, *found* 325.0836.

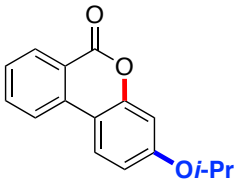

3-isopropoxy-6*H*-benzo[*c*]chromen-6-one (5-93'). Following the general procedure A, **103** and **5-89** were used in HFIP at rt, providing 76% yield (**5-93**: **5-93'**=1:4). Colorless oil. The spectroscopic data of major product **5-93'** is the following: ^{1}H NMR (400 MHz, $CDCl_3$) δ 8.34 (d, *J* = 8.0 Hz, 1H), 7.97 (d, *J* = 8.2 Hz, 1H), 7.91 (d, *J* = 8.8 Hz, 1H), 7.76 (dd, *J* = 8.2, 7.3 Hz, 1H), 7.48 (dd, *J* = 8.2, 7.3 Hz, 1H), 6.87 (dd, *J* = 8.8, 2.5 Hz, 1H), 6.84 (d, *J* = 2.5 Hz, 1H), 4.69-4.57 (m, 1H), 1.39 (d, *J* = 6.1 Hz, 6H) ppm. ^{13}C NMR (101 MHz, $CDCl_3$) δ 161.8, 152.8, 135.4, 135.0, 130.8, 129.1, 127.8, 123.9, 121.2, 120.1, 113.9, 111.0, 103.3, 77.2, 22.0 ppm. IR (neat, cm^{-1}): 1721, 1618, 1456, 1261, 1095, 1032, 762. HRMS *calcd.* for ($C_{16}H_{14}O_3$+1): 255.1016, *found* 255.1013.

Synthesis of 5-90 and 5-87

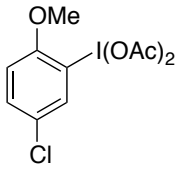

5-chloro-2-methoxy(diacetoxyiodo)benzene (5-90). This compound was prepared according to a related literature procedure.[172] Colorless solid. Yield, 65%. M. P. =

[172] Hossain, M. D.; Kitamura, T. *J. Org. Chem.* **2005**, *70*, 6984.

190.5-192.3 °C. ^{1}H NMR (400 MHz, $CDCl_3$) δ 8.09 (d, *J* = 2.5 Hz, 1H), 7.52 (dd, *J* = 8.9, 2.5 Hz, 1H), 7.09 (d, *J* = 8.9 Hz, 1H), 3.96 (s, 3H), 1.98 (s, 7H) ppm. ^{13}C NMR (101 MHz, $CDCl_3$) δ 177.0, 155.2, 137.1, 134.3, 127.2, 113.5, 112.9, 57.4, 20.5 ppm. IR (neat, cm^{-1}): 1656, 1481, 1271, 1036, 696.

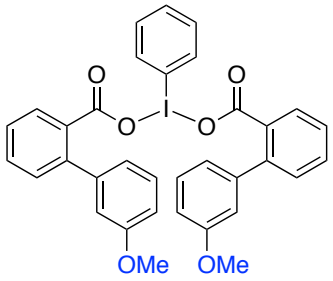

[di(3'-methoxy-[1,1'-biphenyl]-2-carboxyiodo)]benzene (5-87). This compound was prepared according to a related literature procedure.[173] Colorless solid. Yield, 95%. M. P. = 140.2-142.1 °C. ^{1}H NMR (400 MHz, $CDCl_3$) δ 7.72 (dd, *J* = 7.8, 1.4 Hz, 1H), 7.44 (td, *J* = 7.5, 1.5 Hz, 1H), 7.38-7.27 (m, 4H), 7.16-7.07 (m, 1H), 6.93-6.83 (m, 5H) ppm. ^{13}C NMR (101 MHz, $CDCl_3$) δ 174.2, 159.6, 143.6, 141.8, 134.5, 131.5, 131.0, 130.9, 130.5, 130.4, 130.0, 129.3, 127.5, 121.1, 120.5, 113.6, 113.4, 55.5 ppm. IR (neat, cm^{-1}): 1630, 1296, 1127, 759, 439.

Influence on selectivity depending on the iodine (III) reagent utilized

General procedure: A Schlenk tube containing a stirring bar was charged with **5-34** (0.20 mmol), the corresponding hypervalent iodine (III) reagent (0.20 mmol), additive (0.20 mmol), HFIP (2 mL). The reaction mixture was then stirred at room temperature for 16 h. The solvents were concentrated under reduced pressure and the crude was purified by column chromatography on silica gel (eluting with hexanes/ethyl acetate mixtures); the **5-86**:**5-86'** ratio was determined by ^{1}H NMR analysis of the crude mixture.

Plot of 5-86:5-86' ratio as a function of time when 5-16 (20 mol%)

General procedure: A Schlenk tube containing a stirring bar was charged with **5-34** (0.20 mmol), 4-bromoiodobezene (**5-16;** 11.6 mg, 0.04 mmol, 20 mol%), HFIP (2 mL) and AcOOH (83.2 μL, 2.20 equiv, 35% in AcOH). The reaction mixture was then stirred at room temperature. The ratio of **5-86**:**5-86'** was determined by ^{1}H NMR of

[173] Sang, P. J.; Boehshar, M.; Wingert, H.; Kitamura, T. *J. Am. Chem. Soc.* **1988**, *110*, 3272.

different aliquots at the indicated reaction times.

General procedure for the use of 5-87

General procedure: A Schlenk tube containing a stirring bar was charged with **5-87** (0.20 mmol), additive (0.20 mmol), HFIP (2 mL). The reaction mixture was then stirred at room temperature for 16 h. The solvents were concentrated under reduced pressure and the crude was purified by column chromatography on silica gel (eluting with hexanes/ethyl acetate mixtures); the **5-86**:**5-86'** ratio was determined by ^{1}H NMR analysis of the crude mixture.

Selectivity Switch for 5-96

General Procedure: A Schlenk tube containing a stirring bar was charged with **5-96** (0.20 mmol), the corresponding catalyst (0.04 mmol, 20 mol%), HFIP (1.5 mL) and AcO_2H (150 μL, 4.0 equiv, 35% in AcOH). The reaction mixture was then stirred at 40 ºC for 16 h. The solvents were concentrated under reduced pressure and the crude was purified by column chromatography on silica gel (eluting with hexanes/ethyl acetate/dichloromethane mixtures).

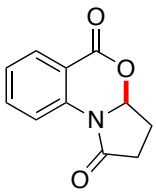

3,3a-dihydro-1*H*-benzo[*d*]pyrrolo[2,1-*b*][1,3]oxazine-1,5(2*H*)-dione (5-53): Following the general procedure, **5-96** and **5-17** were used. Colorless solid, 68% (**5-97**:**5-97'**=1.4:1).

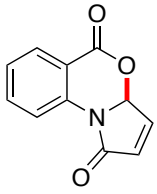

1*H*-benzo[*d*]pyrrolo[2,1-*b*][1,3]oxazine-1,5(3a*H*)-dione (5-97): Following the general procedure, **5-96** and **5-16** were used. Colorless solid, 69% (**5-53**:**5-97**=1:20). M. P. = 152.1-154.0 ^{o}C. ^{1}H NMR (500 MHz, $CDCl_3$) δ 8.10 (dd, *J* = 7.9, 1.6 Hz, 1H), 7.99 (dd, *J* = 8.2, 1.1 Hz, 1H), 7.69 (dd, *J* = 8.2, 7.4 Hz, 1H), 7.30 (dd, *J* = 7.9, 7.4 Hz,

1H), 7.26 (dd, J = 6.1, 1.8 Hz, 1H), 6.50 (dd, J = 6.1, 0.9 Hz, 1H), 6.30 (dd, J = 1.7, 0.9 Hz, 1H) ppm. ^{13}C NMR (126 MHz, $CDCl_3$) δ 166.2, 162.4, 142.4, 137.6, 136.2, 131.9, 131.3, 125.4, 119.3, 114.7, 86.3 ppm. IR (neat, cm^{-1}): 1717, 1599, 1101, 1484, 1392, 750, 520. HRMS *calcd.* for ($C_{11}H_7NO_3$+Na): 224.0318, *found* 224.0126.

5.10.5 Selected Examples of NMR Spectra

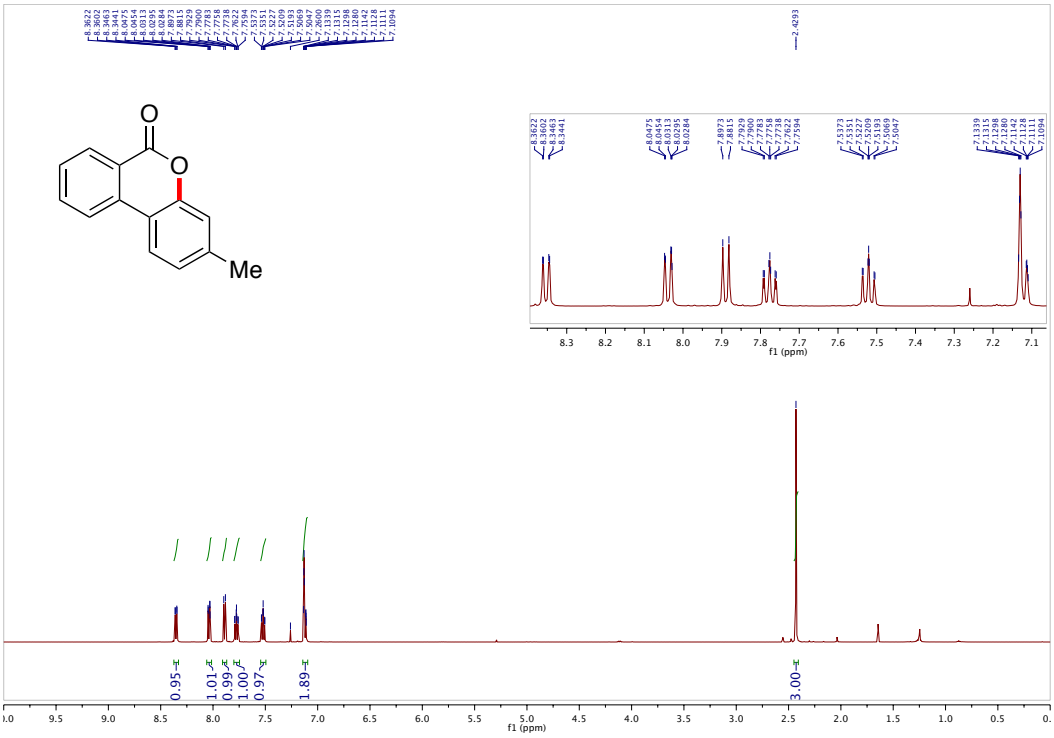

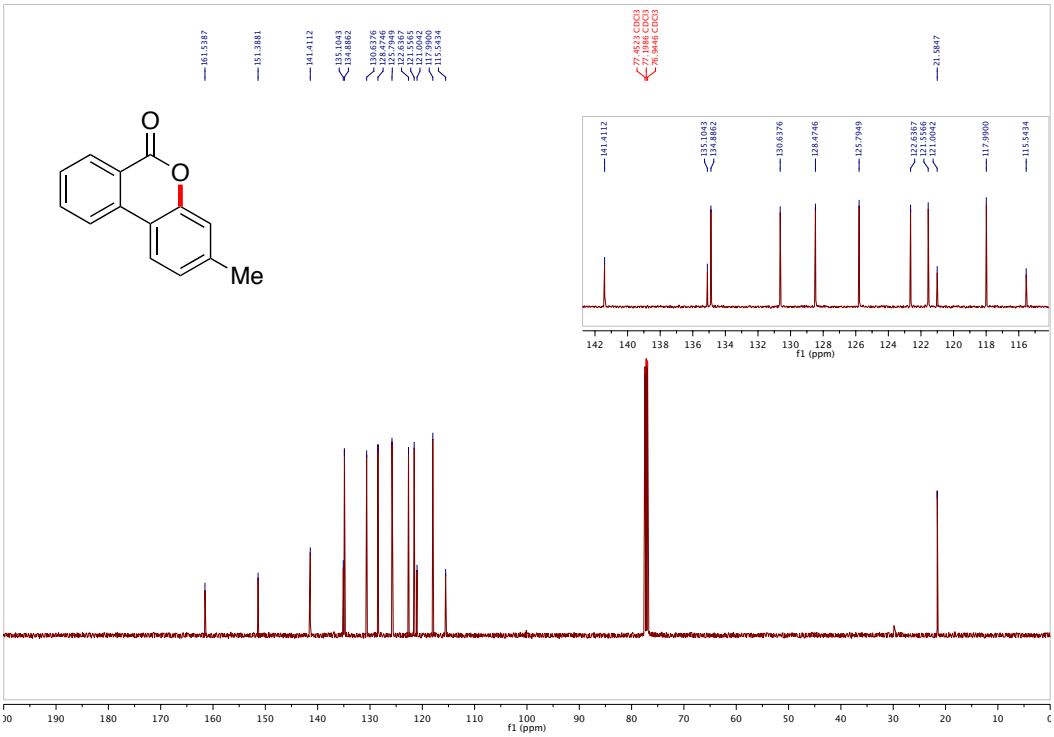
O
O
Me
161.5387
151.3881
141.4112
135.1043
134.8862
130.6376
128.4746
125.7949
122.6387
121.5565
121.0642
117.9900
115.5434
77.6023 CDCl3
77.3886 CDCl3
76.9446 CDCl3
21.5847
f1 (ppm)

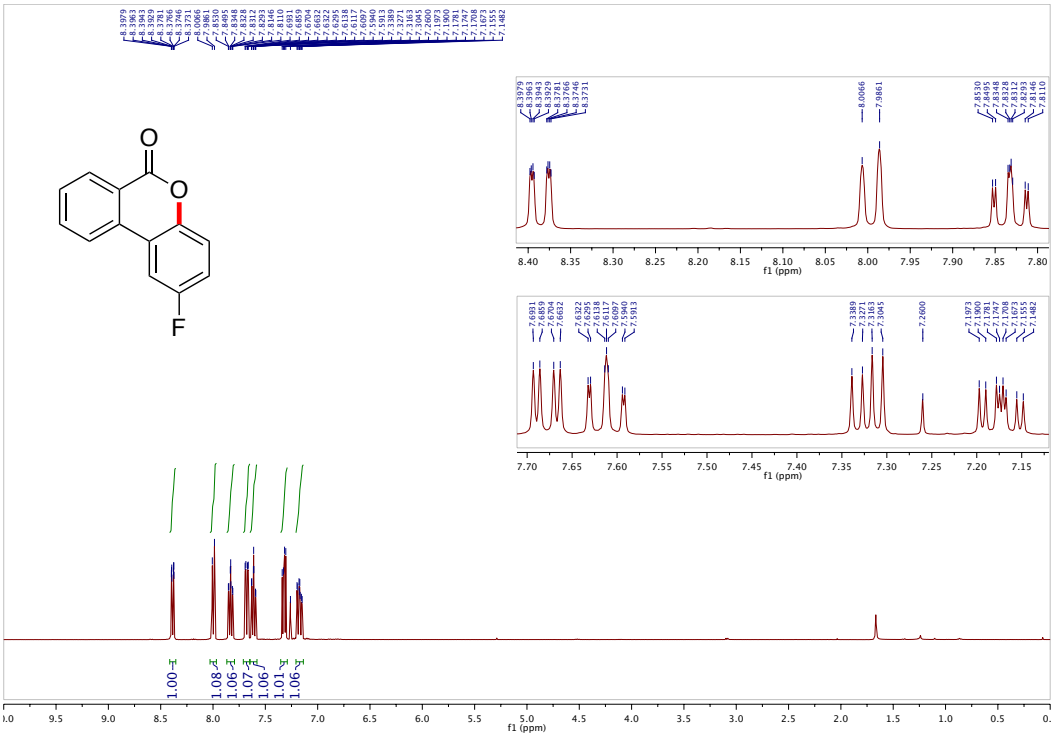
O
O
F
8.0066
7.9861
7.8530
7.8495
7.8348
7.8312
7.8146
7.8110
7.6091
7.6859
7.6704
7.6652
7.6322
7.6298
7.6138
7.6117
7.6090
7.5940
7.5913
7.3389
7.3271
7.3183
7.3045
7.2600
7.1973
7.1960
7.1781
7.1747
7.1708
7.1673
7.1555
7.1548
7.1446
1.00
1.08
1.06
1.07
1.06
1.01
1.06
f1 (ppm)

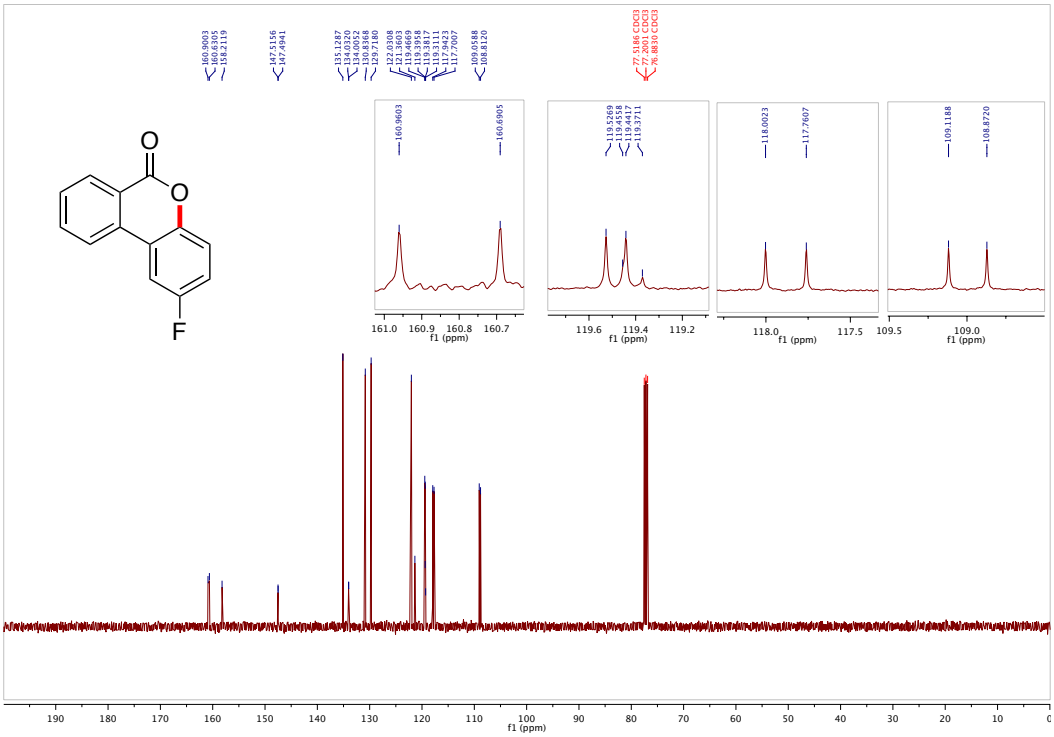
O
O
F
160.9603
160.6305
158.2119
147.5156
147.4941
135.1287
134.1030
134.0052
130.9368
130.8148
122.0308
121.3603
119.4669
119.3838
119.3817
119.3411
118.8453
117.7007
109.0588
108.8120
77.3186 CDCl3
77.0000 CDCl3
76.6814 CDCl3
160.9603
160.6905
119.5269
119.4558
119.4447
119.3711
118.0023
117.7607
109.1188
108.8720
f1 (ppm)

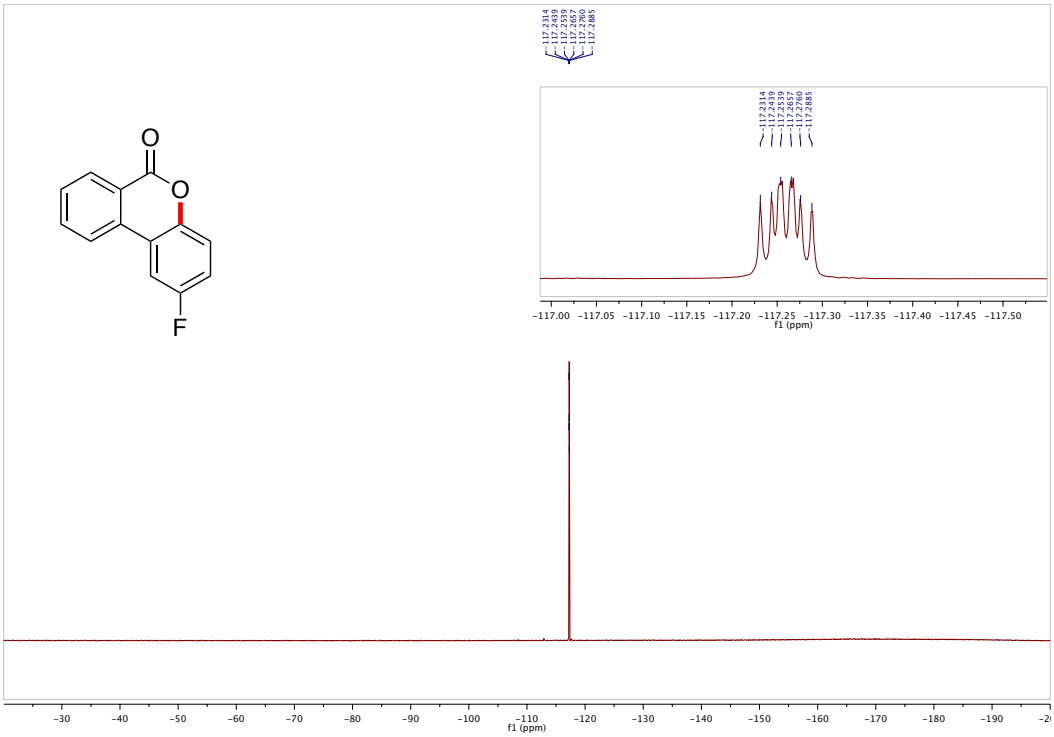
O
O
F
117.2314
117.2459
117.2539
117.2657
117.2760
117.2885
f1 (ppm)

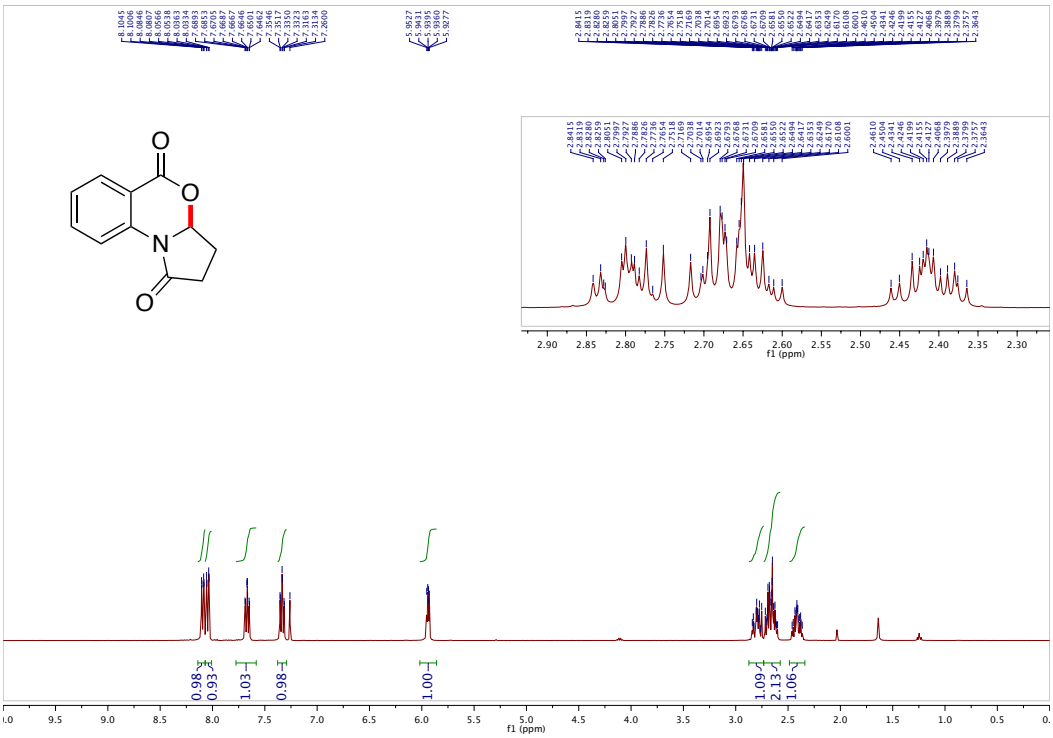
O
O
N
O
0.98
0.93
1.03
0.98
1.00
1.09
2.13
1.06
f1 (ppm)

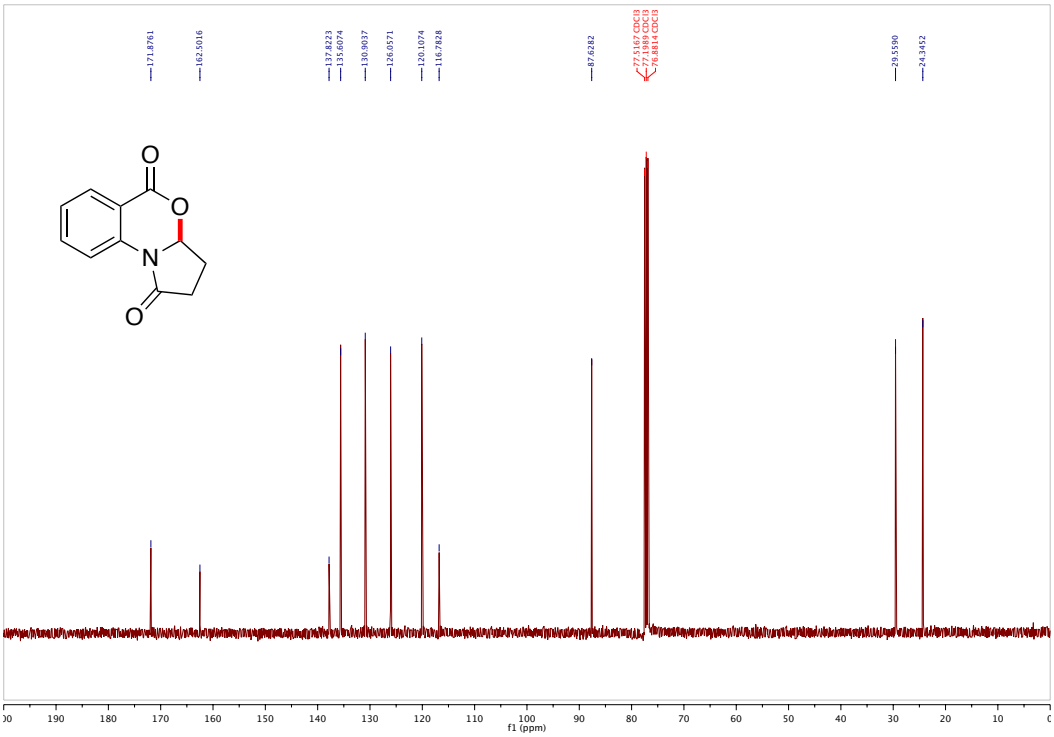
171.8761
162.5016
137.8223
135.6074
130.9037
126.0571
120.1074
116.7828
87.6282
77.5167 CDCl3
77.1984 CDCl3
76.8814 CDCl3
29.5590
24.3452
O
O
N
O
f1 (ppm)

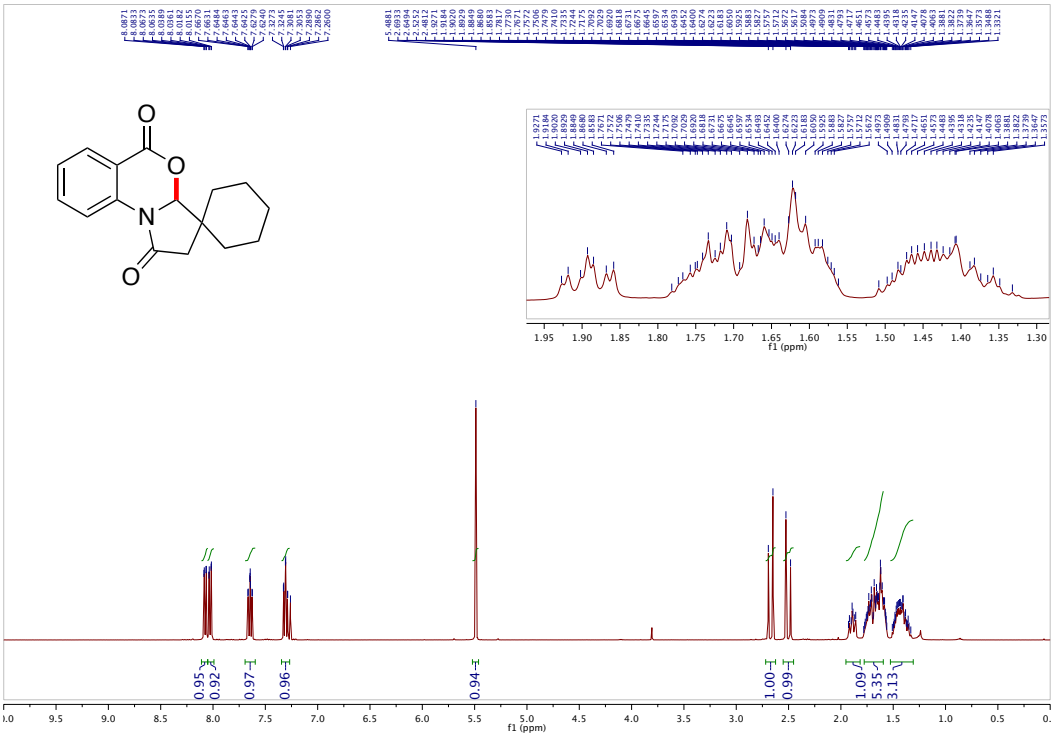
O
O
N
O
f1 (ppm)
0.95
0.92
0.97
0.96
0.94
1.00
0.99
1.09
5.35
3.13

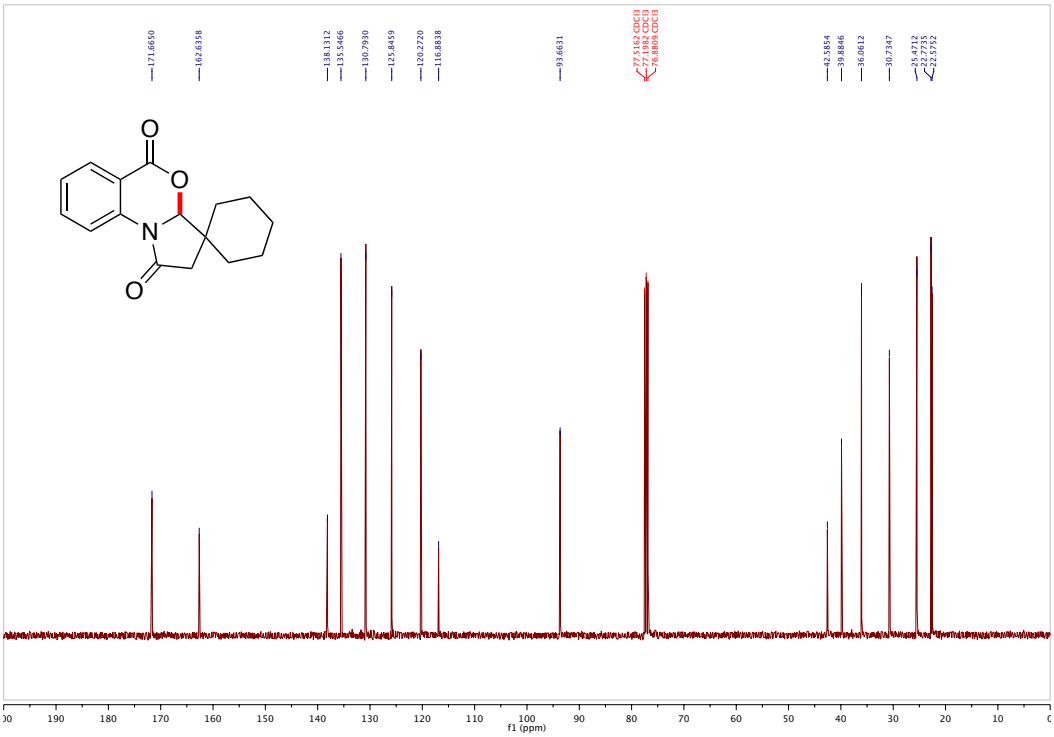
O
O
N
O
f1 (ppm)

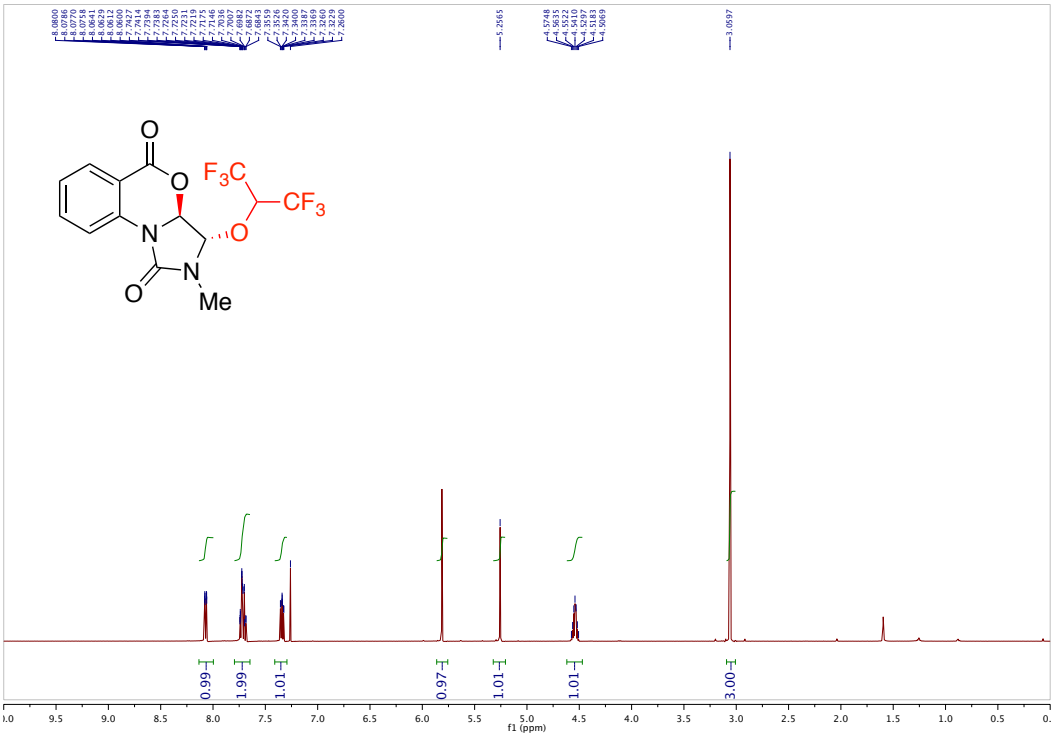
F3C
CF3
O
N
N
Me
0.99
1.99
1.01
0.97
1.01
1.01
3.00
f1 (ppm)

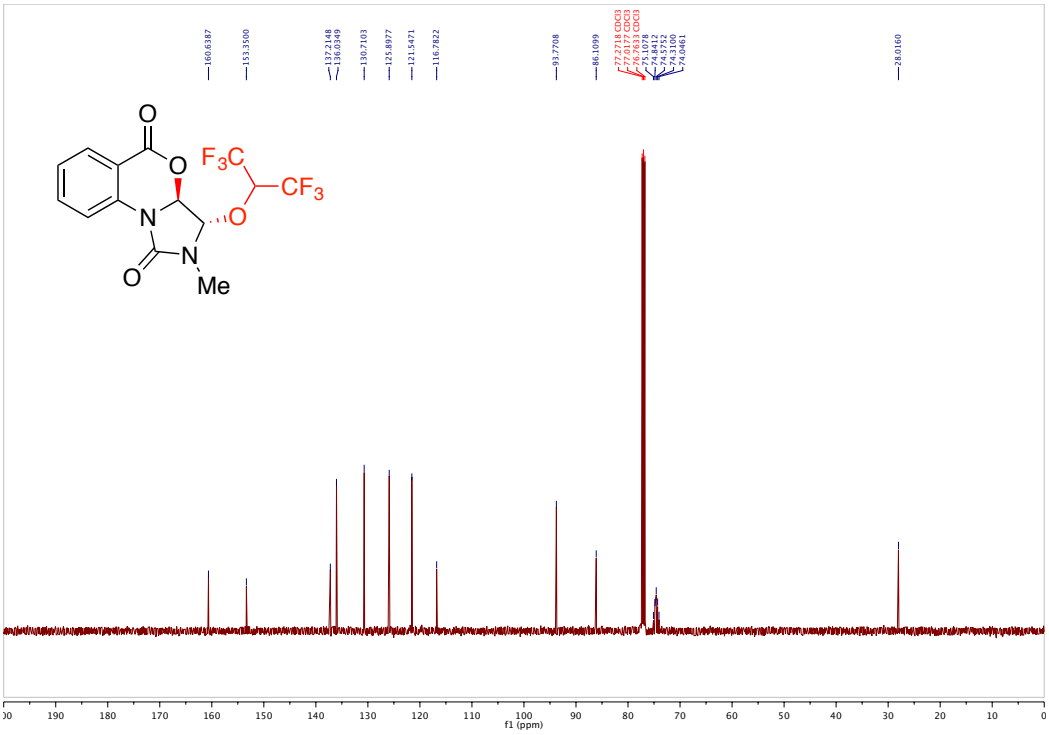
F3C
CF3
O
N
N
Me
f1 (ppm)

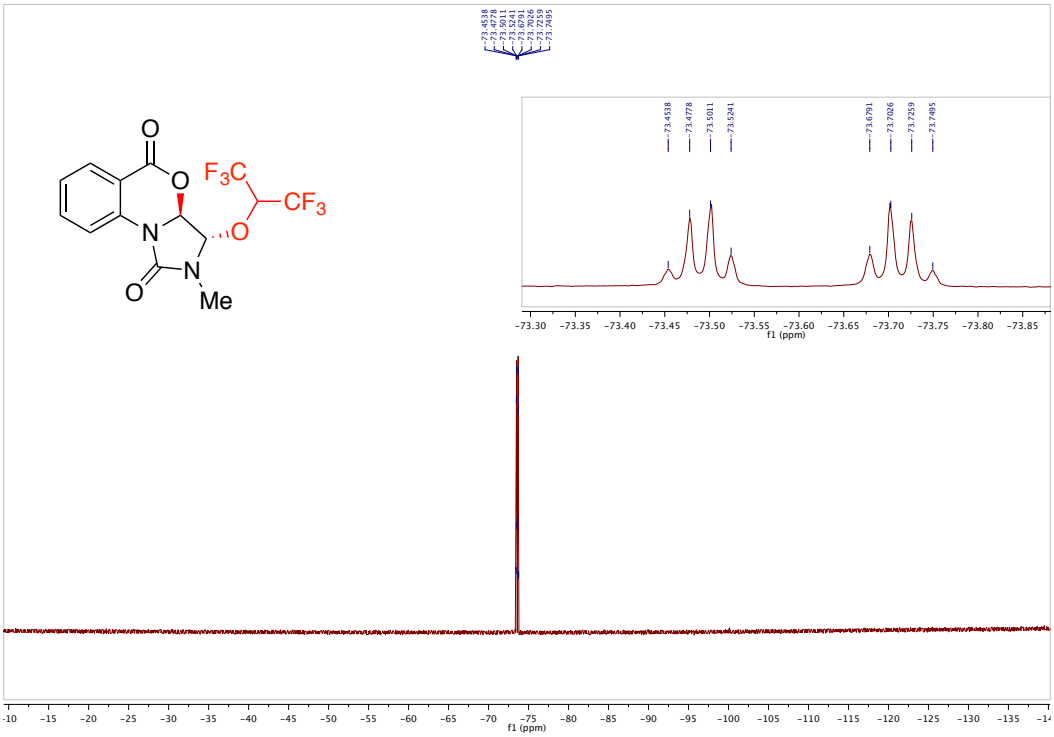
F3C
CF3
O
N
Me
f1 (ppm)

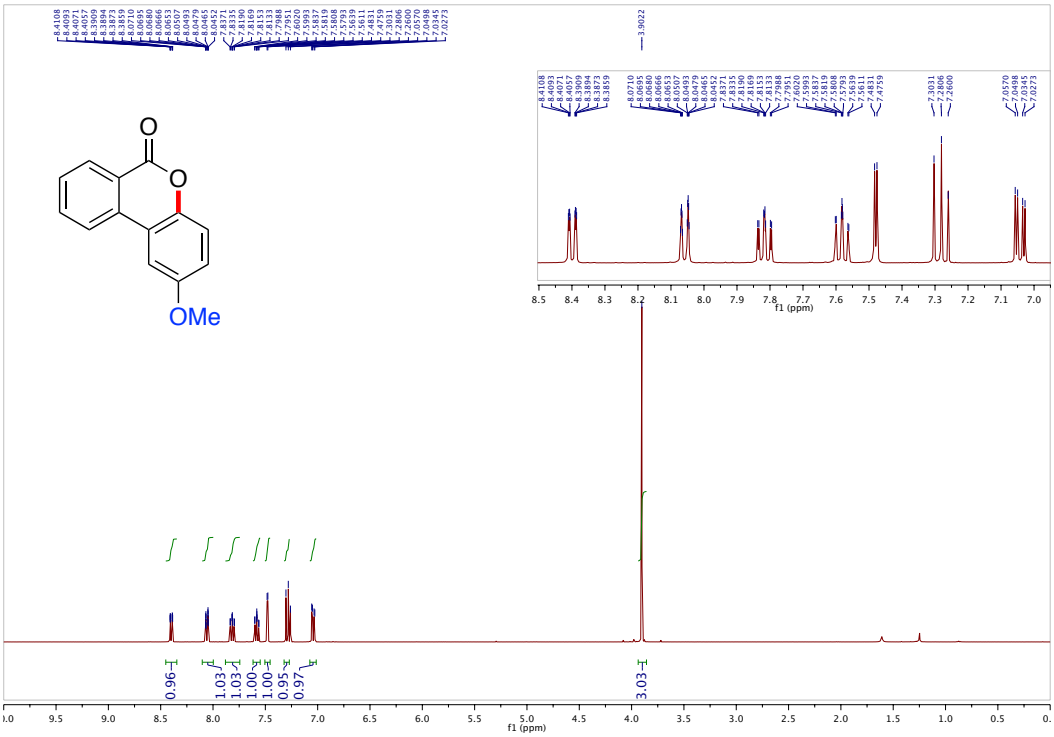
OMe
f1 (ppm)

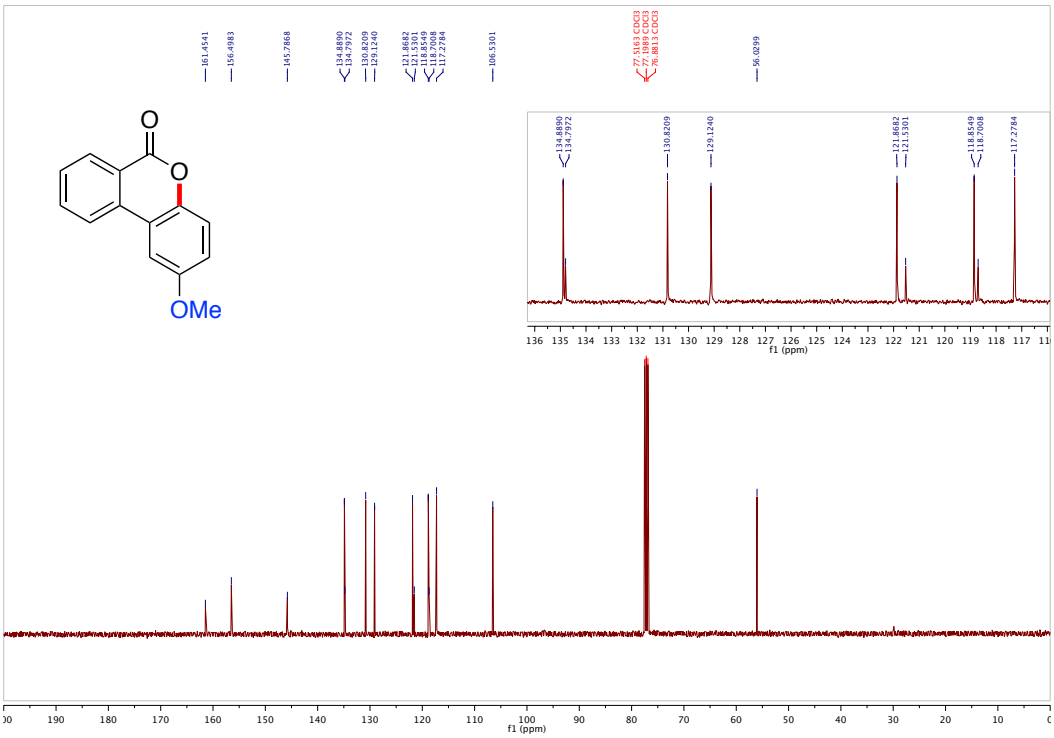
OMe
f1 (ppm)

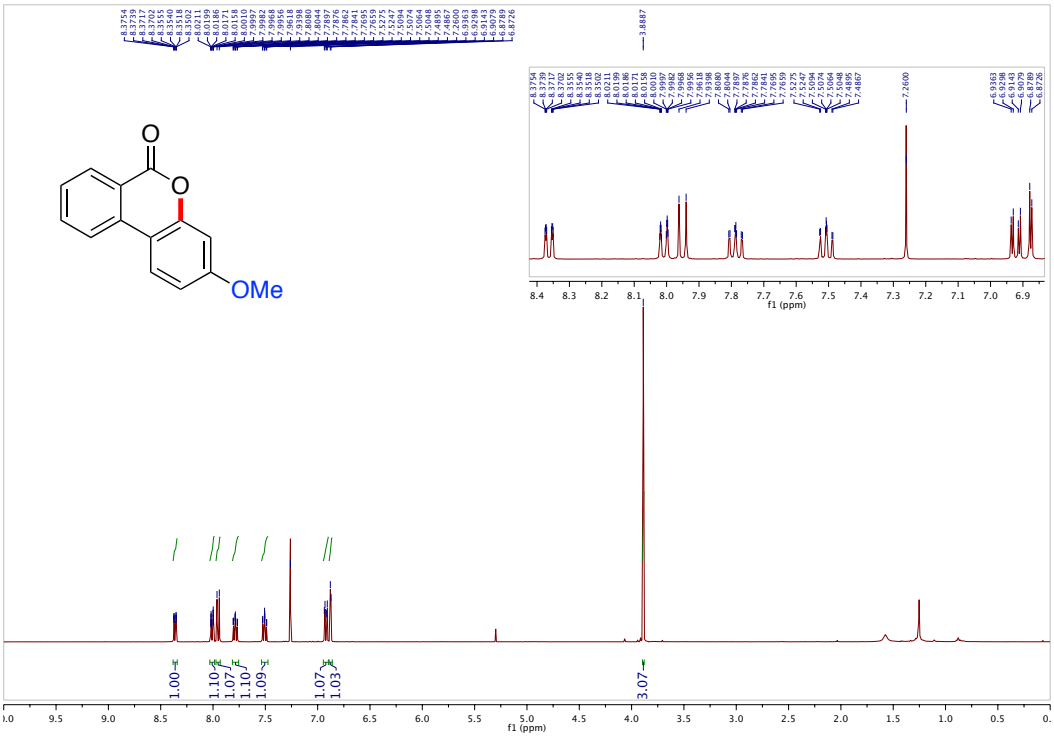
OMe
f1 (ppm)

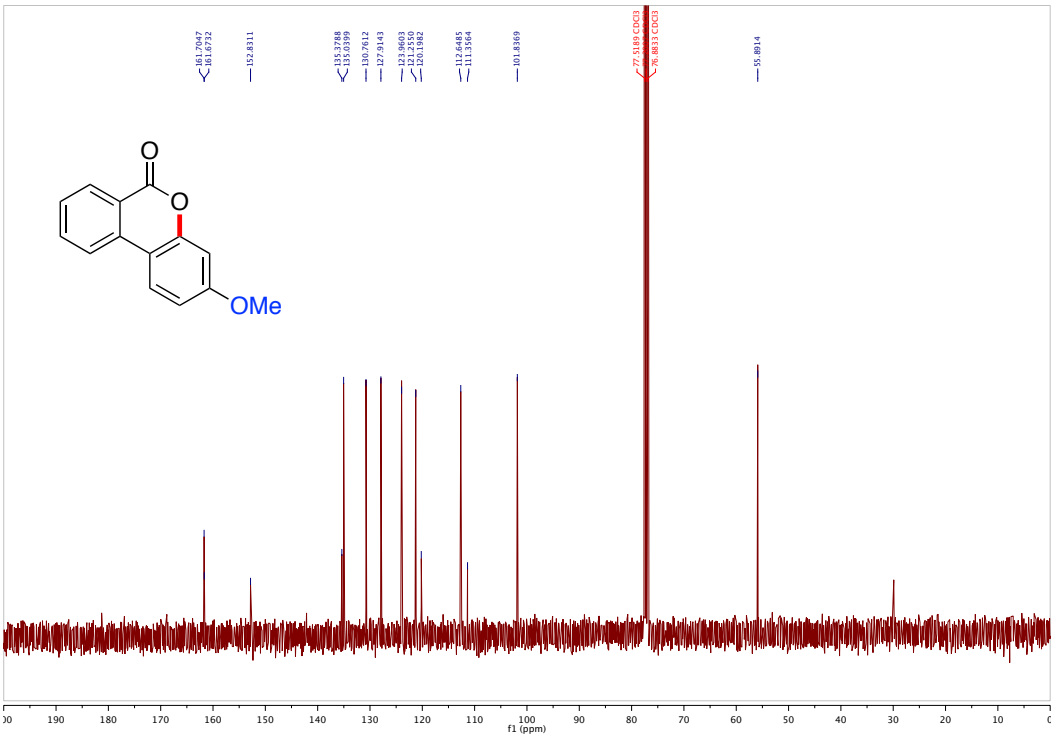
O
O
OMe
f1 (ppm)

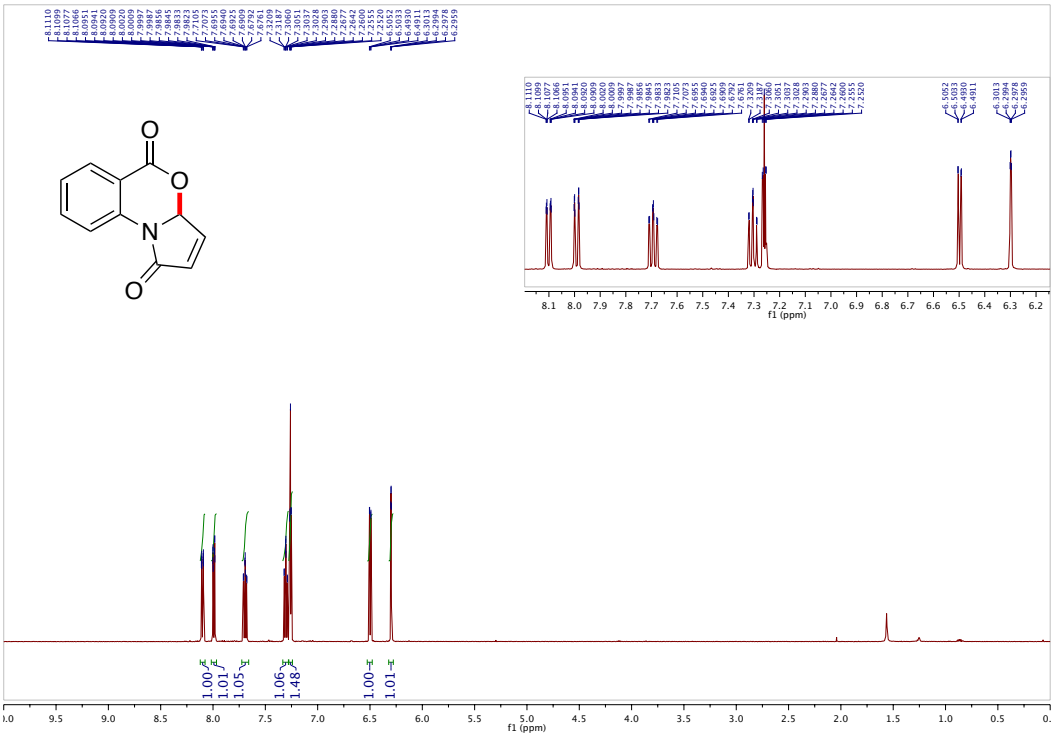
O
O
N
O
f1 (ppm)

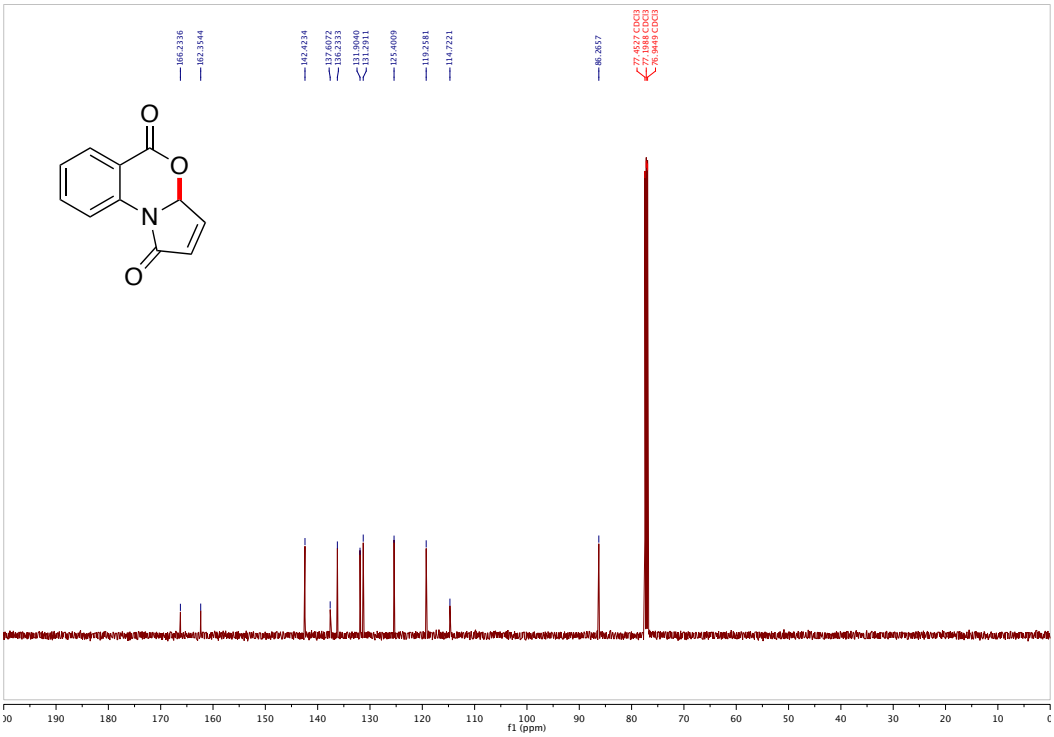
166.2336
162.3544
142.4234
137.6072
136.2333
131.9040
131.2911
125.4009
119.2581
114.7221
86.3857
77.4527 CDCl3
77.0840 CDCl3
76.7153 CDCl3
O
O
N
O
f1 (ppm)

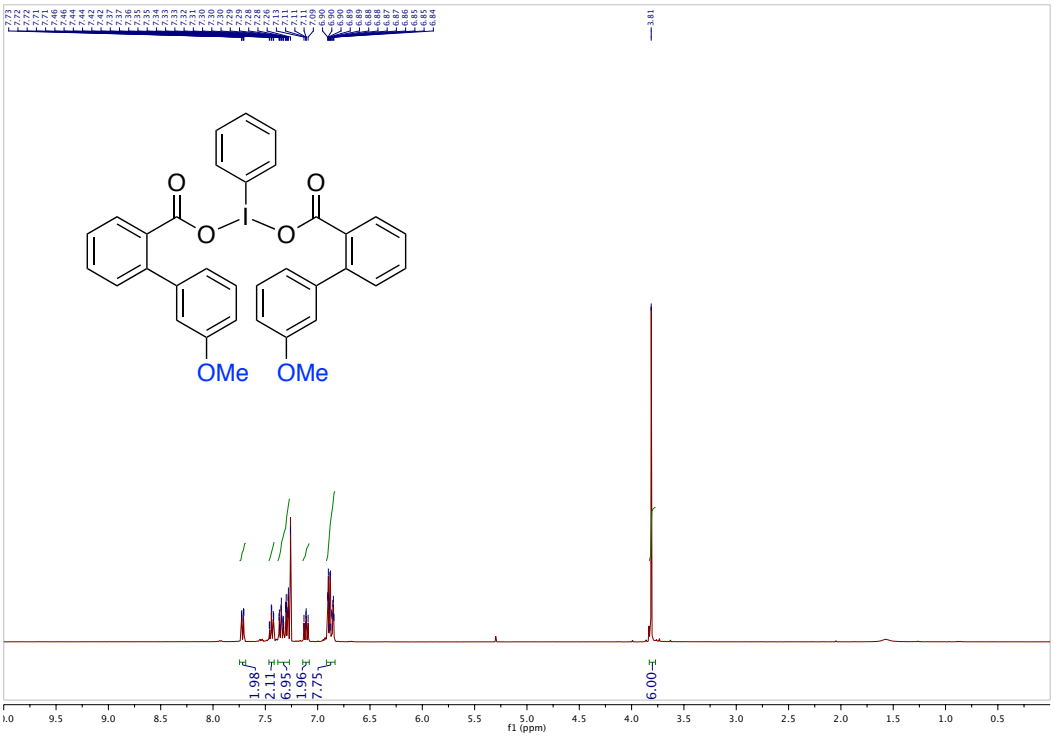
3.81
O
O
O
O
I
OMe
OMe
1.98
2.11
6.95
1.96
7.75
6.00
f1 (ppm)

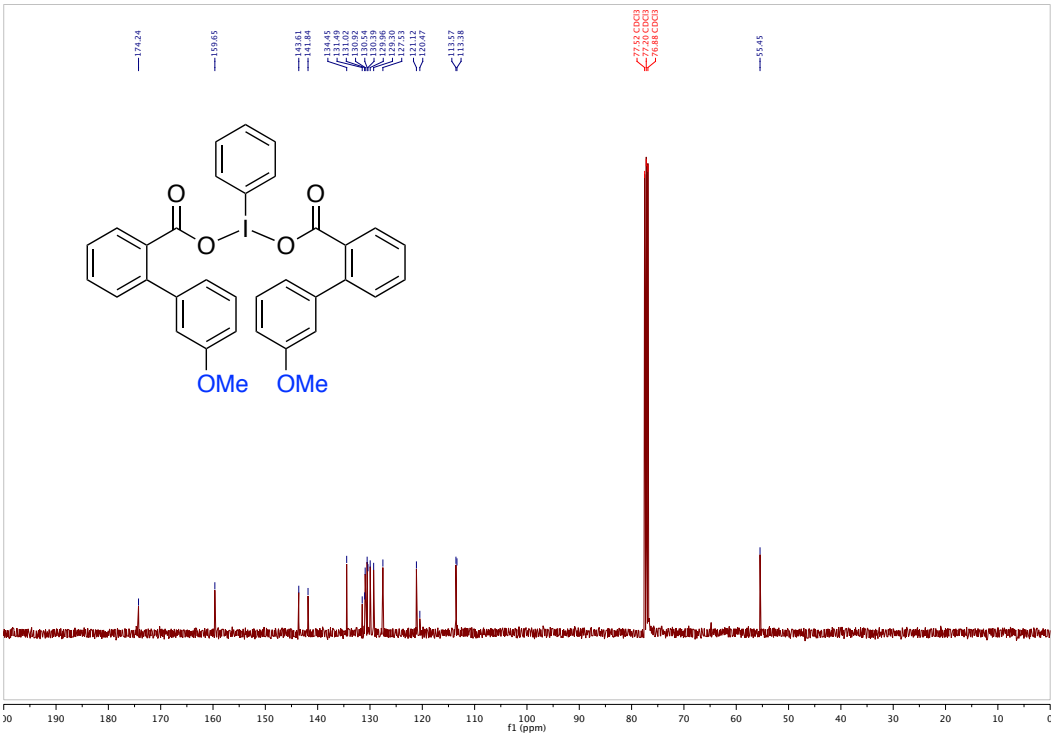

5.11 X-ray Crystallographic Data for 5-50, 5-86', 5-86, 5-53, 5-97 and 5-85

X-Ray Crystallography of 5-50

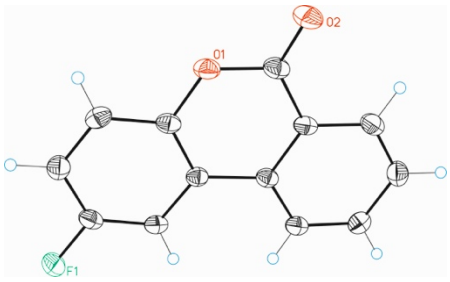

Table 1. Crystal data and structure refinement for **5-50**.

Identification code	**5-50**
Empirical formula	C13 H7 F O2
Formula weight	214.19
Temperature	100(2) K
Wavelength	0.71073 Å

Crystal system Orthorhombic

Space group Pna2(1)

Unit cell dimensions a = 13.795(3) Å a= 90.00 °.

b = 17.654(4) Å b = 90.00 °.

c = 3.7688(8) Å g = 90.00 °.

Volume 917.8(3) Å3

Z 4

Density (calculated) 1.550 Mg/m3

Absorption coefficient 0.118 mm-1

F(000) 440

Crystal size 0.04 x 0.01 x 0.002 mm3

Theta range for data collection 1.87 to 30.02 °.

Index ranges -18 <=h<=16 ,-23 <=k<=23 ,-3 <=l<=5

Reflections collected 7083

Independent reflections 2157 [R(int) = 0.0534]

Completeness to theta =30.02 ° 91.2%

Absorption correction Empirical

Max. and min. transmission 0.9883 and 0.9768

Refinement method Full-matrix least-squares on F2

Data / restraints / parameters 2157 / 1 / 145

Goodness-of-fit on F2 1.051

Final R indices [I>2sigma(I)] R1 = 0.0452 , wR2 = 0.1063

R indices (all data) R1 = 0.0637 , wR2 = 0.1168

Flack parameter x =0.0(11)

Largest diff. peak and hole 0.310 and -0.253 e.Å-3

Table 2. Bond lengths [Å] and angles [°] for **5-50**.

Bond lengths----

C1-F1 1.364(3)

C1-C13 1.367(3)

C1-C2 1.386(3)

C2-C3 1.383(3)

C3-C4 1.387(3)
C4-O3 1.387(3)
C4-C12 1.391(3)
C5-O2 1.207(3)
C5-O3 1.371(3)
C5-C6 1.468(3)
C6-C7 1.398(3)
C6-C11 1.403(3)
C7-C8 1.375(3)
C8-C9 1.392(4)
C9-C10 1.378(3)
C10-C11 1.404(3)
C11-C12 1.466(3)
C12-C13 1.403(3)

Angles----------
F1-C1-C13 118.4(2)
F1-C1-C2 117.6(2)
C13-C1-C2 123.9(2)
C3-C2-C1 117.5(2)
C2-C3-C4 119.6(2)
C3-C4-O3 115.4(2)
C3-C4-C12 122.6(2)
O3-C4-C12 122.1(2)
O2-C5-O3 116.6(2)
O2-C5-C6 125.7(2)
O3-C5-C6 117.6(2)
C7-C6-C11 120.5(2)
C7-C6-C5 118.1(2)
C11-C6-C5 121.3(2)
C8-C7-C6 120.0(2)
C7-C8-C9 119.8(2)
C10-C9-C8 121.0(2)

C9-C10-C11 120.1(2)
C6-C11-C10 118.6(2)
C6-C11-C12 118.0(2)
C10-C11-C12 123.4(2)
C4-C12-C13 117.60(19)
C4-C12-C11 118.7(2)
C13-C12-C11 123.7(2)
C1-C13-C12 118.8(2)
C5-O3-C4 122.20(18)

Table 3. Torsion angles [°] for **5-50**.

F1-C1-C2-C3 179.7(2)
C13-C1-C2-C3 -1.0(4)
C1-C2-C3-C4 1.4(4)
C2-C3-C4-O3 179.5(2)
C2-C3-C4-C12 -0.8(4)
O2-C5-C6-C7 -1.6(4)
O3-C5-C6-C7 179.1(2)
O2-C5-C6-C11 177.4(3)
O3-C5-C6-C11 -2.0(3)
C11-C6-C7-C8 0.3(4)
C5-C6-C7-C8 179.3(2)
C6-C7-C8-C9 -0.6(4)
C7-C8-C9-C10 0.4(4)
C8-C9-C10-C11 0.0(4)
C7-C6-C11-C10 0.1(3)
C5-C6-C11-C10 -178.9(2)
C7-C6-C11-C12 -179.9(2)
C5-C6-C11-C12 1.1(3)
C9-C10-C11-C6 -0.2(3)
C9-C10-C11-C12 179.7(2)

C3-C4-C12-C13 -0.2(3)

O3-C4-C12-C13 179.4(2)

C3-C4-C12-C11 -180.0(2)

O3-C4-C12-C11 -0.4(3)

C6-C11-C12-C4 0.0(3)

C10-C11-C12-C4 -179.9(2)

C6-C11-C12-C13 -179.7(2)

C10-C11-C12-C13 0.3(4)

F1-C1-C13-C12 179.3(2)

C2-C1-C13-C12 0.0(4)

C4-C12-C13-C1 0.6(3)

C11-C12-C13-C1 -179.6(2)

O2-C5-O3-C4 -177.8(2)

C6-C5-O3-C4 1.6(3)

C3-C4-O3-C5 179.1(2)

C12-C4-O3-C5 -0.5(3)

X-Ray Crystallography of 5-86'

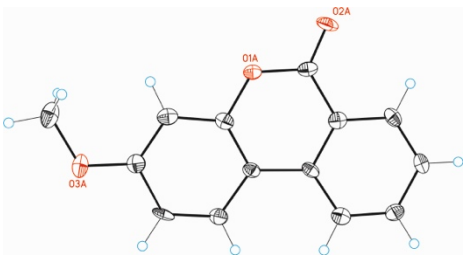

Table 1. Crystal data and structure refinement for **5-86'**.

Identification code	**5-86'**
Empirical formula	C14 H10 O3
Formula weight	226.22
Temperature	100(2) K
Wavelength	0.71073 Å

Crystal system Monoclinic

Space group Pn

Unit cell dimensions a = 16.0795(18) Å a= 90.00 °.

b = 3.8084(4) Å b = 96.927(3) °.

c = 16.6901(17) Å g = 90.00 °.

Volume 1014.59(19) Å3

Z 4

Density (calculated) 1.481 Mg/m3

Absorption coefficient 0.104 mm-1

F(000) 472

Crystal size 0.01 x 0.01 x 0.01 mm3

Theta range for data collection 1.66 to 27.61 °.

Index ranges -20 <=h<=20 ,-2 <=k<=4 ,-14 <=l<=21

Reflections collected 5361

Independent reflections 3106 [R(int) = 0.0249]

Completeness to theta =27.61 ° 98.4%

Absorption correction Empirical

Max. and min. transmission 0.9990 and 0.9990

Refinement method Full-matrix least-squares on F2

Data / restraints / parameters 3106 / 8 / 309

Goodness-of-fit on F2 1.115

Final R indices [I>2sigma(I)] R1 = 0.0757 , wR2 = 0.2349

R indices (all data) R1 = 0.0789 , wR2 = 0.2372

Flack parameter x =1(2)

Largest diff. peak and hole 0.737 and -0.465 e.Å-3

Table 2. Bond lengths [Å] and angles [°] for **5-86'**.

Bond lengths----

O1A-C13A 1.368(8)

O1A-C1A 1.378(7)

C2A-C3A 1.383(10)

C2A-C1A 1.389(9)

C13B-C8B 1.383(9)
C13B-O1B 1.395(7)
C13B-C12B 1.396(8)
O3A-C3A 1.348(8)
O3A-C14A 1.431(8)
C7B-C6B 1.387(9)
C7B-C2B 1.423(9)
C7B-C8B 1.469(8)
C6A-C1A 1.388(8)
C6A-C5A 1.411(8)
C6A-C7A 1.468(8)
C1B-O2B 1.226(8)
C1B-O1B 1.363(7)
C1B-C2B 1.445(9)
C11B-O3B 1.364(8)
C11B-C10B 1.371(9)
C11B-C12B 1.392(9)
C9B-C10B 1.374(9)
C9B-C8B 1.395(9)
O2A-C13A 1.204(8)
C3B-C4B 1.386(9)
C3B-C2B 1.393(8)
C8A-C9A 1.368(9)
C8A-C7A 1.401(8)
O3B-C14B 1.430(8)
C10A-C11A 1.377(9)
C10A-C9A 1.396(9)
C12A-C7A 1.399(8)
C12A-C11A 1.399(9)
C12A-C13A 1.477(8)
C3A-C4A 1.420(9)
C4A-C5A 1.362(9)
C5B-C6B 1.373(9)

C5B-C4B 1.395(9)

Angles----------

C13A-O1A-C1A 122.8(5)

C3A-C2A-C1A 119.0(6)

C8B-C13B-O1B 122.3(5)

C8B-C13B-C12B 123.5(5)

O1B-C13B-C12B 114.2(5)

C3A-O3A-C14A 117.5(5)

C6B-C7B-C2B 118.0(6)

C6B-C7B-C8B 124.0(6)

C2B-C7B-C8B 117.9(6)

C1A-C6A-C5A 116.3(6)

C1A-C6A-C7A 119.1(5)

C5A-C6A-C7A 124.6(5)

O2B-C1B-O1B 115.6(6)

O2B-C1B-C2B 124.8(6)

O1B-C1B-C2B 119.6(6)

O3B-C11B-C10B 116.3(5)

O3B-C11B-C12B 123.5(6)

C10B-C11B-C12B 120.2(6)

C10B-C9B-C8B 120.8(6)

C4B-C3B-C2B 120.6(6)

C1B-O1B-C13B 121.2(5)

C9A-C8A-C7A 120.5(6)

C11B-O3B-C14B 117.3(5)

C11A-C10A-C9A 118.9(6)

C7A-C12A-C11A 121.3(5)

C7A-C12A-C13A 120.6(6)

C11A-C12A-C13A 118.1(6)

O1A-C1A-C6A 121.5(5)

O1A-C1A-C2A 115.0(5)

C6A-C1A-C2A 123.5(6)

O3A-C3A-C2A 125.6(6)
O3A-C3A-C4A 115.5(6)
C2A-C3A-C4A 118.8(6)
C12A-C7A-C8A 117.8(6)
C12A-C7A-C6A 118.2(5)
C8A-C7A-C6A 124.0(6)
C13B-C8B-C9B 116.9(5)
C13B-C8B-C7B 118.7(6)
C9B-C8B-C7B 124.4(6)
C5A-C4A-C3A 120.8(6)
C3B-C2B-C7B 120.0(6)
C3B-C2B-C1B 119.7(6)
C7B-C2B-C1B 120.3(5)
O2A-C13A-O1A 116.9(5)
O2A-C13A-C12A 125.5(6)
O1A-C13A-C12A 117.6(5)
C4A-C5A-C6A 121.6(6)
C11B-C10B-C9B 121.3(6)
C10A-C11A-C12A 119.9(6)
C11B-C12B-C13B 117.3(6)
C8A-C9A-C10A 121.7(6)
C6B-C5B-C4B 120.9(6)
C5B-C6B-C7B 121.3(6)
C3B-C4B-C5B 119.0(5)

Table 3. Torsion angles [°] for **5-86'**.

O2B-C1B-O1B-C13B 179.8(5)
C2B-C1B-O1B-C13B 0.1(8)
C8B-C13B-O1B-C1B 0.2(8)
C12B-C13B-O1B-C1B -179.8(5)
C10B-C11B-O3B-C14B -179.8(5)

C12B-C11B-O3B-C14B -0.2(8)
C13A-O1A-C1A-C6A 2.7(8)
C13A-O1A-C1A-C2A -178.2(5)
C5A-C6A-C1A-O1A -178.6(6)
C7A-C6A-C1A-O1A 0.5(8)
C5A-C6A-C1A-C2A 2.3(9)
C7A-C6A-C1A-C2A -178.5(6)
C3A-C2A-C1A-O1A 178.3(5)
C3A-C2A-C1A-C6A -2.6(9)
C14A-O3A-C3A-C2A 0.0(9)
C14A-O3A-C3A-C4A 178.8(6)
C1A-C2A-C3A-O3A -179.8(6)
C1A-C2A-C3A-C4A 1.5(9)
C11A-C12A-C7A-C8A 1.1(9)
C13A-C12A-C7A-C8A -179.2(5)
C11A-C12A-C7A-C6A -177.9(6)
C13A-C12A-C7A-C6A 1.7(8)
C9A-C8A-C7A-C12A -0.7(9)
C9A-C8A-C7A-C6A 178.3(6)
C1A-C6A-C7A-C12A -2.6(8)
C5A-C6A-C7A-C12A 176.5(6)
C1A-C6A-C7A-C8A 178.4(6)
C5A-C6A-C7A-C8A -2.5(9)
O1B-C13B-C8B-C9B 179.2(5)
C12B-C13B-C8B-C9B -0.8(9)
O1B-C13B-C8B-C7B -0.4(8)
C12B-C13B-C8B-C7B 179.6(5)
C10B-C9B-C8B-C13B 1.3(9)
C10B-C9B-C8B-C7B -179.1(6)
C6B-C7B-C8B-C13B -178.4(6)
C2B-C7B-C8B-C13B 0.3(8)
C6B-C7B-C8B-C9B 2.1(9)
C2B-C7B-C8B-C9B -179.3(5)

O3A-C3A-C4A-C5A -179.1(6)
C2A-C3A-C4A-C5A -0.2(9)
C4B-C3B-C2B-C7B 1.3(9)
C4B-C3B-C2B-C1B 179.9(6)
C6B-C7B-C2B-C3B -2.7(8)
C8B-C7B-C2B-C3B 178.6(5)
C6B-C7B-C2B-C1B 178.7(6)
C8B-C7B-C2B-C1B 0.0(8)
O2B-C1B-C2B-C3B 1.5(10)
O1B-C1B-C2B-C3B -178.8(5)
O2B-C1B-C2B-C7B -179.9(6)
O1B-C1B-C2B-C7B -0.2(9)
C1A-O1A-C13A-O2A 176.7(5)
C1A-O1A-C13A-C12A -3.5(8)
C7A-C12A-C13A-O2A -179.0(6)
C11A-C12A-C13A-O2A 0.7(9)
C7A-C12A-C13A-O1A 1.2(8)
C11A-C12A-C13A-O1A -179.1(5)
C3A-C4A-C5A-C6A -0.1(9)
C1A-C6A-C5A-C4A -1.0(9)
C7A-C6A-C5A-C4A 179.9(6)
O3B-C11B-C10B-C9B 179.9(5)
C12B-C11B-C10B-C9B 0.3(9)
C8B-C9B-C10B-C11B -1.1(9)
C9A-C10A-C11A-C12A 0.5(9)
C7A-C12A-C11A-C10A -1.0(9)
C13A-C12A-C11A-C10A 179.3(6)
O3B-C11B-C12B-C13B -179.4(5)
C10B-C11B-C12B-C13B 0.2(8)
C8B-C13B-C12B-C11B 0.1(9)
O1B-C13B-C12B-C11B -179.9(5)
C7A-C8A-C9A-C10A 0.2(9)
C11A-C10A-C9A-C8A 0.0(10)

C4B-C5B-C6B-C7B -1.1(10)

C2B-C7B-C6B-C5B 2.6(9)

C8B-C7B-C6B-C5B -178.7(6)

C2B-C3B-C4B-C5B 0.3(9)

C6B-C5B-C4B-C3B -0.3(10)

X-Ray Crystallography of 5-86

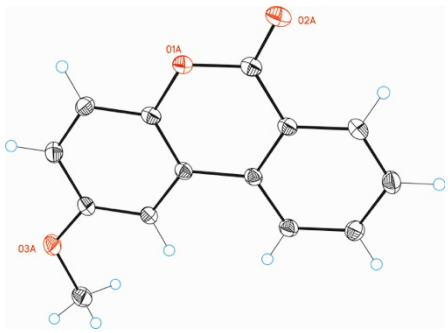

Table 1. Crystal data and structure refinement for **5-86**.

Identification code	**5-86**
Empirical formula	C14 H10 O3
Formula weight	226.22
Temperature	100(2) K
Wavelength	0.71073 Å
Crystal system	Triclinic
Space group	P-1
Unit cell dimensions	a = 7.4113(6) Å a= 83.117(2) °.
	b = 10.7360(8) Å b = 84.142(2) °.
	c = 13.6758(10) Å g = 73.882(2) °.
Volume	1035.14(14) Å3
Z	4
Density (calculated)	1.452 Mg/m3
Absorption coefficient	0.102 mm-1

F(000) 472

Crystal size 0.30 x 0.30 x 0.05 mm3

Theta range for data collection 1.50 to 31.96 °.

Index ranges -10 <=h<=10 ,-15 <=k<=14 ,-19 <=l<=11

Reflections collected 16160

Independent reflections 6272 [R(int) = 0.0400]

Completeness to theta =31.96 ° 87.7%

Absorption correction Empirical

Max. and min. transmission 0.9949 and 0.9700

Refinement method Full-matrix least-squares on F2

Data / restraints / parameters 6272 / 0 / 309

Goodness-of-fit on F2 1.020

Final R indices [I>2sigma(I)] R1 = 0.0551 , wR2 = 0.1377

R indices (all data) R1 = 0.0785 , wR2 = 0.1554

Largest diff. peak and hole 0.647 and -0.275 e.Å-3

Table 2. Bond lengths [Å] and angles [°] for **5-86**.

Bond lengths----

O1A-C1A 1.3651(17)

O1A-C13A 1.3871(16)

O2A-C1A 1.2110(17)

O3A-C10A 1.3718(17)

O3A-C14A 1.4288(19)

C1A-C2A 1.469(2)

C2A-C3A 1.3994(19)

C2A-C7A 1.4017(18)

C3A-C4A 1.380(2)

C4A-C5A 1.399(2)

C5A-C6A 1.3836(19)

C6A-C7A 1.4041(19)

C7A-C8A 1.4626(18)

C8A-C13A 1.3905(19)

C8A-C9A 1.4087(19)
C9A-C10A 1.3861(19)
C10A-C11A 1.401(2)
C11A-C12A 1.379(2)
C12A-C13A 1.3932(19)
O1B-C1B 1.3666(17)
O1B-C13B 1.3872(17)
O2B-C1B 1.2116(18)
O3B-C10B 1.3709(17)
O3B-C14B 1.425(2)
C1B-C2B 1.468(2)
C2B-C3B 1.4038(19)
C2B-C7B 1.4040(19)
C3B-C4B 1.381(2)
C4B-C5B 1.398(2)
C5B-C6B 1.3855(19)
C6B-C7B 1.4009(19)
C7B-C8B 1.4637(18)
C8B-C13B 1.3878(19)
C8B-C9B 1.4073(19)
C9B-C10B 1.3841(19)
C10B-C11B 1.403(2)
C11B-C12B 1.376(2)
C12B-C13B 1.3928(19)

Angles----------
C1A-O1A-C13A 121.90(11)
C10A-O3A-C14A 116.76(11)
O2A-C1A-O1A 117.27(13)
O2A-C1A-C2A 124.79(13)
O1A-C1A-C2A 117.93(12)
C3A-C2A-C7A 120.88(13)
C3A-C2A-C1A 118.15(12)

C7A-C2A-C1A 120.96(12)
C4A-C3A-C2A 120.31(13)
C3A-C4A-C5A 119.08(13)
C6A-C5A-C4A 121.15(13)
C5A-C6A-C7A 120.27(13)
C2A-C7A-C6A 118.31(12)
C2A-C7A-C8A 118.46(12)
C6A-C7A-C8A 123.22(12)
C13A-C8A-C9A 118.39(12)
C13A-C8A-C7A 118.24(12)
C9A-C8A-C7A 123.37(12)
C10A-C9A-C8A 119.97(13)
O3A-C10A-C9A 124.17(13)
O3A-C10A-C11A 115.25(12)
C9A-C10A-C11A 120.58(13)
C12A-C11A-C10A 119.85(13)
C11A-C12A-C13A 119.53(13)
O1A-C13A-C8A 122.44(12)
O1A-C13A-C12A 115.89(12)
C8A-C13A-C12A 121.67(13)
C1B-O1B-C13B 121.94(11)
C10B-O3B-C14B 117.33(12)
O2B-C1B-O1B 117.27(13)
O2B-C1B-C2B 125.10(13)
O1B-C1B-C2B 117.63(12)
C3B-C2B-C7B 120.73(13)
C3B-C2B-C1B 117.98(13)
C7B-C2B-C1B 121.27(12)
C4B-C3B-C2B 120.02(13)
C3B-C4B-C5B 119.42(13)
C6B-C5B-C4B 121.05(13)
C5B-C6B-C7B 120.24(13)
C6B-C7B-C2B 118.54(12)

C6B-C7B-C8B 123.19(12)

C2B-C7B-C8B 118.27(12)

C13B-C8B-C9B 118.46(12)

C13B-C8B-C7B 118.18(12)

C9B-C8B-C7B 123.35(12)

C10B-C9B-C8B 119.94(13)

O3B-C10B-C9B 124.32(13)

O3B-C10B-C11B 115.10(13)

C9B-C10B-C11B 120.58(13)

C12B-C11B-C10B 119.76(13)

C11B-C12B-C13B 119.55(13)

O1B-C13B-C8B 122.67(12)

O1B-C13B-C12B 115.65(12)

C8B-C13B-C12B 121.68(13)

Table 3. Torsion angles [°] for **5-86**.

C13A-O1A-C1A-O2A -179.51(13)

C13A-O1A-C1A-C2A -0.1(2)

O2A-C1A-C2A-C3A -1.6(2)

O1A-C1A-C2A-C3A 179.06(13)

O2A-C1A-C2A-C7A 177.69(14)

O1A-C1A-C2A-C7A -1.6(2)

C7A-C2A-C3A-C4A 0.3(2)

C1A-C2A-C3A-C4A 179.58(14)

C2A-C3A-C4A-C5A -0.6(2)

C3A-C4A-C5A-C6A 0.4(2)

C4A-C5A-C6A-C7A 0.1(2)

C3A-C2A-C7A-C6A 0.3(2)

C1A-C2A-C7A-C6A -179.01(13)

C3A-C2A-C7A-C8A -179.48(13)

C1A-C2A-C7A-C8A 1.2(2)

C5A-C6A-C7A-C2A -0.5(2)

C5A-C6A-C7A-C8A 179.26(13)

C2A-C7A-C8A-C13A 0.9(2)

C6A-C7A-C8A-C13A -178.87(14)

C2A-C7A-C8A-C9A -179.76(13)

C6A-C7A-C8A-C9A 0.5(2)

C13A-C8A-C9A-C10A 0.1(2)

C7A-C8A-C9A-C10A -179.30(13)

C14A-O3A-C10A-C9A 2.4(2)

C14A-O3A-C10A-C11A -177.91(13)

C8A-C9A-C10A-O3A -179.05(13)

C8A-C9A-C10A-C11A 1.2(2)

O3A-C10A-C11A-C12A 178.58(13)

C9A-C10A-C11A-C12A -1.7(2)

C10A-C11A-C12A-C13A 0.8(2)

C1A-O1A-C13A-C8A 2.3(2)

C1A-O1A-C13A-C12A -178.73(13)

C9A-C8A-C13A-O1A 177.91(12)

C7A-C8A-C13A-O1A -2.7(2)

C9A-C8A-C13A-C12A -1.0(2)

C7A-C8A-C13A-C12A 178.46(13)

C11A-C12A-C13A-O1A -178.42(13)

C11A-C12A-C13A-C8A 0.5(2)

C13B-O1B-C1B-O2B 178.17(13)

C13B-O1B-C1B-C2B -2.2(2)

O2B-C1B-C2B-C3B 2.8(2)

O1B-C1B-C2B-C3B -176.79(13)

O2B-C1B-C2B-C7B -178.71(14)

O1B-C1B-C2B-C7B 1.7(2)

C7B-C2B-C3B-C4B 0.0(2)

C1B-C2B-C3B-C4B 178.54(14)

C2B-C3B-C4B-C5B 0.2(2)

C3B-C4B-C5B-C6B 0.0(2)

C4B-C5B-C6B-C7B -0.3(2)

C5B-C6B-C7B-C2B 0.5(2)

C5B-C6B-C7B-C8B -178.41(14)

C3B-C2B-C7B-C6B -0.4(2)

C1B-C2B-C7B-C6B -178.85(13)

C3B-C2B-C7B-C8B 178.62(13)

C1B-C2B-C7B-C8B 0.1(2)

C6B-C7B-C8B-C13B 177.42(14)

C2B-C7B-C8B-C13B -1.5(2)

C6B-C7B-C8B-C9B -2.9(2)

C2B-C7B-C8B-C9B 178.20(13)

C13B-C8B-C9B-C10B 0.4(2)

C7B-C8B-C9B-C10B -179.30(14)

C14B-O3B-C10B-C9B -2.5(2)

C14B-O3B-C10B-C11B 177.33(15)

C8B-C9B-C10B-O3B 178.39(14)

C8B-C9B-C10B-C11B -1.4(2)

O3B-C10B-C11B-C12B -178.78(15)

C9B-C10B-C11B-C12B 1.0(3)

C10B-C11B-C12B-C13B 0.3(2)

C1B-O1B-C13B-C8B 0.9(2)

C1B-O1B-C13B-C12B -178.70(13)

C9B-C8B-C13B-O1B -178.64(13)

C7B-C8B-C13B-O1B 1.1(2)

C9B-C8B-C13B-C12B 0.9(2)

C7B-C8B-C13B-C12B -179.36(14)

C11B-C12B-C13B-O1B 178.29(14)

C11B-C12B-C13B-C8B -1.3(2)

X-Ray Crystallography of 5-53

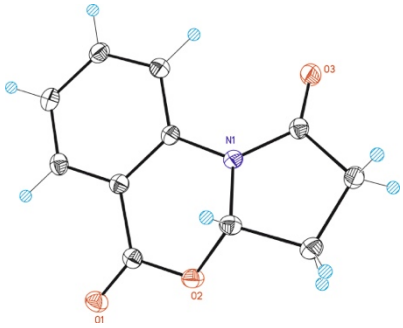

Table 1. Crystal data and structure refinement for **5-53**.

Identification code	**5-53**
Empirical formula	C11 H9 N O3
Formula weight	203.19
Temperature	100(2) K
Wavelength	0.71073 Å
Crystal system	Monoclinic
Space group	P2(1)/c
Unit cell dimensions	a = 8.9408(7) Å a= 90.00 °.
	b = 8.9435(6) Å b = 112.029(2) °.
	c = 11.8253(9) Å g = 90.00 °.
Volume	876.54(11) Å3
Z	4
Density (calculated)	1.540 Mg/m3
Absorption coefficient	0.114 mm-1
F(000)	424
Crystal size	0.25 x 0.15 x 0.15 mm3
Theta range for data collection	2.46 to 28.27 °.
Index ranges	-11 <=h<=11 ,-11 <=k<=11 ,-15 <=l<=13
Reflections collected	7099
Independent reflections	2157 [R(int) = 0.0271]
Completeness to theta =28.27 °	99.4%
Absorption correction	Empirical
Max. and min. transmission	0.9831 and 0.9721

Refinement method Full-matrix least-squares on F2

Data / restraints / parameters 2157 / 0 / 136

Goodness-of-fit on F2 1.040

Final R indices [I>2sigma(I)] R1 = 0.0421 , wR2 = 0.1071

R indices (all data) R1 = 0.0486 , wR2 = 0.1121

Largest diff. peak and hole 0.406 and -0.338 e.Å-3

Table 2. Bond lengths [Å] and angles [°] for **5-53**.

Bond lengths----

N1-C11 1.3774(16)

N1-C1 1.3997(16)

N1-C8 1.4466(16)

O1-C7 1.2084(16)

O2-C7 1.3555(15)

O2-C8 1.4453(15)

O3-C11 1.2164(17)

C1-C2 1.3973(18)

C1-C6 1.4030(17)

C2-C3 1.3888(18)

C3-C4 1.3944(19)

C4-C5 1.3838(19)

C5-C6 1.3961(17)

C6-C7 1.4815(18)

C8-C9 1.5223(18)

C9-C10 1.5305(19)

C10-C11 1.5138(18)

Angles----------

C11-N1-C1 129.27(11)

C11-N1-C8 113.56(10)

C1-N1-C8 116.83(10)

C7-O2-C8 117.09(10)

C2-C1-N1	123.75(11)
C2-C1-C6	120.30(12)
N1-C1-C6	115.95(11)
C3-C2-C1	118.71(12)
C2-C3-C4	121.48(13)
C5-C4-C3	119.54(12)
C4-C5-C6	120.13(12)
C5-C6-C1	119.81(12)
C5-C6-C7	119.19(11)
C1-C6-C7	120.74(11)
O1-C7-O2	118.58(12)
O1-C7-C6	124.06(12)
O2-C7-C6	117.30(11)
O2-C8-N1	110.80(10)
O2-C8-C9	109.29(10)
N1-C8-C9	104.57(10)
C8-C9-C10	104.74(10)
C11-C10-C9	105.42(10)
O3-C11-N1	125.25(12)
O3-C11-C10	127.24(12)
N1-C11-C10	107.51(11)

Table 3. Torsion angles [°] for **5-53**.

C11-N1-C1-C2	-17.9(2)
C8-N1-C1-C2	154.99(12)
C11-N1-C1-C6	162.49(13)
C8-N1-C1-C6	-24.65(16)
N1-C1-C2-C3	-179.52(12)
C6-C1-C2-C3	0.11(19)
C1-C2-C3-C4	1.2(2)
C2-C3-C4-C5	-1.5(2)

C3-C4-C5-C6	0.4(2)
C4-C5-C6-C1	0.96(19)
C4-C5-C6-C7	-173.27(12)
C2-C1-C6-C5	-1.20(19)
N1-C1-C6-C5	178.45(11)
C2-C1-C6-C7	172.95(11)
N1-C1-C6-C7	-7.40(17)
C8-O2-C7-O1	-165.38(11)
C8-O2-C7-C6	17.39(16)
C5-C6-C7-O1	8.41(19)
C1-C6-C7-O1	-165.77(13)
C5-C6-C7-O2	-174.53(11)
C1-C6-C7-O2	11.29(18)
C7-O2-C8-N1	-47.46(14)
C7-O2-C8-C9	-162.17(10)
C11-N1-C8-O2	-134.32(11)
C1-N1-C8-O2	51.71(14)
C11-N1-C8-C9	-16.69(14)
C1-N1-C8-C9	169.34(11)
O2-C8-C9-C10	139.03(11)
N1-C8-C9-C10	20.36(13)
C8-C9-C10-C11	-17.49(14)
C1-N1-C11-O3	-1.6(2)
C8-N1-C11-O3	-174.63(12)
C1-N1-C11-C10	178.54(12)
C8-N1-C11-C10	5.49(15)
C9-C10-C11-O3	-171.83(13)
C9-C10-C11-N1	8.05(14)

X-Ray Crystallography of 5-97

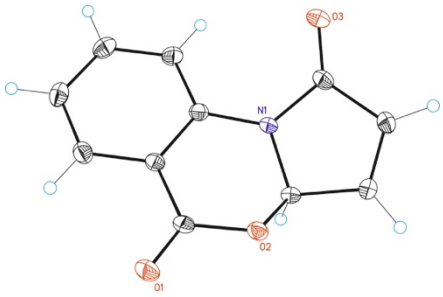

Table 1. Crystal data and structure refinement for **5-97**.

Identification code	**5-97**
Empirical formula	C11 H7 N O3
Formula weight	201.18
Temperature	100(2) K
Wavelength	0.71073 Å
Crystal system	Monoclinic
Space group	P2(1)/c
Unit cell dimensions	a = 9.3860(9) Å α= 90.00 °.
	b = 3.8928(4) Å β = 99.904(3) °.
	c = 23.696(2) Å γ = 90.00 °.
Volume	852.90(15) Å3
Z	4
Density (calculated)	1.567 Mg/m3
Absorption coefficient	0.116 mm-1
F(000)	416
Crystal size	0.40 x 0.10 x 0.06 mm3
Theta range for data collection	1.74 to 29.16 °.
Index ranges	-12 <=h<=12 ,0 <=k<=5 ,0 <=l<=32
Reflections collected	3963
Independent reflections	3963 [R(int) = 0.0000]
Completeness to theta =29.16 °	96.7%
Absorption correction	Empirical
Max. and min. transmission	0.9931 and 0.9550
Refinement method	Full-matrix least-squares on F2

Data / restraints / parameters 3963 / 330 / 272

Goodness-of-fit on F2 1.115

Final R indices [I>2sigma(I)] R1 = 0.0575 , wR2 = 0.1515

R indices (all data) R1 = 0.0768 , wR2 = 0.1692

Largest diff. peak and hole 0.315 and -0.304 e.Å-3

Table 2. Bond lengths [Å] and angles [°] for **5-97**.

Bond lengths----

N1-C1 1.3941(18)

N1-C7 1.3987(18)

N1-C4 1.4440(17)

O3-C1 1.2123(18)

O2-C5 1.3690(18)

O2-C4 1.4407(18)

O1-C5 1.2101(19)

C1-C2 1.483(2)

C2-C3 1.329(2)

C3-C4 1.498(2)

C5-C6 1.479(2)

C6-C11 1.394(2)

C6-C7 1.4045(19)

C7-C8 1.386(2)

C8-C9 1.384(2)

C9-C10 1.394(2)

C10-C11 1.382(2)

N1'-C1' 1.393(4)

N1'-C7' 1.399(4)

N1'-C4' 1.445(4)

O3'-C1' 1.212(4)

O2'-C5' 1.369(4)

O2'-C4' 1.441(5)

O1'-C5' 1.211(4)

C1'-C2'	1.483(5)
C2'-C3'	1.327(5)
C3'-C4'	1.499(5)
C5'-C6'	1.479(4)
C6'-C11'	1.396(4)
C6'-C7'	1.406(4)
C7'-C8'	1.386(4)
C8'-C9'	1.384(5)
C9'-C10'	1.393(5)
C10'-C11'	1.382(5)

Angles----------

C1-N1-C7	129.09(12)
C1-N1-C4	111.41(12)
C7-N1-C4	117.92(11)
C5-O2-C4	116.06(13)
O3-C1-N1	125.01(15)
O3-C1-C2	129.53(15)
N1-C1-C2	105.45(12)
C3-C2-C1	109.74(15)
C2-C3-C4	110.10(14)
O2-C4-N1	111.19(11)
O2-C4-C3	111.16(13)
N1-C4-C3	103.24(11)
O1-C5-O2	117.35(14)
O1-C5-C6	125.26(15)
O2-C5-C6	117.15(12)
C11-C6-C7	119.48(13)
C11-C6-C5	119.31(13)
C7-C6-C5	120.83(13)
C8-C7-N1	123.22(13)
C8-C7-C6	120.47(14)
N1-C7-C6	116.31(12)

C9-C8-C7 119.27(15)
C8-C9-C10 120.80(16)
C11-C10-C9 120.02(15)
C10-C11-C6 119.94(14)
C1'-N1'-C7' 129.7(4)
C1'-N1'-C4' 111.4(3)
C7'-N1'-C4' 117.5(4)
C5'-O2'-C4' 116.7(5)
O3'-C1'-N1' 125.1(6)
O3'-C1'-C2' 129.3(6)
N1'-C1'-C2' 105.5(3)
C3'-C2'-C1' 109.6(4)
C2'-C3'-C4' 110.2(4)
O2'-C4'-N1' 111.2(5)
O2'-C4'-C3' 110.7(6)
N1'-C4'-C3' 103.1(3)
O1'-C5'-O2' 117.1(5)
O1'-C5'-C6' 125.1(5)
O2'-C5'-C6' 117.2(4)
C11'-C6'-C7' 119.6(4)
C11'-C6'-C5' 118.9(4)
C7'-C6'-C5' 121.3(4)
C8'-C7'-N1' 123.6(4)
C8'-C7'-C6' 120.1(4)
N1'-C7'-C6' 115.9(4)
C9'-C8'-C7' 119.3(5)
C8'-C9'-C10' 120.8(5)
C11'-C10'-C9' 119.9(5)
C10'-C11'-C6' 119.8(5)

Table 3. Torsion angles [°] for **5-97**.

C7-N1-C1-O3	-12.2(3)
C4-N1-C1-O3	-177.38(17)
C7-N1-C1-C2	166.99(15)
C4-N1-C1-C2	1.84(18)
O3-C1-C2-C3	176.68(19)
N1-C1-C2-C3	-2.5(2)
C1-C2-C3-C4	2.2(2)
C5-O2-C4-N1	50.12(17)
C5-O2-C4-C3	164.53(12)
C1-N1-C4-O2	118.63(14)
C7-N1-C4-O2	-48.35(18)
C1-N1-C4-C3	-0.64(17)
C7-N1-C4-C3	-167.62(13)
C2-C3-C4-O2	-120.28(15)
C2-C3-C4-N1	-1.00(19)
C4-O2-C5-O1	161.24(14)
C4-O2-C5-C6	-24.04(19)
O1-C5-C6-C11	-4.8(2)
O2-C5-C6-C11	-179.02(14)
O1-C5-C6-C7	168.12(16)
O2-C5-C6-C7	-6.1(2)
C1-N1-C7-C8	34.8(3)
C4-N1-C7-C8	-160.88(15)
C1-N1-C7-C6	-144.82(16)
C4-N1-C7-C6	19.5(2)
C11-C6-C7-C8	1.7(2)
C5-C6-C7-C8	-171.20(15)
C11-C6-C7-N1	-178.70(14)
C5-C6-C7-N1	8.4(2)
N1-C7-C8-C9	179.11(16)
C6-C7-C8-C9	-1.3(3)
C7-C8-C9-C10	0.0(3)
C8-C9-C10-C11	0.8(3)

C9-C10-C11-C6	-0.4(3)
C7-C6-C11-C10	-0.8(2)
C5-C6-C11-C10	172.18(16)
C7'-N1'-C1'-O3'	14.7(18)
C4'-N1'-C1'-O3'	-179.3(12)
C7'-N1'-C1'-C2'	-169.2(10)
C4'-N1'-C1'-C2'	-3.2(11)
O3'-C1'-C2'-C3'	-179.8(14)
N1'-C1'-C2'-C3'	4.3(15)
C1'-C2'-C3'-C4'	-3.7(15)
C5'-O2'-C4'-N1'	-48.2(10)
C5'-O2'-C4'-C3'	-162.2(8)
C1'-N1'-C4'-O2'	-117.5(8)
C7'-N1'-C4'-O2'	50.4(9)
C1'-N1'-C4'-C3'	1.1(10)
C7'-N1'-C4'-C3'	169.0(8)
C2'-C3'-C4'-O2'	120.7(11)
C2'-C3'-C4'-N1'	1.7(12)
C4'-O2'-C5'-O1'	-167.0(10)
C4'-O2'-C5'-C6'	21.7(13)
O1'-C5'-C6'-C11'	9.7(16)
O2'-C5'-C6'-C11'	-179.8(9)
O1'-C5'-C6'-C7'	-165.2(11)
O2'-C5'-C6'-C7'	5.4(14)
C1'-N1'-C7'-C8'	-32.7(16)
C4'-N1'-C7'-C8'	162.0(9)
C1'-N1'-C7'-C6'	140.6(10)
C4'-N1'-C7'-C6'	-24.7(12)
C11'-C6'-C7'-C8'	-5.0(15)
C5'-C6'-C7'-C8'	169.8(10)
C11'-C6'-C7'-N1'	-178.6(9)
C5'-C6'-C7'-N1'	-3.8(13)
N1'-C7'-C8'-C9'	179.2(11)

C6'-C7'-C8'-C9' 6.1(17)

C7'-C8'-C9'-C10' -7(2)

C8'-C9'-C10'-C11' 6(2)

C9'-C10'-C11'-C6' -5(2)

C7'-C6'-C11'-C10' 4.4(17)

C5'-C6'-C11'-C10' -170.5(12)

X-Ray Crystallography of 5-85

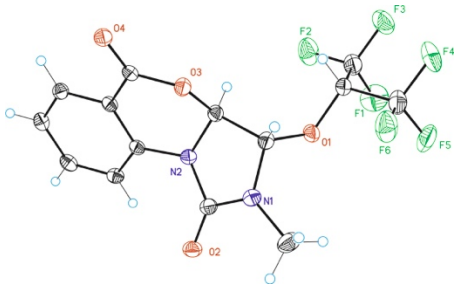

Table 1. Crystal data and structure refinement for **5-85**.

Identification code	**5-85**
Empirical formula	C14 H10 F6 N2 O4
Formula weight	384.24
Temperature	100(2) K
Wavelength	0.71073 Å
Crystal system	Monoclinic
Space group	P2(1)/c
Unit cell dimensions	a = 7.0844(3) Å a= 90.00 °.
	b = 29.4897(11) Å b = 90.5280(10) °.
	c = 7.2945(3) Å g = 90.00 °.
Volume	1523.88(11) Å3
Z	4
Density (calculated)	1.675 Mg/m3
Absorption coefficient	0.169 mm-1

F(000) 776

Crystal size 0.40 x 0.25 x 0.10 mm3

Theta range for data collection 1.38 to 30.14 °.

Index ranges -9 <=h<=9 ,-40 <=k<=37 ,-10 <=l<=9

Reflections collected 13504

Independent reflections 3981 [R(int) = 0.0286]

Completeness to theta =30.14 ° 88.4%

Absorption correction Empirical

Max. and min. transmission 0.9833 and 0.9353

Refinement method Full-matrix least-squares on F2

Data / restraints / parameters 3981 / 0 / 236

Goodness-of-fit on F2 1.079

Final R indices [I>2sigma(I)] R1 = 0.0419 , wR2 = 0.1053

R indices (all data) R1 = 0.0477 , wR2 = 0.1087

Largest diff. peak and hole 0.399 and -0.274 e.Å-3

Table 2. Bond lengths [Å] and angles [°] for **5-85**.

Bond lengths----

N1-C2 1.3712(18)

N1-C1 1.4199(18)

N1-C14 1.4519(18)

N2-C2 1.3972(17)

N2-C10 1.4106(17)

N2-C3 1.4364(17)

O1-C11 1.4054(16)

O1-C1 1.4421(16)

O2-C2 1.2135(17)

O3-C4 1.3658(16)

O3-C3 1.4405(16)

O4-C4 1.2037(16)

C1-C3 1.5322(18)

C4-C5 1.4799(18)

C5-C6 1.3986(18)
C5-C10 1.4013(18)
C6-C7 1.3832(19)
C7-C8 1.397(2)
C8-C9 1.386(2)
C9-C10 1.3898(18)
C11-C12 1.523(2)
C11-C13 1.525(2)
C12-F1 1.329(2)
C12-F3 1.3316(19)
C12-F2 1.3319(19)
C13-F5 1.3283(19)
C13-F4 1.3308(19)
C13-F6 1.339(2)

Angles----------
C2-N1-C1 112.70(11)
C2-N1-C14 123.62(12)
C1-N1-C14 122.55(12)
C2-N2-C10 125.33(11)
C2-N2-C3 111.23(11)
C10-N2-C3 116.71(11)
C11-O1-C1 115.03(10)
C4-O3-C3 115.42(10)
N1-C1-O1 107.65(11)
N1-C1-C3 103.24(11)
O1-C1-C3 110.47(11)
O2-C2-N1 126.80(13)
O2-C2-N2 126.40(13)
N1-C2-N2 106.80(11)
N2-C3-O3 112.47(11)
N2-C3-C1 103.38(11)
O3-C3-C1 108.32(11)

O4-C4-O3 118.27(12)
O4-C4-C5 124.49(12)
O3-C4-C5 117.03(11)
C6-C5-C10 119.70(12)
C6-C5-C4 118.86(12)
C10-C5-C4 121.13(12)
C7-C6-C5 119.78(12)
C6-C7-C8 119.94(13)
C9-C8-C7 120.96(13)
C8-C9-C10 119.07(12)
C9-C10-C5 120.53(12)
C9-C10-N2 123.07(12)
C5-C10-N2 116.38(11)
O1-C11-C12 107.43(12)
O1-C11-C13 108.73(12)
C12-C11-C13 113.41(12)
F1-C12-F3 107.25(14)
F1-C12-F2 107.61(15)
F3-C12-F2 107.17(13)
F1-C12-C11 113.08(13)
F3-C12-C11 111.56(14)
F2-C12-C11 109.90(13)
F5-C13-F4 107.87(13)
F5-C13-F6 107.43(14)
F4-C13-F6 107.45(14)
F5-C13-C11 113.00(13)
F4-C13-C11 111.69(13)
F6-C13-C11 109.16(12)

Table 3. Torsion angles [°] for **5-85**.

C2-N1-C1-O1 -101.87(13)

C14-N1-C1-O1	66.32(17)
C2-N1-C1-C3	14.99(15)
C14-N1-C1-C3	-176.82(13)
C11-O1-C1-N1	-157.24(11)
C11-O1-C1-C3	90.72(13)
C1-N1-C2-O2	171.91(13)
C14-N1-C2-O2	3.9(2)
C1-N1-C2-N2	-7.90(16)
C14-N1-C2-N2	-175.94(13)
C10-N2-C2-O2	26.6(2)
C3-N2-C2-O2	176.71(13)
C10-N2-C2-N1	-153.55(12)
C3-N2-C2-N1	-3.48(15)
C2-N2-C3-O3	-104.45(13)
C10-N2-C3-O3	48.43(15)
C2-N2-C3-C1	12.16(14)
C10-N2-C3-C1	165.05(11)
C4-O3-C3-N2	-50.83(15)
C4-O3-C3-C1	-164.45(10)
N1-C1-C3-N2	-15.71(13)
O1-C1-C3-N2	99.15(12)
N1-C1-C3-O3	103.81(12)
O1-C1-C3-O3	-141.34(11)
C3-O3-C4-O4	-161.66(12)
C3-O3-C4-C5	23.41(16)
O4-C4-C5-C6	6.2(2)
O3-C4-C5-C6	-179.17(11)
O4-C4-C5-C10	-167.25(13)
O3-C4-C5-C10	7.33(18)
C10-C5-C6-C7	1.4(2)
C4-C5-C6-C7	-172.14(12)
C5-C6-C7-C8	-0.2(2)
C6-C7-C8-C9	-0.8(2)

C7-C8-C9-C10 0.6(2)

C8-C9-C10-C5 0.6(2)

C8-C9-C10-N2 -177.53(12)

C6-C5-C10-C9 -1.65(19)

C4-C5-C10-C9 171.80(12)

C6-C5-C10-N2 176.62(12)

C4-C5-C10-N2 -9.94(18)

C2-N2-C10-C9 -51.43(19)

C3-N2-C10-C9 159.95(12)

C2-N2-C10-C5 130.36(13)

C3-N2-C10-C5 -18.26(17)

C1-O1-C11-C12 -137.45(12)

C1-O1-C11-C13 99.44(13)

O1-C11-C12-F1 -57.26(16)

C13-C11-C12-F1 62.92(18)

O1-C11-C12-F3 -178.26(12)

C13-C11-C12-F3 -58.08(18)

O1-C11-C12-F2 63.01(16)

C13-C11-C12-F2 -176.81(13)

O1-C11-C13-F5 61.33(17)

C12-C11-C13-F5 -58.11(18)

O1-C11-C13-F4 -176.82(12)

C12-C11-C13-F4 63.73(17)

O1-C11-C13-F6 -58.15(16)

C12-C11-C13-F6 -177.59(13)

Chapter 6: General Conclusion and Outlook

In this PhD thesis we have established two catalytic protocol towards the synthesis of carboxylic acids by dealing with Ni-catalyzed CO_2 fixation techniques. In chapter 2, we developed a mild, robust and use-friendly Ni-catalyzed cascade reductive cyclization/carboxylation using CO_2 in which the selectivity pattern is dictated by an appropriate substrate and/or ligand selection. The project is distinguished by its good functional group tolerance and excellent selectivity. We carried out mechanistic studies for this protocol, and found that while primary alkyl bromides undergo a traditional organometallic pathway, secondary alkyl bromides follow a radical-type mechanism.

Ni-catalyzed Reductive Cyclization/Carboxylation

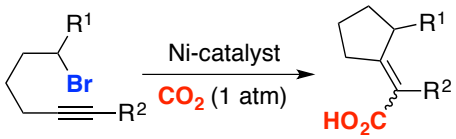

Scheme 6.1. Ni-catalyzed reductive cyclization/carboxylation.

In chapter 3, we described a novel, mild and use-friendly Ni-catalyzed hydrocarboxylation of alkynes at atmospheric pressure of CO_2 that occurs with an exquisite C2 regioselectivity profile using commercially available alcohols as proton source. The protocol tolerates a wide number of functional groups such as ketone, ester, amide, chloride, tosylate, and pivalate among others. The outcomes of mechanistic studies supported a mechanism involving nickelalactone intermediate.

Ni-catalyzed Reductive Hydrocarboxylation

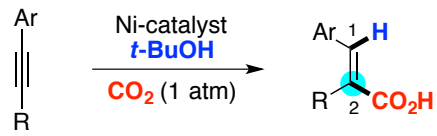

Scheme 6.2. Ni-catalyzed hydrocarboxylation.

Following up with our interest in reductive electrophile-electrophile cross coupling reactions. In chapter 4, we developed a convenient hydroamidation protocol of alkynes with isocyanates that utilizes simple alkyl bromides as hydride source. The transformation occurs under mild reaction conditions with an excellent chemoselectivity profile. Differing from our hydrocarboxylation reactions, we can incorporate isocyanates into alkynes with a C1 selectivity in this hydroamidation. Initial

isotope-labelling studies confirm the intermediacy of well-defined [Ni]-hydride species.

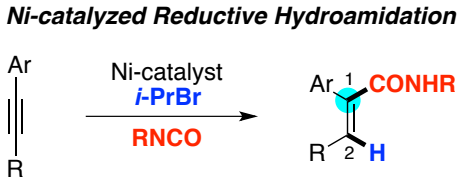

Scheme 6.3. Ni-catalyzed hydroamidation.

In chapter 5, we established a C(sp^2)-H or C(sp^3)-H functionalization/C-O bond forming process catalyzed by *in situ* generated I(III) reagent. The reactions occurred under mild conditions and with an intriguing selectivity switch depending on the catalyst used. We believe that the results of mechanistic studies support the intermediacy of a species like **5-95** species within the catalytic cycle, thus revealing an intimate interplay between the ArI motif and non-innocent additives. This air-insensitive method is a cheap and practical alternative to related metal-catalyzed protocols.

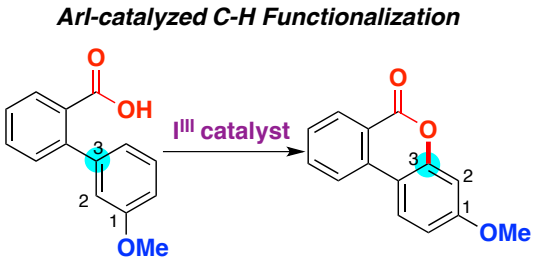

Scheme 6.4. ArI-catalyzed C-H functionalization.